



VALIDATION OF INTELLIGENT COMPACTION TO CHARACTERIZE PAVEMENT FOUNDATION MECHANICAL PROPERTIES

Prepared By
Erol Tutumluer and Maziar Moaveni
University of Illinois at Urbana-Champaign
and
David J. White and Pavana Vennapusa
Ingios Geotechnics, Inc.

Research Report No: 16-01 UILU-ENG-2018

Sponsored by
Illinois State Toll Highway Authority

Report Prepared by
University of Illinois at Urbana-Champaign

February 2018

Technical Report Documentation Page

1. Report No. 16-01 UILU-ENG-2018		2. Government Accession No.		3. Recipient's Catalog No.	
4. Title and Subtitle Validation of Intelligent Compaction to Characterize Pavement Foundation Mechanical Properties				5. Report Date February 2018	
				6. Performing Organization Code N/A	
7. Author(s) Erol Tutumluer, Maziar Moaveni, David White, Pavana Vennapusa				8. Performing Organization Report No. 16-01 UILU-ENG-2018	
9. Performing Organization Name and Address Department of Civil & Environmental Engineering University of Illinois at Urbana-Champaign 205 N. Mathews Ave., MC-250 Urbana, IL 61801				10. Work Unit No. (TRAIS)	
				11. Contract or Grant No. ITHA KC083509	
12. Sponsoring Agency Name and Address Illinois State Toll Highway Authority 2700 Ogden Ave Downers Grove, IL 60515				13. Type of Report and Period Covered Final Report 2016-2018	
				14. Sponsoring Agency Code	
15. Supplementary Notes					
16. Abstract <p>Although intelligent compaction (IC) technologies have been used in the U.S. on over 380 pilot/demonstration projects since year 2000, current specifications lack a detailed framework for calibration (i.e., corrections from independent testing) and validation of results (i.e., accuracy and system quality checks) in terms of mechanical soil properties. The next big leap forward in pavement foundation construction quality could be realized through developing statistically valid relationships between IC measurement values (MVs) and mechanical properties of compacted materials. The main objectives of the research presented herein were to create a synthesis of literature that identifies methods used to compare IC measurements to soil mechanical properties, to develop a criteria or procedure for field validating IC measurements versus soil mechanical properties, and to demonstrate the field calibration process using different IC technology providers. The literature review resulted in a synthesis of information that identifies methods/procedures used to compare IC measurements to soil mechanical properties, and the success of those methods/procedures along with a summary of current IC specifications.</p> <p>As part of the field demonstration phase of this project, in coordination with Illinois State Toll Highway Authority, field testing was conducted on selected test sections on the Elgin O'Hare Western Access Tollway construction project in October 2016, April-May 2017, and in June 2017. Field evaluation was performed on a total of 18 test sections, of which in situ comparison and calibration testing was conducted on 12 test sections. Four different IC-MV technologies were evaluated including: CMV, H MV, MDP, and VIC. Field calibration testing was conducted using LWD, DCP, and static and cyclic APLT testing. To implement IC technologies on near-term Tollway projects, a calibration process and a guide specification were developed. A guide specification is recommended for implementation on upcoming construction projects.</p>					
17. Key Words Intelligent Compaction, Pavement Foundation, Subgrade, Subbase, Quality Control, Quality Assurance, Specifications				18. Distribution Statement No restrictions.	
19. Security Classif. (of this report) Unclassified		20. Security Classif. (of this page) Unclassified		304	22. Price

ACKNOWLEDGMENTS

This publication is based on the results of Illinois State Toll Highway Authority project: Validation of Intelligent Compaction to Characterize Pavement Foundation Mechanical Properties. This research was conducted in cooperation with the Illinois Center for Transportation; the Illinois State Toll Highway Authority, and Ingios Geotechnics, Inc.

The research team appreciates the contribution of the members of the Technical Review Panel (TRP):

- Bill Vavrik (ARA – TRP Chair)
- Steve Gillen (Tollway)
- Dan Gancarz (Tollway)
- Nick Smith (AECOM)
- Sheila Beshears (IDOT Central Bureau of Materials)
- Heather Shoup (IDOT Central Bureau of Materials)
- George Houston (IDOT D-1)
- Supraja Reddy (Interra)
- Tim Seiwert (Plote)
- Todd Ward (STATE Testing)
- Drew Ptak (Geoservices)
- Allen J. DeClerk (Caterpillar)

The research team also extends special appreciation to Bin Feng and Wei Li – Graduate Research Assistants, Marc Allen Killion – CEE Machine Shop, and Greg Renshaw – Illinois Center for Transportation Research Engineer from the University of Illinois at Urbana Champaign, for field and lab testing assistance. Heath Gieselman and Colby VanNimwegen provided field support for Ingios to conduct APLT testing. We also appreciate the help from Tim Kowalski - Hamm Applications Support Manager and Tyler Barton – Shop Technician with WIRTGEN AMERICA, and Michael J. Brunson - Roland Machinery Company for providing roller support. Kenny Rigan – Project Superintendent with Plote, Bob Valentine – Construction Manager helped provide project site access and roller operators for mapping.

DISCLAIMER

The contents of this report reflect the view of the authors, who are responsible for the facts and the accuracy of the data presented herein. The contents do not necessarily reflect the official views or policies of the Illinois State Toll Highway Authority. This report does not constitute a standard, specification, or regulation.

NOTATIONS AND ABBREVIATIONS

A	Vibration amplitude
AASHTO	American Association for State Highway and Transportation Officials
a	Machine acceleration
a_1 , a_2 , and a_3	Regression coefficients
$A_{0.5\Omega}$	Drum acceleration amplitude at half of the operating frequency
A_{Ω}	Amplitude of the vertical drum acceleration at the operating frequency
$A_{2\Omega}$	Drum acceleration amplitude of the first harmonic or twice the operating frequency
$A_{2.5\Omega}$	Drum acceleration amplitude at two and half times the operating frequency
$A_{3\Omega}$	Drum acceleration amplitude at three times the operating frequency
APLT	Automated plate load testing
ASTM	American Society of Testing and Materials
b	Machine internal loss coefficients specific to a machine
B	Contact width of the drum
BCD	Briaud compaction device
BST	Borehole shear test
c'	Effective cohesion
c_u	Undrained cohesion
C	Constant
CBR	California bearing ratio
CCC	Continuous compaction control
CCV	Continuous compaction value
CL	Low plasticity clay
CH	High plasticity clay
CIR	Col in-place recycling
CMV	Compaction meter value
COV	Coefficient of variation
CPT	Cone penetration test
DOT	Department of Transportation
DCP	Dynamic cone penetrometer
DPI	Dynamic penetration index
D-SPA	Dynamic seismic pavement analyzer
E	Elastic modulus
E_{LWD}	Elastic modulus determined using LWD

E_{vib}	Vibratory modulus
F_s	Drum force
F	Shape factor
FDR	Full depth reclamation
FFT	Fast Fourier Transform
FHWA	Federal Highway Administration
FS	Factor of safety
FWD	Falling weight deflectometer
g	Acceleration of gravity
GP	Poorly graded gravel
GPS	Global position system
GW	Well graded gravel
h	Thickness of the base or top layer (in layered analysis)
h_e	Equivalent thickness
HMA	Hot mix asphalt
HMV	Hamm measurement value
IC	Intelligent compaction
IC-MV	Intelligent compaction measurement value
ILT	Illinois Tollway
LWD	Light weight deflectometer
M_r	Resilient modulus
M_{r1}	Resilient modulus of the top layer (in layered analysis)
M_{r2}	Resilient modulus of the bottom layer (in layered analysis)
M_{r-Comp}	Composite resilient modulus
M_{r-Base}	Base or top layer resilient modulus
M_{r-SG}	Subgrade or bottom layer resilient modulus
NG	Nuclear gauge
K_o	Coefficient of lateral earth pressure at rest
k	Modulus of subgrade reaction
k_s	Soil stiffness measurement value
k'_u	Uncorrected modulus of subgrade reaction
k_u	Modulus of subgrade reaction corrected for plate bending (uncorrected for saturation)
k_{u1} or k_{u2}	1 represents value determined during 1 st loading cycle and 2 represents value determined using 2 nd loading cycle
k_1^* , k_2^* , k_3^*	Stress-dependent resilient modulus model parameters

L	Length of the drum
MDP	Machine drive power
MDP*	Machine drive power (rescaled)
MET	Method of equivalent thickness
m	Machine internal loss coefficients specific to a machine
m_d	Drum mass
$m_e r_e$	Eccentric moment of the unbalanced mass
n	Number of measurements
NCHRP	National Cooperative Highway Research Program
P_a	Atmospheric pressure
P_g	Gross power needed to move the machine
PCC	Portland cement concrete
PD	Padfoot drum
PGE	Porous granular embankment
PLT	Plate load test
QC	Quality control
QA	Quality assurance
r	Plate radius
R	Drum radius
R^2	Coefficient of determination
RAP	Recycled asphalt pavement
RC	Relative compaction
RTK	Real time kinematic
RPCC	Recycled portland cement concrete
SBAS	Satellite based augmentation system
SD	Smooth drum
SDG	Soil density gauge
SPA	Seismic pavement analyzer
SWCC	Soil water characteristic curve
V	Roller velocity
VIC	Validated intelligent compaction
VST	Vane shear test
W	Roller weight
w	Moisture content
w_{opt}	Optimum moisture content

x	Applied stress
y	Deflection in inches
σ_0	Applied stress
Z_d	Drum displacement
α	Slope angle (roller pitch from a sensor)
φ	Phase angle
ϕ'	Effective friction angle
ϕ_u	Undrained friction angle
γ_d	Dry density
ν	Poisson ratio
ν_1	Poisson ratio of the top layer (in layered analysis)
ν_2	Poisson ratio of the bottom layer (in layered analysis)
η	Poisson ratio
δ_r	Resilient deflection of plate during the unloading portion of the cycle
θ	Bulk stress
δ_i	Deformation measured during initial loading cycle
δ_r	Deformation measured during reload cycle
σ	Applied stress
σ_1	Applied cyclic stress ($\Delta\sigma_{cyclic}$) used in M_{r-comp} calculations because there is no confining stress at the surface
σ_2	$K_o \sigma_1$
σ_3	σ_2
$\Delta\sigma_{cyclic}$	Cyclic stress
τ_{oct}	Octahedral shear stress

EXECUTIVE SUMMARY

The main objectives of this research were to create a synthesis of literature that identifies methods used to compare intelligent compaction (IC) measurements to soil mechanical properties, to develop a criteria or procedure for field validating IC measurements versus soil mechanical properties, and to demonstrate the field calibration process using different IC technology providers.

The literature review resulted in a synthesis of information that identifies methods/procedures used to compare IC measurements to soil mechanical properties, and the success of those methods/procedures along with a summary of current IC specifications. More than 300 documents were collected. A few key findings were as follows:

- IC technologies have been used in the U.S. on at least 381 pilot/demonstration projects since year 2000.
- A variety of in situ test measurements have been utilized with varying success to correlate IC measurement values (MVs) to independent in situ measurements.
- IC specifications were introduced in Europe in the 1990s. In the U.S., few state highway agencies and the FHWA have developed guide specifications, but not in terms of mechanical soil properties.

As part of the field demonstration phase of this project, in coordination with Illinois State Toll Highway Authority, field testing was conducted on selected test sections on the Elgin O'Hare Western Access Tollway construction project in October 2016, April-May 2017, and in June 2017. Field evaluation was performed on a total of 18 test sections, of which in situ comparison and calibration testing was conducted on 12 test sections. Four different IC-MV technologies were evaluated including: CMV, HMV, MDP, and VIC. Field calibration testing was conducted using LWD, DCP, and static and cyclic APLT testing. Detailed results are presents or all measurements. In brief, the results demonstrated the following:

- Regression relationships between the IC-MVs and in situ test measurements showed simple linear and non-linear (power) regression trends.
- Regression relationships in terms of R^2 values were variable between IC technologies and independent in situ measurements.
- IC-MVs showed variable pavement foundation support conditions.
- Validated IC calibration was performed using stress-dependent M_r values from cyclic automated plate load testing and modulus of subgrade reaction k -values. This testing produced relatively high R^2 values (≥ 0.90) and with relatively low standard error.
- Validated IC maps in a subgrade area identified high subgrade variability that traditional QC/QA inspection did not reveal.

To implement IC technologies on near-term Tollway projects, a calibration process and guide specification were developed. A guide specification is recommended for implementation on upcoming construction projects (likely, as "shadow" evaluations) in 2018/19. The near-term benefits of implementing the findings of this research are expected to be improved contractor efficiencies and more effective QC/QA processes, providing additional information in terms of meeting the pavement design assumptions, and generating baseline data to evaluate future pavement performance.

CONTENTS

ACKNOWLEDGMENTS..... I

DISCLAIMER I

NOTATIONS AND ABBREVIATIONS..... II

EXECUTIVE SUMMARY VI

CHAPTER 1 INTRODUCTION 1

1.1 Problem Statement 1

1.2 Objectives of the study..... 1

 1.2.1 Task 1—Conduct a Comprehensive Literature Review 1

 1.2.2 Task 2—Develop an IC Certification Process 1

 1.2.3 Task 3—Conduct Field Demonstration Projects 1

1.3 Report Organization..... 2

CHAPTER 2 LITERATURE REVIEW 3

2.2 History and Description of IC Measurement Values 3

2.2 Summary of Correlations 8

 2.2.1 Mechanical Properties of Foundation Layers in Embankment and Pavement Design..... 8

 2.2.2 Correlations between Soil Physical and Mechanical Properties and IC Measurements 10

2.3 Summary of Existing Specifications..... 18

2.4 Concluding Remarks 24

CHAPTER 3 FIELD DEMONSTRATION PROJECTS 25

3.1 Review of Current ILT Specifications 25

3.2 Test Sections and Materials 27

3.3 Field Testing Methods 33

 3.3.1 IC Measurement Values 33

 3.3.2 Light Weight Deflectometer (LWD) Testing 36

 3.3.3 Dynamic Cone Penetrometer (DCP) Testing 36

 3.3.4 Automated Plate Load Testing (APLT) 37

 3.3.4 Drive Core Testing 42

3.4 Field Testing Results 43

 3.4.1 Calibration Testing and Analysis – Hamm H11 HMV Measurements 43

 3.4.2 Calibration Testing and Analysis – CMV and MDP Measurements..... 52

 3.4.3 Calibration Testing and Analysis – VIC Measurements 62

3.6 Summary of Key Findings and Observations 71

CHAPTER 4 IC CERTIFICATION PROCESS AND GUIDE SPECIFICATION..... 73

4.1 Specification Overview 73

4.2 Key Components of IC Specifications..... 74

4.2.1 Establishing field QA Target Values with Link to Design Inputs	74
4.2.2 Field Calibration and Certification Process	74
4.2.3. Field Verification/QA Process using IC Stiffness Mapping	76
4.3 Guide Specification Language	77
CHAPTER 5 SUMMARY AND IMPLEMENTATION RECOMMENDATIONS	78
5.1 Summary of Key Findings	78
5.2 Implementation Recommendations	80
REFERENCES	82
APPENDIX A: LIST OF IC REFERENCES	
APPENDIX B: SUMMARY OF COMPACTION REPORTS	
APPENDIX C: SUMMARY OF IN SITU TEST RESULTS	
APPENDIX D: GUIDE SPECIFICATION	

LIST OF FIGURES

Figure 1. Illustration of relationship between subsurface conditions and CMV (reproduced from Thurner and Sandstrom 1980).	4
Figure 2. One-degree-of-freedom lumped parameter model representation of vibratory compactor (reproduced from Kröber 1988).	4
Figure 3. Lumped parameter two-degree-of-freedom spring dashpot model representing vibratory compactor and soil behavior (reproduced from Yoo and Selig 1980).	5
Figure 4. Changes in amplitude spectrum with increasing ground stiffness (reproduced from Schor (reproduced from Scherocman et al. 2007).	6
Figure 5. U.S. map showing IC project locations between 2000 and 2017 and a bar chart of cumulative number of projects for each year [States highlighted in darker color have participated in or conducted at least one IC demo/research/pilot project and points represent the project locations]	7
Figure 6. Simple linear regressions between CMV (amplitude = 1.00 mm) and in-situ point-MVs (LWD modulus and dry unit weight) – silty sand with gravel underlain by relatively stiff fly ash stabilized subgrade (White et al. 2011).	16
Figure 7. Relationships between CMV (theoretical amplitude = 1.50 mm) and in-situ point measurements (LWD modulus, dry unit weight, and CBR determined from DCP) (White et al. 2011)..	17
Figure 8. Illustration of differences in measurement influence depths of different testing devices (reproduced from Vennapusa et al. 2011).	18
Figure 9. Large aggregate base samples: (a) Large RAP (with sizes above 3-in. unfractionated RAP particles), (b) PGE (with four different sizes above 3-in. particles), and (c) RAP Capping Material (maximum 1-in. size)	30
Figure 10. RAP Capping Material (maximum 1-in. size) gradation results.	30
Figure 11. PGE gradation and image analysis results for four large particles above 3-in. diameter according to the approach adopted by Moaveni (2015).	31
Figure 12. Large RAP gradation and image analysis results for five large particles above 3-in. diameter according to the approach adopted by Moaveni (2015).	32
Figure 13. Hamm H11i vibratory smooth drum IC roller	33
Figure 14. Caterpillar CS74B smooth drum IC roller	34
Figure 15. Caterpillar 815F padfoot IC roller	34
Figure 16. Caterpillar CS6 smooth drum roller with retrofit VIC system	35
Figure 17. LWD (left) and DCP (right) testing on compacted CA6 capping layer.	37
Figure 18. (a) APLT setup; (b) setup for measuring in situ resilient modulus using cyclic testing with 12 in. diameter plate, and (d) in situ modulus of subgrade reaction with static testing with 30 in. diameter plate	38
Figure 19. Deflection basis measurement kit positioned at 2r, 3r, and 4r positions (where ‘r’ is the radius of the plate) from the plate center axis.	39
Figure 20. Drive core test equipment.	42
Figure 21. Pictures showing: (a) PGE layer from TS1 (10/13/16); (b) PGE layer from TS3 (10/13/16); and (c) CA6 Capping layer from TS4 (10/14/16).	45

Figure 22. (a) Color-coded spatial map of HMV from TS1; (b) E_{LWD} test measurements across the PGE layer width (red dots are the HMV values); and (c) DCP profiles at two selected test locations shown on the HMV map..... 46

Figure 23. Color-coded spatial map of HMV from TS3 on PGE layer along with DCP profile at test location #53 representing very stiff conditions..... 47

Figure 24. Color-coded spatial map of HMV from TS4 on CA6 capping layer along with DCP profile at test location #60 representing very stiff conditions. 47

Figure 25. Color-coded spatial map of HMV from: (a) TS1 PGE layer from 10/13/16, and (b) TS6 PGE layer from 04/11/17. (Note: The two maps have different zoom scale and zones labeled as “A” and “B” are shown as reference points between the two maps. Average HMV from TS1 = 9.9 and TS6 = 6.2) 48

Figure 26. Color-coded spatial maps of HMV from PGE and overlaid CA6 capping layer: (a) TS6 PGE layer from 04/11/17, and (b) TS8 Ca6 capping layer rom 04/12/17. (Note: The zones labeled as “A” to “D” are shown as reference points between the two maps. Average HMV from TS6 = 6.2 and TS8 = 7.8). 49

Figure 27. Histograms of HMV measurements on PGE layer test sections [TS1, 2, 3, and 6] (left) and CA6 capping layer test sections [TS4, 7, 8, 9, and 12] (right)..... 50

Figure 28. Histograms of E_{LWD} measurements on PGE layer test sections [TS1, 2, 3, and 6] (left) and CA6 capping layer test sections [TS4, 7, 8, 9, and 12] (right)..... 50

Figure 29. Histograms of DCP-CBR measurements of the top layer on PGE layer test sections [TS1, 2, 3, and 6] (left) and CA6 capping layer test sections [TS4, 7, 8, 9, and 12] (right). 51

Figure 30. Histograms of DCP-CBR measurements of the bottom subgrade layer on PGE layer test sections [TS1, 2, 3, and 6] (left) and CA6 capping layer test sections [TS4, 7, 8, 9, and 12] (right). 51

Figure 31. Regression relationships between E_{LWD} and DCP-CBR measurements, and HMV from PGE and CA6 test sections 52

Figure 32. Pictures of embankment fill area (TS5) on 10/14/2017..... 53

Figure 33. Screenshot of elevation map in TS5 embankment fill area..... 54

Figure 34. Screenshot of MDP* summary in TS5 embankment fill area. 54

Figure 35. Screenshot of pass count summary in TS5 embankment fill area. 55

Figure 36. In situ dry density and moisture content measurements from drive core testing overlaid on standard Proctor test results for embankment fill material. 55

Figure 37. GPS referenced MDP* measurements map overlaid with in situ test locations and DCP-CBR profiles at two selected test locations..... 56

Figure 38. Pictures of CA6 capping material from PGE material from TS11 (middle-04/25/17) and CA6 material from TS12 (bottom-05/04/17) 57

Figure 39. Screenshot of CMV and MDP* summary maps for TS10 and TS11 with PGE material..... 58

Figure 40. Screenshot of CMV and MDP* summary maps for TS9 with CA6 capping layer (Note: #3 and #15 are test locations representing very stiff and soft conditions) 59

Figure 41. DCP profiles at test points 3 (very stiff) and 15 (soft) from TS7 60

Figure 42. Histograms of CMV and MDP* measurements from PGE test sections (TS10 and 11) and CA6 test sections (TS7, 9, and 12). 60

Figure 43. Regression relationships between E_{LWD} and DCP-CBR measurements, and CMV measurements.....	61
Figure 44. Regression relationships between E_{LWD} and DCP-CBR measurements, and MDP* measurements.....	62
Figure 45. Pictures of (a) CA6 capping layer on TS13; (b) subgrade on TS14; and (c) PGE layer on TS15.....	63
Figure 46. Summary of calibration results showing predicted versus measured values along with a summary of statistics for each calibration relationship: (a) CMV – M_{r-Comp} at $\Delta\sigma_{cyclic} = 15$ psi, (b) VIC – M_{r-Comp} at $\Delta\sigma_{cyclic} = 15$ psi, (c) CMV – E_{LWD} at $\sigma_o = 14.5$ psi, (d) VIC – E_{LWD} at $\sigma_o = 14.5$ psi.....	65
Figure 47. Summary of calibration results showing predicted versus measured values along with a summary of statistics for each calibration relationship: (a) VIC – $k_{u(1)}$ (b) VIC – $k_{u(2)}$, (c) CMV – $k_{u(1)}$, and (d) CMV – $k_{u(2)}$	66
Figure 48. Color-coded map of M_{r-Comp} values at 20 psi cyclic stress on compacted subgrade along with M_{r-Comp} versus cyclic stress at two select test locations – TS14.	68
Figure 49. Pictures of subgrade during and after proof rolling near southwest corner of TS14.....	69
Figure 50. Color-coded map of M_{r-Comp} values at 20 psi cyclic stress on 6 in. of PGE placed over compacted subgrade along with static plate load test results at two select test locations representing stiff and soft ground conditions – TS15.	70
Figure 51. Preliminary concept of field certification / calibration and verification process in relationship with design assumed mechanical properties.....	75
Figure 52. Flow chart to determine in situ target moduli values based on design input parameters using layered elastic analysis.	76

LIST OF TABLES

Table 1. Summary of key mechanical properties for embankments and pavement foundations 8

Table 2. Summary of test methods to determine mechanical properties of earth materials 9

Table 3. Summary of findings from correlation studies documented in the literature 11

Table 4. Summary of the existing IC specifications 20

Table 5. Summary of existing QC/QA specifications for embankment and pavement foundation materials on the field demonstration project (ILT Contracts I-15-4662, I-14-4644, and I-14-4642) 25

Table 6. Summary of test sections. 27

Table 7. Properties of soil materials tested 29

CHAPTER 1 INTRODUCTION

1.1 PROBLEM STATEMENT

It is believed that earthwork construction and pavement foundation construction quality will be improved using intelligent compaction (IC) measurement values that are statistically validated in terms of mechanical properties of compacted materials. Providing contractors and owners with mechanical property outputs in real-time with nearly 100% spatial coverage of the project will substantially reduce the risk of not meeting the pavement design criteria, thus helping to insure long-term performance. To achieve this goal and advance the current state of the IC technology implementation, the Illinois State Toll Highway Authority sponsored a research project to develop a criteria or procedure for field validating the relationship between IC measurements and soil mechanical properties.

Intelligent compaction (IC) technologies have been used in the U.S. on about 381 research, demonstration, or pilot implementation projects from 2000 till 2016, of which nearly 100 projects were on pavement foundation materials. Many technical articles have been published on this topic since about 1980 with emphasis on sensor measurements, field trials and correlation analysis, data interpretation, and implementation challenges and recommendations. Currently, the Federal Highway Administration (FHWA) has put forth specifications that focus on IC equipment and the procedure/format for data reporting. Existing specifications lack a detailed framework for calibration (i.e., correlations with independent testing) and validation of IC results (i.e., accuracy and system quality checks) in terms of mechanical soil properties (not soil volumetric parameters).

1.2 OBJECTIVES OF THE STUDY

This study has three objectives:

- To create a synthesis of literature and manufacturer information that identifies methods used to compare IC measurements to soil mechanical properties, and the success of those methods;
- To develop a criteria or procedure for field validating the relationship between IC measurements and soil mechanical properties; and
- To demonstrate the field calibration process using three different IC technology providers.

The objectives of this research study were accomplished by performing the following tasks:

1.2.1 Task 1—Conduct a Comprehensive Literature Review

Conduct a thorough review of technical literature and vendor information to evaluate and summarize previous efforts to develop relationships between IC measurements and mechanical properties.

1.2.2 Task 2—Develop an IC Certification Process

Based on the lessons learned in Task 1, develop an implementable process for collecting IC measurements and field verification data to ensure confidence in the relationship between the two sets of data.

1.2.3 Task 3—Conduct Field Demonstration Projects

Arrange field demonstrations for the IC technologies during the 2016 and 2017 Tollway construction seasons. This task required working with the Tollway to identify potential contracts for the field demonstrations, and with the providers of IC technology to coordinate collection of IC measurements and providing data for analyses.

Our goal for the project was to develop guidelines for the Tollway that provide valuable information on how the mechanical properties of earth materials can be measured from IC technologies are directly related the in situ measurements to the assumed design values. Calibrated IC data with high degree of reliability not only provides high quality data to ensure critical mechanical properties have been achieved, but it also provides a rich database with numerous opportunities to how we analyze failures/ future performance of embankment fills and pavement foundations.

1.3 REPORT ORGANIZATION

This report is organized into five chapters. The objectives of the project and key tasks are present in Chapter 1 as described above. In Chapter 2, a synthesis of literature is presented that provides a summary of IC technologies and the various methods/procedures used to compare IC measurements to soil mechanical properties, and the success of those methods/procedures along with a summary of current IC specifications. More than 300 documents were collected, compiled, reviewed, and organized to create the synthesis presented in this chapter. In Chapter 3, a review of the existing ILT specifications for the different pavement foundation layers is summarized to study the quality assurance target values used on the project, a summary of field testing and analysis procedures is provided, and a detailed account of all field results and correlation analysis results are provided. Chapter 4 describes a process for field verification/calibration of IC measurements and guide specification language to implement IC technology. Chapter 5 provides the summary of key findings and recommendations. A list of references reviewed as part of the synthesis, the test bed summary reports, in situ test records, and a guide specification are provided in the appendices of this report.

CHAPTER 2 LITERATURE REVIEW

The objective of this review was to create a synthesis of literature and manufacturer information that identifies methods/procedures used to compare IC measurements to soil mechanical properties, and the success of those methods/procedures along with a summary of current IC specifications. More than 300 documents that have been published on the general topic of IC were collected, compiled, reviewed, and organized to create the synthesis presented in this chapter. A list of these references is provided in Appendix A.

The words “intelligent compaction” (IC) means different things to researchers and practitioners in different industries and agencies. In Europe, the technology was originally referred to as the “continuous compaction control” (CCC) and IC was reserved for rollers with integrated control algorithms that automatically adjust vibration amplitude and/or vibration frequency. The automatic feedback was the “intelligent” aspect and was primarily used to prevent chaotic motion while vibrating on hard ground. CCC and IC definitions were limited only to compactors that vibrated, whereas recent technologies provide measurements in the non-vibratory mode. Consequently, the word “intelligent” became trendy as a shorthand used at meetings and conferences, which is the current terminology in the United States.

Presently, IC represents a catch-all category of compactors with integrated sensors that measure machine-ground interaction properties and various machine operational (e.g., pass count, temperature) and position measurements. In this chapter, and elsewhere in this report, the term IC has been used to reflect the current use of this terminology. In this report we also refer to Validated Intelligent Compaction (VIC), where “validated” indicates that the output has been calibrated to independent engineering measurements.

2.2 HISTORY AND DESCRIPTION OF IC MEASUREMENT VALUES

Several IC measurement systems have been documented in the literature for subgrade and aggregate base materials. A detailed description and evolution of these measurements is well-documented in the technical literature (see Mooney et al. 2010, Mooney and Adam 2007, White et al. 2011). A brief account of this historical development is provided below along with a brief description of the different measurement systems.

The research and development on IC was initiated in the early 1970s by Dr. Heinz Thurner in Sweden with field studies on vibratory smooth drum rollers instrumented with accelerometers. Those initial field tests have shown that the compaction state of the material and soil stiffness was related to ratios of the vibration amplitudes at selected frequencies. The initial testing led to the development of Compaction Meter Value (CMV), and several technical articles have appeared on this topic in the First International Conference on Compaction in Paris in 1980 (Thurner and Sandstrom 1980, Forssblad 1980).

The concept of CMV is illustrated by Thurner and Sandström (1980) as shown in Figure 1. When roller drum interacts with a layer consisting of “soft” rubber material, there would be no first harmonic motion and the CMV is theoretically zero. If the compaction layer consists of sand material, the vibration amplitude of the first harmonic increases with increasing compaction effort (number of passes) and consequently this results in a higher CMV. CMV is an index parameter calculated using Equation 1:

$$CMV = C \cdot \frac{A_{2\Omega}}{A_{\Omega}} \quad (1)$$

where $C = \text{constant}$, $A_{2\Omega} = \text{drum acceleration amplitude of the first harmonic or twice the operating frequency}$, and $A_{\Omega} = \text{amplitude of the vertical drum acceleration at the operating frequency}$ (Thurner and Sandström 1980). The CMV system is currently available on Caterpillar, Dynapac, and Hamm rollers. Hamm reports the value as Hamm Measurement Value (HMV). Each manufacturer may use a different C value and different algorithms in processing the acceleration data. The relationship between CMV and soil density, soil stiffness and soil modulus are empirical and is influenced by roller dimensions (e.g. drum diameter, weight), roller operation parameters (e.g. frequency, amplitude, speed), and soil conditions, i.e., soil type and underlying soil stratigraphy (Sandström and Pettersson 2004).

In the early 1980s, Bomag developed the Omega value as an alternative to CMV. The Omega value is determined by integrating the drum force transmitted to the soil and drum displacement time history over two cycles of vibration, which essentially provides a measure of the energy transmitted to the soil (Kröber 1988). In the late 1990s, Bomag replaced the Omega value with vibratory modulus (E_{vib}) by Bomag. Like the *Omega* value, E_{vib} is also determined by modelling the drum-soil assembly as shown in Figure 2. But the drum force (F_s) and displacement (z_d) behavior is related to E_{vib} (Equation 2) using Lundberg’s theoretical solution for a rigid cylinder resting on a homogeneous, isotropic elastic half-space for a parabolic loading condition across the drum width (Lundberg 1939).

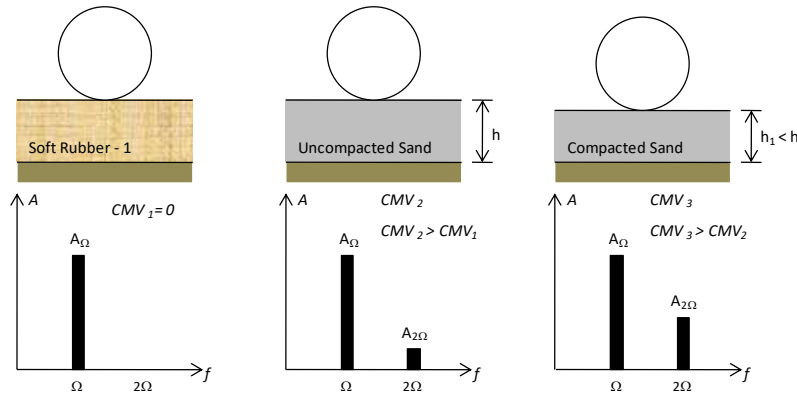


Figure 1. Illustration of relationship between subsurface conditions and CMV (reproduced from Thurner and Sandstrom 1980).

According to Hertz (1895), the contact width of a cylindrical drum (B) can be calculated using the geometry of the drum, applied force, and the material properties (Equation 3). Equations 2 and 3 are numerically solved to determine E_{vib} .

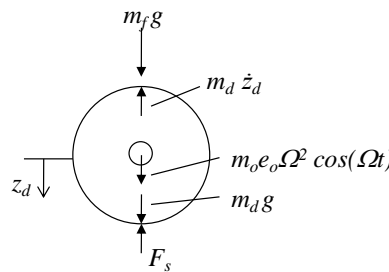


Figure 2. One-degree-of-freedom lumped parameter model representation of vibratory compactor (reproduced from Kröber 1988).

$$z_d = \frac{(1-\nu^2)}{E_{vib}} \cdot \frac{F_s}{L} \cdot \frac{2}{\pi} \cdot \left(1.8864 + \ln \frac{L}{B}\right) \quad (2)$$

$$\text{where } B = \sqrt{\frac{16}{\pi} \cdot \frac{R(1-\nu^2)}{E_{vib}} \cdot \frac{F_s}{L}} \quad (3)$$

where ν = Poisson's ratio of the material, L = length of the drum, B = contact width of the drum, and R = radius of the drum.

During the late 1990s, Ammann introduced the soil stiffness measurement value, k_s , considering a lumped parameter two-degree-of-freedom spring dashpot system described in Figure 3 (Anderegg 1998). The drum inertia force and eccentric force time histories are determined from drum acceleration and eccentric position (neglecting frame inertia). The drum displacement z_d is determined by integrating the measured peak drum accelerations. The soil stiffness k_s is determined using Equation 4 when the drum is near the bottom of its trajectory (i.e. z_d is at maximum). The k_s value represents quasi-static stiffness and is independent of the excitation frequency between 25 to 40 Hz (Anderegg and Kaufmann 2004).

$$k_s = 4\pi^2 f^2 \left(m_d + \frac{m_e r_e \cos(\varphi)}{A} \right) \quad (4)$$

where f is the excitation frequency, m_d is the drum mass, $m_e r_e$ is the eccentric moment of the unbalanced mass, φ is the phase angle, A is vibration amplitude.

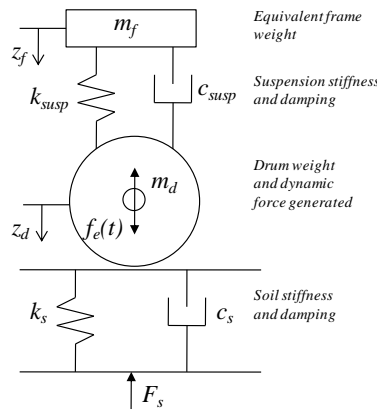


Figure 3. Lumped parameter two-degree-of-freedom spring dashpot model representing vibratory compactor and soil behavior (reproduced from Yoo and Selig 1980).

Sakai introduced the Continuous Compaction Value (CCV) in early 2000 which considers the vibration amplitude that corresponds to six different harmonics. The vibration acceleration signal from the accelerometers mounted on the drum is transformed through the Fast Fourier Transform (FFT) method and then filtered through band pass filters to detect the acceleration amplitude spectrum (Scherocman et al. 2007, Nohse and Kitano 2002). The formula to calculate CCV is presented in Equation 5, and the concept of changes in amplitude spectrum depending on the ground condition is illustrated in Figure 4.

$$CCV = \left[\frac{A_{0.5\Omega} + A_{1.5\Omega} + A_{2\Omega} + A_{2.5\Omega} + A_{3\Omega}}{A_{0.5\Omega} + A_{\Omega}} \right] \times 100 \quad (5)$$

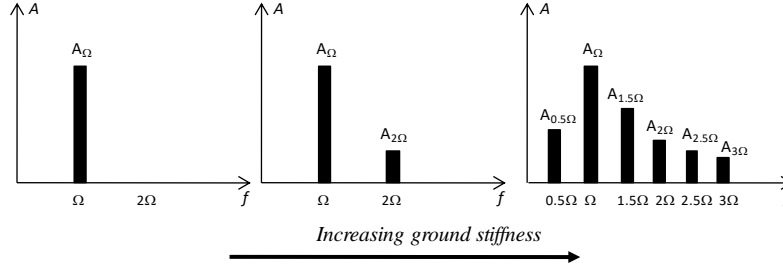


Figure 4. Changes in amplitude spectrum with increasing ground stiffness (reproduced from Schor (reproduced from Scherocman et al. 2007)).

In early 2000, Caterpillar developed the principal of rolling resistance due to drum sinkage, called the machine drive power (MDP). Machine drive power (MDP) technology relates the mechanical performance of the roller during compaction to the properties of the compacted soil. The use of MDP as a measure of soil compaction is a concept originated from study of vehicle-terrain interaction (Bekker 1969). The basic premise of determining soil compaction from changes in equipment response is that the efficiency of mechanical motion pertains not only to the mechanical system but also to the physical properties of the material being compacted. More detailed background information on the MDP system is provided in White et al. (2005). The basic formula for MDP is:

$$MDP = P_g - WV \left(\sin \alpha + \frac{a}{g} \right) - (mV + b) \quad (6)$$

where P_g = gross power needed to move the machine (kJ/s), W = roller weight (kN), a = machine acceleration (m/s^2), g = acceleration of gravity (m/s^2), α = slope angle (roller pitch from a sensor), V = roller velocity (m/s), and m (kJ/m) and b (kJ/s) = machine internal loss coefficients specific to a machine. The second and third terms of Equation 6 account for the machine power associated with sloping grade and internal machine loss, respectively. MDP is a relative value referencing the material properties of the calibration surface, which is generally a hard-compacted surface ($MDP = 0$ kJ/s). Positive MDP values therefore indicate material that is less compacted than the calibration surface, while negative MDP values would indicate material that is more compacted than the calibration surface (i.e. less roller drum sinkage). Currently, the MDP values are index values that range between 1 and 150, where 150 represents a hard-compacted surface with MDP close to 0 kJ/s and 1 represents a soft condition as defined during calibration.

Kimmel and Mooney (2011) documented a “smart pad” method which involves an instrumented roller pad with sensors to monitor normal force, contact stress distribution, and pad deflection. According to Kimmel and Mooney (2011), by combining these measurements, soil stiffness or modulus can be potentially determined.

Validated Intelligent Compaction (VIC) technique is an original approach and was developed by Ingios Geotechnics, Inc. It uses advanced data analytics and requires site specific calibration of the roller sensor measurements using in situ plate load test measurements (i.e., modulus of subgrade reaction, in situ elastic modulus, or in situ resilient modulus). The approach is different from the other measurement values described above, as it requires a field calibration to output mechanistic parameter values that are tied to pavement design parameters, as oppose to index values. Recent field

calibrations on subgrade and base materials using this approach showed coefficient of determination (R^2) > 0.95 are achievable, compared to R^2 of 0.6 using CMV for the same data (White et al. 2014b).

Since the year 2000, IC technology has been utilized on at least 381 roadway construction projects in the U.S. either in a research/demonstration setting or with a pilot specification. The project locations are shown in Figure 5. Of these, most of the projects (220+) involved hot mix asphalt (HMA) construction (full depth HMA or overlay), 75+ project sites involved subgrade and aggregate base materials, and over 25+ project sites involved cold in-place recycling (CIR) or full-depth reclamation (FDR) materials.

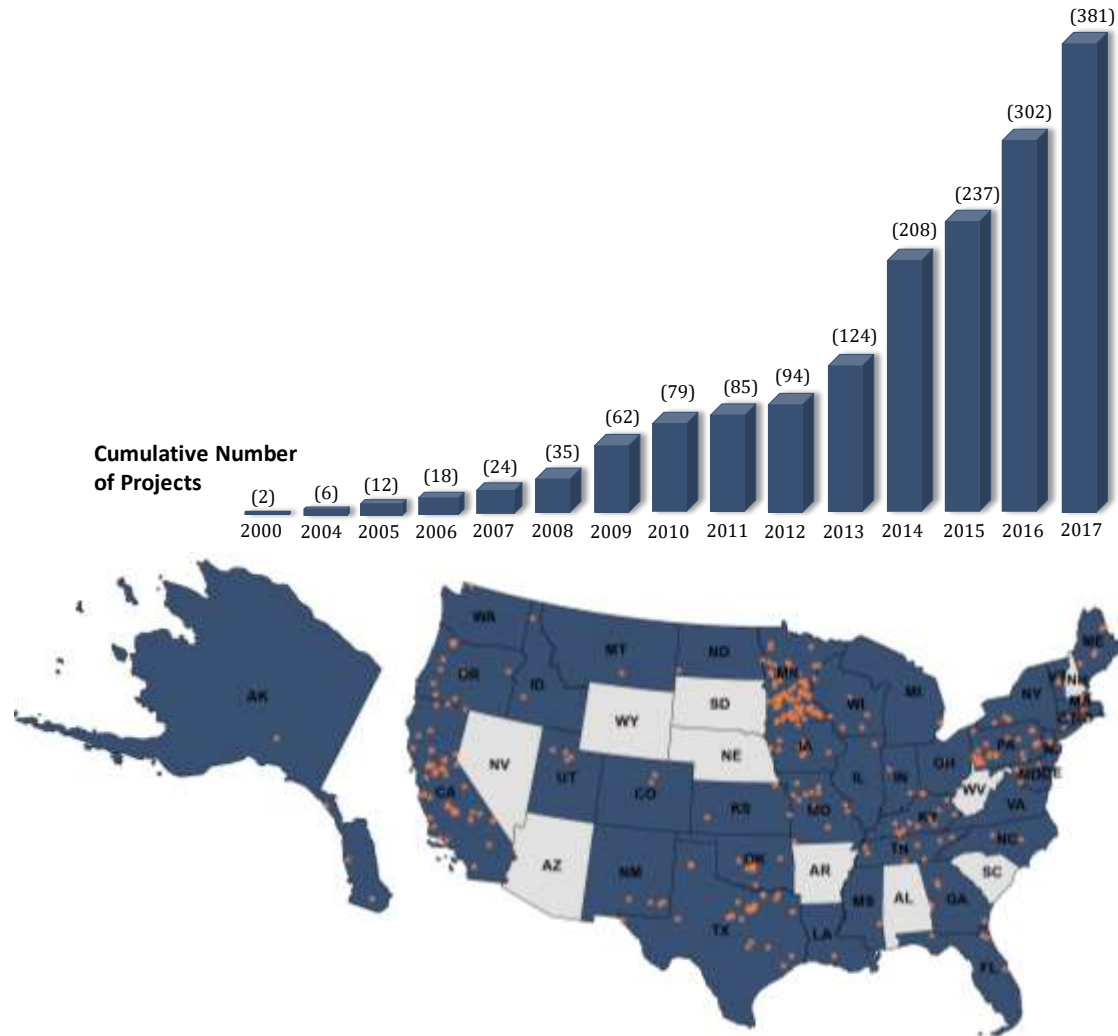


Figure 5. U.S. map showing IC project locations between 2000 and 2017 and a bar chart of cumulative number of projects for each year [States highlighted in darker color have participated in or conducted at least one IC demo/research/pilot project and points represent the project locations]

The projects with HMA involved use of rollers with self-propelled dual drum configuration. On projects with embankment materials and on CIR/FDR materials, most of the projects involved using self-propelled vibratory smooth drum rollers. Self-propelled padfoot rollers have been used on a few projects with Caterpillar’s MDP measurement value, and on a few selected projects with Sakai’s CCV and Ammann’s k_s value.

2.2 SUMMARY OF CORRELATIONS

Since 1980, many technical articles have been published with results from field calibration testing that involved performing various in situ point tests to determine the soil physical and mechanical properties (i.e., dry density, moisture content, stiffness, modulus) using a variety of measurement techniques. Those studies have been compiled and a summary of those correlations are presented in this section. First, the key mechanical properties used to measure pavement foundation layer properties are discussed and then the summary of correlation studies is presented. This information helps establish the basis for the need for validation of IC measurements within a specification.

2.2.1 Mechanical Properties of Foundation Layers in Embankment and Pavement Design

A summary of example mechanical properties used in design of embankment fill layers and pavement foundation subgrade and base layers is provided in Table 1. The embankment fill section is divided into three parts: (1) embankment fill > 3 ft. below pavement, (2) pavement foundation layers ≤ 3ft. of pavement including earth fills in critical areas (e.g., box culverts), and (3) fill materials in critical areas such as box culverts and bridge backfills, etc. Geotechnical design criteria for these conditions are summarized in Table 1. The pavement foundation layer mechanical properties are summarized based on three commonly used pavement design procedures. The associated different field and laboratory test measurements to determine mechanical properties are identified in Table 2, which is highlighted with the test measurements that are utilized in this research during the field testing phase.

Table 1. Summary of key mechanical properties for embankments and pavement foundations

Foundation Layers	Design Procedure	Mechanical Properties*
Embankment fill (> 3ft below pavement layer)	Limit equilibrium slope stability analysis with FS ≥ prescribed value (e.g., 1.5)	Effective cohesion c' and effective friction angle ϕ' , or undrained cohesion c_u or undrained friction angle ϕ_u (accounting for geometric factors and water table)
	Total settlement criteria (e.g., ≤ 2% of fill height)	Modulus of subgrade reaction k -value
	Differential settlement criteria (e.g., ≤ 1 in.)	w% ≥ strain softening condition for post-saturation and ≤ required to achieve strength/stiffness criteria
Pavement foundation layers (subgrade, stabilized subgrade, unbound base and fill ≤3 ft. below bottom of pavement layer) – new construction	1993 AASHTO Guide for Design of Pavement Structures	<u>PCC</u> : k -value for subgrade based on 30-in. plate diameter, composite k -value based on empirical relationships with base layer thickness and elastic modulus (E). <u>HMA</u> : M_r on each layer (base/subbase and subgrade) or empirical relationships with CBR.
	2001 United Facilities Criteria (UFC) 3-260-02 Pavement Design for Airfields	<u>CBR Method for HMA</u> : California Bearing Ratio (CBR) <u>Layered Analysis Method for HMA</u> : M_r on saturated specimens or empirical relationships with CBR, unconfined compressive strength (for stabilized materials), <u>PCC</u> : k -value for subgrade based on 30-in plate diameter and corrected for bending and saturation.
	AASHTOWare™ Pavement ME Design	<u>Level 1</u> : M_r coefficients k_1 , k_2 , and k_3 from AASHTO T307 or NCHRP 1-28A testing, Poisson's ratio (assumed), soil-water characteristic curve (SWCC) fitting parameters from pressure plate (ASTM C1699) or filter paper (ASTM D5298) testing. <u>Levels 2 and 3</u> : M_r based on soil classification, and w_{opt} , maximum γ_d , and SWCC parameters from empirical relationships with gradation parameters.
Fill materials in critical areas (e.g., structural foundations and box culverts)	Total settlement criteria (e.g., ≤ 1% of fill height)	Modulus of subgrade reaction k -value
	Differential settlement criteria (e.g., ≤ 0.5 in.)	w% ≥ strain softening condition for post-saturation and ≤ required to achieve strength/stiffness criteria

*Only properties related to stability are provided and properties related to drainage and freeze-thaw assessment are omitted.

Table 2. Summary of test methods to determine mechanical properties of earth materials

Mechanical Property	Lab/Field	Test Method/Reference	Measurement Devices	Comments
California Bearing Ratio (CBR)	Lab	ASTM D1883	CBR test device	Sample is compacted in lab. Differences in field vs. lab compaction and boundary conditions can influence results.
	Field	ASTM D6951	Dynamic Cone Penetrometer (DCP)	Empirically related to CBR. Can determine individual layer CBR in situ.
Resilient Modulus (M_r)	Lab	AASHTO T-307 NCHRP 1-28A	Repetitive triaxial test device	Sample is compacted in lab. Differences in field vs. lab compaction and boundary conditions can influence results.
	Field	ASTM E1196 AASHTO T-307* NCHRP 1-28A*	Automated Plate Load Test (APLT)	Can <i>directly</i> measure confining stress dependent M_r values to determine k_1 , k_2 , and k_3 values. Test measures composite moduli values, but layered moduli can be determined based on layered analysis.
		ASTM D4694	Falling weight deflectometer (FWD)	Layered analysis can be performed for individual layer moduli determination
		ASTM E2583 ASTM E2835	Light weight deflectometer (LWD)	Results can be empirically correlated to M_r (Nazarian et al. 2014)
		Nazarian et al. (1995)	Seismic pavement analyzer (SPA)	
Elastic Modulus (E)	Field	ASTM D1196 AASHTO T222	Automated Plate Load Test (APLT)	Test measures composite moduli values, but layered moduli can be determined based on layered analysis.
		ASTM E2583	Light weight deflectometer (LWD)	
Modulus of subgrade reaction k -value	Field	AASHTO T222 CRD-C 655-95 ASTM D1196	Automated Plate Load Test (APLT)	Can be determined using 30 in., 18 in., 12 in., and 8 in. diameter plates
Shear strength parameters (c_u , c' , ϕ_u and ϕ')	Lab	ASTM D4767 ASTM D2850	Triaxial testing	Need an undisturbed sample from field for fine-grained soils.
		ASTM D3080	Direct shear testing	For coarse-grained soils only.
	Field	Handy (2002)	Borehole shear test (BST)	Can directly measure the effective shear strength parameters in situ.
		ASTM D5778	Cone penetration test (CPT)	Can provide layered profile along with pore-pressure measurements.
		ASTM D2573	Vane shear test (VST)	Can only measure undrained shear strength parameters.
Soil water characteristic curves (SWCC)	Lab	ASTM C1699	Pressure plate	Can directly measure the SWCC parameters needed in design.
		ASTM D5298	Filter paper	
		ASTM D2325	Tempe cell	

*APLT can be configured to perform in accordance with the stress sequences listed;

NOTE: Highlighted are test methods utilized by the research team during the field demonstration/testing phase of this project.

2.2.2 Correlations between Soil Physical and Mechanical Properties and IC Measurements

Several field studies have been documented since 1980 focusing on correlating IC measurement values (IC-MVs) and in situ point test measurements. The details of these studies are summarized in Table 3 along with project location, IC manufacturer, type of roller drum, soil types, point-MVs, and key findings. The field testing documented in these studies involved performing point measurements in conjunction with obtaining the IC-MVs on calibration test strips with multiple roller passes to large production areas. Most of the studies characterized the strength of the relationships between the point-MVs and IC-MVs using the coefficient of determination (R^2) value. A variety of point-MVs have been documented in the correlation studies, which include:

- Nuclear gauge (NG), electrical soil density gauge (SDG), water balloon method, sand cone replacement method, radio isotope method, “undisturbed” Shelby tube sampling, and drive core samples to determine moisture content and dry unit weight.
- Light weight deflectometer (LWD), soil stiffness gauge (SSG), static plate load test (PLT), falling weight deflectometer (FWD), Briaud compaction (BCD), dynamic seismic pavement analyzer (D-SPA), and Clegg hammer to determine stiffness or modulus.
- Dynamic cone penetrometer (DCP), cone penetration testing (CPT), “undisturbed” Shelby tube sampling, rut depth measurements under heavy test rolling to determine shear strength or California bearing ratio (CBR).

Most of the field studies involved constructing and testing controlled field test sections for research purposes and correlation development, while a few studies were conducted on full-scale earthwork construction projects (White et al. 2008a, 2009a). Based on the findings from a comprehensive correlation study conducted on 17 different soil types from multiple project sites across the U.S. as part of the National Cooperative Highway Research Program (NCHRP) 21-09 project (Mooney et al. 2010), the factors that commonly affect the correlations are as follows:

- Heterogeneity in underlying layer support conditions
- High moisture content variation
- Narrow range of measurements
- Machine operation setting variation (e.g., amplitude, frequency, speed, and roller “jumping”)
- Non-uniform drum/soil contact conditions
- Uncertainty in spatial pairing of point measurements and roller MVs
- Limited number of measurements
- Not enough information to interpret the results
- Intrinsic measurement errors associated with the RICM and in-situ point measurements.

Table 3. Summary of findings from correlation studies documented in the literature

Reference; Project Location	Roller drum type; IC-MV; Soil types	In situ test measurements (Point-MVs)	Key findings and Comments
Forssblad (1980); Sweden.	Dynapac SD; CMV; Fine and coarse rock fill.	Water balloon, PLT, FWD, and surface settlement	Typical values of CMV are provided for different materials, when compacted at near optimum moisture content. CMV represents a composite value in layered soil condition and are influenced by roller speed (higher speeds result in lower CMV). Compaction growth curves of the different point-MV and CMV are presented, which provided good comparisons, but direct correlations are not presented except for between CMV and surface settlement.
Hansbo and Pramborg (1980); Sweden.	Dynapac SD; CMV; Gravelly sand, silty sand, and fine sand.	Sand cone, pressuremeter, PLT, CPT, and DCP	Compaction growth curves showed improvement in CMV and other mechanical properties (i.e., modulus and cone resistance) with increasing pass. Relative compaction measurement was not sensitive to changes in compaction. No direct correlations presented.
Floss et al. (1983); Munich, Germany.	Dynapac Dual SD; CMV; Sandy to silty gravel fill	Water balloon and sand cone, PLT, and DCP	Scatter plots are presented comparing CMV and in situ point-MVs, regression relationships and the strength of the relationships are not presented. The trends generally showed increasing CMV with increasing density, modulus, and DCP penetration blows (per 0.6 m penetration). Correlations with modulus and penetration blows are generally better than density. CMV measurements are dependent on speed, vibration frequency and amplitude, soil type, gradation, water content, and strength of subsoil.
Samaras et al. (1991); Stuttgart, West Germany	Unknown SD; CMV; granular soil	Density, PLT	General trends between CMV and point-MVs are presented, but raw data was not included. Plots are presented showing how wide the scatter is around a regression relationship, which indicated PLT-based initial and reload measurements showed tighter relationships with CMV than dry density measurements.
Adam (1997); Unknown.	Unknown SD; CMV	PLT	Correlation between CMV and PLT modulus (initial) is shown for a material as an example. Soil conditions and testing are not defined. The relationship presented showed $R^2 = 0.99$.
Brandl and Adam (1997); Unknown.	Bomag SD; CMV and Omega	PLT	Correlation between CMV and PLT modulus (initial) showed different regression trends for partial uplift and double jump operating conditions. Regressions in partial uplift and double jump conditions yielded $R^2 = 0.9$ and 0.6 , respectively.
Nohse et al. (1999); Tomei, Japan.	Sakai SD; CMV; Clayey Gravel	Radio-isotope	Results from calibration test strips are presented, which showed average dry density and CMV increased with increasing roller passes. Linear regression relationships with $R^2 > 0.9$ are observed for correlations between dry density and CMV.
Krober et al. (2001); Germany.	Bomag SD; E_{vib} ; Silty gravel	PLT	Correlations between E_{vib} and initial/reload moduli values from PLT showed $R^2 > 0.9$. Initial moduli values and E_{vib} values were similar in magnitude during early compaction passes, while reload moduli values and E_{vib} were similar at near full compaction.
Preisig et al. (2003); Various sites, Sweden.	Ammann SD; k_s (presented as k_B); sandy and silty gravel	PLT	Correlations between k_s and initial/reload moduli values from PLT showed R^2 values of 0.83 and 0.79 , respectively, with linear relationships.
White et al. (2004, 2005); Edwards, IL.	Caterpillar PD; MDP; Lean clay	NG, Drive core, DCP, and Clegg hammer	Correlations between MDP and in-situ test measurements using simple and multiple regression analyses are presented. MDP correlated relatively better with dry unit weight ($R^2 = 0.86$) than with DCP ($R^2 = 0.38$) or Clegg impact value ($R^2 = 0.46$). Including moisture content via multiple regression analysis greatly improves the R^2 values for DCP and Clegg impact value ($R^2 > 0.9$). These results are developed by averaging data over 20m long strip per pass.

Reference; Project Location	Roller drum type; IC-MV; Soil types	In situ test measurements (Point-MVs)	Key findings and Comments
Petersen and Peterson (2006); TH53, Duluth, MN.	Caterpillar SD; CMV and MDP; Fine sand	LWD, DCP, and soil stiffness gauge (SSG)	Weak correlations are obtained on a point-by-point basis comparison between in-situ test measurements and roller measurements, likely due to the depth and stress dependency of soil modulus, and the heterogeneity of the soils. Good correlations are obtained between CMV values and DCP measurements for depths between 200 and 400 mm depth.
White et al. (2006a,b); Edwards, IL.	Caterpillar SD; MDP; Well-graded silty sand	NG and DCP	Average MDP values showed a decreasing (logarithmic) trend, dry unit weight values showed an asymptotic increase, and DCP index showed an asymptotic decrease with increasing roller pass. Correlations between MDP and point-MVs showed good correlations ($R^2 = 0.5$ to 0.9). Incorporating moisture content into analysis is critical to improve correlations for dry unit weight.
Ryden and Mooney (2007); Albertville, MN	Ammann SD; k_s ; clay subgrade	Surface wave testing	Correlation between shear wave velocity (V_s) representing different measurement depths (0 to 1.0 m and 0 to 1.6 m) and k_s are presented based on 10 test locations. The regression relationships showed $R^2 = 0.69$ for 0 to 1.0 m depth and $R^2 = 0.12$ for 0 to 1.6 m depth.
Thompson and White (2007); Edwards, IL.	Caterpillar SD; MDP and CMV; well-graded sand	NG, LWD, DCP, and Clegg hammer	Test results obtained from a test bed area with multiple lift thicknesses and passes are presented. Correlations between MDP and in-situ test measurements using multiple regression analyses are presented by incorporating moisture content. The results were based on averaging several test measurements for each pass and not based spatially paired test data. All multiple regression relationships (incorporating moisture content) showed R^2 values ranging between 0.7 and 0.9 for averaged-MVs.
Rahman et al. (2008); Multiple sites, KS	Bomag SD; E_{vib} ; granular soil	NG, FWD, LWD, DCP, SSG,	Tests were obtained on a proof test section that was well-compacted, and correlations were developed between Evib and point-MVs. It is unclear how the spatial pairing was performed (in terms of the accuracy of the GPS measurements). Regression relationships showed relatively poor correlations between all point-MVs and E_{vib} values. Reasons for poor correlations were attributed to the differences in the measurement influence depths between the IC measurement values and point-MVs. Although not noted in the paper, the E_{vib} values were obtained in the automatic feedback control model, which are affected by the variable amplitude and frequencies and consequently affect the correlations.
Thompson and White (2008); Edwards, IL.	Caterpillar PD; MDP; Silt and lean clay	NG, DCP, Clegg Hammer, and LWD	Correlations between MDP and point-MVs are presented using simple and multiple regression analysis. Averaging the data along the full length of the test strip (per pass) improved the regressions. Multiple regression analysis by incorporating moisture content as a regression parameter further improved the correlations.
White et al. (2007a, 2008a); TH64, Ackley, MN.	Caterpillar SD; CMV; Poorly graded sand and well-graded sand with silt	LWD, DCP, and NG	Project scale correlations by averaging data from different areas on the project are presented, which showed R^2 values ranging from 0.52 for density and 0.79 for DCP index value. Correlations with LWD showed poor correlations because of loose surficial material. The variability observed in the CMV data was like DCP and LWD measurements but not to density measurements.
White et al. (2007b); Edwards, IL.	Caterpillar PD; MDP; Sandy lean clay	NG and DCP	Based on average measurements over the length of the test strip (~20 m); correlations between MDP and point-MVs showed $R^2 = 0.87$ for density and 0.96 for DCP index values.

Reference; Project Location	Roller drum type; IC-MV; Soil types	In situ test measurements (Point-MVs)	Key findings and Comments
White et al. (2008b); FM156, Roanoke, TX.	Dynapac SD and Ammann PD; CMV, k_s ; granular base and lime stabilized subgrade.	NG, LWD, PLT, FWD, D-SPA	CMV measurements showed good repeatability but are influenced by vibration amplitude. High amplitude (i.e., > 1.5 mm) caused drum bouncing and affected the CMV measurements. Increasing amplitude generally showed an increase in CMV. Results showed that FWD modulus point measurements tracked well with variations in CMV in some cases and in some cases, it did not. The reason for poor correlations with FWD measurements in some cases is attributed to the possible influence of heterogeneity observed in the material across the drum width due to moisture segregation. The CMV measurements however were well correlated with variations in moisture content as evidenced by a decrease in CMV with increasing moisture content. D-SPA, PLT, and DCP measurements tracked well with the variations in CMV.
Vennapusa et al. (2009), Edwards, IL.	Caterpillar PD; MDP; Crushed gravel base	DCP and LWD	Correlations were obtained on a test bed with multiple lifts placed on a concrete base and a soft subgrade base. Correlations between MDP and point-MVs yielded $R^2 = 0.66$ to 0.85 for spatially nearest point data, and $R^2 = 0.74$ to 0.92 for averaged data (over the length of concrete pad or soft subgrade pad).
White et al. (2009a,b), TH60, Bigelow, MN.	Caterpillar PD-MDP ₈₀ and SD-CMV; Sandy lean clay to lean clay with sand	Heavy test roller, DCP, LWD, and PLT	Correlations are presented from multiple calibration test strips and production areas from the project. MDP ₈₀ and LWD modulus correlation showed two different trends ($R^2 = 0.35$ and 0.65) over the range of measurements as the MDP ₈₀ reached an asymptotic value of about 150 which is the maximum value on the calibration hard surface. CMV correlation with LWD modulus produced $R^2 = 0.70$, and with rut depth produced $R^2 = 0.64$.
White et al. (2009a); TH36, North St. Paul, MN.	Caterpillar SD; CMV; Granular subbase and select granular base	DCP, SSG, Clegg Hammer, LWD, PLT, FWD, and CPT	Correlations between CMV and point-MVs from calibration and production test areas based on spatially nearest point data are presented. Positive trends are generally observed with $R^2 > 0.5$ (for LWD, FWD, PLT, SSG, and Clegg) with exception of one test bed (FWD, LWD, and CPT) with limited/narrow range of measurements.
White et al. (2009a); US10, Staples, MN	Caterpillar SD; CMV; Poorly graded sand with silt to silty sand	LWD, PLT, and DCP	Correlations between CMV and point-MVs from calibration and production test areas based on spatially nearest point data are presented. Correlations between CMV and point-MVs showed R^2 value ranging from 0.2 to 0.9. The primary factors contributing to scatter are attributed to differences in measurement influence depths, applied stresses, and the loose surface of the sandy soils on the project. Correlations between CMV and LWD or DCP measurements improved using measurements at about 150-mm below the compaction surface.
White et al. (2009a); CSAH 2, Olmsted County, MN	Caterpillar PD; MDP ₈₀ ; Sandy lean clay	LWD	MDP ₈₀ values are influenced by the travel direction of the roller due to localized slope changes and roller speed. Correlations between MDP ₈₀ and LWD generally showed $R^2 > 0.6$ (with exception of one case) when regressions are performed by separating data sets with different travel directions and speed. Data was combined by performing multiple regression analysis incorporating travel speed and direction which showed correlations with $R^2 = 0.93$.

Reference; Project Location	Roller drum type; IC-MV; Soil types	In situ test measurements (Point-MVs)	Key findings and Comments
Mooney et al. (2010); Minnesota, Colorado, North Carolina, Maryland, Florida.	Caterpillar PD – MDP and SD – CMV, Dynapac SD – CMV; Bomag SD – E _{vib} ; Ammann SD – k _s ; Two types of cohesive soils, eleven types of granular soils.	NG, DCP, LWD, FWD, PLT, Clegg hammer, SSG	Simple and multiple regression analysis results are presented. Simple linear correlations between IC-MVs and compaction layer point-MVs are possible for a compaction layer underlain by relatively homogenous and stiff/stable supporting layer. Heterogeneous conditions in the underlying layers, however, can adversely affect the relationships. A multiple regression analysis approach is described that includes parameter values to represent underlying layer conditions to improve correlations. Modulus measurements generally capture the variation in IC-MVs better than traditional dry unit weight measurements. DCP tests are effective in detecting deeper “weak” areas (at depths > 300 mm) that are commonly identified by IC-MVs and not by compaction layer point-MVs. High variability in soil properties across the drum width and soil moisture content contribute to scatter in relationships. Averaging measurements across the drum width, and incorporating moisture content into multiple regression analysis, when statistically significant, can help mitigate the scatter to some extent. Relatively constant machine operation settings are critical for calibration strips (i.e., constant amplitude, frequency, and speed) and correlations are generally better for low amplitude settings (e.g., 0.7 to 1.1 mm).
White et al. (2010a); US219, Springville, NY.	Caterpillar SD and Bomag SD; CMV and MDP, and E _{vib} ; Well-graded gravel.	DCP, LWD, FWD, PLT, BCD, NG, and SDG	Non-linear power, exponential, and logarithmic relationships between IC-MVs and point-MVs. Correlations between IC-MVs and different point-MVs are generally weak when evaluated independently for each test bed due to narrow range of measurements. When data are combined for site wide correlations with a wide measurement range, the correlations improved. IC-MVs generally correlated better with modulus/stiffness and CBR point-MVs than with dry density point-MVs. Correlations between IC-MVs and FWD and PLT measurements showed the strongest correlation coefficients.
White et al. (2010b); US84, Waynesboro, MS.	Caterpillar PD, Sakai SD; MDP and CCV; poorly graded to silty sand	DCP, LWD, FWD, NG, and PLT	
Rinehart et al. (2012); Colorado	SD; CMV; granular soil	NG and LWD	Regression relationships between CMV and in situ point MVs were presented based on testing on calibration test strips and production areas. Results showed R ² of about 0.7 with dry density and 0.63 with LWD modulus.
White et al. (2013); Boone, IA	Caterpillar SD; MDP and CMV; poorly graded gravel	LWD, DCP, FWD	Regression relationships between MDP and CMV vs. in situ point MVs were presented based on 200+ comparative measurements obtained over a wide range of stiffness conditions (very soft to hard) on pavement foundations constructed with a variety of stabilization methods (mechanical and chemical). R ² was highest (0.84) for CMV vs. FWD modulus. R ² value was about 0.54 for CMV vs. LWD modulus, and the low R ² value was attributed to lower measurement influence depth for LWD and measurement range than for FWD. Regression relationships with MDP yielded relatively low R ² values (< 0.4).
Liu et al. (2014); China	SD; CV; rock fill	Density and Relative Compaction	A relatively new IC-MV, called the compaction value (CV) was introduced in this paper, which followed a similar concept as CMV but used the ratio of vertical drum accelerations at four times the fundamental frequencies and two times the fundamental frequency. The CV was correlated with relative compaction and density, which showed R ² of 0.68 to 0.80.

Reference; Project Location	Roller drum type; IC-MV; Soil types	In situ test measurements (Point-MVs)	Key findings and Comments
Vennapusa and White (2014); Jacksonville, FL	Caterpillar SD; MDP and CMV; poorly graded sand and recycled granular materials	DCP, LWD	Results from test strips constructed with poorly graded sand and a recycled asphalt layer over poorly graded sand were used to develop regression relationships between MDP, CMV, and in situ point-MVs. Results showed that MDP correlated well with LWD modulus and CBR measurements averaged over the top 300 mm depth, while CMV measurements correlated well with CBR measurements averaged over the top 800 mm depth, suggesting the differences in the measurement influence depth of the two measurements.
Unpublished report from 2014; Knoxville, TN	SD; VIC; fly ash and gypsum	PLT	Elastic modulus values determined from 18 in. diameter plate with two loading cycles were used for calibration. Calibration records showed R^2 of 0.97. Tests were obtained from about 20 test locations obtained over a large spatial area with moduli values varying between 3 and 50 ksi.
White et al. (2014b); Louisville, KY	SD; VIC; crushed rock, lime stabilized subgrade, and clay subgrade	Cyclic PLT	In situ resilient moduli values determined using 18 in. diameter loading plate from cyclic plate load testing on granular and non-granular materials at about 15 test locations. Calibration showed predicted versus actual resilient modulus with R^2 of 0.96.
Unpublished report from 2016; Knoxville, TN	SD; VIC; fly ash and gypsum	PLT, surface wave testing, DCP	Elastic modulus values determined from 30 in. diameter plate with two loading cycles, shear and compression wave velocities (V_s and V_p) from surface wave testing, and CBR values determined from DCP were used for calibration. Calibration records showed R^2 values ranging 0.90 to 0.99 for predicted vs. actual measurements, for all test measurements except DCP-CBR R^2 values for DCP-CBR varied between 0.6 and 0.93.
Liu et al. (2016); China	SD; CMV; lime stabilized subgrade	Relative compaction	A new measure of compaction, the compaction power per unit volume, was introduced in this study, which was incorporated in the regression relationships to predict dry density along with CMV. The compaction power value was derived from the drum excitation frequency, calculated excitation force, assumed compaction value, speed of roller, and number of roller passes. Results showed that the regression relationships were material specific when compared with just CMV with R^2 of about 0.7 and were not material specific when the compaction power parameter was included in the regression.

In general, results from controlled field studies indicate that statistically valid simple linear or simple non-linear correlations between IC-MVs and compaction layer point-MVs (e.g., modulus or density) are possible when the compaction layer is underlain by a relatively homogenous and stiff/stable supporting layer. For example, Figure 6 presents simple linear regression relationships between CMV and in-situ LWD modulus and dry density point-MVs obtained from a calibration test strip with plan dimensions of 30 m x 2 m (White et al. 2011). The test strip consisted of silty sand with gravel base material underlain by a very stiff fly ash stabilized subgrade layer. For this case, correlations between CMV and both LWD modulus and dry density measurements showed $R^2 > 0.8$.

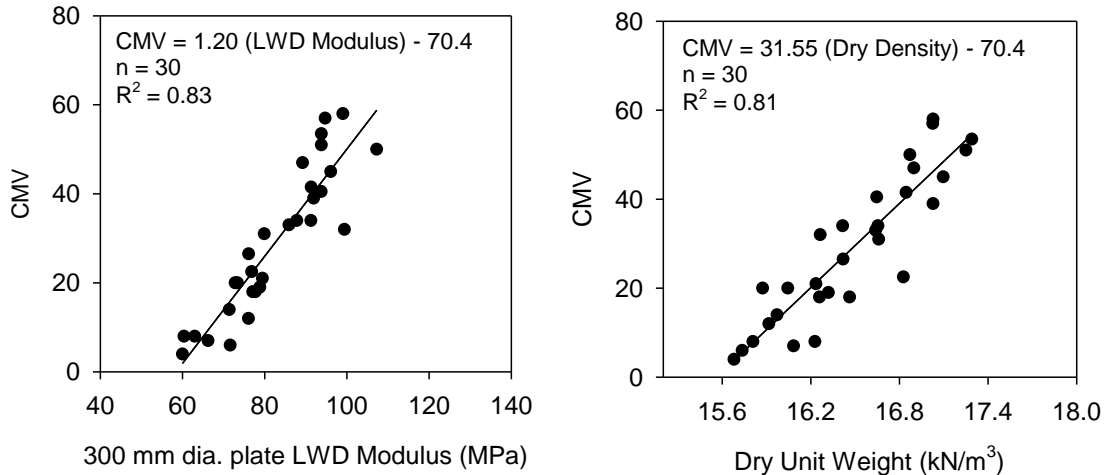


Figure 6. Simple linear regressions between CMV (amplitude = 1.00 mm) and in-situ point-MVs (LWD modulus and dry unit weight) – silty sand with gravel underlain by relatively stiff fly ash stabilized subgrade (White et al. 2011).

On the contrary, many field studies summarized in Table 1 indicate that modulus or stiffness-based measurements (i.e. determined by FWD, LWD, PLT, etc.) generally correlate better with the IC-MVs than compaction layer dry unit weight or CBR measurements. This is illustrated in Figure 7, based on data obtained from several calibration and production test areas with lean clay subgrade, recycled asphalt subbase, recycled concrete base, and crushed limestone base materials compacted with a vibratory smooth drum roller. CBR measurements presented in Figure 7 are obtained from DCP tests using empirical correlations between DCP index values and CBR (White et al. 2011). One of the primary reasons for why modulus measurements correlated better is that modulus measurements represent a composite layered soil response under an applied load which simulates vibratory drum-ground interaction. The density and CBR measurements are average measurements of the compaction layer and do not directly represent a composite layered soil response under loading. Although DCP-CBR measurements did not correlate well in the two cases presented in Figure 7, other field studies (White et al. 2009, Mooney et al. 2010, Vennapusa and White 2014) have indicated that DCP tests are effective in detecting deeper “weak” areas (at depths > 300 mm) that are commonly identified by the IC-MVs and not by point-MVs obtained on the surface. This is primarily because of the differences in measurement influence depths which are reported to be in the range of 0.8 m to 1.5 m for vibratory roller measurements depending on the soil layering, drum mass, and the excitation force (ISSMGE 2005, Rinehart and Mooney 2009, Mooney et al. 2010, Vennapusa et al. 2011, Vennapusa and White 2014), while most point-MVs have influence depths < 0.5 m (Vennapusa et al. 2011, Vennapusa and White 2014, White et al. 2013). The differences in the measurement influence depths for different point-MVs and IC-MVs are illustrated in Figure 8. Statistical multiple regression analysis techniques can be used to account for heterogeneity in the underlying layers if the underlying layer IC-MVs or in-situ point MV measurements have been demonstrated (Mooney et al. 2010).

High variability in soil properties across the drum width and soil moisture content also contribute to scatter in relationships. Averaging point measurements across the drum width, and incorporating moisture content into multiple regression analysis, when statistically significant, can help mitigate the scatter to some extent.

As summarized in Table 3, the new VIC technique was documented in a few recent studies and has shown promise with consistently producing R^2 values > 0.9 with APLT measured field mechanical properties including the modulus of subgrade reaction, initial and reload moduli, and resilient modulus. Validation testing was performed on granular and non-granular pavement foundation materials, coal

combustion by products such as fly ash and gypsum using vibratory smooth drum rollers. The technique has the advantage of using the field calibration to output mechanistic parameter values that are tied to pavement design parameters, as opposed to index values, and is evaluated as part of the field demonstration/testing phase of this research project.

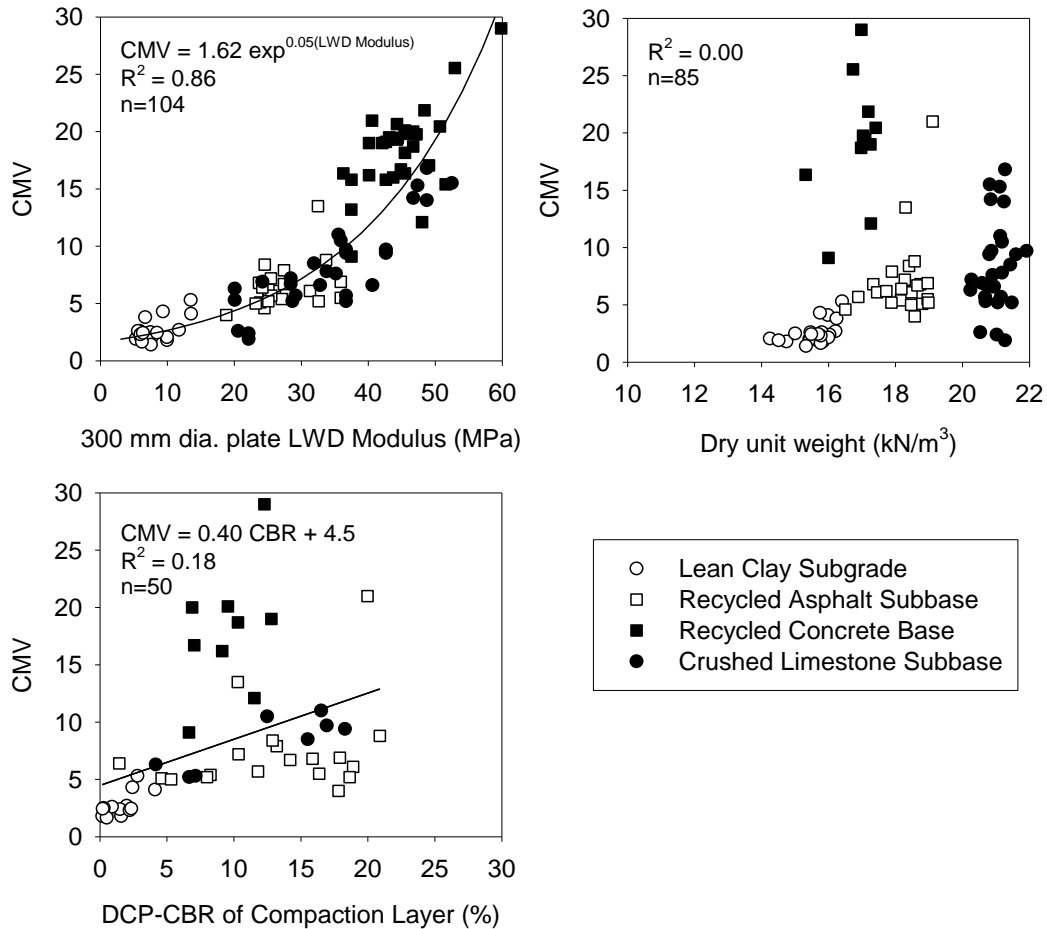


Figure 7. Relationships between CMV (theoretical amplitude = 1.50 mm) and in-situ point measurements (LWD modulus, dry unit weight, and CBR determined from DCP) (White et al. 2011).

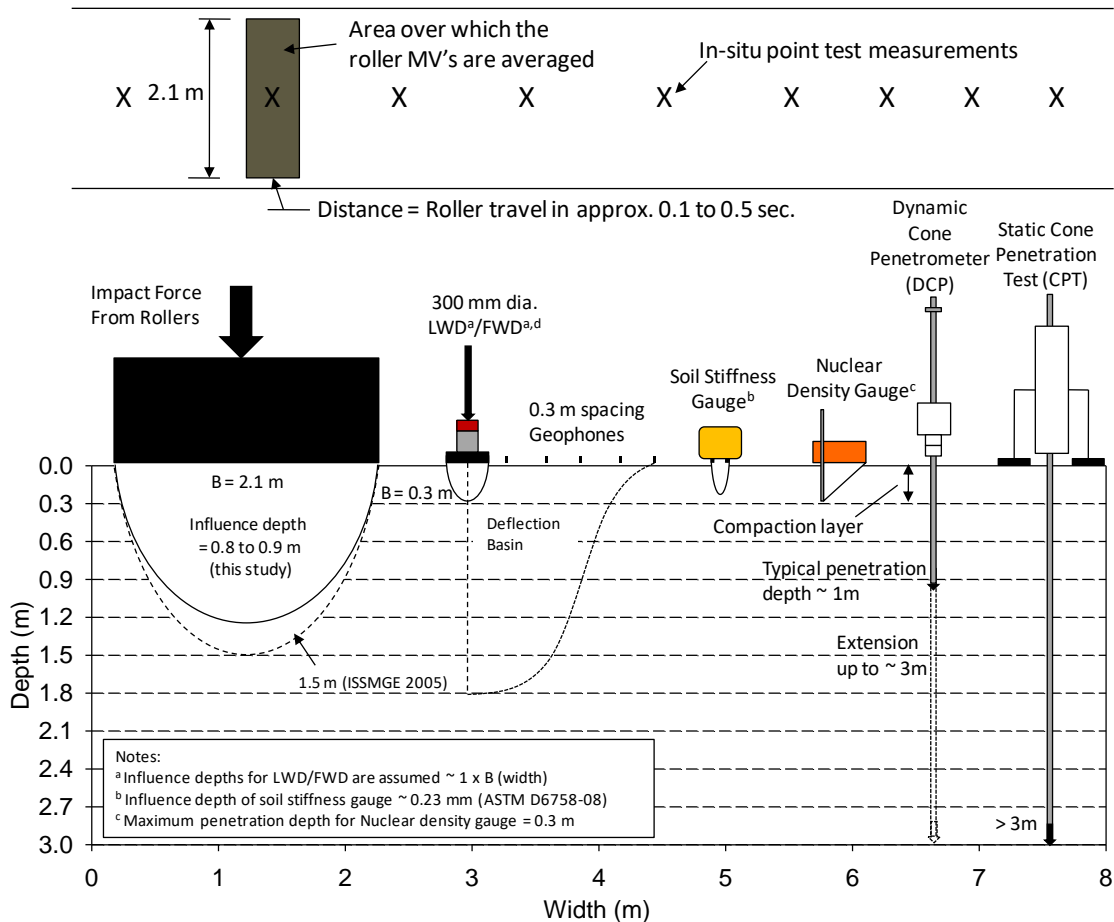


Figure 8. Illustration of differences in measurement influence depths of different testing devices (reproduced from Vennapusa et al. 2011).

2.3 SUMMARY OF EXISTING SPECIFICATIONS

IC specifications have been introduced in Europe (Austria, Germany, and Sweden) in the 1990s, and in 2005, the ISSMGE developed recommended construction specifications based primarily on the Austrian specifications. In the U.S., currently a few state highway agencies and the FHWA have developed specifications to facilitate implementation of IC technologies for embankment and pavement foundation layer materials. A summary of the key elements of the specifications implemented by these different agencies is provided in Table 4. The FHWA has provided a generic specification, and several state DOTs have now adopted the FHWA specification by modifying and customizing it to the QA requirements traditionally accepted in their state.

The ISSMGE and European specifications require performing either static or dynamic plate load tests on calibration strips to determine average target values (typically based on 3 to 5 measurements) and use the same for QA later in production areas. The German, ISSMGE, and Austrian specifications suggest performing at least three static PLTs or dynamic LWDs in locations of low, medium, and high degree of compaction during calibration process. Further, it is specified that linear regression relationships between roller measurement values and plate load test results should achieve a minimum R^2 of 0.49.

In the U.S., state agencies have specified the use of dry density measurements, LWD test measurements, and DCP test measurements for calibration and QA testing. Calibration in the FHWA

(2014) specifications involved performing the point tests at selected locations after consecutive compaction passes and comparing the IC-MVs with the point-MVs via linear regression to establish an IC target value. Also, language is provided in the specification for establishing IC target value using compaction curve data, by conducting compaction passes until an average change of less than 5% between consecutive compaction passes is achieved. It is unclear in some of the state agency specifications that adopted this language, on which method takes precedent in determining the IC target value that is implemented in the production area. The QA is largely based on independent spot testing acceptable to the state. The IC data is being used to evaluate a production area meeting the IC target value established from the calibration, for e.g., the FHWA (2014) specification allows a production area must achieve a minimum of 70% of the IC target value established from calibration over at least 90% of the production area. The current U.S. specifications on IC are method and prescriptive specifications and focus on IC equipment and the procedure/format for data reporting.

Table 4. Summary of the existing IC specifications

Reference	Equipment	Calibration Requirements		Documentation	Compaction Specs	Speed	Freq.
		Area	Location				
FHWA (2014)	Smooth drum or padfoot vibratory roller	225 ft long by 24 ft wide	Material at optimum moisture content and for each material type.	Color-coded IC-MVs including the stiffness response values, location of the roller, number of roller passes, roller speed, vibration frequency, and vibration amplitude	The target IC-MV is determined based on a compaction curve with repetitive roller passes until a less than 5% change in IC-MV is observed between consecutive roller passes. The estimated target density will be peak of the nondestructive readings within the desired moisture range. Another option for linear regression relationships between IC-MV and density measurements is also provided to establish target IC-MV. Production mapping is recommended at the final surface of the fill and the elevation levels at 1.0 ft., 2.0 ft., 4.0 ft., and 8.0 ft. below the final surface as applicable. The magnitude of the evaluation areas may vary with production, but they need to be at least 25,000 ft ² for evaluation and not greater than 100,000 ft ² . A minimum coverage of 90% of the individual construction area shall meet the optimal number of roller passes and 70% of the target IC-MV determined from the test sections. Construction areas not meeting the IC criteria shall be reworked and reevaluated prior to continuing with the operations in that area.		Not specified but requires maintaining the operation parameters constant during mapping.
Georgia DOT (2012)	Smooth drum or padfoot vibratory roller	500 ft long by 24 ft wide	Material at no less than 1% below optimum and for each material type, 8 in. thick lift	Same as FHWA (2014) specification requirements.	Like FHWA (2014) specification requirements. Exceptions/additions include obtaining a minimum of 10 measurements for linear regression analysis and target density being 95% of maximum Proctor density, and the minimum size of the production evaluation area is 5,000 ft ² .		Not specified.
Indiana DOT (2014)	Smooth drum or padfoot vibratory roller	225 ft long by 24 ft wide	Material type specific moisture limits are required. Test section for each material type.	Same as FHWA (2014) specification requirements.	Test sections to be constructed to determine number of roller passes for verification of DCP blow count requirement (specific to each material type) in the top 12 in. lift. Target IC-MV to be determined based on the target DCP criteria and regression analysis. In production areas, a minimum 70% of the mapped construction area shall equal or exceed the target IC-MV. Minimum size of the production evaluation area is 5,000 ft ² and maximum is 75,000 ft ² . Deficiencies exhibiting excessive pumping or rutting or by not meeting the IC-MV target values shall be reworked and retested for acceptance. Deficient areas that do not meet the target IC-MV criteria may be accepted if the target DCP and moisture criteria is met. DCP testing frequency for QA is one test per 1400 yd ³ for each lift.		Not specified.

Reference	Equipment	Calibration Requirements		Documentation	Compaction Specs	Speed	Freq.
		Area	Location				
Iowa DOT (2010)	Self-propelled padfoot roller weighing at least 10,800 kg.	5 m wide x 75 m long compacted for 12 passes.	IC roller shall be used for measurement at vertical intervals of 0.6 m or less in proof areas. Surface shall be relatively smooth and uniform.	Machine model, type, and serial/machine number; roller drum dimensions (width and diameter); roller and drum weights; file name; date stamp; time stamp; RTK based GPS measurements showing Northing, Easting, and Elevation; Roller travel direction; Roller speed; Vibration setting, amplitude, and frequency (if vibration used); Surface temperature; Compaction measurement value	IC measurements in forward direction only on test strips and proof areas. IC data shall be collected and provided for a minimum 80% of the required proof areas. QA in proof areas is based on meeting moisture limits according to the specification.		Constant on test strips and proof areas
KYTC (2015)	Smooth drum or padfoot vibratory roller	Not specified. Cross referenced to KYTC standard specifications section 302.03.04 for test strip construction to determine optimum rolling pattern and target density for base materials.		Same as FHWA (2014) specification requirements.	Any areas a minimum of 50 square feet in area not achieving the 80% of the stiffness value determined by the latest control strip shall be tested by other means approved by the Engineer. If the material doesn't pass the testing is shall be repaired based on current standards to the satisfaction of the Engineer.		Not specified.
MnDOT (2017)	Smooth drum or padfoot vibratory roller	Control strips are specified for full-depth reclamation and cold in-place recycling materials to establish rolling pattern to achieve target density. Minimum 400 square yards.		Displays real-time, color-coded maps of: line work (alignment file), roller drum location, number of roller passes, IC-MV for systems with an accelerometer, displays and store current value for: roller speed, vibration frequency, vibration amplitude, GNSS coordinates, and pass count, and ability to internally store data until data transfer, to automatically transfer data to cloud storage, and to manually transfer data using a removable media device, and allows operator to define, label, and/or select the standardized name of each lot.	Not specified for IC-MVs.		Same during calibration and production compaction

Reference	Equipment	Calibration Requirements		Documentation	Compaction Specs	Speed	Freq.
		Area	Location				
Michigan DOT (2013)	Self-propelled smooth drum vibratory roller	100 ft long by 20 ft wide	Test section for each material type, with at least 2 lifts of material for subbase soils.	Same as FHWA (2014) specification requirements.	Test strip to be constructed to establish a rolling pattern for each subbase and base material type. Initiate test strip with 2 passes and perform density and moisture measurements, and perform additional testing or every 2 consecutive passes, until the maximum density is reached per project specifications. Proof rolling is performed in production areas with the IC roller and QA is based on achieving density and moisture at locations selected by Engineer based on the IC map.	Constant 3 mph	Per vendor recommendation.
TxDOT (2004)	Self-propelled smooth drum vibratory roller	500 ft long by full width of the material course layer	Test section for each material type	Same as FHWA (2014) specification requirements.	Control strip is constructed by proof mapping an existing area and placing the new material layer. Initiate 2 compaction passes and perform density and moisture measurements at 3 random locations and perform additional testing or every 2 consecutive passes at the same 3 test locations, until the maximum density is reached per project specifications. Production compaction is achieved using the same rolling pattern as established from control strip and deliver data to the engineer. Engineer will establish IC-TV, and the IC-TV will be 1.05 times the IC-TV of the previous layer. In case of no control strip, the IC-MV data is color-coded based as "RED" in areas achieving 25% of the average IC-MV data from the control strip, "YELLOW" in areas achieving 25% to 85% of the average IC-MV, and "GREEN" in areas achieving > 85% of the average IC-MV. The color-coded map is used by the engineer to select test locations.	Not specified.	
ISSMGE (2005)	Roller chosen by experience	100 m by the width of the site	Homogenous, even surface. Track overlap \leq 10% drum width.	Rolling pattern, sequence of compaction and measuring passes; amplitude, speed, dynamic measuring values, frequency, jump operation, and corresponding locations	Correlation coefficient \geq 0.7. Minimum value \geq 95% of E_{v1} and mean should be \geq 105% (or \geq 100% during jump mode). Dynamic measuring values should be lower than the specified minimum for \leq 10% of the track. Measured minimum should be \geq 80% of the specified minimum. Standard deviation (of the mean) must be \leq 20% in one pass.	Constant 2–6 km/h (\pm 0.2 km/h)	Constant (\pm 2 Hz)
Austria — RVS 8S.02.6. (1999)	Vibrating roller compactors with rubber wheels and smooth drums suggested	100 m long by the width of the site	No inhomogeneities close to surface (materials or water content). Track overlap \leq 10% drum width.	Compaction run plan, sequence of compaction and measurement runs, velocity, amplitude, frequency, speed, dynamic measuring values, jump operation, and corresponding locations	Correlation coefficient \geq 0.7. Minimum value \geq 95% of E_{v1} , and median should be \geq 105% (or \geq 100% during jump mode). Dynamic measuring values should be lower than the specified minimum for \leq 10% of the track. Measured minimum should be \geq 80% of the set minimum. Measured maximum in a run cannot exceed the set maximum (150% of the determined minimum). Standard deviation (of the median) must be \leq 20% in one pass.	Constant 2–6 km/h (\pm 0.2 km/h)	Constant (\pm 2 Hz)

Reference	Equipment	Calibration Requirements		Documentation	Compaction Specs	Speed	Freq.
		Area	Location				
Germany — ZTVE StB/TP BF-StB (1994)	Self-propelled rollers with rubber tire drive are preferred; towed vibratory rollers with towing vehicle are suitable.	Each calibration area must cover at least 3 partial fields ~20 m. long	Level and free of puddles. Similar soil type, water content, layer thickness, and bearing capacity of support layers. Track overlap \leq 10% machine width.	Dynamic measuring value; frequency; speed; jump operation; amplitude; distance; time of measurement; roller type; soil type; water content; layer thickness; date, time, file name, or registration number; weather conditions; position of test tracks and rolling direction; absolute height or application position; local conditions and embankments in marginal areas; machine parameters; and perceived deviations	The correlation coefficient resulting from a regression analysis must be \geq 0.7. Individual area units (the width of the roller drum) must have a dynamic measuring value within 10% of adjacent area to be suitable for calibration.	Constant	
Sweden — ROAD 94 (1994)	Vibratory or oscillating single-drum roller. Min. linear load 15–30 kN. Roller-mounted compaction meter optional.	Thickness of largest layer 0.2–0.6 m.	Layer shall be homogenous and non-frozen. Protective layers < 0.5 m may be compacted with sub-base.	—	Bearing capacity or degree of compaction requirements may be met. Mean of compaction values for two inspection points \geq 89% for sub-base under roadbase and for protective layers over 0.5 m thick; mean should be \geq 90% for roadbases. Required mean for two bearing capacity ratios varies depending on layer type.	Constant 2.5–4.0 km/h	—

2.4 CONCLUDING REMARKS

As discussed above in this chapter, IC technologies have been used in the U.S. on over 380+ pilot/demonstration projects since year 2000. While in general using the technology presents a significant step forward in the right direction, the current European and U.S. specifications lack detailed framework for calibration (i.e., corrections from independent testing) and validation of results (i.e., accuracy and system quality checks) in terms of mechanical soil properties. Further, the mechanical soil properties that some agencies are using, do not directly link to the pavement design input parameters (e.g., k-value or stress-dependent M_r value). Albeit considerable evidence in the literature from numerous correlation studies that correlating IC-MVs with dry density can be challenging and practically impossible in many cases (see Mooney et al. 2010, White et al. 2011), some states and a version of the current FHWA specification still require the IC data be calibrated with density measurements.

White et al. (2014) recently documented findings from a series of annual workshops conducted with participants from state agencies, academia, industry, and contractors from 2008 to 2012. The workshops identified a list of the IC research and implementation needs and prioritized them, to further successful implementation of the technology. The most recent prioritized list in 2012 was as follows (highest to least priority in that order):

1. Data management and analysis
2. Specifications/guidance
3. In-situ correlations
4. Understanding impact of non-uniformity on performance
5. Standardization of roller outputs and format files
6. Standardization of roller sensor calibration protocols
7. Education program/certification process
8. Understanding roller measurement influence depth
9. Project scale demonstration and case histories
10. In situ testing advancements and new mechanistic based QC/QA
11. Intelligent compaction technology advancements and innovations

The topic of *data management and analysis* became the highest priority in 2012 and is believed to be a result of the agencies getting hands-on experience with the technology and becoming more involved with data aspects. Simplifying the data management and analytics, automating generation of compaction reports, and automating data archival need be resolved to successfully implement the IC technology.

CHAPTER 3 FIELD DEMONSTRATION PROJECTS

As part of the field demonstration phase of this project, field testing was conducted on selected test sections on the Elgin O’Hare Western Access Tollway construction project in October 2016, April-May 2017, and in June 2017. Field evaluation was performed on a total of 18 test sections, of which in situ comparison and calibration testing was conducted on 12 test sections. Tests were conducted on embankment subgrade, subgrade aggregate special or porous granular embankment (PGE), and improved subgrade or CA6 capping layer materials.

Four different IC-MV technologies have been evaluated including: CMV, HMV, MDP, and VIC. The CMV and MDP IC-MVs were obtained from Caterpillar CS74 vibratory smooth drum IC roller, HMV IC-MVs were obtained from Hamm H11 vibratory smooth drum IC roller, and VIC IC-MVs were obtained on a retrofitted Caterpillar CS56 vibratory smooth drum roller. Field calibration testing was conducted using LWD, DCP, and static and cyclic APLT testing.

In this chapter, a review of the existing Illinois Tollway (ILT) specifications for the different pavement foundation layers is summarized to study the quality assurance target values used on the project, a summary of field testing and analysis procedures is provided, and a detailed account of all field results and correlation analysis results are provided.

3.1 REVIEW OF CURRENT ILT SPECIFICATIONS

A summary of the current ILT specifications for embankment fill materials (Zone A only), and PGE and capping layer materials is provided in Table 5. The summary includes the reference, soil property used to assess quality, target value of the property, testing frequency, and the type of test used.

The quality of the general embankment fill and the subgrade layers is assessed based on field target moisture and dry density requirement relative to standard Proctor test, proof rolling, and DCP penetration index criteria. For PGE and capping layers, the quality requirements include assessing quality of the aggregate and the gradation properties.

Table 5. Summary of existing QC/QA specifications for embankment and pavement foundation materials on the field demonstration project (ILT Contracts I-15-4662, I-14-4644, and I-14-4642)

MATERIAL / LAYER	SPECIFICATION REFERENCE	PROPERTY/QUALITY	TARGET VALUE	TESTING FREQUENCY	TYPE OF MISTIC ¹ TEST
Embankment (General Embankment Fill – Zone A only)	IDOT Articles 205.04, 205.06 & Project Procedures Guide [Sampling Schedules]	Lift Thickness	8 in. (loose lift – maximum)	None	NA
		Moisture and Density Curve (<i>note: Standard Proctor per AASHTO T99</i>)	NA	For each major change in embankment material	NA
		Density	Height < 1.5 ft = 95% RC (relative compaction) Height 1.5 ft to 3.0 ft = 1 st lift 90% RC and remaining 95% RC Height > 3 ft = Bottom 1/3 rd height (max 2 ft) to 90% RC, next 1 ft to 93% RC, and the remaining to 95% RC.	1 test every 20,000 Cubic Yards. Confined areas: 1 test per 3 ft of lift	Process Control (Project Inspector)

	Project Specification & Project Procedures Guide [Sampling Schedules]	Moisture	Max. 110% of the optimum moisture for all clay soils Max. 105% of the optimum moisture for all clay loam soils	Not specified	Process Control (Project Inspector)
		Stability (DCP)	Max. 1.5 inches/blow (for general embankment fill)	Not specified in contract (determined by DGE)	Process Control (Project Inspector)
	Subgrade Stability Manual & Project Procedures Guide [Sampling Schedules]	Stability (DCP)	Near top of subgrade (below the modified/improved subgrade ²) the criterion is max. 2 inches/blow in the top 6 in. (See Table 1 in the manual for additional description)	Not specified in contract (determined by DGE)	Process Control (Project Inspector)
		Proofrolling (500 to 1,000 ft sections) using fully loaded tandem axle truck	Rutting < 0.5 in. (<i>note: permanent, based 3 to 4 passes</i>). Additional DCP testing in areas with excess rutting to determine remedial layer thickness.	Not specified in contract (determined by DGE – Currently used on all subgrade that is completed)	Process Control (Project Inspector)
Subgrade Aggregate Special (PGE) & CA6 Capping Material (“Improved Subgrade”)	Project Specifications & IDOT Article 1004.01	Aggregate quality and gradation	RAP does not exceed 50% of the final product. Gradation requirements for sieve sizes: 5 in., 4 in., 2 in., #4, #200 for PGE Gradation requirements for sieve sizes: 1.5 in., 1 in., 1/2 in., #4, #16, #200 for CA6	Tollway Construction Bulletin 15-02	Process Control (Project Inspector)
Subgrade	IDOT Article 301.04 & Project Procedures Guide [Sampling Schedules]	Density	95% RC	1 test per 1500 ft of entire length of subgrade	Process Control (Project Inspector)
		Stability (DCP) (<i>note: DCP per IDOT Test Procedure 501, similar equipment to ASTM D6954</i>)	Max. 0.9 inches/blow (<i>note: not used on current project due to relatively weak soil conditions</i>)	Not specified (determined by DGE)	Process Control (Project Inspector)
Modified Soil with Lime, Portland Cement, Portland Blast-Furnace Slag, or Fly	IDOT Article 302.09 & Project Procedures Guide [Sampling Schedules]	Density	95% RC	1 test per 1500 ft of treated area	Process Control (Project Inspector)
		Stability (DCP)	Max. 0.75 inches/blow	Not specified (determined by DGE)	Process Control (Project Inspector)

NOTES:

¹MISTIC – Materials Integrated System for Test Information and Communication

²Modified/improved subgrade is the 12 in. layer that is directly below the pavement (3 in. of bituminous stabilized base, 3 in. of CA6 capping, and 6 in. of PGE or Subgrade Aggregate Special).

³Not used on the Elgin/O’Hare Tollway projects. The requirements are generic IDOT standard specification requirements. These are modified on the Elgin O’Hare project to use Improved Subgrade over the embankment fill as a target DCP of 0.9 inches/blow could not be met for the soils on the project. Lime modified subgrade use only in pavement test section area.

3.2 TEST SECTIONS AND MATERIALS

Field testing was conducted on 18 test sections spanning periods of October 2016, April-May 2017, and in June 2017. In situ comparison and calibration testing was conducted on 12 of these test sections. On a few sections, contractor trained roller operators performed production mapping. A summary of the 18 test sections along with dates, location, and field notes is provided in Table 6.

In situ tests were conducted on embankment subgrade, subgrade aggregate special or porous granular embankment (PGE), and improved subgrade or CA6 capping layer materials. A summary of the soil index properties of these materials is provided in Table 7. The PGE layer was nominal 6 in. thick and was placed over the subgrade and consisted of poorly graded recycled portland cement concrete (RPCC) material with a maximum particle size of about 5 in. and no fines passing the No. 200 sieve. The CA6 capping layer was about 3 in. thick and was placed on the PGE layer and consisted of well-graded recycled asphalt pavement (RAP) material with a maximum particle size of about 1.5 in. and about 1% passing the No. 200 sieve.

Table 6. Summary of test sections.

Date	TS	Material / Layer	IC Roller	IC-MV	In-Situ Testing	Comments / Notes
10/1/16 to 10/2/16 (Contract 4642)	1	PGE	Hamm H11 Smooth Drum Roller	HMV	LWD and DCP	6 in. PGE layer with RPCC aggregate on WB lane. Testing was performed at 25 points (LWD only) across the PGE layer width, and at 15 points (LWD and DCP) selected based on the IC map.
10/13/16 (Contract 4642)	2	PGE	Hamm H11 Smooth Drum Roller	HMV	LWD and DCP	6 in. PGE layer with RPCC aggregate and a portion overlain with RAP material on EB lane. Testing was performed at 10 points (LWD and DCP) selected based on IC map
10/13/16 (Contract 4642)	3	PGE	Hamm H11 Smooth Drum Roller	HMV	LWD and DCP	6 in. PGE layer with RPCC aggregate on EB lane, including RAMP. Testing was performed at 5 points (LWD and DCP) selected based on IC map only in the ramp area because of stiff conditions.
10/14/16 (Contract 4642)	4	CA6 Capping	Hamm H11 Smooth Drum Roller	HMV	LWD and DCP	3 in. CA6-RAP capping layer over 6 in. PGE layer with RPCC aggregate on EB lane. Testing was performed at 5 points (LWD and DCP) selected based on IC map only in the ramp area because of stiff conditions.
10/15/16 (Contract 4662)	5	Embankment	Caterpillar 815 Padfoot Roller	MDP	DC and DCP	Caterpillar 815 padfoot roller was used on Section 4662 (near York Road) and testing was performed with DCP and DC's after compaction work. Plote performed compaction operations with the roller. Proctor information for the material was obtained from Interra Services. The test section was reportedly re-worked after this testing.
10/14/16 (Contract 4642)	P1	PGE	Hamm H11 Smooth Drum Roller	HMV	None.	Production operations by contractor.
10/17/16 (Contract 4642)	P2	PGE	Hamm H11 Smooth Drum Roller	HMV	None.	Production operations by contractor.
10/18/16 (Contract 4642)	P6	CA6 Capping	Hamm H11 Smooth Drum Roller	HMV	None.	Production operations by contractor.
04/11/17 (Contract 4642)	6	PGE	Hamm H11 Smooth Drum Roller	HMV	LWD and DCP	Remap of test section 1. Testing was performed at 15 points (LWD and DCP) selected based on the IC map.

04/12/17 and 04/18/16 (Contract 4642)	7	CA6 Capping Layer	Hamm H11 Smooth Drum Roller	HMV	LWD and DCP	West of test section 1. CA6 Capping Layer (WB Lane) Between Lively Blvd and Wood Dale Road, just east of Wood Dale overpass. In situ testing at 25 selected locations for calibration with LWD and DCP.
			Caterpillar CS74B Smooth Drum Roller	CMV and MDP		
04/12/17 (Contract 4642)	8	CA6 Capping Layer	Hamm H11 Smooth Drum Roller	HMV	None.	Map over test section 6.
04/18/17 (Contract 4642)	9	CA6 Capping Layer	Hamm H11 Smooth Drum Roller	HMV	LWD and DCP	CA6 Capping Layer (WB Lane) Between Prospect Avenue and Salt Creek Bridge. In situ testing at 15 selected locations for calibration with LWD and DCP on 04/18/16.
			Caterpillar CS74B Smooth Drum Roller	CMV and MDP		
04/25/17 (Contract 4644)	10	PGE	Hamm H11 Smooth Drum Roller	HMV	None.	Project 4644 EB Lane between Lively Blvd and IL83 with PGE placed and compacted on 04/23 and 04/24/17. No in situ testing.
			Caterpillar CS74B Smooth Drum Roller	CMV and MDP		
04/25/17 to 04/26/17 (Contract 4644)	11	PGE	Hamm H11 Smooth Drum Roller	HMV	None.	Project 4644 WB Lane between Lively Blvd and IL83 with PGE placed and compacted on 04/25/17. No in situ testing.
			Caterpillar CS74B Smooth Drum Roller	CMV and MDP		
05/04/17 (Contract 4644)	12	CA6 Capping Layer	Hamm H11 Smooth Drum Roller	HMV	LWD and DCP	Mapping on CA6 layer placed over TS10. Project 4644 EB Lane between Lively Blvd and IL83 with RAP Capping placed on 05/02 to 05/03/17. In situ testing performed at 15 test locations.
			Caterpillar CS74B Smooth Drum Roller	CMV and MDP		
06/21/17	13	CA6 Capping Layer	Ingios VIC outfitted Smooth Drum Roller	VIC	Cyclic APLT, LWD, and DCP	Thorndale Ave (EB), between Hamilton Lakes Dr. and N. Arlington Heights Rd. In situ testing performed at 20 test locations.
06/22/17	14	Subgrade	Ingios VIC outfitted Smooth Drum Roller	VIC		Thorndale Ave (EB), just West of Hamilton Lakes Dr. overpass. In situ testing performed at 6 test locations.
06/23/17	15	PGE	Ingios VIC outfitted Smooth Drum Roller	VIC	Static APLT	PGE placed over TS14 subgrade. In situ testing performed at 10 test locations.

Table 7. Properties of soil materials tested

Parameters	Subgrade (TS14) ¹	Embankment Fill (TS5) ¹	Large RAP Haul Road (TS3) ²	RAP CA6 Capping (TS4) ²	RAP CA6 Capping (TS13) ¹	Subgrade Aggregate or PGE (TS15) ¹	Subgrade Aggregate or PGE (TS1) ²
Classification	Sandy lean clay	Fat Clay	Well graded gravel with sand	Well graded sand with gravel	Well graded gravel with sand	Poorly graded gravel	Well graded gravel
USCS	CL	CH	GW	GW	GW	GP	GW
AASHTO	A-7-6 (9)	NA	A-1-a	A-1-a	A-1-a	A-1-a	A-1-a
<i>Particle-Sizes</i>							
Max. Particle Size (in.)	3/8	NA	6.5	1.5	1.5	5.0	5.9
% Gravel	1		75	43	68	98	79
% Sand	32		25	55	31	2	19
% Silt	36		0	2	1	0	2
% Clay	31						
<i>Atterberg Limits</i>							
Liquid Limit	34	NA	Non-Plastic	Non-Plastic	Non-Plastic	Non-Plastic	Non-Plastic
Plastic Limit	17						
Plasticity Index	17						
<i>Standard Proctor</i>							
Optimum Moisture Content (%)	14.0	16.4	NA	NA	NA	NA	NA
Max. Dry Density (pcf)	114	107.9					

¹Details provided by Interra Services.

²Tests performed by the research team

The gradation results of the large particles (see Figure 9) and accompanying image analyses are provided in Figure 10, 11 and 12. For material less than 3-in. diameter, ASTM C136 was followed. The entire available material in each bucket was sieved. The field imaging method developed at UIUC was followed to identify the sizes of particles above 3 in.

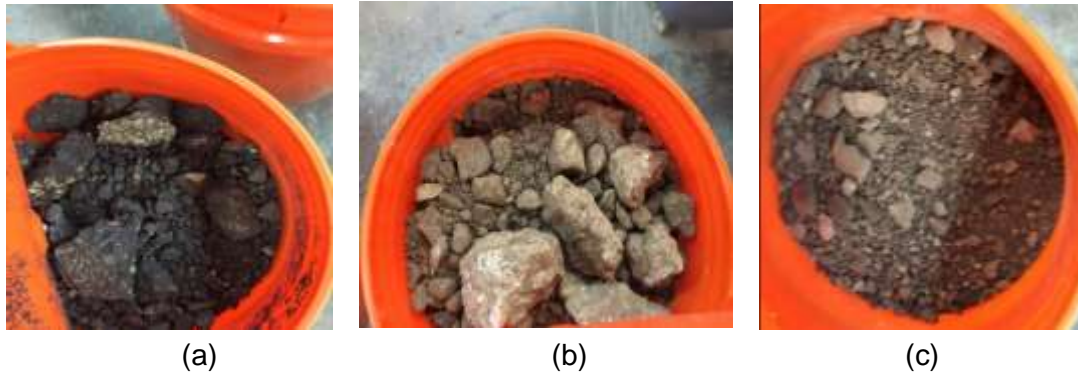


Figure 9. Large aggregate base samples: (a) Large RAP (with sizes above 3-in. unfractured RAP particles), (b) PGE (with four different sizes above 3-in. particles), and (c) RAP Capping Material (maximum 1-in. size)

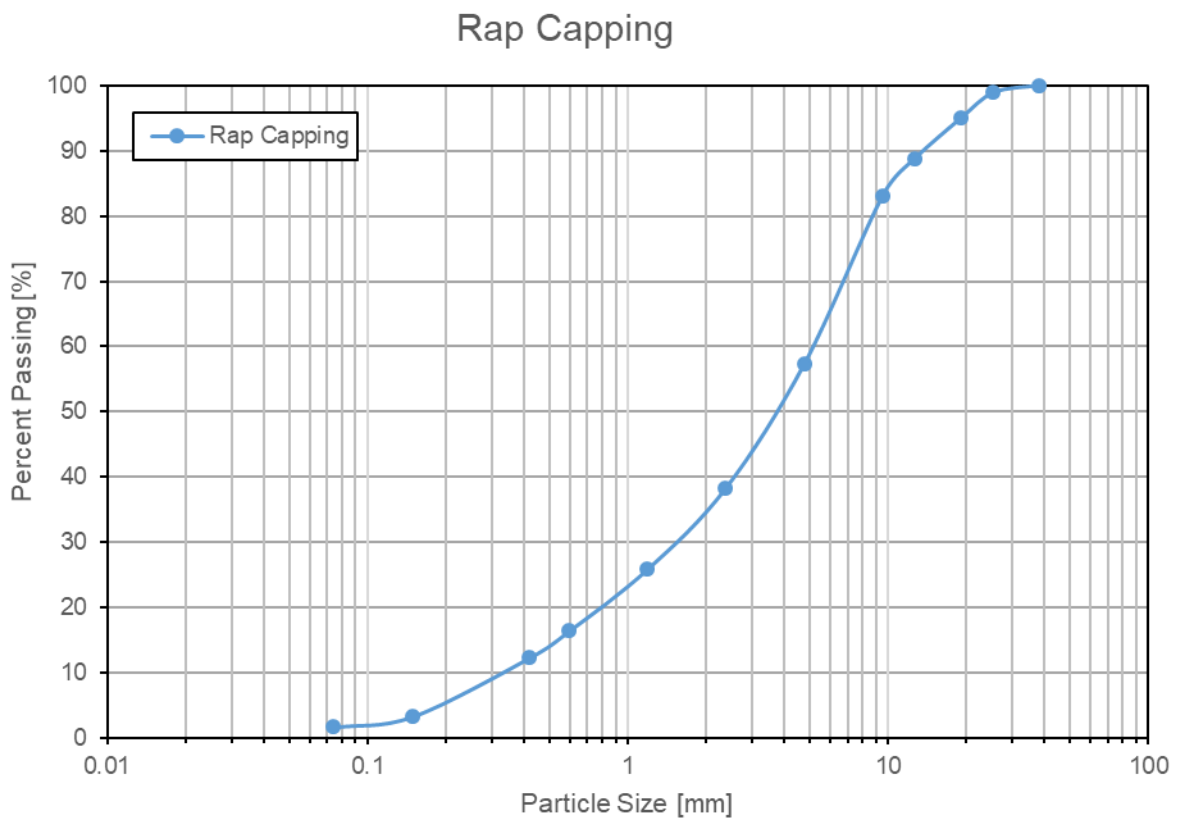


Figure 10. RAP Capping Material (maximum 1-in. size) gradation results

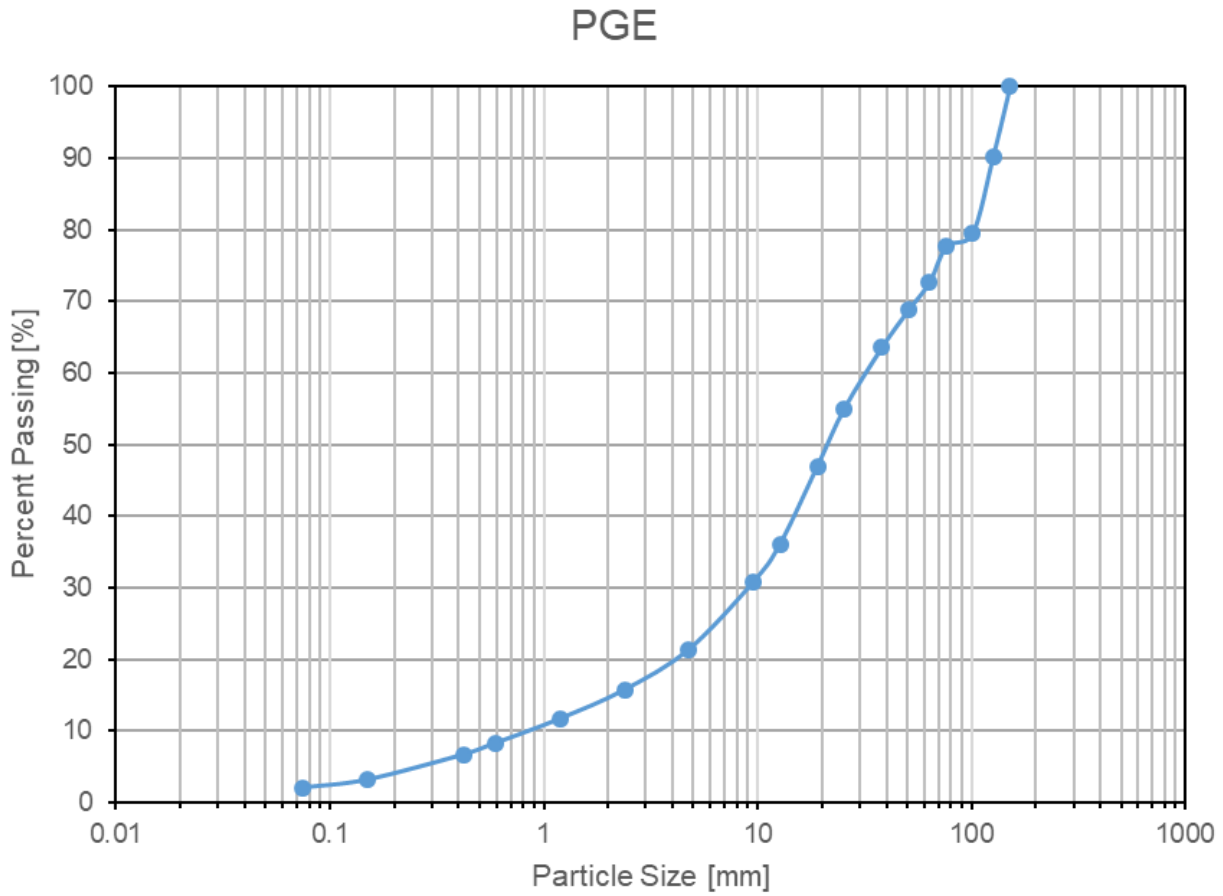


Figure 11. PGE gradation and image analysis results for four large particles above 3-in. diameter according to the approach adopted by Moaveni (2015).

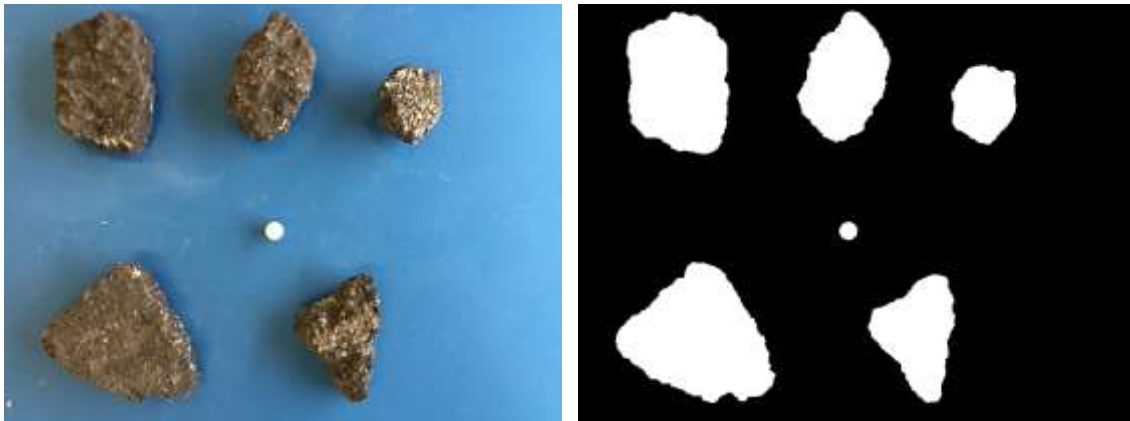
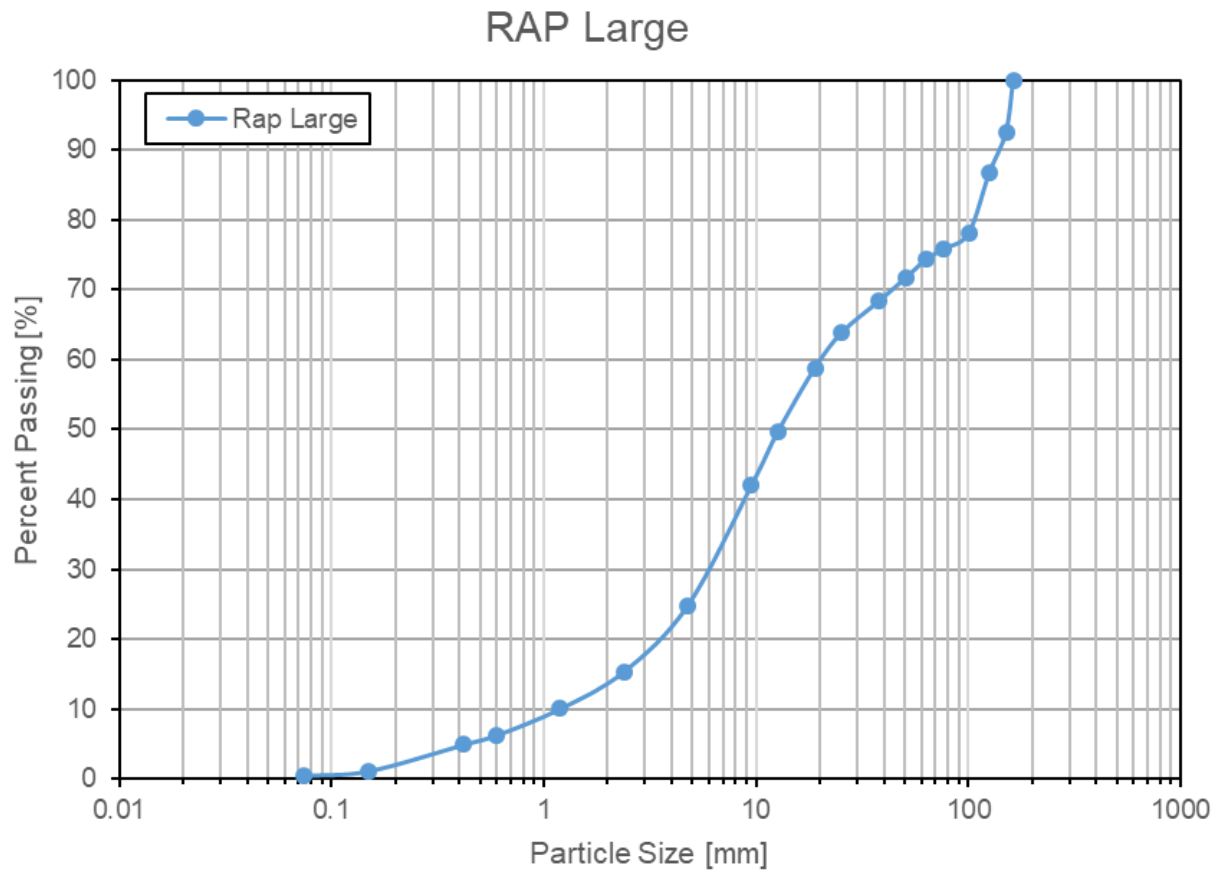


Figure 12. Large RAP gradation and image analysis results for five large particles above 3-in. diameter according to the approach adopted by Moaveni (2015).

3.3 FIELD TESTING METHODS

3.3.1 IC Measurement Values

In this study, four different IC measurement values were evaluated:

- Hamm measurement value (HMV) on Hamm's H11i smooth drum vibratory roller (Figure 13);
- Compaction meter value (CMV) on Caterpillar CS74B smooth drum vibratory roller (Figure 14);
- Machine drive power (MDP) on the CS74 smooth drum roller and Caterpillar 815F padfoot roller (Figure 15), and
- Validated intelligent compaction (VIC) on retrofitted Caterpillar CS56 smooth drum vibratory roller (Figure 16).

The Hamm H11i IC roller weighs about 24,857 lbs. was outfitted with global positioning system (GPS) with corrections from satellite-based augmentation system (SBAS). The Caterpillar CS74B smooth drum vibratory roller weighs about 35,264 lbs. and was outfitted with real-time kinematic (RTK) GPS system that is tied to an onsite GPS base station. The Caterpillar 815 series padfoot vibratory roller weighs about 45,765 lbs. and was also outfitted with RTK-GPS that is tied to an on-site GPS base station. The CS56 smooth drum roller equipped with retrofit VIC system weights about 27,450 lbs. was outfitted with SBAS-GPS.

The IC-MVs are described in Chapter 2, but a brief description as it relates to the field demonstration projects is provided below.



Figure 13. Hamm H11i vibratory smooth drum IC roller



Figure 14. Caterpillar CS74B smooth drum IC roller



Figure 15. Caterpillar 815F padfoot IC roller



Figure 16. Caterpillar CS6 smooth drum roller with retrofit VIC system

3.3.1.1 Hamm Measurement Value (HMV) or Compaction Meter Value (CMV)

The HMV and CMV are similar and are dimensionless compaction parameter values that depend on roller dimensions (i.e., drum diameter and weight), and roller operation parameters (e.g., frequency, amplitude, and speed) and are determined using the dynamic roller response. They are calculated as the ratio of the acceleration of the first harmonic component of the vibration ($A_{2\Omega}$) and the acceleration of the fundamental component of the vibration (A_{Ω}) multiplied by a constant value (C). The C value used depends on the manufacturer. As noted in the literature review, the HMV or CMV measurements are influenced by drum bouncing. Based on past studies, HMV or CMV measurements have a measurement influence depth of about 3 to 5 feet.

In this study, HMV value reported by Hamm on the on-board display was different than what was exported. After a close review of the data and communication with representatives at Hamm, it was determined that the outputted values are 10 times higher than the values displayed on the screen. It was unclear which values (reported on screen or the outputted) were the correct ones to use. For this reason, the HMV values reported as part of correlation analysis with the in situ point measurements show 10x higher values than reported in the color-coded maps in this study.

3.3.1.2 Machine Drive Power (MDP)

The MDP value provides a measure of roller sinkage with units of power (e.g., kJ/s). In this study, the MDP value reported on the machine are index values that range between 1 and 150 and are therefore referred to as MDP* from hereafter. MDP* of 150 value represents a hard-compacted surface with MDP close to 0 kJ/s and MDP* of 1 represents a soft condition as defined during calibration.

3.3.1.3 Validated Intelligent Compaction (VIC)

In this study, the VIC was calibrated to produce stress-dependent M_r values and k -values. The M_r and k -value calibration was performed using APLT testing over a range of ground stiffness

conditions. For comparison purposes, CMV was also simultaneously measured to evaluate the relationships with the in situ point measurements.

3.3.2 Light Weight Deflectometer (LWD) Testing

The LWD was setup with a 11.81-in. diameter plate (Figure 17), and the tests were performed following manufacturer recommendations (Zorn 2003). The elastic modulus values were determined using Equation 7:

$$E_{LWD} = \frac{(1 - \nu^2)\sigma_0 r}{D_0} \times F \quad (7)$$

where E_{LWD} = elastic modulus (psi), D_0 = measured peak plate deformation (in.), ν = Poisson's ratio (assumed as 0.4), σ_0 = applied stress (psi) = 14.5 psi, r = radius of the plate (in.) = 5.9 in., F = shape factor depending on stress distribution (assumed as 8/3 for granular materials). The measurement influence depth of LWD testing is about 1 to 2 ft. based on the criteria of 1 to 1.5 times the diameter of the loading plate (Mooney et al. 2010, Vennapusa et al. 2012).

3.3.3 Dynamic Cone Penetrometer (DCP) Testing

DCP tests were performed in accordance with ASTM D6951-03. The tests involved dropping a 17.6 lb. hammer from a height of 22.6 in. and measuring the resulting penetration depth (Figure 17). A 30-in. penetrating rod was used. California bearing ratio (CBR) values were determined using Equations 8 and 9, whichever is appropriate, where the dynamic penetration index (DPI) is in units of mm/blow.

$$\text{CBR}(\%) = \frac{292}{\text{DPI}^{1.12}} \text{ for all materials except CL soils with CBR} < 10 \quad (8)$$

$$\text{CBR}(\%) = 1 / (0.017019 \times \text{DPI})^2 \text{ for CL soils with CBR} < 10 \quad (9)$$

The DCP test results were used to determine an average CBR of a given layer or for a given depth. For tests conducted on 6 in. of PGE over subgrade and 3 in. of RAP over 6 in. of PGE and subgrade, average CBR of the top and bottom layer are reported. The top layer was either the PGE or PGE + RAP, and the bottom layer was the top 12 in. of the subgrade which represents the top subgrade layer. The average value was reported by calculating the DPI value based on the total number of blows taken to the desired depth.



Figure 17. LWD (left) and DCP (right) testing on compacted CA6 capping layer.

3.3.4 Automated Plate Load Testing (APLT)

APLT was developed recently to directly and rapidly measure the in situ M_r and k values through automated cyclic and static plate load testing, respectively (White and Vennapusa 2017). The major advantages of using in situ cyclic testing to determine M_r using APLT is the ability to perform a conditioning stage like a laboratory M_r test (AASHTO T307-99) and obtain M_r values at various cyclic and confining stresses. APLT was used in this study (Figure 18) to measure the composite resilient modulus (M_{r-Comp}), individual top (aggregate base) and bottom (subgrade) layer resilient modulus (M_{r-Base} and M_{r-SG}), and modulus of subgrade reaction k -value. The data analysis procedures are summarized below.

3.3.4.1 In Situ Composite Resilient Modulus

Cyclic APLT using a 12-in. diameter loading plate was conducted to determine in situ composite resilient modulus (M_{r-Comp}) at six different stress levels, which involved one conditioning sequence with 500 cycles followed by six loading steps with 100 cycles each. Average of the last 5 cycles from each step were used for calculations.



(a)



(b)



(c)

Figure 18. (a) APLT setup; (b) setup for measuring in situ resilient modulus using cyclic testing with 12 in. diameter plate, and (d) in situ modulus of subgrade reaction with static testing with 30 in. diameter plate

The M_{r-Comp} was calculated as the ratio of the cyclic stress divided by the resilient deflection (during unloading) using the Boussinesq's half-space equation:

$$M_{r-Comp} = \frac{(1 - \eta^2) \Delta \sigma_{cyclic} r}{\delta_r} \times F \quad (10)$$

where: M_{r-Comp} = in situ composite resilient modulus (psi), δ_r = the resilient deflection of plate during the unloading portion of the cycle (determined as the average of three measurements along the plate edge), η = Poisson's ratio (assumed as 0.4), $\Delta \sigma_{cyclic}$ = cyclic applied stress (psi), r = radius of the plate (in.), F = shape factor depending on stress distribution (assumed as 8/3 for granular materials). Using the criteria of 1 to 1.5 times the plate diameter for measurement influence depth, the M_{r-Comp} values have an influence depth of about 1 to 1.5 ft.

The M_r parameter is a highly stress-dependent parameter, and most soils exhibit the effects of increasing stiffness with increasing bulk stress and decreasing stiffness with increasing shear stress.

The APLT testing program was designed to assess the in situ composite resilient modulus at six different stress levels. The results were used to model the behavior using the “universal” model (AASHTO 2015):

$$M_r = k_1^* P_a \left(\frac{\theta}{P_a} \right)^{k_2^*} \left(\frac{\tau_{oct}}{P_a} + 1 \right)^{k_3^*} \quad (11)$$

where M_r = in situ resilient modulus (psi); P_a = atmospheric pressure (psi); θ = bulk stress (psi) = $\sigma_1 + \sigma_2 + \sigma_3$; σ_1 = applied cyclic stress ($\Delta\sigma_{cyclic}$) used in M_{r-comp} calculations because there is no confining stress at the surface; $\sigma_2 = K_o \sigma_1$; $\sigma_3 = \sigma_2$, K_o = coefficient of lateral earth pressure at rest = $\eta/(1-\eta)$; η = Poisson’s ratio assumed as 0.4; τ_{oct} = octahedral shear stress (psi) = $\sqrt{(\sigma_1 - \sigma_2)^2 + (\sigma_2 - \sigma_3)^2 + (\sigma_3 - \sigma_1)^2} / 3$; and k_1^* , k_2^* , and k_3^* = regression coefficients determined from in situ testing (these coefficients are presented herein with a * to differentiate with the regression coefficients traditionally developed using laboratory test results).

3.3.4.2. In Situ Layered Resilient Modulus

Individual subgrade and base layer resilient modulus values were determined by obtaining resilient deflections measured at radii of 12 in. ($2r$), 18 in. ($3r$), and 24 in. ($4r$) away from the plate center. The test setup is shown in Figure 18b and it is illustrated as shown in Figure 19 . The layered analysis measurement system was developed specifically for testing unbound materials and provides average resilient deflections measured over one-third (60 degrees) of the circumference of a circle at the selected radii. This method was designed to improve practices that use point measurements, which are often variable from point-to-point for unbound aggregate materials.

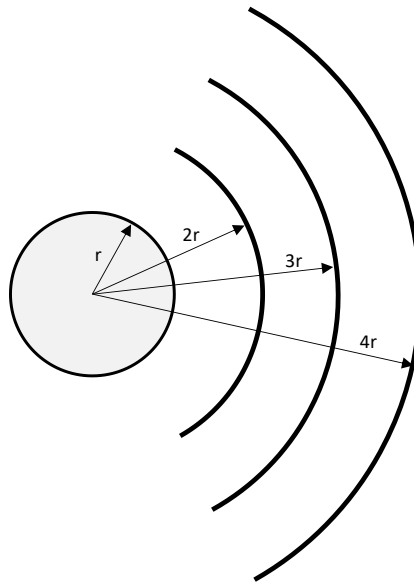


Figure 19. Deflection basis measurement kit positioned at 2r, 3r, and 4r positions (where ‘r’ is the radius of the plate) from the plate center axis.

Equation 12 as suggested by AASHTO (1993) can be used to determine subgrade layer resilient modulus value:

$$M_{r-SG} = \frac{(1 - \nu^2) \cdot P}{\pi \cdot r' \cdot \delta_{r,r'}} \quad (12)$$

where M_{r-SG} is in situ subgrade resilient modulus (psi), $\delta_{r,r'}$ is the resilient deflection (in.) during the unloading portion of the cycle at $r' = 2r$ or $3r$ or $4r$ away from plate center, ν is the Poisson ratio (assumed as 0.4), and P is the cyclic load (lbs.).

AASHTO (1993) suggests that the r' must be far enough away that it provides a good estimate of the subgrade modulus, independent of the effects of any layers above, but also close enough that it does not result in a too small value. A graphical solution is provided in AASHTO (1993) to estimate the minimum radial distance based on an assumed effective modulus of all layers above the subgrade and the $\delta_{r=0}$ value. Salt (1998) indicated that if the modulus values are plotted against radial distance r , in linear elastic materials such as sands and gravels, the modulus values decrease with increasing distance and then level off after a certain distance. The distance at which the modulus values level off can be used as r' in Eq. 4. In some cases, the modulus values decrease and then increase with distance. Such conditions represent either soils with moderate to high moduli with poor drainage at the top of the subgrade or soft soils with low moduli. In those cases, the distance where the modulus is low can be used as r' in Eq. 4. In this study, $r' = 2r$ or $3r$ were used to determine M_{r-SG} .

Ullidtz (1987) described Odemark's method of equivalent thickness (MET) concept which involves transforming a two-layer system into an equivalent thickness h_e with properties of the bottom layer. The h_e is calculated using Equation 13 which can be simplified to Equation 14, if Poisson's ratio (ν) is assumed as the same for the two layers:

$$h_e = h \times \sqrt[3]{\frac{M_{r1}(1 - \nu_1^2)}{M_{r2}(1 - \nu_2^2)}} \quad (13)$$

$$h_e = h \times \sqrt[3]{\frac{M_{r1}}{M_{r2}}} \quad (14)$$

Using the Boussinesq's solution for linear-elastic materials and Odemark's MET method, Equation 15 from AASHTO (1993) can be solved to determine the resilient modulus of the base layer (M_{r-Base}):

$$\delta_c = (1 - \nu^2) \sigma_0 r f \left[\frac{1}{M_{r-SG} \sqrt{1 + \left(\frac{h}{r} \times \sqrt[3]{\frac{M_{r-Base}(1 - \nu_1^2)}{M_{r-SG}(1 - \nu_2^2)}} \right)^2}} + \frac{\left(1 - \frac{1}{\sqrt{1 + \left(\frac{h}{r} \right)^2}} \right)}{M_{r-Base}} \right] \quad (15)$$

where ν_1 and ν_2 are Poisson ratios for base and subgrade layer, respectively (assumed as 0.40 for both layers), and h is the thickness of the base layer (in.). Past research has shown that stress measurements in two-layer systems of aggregate base over compressible subgrade are very similar to those predicted by Boussinesq's analysis (e.g., McMahon and Yoder, 1960; Sowers and Vesic, 1961).

The two-layered analysis using the Odemark method is applicable for conditions with moduli values decreasing with depth (i.e., hard over soft), preferably by a factor of at least two between the consecutive layers (Ullidtz 1987). Ullidtz (1987) also noted that the h_e should be larger than the radius of the loading plate, i.e., $h_e/r > 1$.

The M_{r-SG} and M_{r-Base} values were calculated at different applied stress levels from layered analysis to assess the stress-dependent behavior of each layer. Like in situ composite M_r values, the calculated M_{r-SG} and M_{r-Base} values were used to model the behavior using the “universal” model (AASHTO 2015) shown in Equation 11.

In modeling M_{r-Base} behavior, the bulk stress (θ) values are the same as the σ_{cyclic} stress. In case of M_{r-SG} , the θ values were calculated using the following steps:

- The applied cyclic stress at the base/subgrade interface was calculated using the KENLAYER layered elastic analysis program. The interface stresses are a function M_{r-Base}/M_{r-SG} ratio, thickness of the base layer, radius of the plate, and the applied cyclic stress at the surface (see Huang 2004). The stresses were calculated at the center of the plate.
- The applied vertical stress (σ_1) is calculated by adding the calculated cyclic stress at the interface and confining stress due to the aggregate layer over the subgrade (calculated assuming a total unit weight of 130 pcf and layer thickness).
- The horizontal stresses (σ_2 and σ_3) were calculated using the procedure described under M_{r-Comp} determination discussion, assuming $\nu = 0.4$ for subgrade.
- The bulk stress (θ) values were calculated as the sum of σ_1 , σ_2 , and σ_3 .

The analysis approach described above assumes a flexible loading plate with uniform stress distribution at the surface and the assumption that both subgrade and base layers are linear elastic with homogenous conditions. The calculated stress values at the interface should therefore be considered approximate.

3.3.4.3. Modulus of Subgrade Reaction

Static plate load tests were conducted in general accordance with the AASHTO standard for non-repetitive loading using static plate load test (AASHTO T222-81) to determine k value using a 30-in. diameter loading plate setup shown in Figure 18c. A thin layer of fine silica sand was used as a bedding material for all tests. Using the criteria of 1 to 1.5 times the plate diameter for measurement influence depth, the k values determined using the 30-in. diameter loading plate have an influence depth of about 2.5 to 3.8 ft.

The test standard requires increasing applied stresses up to 30 psi in 5 psi increments. In this study, applied stresses were increased up to a maximum of at least 15 psi in 2.5 psi increments. The test was performed for two loading cycles. Plate deformations were measured at three locations along the edge of the plate. The uncorrected k value was determined using Equation 16.

$$k'_u = \frac{10\text{psi}}{\delta} \quad (16)$$

where k'_u = uncorrected modulus of subgrade reaction (pci), δ = deformation corresponding to the 10-psi loading increment (inches). In this study, a plot of applied stress on x-axis and average plate deflection on y-axis is prepared for the two loading cycles. Then a second order polynomial curve is fit separately for both first and second loading cycles, using model shown in Equation 17:

$$y = a_1x^2 + a_2x + a_3 \quad (17)$$

where y = deflection in inches; x = applied stress in psi; a_1 , a_2 , and a_3 = regression coefficients. To assess the quality of the regression fit, the coefficient of determination (R^2) value is determined. A minimum R^2 value of 0.98 has been established as required to achieve acceptable results.

Using the second order polynomial fit parameters the average plate deflections corresponding to a target applied stress (σ) are computed using the following equations for the first and second load cycles, respectively:

$$\delta_i = a_1\sigma^2 + a_2\sigma \text{ for 1}^{\text{st}} \text{ loading cycle} \quad (18)$$

$$\delta_r = a_1\sigma^2 + a_2\sigma \text{ for 2}^{\text{nd}} \text{ loading cycle} \quad (19)$$

In this study a target applied stress of $\sigma = 10$ psi has been used. The k'_u values calculated for 1st and 2nd loading cycles are reported as $k'_{u(1)}$ and $k'_{u(2)}$, respectively. The k'_u values were then corrected for plate bending to determine k_u following the procedure described in AASHTO T222 and the following Equation for $k'_u \geq 100$ pci and ≤ 1000 pci.

$$k_u = -39.9178 + 5.5076 \times [k'_u]^{0.7019} \quad (20)$$

The k_u values calculated for 1st and 2nd loading cycles are reported as $k_{u(1)}$ and $k_{u(2)}$, respectively.

3.3.4 Drive Core Testing

Drive core testing (see Figure 20) was performed in accordance with ASTM D2937 to determine in situ moisture and dry density of cohesive subgrade materials. The drive cylinders extracted from the subgrade layer were carefully wrapped and sealed in plastic bags, and stored in a cooler in a humid environment, and were transported to the laboratory for processing.

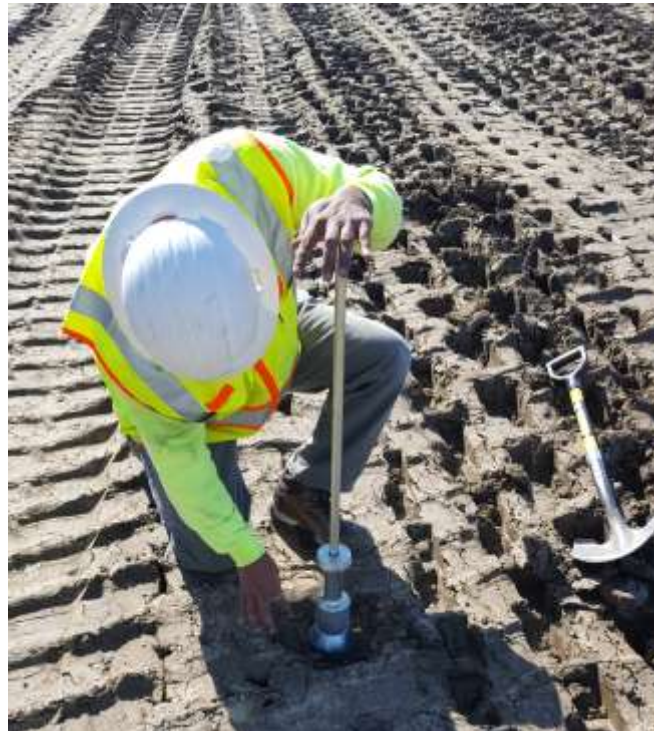


Figure 20. Drive core test equipment.

3.4 FIELD TESTING RESULTS

In this section, results from field testing conducted in different test sections are presented separately for each of the IC-MV technologies along with relevant pictures taken during field testing activities, key observations, color-coded IC-MV maps, selected in situ test measurements, calibration test results, and a statistical summary of IC-MVs and field measurement values. IC-MV maps and individual test results (e.g., DCP profiles) are presented for selected test sections to highlight some of the key observations. All results are included in the Appendices.

The technology providers' software was used to export color-coded images of IC-MVs and export the raw data and perform calibration analysis. For calibration/regression analysis, the GPS coordinates of the in situ point measurement were spatially paired with the GPS referenced IC-MVs from each roller. The in situ test location GPS coordinates were obtained using contractors' RTK-GPS equipment that is tied to an on-site base station or using the rover on the IC roller. The spatial pairing was performed in ArcGIS software. Compaction reports are also generated by the research team for each test section and are included in Appendix B. LWD and DCP test results are summarized in the following sections and raw test results are included in Appendix C.

3.4.1 Calibration Testing and Analysis – Hamm H11 HMV Measurements

HMV IC-MV measurements were obtained from 12 test sections, of which 6 consisted of nominal 6 in. thick PGE layer at the surface and the remaining 6 consisted of nominal 3 in. thick CA6 capping layer placed over the PGE layer at the surface. In situ tests were conducted at a total of 135 test locations for calibration analysis, of which 70 were obtained on PGE test sections and the remaining 135 on CA6 test sections. Test locations were selected using a systematic-random approach.

Pictures of test sections with PGE and CA6 capping layers where HAMM IC-MVs were obtained are shown in Figure 21. A screenshot of HMV IC-MV map from TS1 is shown in Figure 22. On TS1, 25 LWD test measurements were obtained across the pavement width, with either 2 or 3 test measurements in each roller lane. E_{LWD} test results across the pavement width along with the reported HMV value (one at the center of each lane) are also shown for comparison in Figure 22. In addition, DCP profiles showing CBR and cumulative blows with depth are shown for two selected locations with relatively stiff and soft conditions, as identified in the IC-MV map. The initial assessment of these results indicates that the IC-MV maps generally match with the pavement foundation layer parameter values measured using the LWD and DCP point measurements. Similar results are presented in Figure 23 and Figure 24 for TS3 PGE layer test section and TS5 CA6 capping layer test section, respectively.

In Figure 25, HMV IC-MV maps obtained on TS1 in October 2016 are compared with measurements obtained on TS6 in April 2017, in the same area. The two maps are not at the same zoom level, therefore, two locations identified as "A" and "B" are highlighted on each map for reference. Results indicated that average HMV on TS1 was about 9.9 and on TS6 was about 6.2, which suggests the foundation support conditions have weakened in comparison to the Fall 2016 testing, likely due to spring thaw action and saturated subgrade conditions during testing in April 2017. This reduction in foundation support was also confirmed with E_{LWD} measurements which decreased from an average of about 8,083 psi in Fall 2016 to 6,976 psi in April 2017.

In Figure 26, HMV IC-MV map obtained from TS6 on PGE is compared with map obtained from TS8 on CA6 capping layered placed over TS6. Comparison of the two maps reveal that "soft" and "stiff" zones identified on the PGE layer are reflected on the CA6 mapping layer.

Histograms and univariate statistics of HMV measurements obtained from the PGE layer and CA6 capping layer test sections are shown in Figure 27. The coefficient of variation in the HMV values

were 84% and 97% in the PGE and CA6 capping layer test sections. These results indicate high variability.

Similarly, E_{LWD} and DCP-CBR measurement histograms are shown in Figure 28 to Figure 30. For DCP-CBR measurements, average of the top layer, i.e., representing the top 6 in. PGE layer in the PGE test sections and the top 9 in. in the CA6 capping layer test sections, and the average of the top 12 in. of subgrade are presented. DCP-CBR of subgrade was more variable (with COV of 110%) than the DCP-CBR of the top PGE or PGE+CA6 layers (with COV of 64 to 67%).

Regression relationships between the HMV IC-MV and in situ test measurements from all the test sections are shown in Figure 31. Simple linear regression trends were used for all the measurements. The regression relationships, the R^2 value, and the standard error of the estimate are included in the presentation of results. The regression relationship with E_{LWD} showed the highest R^2 value of about 0.63 but presented significant scatter. The regression relationships showed R^2 about 0.14 with DCP-CBR of top layer, and about 0.56 with DCP-CBR of the top 12 in. of the subgrade layer. Results indicate that the HMV measurements are correlated better with subgrade layer measurements (DCP-CBR of subgrade) than the DCP-CBR of the top PGE or PGE+CA6 layer.



(a)

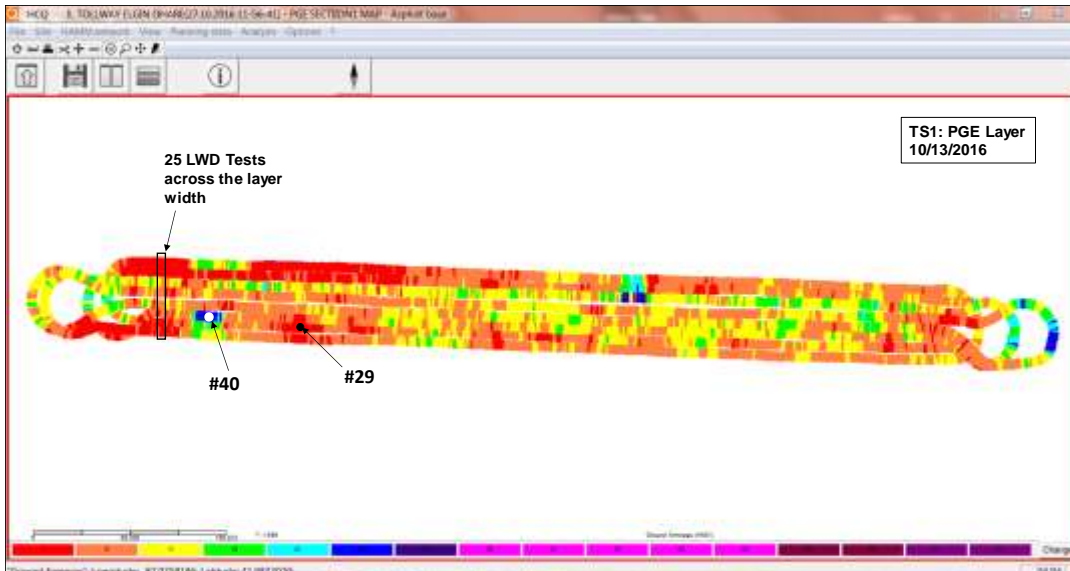


(b)

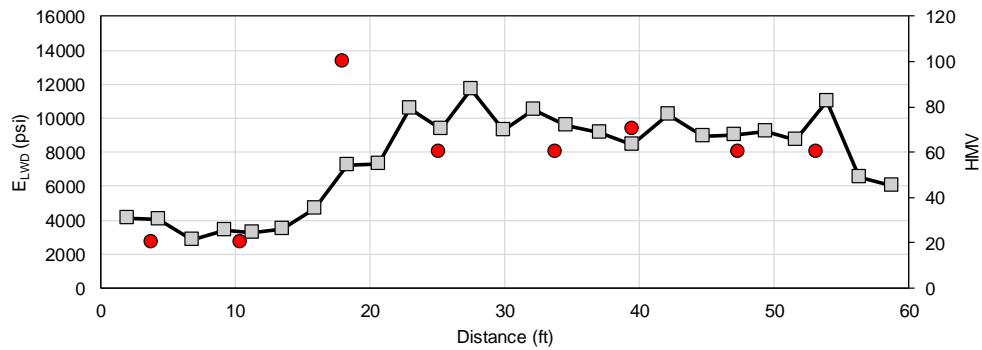


(c)

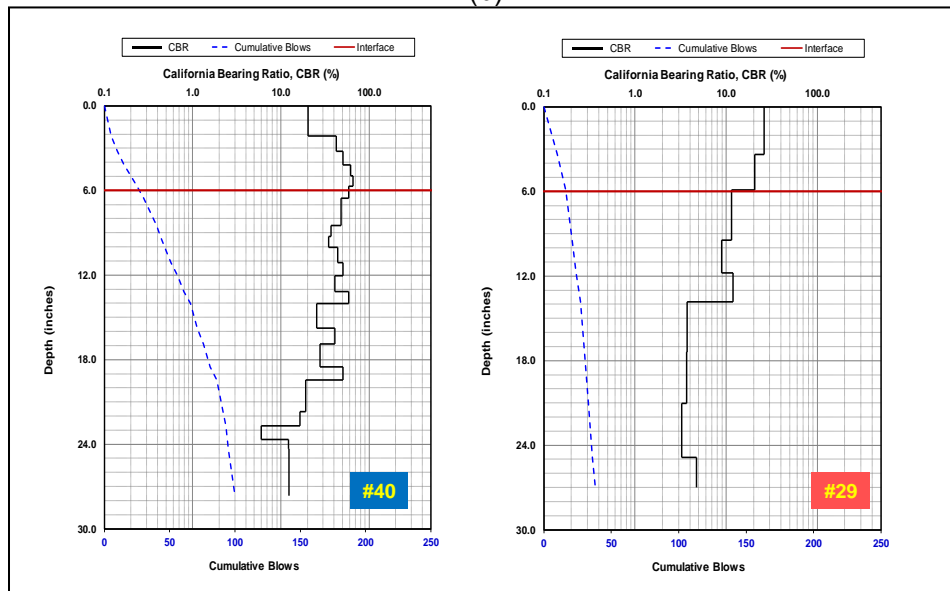
Figure 21. Pictures showing: (a) PGE layer from TS1 (10/13/16); (b) PGE layer from TS3 (10/13/16); and (c) CA6 Capping layer from TS4 (10/14/16).



(a)



(b)



(c)

Figure 22. (a) Color-coded spatial map of HMV from TS1; (b) E_{LWD} test measurements across the PGE layer width (red dots are the HMV values); and (c) DCP profiles at two selected test locations shown on the HMV map.

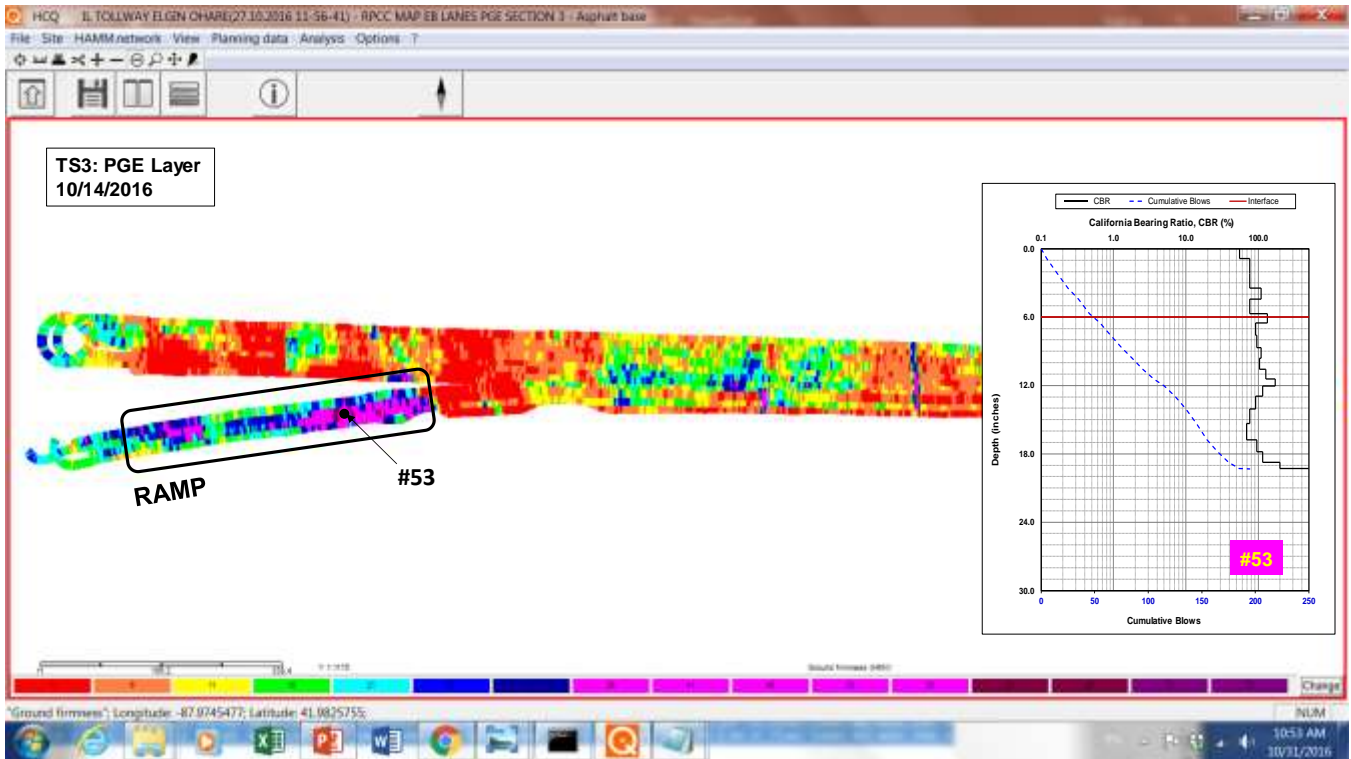


Figure 23. Color-coded spatial map of HMV from TS3 on PGE layer along with DCP profile at test location #53 representing very stiff conditions.

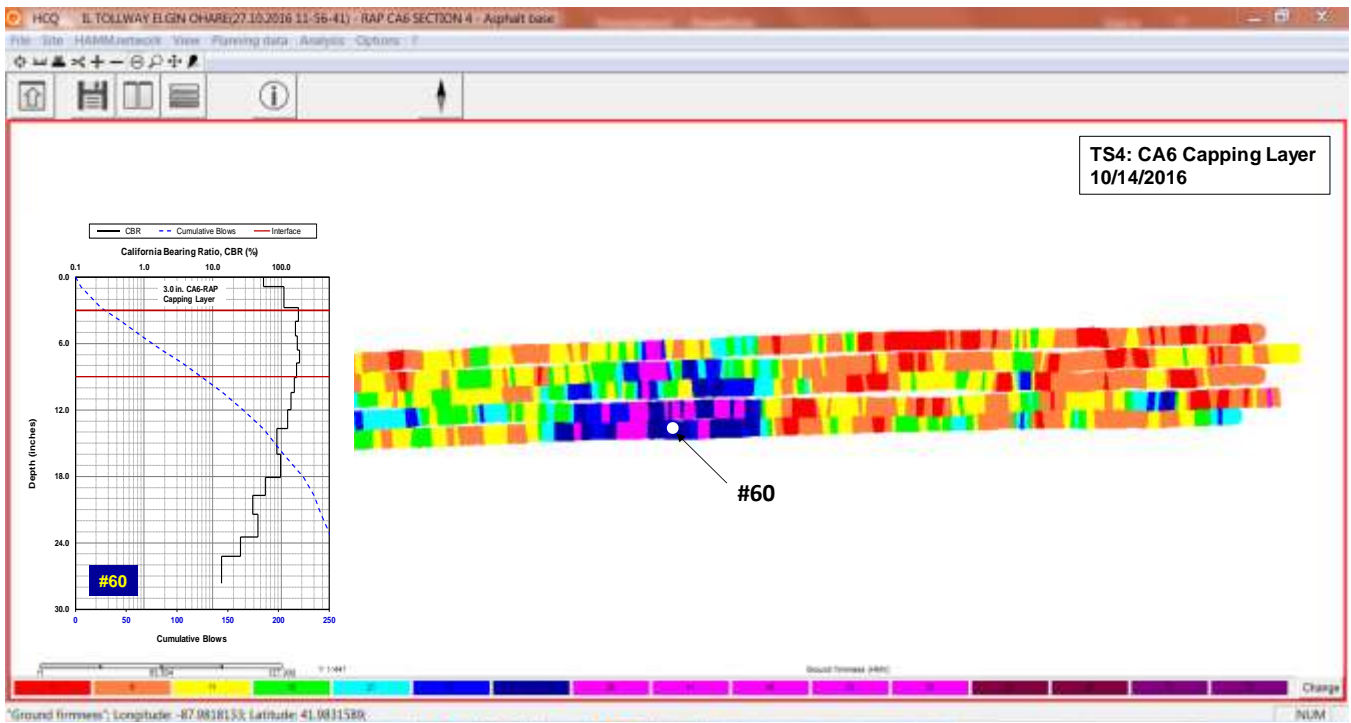
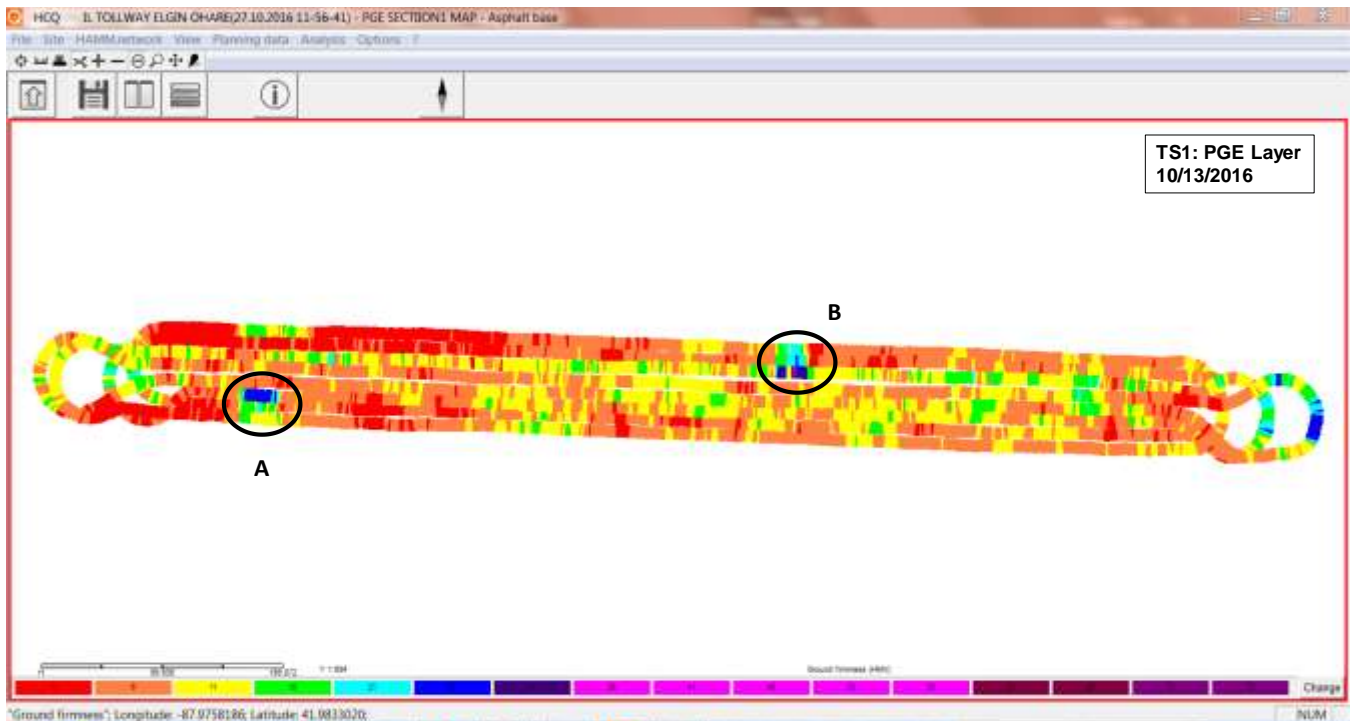
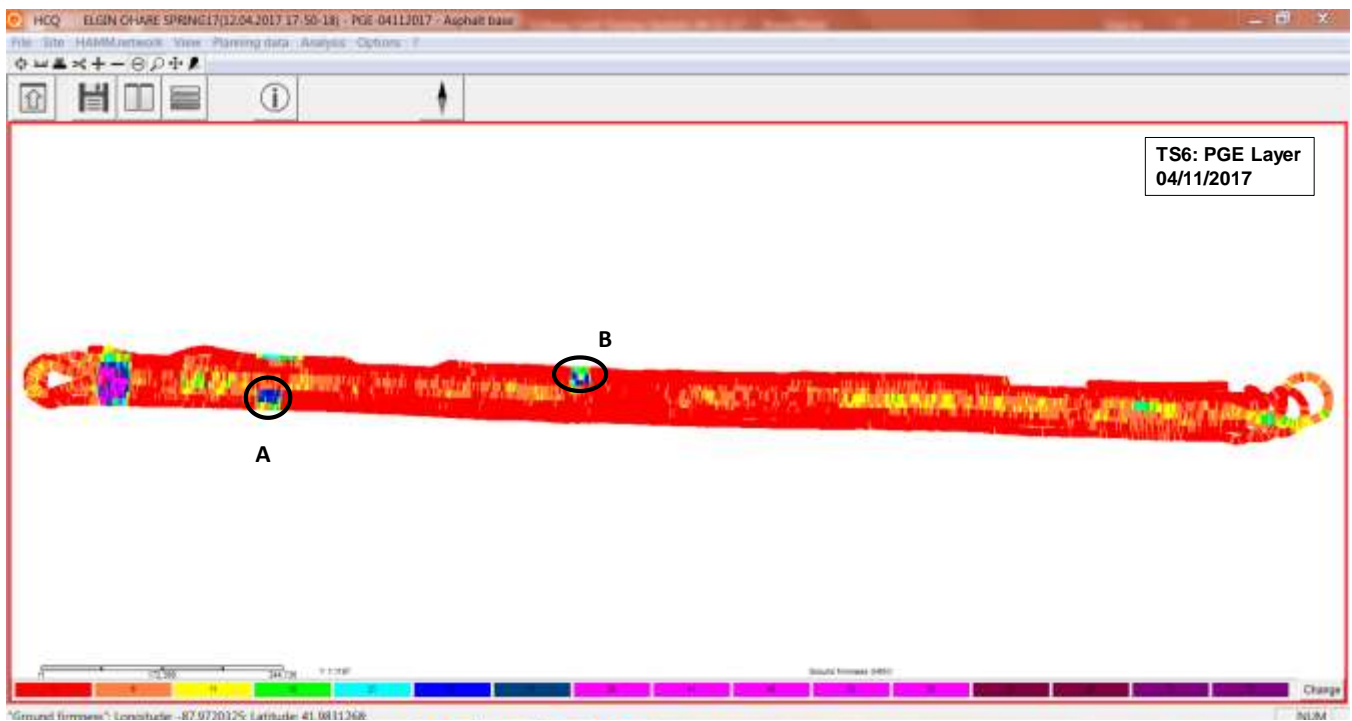


Figure 24. Color-coded spatial map of HMV from TS4 on CA6 capping layer along with DCP profile at test location #60 representing very stiff conditions.

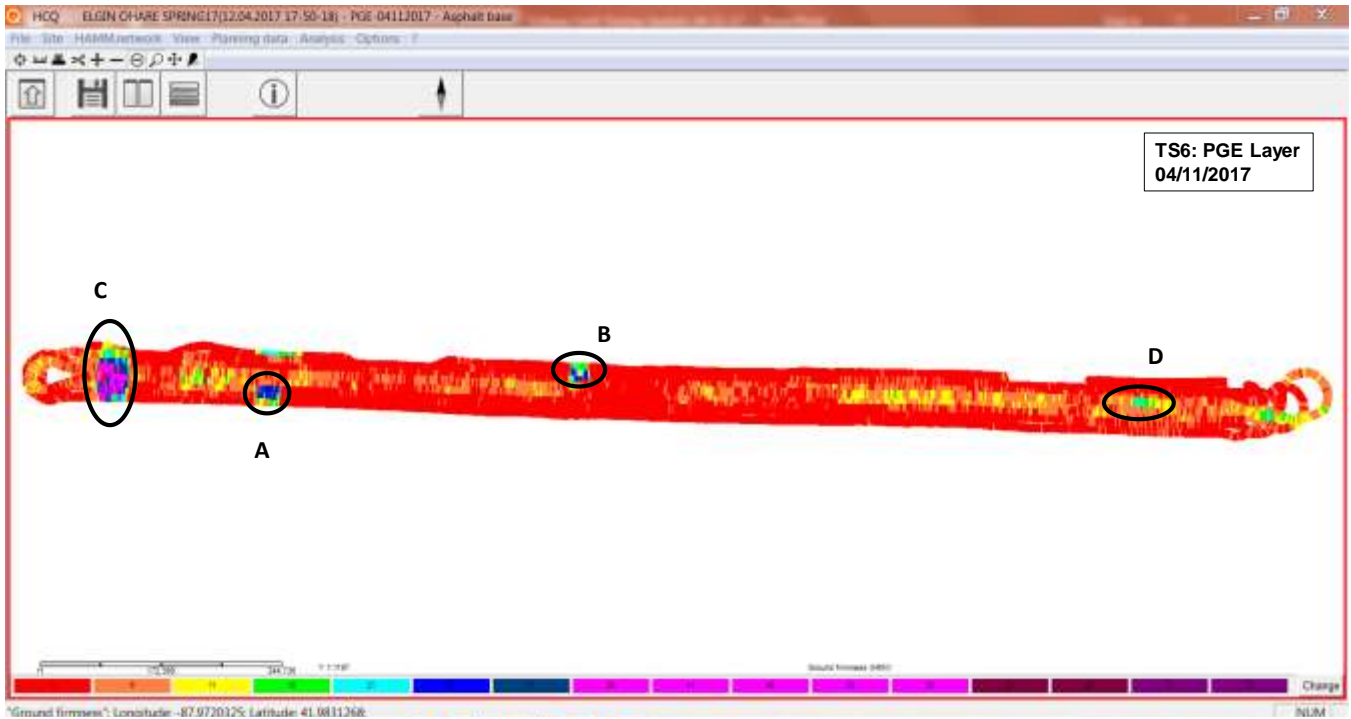


(a)

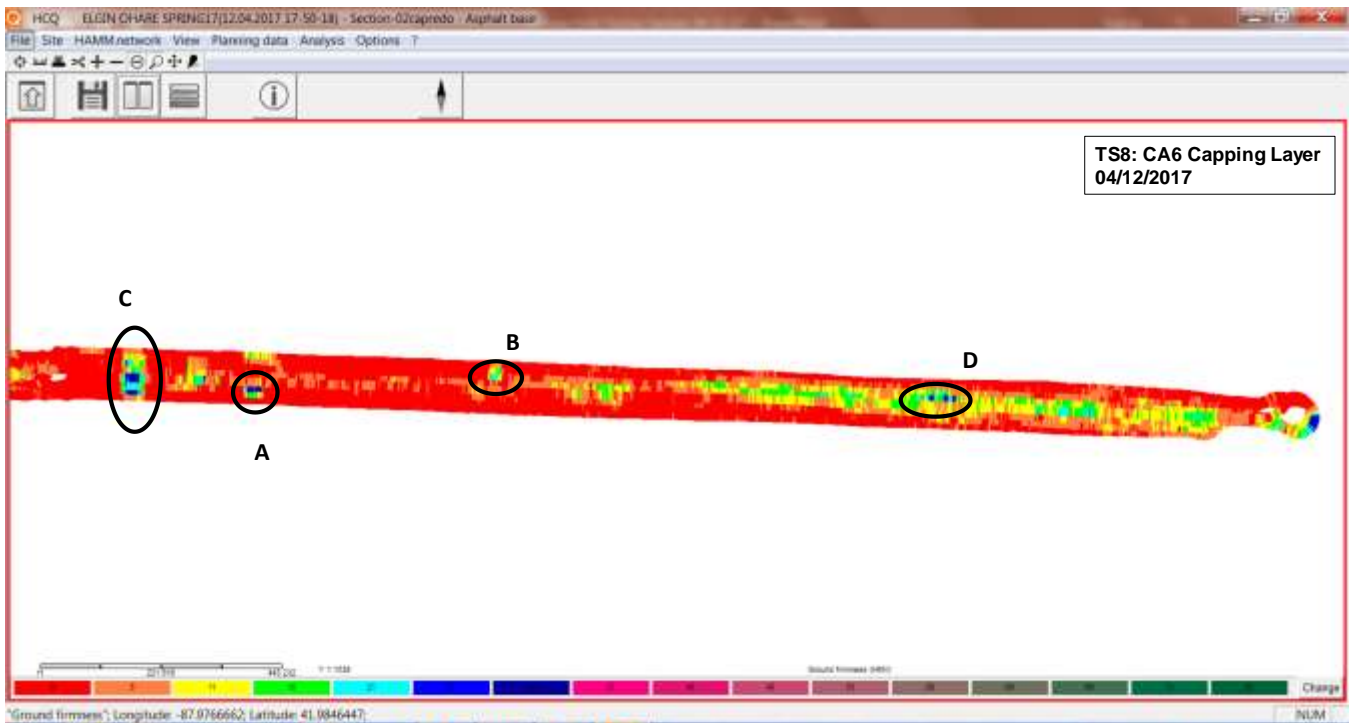


(b)

Figure 25. Color-coded spatial map of HMV from: (a) TS1 PGE layer from 10/13/16, and (b) TS6 PGE layer from 04/11/17. (Note: The two maps have different zoom scale and zones labeled as “A” and “B” are shown as reference points between the two maps. Average HMV from TS1 = 9.9 and TS6 = 6.2)



(a)



(b)

Figure 26. Color-coded spatial maps of HMV from PGE and overlaid CA6 capping layer: (a) TS6 PGE layer from 04/11/17, and (b) TS8 Ca6 capping layer rom 04/12/17. (Note: The zones labeled as “A” to “D” are shown as reference points between the two maps. Average HMV from TS6 = 6.2 and TS8 = 7.8).

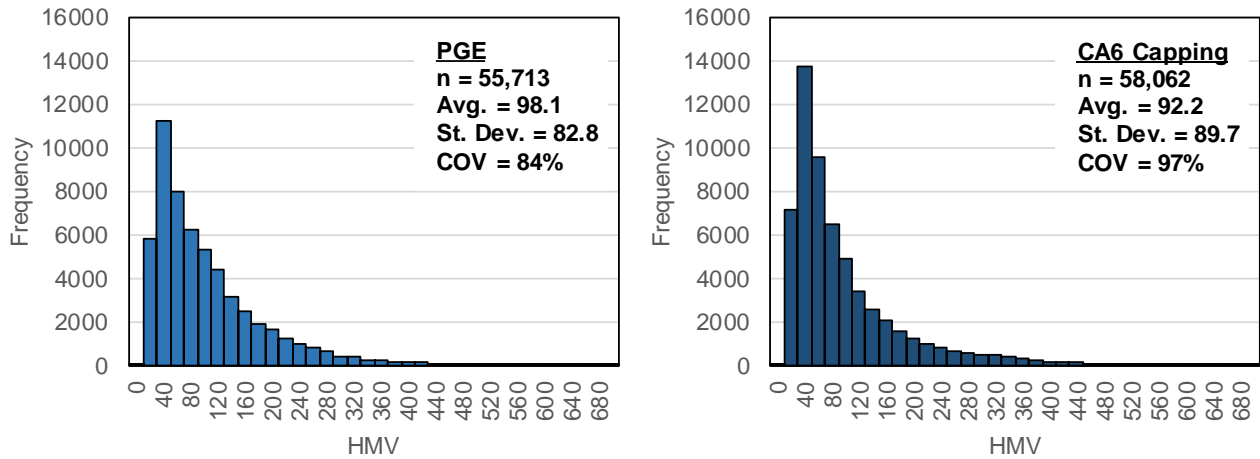


Figure 27. Histograms of HMV measurements on PGE layer test sections [TS1, 2, 3, and 6] (left) and CA6 capping layer test sections [TS4, 7, 8, 9, and 12] (right).

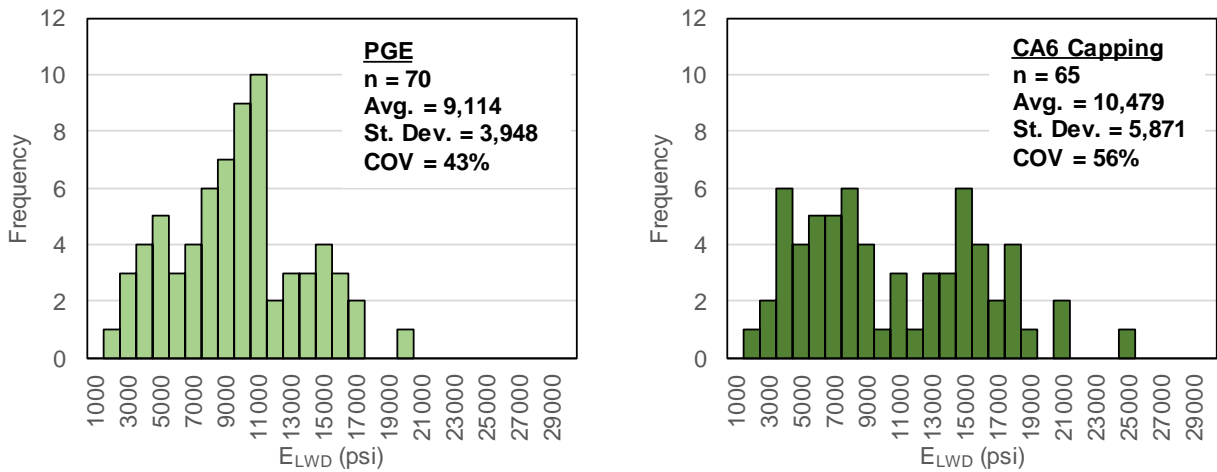


Figure 28. Histograms of E_{LWD} measurements on PGE layer test sections [TS1, 2, 3, and 6] (left) and CA6 capping layer test sections [TS4, 7, 8, 9, and 12] (right).

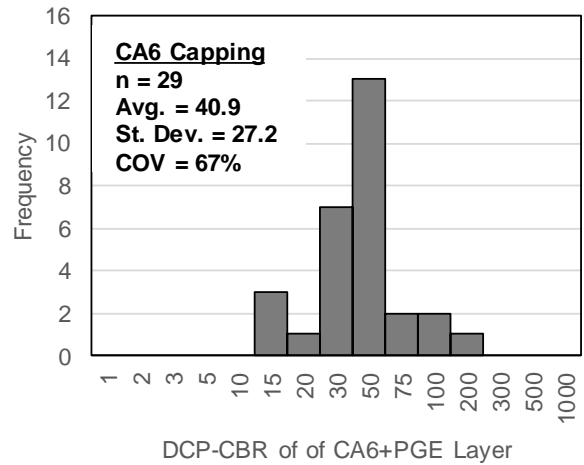
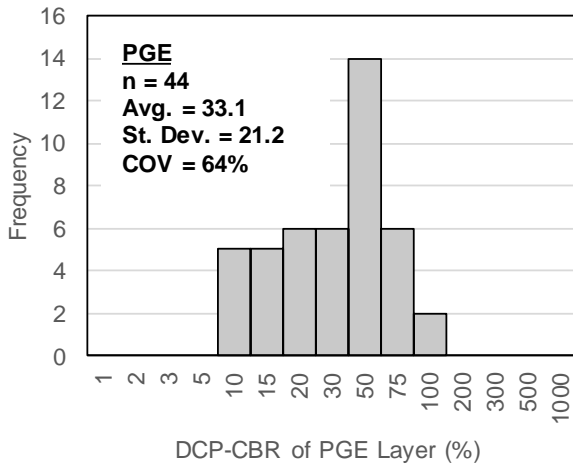


Figure 29. Histograms of DCP-CBR measurements of the top layer on PGE layer test sections [TS1, 2, 3, and 6] (left) and CA6 capping layer test sections [TS4, 7, 8, 9, and 12] (right).

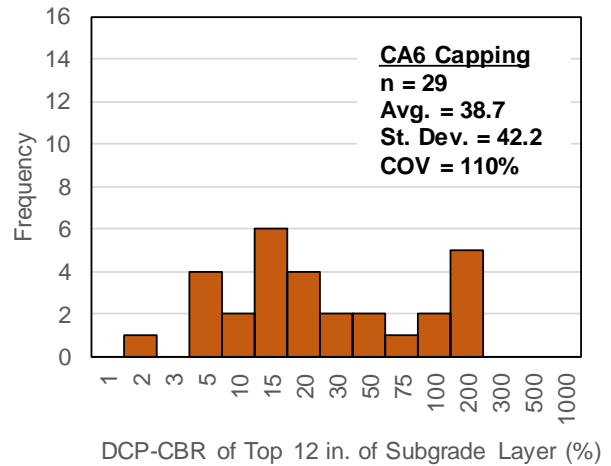
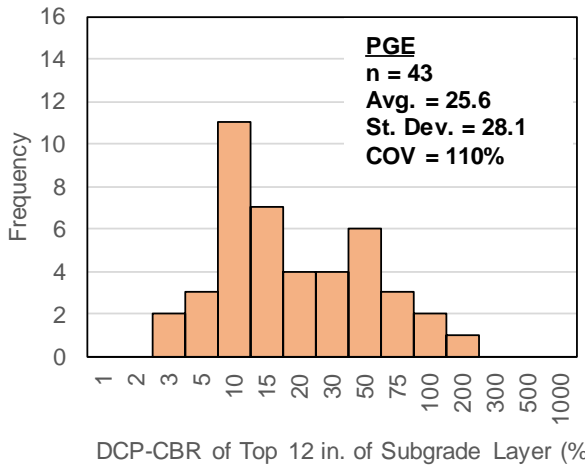


Figure 30. Histograms of DCP-CBR measurements of the bottom subgrade layer on PGE layer test sections [TS1, 2, 3, and 6] (left) and CA6 capping layer test sections [TS4, 7, 8, 9, and 12] (right).

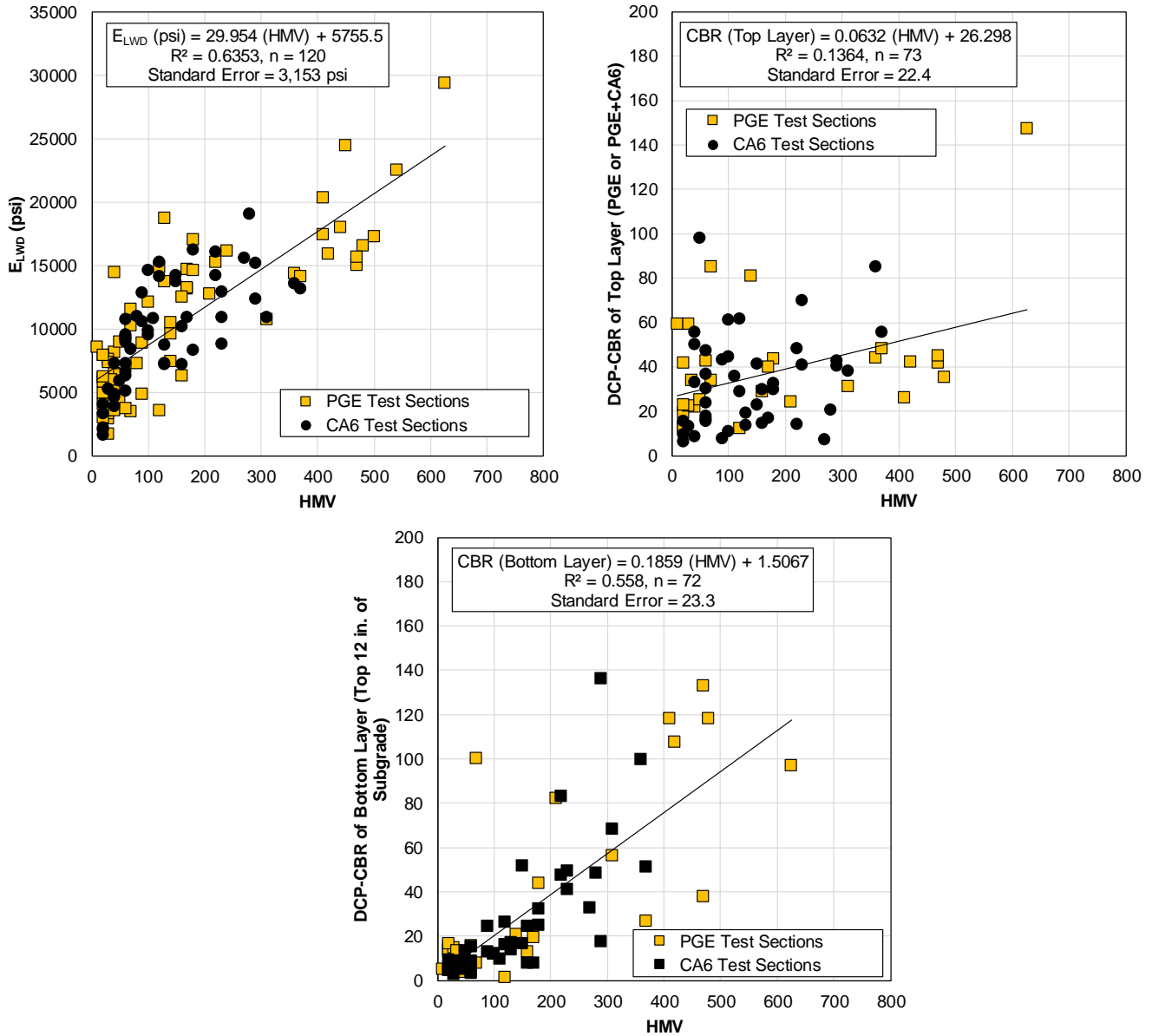


Figure 31. Regression relationships between E_{LWD} and DCP-CBR measurements, and HMV from PGE and CA6 test sections

3.4.2 Calibration Testing and Analysis – CMV and MDP Measurements

3.4.2.1 Caterpillar 815F Padfoot IC roller

The Caterpillar 815 padfoot IC roller was used by the contractor in embankment fill construction areas. The research team conducted field testing in TS5 in October 2016, with in situ drive core and DCP testing. Testing was conducted after compaction operations were completed. Pictures during fill placement and compaction on TS5 are shown in Figure 32. Screen shots of IC data showing maps of elevation, pass count, and MDP* summaries are shown in Figure 33 to Figure 35. In situ drive core test results relative to laboratory Proctor test results are shown in Figure 36, which showed that the embankment fill material was relatively wet and near the zero-air void line. GPS referenced in situ test

locations were compared with the IC data and was found that no IC data was recorded in the area where in situ testing was performed (Figure 37). The reason for this issue could not be resolved. The test area was reportedly later rejected by the field QA inspector and was reworked. No additional analysis was performed on this data.



Figure 32. Pictures of embankment fill area (TS5) on 10/14/2017.

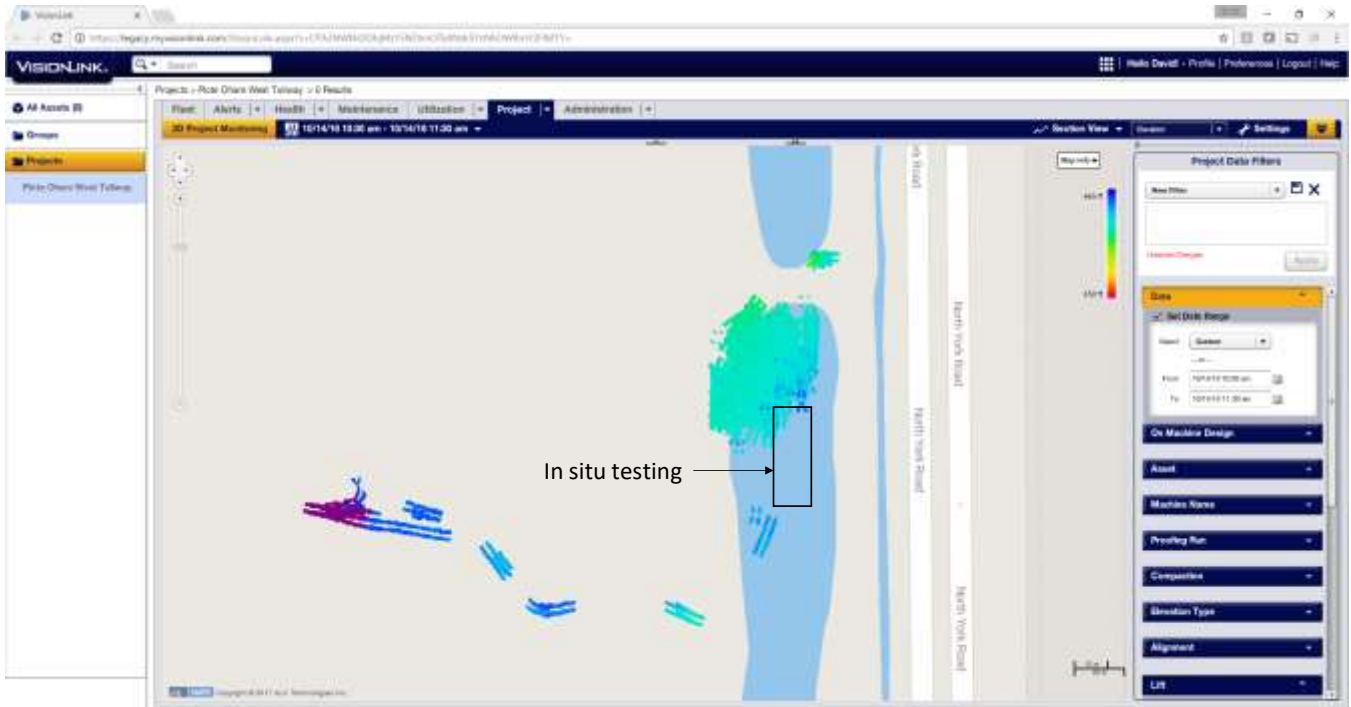


Figure 33. Screenshot of elevation map in TS5 embankment fill area.

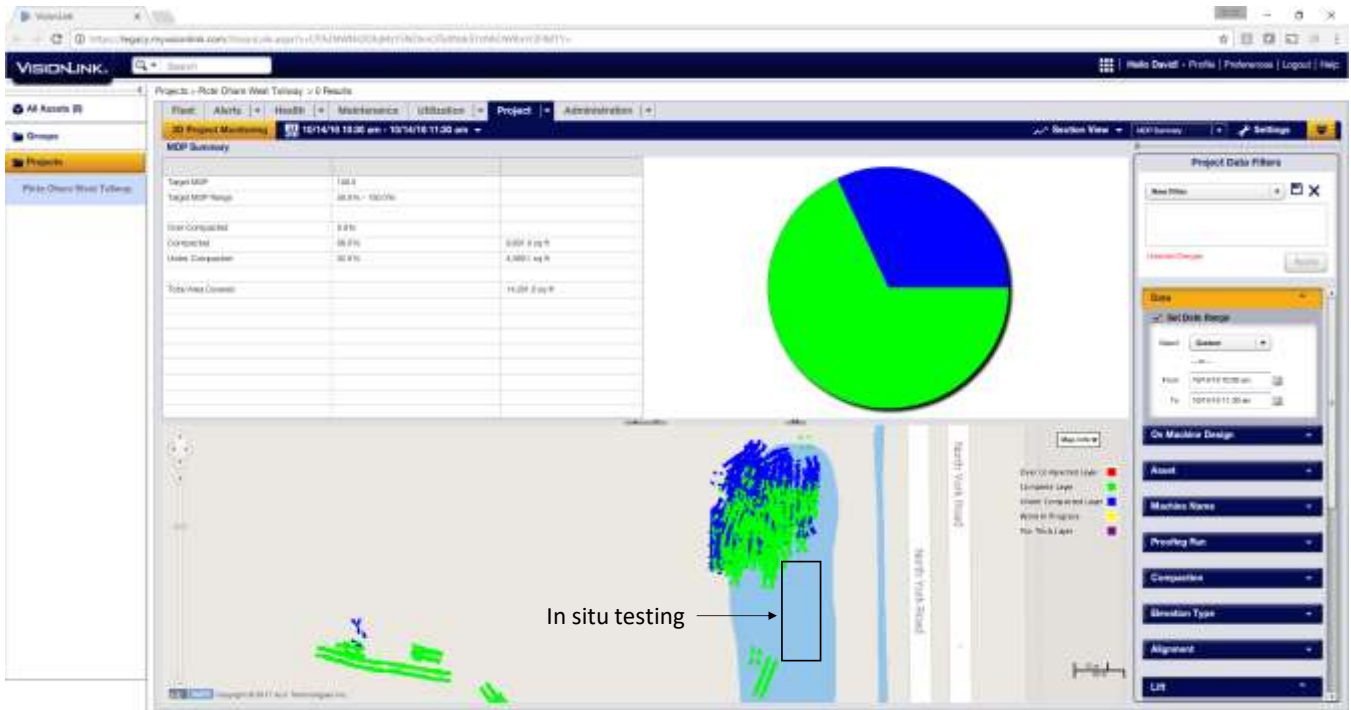


Figure 34. Screenshot of MDP* summary in TS5 embankment fill area.

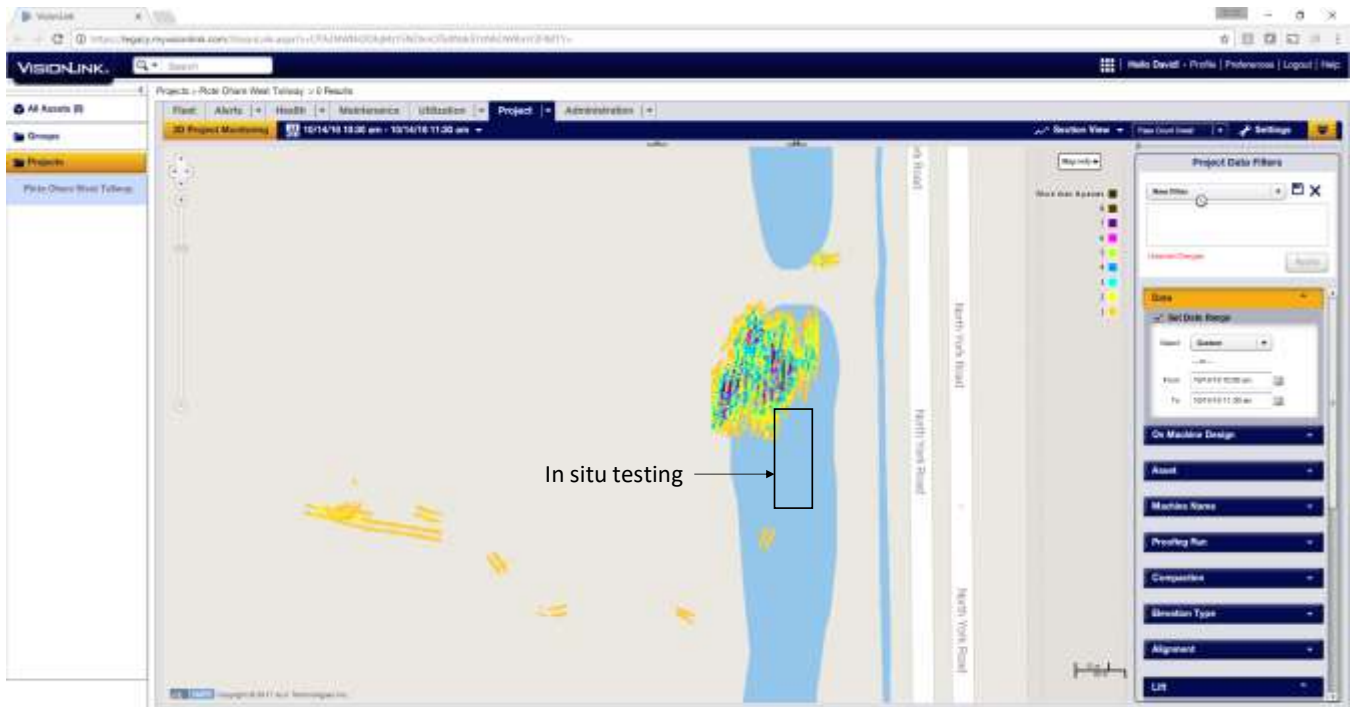


Figure 35. Screenshot of pass count summary in TS5 embankment fill area.

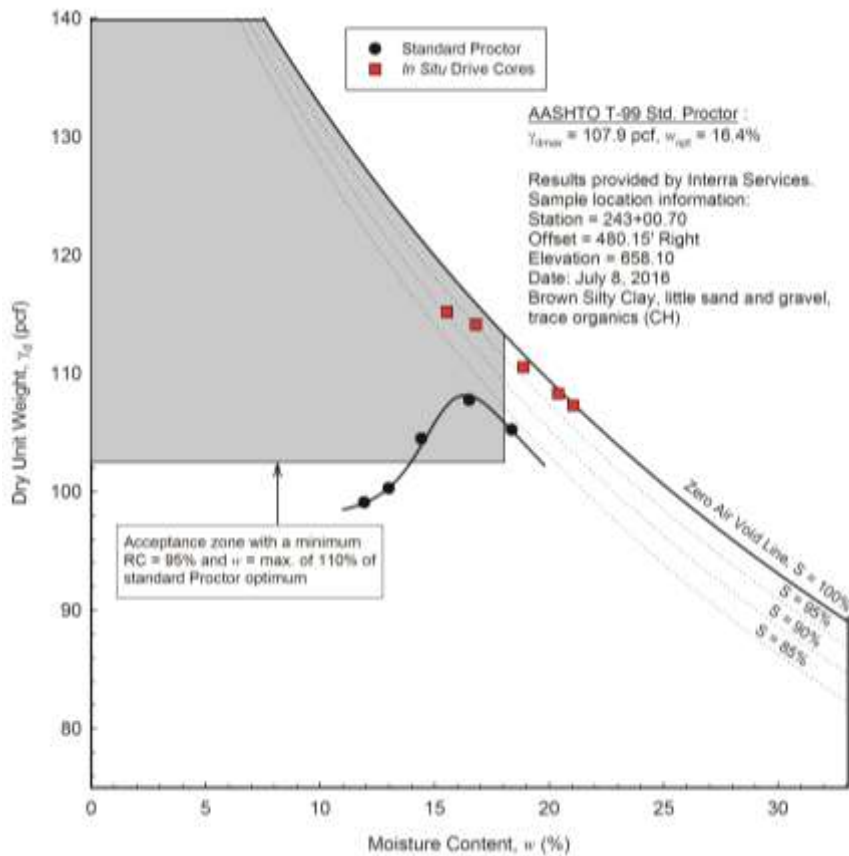


Figure 36. In situ dry density and moisture content measurements from drive core testing overlaid on standard Proctor test results for embankment fill material.

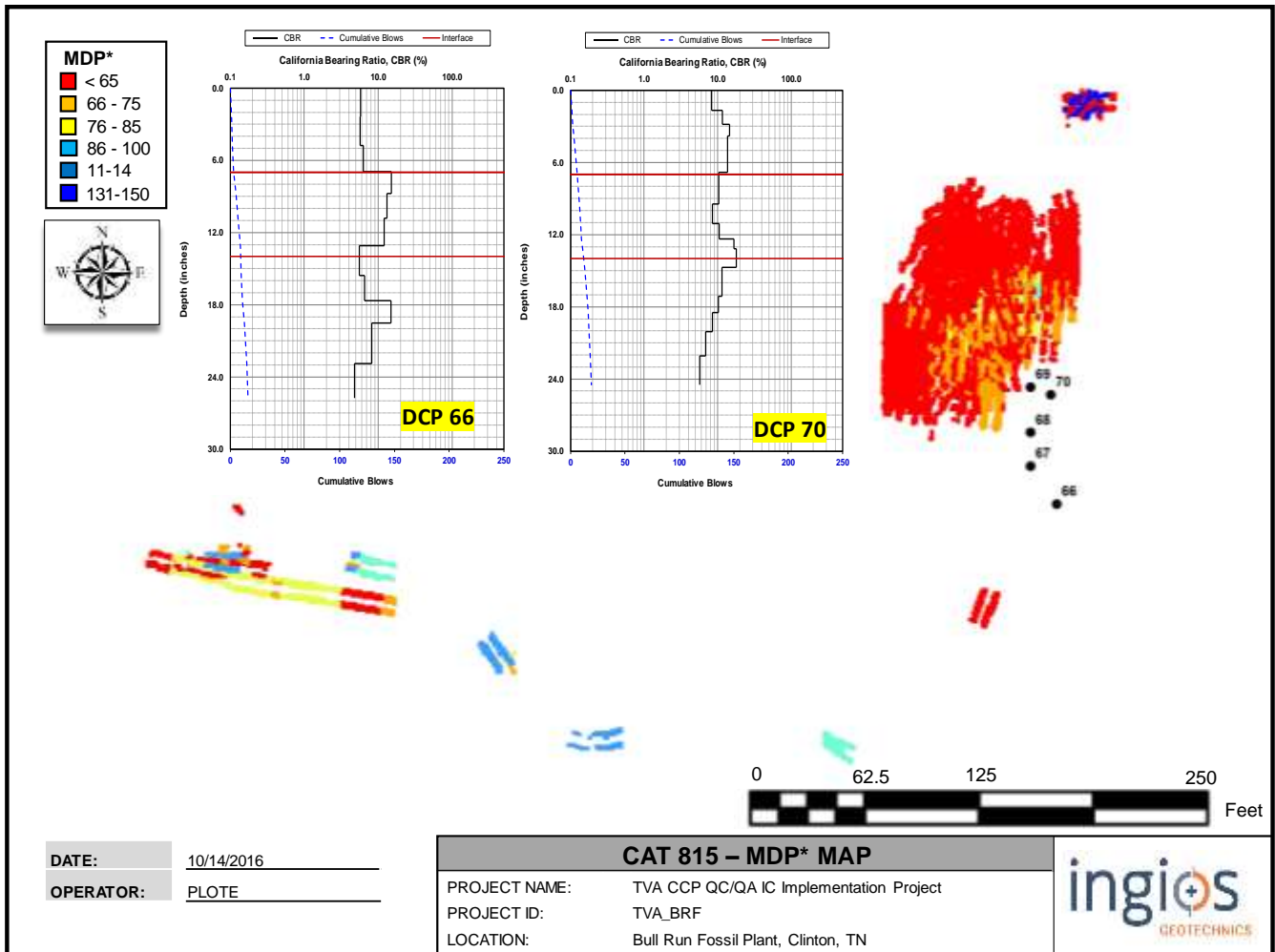


Figure 37. GPS referenced MDP* measurements map overlaid with in situ test locations and DCP-CBR profiles at two selected test locations

3.4.2.2 Caterpillar CS74 Smooth Drum IC roller

CMV and MDP* measurements were obtained at five test sections, of which two consisted of nominal 6 in. thick PGE layer at the surface and the remaining three consisted of nominal 3 in. thick CA6 capping layer placed over the PGE layer at the surface. In situ tests were conducted at a total of 35 test locations for calibration analysis.

Pictures of a test sections with PGE and CA6 capping layers where the IC maps were obtained are shown in Figure 38. Screenshots of the CMV and MDP* maps from TS10 and TS11 with PGE material are shown in Figure 39. The mapping in TS10 and TS11 was performed by the contractor, and no in situ testing was available for those sections. Screenshots of the CMV and MDP* maps from TS7 with CA6 capping layer test section is shown in Figure 40. On TS7, in situ tests were obtained from 15 test locations selected based on the CMV map to capture the variations observed in the map. DCP profiles showing CBR and cumulative blows with depth are shown in Figure 41 for two selected locations with relatively stiff and soft conditions, as identified in the CMV map.

Histograms and univariate statistics of CMV and MDP* measurements obtained from the PGE layer and CA6 capping layer test sections are shown in Figure 42. The coefficient of variation in the CMV values were 50% and 80% in the PGE and CA6 capping layer test sections, respectively. The

MDP* measurements showed lower COV with $\leq 10\%$. As identified in the literature review, MDP* has a relatively shallow measurement influence depth (1 to 2 ft) compared to CMV measurements (3 to 5 ft). The shallow influence depth of MDP* and the fact that the DCP measurements showed variability in the subgrade was greater than in the top PGE and PGE+CA6 layer, and the narrow measurement range of MDP* are likely the reasons why the COV of MDP* was very low.

Regression relationships between the CMV and in situ test measurements from all the test sections are shown in Figure 43. Non-linear power relationship was observed for CMV vs. E_{LWD} with R^2 of 0.65, and for CMV vs. DCP-CBR of the top CA6+PGE layer with R^2 of 0.16. CMV vs. DCP-CBR of the subgrade layer yielded a linear relationship with $R^2 = 0.59$. Like HMV regression relationships, results indicate that CMV is correlated better with subgrade layer measurements (DCP-CBR of subgrade) than the DCP-CBR of the top layer

Comparison between MDP* and in situ test measurements is shown in Figure 44. Regression relationships between the CMV and in situ test measurements from all the test sections are shown in Figure 44. No statistically significant relationship was observed between MDP* and in situ test measurements in the test sections.



Figure 38. Pictures of CA6 capping material from PGE material from TS11 (middle-04/25/17) and CA6 material from TS12 (bottom-05/04/17)



Figure 39. Screenshot of CMV and MDP* summary maps for TS10 and TS11 with PGE material.

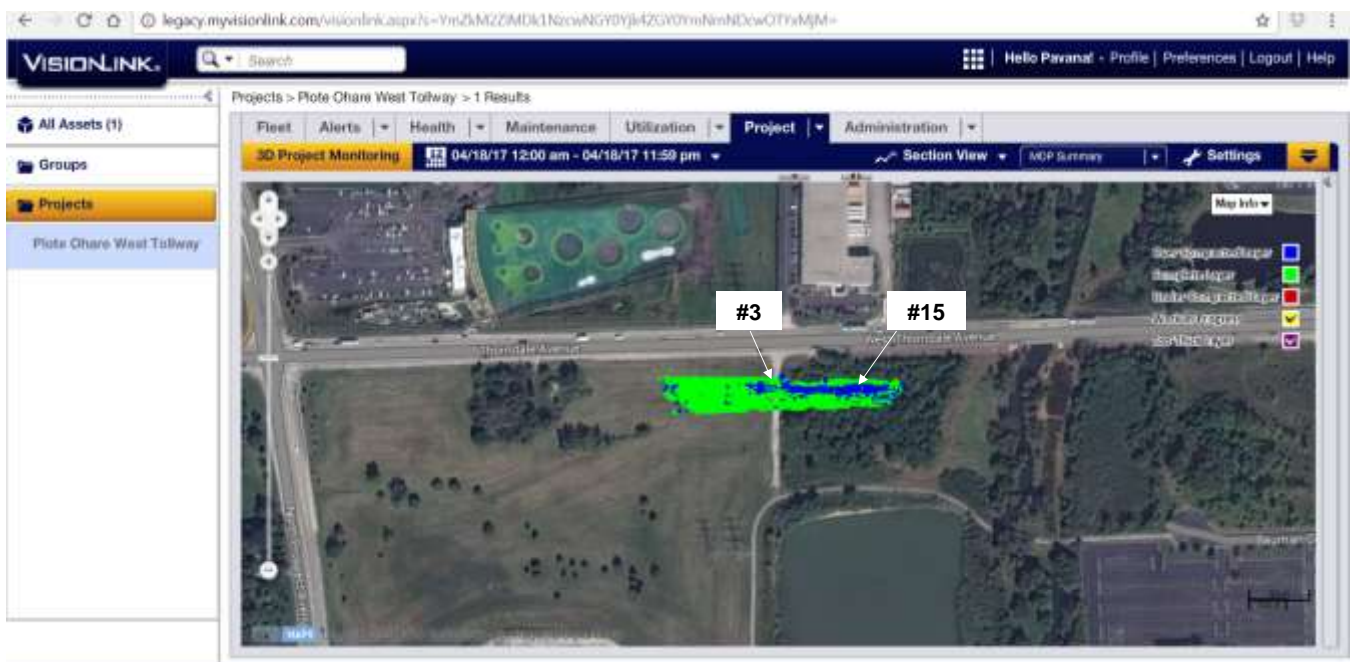
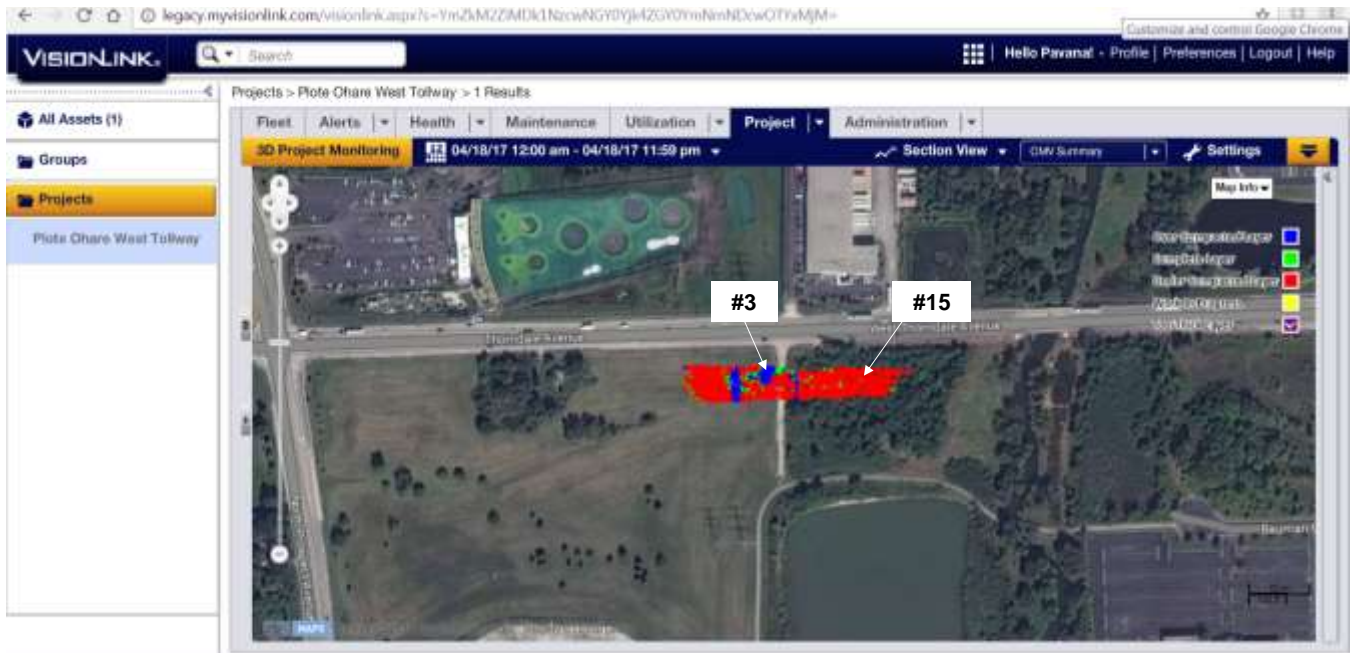


Figure 40. Screenshot of CMV and MDP* summary maps for TS9 with CA6 capping layer (Note: #3 and #15 are test locations representing very stiff and soft conditions)

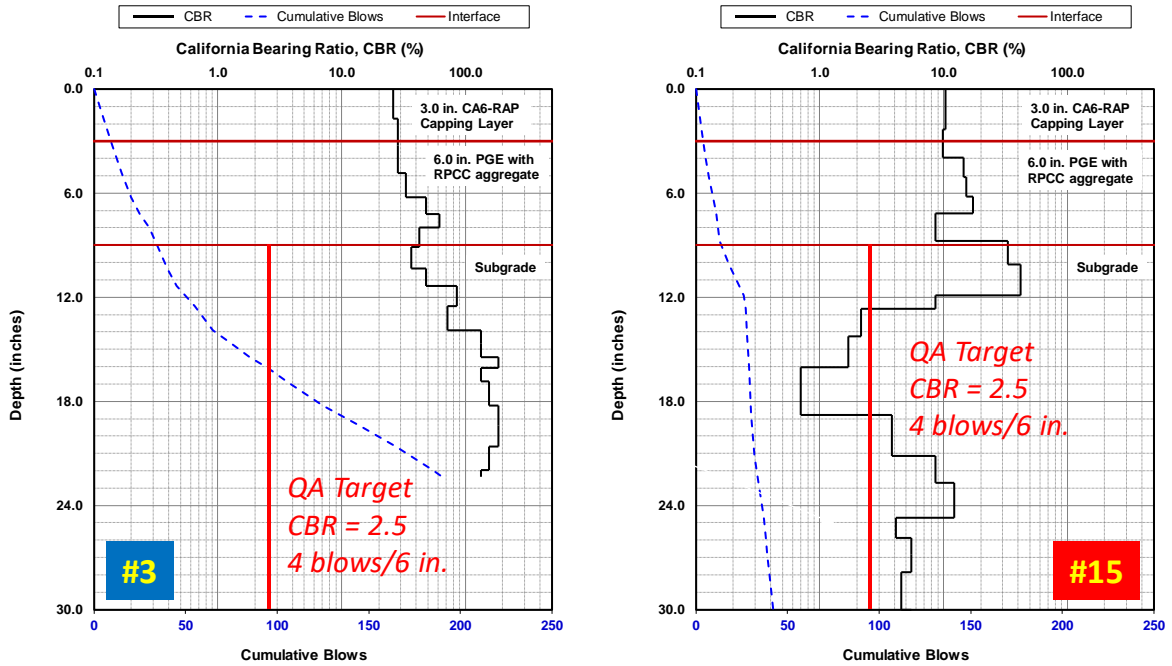


Figure 41. DCP profiles at test points 3 (very stiff) and 15 (soft) from TS7

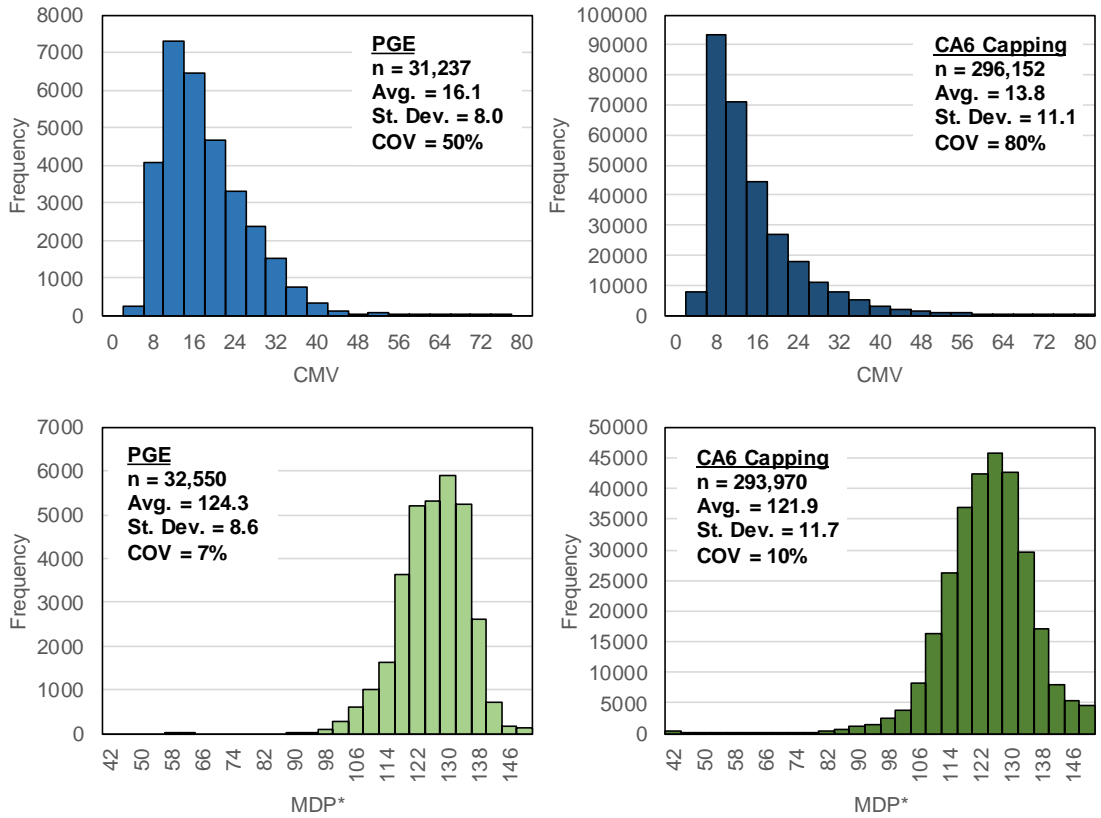


Figure 42. Histograms of CMV and MDP* measurements from PGE test sections (TS10 and 11) and CA6 test sections (TS7, 9, and 12).

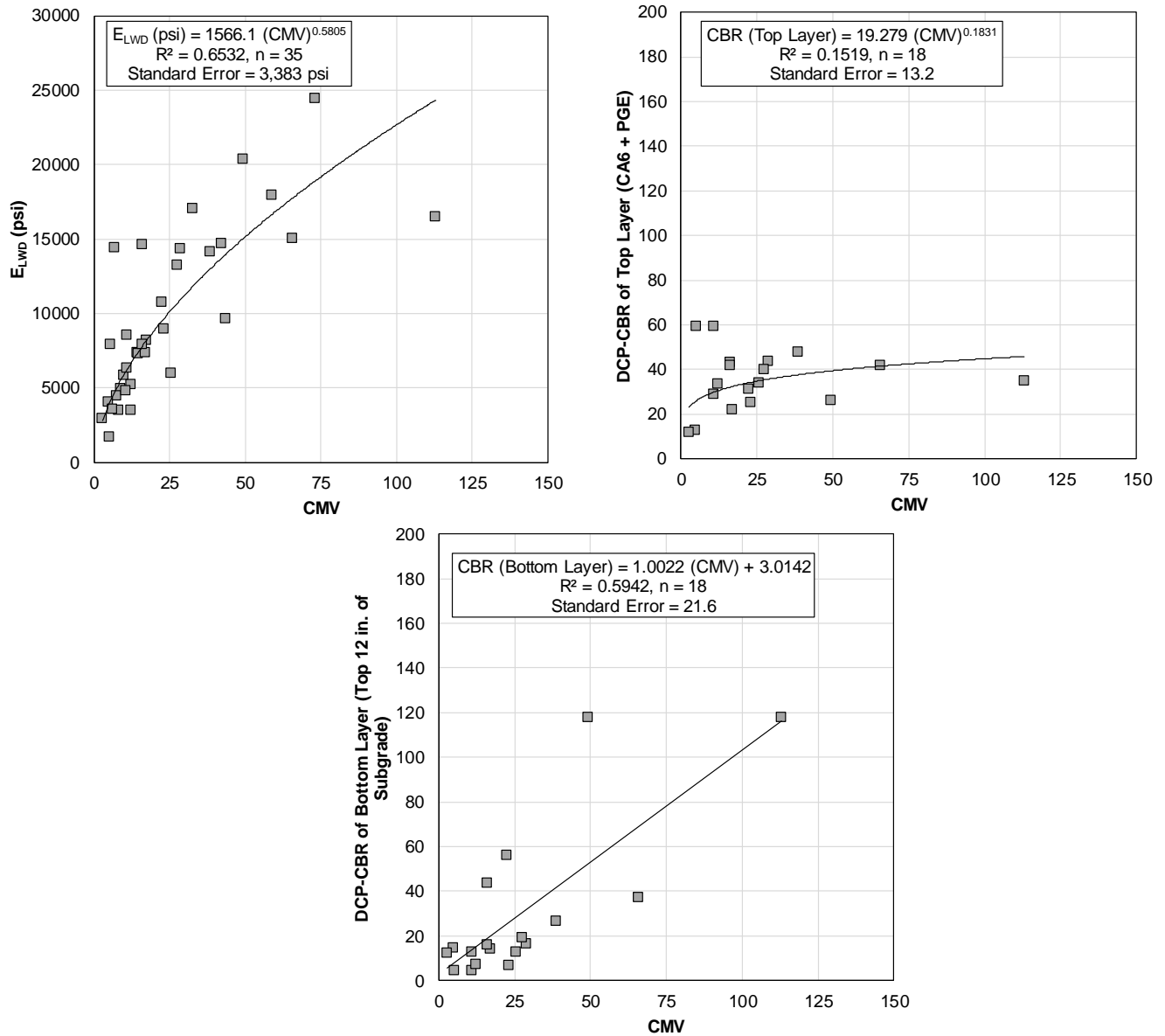


Figure 43. Regression relationships between E_{LWD} and DCP-CBR measurements, and CMV measurements

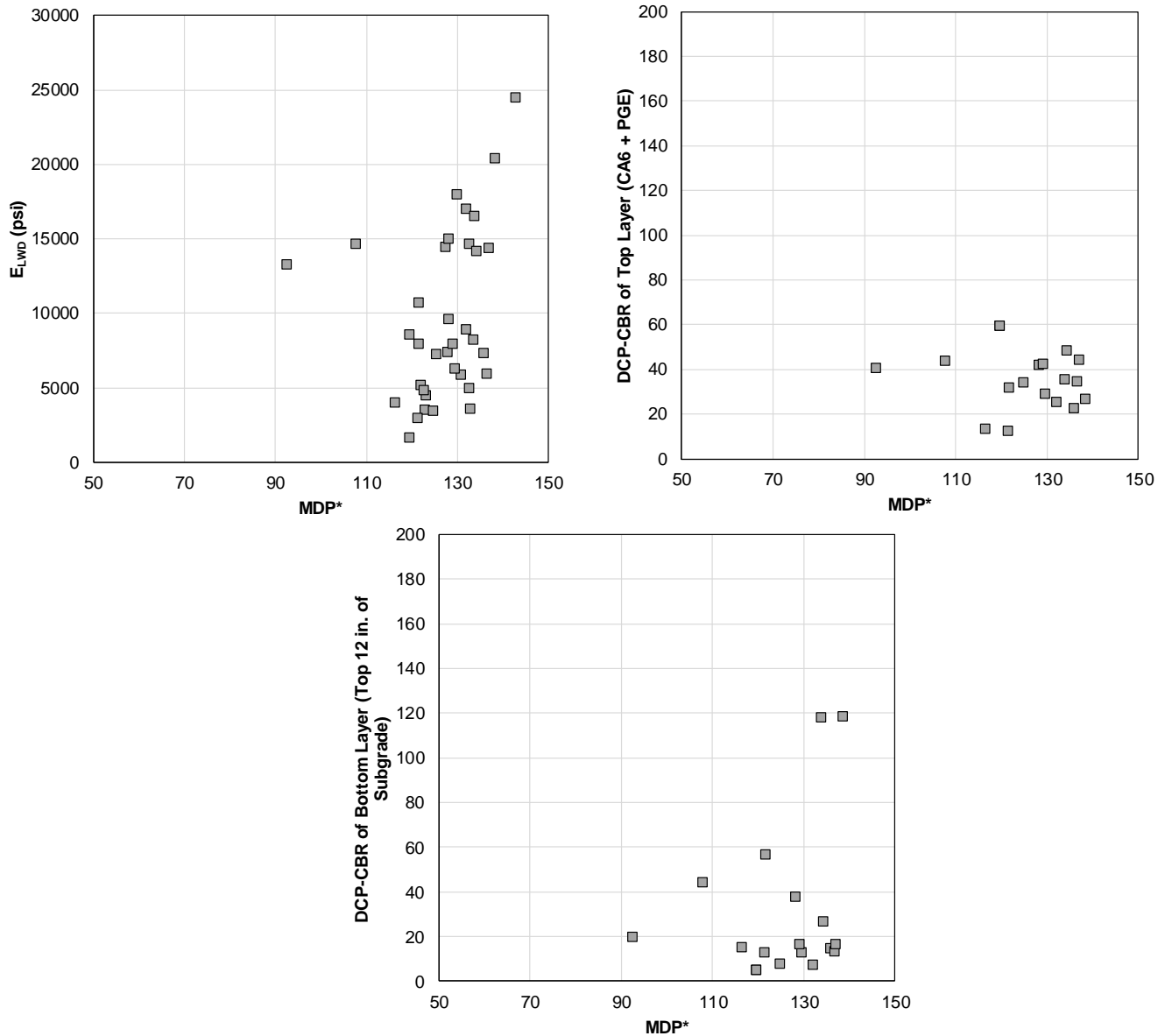


Figure 44. Regression relationships between E_{LWD} and DCP-CBR measurements, and MDP* measurements

3.4.3 Calibration Testing and Analysis – VIC Measurements

VIC field calibration was performed with cyclic APLTs on 3 in. thick RAP base material over 6 in. thick PGE and compacted subgrade material, and directly on compacted subgrade material to capture a wide range of stiffness conditions. Static 30 in. APLTs were performed on 6 in. PGE over compacted subgrade to calibrate with static *k* measurements. CMV measurements were also simultaneously obtained for field calibration. Pictures of test sections where VIC calibration was performed are shown in Figure 45.



(a)



(b)



(c)

Figure 45. Pictures of (a) CA6 capping layer on TS13; (b) subgrade on TS14; and (c) PGE layer on TS15.

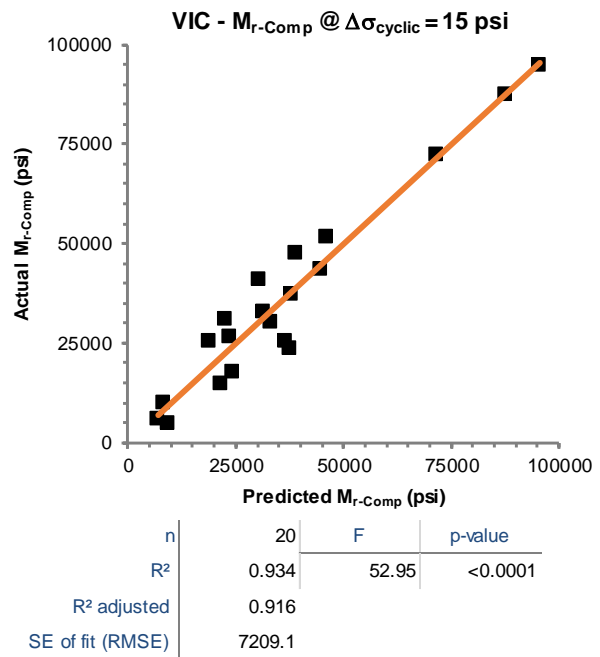
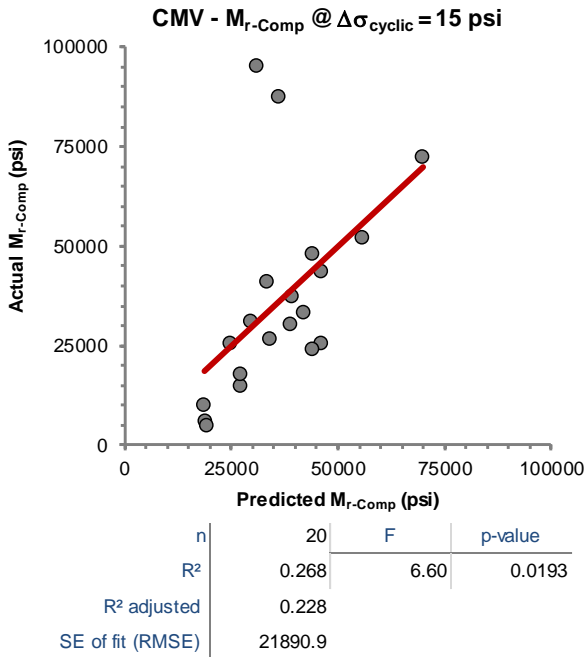
Results of both VIC and CMV calibrations with cyclic APLT measurements showing measured versus predicted M_{r-Comp} values at 15 psi cyclic stress are shown in Figure 46. The 15-psi cyclic stress level is selected here as an example, to match with the stress level applied with LWD test measurements, but M_{r-Comp} at all other stress levels measured (5 psi to 40 psi) showed similar trends and R^2 values, and are included in Appendix C. E_{LWD} measurements were also obtained at these test locations, and the calibration results are also shown in Figure 46.

VIC – M_{r-Comp} calibration measurements showed R^2 of 0.92 and a standard error of about 7,200 psi for M_{r-Comp} values that ranged between 4,800 and 95,000 psi. For the same M_{r-Comp} data set, the CMV calibration measurements showed R^2 of 0.23 and a standard error of about 21.9 ksi. The two points that fell far away from the best fit regression line are test locations that where the roller drum experienced jumping because of relatively stiff conditions. As noted earlier in the literature review, it is well-documented that the CMV measurements are influenced by drum bouncing (Brandl and Adam 1997, Mooney et al. 2010, Vennapusa et al. 2011).

The VIC – E_{LWD} calibration showed R^2 of 0.7 with standard error of about 3,500 psi for E_{LWD} values that ranged between 700 psi to 21,300 psi. For the same E_{LWD} dataset, the CMV calibration showed R^2 of 0.56 with standard error of about 4,200 psi. Results show that the E_{LWD} measurements were on average about 3 times lower than the M_{r-Comp} values obtained at similar applied stress (~15 psi). It must be noted here that the moduli values obtained from LWD are not the same as M_r . This is because LWD measures peak deflections and not rebound deflections, and conditioning cycles (which can take up to several 100 cycles) are not applied with LWD, which contributes to the quality of the data that can be obtained from an LWD test device. LWD testing method, although provides a rapid measurement, should therefore not be considered a direct measure of M_r or compared directly with the design input parameter value. It is also a well-documented that moduli values provided by different LWD manufacturer can be significantly different (on the order of 2 to 3 times) because of differences in the measured/calculated deflections and applied stresses (Vennapusa and White 2008, Vennapusa et al. 2011).

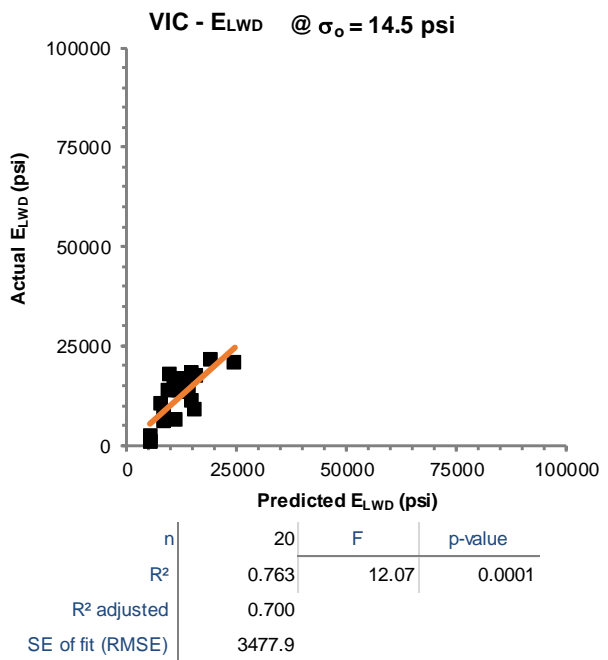
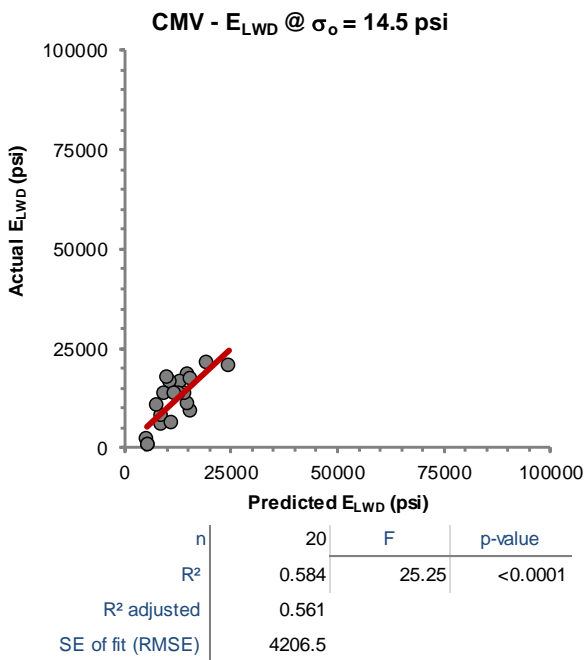
Results of VIC and CMV measurement calibration with static APLT measurements showing measured versus predicted $k_{u(1)}$ and $k_{u(2)}$ values are shown in Figure 47. The VIC – $k_{u(1)}$ calibration measurements showed R^2 of 0.92 and a standard error of about 25 pci for $k_{u(1)}$ values that ranged between 26 and 305 pci. Similarly, the VIC – $k_{u(2)}$ calibration measurements showed R^2 of 0.93 and a standard error of about 195 pci for $k_{u(2)}$ values that ranged between 212 and 2,291 pci. On the other hand, the CMV – $k_{u(1)}$ calibration measurements showed R^2 of 0.71 and a standard error of about 47 pci for $k_{u(1)}$ values that ranged between 26 and 305 pci. Similarly, the CMV – $k_{u(2)}$ calibration measurements showed R^2 of 0.74 and a standard error of about 384 pci for $k_{u(2)}$ values that ranged between 212 and 2,291 pci.

Results from the calibration testing and the analysis showed that VIC calibration with both M_{r-comp} and k_u measurements obtained from APLT produced high R^2 values (≥ 0.90) and with relatively low standard error. Higher R^2 values and low standard errors suggest higher reliability in future predictions of the respective measurement values in a production area. Following VIC calibration, M_{r-Comp} maps at different stress levels and k_u maps were produced at this site, with the objective of demonstrating the ability to spatially assess the compacted layer properties in terms of mechanical property values (i.e., M_r or k) and directly comparing them with the design target values.



(a)

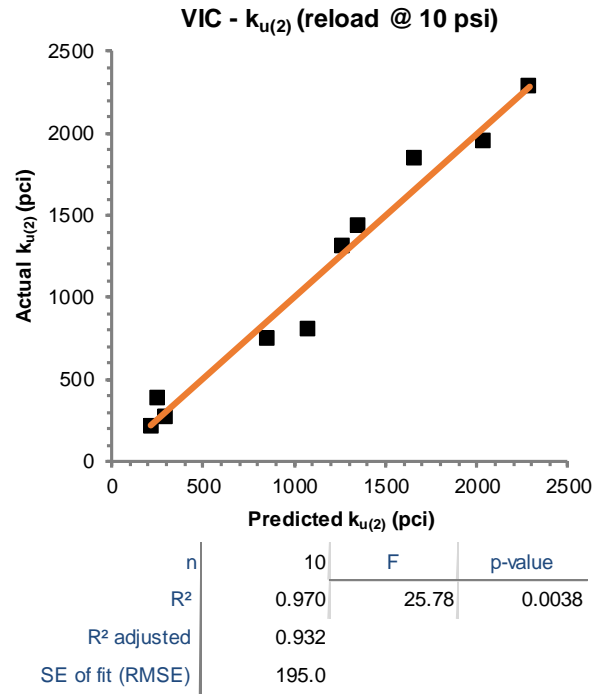
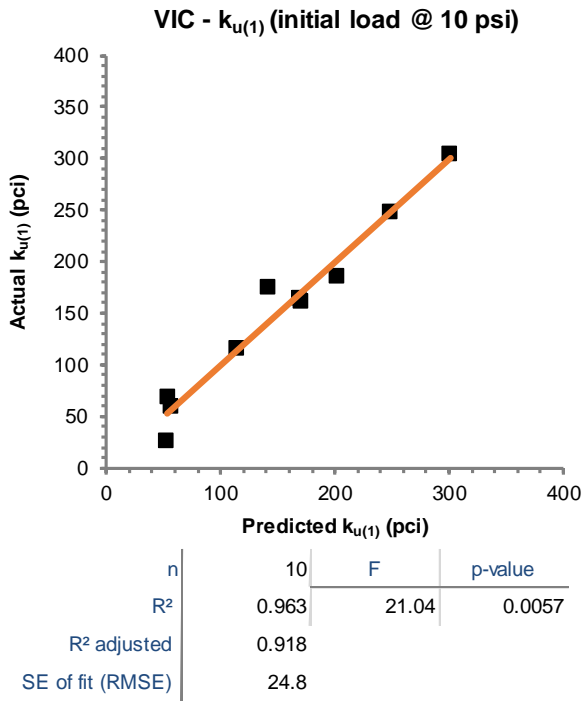
(b)



(c)

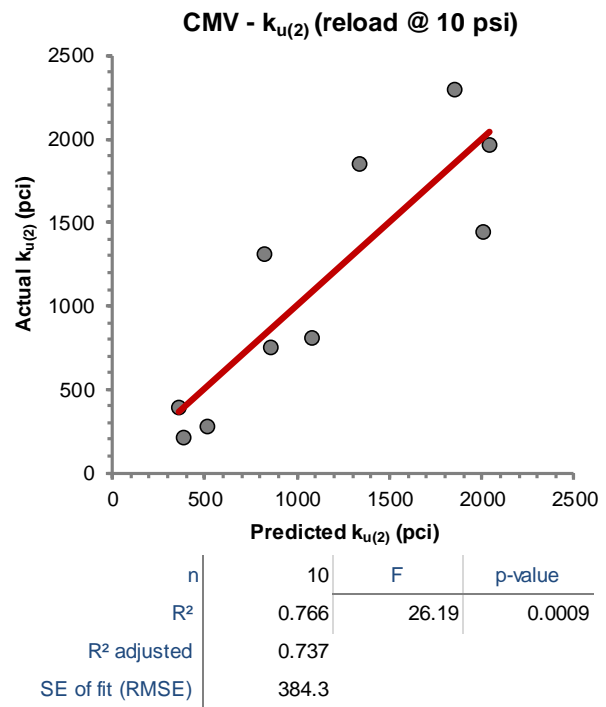
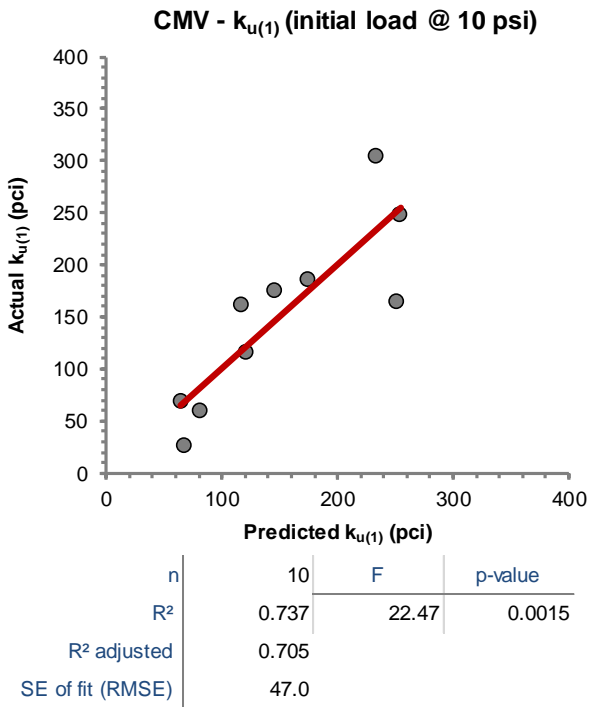
(d)

Figure 46. Summary of calibration results showing predicted versus measured values along with a summary of statistics for each calibration relationship: (a) CMV – M_{r-Comp} at $\Delta\sigma_{cyclic} = 15$ psi, (b) VIC – M_{r-Comp} at $\Delta\sigma_{cyclic} = 15$ psi, (c) CMV – E_{LWD} at $\sigma_o = 14.5$ psi, (d) VIC – E_{LWD} at $\sigma_o = 14.5$ psi



(a)

(b)



(c)

(d)

Figure 47. Summary of calibration results showing predicted versus measured values along with a summary of statistics for each calibration relationship: (a) VIC – $k_{u(1)}$ (b) VIC – $k_{u(2)}$, (c) CMV – $k_{u(1)}$, and (d) CMV – $k_{u(2)}$

An example M_{r-Comp} map at 20 psi cyclic stress on a compacted subgrade area is presented in Figure 48. Average M_{r-Comp} of the entire area was about 24.3 ksi with a COV of about 78%. In addition, M_{r-Comp} versus cyclic stress results from two selected test locations (labeled as A and B) representing stiff and soft conditions in the area are also included in Figure 48 for reference. Test location A with relatively stiff conditions showed that the M_{r-Comp} values increased with increasing cyclic stress up to about 19 psi and then decreased with increasing stress. On the other hand, at test location B with relatively soft conditions, the M_{r-Comp} values generally decreased with increasing cyclic stress.

Subgrade conditions under proof-rolling at test location B showed rutting, which is confirmed with the relatively low M_{r-Comp} values (~5 ksi at 15 psi cyclic stress) near that test location. Decreasing M_{r-Comp} with increasing stress is a characteristic of wet or soft cohesive subgrade soils, and test location B is representative of such a condition. On the other hand, an increase in M_{r-Comp} with increasing stress is a characteristic of either granular materials or relatively dry cohesive subgrade soils. Test location A is representative of such a condition. The decrease in modulus beyond 19 psi stress, which is considered a “break point” (BP) stress, is likely because of deeper soil conditions that are wetter than the near surface subgrade materials.

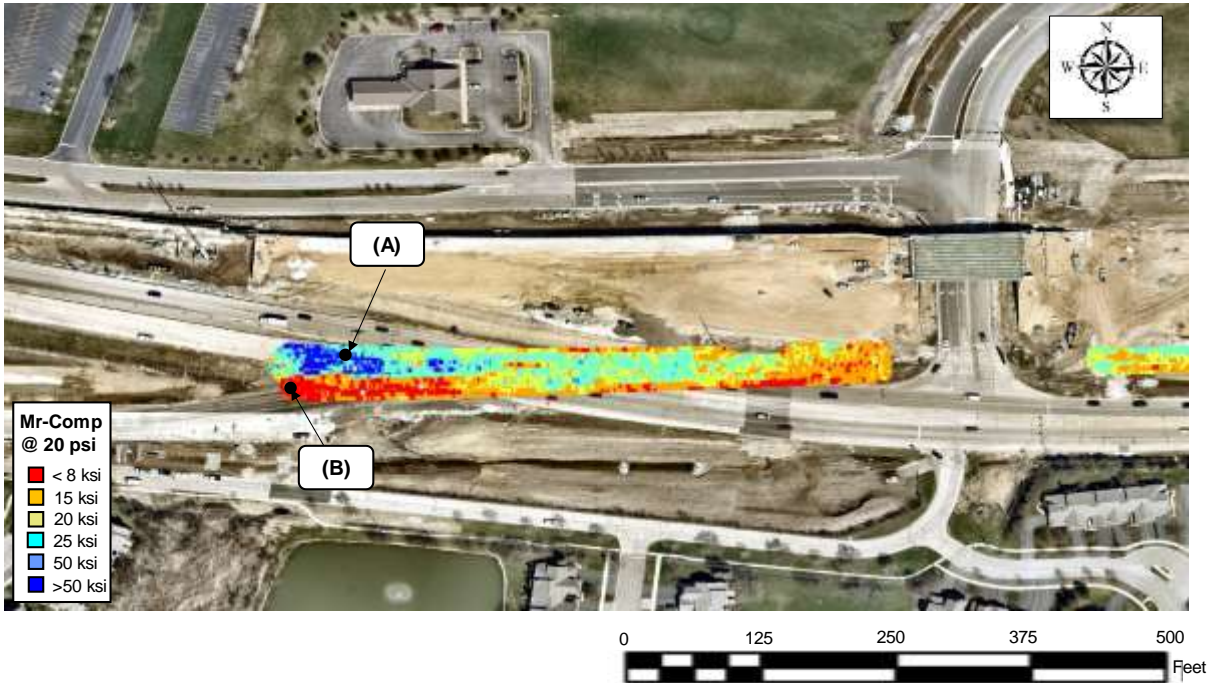
The sharp contrast seen in the M_{r-Comp} map (Figure 48) with a clear boundary of the “red” area, especially near the west half of the test area, is related to how the construction progressed in the area. The final subgrade layer in the area was constructed over nearly a 20+ ft. embankment constructed next to a retaining wall. The south half of the test area was constructed later than the northern half and in a narrow space due to limitations with how the material could be sloped and matched with the progress of the retaining wall construction. The narrow space limitation could be linked to lack of adequate compaction during fill placement in the area.

As VIC measurements were only obtained for research purposes, the mapping results were not used at this site to make field quality assurance decisions. About a 100-ft. long x 30-ft. portion near test location B was recompacted as part of the quality assurance evaluation of the subgrade, as it showed rutting under proof rolling. Pictures of the subgrade during proof rolling near test location B is show in Figure 49.

Immediately after the subgrade repair work, 6 in. PGE layer was placed above the subgrade layer. M_{r-Comp} map of the PGE layer is presented in Figure 50, which showed reflections of the underlying subgrade layer properties when compared with M_{r-Comp} map presented in Figure 48. Average M_{r-Comp} of the entire area was about 28.8 ksi with a COV of about 43%. On average, the M_{r-Comp} on the PGE layer was slightly higher than on the subgrade and the COV is reduced from 78% to 43%.

Static 30 in. plate load tests were conducted on the PGE layer, and results from two select locations (C and D) are presented in Figure 50. Test location C was in a location with relatively stiff subgrade condition and produced $k_{u(1)}$ of 185 pci and $k_{u(2)}$ of 1,847 pci, while test location D was in a location with relatively soft conditions and produced $k_{u(1)}$ of 26 pci and $k_{u(2)}$ of 212 pci. The predicted M_{r-Comp} at test locations C and D were 21.6 ksi and 14.1 ksi, respectively.

MAP ID:	ILT_SG_TS14	Property:	Mr-Comp at 20 psi	Machine:	CS56
Surface Material:	Subgrade	Mean:	24,270	Drum Configuration:	Smooth
Mapping Time:	0.8 hrs	Standard Deviation:	19,026	Vibration Settings:	f = 30 Hz, low amp
No. of Measurements:	5,621	Coeff. Of Variation:	78%	Speed:	3 mph (nominal)



DATE:	06/21/2017	Ingios VICM Compaction Record – XMV Mr-Comp @ 20 psi Cyclic Stress		
OPERATOR:	DW (Ingios)	PROJECT NAME:	Validation of Intelligent Compaction to Characterize Pavement Foundation Mechanical Properties	
		PROJECT ID:	ILT_IC Project	
		LOCATION ID:	Elgin O'Hare Expressway, Elgin, IL	

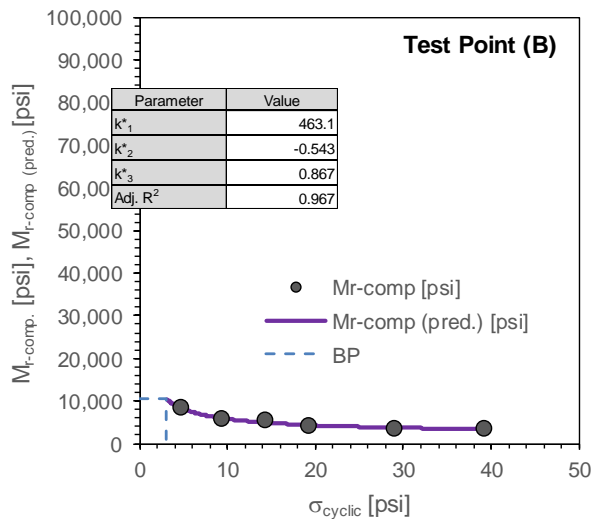
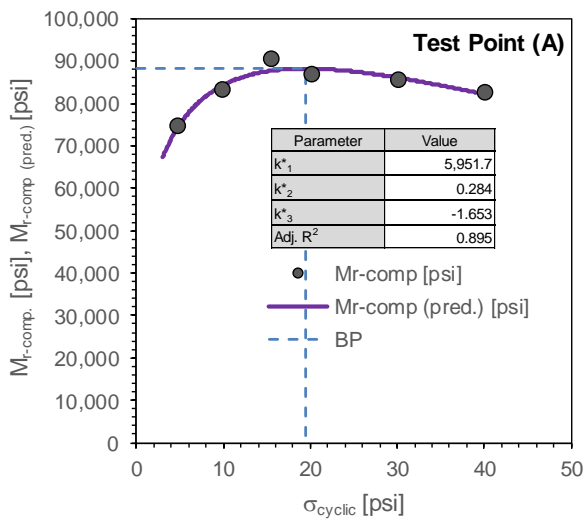


Figure 48. Color-coded map of Mr-Comp values at 20 psi cyclic stress on compacted subgrade along with Mr-Comp versus cyclic stress at two select test locations – TS14.



Figure 49. Pictures of subgrade during and after proof rolling near southwest corner of TS14

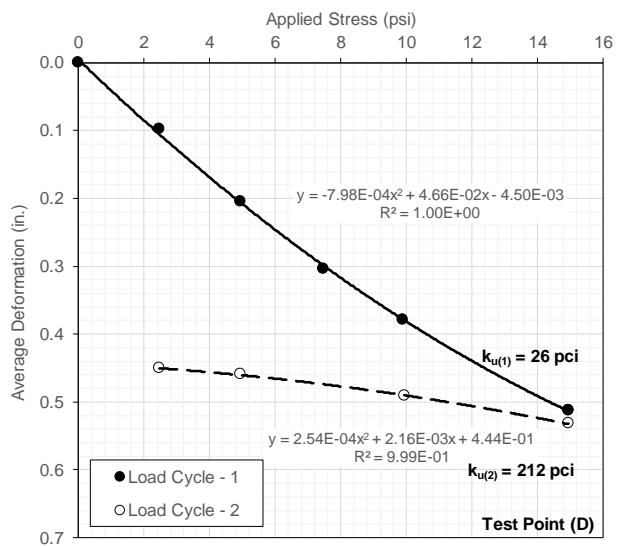
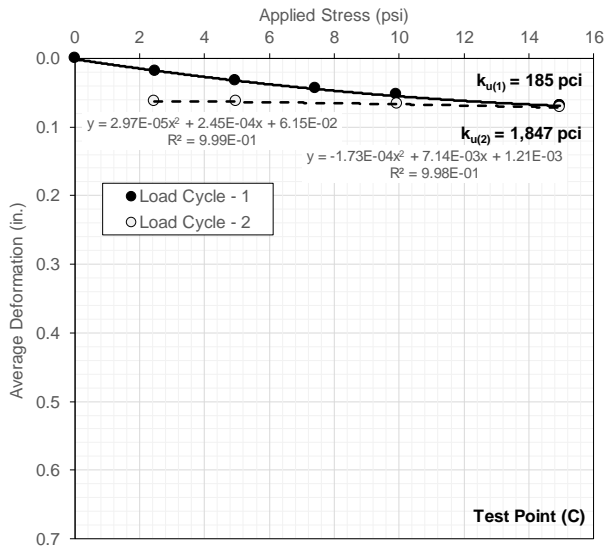
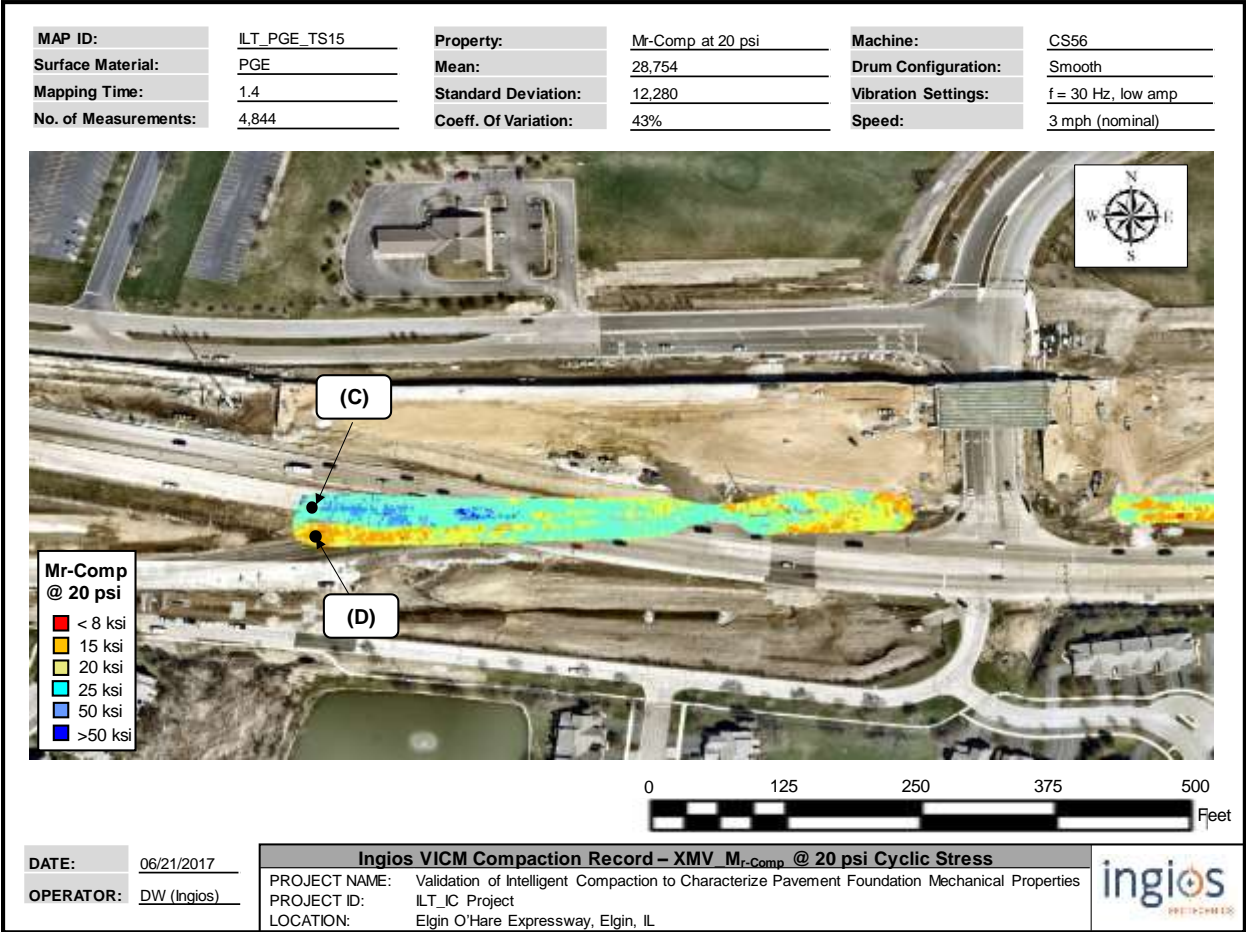


Figure 50. Color-coded map of Mr-Comp values at 20 psi cyclic stress on 6 in. of PGE placed over compacted subgrade along with static plate load test results at two select test locations representing stiff and soft ground conditions – TS15.

3.6 SUMMARY OF KEY FINDINGS AND OBSERVATIONS

Field testing was conducted on several test sections with support from the Illinois State Toll Highway Authority on the Elgin O'Hare Western Access Tollway construction project in October 2016, April-May 2017, and in June 2017. Field evaluation was performed on a total of 18 test sections, of which in situ comparison and calibration testing was conducted on 12 test sections. Four different IC-MV technologies were evaluated including: CMV, H MV, MDP, and VIC. The CMV and MDP IC-MVs were obtained from Caterpillar CS74 vibratory smooth drum IC roller, H MV IC-MVs were obtained from Hamm H11 vibratory smooth drum IC roller, and VIC IC-MVs were obtained on a retrofitted Caterpillar CS56 vibratory smooth drum roller. In situ tests included as part of calibration testing were LWD, DCP, and static and cyclic APLT testing.

Tests were conducted on embankment subgrade, PGE, and CA6 capping layer materials. The PGE layer was nominal 6 in. thick and was placed over the subgrade and consisted of poorly graded RPCC material with a maximum particle size of about 5 in. and no fines passing the No. 200 sieve. The CA6 capping layer was about 3 in. thick and was placed on the PGE layer and consisted of well-graded RAP material with a maximum particle size of about 1.5 in. and about 1% passing the No. 200 sieve.

Key findings from calibration testing performed between H MV-IC MVs and in situ point measurements are as follows:

- Regression relationships between the H MV IC-MV and in situ test measurements showed simple linear regression trends. The regression relationship with E_{LWD} yielded the highest R^2 value of about 0.63 but presented significant scatter. The regression relationships yielded R^2 about 0.14 with DCP-CBR of the top layer, and about 0.56 with DCP-CBR of the top 12 in. of the subgrade layer. Results indicate that the H MV measurements are correlated better with subgrade layer measurements (DCP-CBR of subgrade) than the DCP-CBR of the top PGE or PGE+CA6 layer.
- Comparison between H MV measurements obtained from the same test section with PGE layer material shortly after construction in October 2016 and then after spring-thaw in April 2017 indicated that the foundation support conditions were weaker during the spring-thaw. The average H MV in the area was about 9.9 in October 2016 and reduced to 6.2 in April 2017. This reduction in foundation support was also confirmed with E_{LWD} measurements which decreased from an average of about 8,083 psi in October 2016 to 6,976 psi in April 2017.
- Comparison of H MV measurements obtained from the same area on the PGE layer material and overlaid CA6 capping layer indicated that "hard" and "soft" areas identified in the bottom layer were reflected on the top layer map.

Key findings from calibration testing performed between CMV and MDP* (from CS74B smooth drum vibratory roller) and in situ point measurements are as follows:

- Regression relationships between the CMV and E_{LWD} yielded a non-linear power relationship with R^2 of 0.65. CMV vs. DCP-CBR of the top CA6+PGE layer also yielded a power relationship with R^2 of 0.16, while CMV vs. DCP-CBR of the subgrade layer yielded a linear relationship with $R^2 = 0.59$. Like H MV regression relationships, results indicate that CMV is correlated better with subgrade layer measurements (DCP-CBR of subgrade) than the DCP-CBR of the top layer.
- Variability in CMV measurements (as measured by COV) was 50% and 80% in the PGE and CA6 capping layer test sections, respectively. The MDP* measurements showed lower COV with $\leq 10\%$. As identified in the literature review, MDP* has a relatively shallow

measurement influence depth (1 to 2 ft) compared to CMV measurements (3 to 5 ft). The shallow influence depth of MDP* and the fact that the DCP measurements showed variability in the subgrade was greater than in the top PGE and PGE+CA6 layer, and the narrow measurement range of MDP* are likely the reasons why the COV of MDP* was comparatively low.

- Although the literature shows other projects where MDP* was statistically meaningful for a range of parameter values, regression relationships comparing MDP* and in situ test measurements did not yield a statistically meaningful relationship for the test sections in this study.

VIC calibration was performed using stress-dependent M_r values from cyclic APLT testing and modulus of subgrade reaction k_u -values from two loading cycles. Key findings and observations from this calibration testing are as follows:

- Results from the VIC calibration with both M_{r-comp} and k_u measurements obtained from APLT produced relatively high R^2 values (≥ 0.90) and with relatively low standard error. Higher R^2 values and low standard errors suggest higher reliability in future predictions of the respective measurement values in a production area.
- The VIC – E_{LWD} calibration showed R^2 of 0.7 while the CMV – E_{LWD} calibration showed R^2 of 0.56.
- The CMV calibration with M_{r-comp} produced R^2 of 0.23 and k_u produced R^2 of about 0.71-0.74.
- Results show that the E_{LWD} measurements were on average about 3x lower than the M_{r-comp} values obtained at similar applied stress (~15 psi). The moduli values obtained from LWD measurements are not the same as in situ resilient modulus, M_r . This is because LWD measures peak deflections and not rebound deflections, and conditioning cycles (which can take up to several 100 cycles) are not applied with LWD, which limits the usefulness of the E_{LWD} data as a pavement design verification value.
- VIC – M_{r-comp} maps in a subgrade area identified a sharp contrast with a clear boundary of relatively low M_r and high M_r values. The sharp contrast and the relatively low M_r values was linked to the construction materials and process control followed in the area. Traditional QC/QA inspection did not reveal the very high variability in M_r in the test area.
- A comparison of VIC – M_{r-comp} map obtained on PGE layer with the map obtained on the underlying subgrade layer showed reflections of the soft and stiff areas in the subgrade layer. The average M_{r-comp} increased slightly on the PGE layer (from 24.2 ksi on the subgrade to 28.8 ksi on the PGE) while the COV decreased from about 78% on the subgrade to about 43% on the PGE layer.

CHAPTER 4 IC CERTIFICATION PROCESS AND GUIDE SPECIFICATION

4.1 SPECIFICATION OVERVIEW

In this chapter, guidance for future IC specification for pavement foundation subgrade (and improved subgrade), subbase, and base layer materials, with focus on the certification process is provided. Key attributes of the IC specifications typically include the following:

- Descriptions of the rollers and configurations,
- Guidelines for roller operations (speed, vibration frequency, vibration amplitude, and roller overlap),
- Records to be reported (time of measurement, roller operations/mode, soil type, moisture content, layer thickness, etc.),
- Repeatability and reproducibility measurements for IC measurement,
- Ground conditions (smoothness, levelness, isolated soft/wet spots)
- Calibration/certification procedures for rollers and selection of calibration areas,
- Regression analysis between IC measurements and point measurements,
- Number and locations of QC and QA tests,
- Operator training,
- Acceptance procedures/corrective actions based on achievement of required IC measurements (e.g., minimum value and uniformity), and
- Basis of payment

Common language for many of these attributes can be adopted from the current specifications, although language describing the calibration procedures, certification requirements, use of the IC measures for QC versus QA, and reporting requirements are poorly defined in the current specifications. Field calibration of the IC-MVs with mechanical property values with an independent certification process is an important task to successfully implement IC for field verification/QA. Some key aspects that are considered in developing the certification process are as follows:

- Uncertainty associated with the IC-MV versus mechanical property relationships: This is with R^2 values and standard error in prediction values. The higher the R^2 value and the lower the standard error in prediction values, the higher is the confidence in the mechanical property target value and subsequent identification of areas of non-compliance. Based on the review of literature, authors' experience, and field demonstration projects conducted as part of this project, R^2 values > 0.9 is achievable.
- Impacts of factors affecting the IC-MVs: Numerous factors such as machine operational parameters (i.e., speed, frequency, and amplitude) affect the IC-MVs. In general, the operational parameters used during field calibration work should be the same as the parameters used in the production area. Other factors such as soil layering, in situ moisture content, and post-construction saturation are key factors and should be considered in a specification. An approach to link design values for individual layers versus composite values measured by the IC is needed to address this issue. This issue is particularly important for pavement foundation layer construction.

- Impact of factors affecting the in situ test measurements: Impacts of soil layering and moisture content are important to assess in case of in situ test measurements, like the IC-MVs. An approach to link design values for individual layers versus composite values measured is needed to address this issue.

4.2 KEY COMPONENTS OF IC SPECIFICATIONS

The new specification will primarily involve developing a process that will ensure obtaining repeatable IC measurements with high degree of confidence in relating mechanical properties of compacted materials to the IC-MVs, and then use the calibrated IC-MVs for site wide QA. The process involves three key components as illustrated graphically in Figure 51: (a) Design – where target values are determined for field QA, based on design input parameters assumed for pavement thickness design, (b) field calibration and certification, and (c) site-wide verification or QA.

The part (a) design component does not have to be fully included in the specification but is a process that the agency must undertake to develop the target value that is to be used in the specification. This will help establish the methods and means required to conduct the in situ test measurement for calibration of IC-MVs. This process is important because the pavement design input properties either relate to composite pavement layer properties or individual layer properties, and the method followed to determine these properties (i.e., static or cyclic test and plate size, etc.) will affect the target value.

4.2.1 Establishing field QA Target Values with Link to Design Inputs

The target value determination will depend on the pavement design methodology followed and the input parameters used in the design. For example, a rigid pavement design per AASHTO (1993) or PCA (1984) requires modulus of subgrade reaction k -value or a composite modulus of subgrade reaction k_{comp} -value as the key foundation input parameter. These values are obtained from a static plate load test performed using a 30-in. diameter loading plate. As another example, in AASHTO Ware ME Pavement Design (AASHTO 2015), the key input parameter is resilient modulus (M_r). M_r is a stress-dependent parameter and therefore should be tied to a representative stress condition depending on the layer that is being tested. Further, if the design assumed individual layer properties, a target composite value for a given plate size should be determined. A flow chart of that process is illustrated in Figure 52.

4.2.2 Field Calibration and Certification Process

The specification should require the IC-MV system is certified and independently calibrated such that the outputs and the display are a measure of the stiffness/modulus values as defined in Section 4.1.1. This calibration record must be certificated by an independent professional. Certified calibration test results comparing predicted and measured IC stiffness measured values should demonstrate a coefficient of determination (R^2) ≥ 0.90 . In addition, the IC results must be displayed to the roller operator on a color-coded computer screen in real-time and the data must be saved on board for viewing. Results should also be available for viewing remotely during the rolling operations. The color-coding should be adjustable and should be selected by the Engineer, about the target value.

During the field calibration process, the IC machine must be operated using the same operational parameter settings (i.e., speed, amplitude, frequency, and direction of travel) as would be used in production mapping. Operate the machine according to the IC technology provider and roller manufacturer's recommendations to provide reliable and repeatable measurements. A minimum of 12 test points will be required to establish the IC stiffness calibration. Calibration should be performed over the full range of ground stiffness conditions anticipated on the project site. Check, verify and expand the

field calibrated results for the IC equipment to ensure proper performance. If the IC results fall outside the limits set initial field calibration, additional tests shall be performed to further expand the calibration.

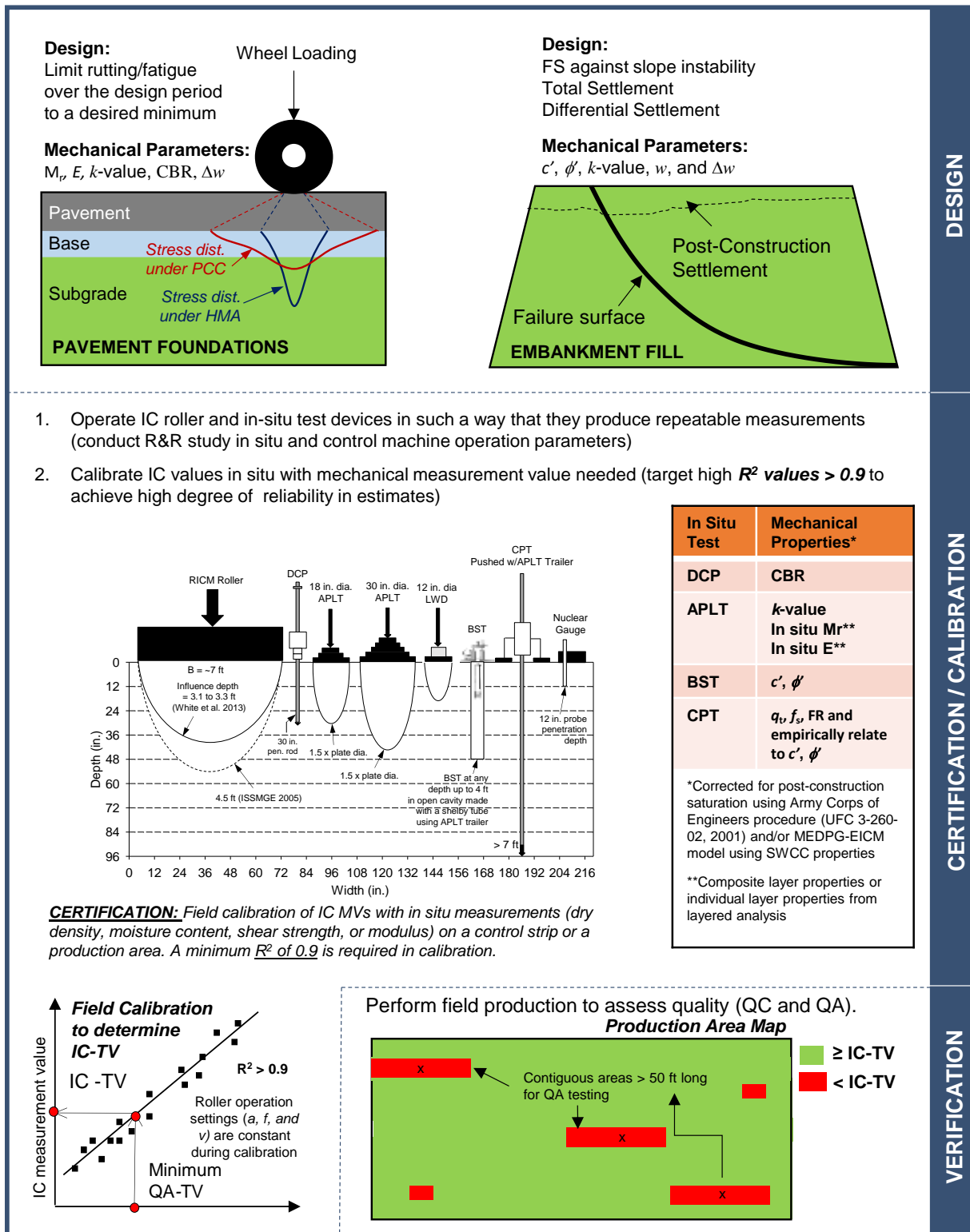


Figure 51. Preliminary concept of field certification / calibration and verification process in relationship with design assumed mechanical properties.

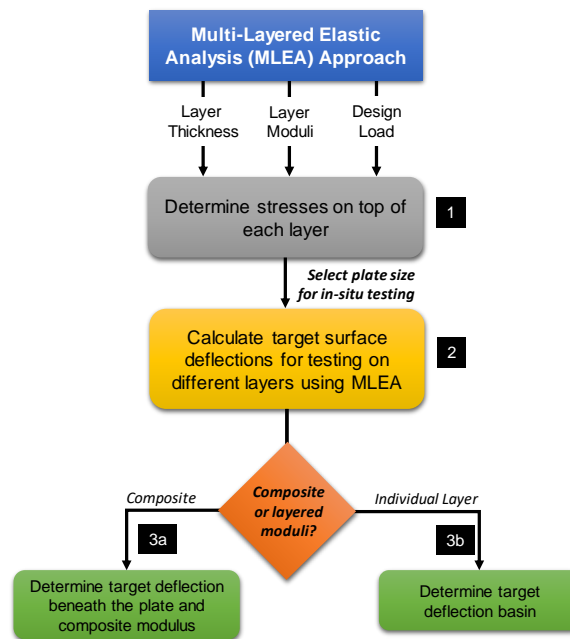


Figure 52. Flow chart to determine in situ target moduli values based on design input parameters using layered elastic analysis.

4.2.3. Field Verification/QA Process using IC Stiffness Mapping

The IC stiffness mapping should be performed on all compaction layers, and prior to placing of new fill layer. The mapping area (i.e., lot size) can be defined in the specification per agencies current state-of-the practice. Mapping must be performed in such a way that it covers the full extent of the compaction work area. Overlapping between adjacent roller lanes shall be limited to 10% or less. Keep roller speed and vibration settings (frequency and amplitude) constant during roller operations and within range of what was used during calibration. Permitted variation in vibration frequency is +/-2Hz and permitted variation in roller speed is +/- 0.5 mph of the settings used during the calibration. Record IC stiffness mapping results in the forward direction only unless the roller is calibrated for mapping in reverse direction.

In the event of equipment breakdowns/IC system malfunctions/GPS problems, the Contractor should have a contingency plan to acquire the equipment or unit necessary in a reasonable time-frame acceptable by the agency. The IC stiffness mapping data shall be collected and provided for a minimum defined area acceptable to the agency (e.g., 80 to 90%) of all compaction layers.

The acceptance or QA using the IC stiffness mapping results should be based on:

- a defined amount of mapping area (~80 to 90%) achieving the minimum target value, and
- the COV of the measurements are less than a defined target (e.g., 25%) and there are no spatially contiguous areas (> 100 ft²) with values less than the target value.
- Independent QA testing (using the same testing utilized for calibration) can be used in to verify the IC stiffness mapping results in areas with low values and apply corrective actions.

The advantage of this type of verification approach is that it allows for the assignment of acceptable risk (statistical calculation that can be linked to measurement frequency and quality of the correlations) and creates a framework for incentive-based pay to the contractor.

4.3 GUIDE SPECIFICATION LANGAUAGE

A guide specification was drafted and is provided in Appendix D. The specification pulls language from various specifications studied from the synthesis effort and incorporates key features of the calibration process as studies in this research effort.

CHAPTER 5 SUMMARY AND IMPLEMENTATION RECOMMENDATIONS

5.1 SUMMARY OF KEY FINDINGS

As part of this study, a detailed literature review was conducted to create a synthesis information that identifies methods/procedures used to compare IC measurements to soil mechanical properties, and the success of those methods/procedures along with a summary of current IC specifications. More than 300 documents were collected that have been published on the general topic of IC. Key findings from the literature review are as follows:

- IC technologies have been used in the U.S. on at least 381 pilot/demonstration projects since year 2000. Of these, most of the projects (220+) involved HMA construction (full depth HMA or overlay), 75+ project sites involved subgrade and aggregate base materials, and over 25+ project sites involved CIR/FDR materials.
- Several field studies have been documented since 1980 focusing on correlating IC-MVs and in situ point test measurements. A variety of in situ test measurements have been utilized in these correlation studies to measure dry density, moisture content, elastic modulus, resilient modulus, modulus of subgrade reaction, CBR, dynamic modulus, shear strength, etc.
- In general, results from controlled field studies show that statistically valid simple linear or simple non-linear correlations between IC-MVs and compaction layer point-MVs (e.g., modulus or density) are possible when the compaction layer is underlain by a relatively homogenous and stiff/ stable supporting layer. Many field studies indicate that modulus or stiffness-based measurements (i.e. determined by FWD, LWD, PLT, etc.) generally correlate better with the IC-MVs than compaction layer dry unit weight or CBR measurements.
- IC specifications were introduced in Europe (Austria, Germany, and Sweden) in the 1990s, and in 2005, the ISSMGE developed recommended construction specifications based primarily on the Austrian specifications. In the U.S., few state highway agencies and the FHWA have developed specifications to facilitate implementation of IC technologies for embankment and pavement foundation layer materials, but not in terms of mechanical soil properties.
- Current European and U.S. specifications lack detailed framework for calibration (i.e., corrections from independent testing) and validation of results (i.e., accuracy and system quality checks) in terms of mechanical soil properties. The current U.S. specifications on IC are method and prescriptive specifications and focus on IC equipment features and the procedure/format for data reporting.
- The mechanical soil properties that some agencies are using, do not directly link to the pavement design input parameters (e.g., k-value or stress-dependent M_r value). Some states specifications and a version of the current FHWA specification require the IC data be calibrated to density measurements., though the technical literature shows that correlating IC-MVs to dry density (or percent compaction) is challenging and practically impossible in many cases.
- Investigating IC implementation barriers, key challenges include: (1) simplifying the data management and analytics, (2) automating generation of compaction reports, and (3) automating data archival.

Field testing was conducted on several test sections with support from the Illinois State Toll Highway Authority on the Elgin O'Hare Western Access Tollway construction project in October 2016, April-May 2017, and in June 2017. Field evaluations were performed on a total of 18 test sections, of which in situ comparison and calibration testing was conducted on 12 test sections. Four different IC-MV technologies were evaluated including: CMV, HMV, MDP, and VIC. The CMV and MDP IC-MVs were obtained from Caterpillar CS74 vibratory smooth drum IC roller, HMV IC-MVs were obtained from Hamm H11 vibratory smooth drum IC roller, and VIC IC-MVs were obtained on a retrofitted Caterpillar CS56 vibratory smooth drum roller. In situ tests included as part of calibration testing were LWD, DCP, and static and cyclic APLT testing.

Tests were conducted on embankment subgrade, PGE, and CA6 capping layer materials. The PGE layer was nominal 6 in. thick and was placed over the subgrade and consisted of poorly graded RPCC material with a maximum particle size of about 5 in. and no fines passing the No. 200 sieve. The CA6 capping layer was about 3 in. thick and was placed on the PGE layer and consisted of well-graded RAP material with a maximum particle size of about 1.5 in. and about 1% passing the No. 200 sieve.

Key findings from calibration testing performed between HMV-IC MVs and in situ point measurements are as follows:

- Regression relationships between the HMV IC-MV and in situ test measurements showed simple linear regression trends. The regression relationship with E_{LWD} yielded the highest R^2 value of about 0.63 but presented significant scatter. The regression relationships yielded R^2 about 0.14 with DCP-CBR of the top layer, and about 0.56 with DCP-CBR of the top 12 in. of the subgrade layer. Results indicate that the HMV measurements are correlated better with subgrade layer measurements (DCP-CBR of subgrade) than the DCP-CBR of the top PGE or PGE+CA6 layer.
- Comparison between HMV measurements obtained from the same test section with PGE layer material shortly after construction in October 2016 and then after spring-thaw in April 2017 indicated that the foundation support conditions were weaker during the spring-thaw. The average HMV in the area was about 9.9 in October 2016 and reduced to 6.2 in April 2017. This reduction in foundation support was also confirmed with E_{LWD} measurements which decreased from an average of about 8,083 psi in October 2016 to 6,976 psi in April 2017.
- Comparison of HMV measurements obtained from the same area on the PGE layer material and overlaid CA6 capping layer indicated that "hard" and "soft" areas identified in the bottom layer were reflected on the top layer map.

Key findings from calibration testing performed between CMV and MDP* (from CS74B smooth drum vibratory roller) and in situ point measurements are as follows:

- Regression relationships between the CMV and E_{LWD} yielded a non-linear power relationship with R^2 of 0.65. CMV vs. DCP-CBR of the top CA6+PGE layer also yielded a power relationship with R^2 of 0.16, while CMV vs. DCP-CBR of the subgrade layer yielded a linear relationship with $R^2 = 0.59$. Like HMV regression relationships, results indicate that CMV is correlated better with subgrade layer measurements (DCP-CBR of subgrade) than the DCP-CBR of the top layer.
- Variability in CMV measurements (as measured by COV) was 50% and 80% in the PGE and CA6 capping layer test sections, respectively. The MDP* measurements showed lower COV with $\leq 10\%$. As identified in the literature review, MDP* has a relatively shallow measurement influence depth (1 to 2 ft) compared to CMV measurements (3 to 5 ft). The shallow influence depth of MDP* and the fact that the DCP measurements showed

variability in the subgrade was greater than in the top PGE and PGE+CA6 layer, and the narrow measurement range of MDP* are likely the reasons why the COV of MDP* was comparatively low.

- Although the literature shows other projects where MDP* was statistically meaningful for a range of parameter values, regression relationships comparing MDP* and in situ test measurements did not yield a statistically meaningful relationship for the test sections in this study.

VIC calibration was performed using stress-dependent M_r values from cyclic APLT testing and modulus of subgrade reaction k_U values from two loading cycles. Key findings and observations from this calibration testing are as follows:

- Results from the VIC calibration with both M_{r-comp} and k_U measurements obtained from APLT produced relatively high R^2 values (≥ 0.90) and with relatively low standard error. Higher R^2 values and low standard errors suggest higher reliability in future predictions of the respective measurement values in a production area.
- The VIC – E_{LWD} calibration showed R^2 of 0.7 while the CMV – E_{LWD} calibration showed R^2 of 0.56.
- The CMV calibration with M_{r-Comp} produced R^2 of 0.23 and k_U produced R^2 of about 0.71-0.74.
- Results show that the E_{LWD} measurements were on average about 3x lower than the M_{r-Comp} values obtained at similar applied stress (~15 psi). The moduli values obtained from LWD measurements are not the same as in situ resilient modulus, M_r . This is because LWD measures peak deflections and not rebound deflections, and conditioning cycles (which can take up to several 100 cycles) are not applied with LWD, which limits the usefulness of the E_{LWD} data as a pavement design verification value.
- VIC – M_{r-Comp} maps in a subgrade area identified a sharp contrast with a clear boundary of relatively low M_r and high M_r values. The sharp contrast and the relatively low M_r values was linked to the construction materials and process control followed in the area. Traditional QC/QA inspection did not reveal the very high variability in M_r in the test area.
- A comparison of VIC – M_{r-Comp} map obtained on PGE layer with the map obtained on the underlying subgrade layer showed reflections of the soft and stiff areas in the subgrade layer. The average M_{r-Comp} increased slightly on the PGE layer (from 24.2 ksi on the subgrade to 28.8 ksi on the PGE) while the COV decreased from about 78% on the subgrade to about 43% on the PGE layer.

5.2 IMPLEMENTATION RECOMMENDATIONS

This project has demonstrated that intelligent compaction technologies are effective at mapping compaction conditions and providing verification of project design values in terms of mechanical properties (e.g., modulus) of compacted materials as part of a continuous quality control/acceptance process. The synthesis of literature completed for this project revealed that very little information is available demonstrating how the intelligent compaction studies have been validated in terms of mechanistic design values. This project set out to demonstrate that calibrating the IC-MVs to mechanical properties is possible with well-designed calibration testing program. Following calibration, the in situ test results revealed the compaction layers and pavement foundation material are both highly non-uniform and have built-in defects (low stiffness ‘soft’ areas and high spatial variability) that are not addressed with conventional QC/QA observation and spot testing. A draft guide specification was

developed as part of this project and is recommended for implementation on upcoming construction projects (likely, as “shadow” evaluations) in 2018/19.

Although several test sections were studied as part of this project, no comprehensive (project level) study has been completed using validated intelligent compaction results for the range of pavement foundation materials (recycled materials, stabilized materials, subgrades, etc.) used on Tollway construction projects. Therefore, to further implement this technology additional research is recommended to: (1) monitor and gather data from the VIC technologies used on the proposed 2018/19 projects; and (2) to study more broadly the range of materials, subgrade, aggregate bases, and stabilized pavement foundations used by the Tollway. With this information, the Tollway will be able to more fully understand the limitations and implementation requirements for the technology, how varied materials can be effectively used to construct uniform and stable pavement foundations, and accordingly refine the guide specification.

The near-term benefits of implementing the finding of this research on upcoming construction project are expected to be improved contractor efficiencies and more effective QC/QA processes, providing additional information in terms of meeting the pavement design assumptions, and generating baseline data to evaluate future pavement performance.

REFERENCES

- AASHTO T307-99 (2000). "Standard Method of Test for Determining the Resilient Modulus of Soils and Aggregate Materials", Standard Specifications for Transportation Materials and Methods of Sampling and Testing, Twentieth Edition, American Association of State Highway and Transportation Officials, Washington, DC.
- AASHTO. (1993). AASHTO Guide for Design of Pavement Structures, Published by the American Association of State Highway and Transportation Officials, Washington, D.C.
- AASHTO. (2015). Mechanistic-empirical pavement design guide: A manual of practice, 2nd edition, American Association of Highway and Transportation Officials, Washington, D.C.
- AASHTO T222-81 (2012). "Standard Method of Test for Non-repetitive Static Plate Load Test of Soils and Flexible Pavement Components for Use in Evaluation and Design of Airport and Highway Pavements", Standard Specifications for Transportation Materials and Methods of Sampling and Testing, Thirty Second Edition, American Association of State Highway and Transportation Officials, Washington, DC.
- Adam, D. (1997). "Continuous compaction control (CCC) with vibratory rollers," Proc., GeoEnvironment 97, 245 – 250, November, Melbourne, Australia. Balkema, Rotterdam.
- Anderegg, R. (1998). "Nichtlineare Schwingungen bei dynamischen Bodenverdichtern." Ph.D. Dissertation, Eidgenossische Technische Hochschule Zurich (in German).
- Anderegg R., and Kaufmann, K. (2004). "Intelligent compaction with vibratory rollers - feedback control systems in automatic compaction and compaction control," Transportation Research Record No. 1868, Journal of the Transportation Research Board, 124-134.
- ASTM. (2007). Standard Test Method for Use of the Dynamic Cone Penetrometer in Shallow Pavement Applications - ASTM D6951-03. West Conshohocken, Pennsylvania: American Standard for Testing Methods.
- Bekker, M. (1969). Introduction to Terrain-Vehicle Systems, The University of Michigan Press, Ann Arbor, Michigan (USA).
- Brandl, H., and Adam, D. (1997). "Sophisticated Continuous Compaction Control of Soils and Granular Materials" Proc., XIVth Intl. Conf. on Soil Mechanics & Foundation Engineering, Vol. 1, September, Hamburg, Germany.
- Camargo, F., Larsen, B., Chadbourn, B., Roberson, R., and Siekmeier, J. (2006). "Intelligent compaction: a Minnesota case history." Proc., 54th Annual University of Minnesota Geotechnical Conference, February, Minneapolis, CD-ROM.
- FHWA. (2014). "Intelligent compaction technology for soils applications," Federal Highway Administration, Washington, DC.
- Floss, R., Gruber, N. and Obermayer, J. (1983). "A dynamical test method for continuous compaction control." Proc. 8th European Conf. on Soil Mechanics and Foundation Engineering, Rathmayer, H.G., and Saari, K.H.O., Eds., May, Helsinki, 25-30.
- Forssblad, L. (1980). "Compaction meter on vibrating rollers for improved compaction control", Proc., Intl. Conf. on Compaction, Vol. II, 541-546, Paris.
- Georgia DOT. (2012). "Intelligent Compaction for Soils – Special Provision – PROJECT No. STP00-0001-00(817), Clayton/Fulton Counties, P. I. NO. 0001817, Section 999- Miscellaneous", Department of Transportation, State of Georgia, GA.

- Hansbo, S., and Pramborg, B. (1980). "Compaction control." Proc., Intl. Conf. on Compaction, Vol. II, 559-564, Paris.
- Hertz, H. (1895). Über die Berührung fester elastischer Körper, Gesammelte Werke, Bd. 1. Leipzig.
- Huang, Y. H. (2004). Pavement analysis and design, Second Edition, Pearson Education, Inc., Upper Saddle River, NJ.
- Indiana DOT (2014). "Quality Control/Quality Assurance, QC/QA, Soil Embankment," Indiana Department of Transportation, IN.
- Iowa DOT. (2010). Special provisions for intelligent compaction – Embankment SP-090063 (New), Sac County NHSX-020-2(89)--3H-81 (Effective Date April 20, 2010), Iowa DOT, Ames, Iowa, USA.
- ISSMGE. (2005). Geotechnics for pavements in transportation infrastructure, roller-integrated continuous compaction control (CCC), Technical Contractual Provisions – Recommendations, International Society for Soil Mechanics Geotechnical Engineering.
- Kimmel, S.C., Mooney, M.A. (2011). "Real-time soil compaction monitoring through pad strain measurements: modeling to inform strain gage placement," Proc. SPIE 7981, Sensors and Smart Structures Technologies for Civil, Mechanical, and Aerospace Systems 2011, 79815F (April 18, 2011); doi:10.1117/12.882649.
- Kröber, W. (1988). Untersuchung der dynamischen Vorgänge bei der Vibrations- verdichtung von Böden. Dissertation. Schriftenreihe, Heft 11, Lehrstuhl und Prüfamnt für Grundbau, Bodenmechanik und Felsmechanik der Technischen Universität München. In German.
- Kröber, W., Floss, E., Wallrath, W. (2001). "Dynamic soil stiffness as quality criterion for soil compaction," Geotechnics for Roads, Rail Tracks and Earth Structures, A.A. Balkema Publishers, Lisse /Abingdon/ Exton (Pa) /Tokyo, 189-199.
- KYTC. (2015). "Special Note for Intelligent Compaction of Aggregate Bases and Soils," Kentucky Transportation Cabinet, Lexington, KY.
- Liu, D., Li, Z., Lian, Z. (2014). "Compaction quality assessment of earth-rock dam materials using roller-integrated compaction monitoring technology." Automation in Construction, Vol. 44, 234-246.
- Liu, D., Lin, M., and Li, S. (2016). Real-time quality monitoring and control of highway compaction. Automation in Construction, 62, 114-123.
- Lundberg, G., (1939). "Elastische Berührung Zweier Halbräume." Forschung auf dem Gebiete des Ingenieurwesens, Band 10, 201-211, Göteborg. In German.
- Preisig, M., Caprez, M., and Amann, P. (2003). "Validation of continuous compaction control (CCC) methods." Workshop on Soil Compaction, September, Hamburg.
- Petersen, D., Siekmeier, J., Nelson, C., Peterson, R. (2006). "Intelligent soil compaction – technology, results and a roadmap toward widespread use." Transportation Research Record No. 1975, 81-88.
- Michigan DOT (2013). "Intelligent Compaction Mapping of Subbase and Aggregate Base – Special Provision", Michigan Department of Transportation, MI.
- MnDOT (2017). "2016 Quality Management Special – Intelligent Compaction (IC) Method," Minnesota Department of Transportation, St. Paul, MN.
- Moaveni, M., 2015, *Advanced Image Analysis and Techniques for Degradation Characterization of Aggregates*, PhD Dissertation, University of Illinois, Urbana.
- Mooney, M. A., and Adam, D. (2007). "Vibratory roller integrated measurement of earthwork compaction: An overview." Proc., 7th International Symposium on Field Measurements in

Geomechanics: FMGM 2007, ASCE, Boston, MA.

- Mooney, M. A., Rinehart, R., White, D.J., Vennapusa, P., Facas, F., and O. Musimbi. (2010). "Intelligent soil compaction systems," NCHRP Report 676, National Cooperative Highway Research Program, Washington, DC, USA.
- Newman, K., and White, D. (2008). "Rapid assessment of cement/fiber stabilized soil using roller-integrated compaction monitoring." Transportation Research Record No. 2059, 95-102.
- Nohse, Y., Uchiyama, K., Kanamori, Y., Kase, J., Kawai, Y., Masumura, K., and Tateyama, K. (1999). "An attempt applying a new control system for the vibratory compaction using GPS and CMV in the embankment construction (Part 1)." Proc. of the 13th Intl. Conf. of the ISTVS: Okinawa, Japan, 295-300.
- Nohse, Y., Kitano, M. (2002). "Development of a new type of single drum vibratory roller." Proc., 14th Intl. Conf. of the Intl. Soc. for Terrain-Vehicle Systems, Vicksburg, MS, October.
- Petersen, D., Siekmeier, J., Nelson, C., Peterson, R. (2006). "Intelligent soil compaction – technology, results and a roadmap toward widespread use." Transportation Research Record No. 1975, Journal of the Transportation Research Board, 81-88.
- Rahman, F., Hossain, M., Hunt, M., Romanoschi, S.A. (2008). "Soil stiffness evaluation for compaction control of cohesionless embankments." Geotech. Test. J., 31(5).
- Rinehart R.V., Mooney, M.A., Facas N.F., Musimbi O.M.(2012) "Examination of Roller-Integrated Continuous Compaction Control on Colorado Test Site", Journal of the Transportation Research Board, No. 2310, Transportation Research Board of the National Academies, Washington.
- ROAD 94. (1994). General technical construction specification for roads – Unbound Pavement Layers, Road and Traffic Division, Sweden.
- RVS 8S.02.6. (1999). Continuous compactor integrated compaction – Proof (proof of compaction), Technical Contract Stipulations RVS 8S.02.6 – Earthworks, Federal Ministry for Economic Affairs, Vienna.
- Ryden, N. and Mooney, M. (2007). "Surface Wave Testing to Investigate the Nature of Roller Determined Soil Stiffness," Proc. Symp. on the Application of Geophysics to Engineering and Environmental Problems: SAGEEP 2007, Denver, Colorado, April, 1388-1394.
- Samaras, A., Lamm, R., and Treiterer, J. (1991). "Application of continuous dynamic compaction control for earthworks in railroad construction." Transportation Research Record No. 1309, 42-46.
- Sandström A.J., and Pettersson, C.B. (2004). "Intelligent systems for QA/QC in soil compaction", Proc., 83rd Annual Transportation Research Board Meeting, January 11-14. Washington, D.C.
- Scherocman, J., Rakowski, S., and Uchiyama, K. (2007). "Intelligent compaction, does it exist?" 2007 Canadian Technical Asphalt Association (CTAA) Conference, Victoria, BC, July.
- Texas DOT. (2004). "Special Specification 2304 – Intelligent Compaction of Soil and Flexible Base," Texas Department of Transportation, Austin, TX.
- Thompson, M., and White, D. (2007). "Field calibration and spatial analysis of compaction monitoring technology measurements." Transportation Research Record No. 2004, 69-79.
- Thompson, M., and White, D. (2008). "Estimating compaction of cohesive soils from machine drive power." Journal of Geotechnical and Geoenvironmental Engineering, ASCE, 134(12), 1771-1777.
- Thompson, M., White, D., Gieselman, H., and Siekmeier, J. (2008). "Variable feedback control intelligent compaction to evaluate subgrade and granular pavement layers – Field study at Minnesota US 14." Proc., 87th Annual Transportation Research Board Meeting, Washington, D.C.

- Thurner, H. (1993). "Continuous compaction control - specifications and experience." Proc., XII IRF World Congress, 951-956, Madrid.
- Thurner, H. and Sandström, Å. (1980). "A new device for instant compaction control." Proc., Intl. Conf. on Compaction, Vol. II, 611-614, Paris.
- UFC 3-260-02 (2001). "Pavement Design for Airfields," Unified Facilities Criteria (UFC), Department of Defense, Washington, D.C.
- Ullidtz, P. (1987). Pavement Analysis, Elsevier, New York, NY.
- Vennapusa, P., White, D.J., Gieselman, H. (2009). "Influence of support conditions on roller-integrated machine drive power measurements for granular base." Intl. Foundation Congress and Equipment Expo (IFCEE) 2009, 15-19 March, Orlando, Florida.
- Vennapusa, P., White, D.J., Morris, M. (2010). "Geostatistical analysis of spatial referenced roller-integrated compaction measurements." Journal of Geotechnical and Geoenvironmental Engineering, ASCE, 136(6), 813-822.
- Vennapusa, P., White, D. J., Siekmeier, J., Embacher, R., (2012). "In situ mechanistic characterizations of granular pavement foundation layers." Intl. J. of Pavement Engineering, 13(1), 52-67.
- Vennapusa, P., and White, D.J. (2014). "Interpretation of Dual-Integrated Compaction Measurements on Layered Granular Fill", Geo-Congress 2014 – Geo-Characterization and Modeling for Sustainability, ASCE, Feb 23-26, Atlanta.
- White, D.J, Jaselskis, E., Schaefer, V., Cackler, T., Drew, I., and Li, L. (2004). Field Evaluation of Compaction Monitoring Technology: Phase I, Final Report, Iowa DOT Project TR-495, Iowa State University, Ames, Iowa.
- White, D.J, Jaselskis, E., Schaefer, V., and Cackler, E. (2005). "Real-time compaction monitoring in cohesive soils from machine response." Transportation Research Record No. 1936, 173-180.
- White, D.J, Morris, M., Thompson, M. (2006a). Power-based compaction monitoring using vibratory padfoot, Proc., GeoCongress 2006: Geotechnical Engineering in the Information Technology Age, Atlanta, USA, CD-ROM.
- White, D.J., Thompson, M., Jovaag, K., Morris, M., Jaselskis, E., Shaefer, V., and Cackler, T. (2006b). Field Evaluation of Compaction Monitoring Technology: Phase II, Final Report, Iowa DOT Project TR-495, March, Ames, Iowa, USA.
- White, D.J, Thompson, M., Vennapusa, P. (2007). Field Validation of Intelligent Compaction Monitoring Technology for Unbound Materials, Mn/DOT Report No. MN/RC 2007-10, Minnesota Department of Transportation, St. Paul, Minnesota.
- White, D.J, Thompson, M., Vennapusa, P. (2007). Field study of compaction monitoring systems: self-propelled non-vibratory 825G and vibratory smooth drum CS-533 E rollers, Final Report, Center of Transportation Research and Education, Iowa State University, Ames, Iowa.
- White, D., Thompson, M., Vennapusa, P., and Siekmeier, J. (2008a). "Implementing intelligent compaction specifications on Minnesota TH 64: Synopsis of measurement values, data management, and geostatistical analysis." Transportation Research Record: Journal of the Transportation Research Board, 2045, 1-9.
- White, D.J., Vennapusa, P., Gieselman, H., Johanson, L., Goldsmith, R. (2008b). Accelerated Implementation of Intelligent Compaction Monitoring Technology for Embankment Subgrade Soils, Aggregate Base, and Asphalt Pavement Materials TPF-5(128) – Texas IC Demonstration Field Project, Report submitted to The Transtec Group, FHWA, November.

- White, D., and Thompson, M. (2008). "Relationships between in-situ and roller-integrated compaction measurements for granular soils." *Journal of Geotechnical and Geoenvironmental Engineering*, ASCE, 134 (12), 1763-1770.
- White, D.J., Vennapusa, P., Zhang, J., Gieselman, H., Morris, M. (2009a). Implementation of Intelligent Compaction Performance Based Specifications in Minnesota, EERC Publication ER09-03, MN/RC 2009-14, Minnesota Department of Transportation, St. Paul, Minnesota, March.
- White, D.J., Vennapusa, P., Gieselman, H., Johanson, L., Siekmeier, J. (2009b). "Alternatives to heavy test rolling for cohesive subgrade assessment," Eighth Intl. Conf. on the Bearing Capacity of Roads, Railways, and Airfields (BCR2A'09), June 29 – July 2, Champaign, Illinois.
- White, D.J., Vennapusa, P., Gieselman, H., Zhang, J., Goldsmith, R., Johanson, L., Quist, S. (2010a). Accelerated Implementation of Intelligent Compaction Monitoring Technology for Embankment Subgrade Soils, Aggregate Base, and Asphalt Pavement Materials TPF-5(128) - NY IC Demonstration Field Project, EERC Publication ER10-01, Report submitted to The Transtec Group, FHWA, January.
- White, D.J., Vennapusa, P., Gieselman, H., Fleming, B., Quist, S., Johanson, L. (2010b). Accelerated Implementation of Intelligent Compaction Monitoring Technology for Embankment Subgrade Soils, Aggregate Base, and Asphalt Pavement Materials TPF-5(128) – Mississippi IC Demonstration Field Project, ER10-03, Report submitted to The Transtec Group, FHWA, January.
- White, D.J., Vennapusa, P., Gieselman, H. (2011). "Field Assessment and Specification Review for Roller-Integrated Compaction Monitoring Technologies." Special Issue: Advances in Instrumentation and Monitoring in Geotechnical Engineering in *Advances in Civil Engineering Journal*, Hindawi Publishing Corporation, Volume 2011, Article ID 783836.
- White, D.J., Becker, P., Vennapusa, P., Dunn, M., and White, C. (2013). "Soil Stiffness Assessment of Stabilized Pavement Foundations." *Transportation Research Record*, Journal of Transportation Research Board, 2235, 99-109.
- White, D. J., Vennapusa, P., and Dunn, M. (2014a). "A Road Map for Implementation of Intelligent Compaction Technology." *Geo-Congress 2014 – Geo-Characterization and Modeling for Sustainability*, ASCE, Feb 23-26, Atlanta.
- White, D.J., Vennapusa, P., Cackler, T. (2014b). "ICM Report – Ohio River Bridges East End Crossing I-265, Section 6, Sta. 350+00 to 400+00", Report submitted for Walsh Vinci Construction, Inc., by Ingios Geotechnics, Inc. (unpublished report).
- White, D.J., and Vennapusa, P. (2017). "In situ resilient modulus for geogrid-stabilized aggregate layer: A case study using automated plate load testing," *Transportation Geotechnics*, Vol. 11, 120-132.
- Yoo, T., Selig. E. (1979). "Dynamics of vibratory-roller compaction," *Journal of the Geotechnical Engineering Division*, ASCE, 105(10), pp. 1211–1231.
- Zorn, G. (2003). Operating manual: light drop-weight tester. ZFG2000, Zorn Stendal, Germany.
- ZTVE StB/TP BF-StB. (1994). Surface Covering Dynamic Compaction Control Methods – German Specifications and Regulations, Additional Technical Contractual Conditions and Guidelines for Earthwork in Road Construction and Technical Testing Instructions for Soil and Rock in Road Construction, Research Society of Road and Traffic, Germany.

APPENDIX A: LIST OF IC REFERENCES

Intelligent Compaction Technical Publications [1980-2017]

Journal and Conference Papers (organized by publication date)

1980

1. Forssblad, L. (1980). "Compaction meter on vibrating rollers for improved compaction control", *Proc., Intl. Conf. on Compaction*, Vol. II, 541-546, Paris.
2. Hansbo, S., and Pramborg, B. (1980). "Compaction control." *Proc., Intl. Conf. on Compaction*, Vol. II, 559-564, Paris.
3. Machet, J.M. (1980). "Compactor-mounted control devices", *Proc., Intl. Conf. on Compaction*, Vol. II, 577-581, Paris.
4. Machet, J.M., and Sanejouand, R. (1980). "Modules mathematiques dans le domaine du compactage par vibration", *Proc., Intl. Conf. on Compaction*, Vol. II, Paris.
5. Thurner, H. (1980). "The compactometer principle: Contribution to the discussion in Session IV." *Proc., Intl. Conf. on Compaction*, Vol. II, Paris.
6. Thurner, H. and Sandström, Å. (1980). "A new device for instant compaction control." *Proc., Intl. Conf. on Compaction*, Vol. II, 611-614, Paris.
7. Yoo, T., and Selig, E. (1980). "New concepts for vibratory compaction of soil", *Proc., Intl. Conf. on Compaction*, Vol. II, 703-707, Paris.

1983

8. Floss, R., Gruber, N., and Obermayer, J. (1983). "A dynamical test method for continuous compaction control." *Proc. 8th European Conf. on Soil Mechanics and Foundation Engineering*, Rathmayer, H.G., and Saari, K.H.O., Eds., May, Helsinki, 25-30.

1984

9. Mayne, P.W., Jones, J.S., and Dumas, J. (1984). "Ground response to dynamic compaction." *ASCE Journal of Geotechnical Engineering*, 110(6), p. 757-774.

1991

10. Samaras, A., Lamm, R., and Treiterer, J. (1991). "Application of continuous dynamic compaction control for earthworks in railroad construction." *Transportation Research Record No. 1309, Journal of the Transportation Research Board*, National Academy Press, 42-46.
11. Thurner, H. and Sandström, Å. (1991). "Quality assurance in soil compaction," *Proc., XIXth PIARC World Road Congress*, 468-477, Marrakesh.

1992

12. Pietzsch, D., and Poppy, W. (1992). "Simulation of soil compaction with vibratory rollers", *Journal of Terramechanics*, 29(6), 585-597.

1993

13. Sandström, Å. (1993). "Oscillatory compaction." *Proc., XII IRF World Road Congress*, 957-961, May, Madrid.
14. Thurner, H. (1993). "Continuous compaction control - specifications and experience." *Proc., XII IRF World Congress*, 951-956, Madrid.
15. Watts, K.S. and Charles, J.A. (1993). "Initial assessment of a new rapid impact ground compactor." *Proceedings of the Conference on Engineered Fills*, London, Paper No. 32.

1995

16. Tateyama, K., Nakajima, S., and Fujiyama, T. (1995). "The evaluation of ground properties and its application to the automatic control of vibratory soil compactors," *Automation and Robotics in Construction XII*, Bundy, McCrea, and Szymanski (Eds), 563 – 570.

1997

17. Adam, D. (1997). "Flächendeckende dynamische verdichtungs kontrolle (FDVK) mitvibrationswalzen sonderdruck (Surface covering dynamic compaction control with vibration rollers – special edition." *Österreichische Geotechniktagung (Austrian Geotechnique Conference)*, 26 and 27 May, Vienna.
18. Adam, D. (1997). "Continuous compaction control (CCC) with vibratory rollers," *Proc., GeoEnvironment 97*, 245 – 250, November, Melbourne, Australia. Balkema, Rotterdam.
19. Adam, D., and Brandl, H. (1997). "Roller-Integrated Continuous Compaction Control of Soils", *Proc., 3rd Intl. Conf. on Soil Dynamics (ICSD-III)*, August, Tiberias, Israel.
20. Brandl, H., and Adam, D. (1997). "Sophisticated Continuous Compaction Control of Soils and Granular Materials" *Proc., XIVth Intl. Conf. on Soil Mechanics & Foundation Engineering*, Vol. 1, September, Hamburg, Germany.
21. Braithwaite, E.J and du Preez, R.W. (1997). "Rapid Impact Compaction in Southern Africa." Proceedings of the Conference on Geology for Engineering, Urban Planning and the Environment. South African Institute of Engineering Geologists, 13-14 November 1997.

1998

22. Adam, D., and Kopf, F. (1998). "Application of continuous compaction control (CCC) to waste disposal liners", *Proc. 3rd Intl. Congress on Environmental Geotechnics*, September, Lisboa, Portugal.
23. Merrifield, C.M., Cruickshank, M. and Parvizi, M. (1998). "Modelling of low energy dynamic compaction." Proceedings of the International Centrifuge Conference Centrifuge 98, Tokyo, 819-824.
24. Neilson, R.D., Rodger, A.A., Oliver, K.D., Wright, R.H. and Elliott, R.M. (1998). "Vibration assessment of high speed dynamic compaction." In B.O. Skipp (Eds.), *Ground Dynamics and Man-Made Processes* (p. 143-154). London: Thomas Telford.
25. Uchiyama, K., Kanamori, Y., Nohse, Y., and Mitsui, A. (1998). "Influence of soil compaction of vibrating rollers with different vibration mechanisms." *Proc., of the 5th Asia-Pacific Regional Conf., of the ISTVS: Okinawa*, Japan, November, 112-119.

1999

26. Adam, D., (1999). "Elastic plastic modelling of homogeneous and layered soil under dynamic loading". *Proc. Of COST 337 & ETC 11 Workshop on Modelling and Advanced Testing for Unbound Granular Materials*, January, Lisboa, Portugal.
27. Adam, D. (1999). "Flächendeckende dynamische verdichtungskontrolle mit vibrationswalzen. (Continuous Compaction Control with vibratory rollers)". *Austrian Engineer and Architect Magazine* 144, Class Number 2, Vienna, 65-74 (in German).
28. Adam, D. (1999). "Geotechnics of the Austrian-Hungarian Highway A4", *Geotechnical Engineering for Transportation Infrastructure*, Barends et al. (eds), Balkema, Rotterdam.
29. Nohse, Y., Uchiyama, K., Kanamori, Y., Kase, J., Kawai, Y., Masumura, K., and Tateyama, K. (1999). "An attempt applying a new control system for the vibratory compaction using GPS and CMV in the embankment construction (Part 1)." *Proc. of the 13th Intl. Conf. of the ISTVS: Okinawa*, Japan, 295-300.

2000

30. Adam, D., and Kopf, F. (2000). "Sophisticated compaction technologies and continuous compaction control," *Workshop on Compaction of Soils and Granular Materials, Modeling of Compacted Materials, Compaction Management and Continuous Control*, International Society of Soil Mechanics and Geotechnical Engineering (European Technical Committee), 207 - 220, Paris.
31. Adam, D., and Kopf, F. (2000). "Sophisticated roller compaction technologies and roller-integrated compaction control." *Compaction of Soils, Granulates and Powders*, A.A.Balkema, Rotterdam, Brookfield, 113-132.
32. Anderegg, R., (2000). "ACE Ammann Compaction Expert – automatic control of the compaction." *Workshop on Compaction of Soils and Granular Materials, Modeling of Compacted Materials, Compaction Management and Continuous Control*, International Society of Soil Mechanics and Geotechnical Engineering (European Technical Committee), 229-236, Paris.
33. Floss, R. and Kloubert, H., (2000), "Newest Developments in Compaction Technology," *Workshop on Compaction of Soils and Granular Materials, Modeling of Compacted Materials, Compaction Management*

and Continuous Control, International Society of Soil Mechanics and Geotechnical Engineering (European Technical Committee), Paris.

34. Thurner, H., Sandström, Å. (2000). "Continuous Compaction Control, CCC." *Workshop on Compaction of Soils and Granular Materials, Modeling of Compacted Materials, Compaction Management and Continuous Control*, International Society of Soil Mechanics and Geotechnical Engineering (European Technical Committee), 237-246, Paris.

2001

35. Adam, D. (2001). "Sophisticated compaction of soil, earth structures, roads and rail tracks." *Proc., 5th Intl. Geotech. Conf. Geotechnical Structures Optimization*, September, Bratislava, Slovakia.
36. Adam, D., Markiewicz, R. (2001). "Compaction behaviour and depth effect of the polygon-drum," *Geotechnics for Roads, Rail Tracks and Earth Structures*, A.A.Balkema Publishers, Lisse /Abingdon/ Exton (pa) /Tokyo, 27-36.
37. Brandl, H. (2001). "The importance of optimum compaction of soil and other granular material," *Geotechnics for Roads, Rail Tracks and Earth Structures*, A.A.Balkema Publishers, Lisse /Abingdon/ Exton (Pa) /Tokyo, 47-66.
38. Brandl, H. (2001). "Compaction of soil and other granular material – interactions," *Geotechnics for Roads Rail Tracks and Earth Structures*, A.A.Balkema Publishers, Lisse /Abingdon/ Exton (Pa) /Tokyo, 3-11.
39. Kröber, W., Floss, E., Wallrath, W. (2001). "Dynamic soil stiffness as quality criterion for soil compaction," *Geotechnics for Roads, Rail Tracks and Earth Structures*, A.A.Balkema Publishers, Lisse /Abingdon/ Exton (Pa) /Tokyo, 189-199.
40. Minchin, R.E. Thomas, H.R. Swanson, D.C. (2001). "Theory behind a vibration-based quality-based asphalt density measuring system," *Transportation Research Record No. 1761, Journal of the Transportation Research Board*, National Academy of Press, 70-78.
41. Mooney, M., Bouton, C., and Pan, J. (2001). "Measurement of acceleration during vibratory compaction of unsaturated soils." *Proc. of 10th Int. Conf. Soil Dynamics & Earthquake Engineering*, Philadelphia, Pa.

2002

42. Kloubert, H. (2002). "Asphalt manager with high efficient compaction system for better roads," *Proc., Intl. Conf. on Bituminous Mixtures and Pavements*, Thessaloniki, Greece.
43. Mooney, M., Gorman, P.B., Chan, G., and Srour, C. (2002). "Observed changes in vibratory roller signature during soil compaction." *Proc., 1st European Conf. on Structural Health Monitoring*, Balageas D. L. (Ed), July, Paris, France.
44. Mooney, M., Chan, G.B., Farouk, E. and Pan, J. (2002). "Health monitoring during vibratory compaction of soil", *Proc., 9th Intl. Symp. on Smart Structures and Materials*, San Diego, CA. March 18-22, Vol. 4696, 112-123.
45. Nohse, Y., Kitano, M. (2002). "Development of a new type of single drum vibratory roller." *Proc., 14th Intl. Conf. of the Intl. Soc. for Terrain-Vehicle Systems*, Vicksburg, MS, October.

2003

46. Adam, D., Brandl, H. (2003). "Sophisticated roller integrated continuous compaction control." *Proc., 12th Asian Regional Conf. on Soil Mechanics and Geotechnical Engineering - Geotechnical Infrastructure for the New Millennium*, August, Singapore.
47. Gorman, P. and Mooney, M. (2003). "Monitoring roller vibration during compaction of crushed rock," *Proc., 20th Intl. Symp. on Automation and Robotics in Construction*, Eindhoven, Netherlands, Ger Maas & Frans van Gassel, Eds., 415-419.
48. Minchin, R. E., Thomas, H, R. (2003). "Validation of vibration-based onboard asphalt density measuring system." *J. Const. Eng. and Mgmt.*, 129(1), February. 1-7.
49. Preisig, M., Caprez, M., and Amann, P. (2003). "Validation of continuous compaction control (CCC) methods." *Workshop on Soil Compaction*, September, Hamburg.

2004

50. Adam, D., and Kopf, F. (2004). "Operational devices for compaction optimization and quality control (Continuous Compaction Control & Light Falling Weight Device)." *Proc., of the Intl. Seminar on Geotechnics in Pavement and Railway Design and Construction*, December, Athens, Greece (Invited paper), 97-106.

51. Anderegg R., and Kaufmann, K. (2004). "Intelligent compaction with vibratory rollers - feedback control systems in automatic compaction and compaction control," *Transportation Research Record No. 1868, Journal of the Transportation Research Board*, National Academy Press, 124-134.
52. Brandl, H., Adam, D. (2004). "Continuous compaction control (CCC) for fill dams and roller compacted concrete dams," *New Developments in Dam Engineering – Proc., 4th Intl. Conf. on Dam Engineering*, October, Nanjing, China (Keynote paper), 17-44.
53. Kloubert, H. (2004). "Intelligent VARIOCONTROL rollers with integrated quality control system for soil compaction: principle, measurement, applications." *Proc., 83rd Annual Transportation Research Board Meeting, Workshop 414*, January 11-14. Washington, D.C.
54. Sandström A.J., and Pettersson, C.B. (2004). "Intelligent systems for QA/QC in soil compaction", *Proc., 83rd Annual Transportation Research Board Meeting*, January 11-14. Washington, D.C.

2005

55. Adam, D., and Kopf, F. (2005). *Flächendeckende Dynamische Verdichtungskontrolle (FDVK) - Kalibrierung und Anwendung gemäß RVS 8S.02.6 (Continuous Compaction Control (CCC) - calibration and application according to the Austrian specification RVS 8S.02.6)*, Austrian Engineer and Architect Magazine 150, Class Number 4-5/2005, Vienna. (in German).
56. Mooney, M. A., Gorman, P. B. and Gonzalez, J. N. (2005). "Vibration Based Health Monitoring During Earthwork Construction," *Structural Health Monitoring*, 4(2), 137-152.
57. Mooney, M.A., Bouton, C.O. (2005). "Vibratory plate loading of compacted and instrumented field soil beds." *Geotech. Test. J.*, 28(3), 221-230.
58. Minchin, R., Swanson, D., and Thomas, H. (2005). "Computer methods in intelligent compaction." *Proc., 2005 Intl. Conf. on Computing in Civil Engineering*, Cancun, CD-ROM.
59. Rinehart, R. and Mooney, M. (2005). "Instrumentation of a Roller Compactor to Monitor Earthwork Compaction," *Proc. 22nd Int. Symp. Automation and Robotics in Construction*, Sept. 11-14, Ferrara, Italy.
60. White, D.J, Jaselskis, E., Schaefer, V., and Cackler, E. (2005). "Real-time compaction monitoring in cohesive soils from machine response." *Transportation Research Record No. 1936*, National Academy Press, 173-180.
61. Yongfeng, J., Guangfeng, L., Yindi, F., Zongyi, L. (2005). "Intelligent compaction control based on fuzzy neural network." *Proc., 6th Intl. Conf. on Parallel and Distributed Computing, Application, and Technologies (PDCAT'05)*, IEEE Computer Society, 5-8 December, Dalian, China.

2006

62. Anderegg, R., von Felten, D., and Kaufmann, K. (2006). "Compaction monitoring using intelligent soil compactors." *Proc., GeoCongress 2006: Geotechnical Engineering in the Information Technology Age*, February, Atlanta, CD-ROM.
63. Camargo, F., Larsen, B., Chadbourn, B., Roberson, R., and Siekmeier, J. (2006). "Intelligent compaction: a Minnesota case history." *Proc., 54th Annual University of Minnesota Geotech. Conf.*, February, Minneapolis, CD-ROM
64. Hossain, M., Mulandi, J., Keach, L., Hunt, M., and Romanoschi, S. (2006). "Intelligent compaction control." *Proc., 2006 Airfield and Highway Pavement Specialty Conf.*, ASCE, May, Atlanta, Ga.
65. Mooney, M., Rinehart, R., and van Susante, P. (2006). "The Influence of Heterogeneity on Vibratory Roller Compactor Response," *Proc., GeoCongress 2006: Geotechnical Engineering in the Information Technology Age*, February, Atlanta, CD-ROM.
66. Petersen, D., Siekmeier, J., Nelson, C., Peterson, R. (2006). "Intelligent soil compaction – technology, results and a roadmap toward widespread use." *Transportation Research Record No. 1975, Journal of the Transportation Research Board*, National Academy Press, 81-88.
67. Tawfik, E. (2006). "Validation of numerical evaluation of dynamic response of lumped parameter systems using Runge-Kutta-Nystrom (R-K-N) method." *Proc., GeoCongress 2006: Geotechnical Engineering in the Information Technology Age*, February, Atlanta, CDROM.
68. White, D.J, Morris, M., and Thompson, M. (2006), "Power-based compaction monitoring using vibratory padfoot," *Proc., GeoCongress 2006: Geotechnical Engineering in the Information Technology Age*, Atlanta, CD-ROM.

2007

69. Mooney, M. A., and Adam, D. (2007). "Vibratory roller integrated measurement of earthwork compaction: An overview." *Proc., 7th Intl. Symp. on Field Measurements in Geomechanics: FMGM 2007*, ASCE, Boston, Ma.
70. Mooney, M. A. and Rinehart, R. (2007). "Field Monitoring of Roller Vibration during Compaction of Subgrade Soil," *Journal of Geotechnical and Geoenvironmental Engineering*, ASCE, 133(3), 257-265.
71. Ryden, N. and Mooney, M. (2007). "Surface Wave Testing to Investigate the Nature of Roller Determined Soil Stiffness," *Proc. Symp. on the Application of Geophysics to Engineering and Environmental Problems: SAGEEP 2007*, Denver, Colorado, April, 1388-1394.
72. Scherocman, J., Rakowski, S., and Uchiyama, K. (2007). "Intelligent compaction, does it exist?" 2007 *Canadian Technical Asphalt Association (CTAA) Conference*, Victoria, BC, July.
73. Thompson, M., and White, D. (2007). "Field calibration and spatial analysis of compaction monitoring technology measurements." *Transportation Research Record No. 2004, Journal of the Transportation Research Board*, National Academy Press, 69-79.

2008

74. Commuri, S., Mai, A., Zaman, M. (2008). "Neural Network-Based Intelligent compaction Analyzer for Estimating Compaction Quality of Hot Asphalt Mixes." *Proc., 17th World Congress – The Intl. Federation of Automatic Control*, Seoul, Korea, July 6-11.
75. Commuri, S., Zaman, M. (2008). "A novel neural network-based asphalt compaction analyzer," *Int. J. of Pavement Engineering*, 9(3), 177-188.
76. Kauffman, K., Anderegg, R. (2008). "3D-Construction Applications III GPS-based Compaction Technology", *1st Intl. Conf. on Machine Control & Guidance 2008*, ETH Zurich, Switzerland.
77. Newman, K., and White, D. (2008). "Rapid assessment of cement/fiber stabilized soil using roller-integrated compaction monitoring." *Transportation Research Record: Journal of the Transportation Research Board*, National Academy Press (accepted).
78. Rahman, F., Hossain, M., Hunt, M., Romanoschi, S.A. (2008). "Soil stiffness evaluation for compaction control of cohesionless embankments." *Geotech. Test. J.*, 31(5).
79. Rinehart, R., and Mooney, M. (2008). "Instrumentation of a roller compactor to monitor vibration behavior during earthwork compaction." *Journal of Automation in Construction*, 17(2), 144-150.
80. Rinehart, R.V., Mooney, M.A. and Berger, J.R. (2008). "In-Ground Stress-Strain beneath Center and Edge of Vibratory Roller Compactor." *Proc. 1st Intl. Conf. Transportation Geotechnics*, Nottingham, U.K., Aug. 25-27.
81. Thompson, M., and White, D. (2008). "Estimating compaction of cohesive soils from machine drive power." *J. of Geotech. and Geoenviron. Engg*, ASCE, 134(12), 1771-1777.
82. Thompson, M., White, D., Gieselman, H., and Siekmeier, J. (2008). "Variable feedback control intelligent compaction to evaluate subgrade and granular pavement layers – Field study at Minnesota US 14." *Proc., 87th Annual Transportation Research Board Meeting*, Washington, D.C.
83. van Susante, P. and Mooney, M.A. (2008). "Capturing Nonlinear Roller Compactor Behavior through Lumped Parameter Modeling." *J. Engr. Mechanics*, ASCE, 2008, 134(8), 684-693.
84. White, D., and Thompson, M. (2008). "Relationships between in-situ and roller-integrated compaction measurements for granular soils." *J. of Geotech. and Geoenviron. Engrg*, ASCE, 134(12), 1763-1770.
85. White, D., Thompson, M., Vennapusa, P., and Siekmeier, J. (2008). "Implementing intelligent compaction specifications on Minnesota TH 64: Synopsis of measurement values, data management, and geostatistical analysis." *Transportation Research Record: Journal of the Transportation Research Board*, 2045, 1-9.
86. White, D., Vennapusa, P., Gieselman, H. (2008). "Roller-integrated compaction monitoring technology: Field evaluation, spatial visualization, and specifications." *Proc., 12th Intl. Conf. of Intl. Assoc. for Computer Methods and Advances in Geomechanics (IACMAG)*, 1-6 October, Goa, India.

2009

87. Commuri, S., Mai, A. (2009). "Field validation of the intelligent asphalt compaction analyzer." *Proc. 17th Mediterranean Conf. on Control & Automation*, June 24-26, Makedonia Palace, Thessaloniki, Greece.
88. Commuri, S., Mai, A., Zaman, M. (2009). "Calibration Procedures for the Intelligent Asphalt Compaction Analyzer," *ASTM Journal of Testing and Evaluation*, 37(5), 454-462.

89. Facas, N., Mooney, M.A., and Furrer, R. (2009). "Geostatistical Analysis of Roller-Integrated Continuous Compaction Control Data." *Proc. 8th Intl. Conf. Bearing Capacity of Roads, Railways and Airfields*, June 29-Aug 2, Urbana-Champaign, IL.
90. Mooney, M.A., and Rinehart, R.V. (2009). "In-Situ Soil Response to Vibratory Loading and its Relationship to Roller-Measured Soil Stiffness." *J. Geotech. & Geoenv. Engineering*, ASCE, 135(8), 1022-1031.
91. Rinehart, R.V. and Mooney, M.A. (2009). "Measurement Depth of Vibratory Roller-Measured Soil Stiffness." *Géotechnique*, 59(7), 609-619.
92. Rinehart, R.V., Berger, J.R., and Mooney, M.A. (2009) "Comparison of Stress States and Paths- Vibratory Roller-Measured Soil Stiffness and Resilient Modulus Testing" *Journal of the Transportation Research Board*, No. 2116, Transportation Research Board of the National Academies, Washington.
93. Tehrani, F.S., and Meehan, C.K. "Continuous compaction control: Preliminary data from a Delaware case study." *Eighth Intl. Conf. on the Bearing Capacity of Roads, Railways, and Airfields (BCR2A'09)*, June 29 – July 2, Champaign, Illinois.
94. Vennapusa, P., White, D.J., Gieselmann, H. (2009). "Influence of support conditions on roller-integrated machine drive power measurements for granular base." *Intl. Foundation Congress and Equipment Expo (IFCEE) 2009*, 15-19 March, Orlando, Florida.
95. White, D.J., Vennapusa, P., Gieselmann, H., Johanson, L., Siekmeier, J. (2009). "Alternatives to heavy test rolling for cohesive subgrade assessment," *Eighth Intl. Conf. on the Bearing Capacity of Roads, Railways, and Airfields (BCR2A'09)*, June 29 – July 2, Champaign, Illinois.

2010

96. Facas, N., Mooney, M.A. (2010). "Positioning reporting error of intelligent compaction and continuous compaction control roller measured soil properties," *J. of Testing and Evaluation*, ASTM, 38(1).
97. Facas, N., Mooney, M.A., Furrer, R. (2010). "Anisotropy in the Spatial Distribution of Roller-Measured Soil Stiffness." *Intl. J. of Geomechanics*, 10(4).
98. Facas, N., van Susante, P., Mooney, M.A. (2010). "Influence of Rocking Motion on Vibratory Based Roller Measurement of Soil Stiffness." *J. Eng. Mech.*, Vol. 136, 898-905.
99. Vennapusa, P., White, D.J., Morris, M. (2010). "Geostatistical analysis of spatial referenced roller-integrated compaction measurements." *J. Geotech. Geoenviron. Engrg.*, ASCE, 136(6), 813-822.
100. Beainy, F., Commuri, S., and Zaman, M. (2010) "Asphalt Compaction Quality Control Using Artificial Neural Network" *49th IEEE Conference on Decision and Control 2010*, Atlanta, GA, USA

2011

101. White, D.J., Vennapusa, P., Gieselmann, H. (2011). "Field Assessment and Specification Review for Roller-Integrated Compaction Monitoring Technologies." *Special Issue: Advances in Instrumentation and Monitoring in Geotechnical Engineering in Advances in Civil Engineering Journal*, Hindawi Publishing Corporation, Volume 2011, Article ID 783836.
102. Vennapusa, P., White, D. J., Siekmeier, J., Embacher, R., (2011). "In situ mechanistic characterizations of granular pavement foundation layers." *Intl. J. of Pavement Engineering*, First published on: 15 April 2011 (iFirst).
103. Gallivan, L., Chang, G.K., Horan, R.D. (2011). "Intelligent Compaction for Improving Roadway Construction." *Proc., 2011 GeoHunan Intl. Conf.*, Hunan, China.
104. Commuri, S., Mai, A.T., Zaman, M. (2011). "Neural Network-Based Intelligent Compaction Analyzer for Estimating Compaction Quality of Hot Asphalt Mixes," *ASCE J. of Constr. Engrg., and Mgmt.*, 137(9), 634-644.
105. Beainy, F., Commuri, S., Zaman, M. (2011). "Quality Assurance of Hot Mix Asphalt Pavements Using the Intelligent Asphalt Compaction Analyzer." *ASCE J. of Constr. Engrg., and Mgmt.*, (in press).
106. Xu, Q., Chang, G.K., Gallivan, L., Horan, R.D. (2011). "Data analysis for hot-mix asphalt intelligent compaction." *Proc., 90th Annual Transportation Research Board Meeting*, Paper No. 11-1262, Washington, D.C. (CD-ROM).
107. Gallivan, L., Chang, G.K., Xu, Q., Horan, R.D. (2011). "Validation of Intelligent Compaction Measurement Systems for Practical Implementation." *Proc., 90th Annual Transportation Research Board Meeting*, Paper No. 11-0854, Washington, D.C. (CD-ROM).
108. Singh, D., Beainy, F., Mai, A., Commuri, S., Zaman, Z. (2011). "In-situ assessment of stiffness during the construction of HMA pavements." *Intl., J. of Pavement Research and Technology*, 4(3).

109. Mooney, M., Facas, N., Musimbi, O. (2011). "Estimation of Pavement Earthwork Moduli from Vibratory Roller Measurements," *Proc., 90th Annual Transportation Research Board Meeting*, Paper No. 11-1090, Washington, D.C. (CD-ROM).
110. Facas, N., Rinehart, R., Mooney, M. (2011). "Development and Evaluation of Relative Compaction Specifications Using Roller-Based Measurements." *Geotechnical Testing Journal, ASTM*, 34(6), 634-642.
111. Heersink, D.K., Furrer, R. (2011). "Spatial analysis of modern soil compaction roller measurement values." *Procedia Environmental Sciences*, Volume 7, 8-13.
112. Miller, S.R., Hartmann, T. (2011). "Measuring and visualizing hot mix asphalt concrete paving operations." *Automation in Construction*, 20(4), 474-481.
113. Gallivan, V.L., Chang, G.K., and R.D. Horan. "Practical Implementation of Intelligent Compaction Technology in Hot Mix Asphalt Pavements." *Journal of the Association of Asphalt Paving Technologies*, Vol. 80 (in press).
114. Daniel K. H., Reinhard F. (2011) "Spatial analysis of modern soil compaction roller measurement values" *1st Spatial Statistics Conference 2011*, *Procedia Environmental Sciences* 7 (2011) 1–11.e

2012

115. Xu, Q., Chang, G.K., Gallivan, L., Horan, R.D. (2012). "Influences of intelligent compaction uniformity on pavement performances of hot mix asphalt." *Construction and Building Materials*, Vol. 30, 746-752.
116. Rinehart, R., Mooney, M., Facas, N., Musimbi, O. (2012). "Examination of roller-integrated continuous compaction control on a Colorado test site." *Proc., 91st Annual Transportation Research Board Meeting*, Paper No. 12-4464, Washington, D.C. (CD-ROM).
117. Beainy, F., Commuri, S., Zaman, M. (2012). "Quality assurance of hot mix asphalt pavements using the intelligent asphalt compaction analyzer." *Journal of Construction Engineering and Management*, ASCE, 138(2).
118. Facas N., Mooney M.(2012) "Characterizing the Precision Uncertainty in Vibratory Roller Measurement Values" *Journal of Testing and Evaluation*, ASTM 40(1), DOI: 10.1520/JTE103507
119. Gallivan, L., Chang, G. (2012) "Harmonization and Standardization of Intelligent Compaction Technologies for Practical Implementation." *57th Annual conference of the Canadian technical asphalt association* Vancouver British Columbia, Canada p. 349-365.
120. Horan R.D., Chang G.K., Xu Q, Gallivan V.L. (2012) "Improving Quality Control of Hot-Mix Asphalt Paving with Intelligent Compaction Technology" *Journal of the Transportation Research Board*, No. 2268, Transportation Research Board of the National Academies, Washington. pp 82-91, DOI: 10.3141/2268-10
121. Horan R.D., Chang G.K., Xu Q., Gallivan V.L. (2012) "Improving quality control of hot mix asphalt using intelligent compaction technology" *Proceedings of Transportation Research Board Meeting*, Paper Number: 12-0916.
122. Xu Q., Chang G.K., Gallivan V.L. (2012) "Development of a systematic method for intelligent compaction data analysis and management" *Construction and Building Material* 37 (2012) 470-480
123. Hwang J., Yun H., Kim J., Suh Y., Hong S., Lee D. (2012) "Development of Soil Compaction Analysis Software (SCAN) Integrating a Low Cost GPS Receiver and Compactometer" *Journal of Sensor*, ISSN 1424-8220
124. Rinehart R.V., Mooney, M.A., Facas N.F., Musimbi O.M. (2012) "Examination of Roller-Integrated Continuous Compaction Control on Colorado Test Site", *Journal of the Transportation Research Board*, No. 2310, Transportation Research Board of the National Academies, Washington.
125. Liu, D., Sun, J., Zhong, D., and Song, L. (2012). "Compaction Quality Control of Earth-Rock Dam Construction Using Real-Time Field Operation Data." *J. Constr. Eng. Manage.*, 138(9), 1085–1094.

2013

126. Andrew J. G., William B. D., Michael H., John S., Lee P.(2013) "Locating Soil Tests with Intelligent Compaction Data and Geographic Information System Technology" *Journal of the Transportation Research Board*, No2310, Transportation Research Board of the National Academies, Washington.
127. Heersink D.K., Furrer R. (2013) "Sequential spatial analysis of large datasets with applications to modern earthwork compaction roller measurement values" *Journal of Science Direct*, *Spatial Statistics* 6(2013), 41-56.
128. Heersink D.K., Furrer R. Mooney M.A. (2013) "Intelligent Compaction and Quality Assurance of Roller Measurement Values utilizing Backfitting and Multiresolution Scale Space Analysis", arXiv: 1302.4631.

129. Xia J., (2013) "Research on the key technology of Road Machinery Intelligent" *Applied Mechanics and Materials Vols. 373-375 (2013) pp 142-145*.
130. Xu Q., Chang G.K. (2013) "Evaluation of intelligent compaction for asphalt material" *Automation in Construction*, Vol. 30, 104-112.
131. Hiroshi F., Tetsuo F. (2013) "Development of soil stiffness evaluation equipment ALFA-system using acceleration response of vibratory roller" *International Association for Automation and Robotics in Construction*.
132. White D.J., Christopher B.R., Sanchez R.L. (2013) "Performance Based QC/QA Specifications for TVA's CCP stacking facilities: Part II. Proposed Specifications" *2013 World of Coal Ash (WOCA) Conference* Lexington, KY.
133. Vennapusa P., White D.J., Schramm S. (2013) "Roller-Integrated Compaction Monitoring for Hot-Mix Asphalt Overlay Construction" *Journal of Transportation Engineering*, ASCE 139(12).
134. White, D.J., Becker, P., Vennapusa, P., Dunn, M., and White, C. (2013). "Soil Stiffness Assessment of Stabilized Pavement Foundations." *Transportation Research Record, Journal of Transportation Research Board*, 2235, 99-109.
135. Beainy, F., Commuri, S., Zaman, M., and Syed, I. (2013). "Viscoelastic-Plastic Model of Asphalt-Roller Interaction." *Intl. Journal of Geomechanics*, Vol. 13, No. 5, 581-594.
136. Cacciola, D., Meehan, C., and Khosravi, M. (2013), "An Evaluation of Specification Methodologies for Use with Continuous Compaction Control Equipment." *Geo-Congress 2013*: pp. 413-416.
137. Meehan, C.L., Khosravi, M., and Cacciola, D.V. (2013). "Monitoring Field Lift Thickness Using Compaction Equipment Instrumented with Global Positioning System (GPS) Technology," *Geotechnical Testing Journal*, 36(5).

2014

138. Xu, Q., Chang, G., and Gallivan, L. (2014). "A Sensing-Information-Statistics Integrated Model Predicting Material Density with Intelligent Construction System", IEEE/ASME Transactions on Mechatronics, IEEE XPLore publication.
139. Xu, Qinwu, and Chang, G. (2014). "Experimental and Numerical Study of Asphalt Material Geospatial Heterogeneity with Intelligent Compaction Technology on Roads", *Construction & Building Materials*, Vol. 72, 189-198.
140. Chang, G.K., Gallivan, L., Xu, Q. (2014). "Assess asphalt in-place density with intelligent compaction measurements", *12th International Conference on Asphalt Pavements, ISAP 2014*, Raleigh, NC.
141. Vennapusa, P., and White, D.J. (2014). "Interpretation of Dual-Integrated Compaction Measurements on Layered Granular Fill", *Geo-Congress 2014 – Geo-Characterization and Modeling for Sustainability*, ASCE, Feb 23-26, Atlanta.
142. White, D. J., Vennapusa, P., and Dunn, M. (2014). "A Road Map for Implementation of Intelligent Compaction Technology." *Geo-Congress 2014 – Geo-Characterization and Modeling for Sustainability*, ASCE, Feb 23-26, Atlanta.
143. Becker, P., White, D.J., Vennapusa, P., and Dunn, M. (2014). "Freeze-Thaw Performance Assessment of Stabilized Pavement Foundations." *Proc. of 2014 Annual Transportation Research Board Meeting*, Washington, D.C.
144. Beainy, F., Commuri, S., and Zaman, M. (2014). "Dynamical Response of Vibratory Rollers during the Compaction of Asphalt Pavements." *J. Eng. Mech.*, 140(7), 04014039.
145. Dondi, G., Sangiorgi, C., and Lantieri, C. (2014). "Applying Geostatistics to Continuous Compaction Control of Construction and Demolition Materials for Road Embankments." *J. Geotech. Geoenviron. Eng.*, 140(3), 06013005.
146. Liu, D., Li, Z., Lian, Z. (2014). "Compaction quality assessment of earth-rock dam materials using roller-integrated compaction monitoring technology." *Automation in Construction*, Vol. 44, 234-246.
147. D.H. Liu, A.G. Wang, Y.G. Liu, B.Y. Li, Real-time monitoring and assessment of compaction quality for earth-rock dam basing on roller vibration behavior analysis, *J. Hydraul. Eng.* 45 (2), 60–67.

148. Barman, M., Nazari, M., Imran, S.A., Commuri, S., Zaman, M., Beainy, F., Singh, D. (2014). "Application of Intelligent Compaction Technique in Real-Time Evaluation of Compaction Level during Construction of Subgrade." *Presented at the 93rd Annual Transportation Research Board Meeting*, Washington, D.C.
149. Imran, S.A., Beainy, F., Commuri, S., and Zaman, M. (2014). "Dynamical model of asphalt-roller interaction during compaction," *Informatics in Control, Automation and Robotics (ICINCO)*, Vienna, Austria.
150. Singh, D., Beainy, F., Commuri, S., and Zaman, M. (2014) Application of Intelligent Compaction Technology for Estimation of an Effective Modulus for a Multilayered Asphalt Pavement. *Recent Developments in Evaluation of Pavements and Paving Materials*: pp. 51-58.
151. Correia, A.G., Parente, M. (2014). "Intelligent Compaction Technology for Geomaterials: A demonstration project." *Transport Research Arena 2014*, Paris.
152. White, D.J. (2014). "Geotechnical IT Revolution: Intelligent Compaction and Beyond." *GeoStrata-Geoinstitute of ASCE*, Vol. 18, No. 5, 42-48.
153. Hofer, T. "Continuous Asphalt Density Measurements on a Roller," *Presented at the 93rd Annual Transportation Research Board Meeting*, Washington, D.C.

2015

154. Barman, M., Imran, S., Nazari, M., Commuri, S., and Zaman, M. (2015). "Intelligent Compaction of Stabilized Subgrade of Flexible Pavement." *IFCEE 2015*: pp. 2554-2566.
155. White, D.J., Vennapusa, P., Hageman, E., Christopher, B., McClung, N., Sanchez, R. (2015). "Effects of Micromorphology and Chemical Composition on Densification of CCPs", *2015 World of Coal Ash (WOCA) Conference*, May 4-7, Nashville, Tennessee.
156. White, D.J., Vennapusa, P., Hageman, E., Christopher, B., McClung, N., Sanchez, R. (2015). "Assessment of New QC/QA Compaction Monitoring Program at TVA's Coal Combustion Product Stacking Facilities: A Case Study", *2015 World of Coal Ash (WOCA) Conference*, May 4-7, Nashville, Tennessee.
157. Singh, D., Beainy, F., Commuri, S., and Zaman, M. (2015). "Application of Intelligent Compaction Technology for Estimation of Effective Modulus for a Multilayered Asphalt Pavement." *Journal of Testing and Evaluation*, 10.1520/JTE20130305, 20130305.
158. Cai, H., Kuczek, T., Dunston, P.S. (2015). "Field Experiment for Correlating Intelligent Compaction Data to In-Situ Soil Compaction Quality Measurements," *Presented at the 94th Annual Transportation Research Board Meeting*, Washington, D.C.
159. Kassem, E., Liu, W., Scullion, T., Masad, E., Chowdhury, A. (2015). "Development of compaction monitoring system for asphalt pavements," *Construction and Building Materials*, Vol. 96, 334-345.
160. Neff, A., McAdams, M., Wang, J., Mooney, M. (2015). "Analysis of center of gravity roller drum soil stiffness on compacted layered earthwork," *Canadian Geotechnical Journal*, Vol. 52, No. 4, 459-468.
161. Nie, Z., Wang, X., and Jiao, T. (2015). "Anomalous Data Detection for Roller-Integrated Compaction Measurement." *Int. J. Geomech.* , 10.1061/(ASCE)GM.1943-5622.0000498 , B4015004.
162. Kenneally, B., Musimbi, O.M., Wang, J., Mooney, M. A. (2015). "Finite element analysis of vibratory roller response on layered soil systems." *Computers and Geotechnics*, Vol. 67, 73-82.

2016

163. Kumar, S. A., Aldouri, R., Nazarian, S., & Si, J. (2016). Accelerated assessment of quality of compacted geomaterials with intelligent compaction technology. *Construction and Building Materials*, 113, 824-834.
164. Kumar, S. A., Mazari, M., Garibay, J., Aldouri, R. E., Nazarian, S., & Si, J. (2016). Compaction Quality Monitoring of Lime-Stabilized Clayey Subgrade Using Intelligent Compaction Technology. *In 2016 International Conference on Transportation and Development*, American Society of Civil Engineers, 778-790.
165. Hu, W., Huang, B., Shu, X., & Woods, M. (2016). Utilizing intelligent compaction meter values to evaluate construction quality of asphalt pavement layers. *Road Materials and Pavement Design*, 1-12.
166. Imran, S. A., Barman, M., Nazari, M., Commuri, S., Zaman, M., & Singh, D. (2016). Continuous Monitoring of Subgrade Stiffness during Compaction. *Transportation Research Procedia*, 17, 617-625.

167. Mazari, M., Beltran, J., Aldouri, R., Chang, G., Si, J., & Nazarian, S. (2016). Evaluation and Harmonization of Intelligent Compaction Systems. In *International Conference on Transportation and Development 2016* (pp. 838-846).
168. Barman, M., Nazari, M., Imran, S. A., Commuri, S., & Zaman, M. (2016). Quality Improvement of Subgrade through Intelligent Compaction. *Transportation Research Record: Journal of the Transportation Research Board*, (2579), 59-69.
169. Barman, M., Nazari, M., Imran, S. A., Commuri, S., Zaman, M., Beainy, F., & Singh, D. (2016). Quality control of subgrade soil using intelligent compaction. *Innovative Infrastructure Solutions*, 1(1), 23.
170. Hu, W., Shu, X., Huang, B., & Woods, M. (2016). Field investigation of intelligent compaction for hot mix asphalt resurfacing. *Frontiers of Structural and Civil Engineering*, 1-9.
171. Anjan Kumar, S., Mazari, M., Garibay, J., Aldouri, R. E., Nazarian, S., & Si, J. (2016). Compaction Quality Monitoring of Lime-Stabilized Clayey Subgrade Using Intelligent Compaction Technology. In *International Conference on Transportation and Development 2016* (pp. 778-790).
172. Vennapusa, P. K., & White, D. J. (2016). Influence of Foundation Support Conditions on the Intelligent Compaction Measurements for Hot-Mix Asphalt. In *Geo-Chicago 2016* (pp. 550-559).
173. Vennapusa, P. K., & White, D. J. (2016). Machine Drive Power Based Roller-Integrated Compaction Measurements for Cohesive Embankment Construction. In *Geo-Chicago 2016* (pp. 571-580).
174. Savan, C. M., Ng, K. W., & Ksaibati, K. (2016). Benefit-cost analysis and application of intelligent compaction for transportation. *Transportation Geotechnics*, 9, 57-68.
175. Liu, D., Lin, M., & Li, S. (2016). Real-time quality monitoring and control of highway compaction. *Automation in Construction*, 62, 114-123.
176. Xu, Q., & Chang, G. K. (2016). Adaptive quality control and acceptance of pavement material density for intelligent road construction. *Automation in Construction*, 62, 78-88.
177. Herrera, C., & Caicedo, B. (2016). Finite Difference Time Domain Simulations of Dynamic Response of Thin Multilayer Soil in Continuous Compaction Control. *Procedia Engineering*, 143, 411-418.
178. Kuenzel, R., Teizer, J., Mueller, M., & Blikle, A. (2016). SmartSite: Intelligent and autonomous environments, machinery, and processes to realize smart road construction projects. *Automation in Construction*, 71, 21-33.
179. Masad, E., Scarpas, A., Rajagopal, K. R., Kassem, E., Koneru, S., & Kasbergen, C. (2016). Finite element modelling of field compaction of hot mix asphalt. Part II: Applications. *International Journal of Pavement Engineering*, 17(1), 24-38.
180. Olague, P. B. and Kreinovich, V. (2016). Why half frequency in intelligent compaction, *Proceedings of the 4th International Conference on Mathematical and Computer Modeling*, Omsk, Russia.
181. Tateyama, K. (2016). Achievement and Future Prospects of ICT Construction in Japan. *Journal of Robotics and Mechatronics*, 28(2), 123-128.

2017

182. Hu, W., Shu, X., Huang, B., & Woods, M. (2017). Utilizing intelligent compaction meter values to evaluate construction quality of asphalt pavement layers. *Road Materials and Pavement Design*, Vol. 18, Issue 4, 980-991.
183. Cai, H., Kuczek, T., Dunston, P.S., and Li, S. Correlating Intelligent Compaction Data to In Situ Soil Compaction Quality Measurements, *Journal of Construction Engineering and Management*, Vol 143, Issue 8, 04017038.
184. Imran, S. A., Commuri, S., Barman, M., Zaman, M., & Beainy, F. (2017). Modeling the Dynamics of Asphalt–Roller Interaction during Compaction. *Journal of Construction Engineering and Management*, 143(7), 04017015.
185. Meehan, C. L., Cacciola, D. V., Tehrani, F. S., & Baker, W. J. (2017). Assessing soil compaction using continuous compaction control and location-specific in situ tests. *Automation in Construction*, 73, 31-44.
186. Zhang, Z., Huang, S., & Zhang, K. (2017). Accurate detection method for compaction uniformity of asphalt pavement. *Construction and Building Materials*, 145, 88-97.

187. White, D. J., Vennapusa, P., FitzPatrick, B., Hill, J.F., and McClung, N. (2017). "In situ characterization of lime-treated fly ash stack at TVA's Gallatin Ash Stacking Facility," *2017 World of Coal Ash (WOCA) Conference*, Lexington, KY.
188. White, D. J., Vennapusa, P., Hill, J.F., Eric Hageman, McClung, N., FitzPatrick, B., (2017). "Validated integrated compaction monitoring at TVA's KIF coal combustion product stacking facility," *USSD 2017 Annual Meeting*, Anaheim, CA.

Research Reports (Organized by publication date)

1978

1. Thurner, H., Forssblad, L. (1978). *Compaction meter on vibrating rollers*, Research Bulletin of Dynapac AB. No. 8022, Solna.

1980

2. Thurner, H., Sandström, Å. (1980). *Compaction meter on vibrating roller*, Dynapac Research, Solna.

1982

3. Geodynamik. (1982). *Compactometer, compaction meter for vibratory rollers ALFA-030*, Internal Report, Geodynamik, Stockholm, Sweden.

1984

4. Forssblad, L. (1984). *Compaction control using vibratory rollers equipped with compaction meter –studies at Arlanda airport*, Research Bulletin No. 8031, Dynapac, Sweden.

1985

5. Hoover, J.M. (1985). *In-situ stability of smooth-drum vibratory compacted soils with Bomag Terrameter*, Engineering Research Institute, ERI Project No. 1722, Iowa State University, Ames, Iowa, March.

1989

6. DYNAPAC (1989). *Compaction and paving, theory and practice*, Karlskrona, Sweden.

1991

7. Floss, R. (1991). "Dynamische verdichtungsprüfung bei erd- und straßenbauten (Dynamic compression check with earth constructions and road constructions)," Notebook 612, Research and Traffic Technology, Federal Ministry for Traffic, Germany (in German).

1992

8. Snowdon, R. (1992). *Compaction monitoring devices for earthworks*, Transport Research Laboratory, Research report No. 361, Crowthorne, Berkshire.

1994

9. Sandström, Å. (1994). *Numerical simulation of a vibratory roller on cohesionless soil*, Internal Report, Geodynamik, Stockholm, Sweden.

1996

10. SAKAI (1996). *Compaction equipment, theory and practice*, Takayanagi, Japan.

1999

11. AMMANN (1999). *Einige Aspekte der Verdichtung*, Langenthal, Schweiz
12. Kopf, F., (1999). *Continuous Compaction Control (CCC) During compaction of soils by means of dynamic rollers with different kinds of excitation*, Ph.D. Dissertation, Technical University of Vienna, Faculty of Civil Engineering, Vienna, Austria.

2000

13. Adam, D., and Brandl, H. (2000). *Flächendeckende dynamische verdichtungskontrolle (FDVK) mit vibrationswalzen - vrunlagenforschung und praktische anwendung (Continuous Compaction Control with vibratory rollers - basic research and practical application)*, Road Research Publications Number 506, Research Project No. 3.147, Federal Ministry of Economic Affairs, Vienna (in German).
14. Adam, D., and Brandl, H. (2000). *Flächendeckende dynamische verdichtungskontrolle (FDVK) mit vibrationswalzen - vrunlagenforschung und praktische anwendung (Continuous Compaction Control with vibratory rollers - basic research and practical application)*, Road Research Publications Number 506, Research Project No. 3.147, Federal Ministry of Economic Affairs, Vienna (in German).

2002

15. Adam, D., Brandl, H. (2002). "Roller-integrated continuous compaction control of soils" *Annuaire del'universite d'architecture, de genie civil et de geodesie - Sofia, Bulgaria* (in French).
16. Adam, D., Brandl, H., and Kopf, F. (2002). *Flächendeckende Dynamische Verdichtungskontrolle (FDVK) mit unterschiedlich angeregten dynamischen Walzen - Grundlagenforschung und praktische Anwendung (Continuous Compaction Control with differently excited rollers - basic research and practical application)*, Road Research Publications Number 517, Research Project No. 3.176, Federal Ministry for Traffic, Innovation and Technology, Vienna (in German).
17. AMMANN (2002). *European and U.S. Patents on the ACE-System*, AMMAN Verdichtung AG, Langenthal, Switzerland.

2003

18. AMMANN (2003). *ACE-Soil Compaction and Compaction Control – CD ROM*, AMMAN, Verdichtung AG, Langenthal, Switzerland.
19. Briaud, J. L., Seo, J. (2003). *Intelligent Compaction: Overview and Research Needs*, Texas A&M University.
20. Dumas, C., Mansukhani, S., Porbaha, A., Short, R., Cannon, R., McLain, K. Putcha, S., Macnab, A., Lwin, M., Pelnik, T.W., Brown, D., Christopher, B.C. (2003). *Innovative Technology for Accelerated Construction of Bridge and Embankment Foundations in Europe*, FHWA-PL-03-014., FHWA, Washington, D.C.
21. Mooney, M.A., Gorman, P.B., Tawfik, E.F., Gonzalez, J.N. and Akanda, A.S. (2003). *Exploring Vibration-Based Intelligent Soil Compaction*, Oklahoma Department of Transportation Report, Item 2146.

2004

22. Adam, D., and Kopf, F. (2004). *Anwendung der Flächendeckenden Dynamischen Verdichtungskontrolle (FDVK) im Deponiebau (Application of Continuous Compaction Control (CCC) for landfill construction)*, Österreichische Wasser- und Abfallwirtschaft Heft (in German).
23. White, D.J, Jaselskis, E., Schaefer, V., Cackler, T., Drew, I., and Li, L. (2004). *Field Evaluation of Compaction Monitoring Technology: Phase I*, Final Report, Iowa DOT Project TR-495, Iowa State University, Ames, Ia.

2005

24. Adam, D., Brandl, H., and Kopf, F. (2005). *Continuous Compaction Control (CCC) with differently excited rollers*, Schriftenreihe der Straßenforschung Heft 553, Forschungsvorhaben Nr. 3.176 (Road Research Publications No. 553, Research Project No. 3.176), Federal Ministry of Traffic, Innovation, and Technology, Vienna (in German).
25. Petersen, D. (2005). *Continuous compaction control – MnROAD demonstration*, Mn/DOT Report MN/RC – 2005-07, CNA Consulting Engineers, Minneapolis, Mn.

2006

26. Petersen, L., and Peterson, R. (2006). *Intelligent Compaction and In-Situ Testing at Mn/DOT TH53*, Final Report MN/RC-2006-13, May, Minnesota Department of Transportation, St. Paul, Mn.
27. Sebesta, S., Estakhri, C., Scullion, T., Liu W. (2006). *New technologies for evaluating flexible pavement construction: Year 1 report*, FHWA/TX-06/0-4774-1, Texas Transportation Institute, The Texas A&M University System, College Station, Tx.
28. Scullion, T., Sebesta, S., Rich, D., and Liu, W. (2006). *Field evaluation of new technologies for measuring pavement quality*, FHWA/TX-06/0-4774-2, Texas Transportation Institute, The Texas A&M University System, College Station, Tx.
29. White, D.J, Thompson, M., Jovaag, K., Morris, M., Jaselskis, E., Schaefer, V. and Cackler, E. (2006). *Field evaluation of compaction monitoring technology: Phase II*. Final Report, Iowa DOT Project TR-495, Iowa State University, Ames, Ia.

30. Zambrano, C., Drnevich, V., Bourdeau, P. (2006). *Advanced Compaction Quality Control*, Indiana DOT Final Report FHWA/IN/JTRP – 2006/10, Purdue University.

2007

31. Maupin, G.W. (2007). *Preliminary Field Investigation of Intelligent Compaction of Hot-Mix Asphalt*, Research Report VTRC 08-R7, Virginia Transportation Research Council, Charlottesville, VA, November.
32. White, D.J., Thompson, M., Vennapusa, P. (2007). *Field Validation of Intelligent Compaction Monitoring Technology for Unbound Materials*, Mn/DOT Report No. MN/RC 2007-10, Iowa State University, Ia.
33. White, D.J., Thompson, M., Vennapusa, P. (2007). *Field study of compaction monitoring systems: self-propelled non-vibratory 825G and vibratory smooth drum CS-533 E rollers*, Final Report, Center of Transportation Research and Education, Iowa State University, Ames, Ia.

2008

34. Labuz, J.F., Guzina, B., Khazanovich, L. (2008). *Intelligent Compaction Implementation: Research Assessment*, Final Report MN/RC 2008-22, Minnesota Department of Transportation, St. Paul, MN.
35. Newman, K., Rushing, J.F., and White, D. J. (2008). *Rapid Soil Stabilization for Contingency Airfield Construction*, Army Corps of Engineers Report.
36. Rahman, F., Hossain, M., Ramanoschi, S. (2008). *Intelligent Compaction Control of Highway Embankment Soil in Kansas*. Final Report No. K-TRAN: KSU-06-07, Kansas State University, Manhattan, Kansas, March.
37. White D.J., (2008). *Report of the Workshop on Intelligent Compaction for Soils and HMA*, ER08-01, Earthworks Engineering Research Center, Iowa State University, Ames, Iowa.
38. White, D.J., Vennapusa, P. (2008). *Accelerated Implementation of Intelligent Compaction Monitoring Technology for Embankment Subgrade Soils, Aggregate Base, and Asphalt Pavement Materials TPF-5(128) – Mn/DOT HMA IC Demonstration*, Report submitted to The Transtec Group, FHWA, June.
39. White, D. J., Vennapusa, P., Gieselman, H. (2008). *Investigation of Dual Roller-Integrated MDP/CMV Compaction Monitoring Technologies and Measurement Influence Depth*, Center of Transportation Research and Education, Iowa State University, Ames, Iowa, August.
40. White, D.J., Vennapusa, P., Gieselman, H., Johanson, L., Goldsmith, R. (2008). *Accelerated Implementation of Intelligent Compaction Monitoring Technology for Embankment Subgrade Soils, Aggregate Base, and Asphalt Pavement Materials TPF-5(128) – Texas IC Demonstration Field Project*, Report submitted to The Transtec Group, FHWA, November.

2009

41. Chang, G., Xu, Q., Horan, B., Michael, L. (2009). *Accelerated Implementation of Intelligent Compaction Monitoring Technology for Embankment Subgrade Soils, Aggregate Base, and Asphalt Pavement Materials TPF-5(128) – Maryland HMA IC Demonstration*, Report submitted to FHWA, September.
42. Chang, G., Xu, Q., Horan, B., Michael, L. (2009). *Accelerated Implementation of Intelligent Compaction Monitoring Technology for Embankment Subgrade Soils, Aggregate Base, and Asphalt Pavement Materials TPF-5(128) – Clayton County, Georgia HMA IC Demonstration*, Report submitted to FHWA, March.
43. Petersen, D.L., Morgan, J., Graettinger, A. (2009). *Mn/DOT Intelligent Compaction Implementation Plan: Procedures to Use and Manage IC Data in Real Time*. Final Report MN/RC 2009-35, Minnesota Department of Transportation, St. Paul, Minnesota, December.
44. White, D.J., Vennapusa, P. (2009). *Report of the Workshop on Intelligent Technologies for Earthworks*, EERC Publication ER09-02, Earthworks Engineering Research Center, Iowa State University, Ames, Iowa.
45. White, D.J., Vennapusa, P., Zhang, J., Gieselman, H., Morris, M. (2009). *Implementation of Intelligent Compaction Performance Based Specifications in Minnesota*, EERC Publication ER09-03, MN/RC 2009-14, Minnesota Department of Transportation, St. Paul, Minnesota, March.
46. White, D.J., Vennapusa, P., Gieselman, H., Johanson, L., Goldsmith, R. (2009). *Accelerated Implementation of Intelligent Compaction Monitoring Technology for Embankment Subgrade Soils, Aggregate Base, and Asphalt Pavement Materials TPF-5(128) – Kansas IC Demonstration Field Project*, Report submitted to The Transtec Group, FHWA, May.

2010

47. Chang, G., Xu, Q., Horan, B., Michael, L. (2010). *Accelerated Implementation of Intelligent Compaction Monitoring Technology for Embankment Subgrade Soils, Aggregate Base, and Asphalt Pavement Materials TPF-5(128) – US52 West Lafayette, Indiana HMA IC Demonstration*, Report submitted to FHWA, March.

48. Chang, G., Xu, Q., (2010). *Accelerated Implementation of Intelligent Compaction Monitoring Technology for Embankment Subgrade Soils, Aggregate Base, and Asphalt Pavement Materials TPF-5(128) – FM1281, El Paso, Texas, HMA IC Demonstration*, Report submitted to FHWA, June.
49. Chang, G., Xu, Q., Horan, B., Michael, L. (2010). *Accelerated Implementation of Intelligent Compaction Monitoring Technology for Embankment Subgrade Soils, Aggregate Base, and Asphalt Pavement Materials TPF-5(128) – IH39, Mosinee, Wisconsin HMA IC Demonstration*, Report submitted to FHWA, June.
50. Chang, G., Xu, Q., Horan, B., Michael, L. (2010). *Accelerated Implementation of Intelligent Compaction Monitoring Technology for Embankment Subgrade Soils, Aggregate Base, and Asphalt Pavement Materials TPF-5(128) – US219, Summerhill, Pennsylvania HMA IC Demonstration*, Report submitted to FHWA, October.
51. Chang, G., Xu, Q., Horan, B., Michael, L. (2010). *Accelerated Implementation of Intelligent Compaction Monitoring Technology for Embankment Subgrade Soils, Aggregate Base, and Asphalt Pavement Materials TPF-5(128) – I-66, Fauquier County, Virginia HMA IC Demonstration*, Report submitted to FHWA, October.
52. Commuri, S. (2010). *Intelligent Asphalt Compaction Analyzer – Phase I Report*, Highways for LIFE Technology Partnerships Programs, FHWA, Washington, D.C.
53. Commuri, S., Zaman, M., Singh, D., Mai, A., Beainy, F. (2010). *Continuous Real Time Measurement of Pavement Quality during Construction*, Final Report, Oklahoma Transportation Center, Stillwater, OK.
54. Mooney, M., Rinehart, R., White, D.J., Vennapusa, P., Facas, N., Musimbi, O. (2010). *Intelligent Soil Compaction Systems*, NCHRP 21-09 Final Report, National Cooperative Highway Research Program, Washington, D.C. (in print).
55. Petersen, D.L., Hartman, M.A. (2010). *2008 MnROAD Unbound Quality Control Construction Report*, Final Report Mn/RC 2010-32, Minnesota Dept. of Transportation, St. Paul, MN.
56. Quintus, V.L.H., Rao, C., Bhattacharya, B., Titi, H., English, R. (2010). *Evaluation of Intelligent Compaction Technology for Densification of Roadway Subgrades and Structural Layers*, WHRP Project No. 0092-08-07 (Draft Final Report), Prepared by Applied Research Associates and University of Wisconsin at Milwaukee, November.
57. White, D.J., Vennapusa, P. (2010). *Report of the Webinar Workshop on Intelligent Compaction for Earthworks and HMA*, ER10-02, 3rd Annual Workshop Organized by the Earthworks Engineering Research Center at Iowa State University and the Iowa Department of Transportation, March 1-2, 2010, Ames, Iowa.
58. White, D.J., Vennapusa, P., Gieselman, H., Zhang, J., Goldsmith, R., Johanson, L., Quist, S. (2010). *Accelerated Implementation of Intelligent Compaction Monitoring Technology for Embankment Subgrade Soils, Aggregate Base, and Asphalt Pavement Materials TPF-5(128) - NY IC Demonstration Field Project*, EERC Publication ER10-01, Report submitted to The Transtec Group, FHWA, January.
59. White, D.J., Vennapusa, P., Gieselman, H., Fleming, B., Quist, S., Johanson, L. (2010). *Accelerated Implementation of Intelligent Compaction Monitoring Technology for Embankment Subgrade Soils, Aggregate Base, and Asphalt Pavement Materials TPF-5(128) – Mississippi IC Demonstration Field Project*, ER10-03, Report submitted to The Transtec Group, FHWA, January.
60. White, D.J., Vennapusa, P. (2010). *A Review of Roller-Integrated Compaction Monitoring Technologies for Earthworks*. Report No. ER10-04, Prepared by the Earthworks Engineering Research Center at Iowa State University, Report submitted to The Transtec Group, FHWA, April.
61. White, D.J., Gieselman, H., Douglas, S., Zhang, J., Vennapusa, P. (2010). *-Situ Compaction Measurements for Geosynthetic Stabilized Subbase: Weirton, West Virginia*. ER10-05, Prepared by the Earthworks Engineering Research Center at Iowa State University, Report submitted to Tensar, Inc.
62. White, D.J., Vennapusa, P., Gieselman, H., Zhang, J., Eidem, M. (2010). *Accelerated Implementation of Intelligent Compaction Monitoring Technology for Embankment Subgrade Soils, Aggregate Base, and Asphalt Pavement Materials TPF-5(128) – North Dakota IC Demonstration Field Project*, ER10-08, Report submitted to The Transtec Group, FHWA, November.
63. White, D.J., Vennapusa, P., Gieselman, H. (2010). *Iowa DOT Intelligent Compaction Research and Implementation – Phase I*, ER-10-06, Final Report, Earthworks Engineering Research Center, Iowa State University, Ames, Iowa, December.
64. Mallela, J., Littleton, P., Hoffman, G. (2010). *Minnesota Demonstration Project: Reconstruction of Trunk Highway 36 in North St. Paul*, Report submitted by Applied Research Associates, Inc., FHWA, Washington, D.C., June.

2011

65. White, D.J., Vennapusa, P., Gieselmann, H., Quist, S., Harland, J. (2011). *Iowa DOT Roller Integrated Compaction Monitoring Technology Research and Implementation - PHASE II (HMA)*. Report No. ER11-01, Report submitted to the Iowa Department of Transportation, June.
66. Chang, G., Xu, Q., Rutledge, J., Horan, B., Michael, L., White, D.J., and Vennapusa, P. *Accelerated Implementation of Intelligent Compaction Technology for Embankment Subgrade Soils, Aggregate Base, and Asphalt Pavement Materials – Final Report*, FHWA-IF-12-002, Federal Highway Administration, Washington, D.C., July.

2013

67. Mooney, M., Facas, N. (2013). *Extraction of Layer Properties from Intelligent Compaction Data*, Final Report for Highway IDEA Project 145, Transportation Research Board, Washington, D.C.

2014

68. Chang, G., Xu, Q., Ruteledge, J., and Garber, S. (2014). *A Study on Intelligent Compaction and In-Place Asphalt Density*, FHWA-HIF-14-017. Federal Highway Administration, Washington, D.C.
69. Carrasco, C., Terado, C., and Wang, H. *Numerical Simulation of Intelligent Compaction Technology for Construction Quality Control*, CAIT-UTC-029 Final Report, The State University of New Jersey, Piscataway, NJ.

2015

70. Yoon, S., Hastak, M., & Lee, J. (2015). *Intelligent compaction of asphalt pavement implementation* (Joint Transportation Research Program Publication No. FHWA/IN/JTRP-2015/05). West Lafayette, IN: Purdue University.
71. Savan, C., Ng., K.W., Ksaibati, K. (2015). *Implementation of Intelligent Compaction Technologies for Road Constructions in Wyoming*, University of Wyoming, Laramie, WY.

2016

72. Gautreau, G. P., Abu-Farsakh, M., & Cooper III, S. B. (2016). *Field Evaluation of Roller Integrated Intelligent Compaction Monitoring*, Final Report No. FHWA/LA. 15/555, Louisiana Transportation Research Center (LTRC), Baton Rouge, LA.
73. Ghazanfari, E., and Dewoolkar, M. (2017). *Suitability of Intelligent Compaction for Relatively Smaller-Scale Projects in Vermont*, Final Report No. SPR-RSCH018-744, Vermont Agency of Transportation, Montpelier, VT.

Magazine Articles/Technology Transfer Articles (organized by publication date)

1996

1. Geistlinger, L. (1996). "Onboard compaction meters make inroads into U.S. market", *Roads & Bridges Magazine*, 34(8), August, 40 – 42. <http://www.roadsbridges.com/Onboard-Compaction-Meters-Make-Inroads-into-U-S-Market-article445>

2002

2. Peterson, A. (2002). "Making a Difference," *World Highways/ Routes du Monde*, 11(8), 34-42.

2004

3. Wilson, S. (2004). "Never Guess Again – Intelligent Compaction Making Precision Commonplace at the Job Site," *Roads & Bridges Magazine*, 42(8), 22-25, August. <http://www.roadsbridges.com/rb/index.cfm/powergrid/rfah=cfap=/CFID/3211407/CFTOKEN/89068603/fuseaction/showArticle/articleID/5396>
4. White, D.J., Cackler, T. (2004). "Soil Compaction Monitoring Technology – Tech Transfer Summary." Partnership for Geotechnical Advancement, Iowa State University, Ames, Iowa, September. <http://www.intrans.iastate.edu/pubs/t2summaries/compaction.pdf>

2005

5. Hildebrandt, P. (2005). "Compaction: Business as Usual But with New Options," *Grading & Excavation Contractor*, July/August. <http://www.gradingandexcavation.com/july-august-2005/compaction-business-usual.aspx>

2006

6. Moore, W. (2006). "Intelligent Compaction: Outsmarting Soil and Asphalt", *Construction Equipment*, April 1. <http://www.constructionwriters.org/pdf/2007-awards/cex0604intcompaction.pdf>
7. Kronick, D. (2006). "Intelligent Compaction: The Next Big Thing?", *Technology Exchange*, Vol. 14, Newsletter of the Minnesota Local Technical Assistance Program, Regents of the University of Minnesota, St. Paul, MN. <http://www.mnltap.umn.edu/publications/exchange/2006-4/2006-4-1-1.html>
8. White, D.J. (2006). "Field Evaluation of Compaction Monitoring Technology – Tech Transfer Summary." Partnership for Geotechnical Advancement, Iowa State University, Ames, Iowa, March. http://www.intrans.iastate.edu/pubs/t2summaries/compaction_2.pdf

2007

9. White, D.J., Vennapusa, P., Thompson, M. (2007). "Field Validation of Intelligent Compaction Monitoring Technologies for Unbound Materials – Tech Transfer Summary." Partnership for Geotechnical Advancement, Iowa State University, Ames, Iowa, June. http://www.intrans.iastate.edu/pubs/t2summaries/intel_compaction.pdf

2008

10. Embacher, R., Moe, C., Labuz, J.F. (2008). "Putting Research into Practice: Intelligent Compaction Implementation – Research Assessment." Research Services Section, Minnesota Department of Transportation, St. Paul, Mn. <http://www.lrrb.org/pdf/200822ts.pdf>
11. Horan, B. (2008). "Intelligent Compaction – A new tool for improving asphalt pavement compaction", *Asphalt Magazine*, Published by the Asphalt Institute, March 10. http://www.asphaltmagazine.com/singlenews.asp?item_ID=1453&comm=0&list_code_int=mag01-int
12. Federal Highway Administration. (2008). "Asphalt Contractor Technology Partnerships", Cygnus Interactive, July 8. <http://www.forconstructionpros.com/article/article.jsp?siteSection=25&id=10363&pageNum=1>

2009

13. Hampton, T.V. (2009). "Intelligent Compaction Is on a Roll", Featured in Ground Control – Engineering News Record Magazine, July 13, Published by The McGraw-Hill Companies. http://southeast.construction.com/features/2009/0901_IntelligentCompaction.asp
14. Greschner, A. (2009). "Intelligent Compaction Goes Global", MENA Infrastructure, Issue 3 <http://www.menainfra.com/article/Intelligent-compaction-goes-global/>
15. Kirschbaum, I.V., Winkelstrater, H. (2009). "Increasing compaction efficiency on soils - and saving costs - using cutting-edge technology", European Infrastructure, Issue 8 <http://www.euinfrastructure.com/article/Increasing-compaction-efficiency-on-soils---and-saving-costs---using-cutting-edge-technology/>
16. Siekmeier, J., Moe, C., White, D.J. (2009). "Field Validation of Intelligent Compaction", Research Services Section, Minnesota Department of Transportation, St. Paul, Mn. <http://www.lrrb.org/pdf/200710TS.pdf>
17. Siekmeier, J., Moe, C., White, D.J. (2009). "Putting Research into Practice: Intelligent Compaction Performance-Based Specifications in Minnesota – Technical Summary", Research Services Section, Minnesota Department of Transportation, St. Paul, Mn. <http://www.lrrb.org/pdf/200914TS.pdf>

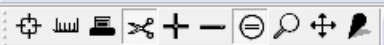
2010

18. Chang, G., Xu, Q. (2010). "Intelligent Compaction Field Demonstration – Tech Brief." Transportation Pooled Fund Program (TPF), FHWA, Washington, D.C. http://www.intelligentcompaction.com/downloads/Reports/IC%20Tech%20Brief_FieldDemo_v2.3.pdf
19. Embacher, R., Moe, C., Petersen, L. (2010). "Managing Intelligent Compaction Data," Research Services Section, Minnesota Department of Transportation, St. Paul, Mn. <http://www.lrrb.org/pdf/200935TS.pdf>
20. FHWA (2010). "The Exploratory Advanced Research Program Fact Sheet: Real-Time Measurement of Soil

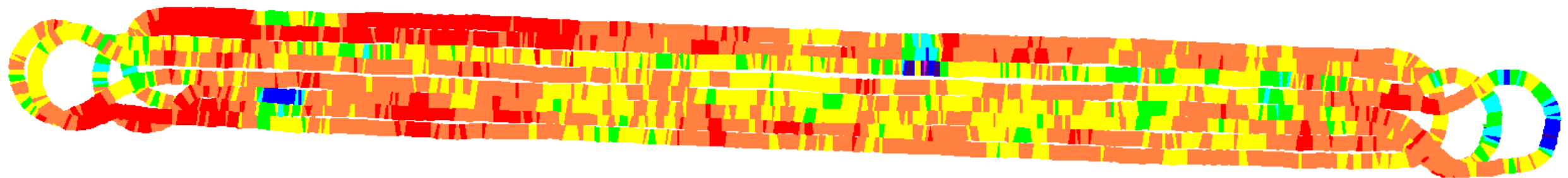
Stiffness During Static Compaction”, Publication No. FHWA-HRT-09-047 HRTM-04/06-09(1M)E, FHWA, Washington, D.C. <http://www.fhwa.dot.gov/advancedresearch/pubs/soilcompact.pdf>

21. Gallivan, L. (2010). “Intelligent Compaction – Onboard Technology Makes Compaction More Accurate”, Highways for Life, FHWA, Washington, D.C., June 14.
<http://www.fhwa.dot.gov/hfl/innovations/intelligentcompaction.cfm>
22. White, D.J., Vennapusa, P., Gieselman, H. (2010). “Iowa’s Intelligent Compaction Research and Implementation.” Iowa DOT Research and Technology Bureau News Letter, November.
<http://www.iowadot.gov/research/pdf/newsnovember2010.pdf>

APPENDIX B: SUMMARY OF COMPACTION REPORTS



TS1: PGE Layer
10/13/2016



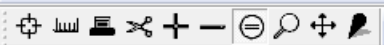
ft 99.936 199.872 Y 1:894

Ground firmness (HNV)

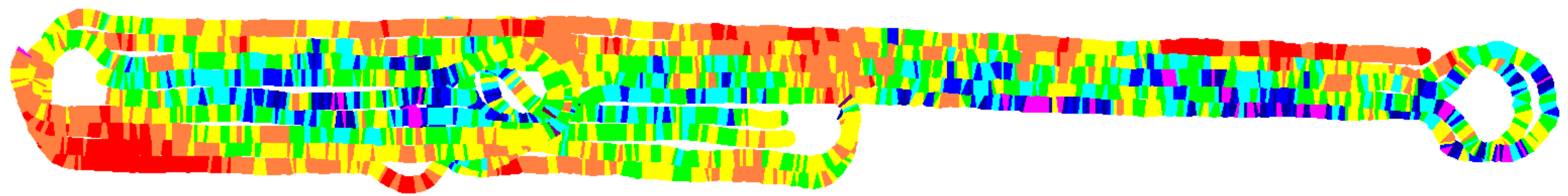


"Ground firmness": Longitude: -87.9758186; Latitude: 41.9833020;

NUM

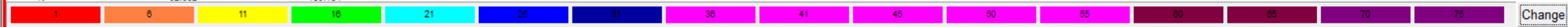


TS2: PGE Layer
10/13/2016



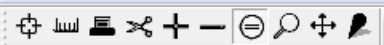
ft 92.592 185.184 Y 1:843

Ground firmness (HNV)

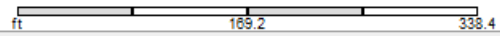
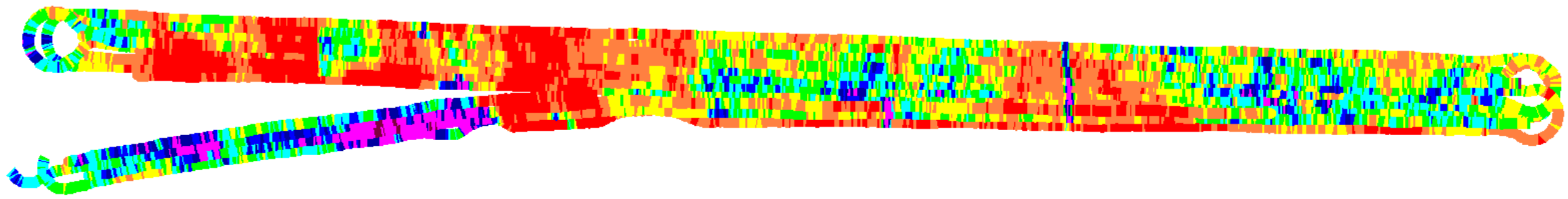


"Ground firmness"; Longitude: -87.9743512; Latitude: 41.9829242;

NUM

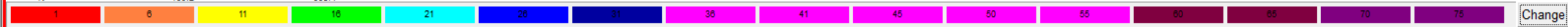


TS3: PGE Layer
10/14/2016



Y 1:1175

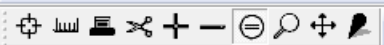
Ground firmness (HMV)



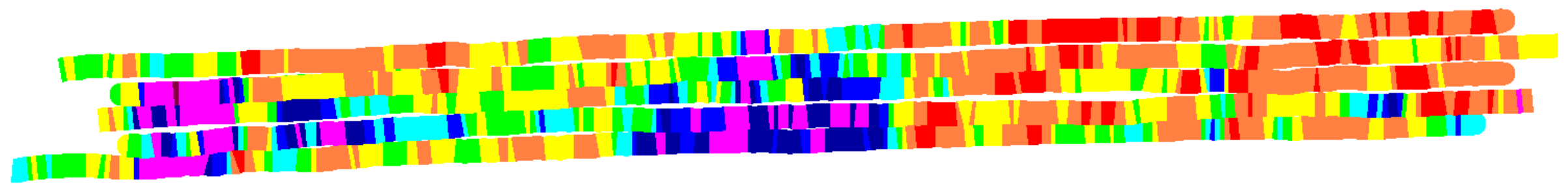
Change

"Ground firmness"; Longitude: -87.9745477; Latitude: 41.9825755;

NUM



TS4: CA6 Capping Layer
10/14/2016



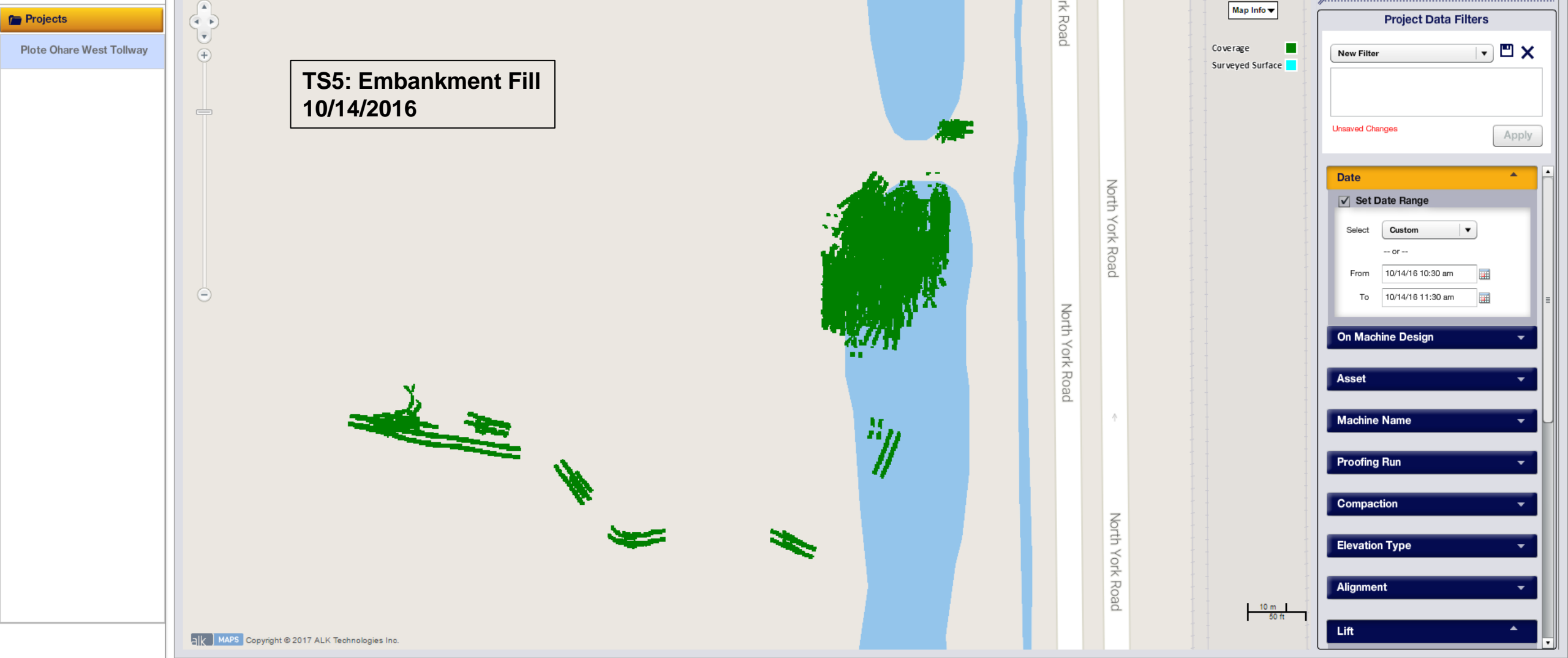
ft 63.504 127.008 Y 1:441

Ground firmness (HNV)



"Ground firmness"; Longitude: -87.9818133; Latitude: 41.9831589;

NUM



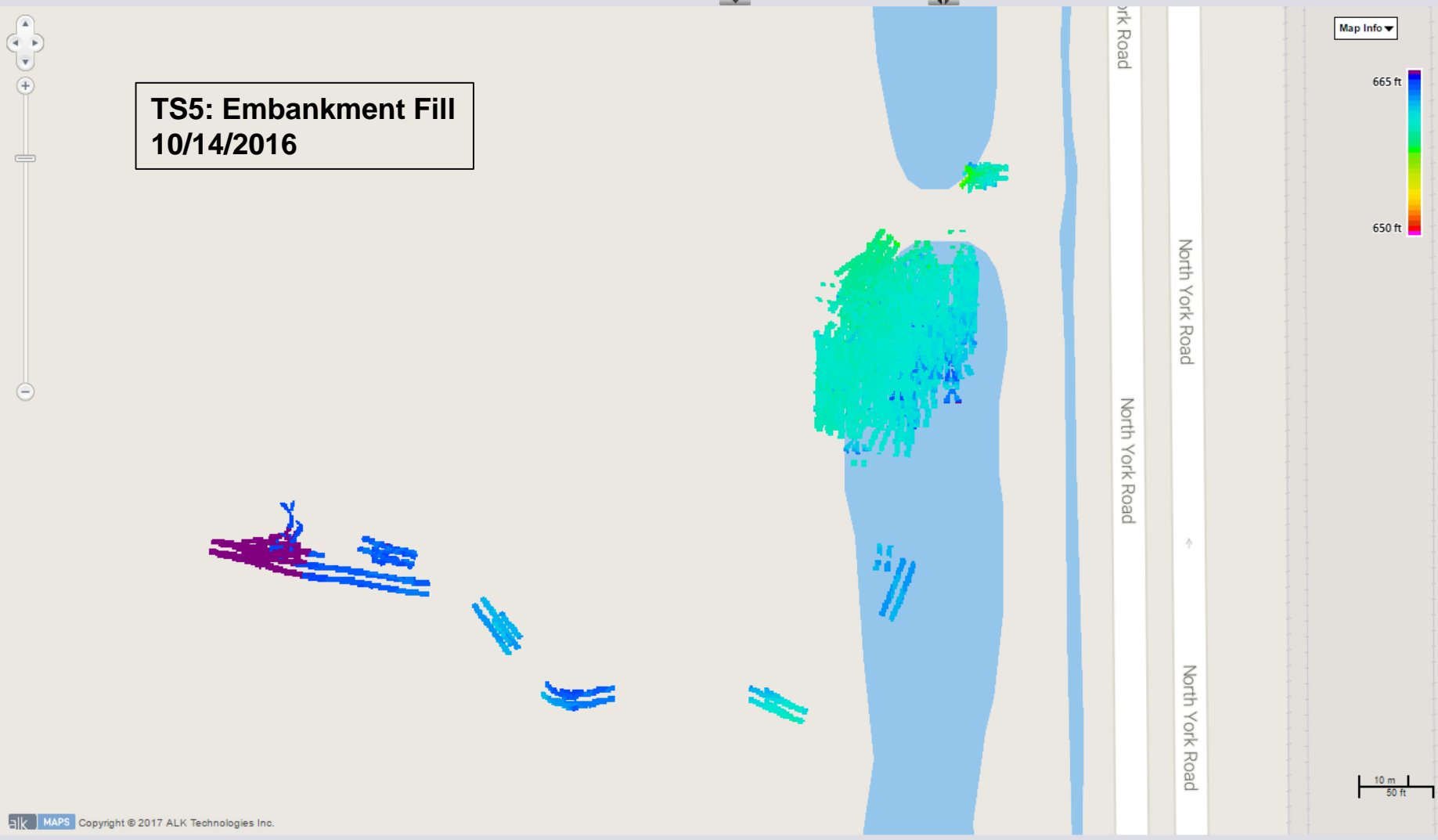
Projects > Plote Ohare West Tollway > 0 Results

Fleet Alerts Health Maintenance Utilization Project Administration

3D Project Monitoring 10/14/16 10:30 am - 10/14/16 11:30 am

Section View Elevation Settings

- All Assets (0)
- Groups
- Projects
- Plote Ohare West Tollway



TS5: Embankment Fill
10/14/2016

Project Data Filters

New Filter [X]

Unsaved Changes [Apply]

Date

Set Date Range

Select: Custom

-- or --

From: 10/14/16 10:30 am

To: 10/14/16 11:30 am

On Machine Design

Asset

Machine Name

Proofing Run

Compaction

Elevation Type

Alignment

Lift

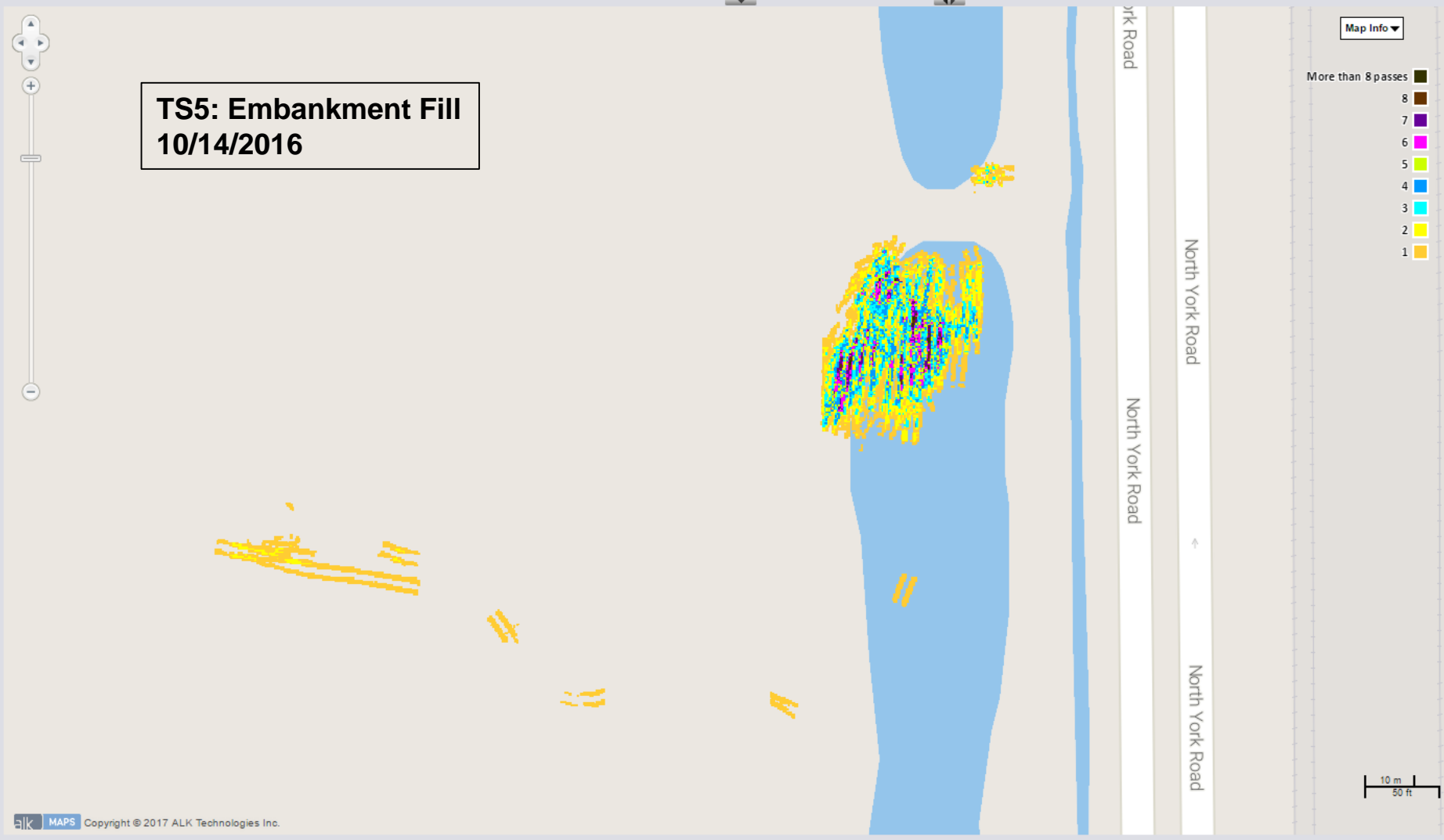
Projects > Plote Ohare West Tollway > 0 Results

Fleet Alerts Health Maintenance Utilization Project Administration

3D Project Monitoring 10/14/16 10:30 am - 10/14/16 11:30 am

Section View Pass Count Detail Settings

- All Assets (0)
- Groups
- Projects
- Plote Ohare West Tollway



Project Data Filters

New Filter

Unsaved Changes

Apply

Date

Set Date Range

Select Custom

-- or --

From 10/14/16 10:30 am

To 10/14/16 11:30 am

On Machine Design

Asset

Machine Name

Proofing Run

Compaction

Elevation Type

Alignment

Lift

Projects > Plote Ohare West Tollway > 0 Results

- All Assets (0)
- Groups
- Projects
 - Plote Ohare West Tollway

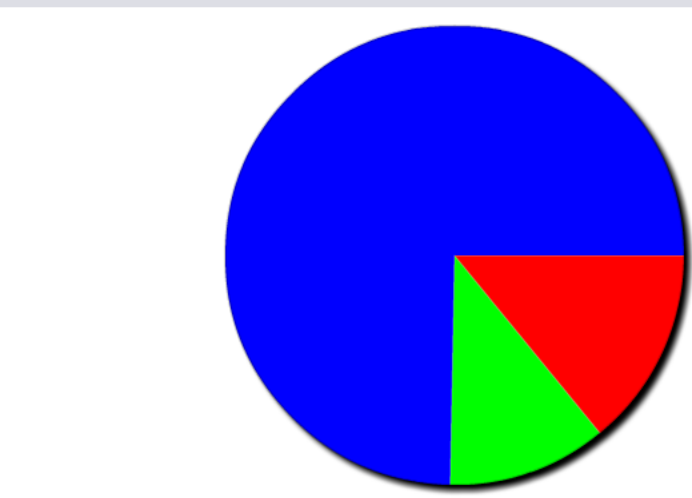
Fleet | Alerts | Health | Maintenance | Utilization | Project | Administration

3D Project Monitoring | 10/14/16 10:30 am - 10/14/16 11:30 am

Section View | Pass Count Summary | Settings

Pass Count Summary

Target Pass Count	4	
Over Pass Target	14.1%	1,715.9 sq ft
Equals Pass Target	11.2%	1,368.7 sq ft
Under Pass Target	74.7%	9,104.6 sq ft
Total Area Covered		12,189.2 sq ft



Project Data Filters

New Filter [X]

Unsaved Changes [Apply]

Date

Set Date Range

Select: Custom

From: 10/14/16 10:30 am

To: 10/14/16 11:30 am

On Machine Design

Asset

Machine Name

Proofing Run

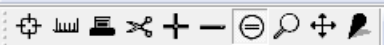
Compaction

Elevation Type

Alignment

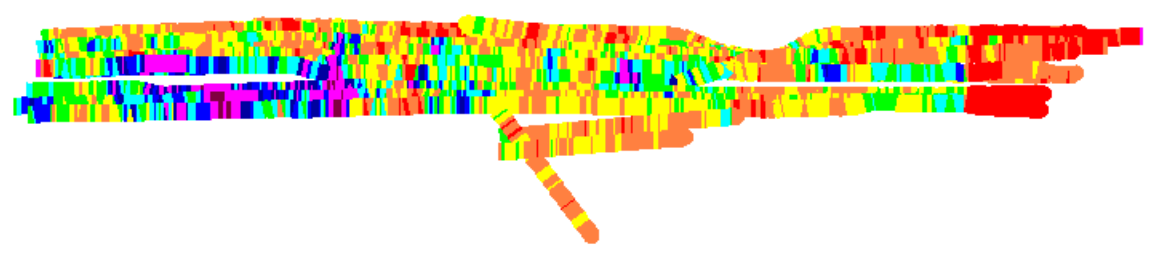
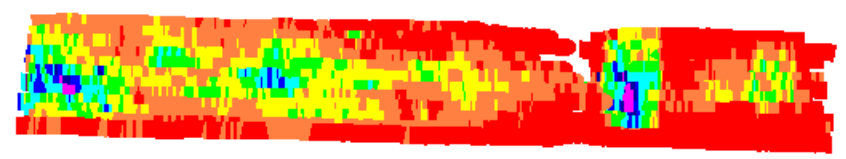
Lift





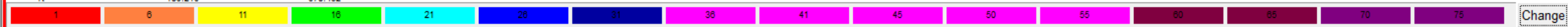
Production Map 1 By Plote (10/14/16)

PGE Material



ft 189.216 378.432 Y 1:1314

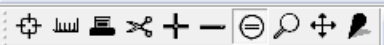
Ground firmness (HMV)



Change

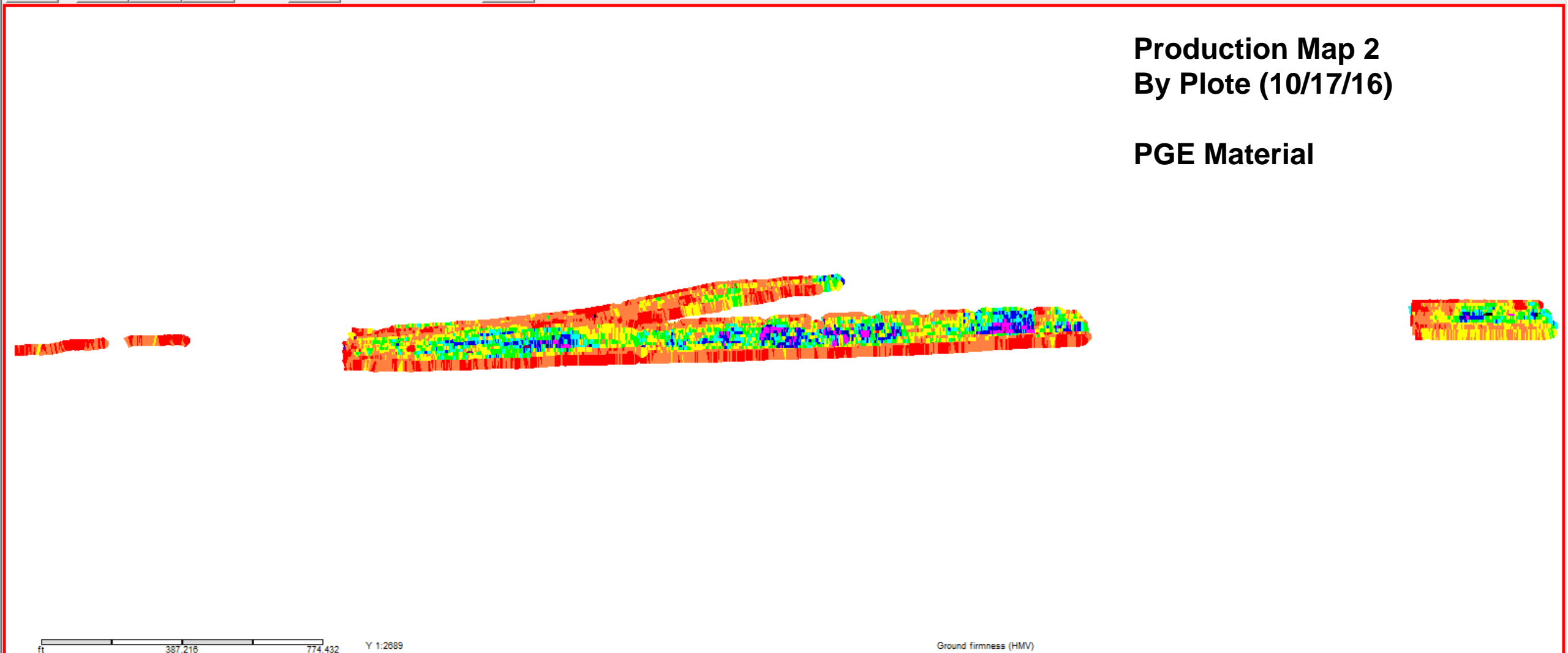
"Ground firmness"; Longitude: -87.9772549; Latitude: 41.9827589;

NUM



Production Map 2 By Plote (10/17/16)

PGE Material

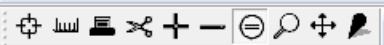


ft 387.216 774.432 Y 1:2689

Ground firmness (HNV)

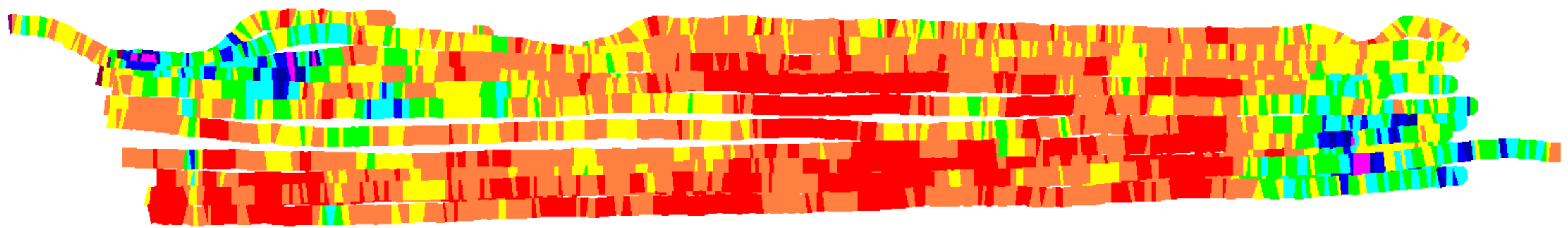


Change



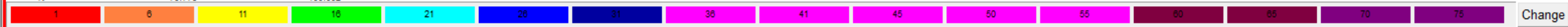
Production Map 3 By Plote (10/17/16)

PGE Material



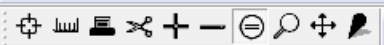
ft 79.776 159.552 Y 1:554

Ground firmness (HNV)



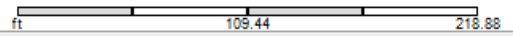
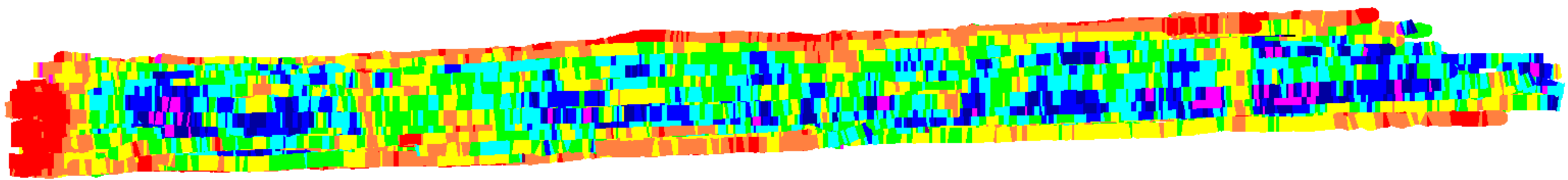
"Ground firmness"; Longitude: -87.9920040; Latitude: 41.9831337;

NUM



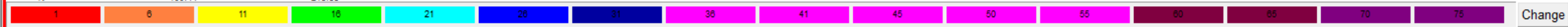
Production Map 4 By Plote (10/18/16)

CA6 Base Material



Y 1:760

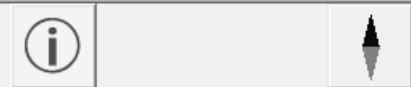
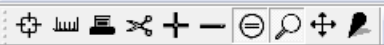
Ground firmness (HNV)



Change

"Ground firmness"; Longitude: -87.9883214; Latitude: 41.9830931;

NUM

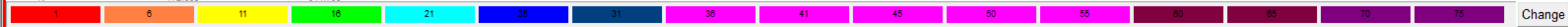


TS6: PGE Layer
04/11/2017



ft 172.368 344.736 Y 1:1197

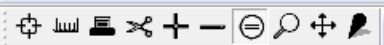
Ground firmness (HNV)



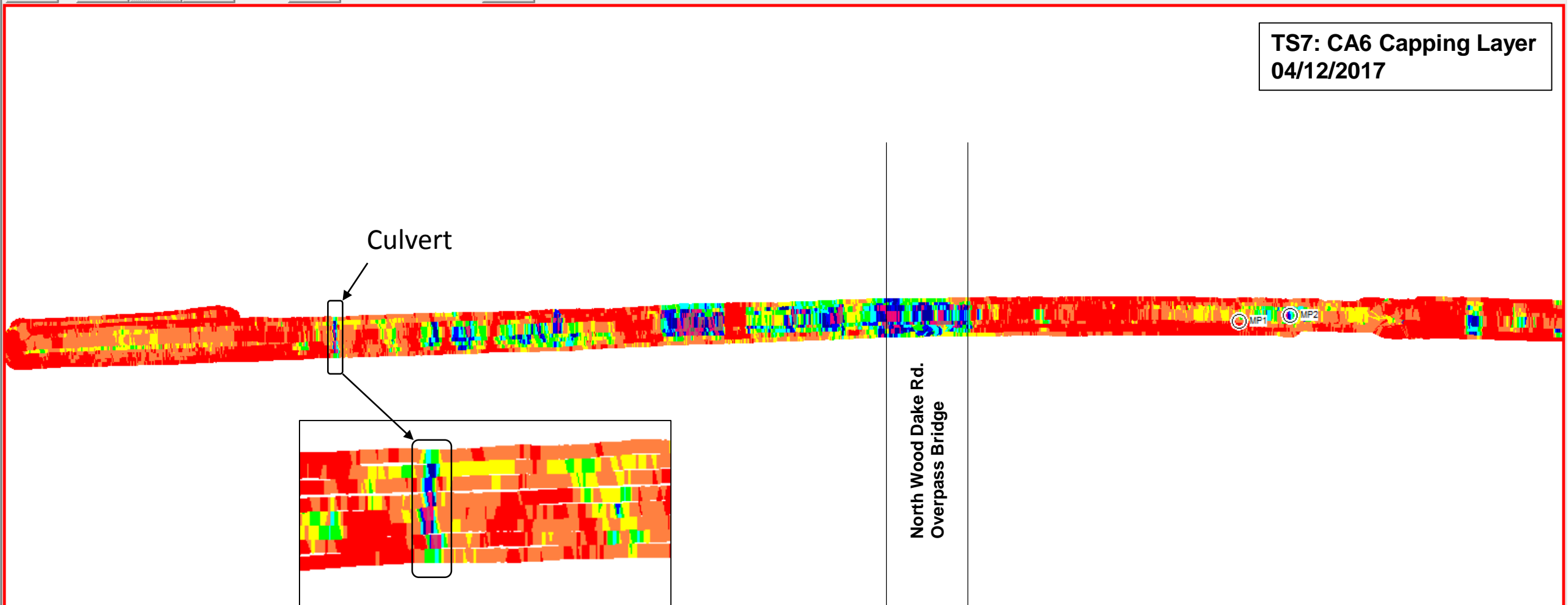
Change

"Ground firmness"; Longitude: -87.9720325; Latitude: 41.9831268;

NUM



TS7: CA6 Capping Layer
04/12/2017



Culvert

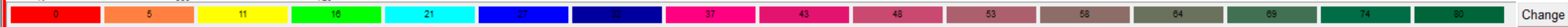
North Wood Lake Rd.
Overpass Bridge

MP1 MP2

ft 0 360 720

Y 1:2500

Ground firmness (HMV)



Change

Projects > Plote Ohare West Tollway > 1 Results

Fleet Alerts Health Maintenance Utilization Project Administration

3D Project Monitoring 12 04/18/17 12:00 am - 04/18/17 11:59 pm

Section View CMV Summary Settings



TS7: CA6 Capping Layer
04/12/2017

N. Wooddale
Rd. Overpass

Driveway
Entrance

- Over Compacted Layer [Blue square]
- Complete Layer [Green square]
- Under Compacted Layer [Red square]
- Work In Progress [Yellow square]
- Too Thick Layer [Purple square]

All Assets (1)

Groups

Projects

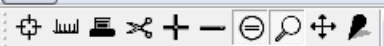
Plote Ohare West Tollway

Projects > Plote Ohare West Tollway > 1 Results

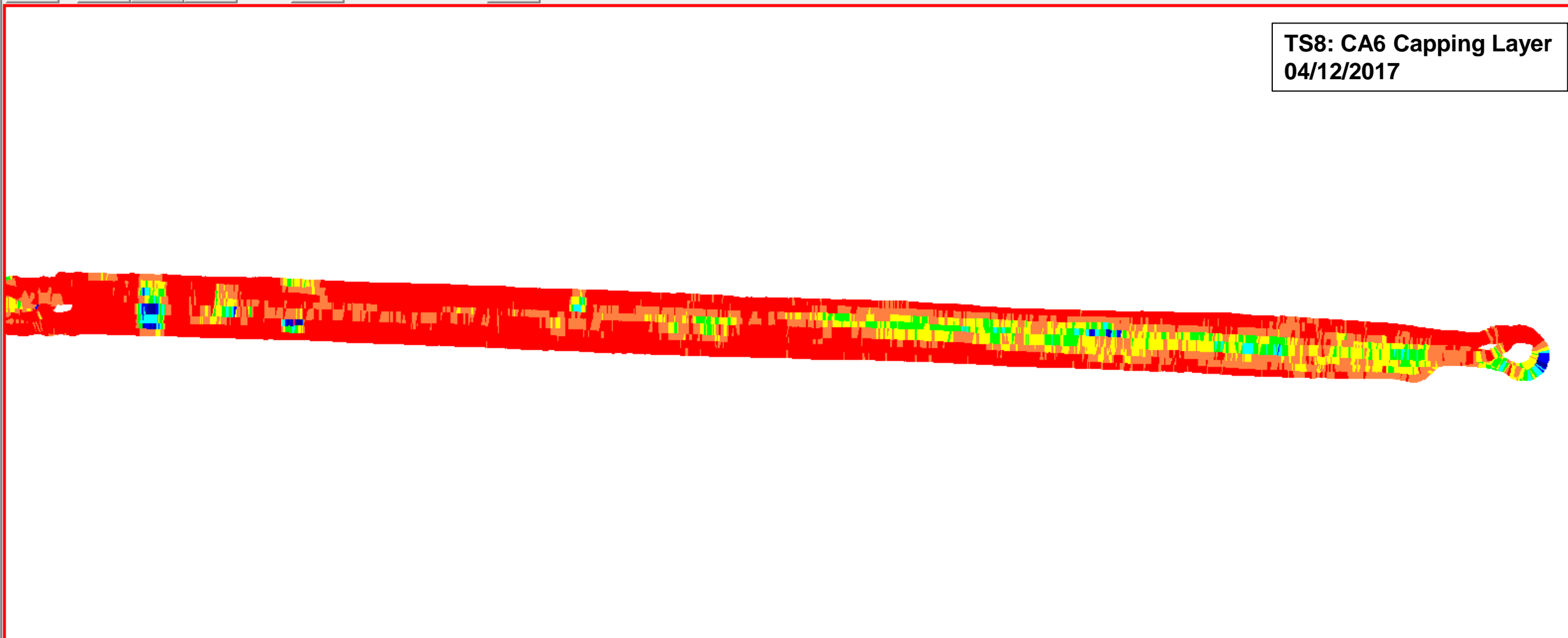
Fleet Alerts Health Maintenance Utilization **Project** Administration

3D Project Monitoring 12 04/18/17 12:00 am - 04/18/17 11:59 pm Section View MDP Summary Settings

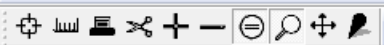




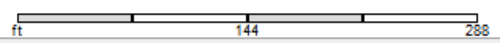
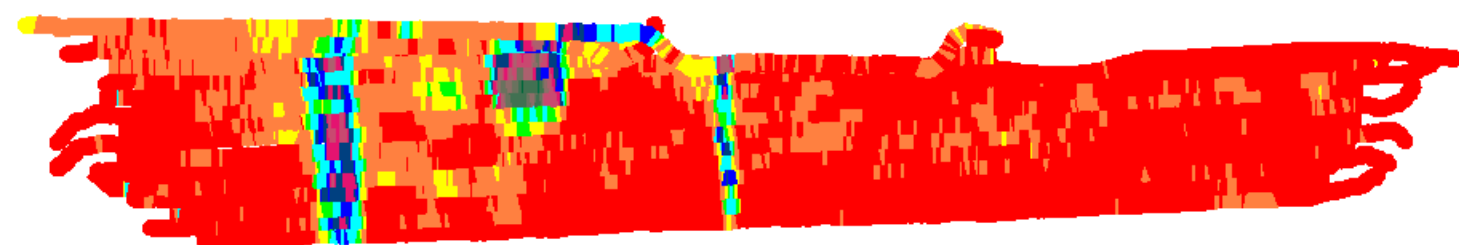
TS8: CA6 Capping Layer
04/12/2017



"Ground firmness"; Longitude: -87.9766662; Latitude: 41.9846447;

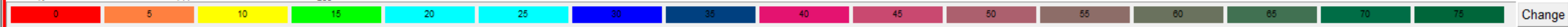


TS9: CA6 Capping Layer
04/12/2017



Y 1:1000

Ground firmness (HNV)



Change

Projects > Plote Ohare West Tollway > 1 Results

All Assets (1)

Groups

Projects

Plote Ohare West Tollway

Fleet | Alerts | Health | Maintenance | Utilization | Project | Administration

3D Project Monitoring

12 04/18/17 12:00 am - 04/18/17 11:59 pm

Section View

CMV Summary

Settings



TS9: CA6 Capping Layer
04/12/2017

- Over Compacted Layer ■
- Complete Layer ■
- Under Compacted Layer ■
- Work In Progress ■
- Too Thick Layer ■

Projects > Plote Ohare West Tollway > 1 Results

All Assets (1)

Groups

Projects

Plote Ohare West Tollway

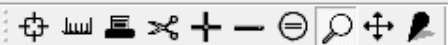
Fleet Alerts Health Maintenance Utilization Project Administration

3D Project Monitoring 12 04/18/17 12:00 am - 04/18/17 11:59 pm

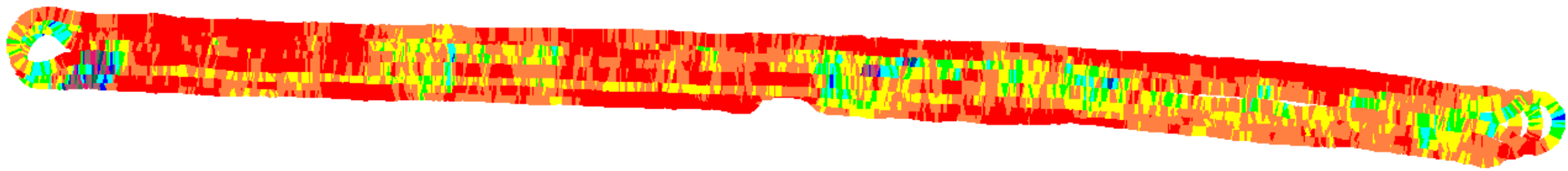
Section View MDP Summary Settings



TS9: CA6 Capping Layer
04/12/2017

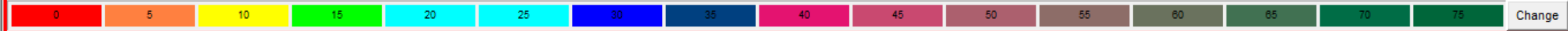


TS10: PGE Layer
04/25/2017



ft 0 138.648 273.296 Y 1:1178

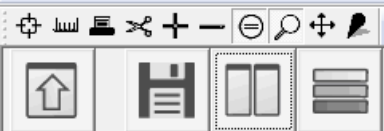
Ground firmness (HNV)



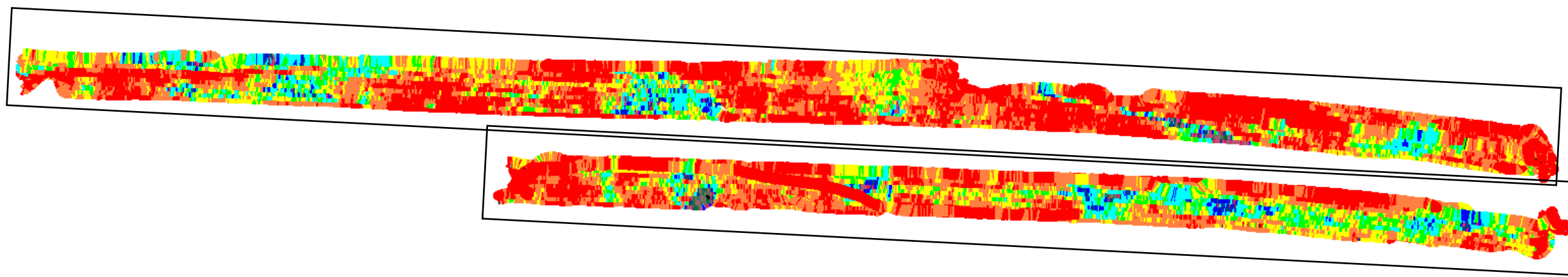
Change

"Ground firmness"; Longitude: -87.9649429; Latitude: 41.9827495;

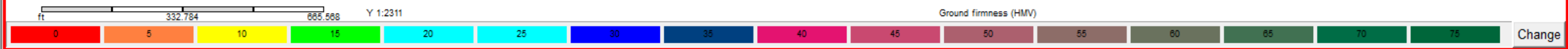
NUM



Test Section 11 – PGE 04/26/17



Test Section 12 – RAP 05/04/17



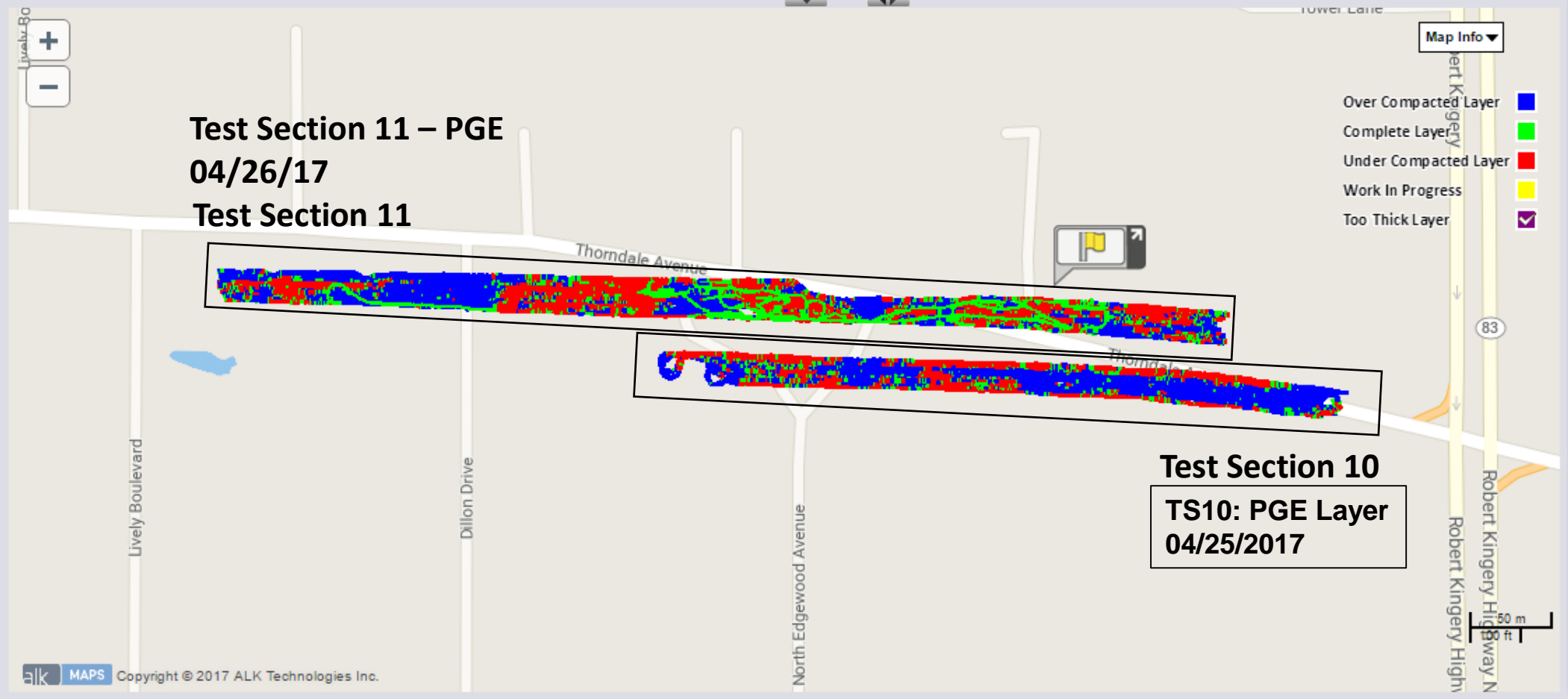
Projects > Plote Ohare West Tollway > 1 Results

Fleet Alerts Health Maintenance Utilization Project Administration

3D Project Monitoring 12 04/24/17 12:00 am - 04/27/17 11:59 pm

Section View CMV Summary Settings

- All Assets (1)
- Groups
- Projects
- Plote Ohare West Tollway



alk MAPS Copyright © 2017 ALK Technologies Inc.

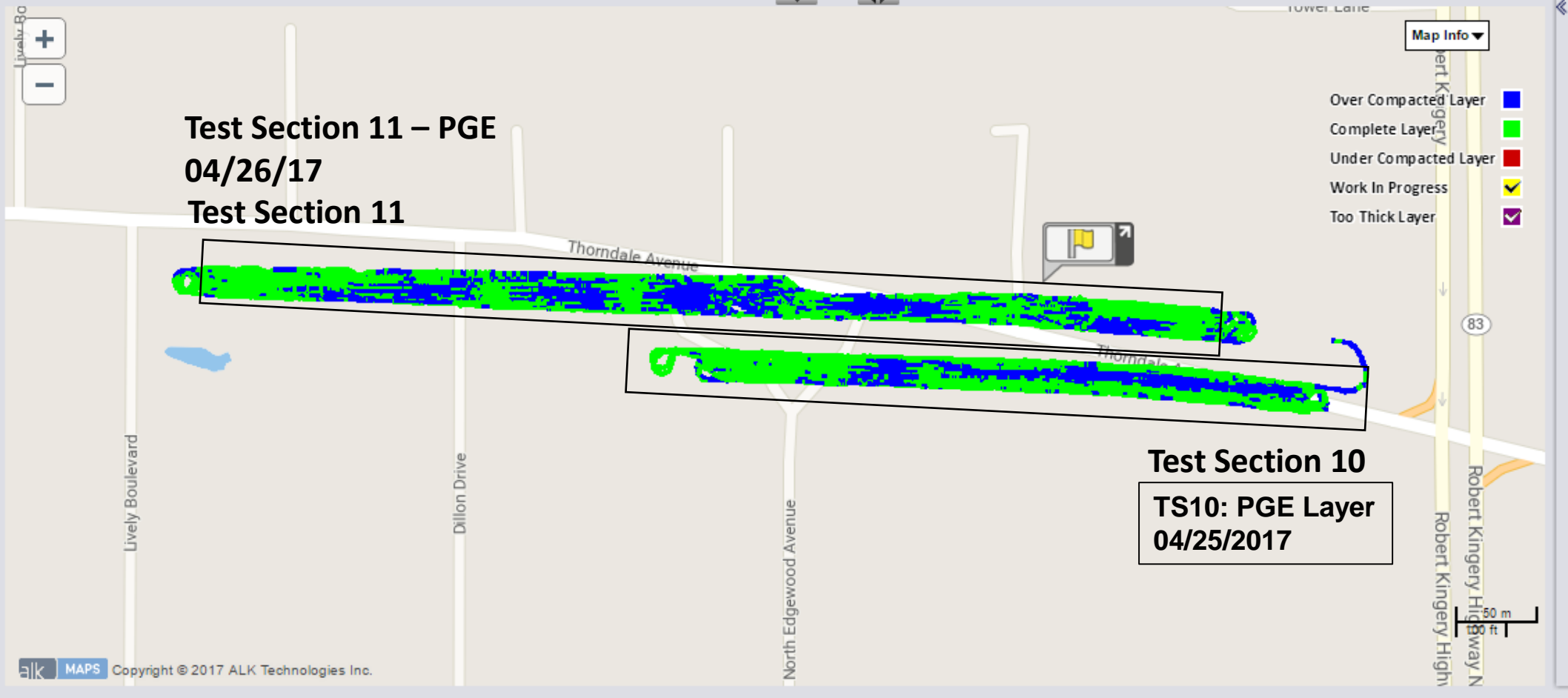
Projects > Plote Ohare West Tollway > 1 Results

Fleet Alerts Health Maintenance Utilization **Project** Administration

3D Project Monitoring 12 04/24/17 12:00 am - 04/27/17 11:59 pm

Section View MDP Summary Settings

- All Assets (1)
- Groups
- Projects
- Plote Ohare West Tollway



VIC Calibration Report

06/21/2017 to 06/23/2017

On Site Personnel

David J. White, Ph.D., P.E. (Ingios)
Pavana Vennapusa, Ph.D., P.E. (Ingios)
Heath Gieselman, M.S. (Ingios)
James Colby Van Nimwegen (Ingios)

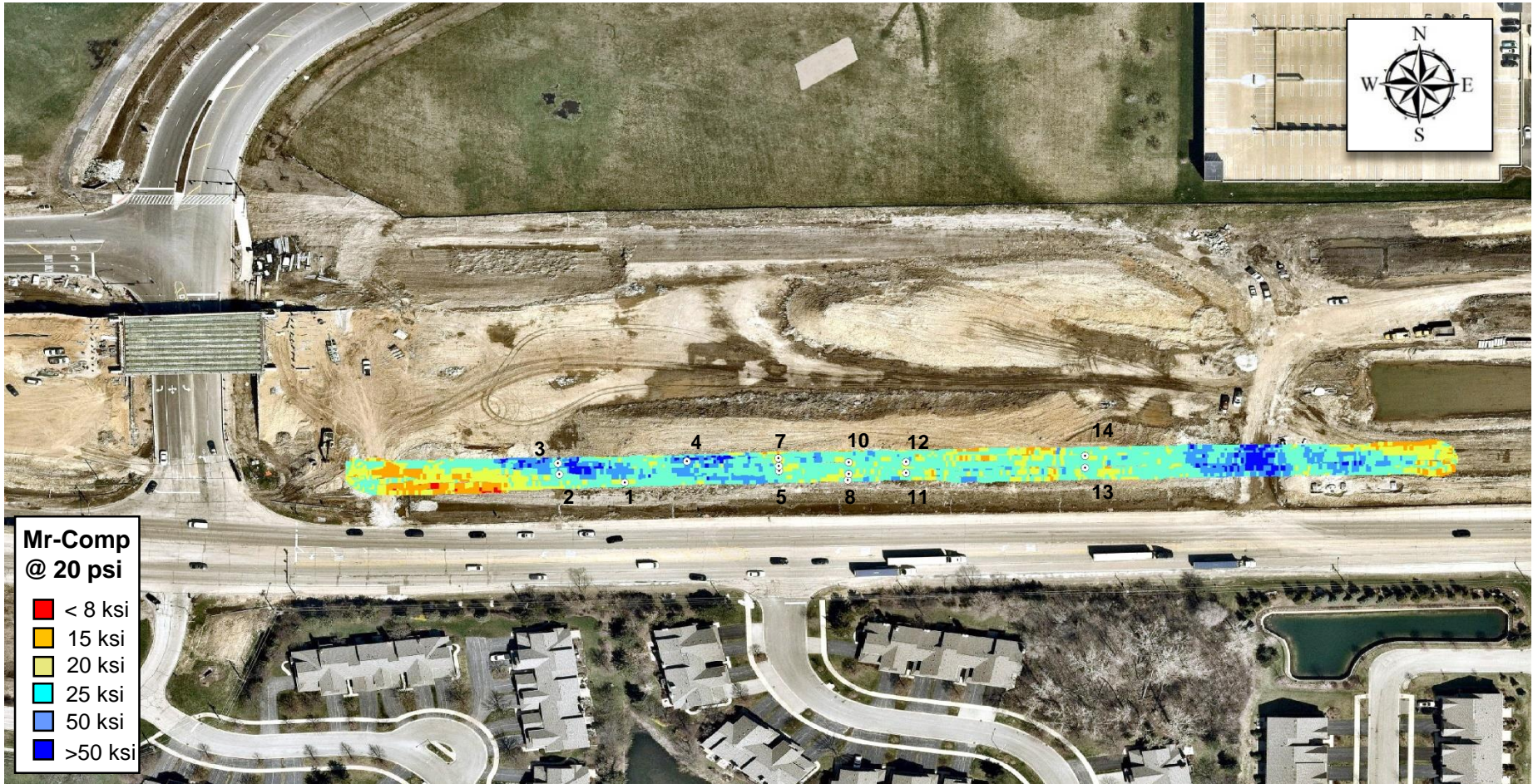
PROJECT NAME: Validation of Intelligent Compaction to Characterize
Pavement Foundation Mechanical Properties
PROJECT ID: ILT_IC Project
LOCATION: Elgin O'Hare Expressway, Elgin, IL



MAP ID: ILT_RAP_TS13
Surface Material: RAP Capping Layer
Mapping Time: 1.2 hrs
No. of Measurements: 4,162

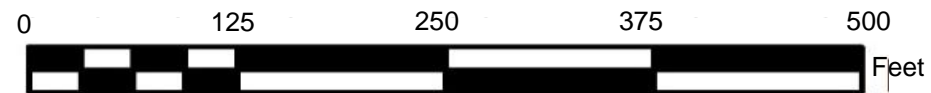
Property: Mr-Comp at 20 psi
Mean: 35,744 psi
Standard Deviation: 18,750 psi
Coeff. Of Variation: 52%

Machine: CS56
Drum Configuration: Smooth
Vibration Settings: f = 30 Hz, low amp
Speed: 3 mph (nominal)



Mr-Comp @ 20 psi

- < 8 ksi
- 15 ksi
- 20 ksi
- 25 ksi
- 50 ksi
- >50 ksi



DATE: 06/21/2017
OPERATOR: DW (Ingios)

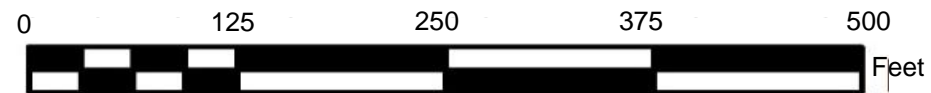
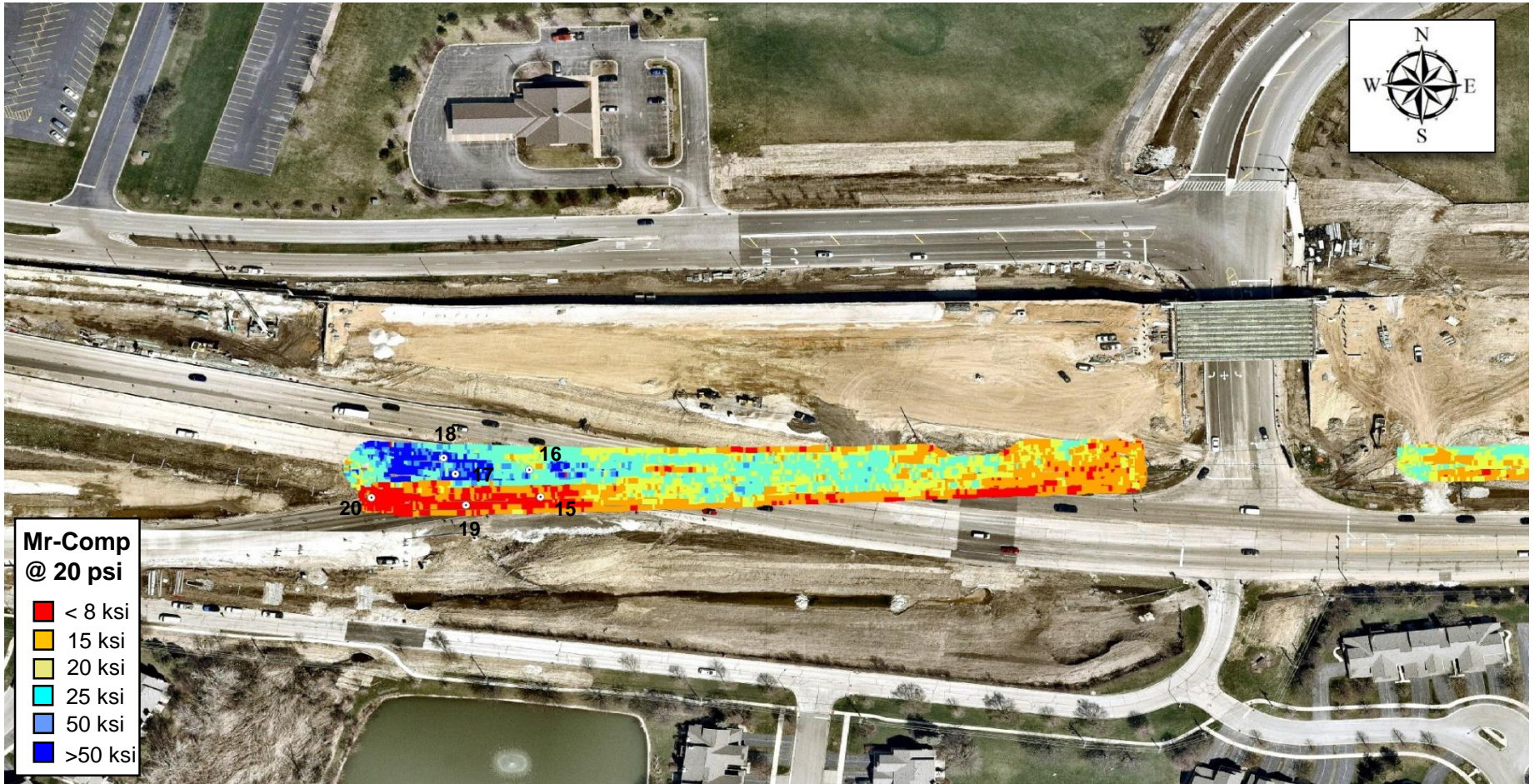
VIC Compaction Record – VIC Mr-Comp @ 20 psi Cyclic Stress
PROJECT NAME: Validation of Intelligent Compaction to Characterize Pavement Foundation Mechanical Properties
PROJECT ID: ILT_IC Project
LOCATION: Elgin O'Hare Expressway, Elgin, IL



MAP ID: ILT_SG_TS14
 Surface Material: Subgrade
 Mapping Time: 0.8 hrs
 No. of Measurements: 5,621

Property: Mr-Comp at 20 psi
 Mean: 24,270
 Standard Deviation: 19,026
 Coeff. Of Variation: 78%

Machine: CS56
 Drum Configuration: Smooth
 Vibration Settings: f = 30 Hz, low amp
 Speed: 3 mph (nominal)



DATE: 06/21/2017
 OPERATOR: DW (Ingios)

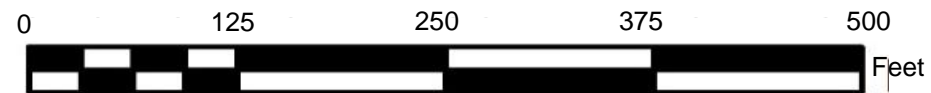
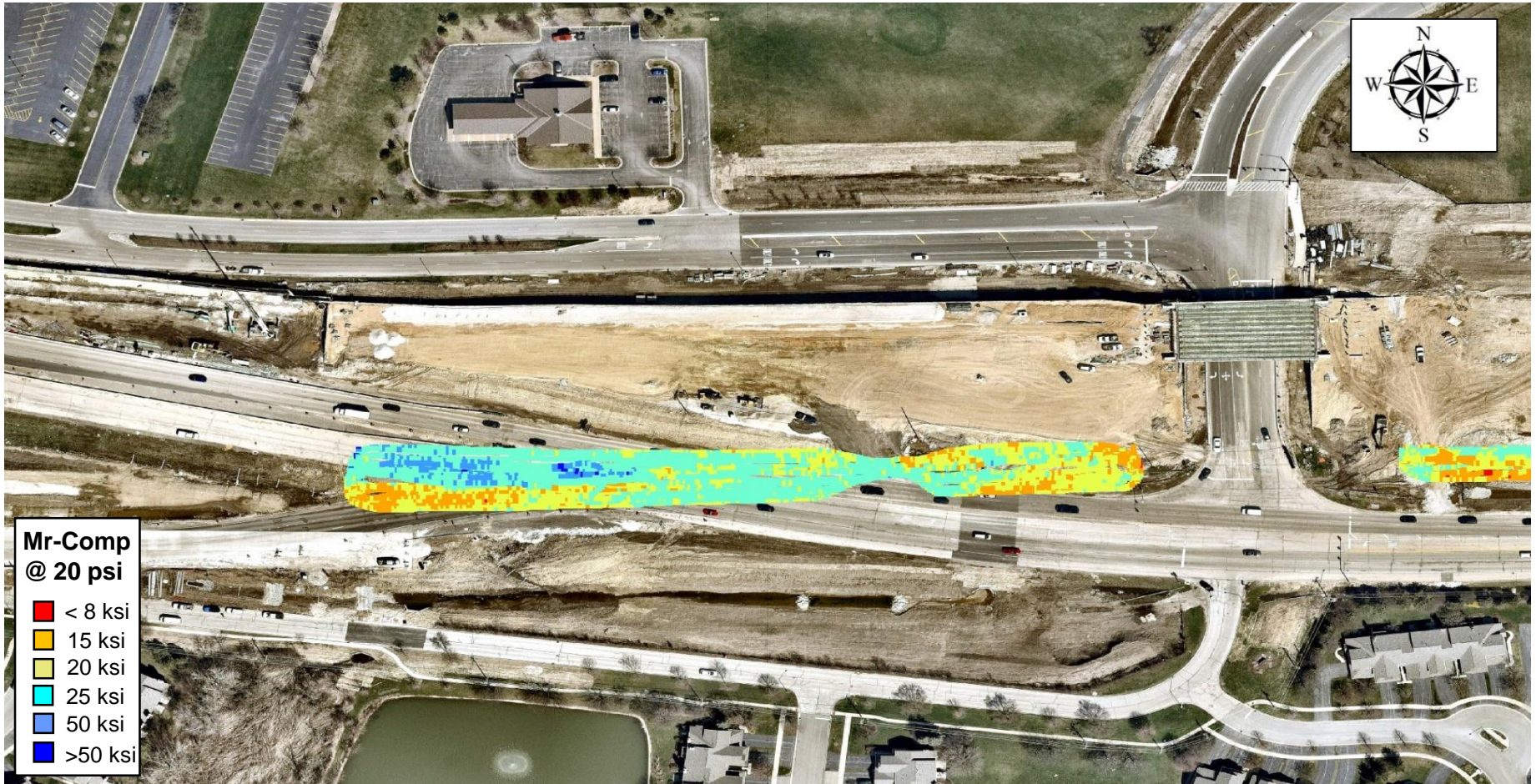
VIC Compaction Record – VIC Mr-Comp @ 20 psi Cyclic Stress
 PROJECT NAME: Validation of Intelligent Compaction to Characterize Pavement Foundation Mechanical Properties
 PROJECT ID: ILT_IC Project
 LOCATION: Elgin O'Hare Expressway, Elgin, IL



MAP ID: ILT_PGE_TS15
 Surface Material: PGE
 Mapping Time: 1.4
 No. of Measurements: 4,844

Property: Mr-Comp at 20 psi
 Mean: 28,754
 Standard Deviation: 12,280
 Coeff. Of Variation: 43%

Machine: CS56
 Drum Configuration: Smooth
 Vibration Settings: f = 30 Hz, low amp
 Speed: 3 mph (nominal)



DATE: 06/22/2017
 OPERATOR: DW (Ingios)

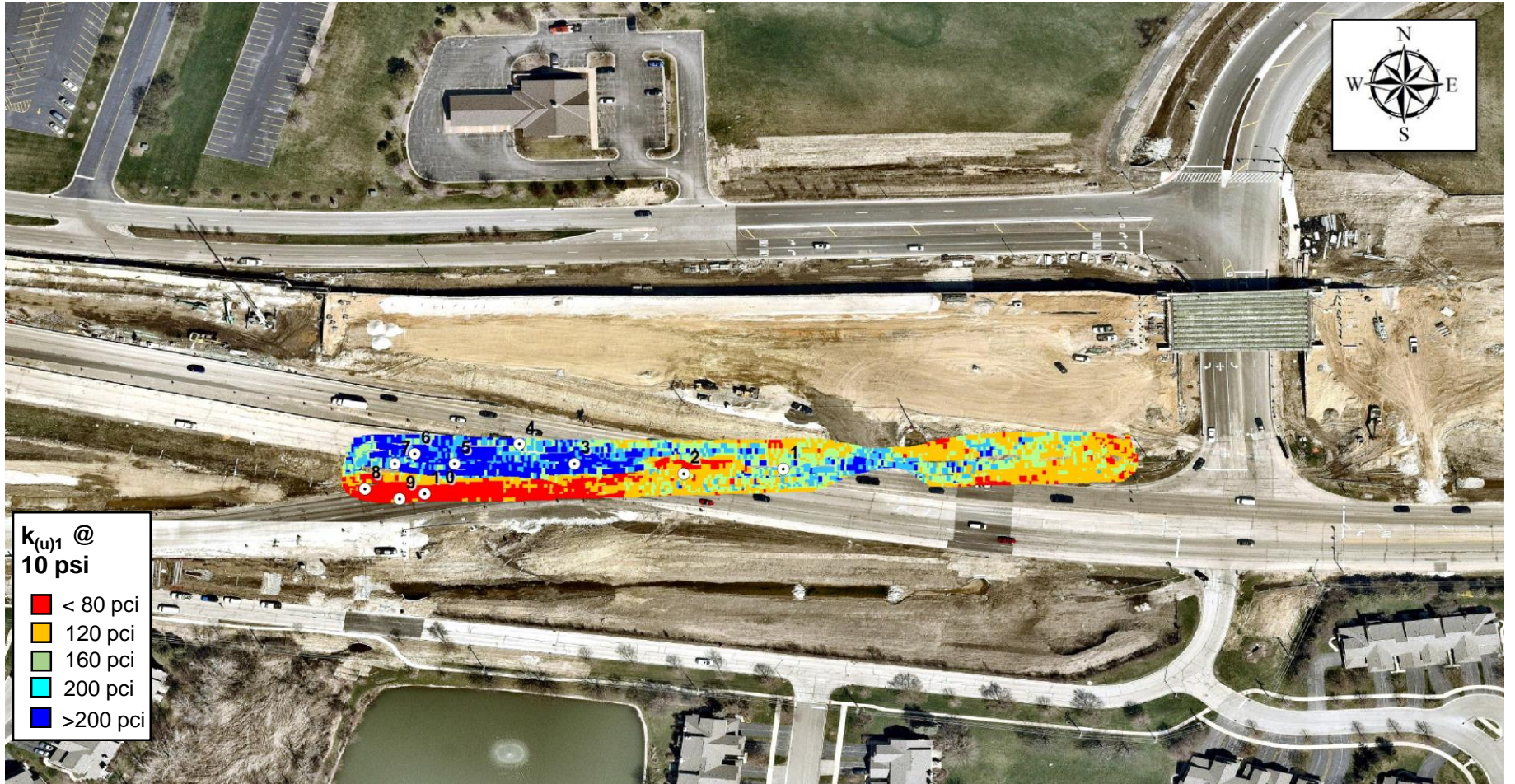
VIC Compaction Record – VIC Mr-Comp @ 20 psi Cyclic Stress
 PROJECT NAME: Validation of Intelligent Compaction to Characterize Pavement Foundation Mechanical Properties
 PROJECT ID: ILT_IC Project
 LOCATION: Elgin O'Hare Expressway, Elgin, IL



MAP ID: ILT_PGE_TS15
 Surface Material: PGE
 Mapping Time: 1.4
 No. of Measurements: 4,844

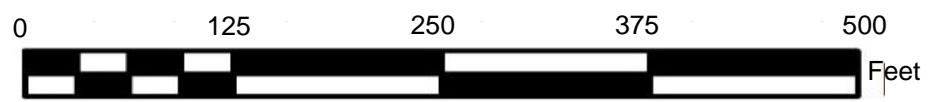
Property: $k_{(u)1}$ @ 10 psi
 Mean: 136
 Standard Deviation: 72
 Coeff. Of Variation: 53%

Machine: CS56
 Drum Configuration: Smooth
 Vibration Settings: f = 30 Hz, low amp
 Speed: 3 mph (nominal)



$k_{(u)1}$ @ 10 psi

- < 80 pci
- 120 pci
- 160 pci
- 200 pci
- > 200 pci



DATE: 06/22/2017
 OPERATOR: DW (Ingios)

VIC Compaction Record – VIC $k_{(u)1}$ @ 10 psi Stress

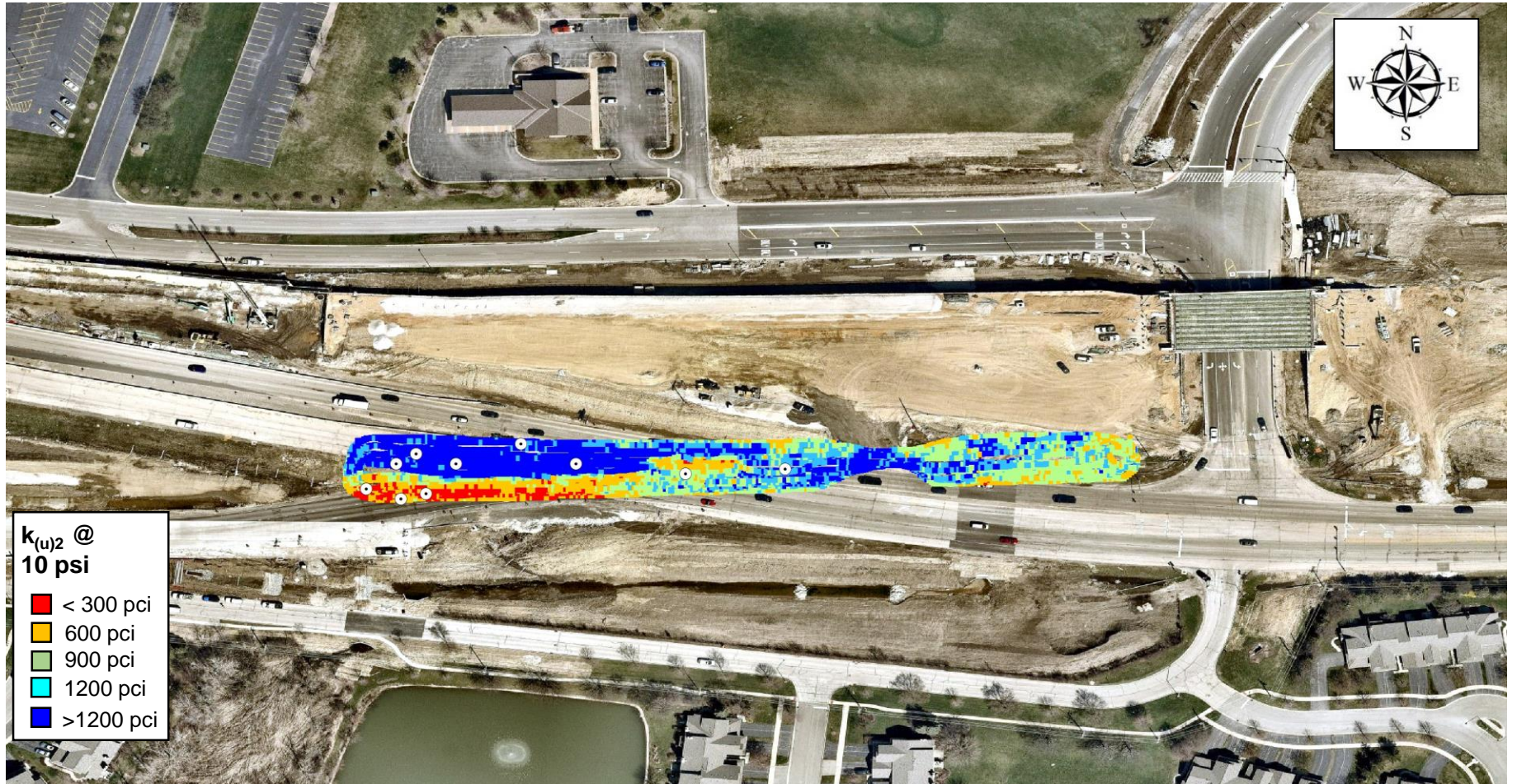
PROJECT NAME: Validation of Intelligent Compaction to Characterize Pavement Foundation Mechanical Properties
 PROJECT ID: ILT_IC Project
 LOCATION: Elgin O'Hare Expressway, Elgin, IL



MAP ID: ILT_PGE_TS15
 Surface Material: PGE
 Mapping Time: 1.4
 No. of Measurements: 4,844

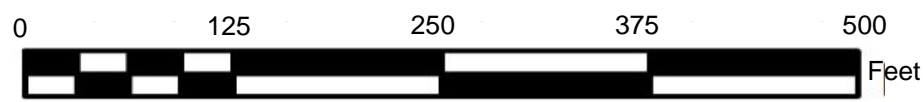
Property: $k_{(u)2}$ @ 10 psi
 Mean: 1,012
 Standard Deviation: 596
 Coeff. Of Variation: 59%

Machine: CS56
 Drum Configuration: Smooth
 Vibration Settings: f = 30 Hz, low amp
 Speed: 3 mph (nominal)



$k_{(u)2}$ @ 10 psi

- < 300 pci
- 600 pci
- 900 pci
- 1200 pci
- >1200 pci



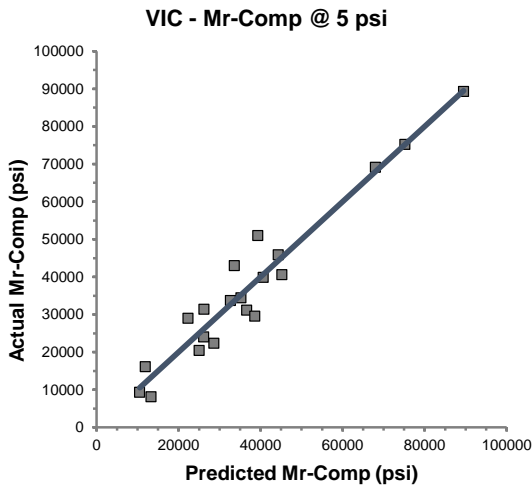
DATE: 06/22/2017
 OPERATOR: DW (Ingios)

VIC Compaction Record – VIC $k_{(u)2}$ @ 10 psi Stress

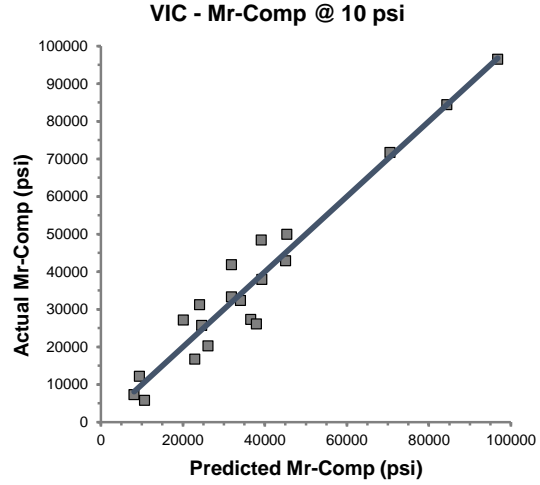
PROJECT NAME: Validation of Intelligent Compaction to Characterize Pavement Foundation Mechanical Properties
 PROJECT ID: ILT_IC Project
 LOCATION: Elgin O'Hare Expressway, Elgin, IL



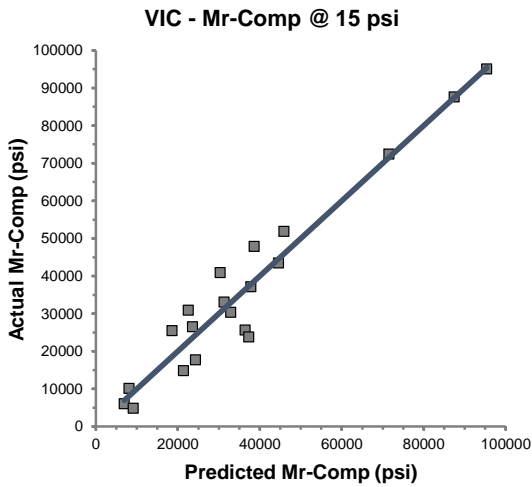
CAL ID	ILT_June2017	TESTED BY	DW, PV, HG, JV	INPUT BY	PV
TESTED DATE	06/21/17 to 06/22/17	TESTED TIMES	2:00 PM to 2:00 AM	INPUT DATE	6/22/2017
Notes	Calibration data obtained from in situ testing and mapping performed on TS13 (RAP Capping Layer) and TS14 (Subgrade). In situ Mr-Comp determined using APLT setup with 12 in. diameter plate at multiple stress levels (5 psi to 40 psi).				



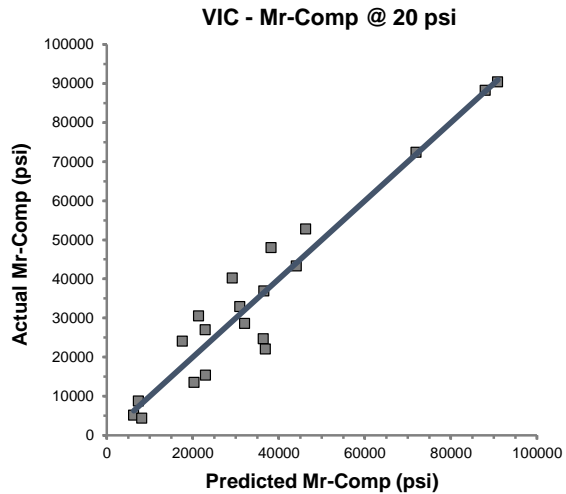
n	20	F	p-value
R ²	0.936	54.47	<0.0001
R ² adjusted	0.918		
SE of fit (RMSE)	6025.2		



n	20	F	p-value
R ²	0.941	59.49	<0.0001
R ² adjusted	0.925		
SE of fit (RMSE)	6599.8		



n	20	F	p-value
R ²	0.934	52.95	<0.0001
R ² adjusted	0.916		
SE of fit (RMSE)	7209.1		



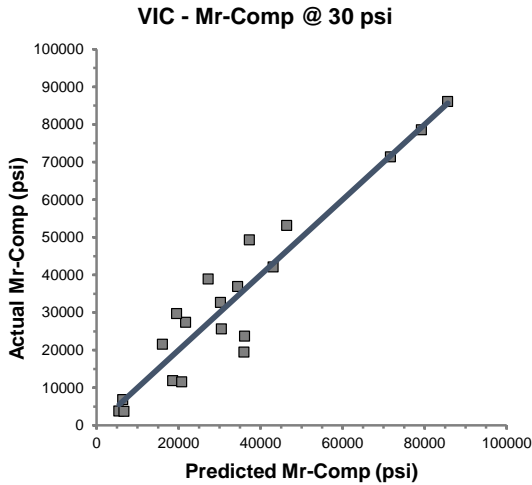
n	20	F	p-value
R ²	0.924	45.69	<0.0001
R ² adjusted	0.904		
SE of fit (RMSE)	7716.7		

VIC Calibration Data Record

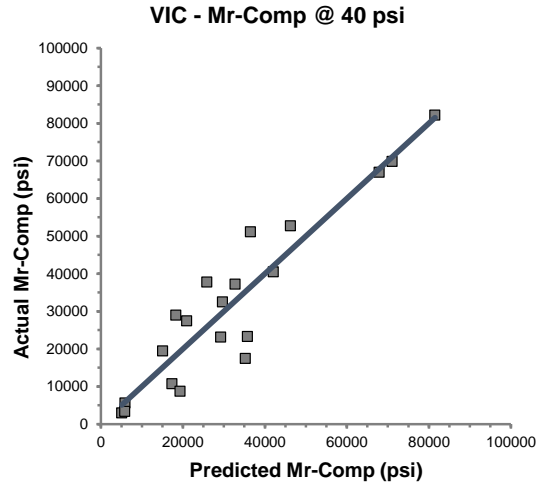
Project Name: Illinois Tollway - IC Research
Project ID: Elgin O'Hare Extension - IL Tollway
Location: IL390 (West of O'Hare), Itasca, IL



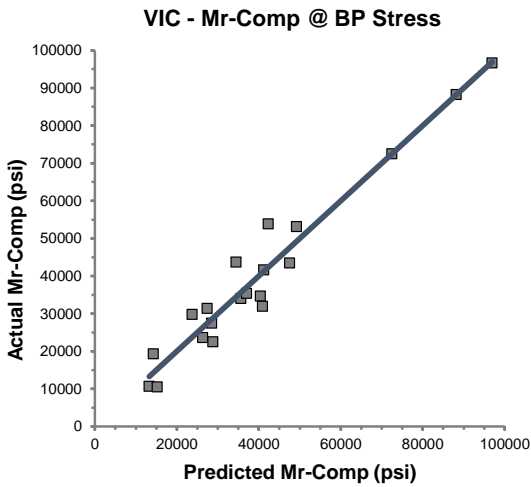
CAL ID	ILT_June2017	TESTED BY	DW, PV, HG, JV	INPUT BY	PV
TESTED DATE	06/21/17 to 06/22/17	TESTED TIMES	2:00 PM to 2:00 AM	INPUT DATE	6/22/2017
Notes	Calibration data obtained from in situ testing and mapping performed on TS13 (RAP Capping Layer) and TS14 (Subgrade). In situ Mr-Comp determined using APLT setup with 12 in. diameter plate at multiple stress levels (5 psi to 40 psi).				



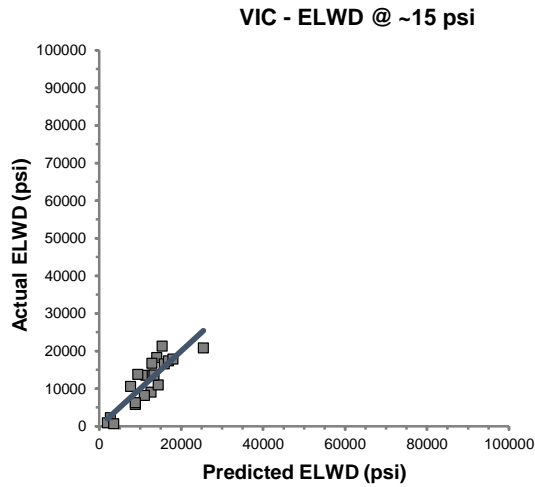
n	20	F	33.79	p-value	<0.0001
R ²	0.900				
R ² adjusted	0.873				
SE of fit (RMSE)	8544.5				



n	20	F	25.50	p-value	<0.0001
R ²	0.872				
R ² adjusted	0.838				
SE of fit (RMSE)	9246.7				



n	20	F	68.90	p-value	<0.0001
R ²	0.948				
R ² adjusted	0.935				
SE of fit (RMSE)	5924.3				



n	20	F	12.07	p-value	0.0001
R ²	0.763				
R ² adjusted	0.700				
SE of fit (RMSE)	3477.9				

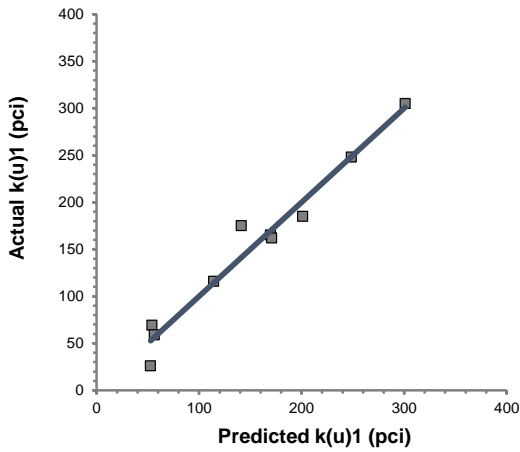
VIC Calibration Data Record

Project Name: Illinois Tollway - IC Research
Project ID: Elgin O'Hare Extension - IL Tollway
Location: IL390 (West of O'Hare), Itasca, IL



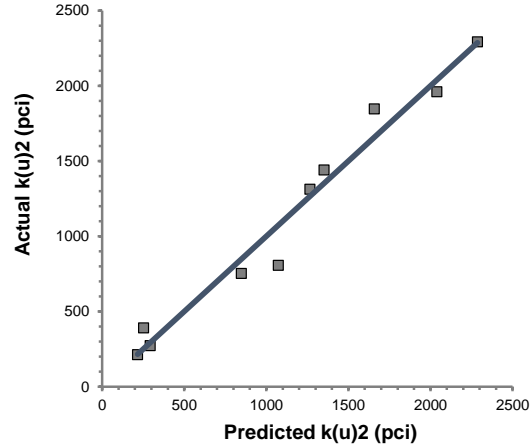
CAL ID	ILT_June2017	TESTED BY	DW, PV, HG, JV	INPUT BY	PV
TESTED DATE	06/21/17 to 06/22/17	TESTED TIMES	2:00 PM to 2:00 AM	INPUT DATE	6/22/2017
Notes	Calibration data obtained from in situ testing and mapping performed on TS13 (RAP Capping Layer) and TS14 (Subgrade). In situ Mr-Comp determined using APLT setup with 12 in. diameter plate at multiple stress levels (5 psi to 40 psi).				

VIC - k(u)1 (initial load @ 10 psi)



n	10	F	21.04	p-value	0.0057
R ²	0.963				
R ² adjusted	0.918				
SE of fit (RMSE)	24.8				

VIC - k(u)2 (reload @ 10 psi)



n	10	F	25.78	p-value	0.0038
R ²	0.970				
R ² adjusted	0.932				
SE of fit (RMSE)	195.0				

VIC Calibration Data Record

Project Name: Illinois Tollway - IC Research
Project ID: Elgin O'Hare Extension - IL Tollway
Location: IL390 (West of O'Hare), Itasca, IL



APPENDIX C: SUMMARY OF IN SITU TEST RESULTS

Summary of LWD Testing Results

Date	TS	PT	Material	S _{avg} (mm)	s/v	E _{vd} (Mpa)	E _{LWD} (Mpa)	E _{LWD} (psi)
10/12/2016	1	1	RPCC - PGE	1.182	6.083	19.0	28.4	4,123
10/12/2016	1	2	RPCC - PGE	1.198	6.041	18.8	28.0	4,068
10/12/2016	1	3	RPCC - PGE	1.715	7.212	13.1	19.6	2,842
10/12/2016	1	4	RPCC - PGE	1.437	6.889	15.7	23.4	3,391
10/12/2016	1	5	RPCC - PGE	1.481	6.65	15.2	22.7	3,291
10/12/2016	1	6	RPCC - PGE	1.415	6.533	15.9	23.7	3,444
10/12/2016	1	7	RPCC - PGE	1.036	5.185	21.7	32.4	4,704
10/12/2016	1	8	RPCC - PGE	0.676	3.646	33.3	49.7	7,209
10/12/2016	1	9	RPCC - PGE	0.666	4.183	33.8	50.5	7,317
10/12/2016	1	10	RPCC - PGE	0.46	3.577	48.9	73.0	10,594
10/12/2016	1	11	RPCC - PGE	0.52	3.114	43.3	64.6	9,372
10/12/2016	1	12	RPCC - PGE	0.416	3.583	54.1	80.8	11,715
10/12/2016	1	13	RPCC - PGE	0.525	3.182	42.9	64.0	9,282
10/12/2016	1	14	RPCC - PGE	0.463	3.231	48.6	72.6	10,525
10/12/2016	1	15	RPCC - PGE	0.511	3.276	44.0	65.8	9,537
10/12/2016	1	16	RPCC - PGE	0.532	3.354	42.3	63.2	9,160
10/12/2016	1	17	RPCC - PGE	0.577	3.577	39.0	58.2	8,446
10/12/2016	1	18	RPCC - PGE	0.478	3.084	47.1	70.3	10,195
10/12/2016	1	19	RPCC - PGE	0.544	3.049	41.4	61.8	8,958
10/12/2016	1	20	RPCC - PGE	0.543	3.263	41.4	61.9	8,975
10/12/2016	1	21	RPCC - PGE	0.528	3.202	42.6	63.6	9,230
10/12/2016	1	22	RPCC - PGE	0.561	3.619	40.1	59.9	8,687
10/12/2016	1	23	RPCC - PGE	0.443	3.158	50.8	75.8	11,001
10/12/2016	1	24	RPCC - PGE	0.746	3.278	30.2	45.0	6,533
10/12/2016	1	25	RPCC - PGE	0.806	3.777	27.9	41.7	6,046
10/12/2016	1	26	RPCC - PGE	0.675	3.954	33.3	49.8	7,220
10/12/2016	1	27	RPCC - PGE	0.733	4.317	30.7	45.8	6,648
10/12/2016	1	28	RPCC - PGE	0.513	3.134	43.9	65.5	9,500
10/12/2016	1	29	RPCC - PGE	0.528	2.767	42.6	63.6	9,230
10/12/2016	1	30	RPCC - PGE	0.775	4.562	29.0	43.4	6,288
10/12/2016	1	31	RPCC - PGE	0.672	3.684	33.5	50.0	7,252
10/12/2016	1	32	RPCC - PGE	0.45	3.299	50.0	74.7	10,830
10/12/2016	1	33	RPCC - PGE	0.493	3.025	45.6	68.2	9,885
10/12/2016	1	34	RPCC - PGE	0.354	2.682	63.6	94.9	13,766
10/12/2016	1	35	RPCC - PGE	0.587	3.17	38.3	57.2	8,302
10/12/2016	1	36	RPCC - PGE	0.477	3.136	47.2	70.4	10,217
10/12/2016	1	37	RPCC - PGE	0.672	4.002	33.5	50.0	7,252
10/12/2016	1	38	RPCC - PGE	0.557	3.248	40.4	60.3	8,749

Date	TS	PT	Material	S _{avg} (mm)	s/v	E _{vd} (Mpa)	E _{LWD} (Mpa)	E _{LWD} (psi)
10/12/2016	1	39	RPCC - PGE	0.454	3.266	49.6	74.0	10,734
10/12/2016	1	40	RPCC - PGE	0.553	2.824	40.7	60.8	8,812
10/12/2016	2	41	RAP (Access Road)	0.256	2.599	87.9	131.3	19,036
10/12/2016	2	42	RAP (Access Road)	0.3	2.806	65.8	112.0	16,244
10/12/2016	2	43	RAP (Access Road)	0.342	2.971	75.0	98.2	14,249
10/12/2016	2	44	RAP (Access Road)	0.303	2.991	74.3	110.9	16,083
10/12/2016	2	45	RAP (Access Road)	0.312	2.974	72.1	107.7	15,619
10/12/2016	2	46	RAP (Access Road)	0.38	3.223	59.2	88.4	12,824
10/12/2016	2	47	RPCC - PGE	0.447	2.906	50.3	75.2	10,902
10/12/2016	2	48	RPCC - PGE	0.321	2.394	70.1	104.7	15,182
10/12/2016	2	49	RPCC - PGE	0.32	2.705	70.3	105.0	15,229
10/12/2016	2	50	RPCC - PGE	0.46	2.785	48.9	73.0	10,594
10/12/2016	3	51	RPCC - PGE (RAMP)	0.369	3.101	61.0	91.1	13,207
10/12/2016	3	52	RPCC - PGE (RAMP)	0.448	3.353	50.2	75.0	10,878
10/12/2016	3	53	RPCC - PGE (RAMP)	0.359	2.651	62.7	93.6	13,575
10/12/2016	3	54	RPCC - PGE (RAMP)	0.343	2.897	65.6	98.0	14,208
10/12/2016	3	55	RPCC - PGE (RAMP)	0.395	2.832	57.0	85.1	12,337
10/13/2016	4	56	RAP - CA6 CAP	0.39	4.768	57.7	86.2	12,496
10/13/2016	4	57	RAP - CA6 CAP	0.463	3.944	48.6	72.6	10,525
10/13/2016	4	58	RAP - CA6 CAP	0.473	4.856	47.6	71.0	10,303
10/13/2016	4	59	RAP - CA6 CAP	0.549	5.545	41.0	61.2	8,877
10/13/2016	4	60	RAP - CA6 CAP	0.166	3.018	135.5	202.4	29,357
10/13/2016	4	61	RAP - CA6 CAP	0.243	3.135	92.6	138.3	20,055
10/13/2016	4	62	RAP - CA6 CAP	0.302	3.344	74.5	111.3	16,137
10/13/2016	4	63	RAP - CA6 CAP	0.32	4.134	70.3	105.0	15,229
10/13/2016	4	64	RAP - CA6 CAP	1.316	7.056	17.1	25.5	3,703
10/13/2016	4	65	RAP - CA6 CAP	0.279	3.135	80.7	120.4	17,467
4/11/2017	6	1	RPCC - PGE	0.345	2.782	65.2	97.4	14,125
4/11/2017	6	2	RPCC - PGE	2.206	7.39	10.2	15.2	2,209
4/11/2017	6	3	RPCC - PGE	0.825	6.212	27.3	40.7	5,907
4/11/2017	6	4	RPCC - PGE	3.037	8.357	7.4	11.1	1,605
4/11/2017	6	5	RPCC - PGE	2.393	7.377	9.4	14.0	2,036
4/11/2017	6	6	RPCC - PGE	1.052	6.722	21.4	31.9	4,632
4/11/2017	6	7	RPCC - PGE	1.243	5.676	18.1	27.0	3,921
4/11/2017	6	8	RPCC - PGE	0.334	3.212	67.4	100.6	14,591
4/11/2017	6	9	RPCC - PGE	0.666	4.651	33.8	50.5	7,317
4/11/2017	6	10	RPCC - PGE	0.932	5.26	24.1	36.1	5,229
4/11/2017	6	11	RPCC - PGE	1.011	5.198	22.3	33.2	4,820
4/11/2017	6	12	RPCC - PGE	0.529	4.423	42.5	63.5	9,212
4/11/2017	6	13	RPCC - PGE	0.96	4.122	23.4	35.0	5,076
4/11/2017	6	14	RPCC - PGE	0.377	2.762	59.7	89.1	12,926
4/11/2017	6	15	RPCC - PGE	0.447	3.326	50.3	75.2	10,902

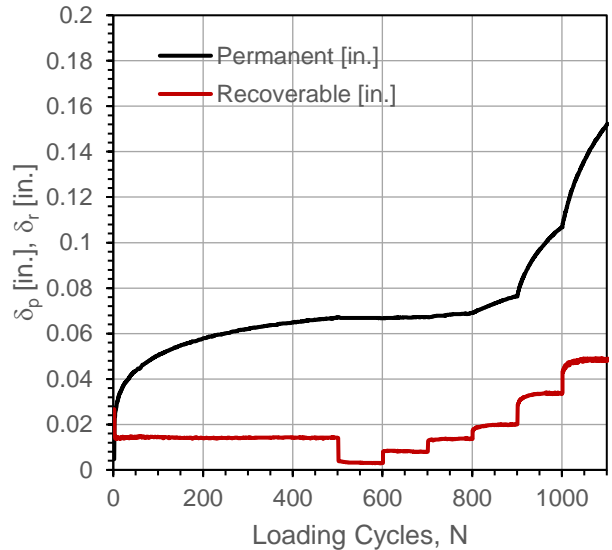
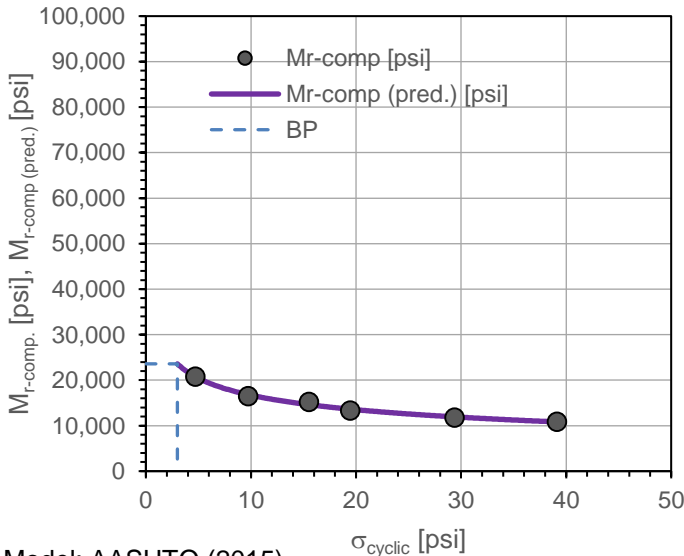
Date	TS	PT	Material	S _{avg} (mm)	s/v	E _{vd} (Mpa)	E _{LWD} (Mpa)	E _{LWD} (psi)
4/12/2017	7	16	CA6-RAP Capping	0.199	3.062	113.1	168.8	24,489
4/12/2017	7	17	CA6-RAP Capping	0.594	5.45	37.9	56.6	8,204
4/12/2017	7	18	CA6-RAP Capping	0.934	6.813	24.1	36.0	5,218
4/12/2017	7	19	CA6-RAP Capping	0.983	7.207	22.9	34.2	4,958
4/12/2017	7	20	CA6-RAP Capping	0.286	3.629	78.7	117.5	17,039
4/12/2017	7	21	CA6-RAP Capping	1.09	7.676	20.6	30.8	4,471
4/12/2017	7	22	CA6-RAP Capping	0.658	5.328	34.2	51.1	7,406
4/12/2017	7	23	CA6-RAP Capping	0.239	3.4	94.1	140.6	20,390
4/12/2017	7	24	CA6-RAP Capping	0.355	3.561	63.4	94.6	13,728
4/12/2017	7	25	CA6-RAP Capping	0.846	6.917	26.6	39.7	5,760
4/12/2017	7	26	CA6-RAP Capping	0.423	5.159	53.2	79.4	11,521
4/12/2017	7	27	CA6-RAP Capping	0.961	7.731	23.4	35.0	5,071
4/12/2017	7	28	CA6-RAP Capping	0.282	3.389	79.8	119.1	17,281
4/12/2017	7	29	CA6-RAP Capping	0.307	2.992	73.3	109.4	15,874
4/12/2017	7	30	CA6-RAP Capping	0.382	3.793	58.9	88.0	12,757
4/12/2017	7	31	CA6-RAP Capping	0.64	6.038	35.2	52.5	7,614
4/12/2017	7	32	CA6-RAP Capping	0.26	3.19	86.5	129.2	18,743
4/12/2017	7	33	CA6-RAP Capping	1.689	9.564	13.3	19.9	2,885
4/12/2017	7	34	CA6-RAP Capping	0.757	6.085	29.7	44.4	6,438
4/12/2017	7	35	CA6-RAP Capping	0.328	3.482	68.6	102.4	14,858
4/12/2017	7	36	CA6-RAP Capping	0.401	4.33	56.1	83.8	12,153
4/12/2017	7	37	CA6-RAP Capping	0.797	5.067	28.2	42.2	6,115
4/12/2017	7	38	CA6-RAP Capping	0.37	4.084	60.8	90.8	13,171
4/12/2017	7	39	CA6-RAP Capping	1.479	7.538	15.2	22.7	3,295
4/12/2017	7	40	CA6-RAP Capping	0.763	6.332	29.5	44.0	6,387
4/18/2017	9	1	CA6-RAP Capping	0.833	6.296	27.0	40.3	5,850
4/18/2017	9	2	CA6-RAP Capping	2.875	9.789	7.8	11.7	1,695
4/18/2017	9	3	CA6-RAP Capping	0.295	3.26	76.3	113.9	16,520
4/18/2017	9	4	CA6-RAP Capping	0.332	3.673	67.8	101.2	14,679
4/18/2017	9	5	CA6-RAP Capping	0.505	4.215	44.6	66.5	9,650
4/18/2017	9	6	CA6-RAP Capping	0.271	3.379	83.0	124.0	17,983
4/18/2017	9	7	CA6-RAP Capping	0.337	3.185	66.8	99.7	14,461
4/18/2017	9	8	CA6-RAP Capping	0.668	5.314	33.7	50.3	7,295
4/18/2017	9	9	CA6-RAP Capping	0.615	5.104	36.6	54.6	7,924
4/18/2017	9	10	CA6-RAP Capping	1.008	6.47	22.3	33.3	4,835
4/18/2017	9	11	CA6-RAP Capping	1.212	7.092	18.6	27.7	4,021
4/18/2017	9	12	CA6-RAP Capping	0.324	3.699	69.4	103.7	15,041
4/18/2017	9	13	CA6-RAP Capping	1.381	7.706	16.3	24.3	3,529
4/18/2017	9	14	CA6-RAP Capping	1.366	7.24	16.5	24.6	3,568
4/18/2017	9	15	CA6-RAP Capping	1.644	8.483	13.7	20.4	2,964
5/4/2017	12	1	CA6-RAP Capping	0.57	6.312	39.5	58.9	8,550
5/4/2017	12	2	CA6-RAP Capping	0.333	4.531	67.6	100.9	14,634

Date	TS	PT	Material	S _{avg} (mm)	s/v	E _{vd} (Mpa)	E _{LWD} (Mpa)	E _{LWD} (psi)
5/4/2017	12	3	CA6-RAP Capping	0.453	5.201	49.7	74.2	10,758
5/4/2017	12	4	CA6-RAP Capping	0.663	5.638	33.9	50.7	7,350
5/4/2017	12	5	CA6-RAP Capping	1.398	8.577	16.1	24.0	3,486
5/4/2017	12	6	CA6-RAP Capping	0.773	6.31	29.1	43.5	6,304
5/4/2017	12	7	CA6-RAP Capping	0.613	5.284	36.7	54.8	7,950
5/4/2017	12	8	CA6-RAP Capping	0.815	6.996	27.6	41.2	5,979
5/4/2017	12	9	CA6-RAP Capping	0.339	3.52	66.4	99.1	14,375
5/4/2017	12	10	CA6-RAP Capping	0.545	4.827	41.3	61.7	8,942
5/4/2017	12	11	CA6-RAP Capping	0.344	3.9	65.4	97.7	14,167
5/4/2017	12	12	CA6-RAP Capping	0.786	6.303	28.6	42.7	6,200
5/4/2017	12	13	CA6-RAP Capping	0.367	0.367	61.3	91.6	13,279
5/4/2017	12	14	CA6-RAP Capping	1.367	7.641	16.5	24.6	3,565
5/4/2017	12	15	CA6-RAP Capping	0.311	3.337	72.4	108.0	15,670
6/21/2017	13	1	CA6-RAP Capping	0.842	6.993	26.7	39.9	5,788
6/21/2017	13	2	CA6-RAP Capping	0.538	4.936	41.8	62.5	9,058
6/21/2017	13	3	CA6-RAP Capping	0.267	2.89	84.3	125.8	18,252
6/21/2017	13	4	CA6-RAP Capping	0.445	4.432	50.6	75.5	10,951
6/21/2017	13	5	CA6-RAP Capping	0.361	4.625	62.3	93.1	13,499
6/21/2017	13	6	CA6-RAP Capping	0.294	3.67	76.5	114.3	16,576
6/21/2017	13	7	CA6-RAP Capping	0.229	2.921	98.3	146.7	21,281
6/21/2017	13	8	CA6-RAP Capping	0.598	5.712	37.6	56.2	8,149
6/21/2017	13	9	CA6-RAP Capping	0.462	5.291	48.5	72.7	10,548
6/21/2017	13	10	CA6-RAP Capping	0.292	3.852	77.1	115.1	16,689
6/21/2017	13	11	CA6-RAP Capping	0.785	5.34	28.7	42.8	6,208
6/21/2017	13	12	CA6-RAP Capping	0.354	3.839	63.6	94.9	13,766
6/21/2017	13	13	CA6-RAP Capping	0.281	3.394	80.1	119.6	17,343
6/21/2017	13	14	CA6-RAP Capping	0.36	4.265	62.5	93.3	13,537
6/21/2017	14	15	Subgrade	1.306	6.507	17.2	15.2	2,198
6/21/2017	14	16	Subgrade	0.138	2.296	163.0	143.4	20,801
6/21/2017	14	17	Subgrade	0.161	2.385	139.8	122.9	17,830
6/21/2017	14	18	Subgrade	0.211	2.576	106.6	93.8	13,605
6/21/2017	14	19	Subgrade	3.294	8.61	6.8	6.0	871
6/21/2017	14	20	Subgrade	4.276	7.681	5.3	4.6	671

Automated Plate Load Test [APLT]

Test:	In-situ Resilient Modulus [Mr]: Cyclic Loading, Composite, Stress-Dependent (5, 10, 15, 20, 30, 40)				
Date:	6/21/2017	Time:	7:59:42 PM	Test ID	ILT_12_Mr_pt1
Tested By	DW, HG, PV, JV	Location:	TS_13_RAP	Sta.	NA
Latitude,N:	41.983734	Longitude,W:	88.011536	Elev. (ft):	720
Comments:	RAP CA6 testing, east bound Thorndale Ave. b/w/ Hamilton Lakes Dr. and No. Arlington Heights Rd.				

Step	N	σ_{cyclic} [psi]	M_{r-comp} [psi]	M_{r-comp} (pred.) [psi]	δ_p [in.]	$\Delta\delta_p$ [in.]	$d = \Delta\log(\delta_p) / \Delta\log(N)$	Near-linear Elastic
Conditioning	500	15.53	---	---	0.0670	---	0.215	---
1	100	4.71	20,827	20,758	0.0667	-0.0003	-0.202	Y
2	100	9.73	16,487	16,823	0.0672	0.0002	0.407	Y
3	100	15.53	15,213	14,613	0.0691	0.0022	0.711	N
4	100	19.45	13,370	13,624	0.0765	0.0095	0.874	N
5	100	29.40	11,797	11,924	0.1069	0.0399	0.803	N
6	100	39.14	10,892	10,826	0.1518	0.0848	0.886	N



Model: AASHTO (2015)

$$M_{r-comp} = k_1^* P_a \left(\frac{\theta}{P_a}\right)^{k_2^*} \left(1 + \frac{\tau_{oct}}{P_a}\right)^{k_3^*}$$

Parameter	Value	P-Value
k_1^*	1,320.1	1.93E-07
k_2^*	-0.273	2.35E-02
k_3^*	-0.242	6.21E-01
Adj. R^2	0.989	
Std. Error [psi]	373	

M_{r-comp} (pred.)-BP [psi]	23,584
$\sigma_{cyclic-BP}$ [psi]	3.0



In-situ Resilient Modulus [Mr]: Cyclic Loading, Composite, Stress-Dependent

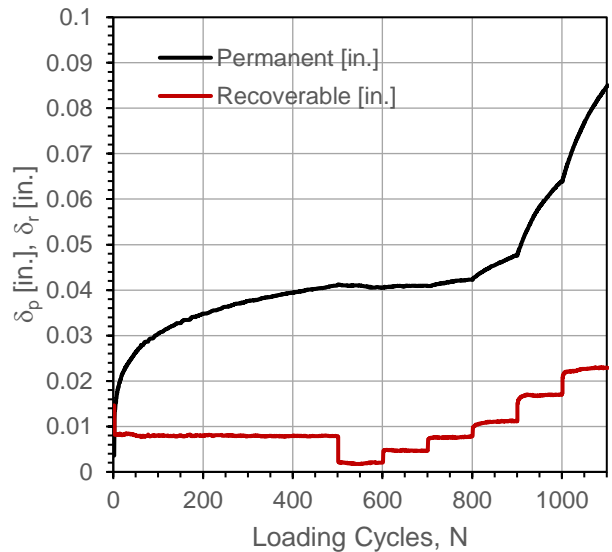
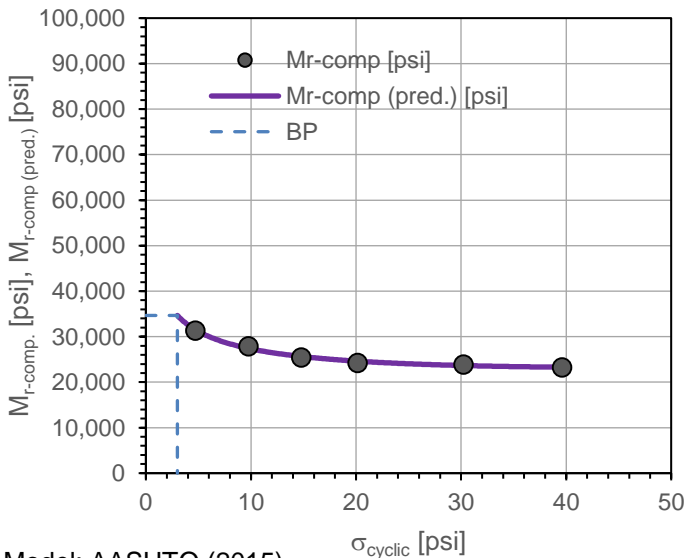
Project Name: Illinois Tollway - IC Research
 Project ID: Elgin O'Hare Extension - IL Tollway
 Location: IL390 (West of O'Hare), Itasca, IL



Automated Plate Load Test [APLT]

Test:	In-situ Resilient Modulus [Mr]: Cyclic Loading, Composite, Stress-Dependent (5, 10, 15, 20, 30, 40)				
Date:	6/21/2017	Time:	7:30:17 PM	Test ID	ILT_12_Mr_pt2
Tested By	DW, HG, PV, JV	Location:	TS_13_RAP	Sta.	NA
Latitude,N:	41.983780	Longitude,W:	88.011421	Elev. (ft):	717
Comments:	RAP CA6 testing, east bound Thorndale Ave. b/w Hamilton Lakes Dr. and No. Arlington Heights Rd.				

Step	N	σ_{cyclic} [psi]	M_{r-comp} [psi]	M_{r-comp} (pred.) [psi]	δ_p [in.]	$\Delta\delta_p$ [in.]	$d = \Delta\log(\delta_p) / \Delta\log(N)$	Near-linear Elastic
Conditioning	500	14.80	---	---	0.0410	---	0.219	---
1	100	4.71	31,345	31,518	0.0405	-0.0005	-0.447	Y
2	100	9.78	27,928	27,415	0.0410	-0.0001	0.290	Y
3	100	14.80	25,449	25,647	0.0423	0.0013	0.742	N
4	100	20.16	24,266	24,612	0.0477	0.0067	0.727	N
5	100	30.23	23,912	23,651	0.0639	0.0229	0.809	N
6	100	39.61	23,233	23,282	0.0848	0.0437	0.896	N



Model: AASHTO (2015)

$$M_{r-comp} = k_1^* P_a \left(\frac{\theta}{P_a}\right)^{k_2^*} \left(1 + \frac{\tau_{oct}}{P_a}\right)^{k_3^*}$$

Parameter	Value	P-Value
k_1^*	1,937.9	2.57E-08
k_2^*	-0.236	6.56E-03
k_3^*	0.660	6.99E-02
Adj. R^2	0.986	
Std. Error [psi]	360	

M_{r-comp} (pred.)-BP [psi]	34,664
$\sigma_{cyclic-BP}$ [psi]	3.0



In-situ Resilient Modulus [Mr]: Cyclic Loading, Composite, Stress-Dependent

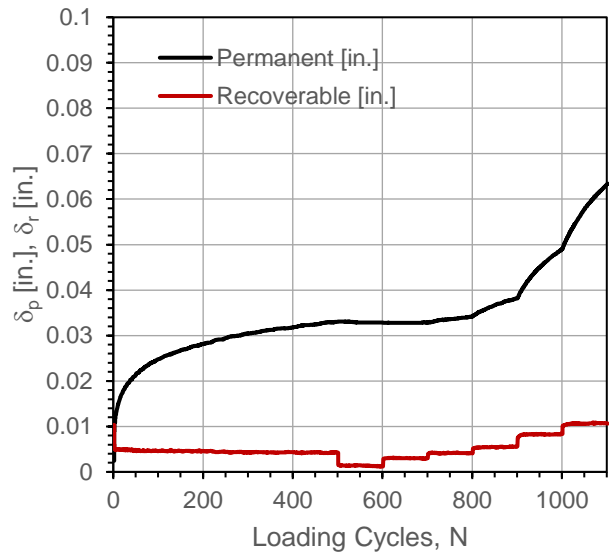
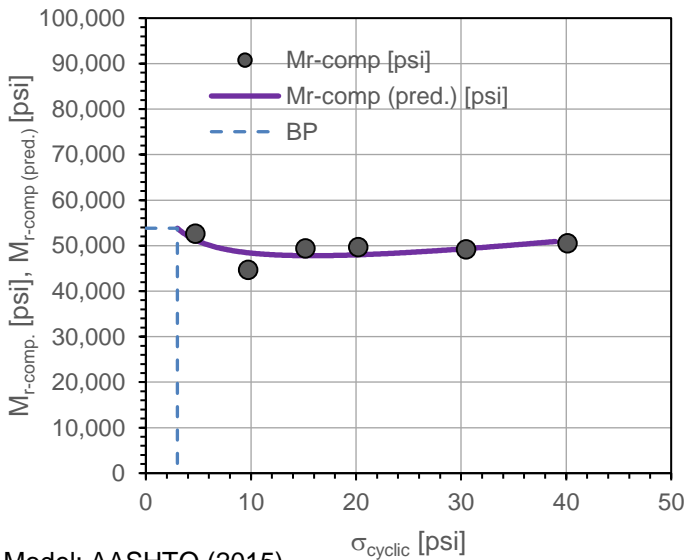
Project Name: Illinois Tollway - IC Research
 Project ID: Elgin O'Hare Extension - IL Tollway
 Location: IL390 (West of O'Hare), Itasca, IL



Automated Plate Load Test [APLT]

Test:	In-situ Resilient Modulus [Mr]: Cyclic Loading, Composite, Stress-Dependent (5, 10, 15, 20, 30, 40)				
Date:	6/21/2017	Time:	7:00:43 PM	Test ID:	ILT_12_Mr_pt3
Tested By:	DW, HG, PV, JV	Location:	TS_13_RAP	Sta.:	NA
Latitude, N:	41.983810	Longitude, W:	88.011452	Elev. (ft):	727
Comments:	RAP CA6 testing, east bound Thorndale Ave. b/w Hamilton Lakes Dr. and No. Arlington Heights Rd.				

Step	N	σ_{cyclic} [psi]	M_{r-comp} [psi]	M_{r-comp} (pred.) [psi]	δ_p [in.]	$\Delta\delta_p$ [in.]	$d = \Delta\log(\delta_p) / \Delta\log(N)$	Near-linear Elastic
Conditioning	500	15.20	---	---	0.0330	---	0.219	---
1	100	4.70	52,637	51,263	0.0328	-0.0002	-0.447	Y
2	100	9.75	44,746	48,434	0.0328	-0.0002	0.032	Y
3	100	15.20	49,406	47,801	0.0341	0.0011	0.545	Y
4	100	20.21	49,710	47,989	0.0382	0.0052	0.747	N
5	100	30.49	49,196	49,339	0.0490	0.0160	0.851	N
6	100	40.15	50,514	51,153	0.0632	0.0302	0.883	N



Model: AASHTO (2015)

$$M_{r-comp} = k_1^* P_a \left(\frac{\theta}{P_a}\right)^{k_2^*} \left(1 + \frac{\tau_{oct}}{P_a}\right)^{k_3^*}$$

Parameter	Value	P-Value
k_1^*	3,175.3	9.07E-07
k_2^*	-0.148	3.09E-01
k_3^*	1.026	3.03E-01
Adj. R ²	0.200	
Std. Error [psi]	1,386	

M_{r-comp} (pred.)-BP [psi]	53,828
$\sigma_{cyclic-BP}$ [psi]	3.0

No image.

In-situ Resilient Modulus [Mr]: Cyclic Loading, Composite, Stress-Dependent

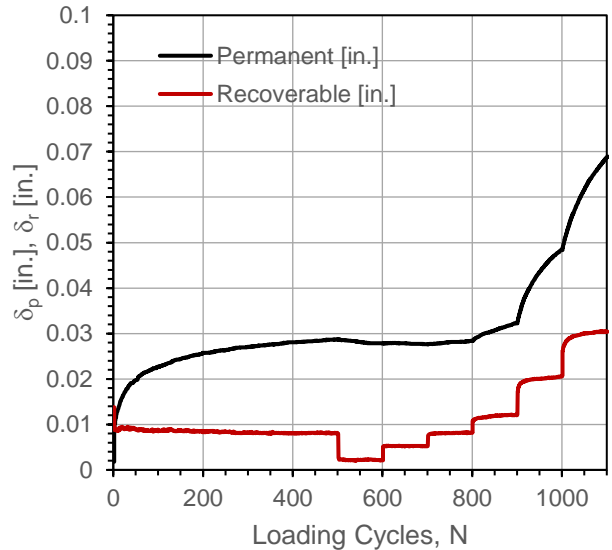
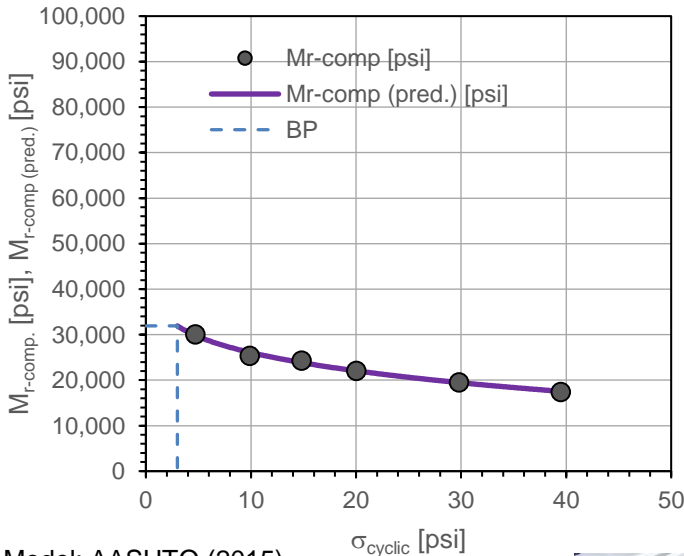
Project Name: Illinois Tollway - IC Research
 Project ID: Elgin O'Hare Extension - IL Tollway
 Location: IL390 (West of O'Hare), Itasca, IL



Automated Plate Load Test [APLT]

Test:	In-situ Resilient Modulus [Mr]: Cyclic Loading, Composite, Stress-Dependent (5, 10, 15, 20, 30, 40)				
Date:	6/21/2017	Time:	6:27:05 PM	Test ID:	ILT_12_Mr_pt4
Tested By:	DW, HG, PV, JV	Location:	TS_14_SG	Sta.:	NA
Latitude, N:	41.983803	Longitude, W:	88.011017	Elev. (ft):	729
Comments:	RAP CA6 testing, east bound Thorndale Ave. b/w Hamilton Lakes Dr. and No. Arlington Heights Rd.				

Step	N	σ_{cyclic} [psi]	M_{r-comp} [psi]	M_{r-comp} (pred.) [psi]	δ_p [in.]	$\Delta\delta_p$ [in.]	$d = \Delta\log(\delta_p) / \Delta\log(N)$	Near-linear Elastic
Conditioning	500	14.84	---	---	0.0287	---	0.204	---
1	100	4.72	30,071	29,820	0.0279	-0.0008	-0.706	Y
2	100	9.88	25,383	26,122	0.0277	-0.0010	-0.203	Y
3	100	14.84	24,353	23,851	0.0284	-0.0002	0.527	Y
4	100	20.03	22,053	22,045	0.0324	0.0037	0.678	N
5	100	29.82	19,562	19,467	0.0484	0.0198	0.770	N
6	100	39.49	17,442	17,542	0.0687	0.0400	0.856	N



Model: AASHTO (2015)

$$M_{r-comp} = k_1^* P_a \left(\frac{\theta}{P_a}\right)^{k_2^*} \left(1 + \frac{\tau_{oct}}{P_a}\right)^{k_3^*}$$

Parameter	Value	P-Value
k_1^*	2,058.7	6.22E-08
k_2^*	-0.113	9.63E-02
k_3^*	-0.959	5.93E-02
Adj. R^2	0.989	
Std. Error [psi]	467	

M_{r-comp} (pred.)-BP [psi]	31,928
$\sigma_{cyclic-BP}$ [psi]	3.0



In-situ Resilient Modulus [Mr]: Cyclic Loading, Composite, Stress-Dependent

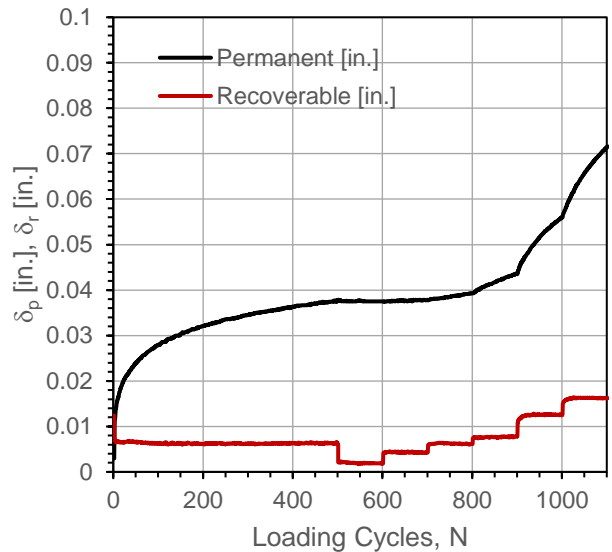
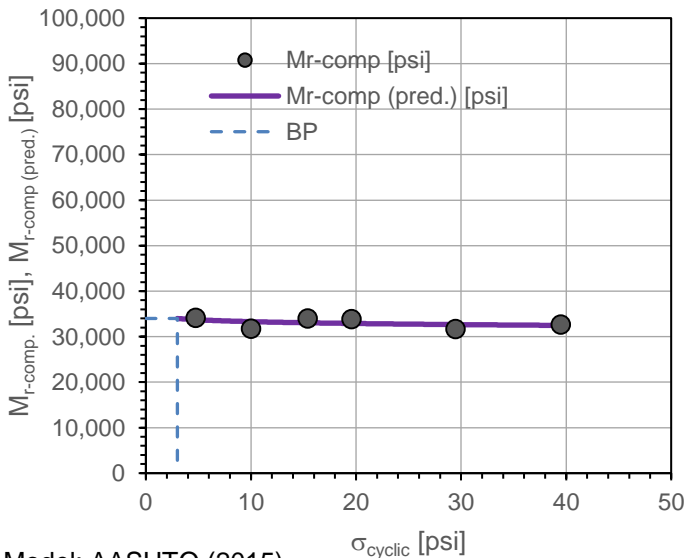
Project Name: Illinois Tollway - IC Research
 Project ID: Elgin O'Hare Extension - IL Tollway
 Location: IL390 (West of O'Hare), Itasca, IL



Automated Plate Load Test [APLT]

Test:	In-situ Resilient Modulus [Mr]: Cyclic Loading, Composite, Stress-Dependent (5, 10, 15, 20, 30, 40)				
Date:	6/21/2017	Time:	5:22:26 PM	Test ID:	ILT_12_Mr_pt5
Tested By:	DW, HG, PV, JV	Location:	TS_13_RAP	Sta.:	NA
Latitude,N:	41.983772	Longitude,W:	88.010727	Elev. (ft):	721
Comments:	RAP CA6 testing, east bound Thorndale Ave. b/w Hamilton Lakes Dr. and No. Arlington Heights Rd.				

Step	N	σ_{cyclic} [psi]	M_{r-comp} [psi]	M_{r-comp} (pred.) [psi]	δ_p [in.]	$\Delta\delta_p$ [in.]	$d = \Delta\log(\delta_p) / \Delta\log(N)$	Near-linear Elastic
Conditioning	500	15.42	---	---	0.0376	---	0.227	---
1	100	4.75	34,162	33,735	0.0375	-0.0001	-0.215	Y
2	100	10.03	31,738	33,298	0.0379	0.0002	0.388	Y
3	100	15.42	33,999	33,045	0.0392	0.0016	0.586	Y
4	100	19.59	33,914	32,903	0.0436	0.0060	0.818	N
5	100	29.47	31,674	32,657	0.0560	0.0184	0.758	N
6	100	39.48	32,713	32,479	0.0713	0.0337	0.866	N



Model: AASHTO (2015)

$$M_{r-comp} = k_1^* P_a \left(\frac{\theta}{P_a}\right)^{k_2^*} \left(1 + \frac{\tau_{oct}}{P_a}\right)^{k_3^*}$$

Parameter	Value	P-Value
k_1^*	2,284.6	4.29E-07
k_2^*	-0.017	8.64E-01
k_3^*	-0.007	9.92E-01
Adj. R^2	-0.053	
Std. Error [psi]	465	

M_{r-comp} (pred.)-BP [psi]	34,002
$\sigma_{cyclic-BP}$ [psi]	3.0



In-situ Resilient Modulus [Mr]: Cyclic Loading, Composite, Stress-Dependent

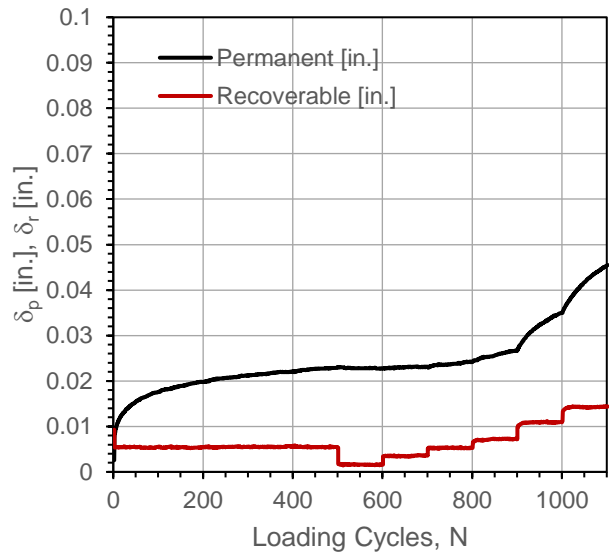
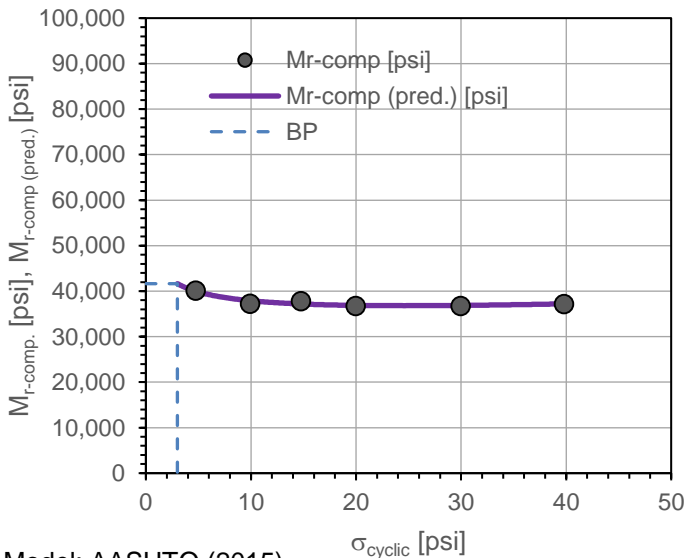
Project Name: Illinois Tollway - IC Research
 Project ID: Elgin O'Hare Extension - IL Tollway
 Location: IL390 (West of O'Hare), Itasca, IL



Automated Plate Load Test [APLT]

Test:	In-situ Resilient Modulus [Mr]: Cyclic Loading, Composite, Stress-Dependent (5, 10, 15, 20, 30, 40)				
Date:	6/21/2017	Time:	4:52:56 PM	Test ID:	ILT_12_Mr_pt6
Tested By:	DW, HG, PV, JV	Location:	TS_13_RAP	Sta.:	NA
Latitude,N:	41.983776	Longitude,W:	88.010727	Elev. (ft):	710
Comments:	RAP CA6 testing, east bound Thorndale Ave. b/w Hamilton Lakes Dr. and No. Arlington Heights Rd.				

Step	N	σ_{cyclic} [psi]	M_{r-comp} [psi]	M_{r-comp} (pred.) [psi]	δ_p [in.]	$\Delta\delta_p$ [in.]	$d = \Delta\log(\delta_p) / \Delta\log(N)$	Near-linear Elastic
Conditioning	500	14.78	---	---	0.0230	---	0.198	---
1	100	4.74	40,146	39,993	0.0228	-0.0003	-0.255	Y
2	100	9.93	37,282	37,907	0.0231	0.0001	0.397	Y
3	100	14.78	37,837	37,182	0.0243	0.0013	0.493	Y
4	100	19.99	36,788	36,875	0.0267	0.0037	0.642	Y
5	100	29.95	36,776	36,872	0.0351	0.0121	0.694	N
6	100	39.80	37,222	37,210	0.0454	0.0223	0.829	N



Model: AASHTO (2015)

$$M_{r-comp} = k_1^* P_a \left(\frac{\theta}{P_a} \right)^{k_2^*} \left(1 + \frac{\tau_{oct}}{P_a} \right)^{k_3^*}$$

Parameter	Value	P-Value
k_1^*	2,570.6	1.61E-08
k_2^*	-0.109	3.98E-02
k_3^*	0.522	9.11E-02
Adj. R^2	0.867	
Std. Error [psi]	436	

M_{r-comp} (pred.)-BP [psi]	41,643
$\sigma_{cyclic-BP}$ [psi]	3.0

No image.

In-situ Resilient Modulus [Mr]: Cyclic Loading, Composite, Stress-Dependent

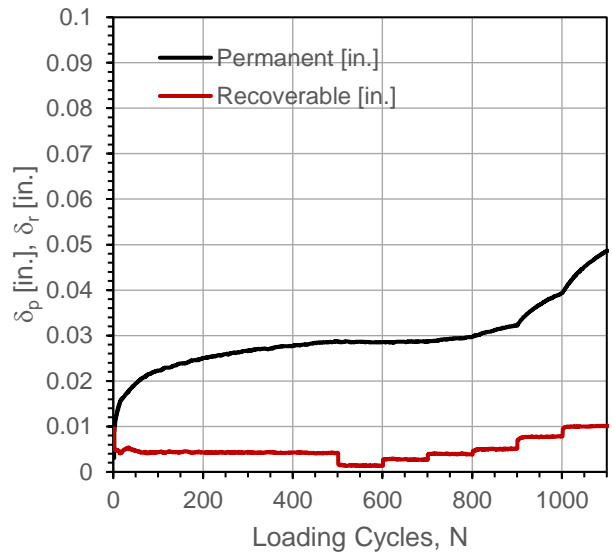
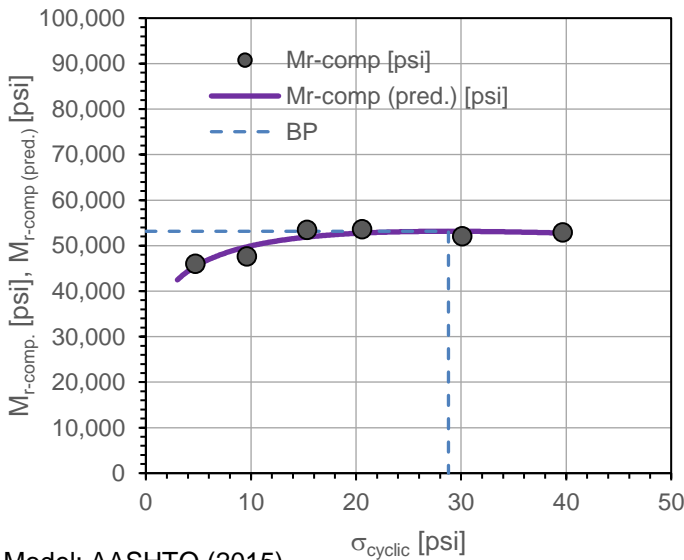
Project Name: Illinois Tollway - IC Research
 Project ID: Elgin O'Hare Extension - IL Tollway
 Location: IL390 (West of O'Hare), Itasca, IL



Automated Plate Load Test [APLT]

Test:	In-situ Resilient Modulus [Mr]: Cyclic Loading, Composite, Stress-Dependent (5, 10, 15, 20, 30, 40)				
Date:	6/21/2017	Time:	5:55:14 PM	Test ID:	ILT_12_Mr_pt7
Tested By:	DW, HG, PV, JV	Location:	TS_13_RAP	Sta.:	NA
Latitude, N:	41.983814	Longitude, W:	88.010719	Elev. (ft.):	725
Comments:	RAP CA6 testing, east bound Thorndale Ave. b/w Hamilton Lakes Dr. and No. Arlington Heights Rd.				

Step	N	σ_{cyclic} [psi]	M_{r-comp} [psi]	M_{r-comp} (pred.) [psi]	δ_p [in.]	$\Delta\delta_p$ [in.]	$d = \Delta\log(\delta_p) / \Delta\log(N)$	Near-linear Elastic
Conditioning	500	15.33	---	---	0.0287	---	0.196	---
1	100	4.72	46,014	45,442	0.0285	-0.0001	-0.153	Y
2	100	9.63	47,662	49,741	0.0287	0.0000	0.174	Y
3	100	15.33	53,495	51,890	0.0297	0.0010	0.575	Y
4	100	20.58	53,609	52,772	0.0322	0.0035	0.652	N
5	100	30.12	52,103	53,147	0.0393	0.0107	0.673	N
6	100	39.68	52,961	52,760	0.0486	0.0199	0.865	N



Model: AASHTO (2015)

$$M_{r-comp} = k_1^* P_a \left(\frac{\theta}{P_a}\right)^{k_2^*} \left(1 + \frac{\tau_{oct}}{P_a}\right)^{k_3^*}$$

Parameter	Value	P-Value
k_1^*	3,379.1	2.19E-07
k_2^*	0.179	9.97E-02
k_3^*	-0.760	2.40E-01
Adj. R^2	0.791	
Std. Error [psi]	1,358	

M_{r-comp} (pred.)-BP [psi]	53,154
$\sigma_{cyclic-BP}$ [psi]	28.8



In-situ Resilient Modulus [Mr]: Cyclic Loading, Composite, Stress-Dependent

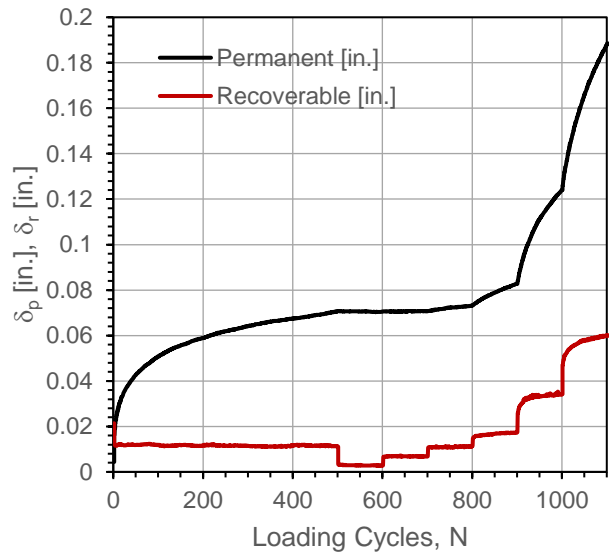
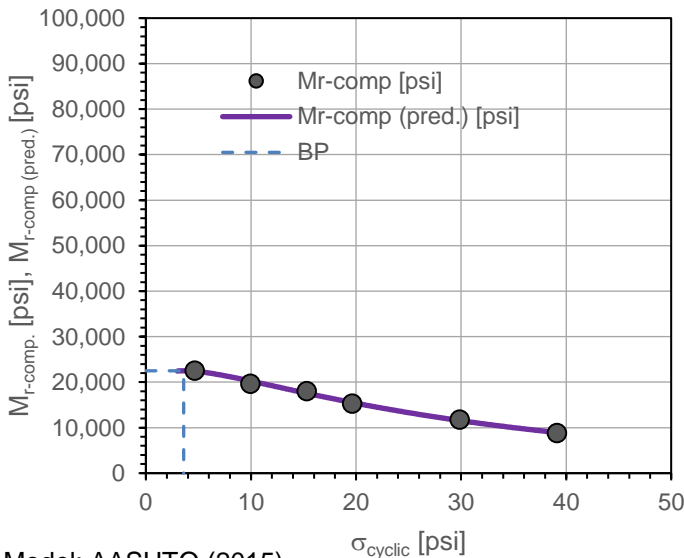
Project Name: Illinois Tollway - IC Research
 Project ID: Elgin O'Hare Extension - IL Tollway
 Location: IL390 (West of O'Hare), Itasca, IL



Automated Plate Load Test [APLT]

Test:	In-situ Resilient Modulus [Mr]: Cyclic Loading, Composite, Stress-Dependent (5, 10, 15, 20, 30, 40)				
Date:	6/21/2017	Time:	3:48:58 PM	Test ID:	ILT_12_Mr_pt8
Tested By:	DW, HG, PV, JV	Location:	TS_13_RAP	Sta.:	NA
Latitude, N:	41.983749	Longitude, W:	88.010483	Elev. (ft):	708
Comments:	RAP CA6 testing, east bound Thorndale Ave. b/w Hamilton Lakes Dr. and No. Arlington Heights Rd.				

Step	N	σ_{cyclic} [psi]	M_{r-comp} [psi]	M_{r-comp} (pred.) [psi]	δ_p [in.]	$\Delta\delta_p$ [in.]	$d = \Delta\log(\delta_p) / \Delta\log(N)$	Near-linear Elastic
Conditioning	500	15.31	---	---	0.0707	---	0.251	---
1	100	4.67	22,574	22,387	0.0705	-0.0002	-0.254	Y
2	100	9.97	19,694	20,250	0.0708	0.0000	0.110	Y
3	100	15.31	18,043	17,562	0.0732	0.0025	0.690	N
4	100	19.65	15,285	15,518	0.0829	0.0122	0.856	N
5	100	29.87	11,803	11,565	0.1240	0.0532	0.850	N
6	100	39.14	8,813	8,926	0.1878	0.1171	0.889	N



Model: AASHTO (2015)

$$M_{r-comp} = k_1^* P_a \left(\frac{\theta}{P_a}\right)^{k_2^*} \left(1 + \frac{\tau_{oct}}{P_a}\right)^{k_3^*}$$

Parameter	Value	P-Value
k_1^*	1,953.8	1.47E-07
k_2^*	0.156	8.43E-02
k_3^*	-4.158	2.24E-03
Adj. R ²	0.993	
Std. Error [psi]	418	

M_{r-comp} (pred.)-BP [psi]	22,498
$\sigma_{cyclic-BP}$ [psi]	3.6



In-situ Resilient Modulus [Mr]: Cyclic Loading, Composite, Stress-Dependent

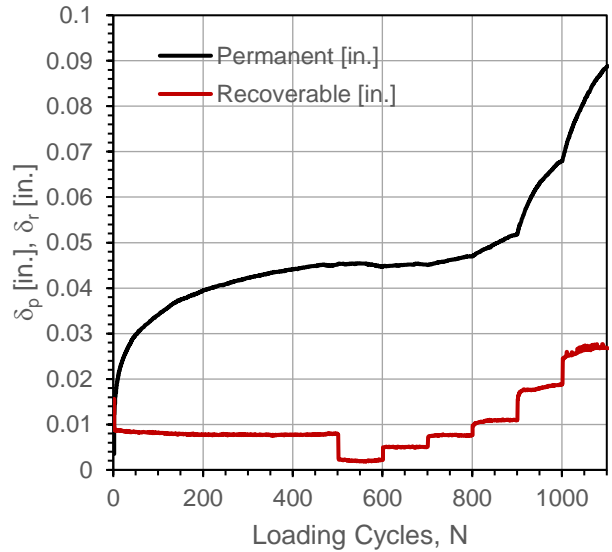
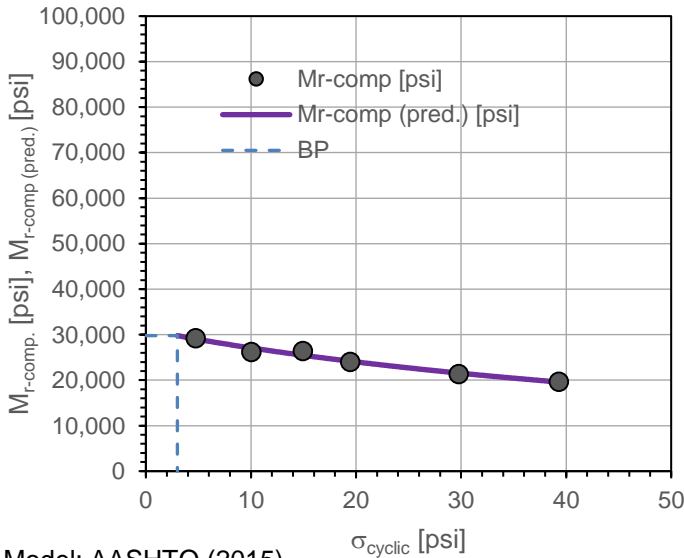
Project Name: IC
 Project ID: ILT
 Location: Itasca, IL



Automated Plate Load Test [APLT]

Test:	In-situ Resilient Modulus [Mr]: Cyclic Loading, Composite, Stress-Dependent (5, 10, 15, 20, 30, 40)				
Date:	6/21/2017	Time:	3:09:00 PM	Test ID:	ILT_12_Mr_pt9
Tested By:	DW, HG, PV, JV	Location:	TS_13_RAP	Sta.:	NA
Latitude,N:	41.983768	Longitude,W:	88.010498	Elev. (ft):	707
Comments:	RAP CA6 testing, east bound Thorndale Ave. b/w Hamilton Lakes Dr. and No. Arlington Heights Rd.				

Step	N	σ_{cyclic} [psi]	M_{r-comp} [psi]	M_{r-comp} (pred.) [psi]	δ_p [in.]	$\Delta\delta_p$ [in.]	$d = \Delta\log(\delta_p) / \Delta\log(N)$	Near-linear Elastic
Conditioning	500	14.96	---	---	0.0452	---	0.220	---
1	100	4.75	29,248	29,050	0.0447	-0.0005	-0.223	Y
2	100	10.04	26,208	27,074	0.0451	0.0000	0.340	Y
3	100	14.96	26,461	25,472	0.0470	0.0018	0.741	N
4	100	19.47	24,017	24,153	0.0519	0.0067	0.737	N
5	100	29.77	21,350	21,566	0.0679	0.0228	0.776	N
6	100	39.32	19,651	19,584	0.0887	0.0435	0.830	N



Model: AASHTO (2015)

$$M_{r-comp} = k_1^* P_a \left(\frac{\theta}{P_a}\right)^{k_2^*} \left(1 + \frac{\tau_{oct}}{P_a}\right)^{k_3^*}$$

Parameter	Value	P-Value
k_1^*	2,102.2	1.66E-07
k_2^*	-0.005	9.48E-01
k_3^*	-1.276	6.66E-02
Adj. R^2	0.964	
Std. Error [psi]	668	

M_{r-comp} (pred.)-BP [psi]	29,786
$\sigma_{cyclic-BP}$ [psi]	3.0

No image.

In-situ Resilient Modulus [Mr]: Cyclic Loading, Composite, Stress-Dependent

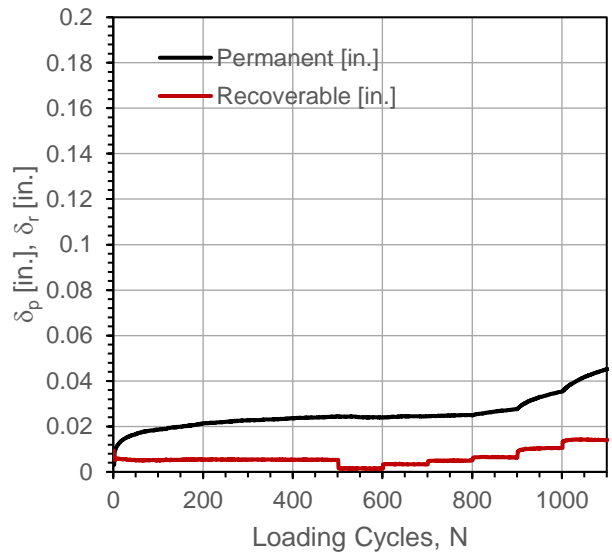
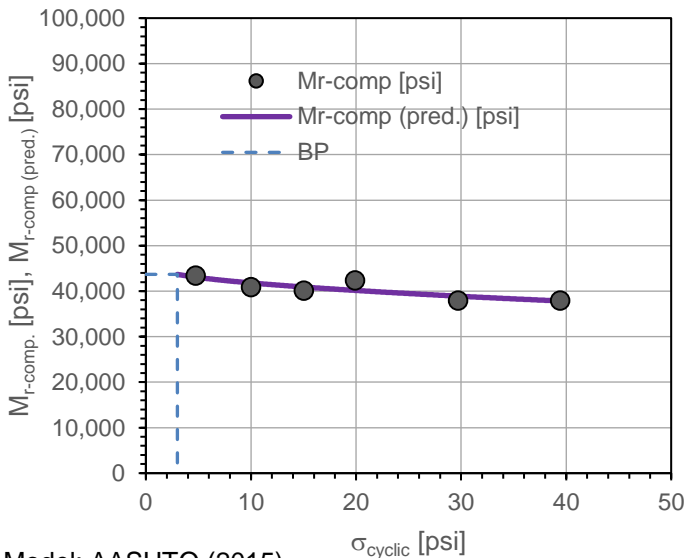
Project Name: Illinois Tollway - IC Research
 Project ID: Elgin O'Hare Extension - IL Tollway
 Location: IL390 (West of O'Hare), Itasca, IL



Automated Plate Load Test [APLT]

Test:	In-situ Resilient Modulus [Mr]: Cyclic Loading, Composite, Stress-Dependent (5, 10, 15, 20, 30, 40)				
Date:	6/21/2017	Time:	4:20:35 PM	Test ID:	ILT_12_Mr_pt10
Tested By:	DW, HG, PV, JV	Location:	TS_13_RAP	Sta.:	NA
Latitude, N:	41.983788	Longitude, W:	88.010468	Elev. (ft.):	715
Comments:	RAP CA6 testing, east bound Thorndale Ave. b/w Hamilton Lakes Dr. and No. Arlington Heights Rd.				

Step	N	σ_{cyclic} [psi]	M_{r-comp} [psi]	M_{r-comp} (pred.) [psi]	δ_p [in.]	$\Delta\delta_p$ [in.]	$d = \Delta\log(\delta_p) / \Delta\log(N)$	Near-linear Elastic
Conditioning	500	15.04	---	---	0.0244	---	0.190	---
1	100	4.73	43,458	43,079	0.0239	-0.0006	-0.401	Y
2	100	10.00	40,907	41,809	0.0245	0.0001	0.425	Y
3	100	15.04	40,123	40,907	0.0249	0.0005	0.467	Y
4	100	19.91	42,379	40,166	0.0277	0.0032	0.620	Y
5	100	29.71	37,994	38,903	0.0353	0.0109	0.735	N
6	100	39.44	37,933	37,843	0.0451	0.0207	0.810	N



Model: AASHTO (2015)

$$M_{r-comp} = k_1^* P_a \left(\frac{\theta}{P_a}\right)^{k_2^*} \left(1 + \frac{\tau_{oct}}{P_a}\right)^{k_3^*}$$

Parameter	Value	P-Value
k_1^*	2,956.0	3.04E-07
k_2^*	-0.020	8.29E-01
k_3^*	-0.290	6.48E-01
Adj. R^2	0.641	
Std. Error [psi]	1,144	

M_{r-comp} (pred.)-BP [psi]	43,693
$\sigma_{cyclic-BP}$ [psi]	3.0



In-situ Resilient Modulus [Mr]: Cyclic Loading, Composite, Stress-Dependent

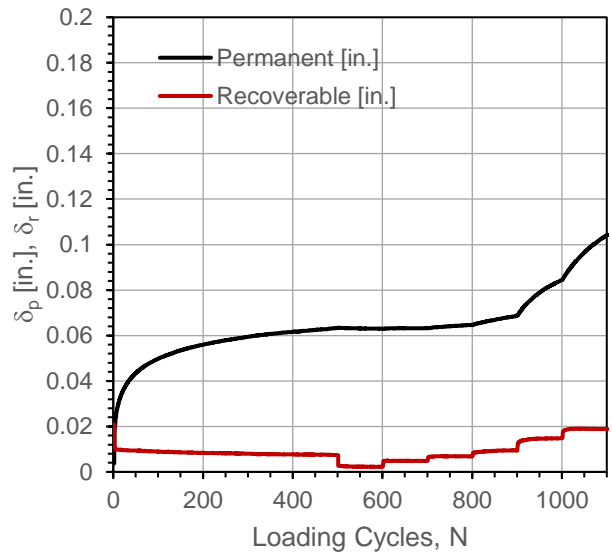
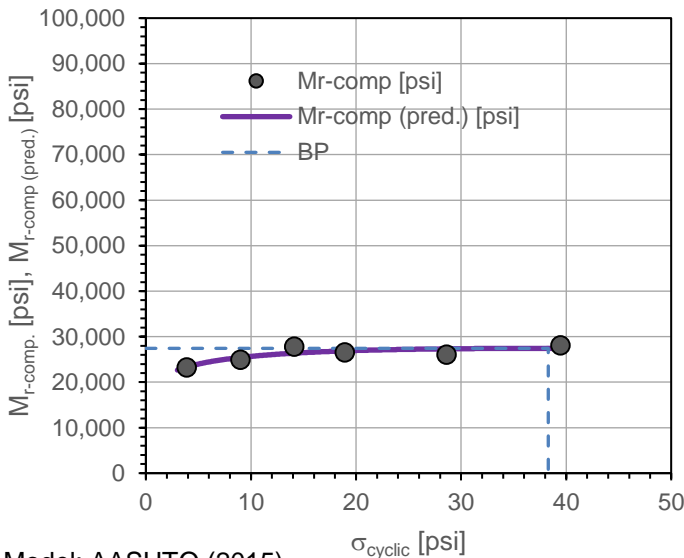
Project Name: Illinois Tollway - IC Research
 Project ID: Elgin O'Hare Extension - IL Tollway
 Location: IL390 (West of O'Hare), Itasca, IL



Automated Plate Load Test [APLT]

Test:	In-situ Resilient Modulus [Mr]: Cyclic Loading, Composite, Stress-Dependent (5, 10, 15, 20, 30, 40)				
Date:	6/21/2017	Time:	2:38:42 PM	Test ID:	ILT_12_Mr_pt11
Tested By:	DW, HG, PV, JV	Location:	TS_13_RAP	Sta.:	NA
Latitude, N:	41.983776	Longitude, W:	88.010300	Elev. (ft.):	695
Comments:	RAP CA6 testing, east bound Thorndale Ave. b/w Hamilton Lakes Dr. and No. Arlington Heights Rd.				

Step	N	σ_{cyclic} [psi]	M_{r-comp} [psi]	M_{r-comp} (pred.) [psi]	δ_p [in.]	$\Delta\delta_p$ [in.]	$d = \Delta\log(\delta_p) / \Delta\log(N)$	Near-linear Elastic
Conditioning	500	14.12	---	---	0.0633	---	0.209	---
1	100	3.89	23,296	23,330	0.0630	-0.0003	-0.363	Y
2	100	9.01	24,958	25,431	0.0632	-0.0001	0.238	Y
3	100	14.12	27,809	26,378	0.0647	0.0014	0.562	Y
4	100	18.95	26,563	26,872	0.0687	0.0054	0.776	N
5	100	28.62	26,100	27,325	0.0845	0.0211	0.854	N
6	100	39.46	28,115	27,427	0.1041	0.0408	0.941	N



Model: AASHTO (2015)

$$M_{r-comp} = k_1^* P_a \left(\frac{\theta}{P_a}\right)^{k_2^*} \left(1 + \frac{\tau_{oct}}{P_a}\right)^{k_3^*}$$

Parameter	Value	P-Value
k_1^*	1,720.6	6.12E-07
k_2^*	0.130	2.12E-01
k_3^*	-0.446	5.10E-01
Adj. R^2	0.668	
Std. Error [psi]	894	

M_{r-comp} (pred.)-BP [psi]	27,428
$\sigma_{cyclic-BP}$ [psi]	38.3



In-situ Resilient Modulus [Mr]: Cyclic Loading, Composite, Stress-Dependent

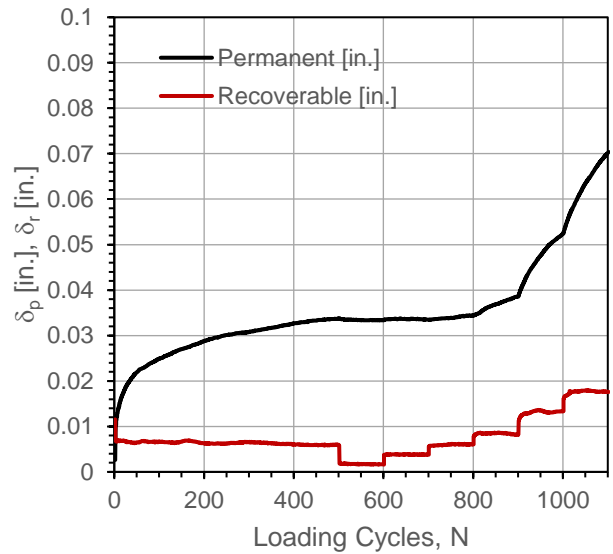
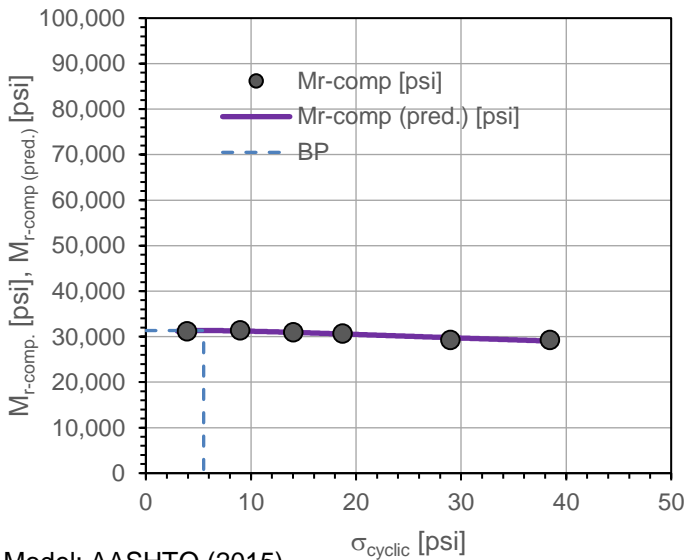
Project Name: Illinois Tollway - IC Research
 Project ID: Elgin O'Hare Extension - IL Tollway
 Location: IL390 (West of O'Hare), Itasca, IL



Automated Plate Load Test [APLT]

Test:	In-situ Resilient Modulus [Mr]: Cyclic Loading, Composite, Stress-Dependent (5, 10, 15, 20, 30, 40)				
Date:	6/21/2017	Time:	2:08:29 PM	Test ID:	ILT_12_Mr_pt12
Tested By:	DW, HG, PV, JV	Location:	TS_13_RAP	Sta.:	NA
Latitude, N:	41.983810	Longitude, W:	88.010292	Elev. (ft):	707
Comments:	RAP CA6 testing, east bound Thorndale Ave. b/w Hamilton Lakes Dr. and No. Arlington Heights Rd.				

Step	N	σ_{cyclic} [psi]	M_{r-comp} [psi]	M_{r-comp} (pred.) [psi]	δ_p [in.]	$\Delta\delta_p$ [in.]	$d = \Delta\log(\delta_p) / \Delta\log(N)$	Near-linear Elastic
Conditioning	500	14.03	---	---	0.0337	---	0.226	---
1	100	3.92	31,230	31,310	0.0334	-0.0003	-0.384	Y
2	100	8.98	31,392	31,248	0.0335	-0.0002	0.070	Y
3	100	14.03	30,973	30,938	0.0344	0.0007	0.560	Y
4	100	18.73	30,702	30,587	0.0386	0.0049	0.834	N
5	100	28.98	29,291	29,773	0.0524	0.0187	0.816	N
6	100	38.46	29,311	29,035	0.0701	0.0364	0.886	N



Model: AASHTO (2015)

$$M_{r-comp} = k_1^* P_a \left(\frac{\theta}{P_a}\right)^{k_2^*} \left(1 + \frac{\tau_{oct}}{P_a}\right)^{k_3^*}$$

Parameter	Value	P-Value
k_1^*	2,192.0	1.03E-08
k_2^*	0.024	3.58E-01
k_3^*	-0.426	7.59E-02
Adj. R^2	0.902	
Std. Error [psi]	283	

M_{r-comp} (pred.)-BP [psi]	31,346
$\sigma_{cyclic-BP}$ [psi]	5.5



In-situ Resilient Modulus [Mr]: Cyclic Loading, Composite, Stress-Dependent

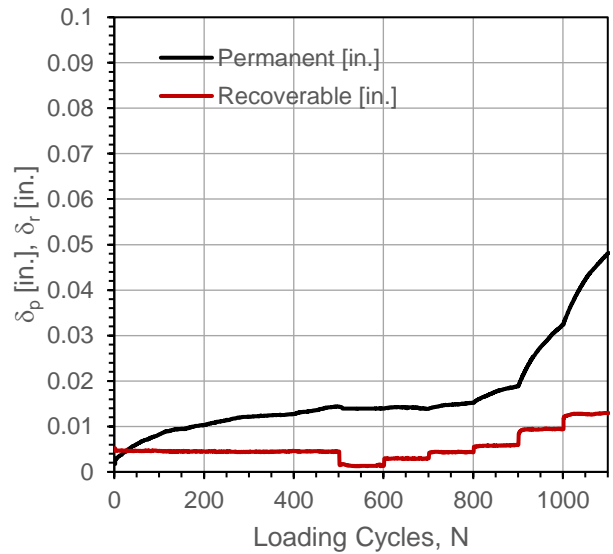
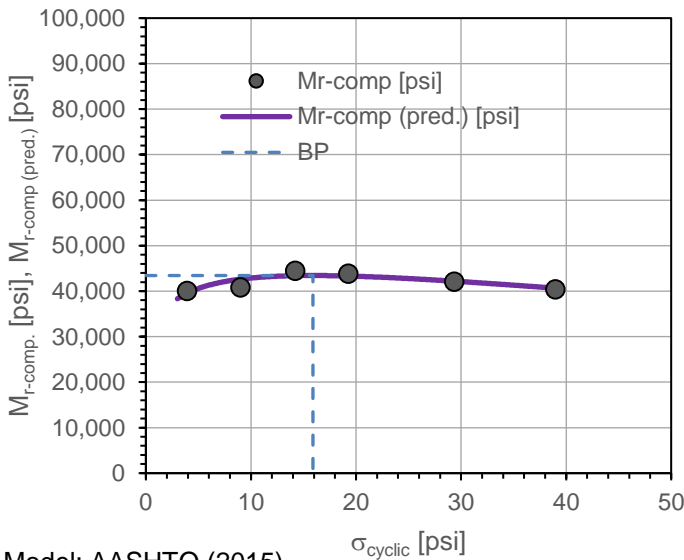
Project Name: Illinois Tollway - IC Research
 Project ID: Elgin O'Hare Extension - IL Tollway
 Location: IL390 (West of O'Hare), Itasca, IL



Automated Plate Load Test [APLT]

Test:	In-situ Resilient Modulus [Mr]: Cyclic Loading, Composite, Stress-Dependent (5, 10, 15, 20, 30, 40)				
Date:	6/21/2017	Time:	12:58:08 PM	Test ID:	ILT_12_Mr_pt13
Tested By:	DW, HG, PV, JV	Location:	TS_13_RAP	Sta.:	NA
Latitude, N:	41.983826	Longitude, W:	88.009705	Elev. (ft):	700
Comments:	RAP CA6 testing, east bound Thorndale Ave. b/w Hamilton Lakes Dr. and N. Arlington Heights Rd.				

Step	N	σ_{cyclic} [psi]	M_{r-comp} [psi]	M_{r-comp} (pred.) [psi]	δ_p [in.]	$\Delta\delta_p$ [in.]	$d = \Delta\log(\delta_p) / \Delta\log(N)$	Near-linear Elastic
Conditioning	500	14.21	---	---	0.0143	---	0.361	---
1	100	3.92	40,057	39,555	0.0139	-0.0004	-0.211	Y
2	100	9.02	40,840	42,634	0.0139	-0.0004	-0.035	Y
3	100	14.21	44,526	43,399	0.0153	0.0010	0.547	Y
4	100	19.27	43,840	43,318	0.0189	0.0046	0.740	N
5	100	29.35	42,138	42,189	0.0323	0.0180	0.847	N
6	100	38.97	40,419	40,664	0.0480	0.0337	0.832	N



Model: AASHTO (2015)

$$M_{r-comp} = k_1^* P_a \left(\frac{\theta}{P_a}\right)^{k_2^*} \left(1 + \frac{\tau_{oct}}{P_a}\right)^{k_3^*}$$

Parameter	Value	P-Value
k_1^*	3,027.8	1.70E-07
k_2^*	0.156	7.41E-02
k_3^*	-1.075	8.41E-02
Adj. R^2	0.636	
Std. Error [psi]	930	

M_{r-comp} (pred.)-BP [psi]	43,433
$\sigma_{cyclic-BP}$ [psi]	15.9



In-situ Resilient Modulus [Mr]: Cyclic Loading, Composite, Stress-Dependent

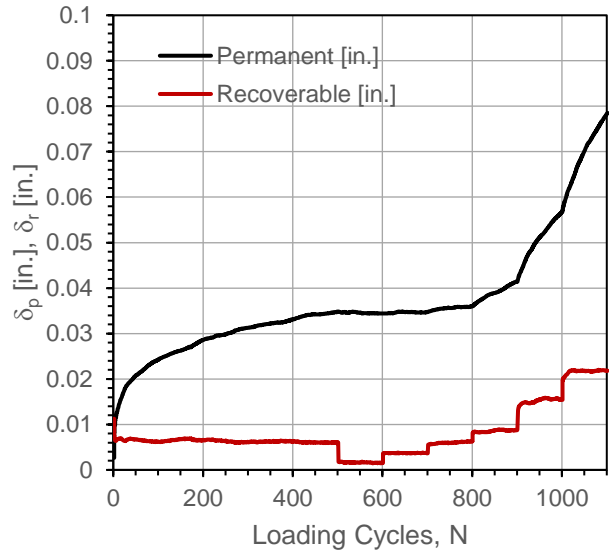
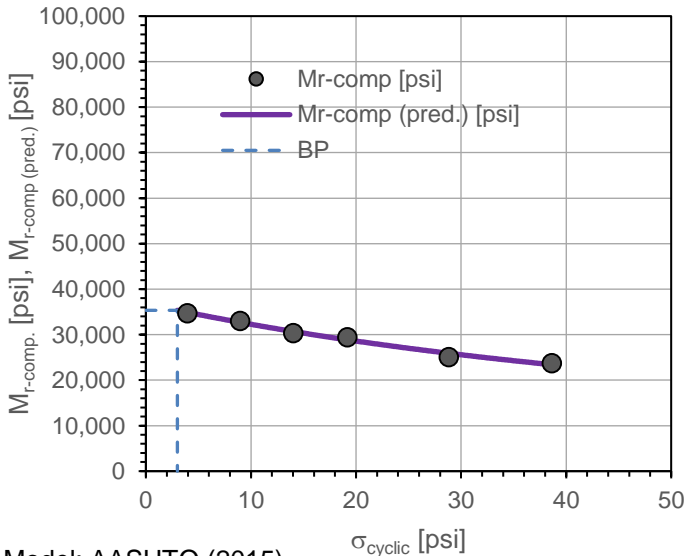
Project Name: Illinois Tollway - IC Research
 Project ID: Elgin O'Hare Extension - IL Tollway
 Location: IL390 (West of O'Hare), Itasca, IL



Automated Plate Load Test [APLT]

Test:	In-situ Resilient Modulus [Mr]: Cyclic Loading, Composite, Stress-Dependent (5, 10, 15, 20, 30, 40)				
Date:	6/21/2017	Time:	1:41:32 PM	Test ID:	ILT_12_Mr_pt14
Tested By:	DW, HG, PV, JV	Location:	TS_13_RAP	Sta.:	NA
Latitude, N:	41.983845	Longitude, W:	88.009689	Elev. (ft.):	707
Comments:	RAP CA6 testing, east bound Thorndale Ave. b/w Hamilton Lakes Dr. and No. Arlington Heights Rd.				

Step	N	σ_{cyclic} [psi]	M_{r-comp} [psi]	M_{r-comp} (pred.) [psi]	δ_p [in.]	$\Delta\delta_p$ [in.]	$d = \Delta\log(\delta_p) / \Delta\log(N)$	Near-linear Elastic
Conditioning	500	14.04	---	---	0.0348	---	0.250	---
1	100	3.94	34,753	34,912	0.0344	-0.0004	-0.354	Y
2	100	8.99	33,063	32,691	0.0347	-0.0001	0.350	Y
3	100	14.04	30,383	30,693	0.0360	0.0012	0.518	Y
4	100	19.18	29,438	28,867	0.0415	0.0067	0.762	N
5	100	28.85	25,067	25,902	0.0567	0.0219	0.832	N
6	100	38.66	23,786	23,396	0.0782	0.0434	0.852	N



Model: AASHTO (2015)

$$M_{r-comp} = k_1^* P_a \left(\frac{\theta}{P_a}\right)^{k_2^*} \left(1 + \frac{\tau_{oct}}{P_a}\right)^{k_3^*}$$

Parameter	Value	P-Value
k_1^*	2,510.1	1.08E-07
k_2^*	0.001	9.78E-01
k_3^*	-1.325	3.41E-02
Adj. R^2	0.981	
Std. Error [psi]	593	

M_{r-comp} (pred.)-BP [psi]	35,349
$\sigma_{cyclic-BP}$ [psi]	3.0



In-situ Resilient Modulus [Mr]: Cyclic Loading, Composite, Stress-Dependent

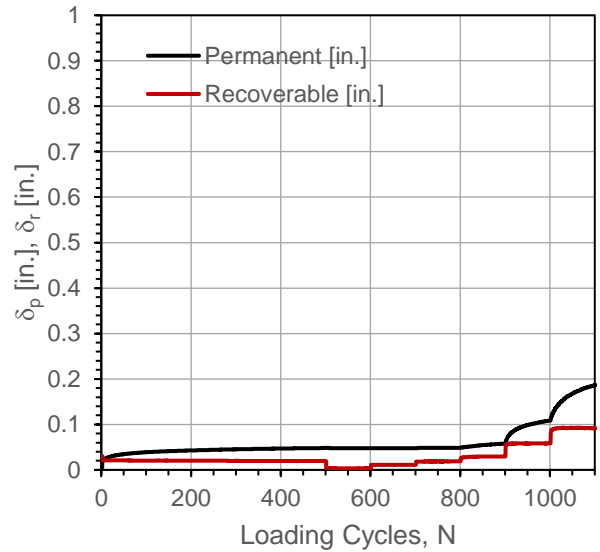
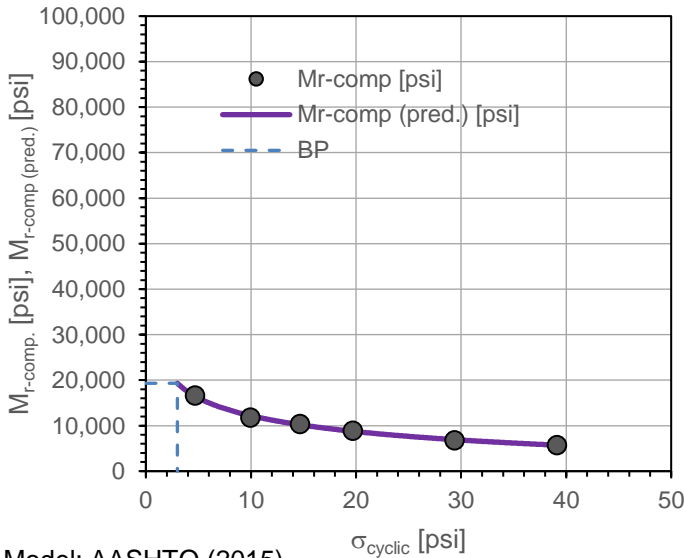
Project Name: Illinois Tollway - IC Research
 Project ID: Elgin O'Hare Extension - IL Tollway
 Location: IL390 (West of O'Hare), Itasca, IL



Automated Plate Load Test [APLT]

Test:	In-situ Resilient Modulus [Mr]: Cyclic Loading, Composite, Stress-Dependent (5, 10, 15, 20, 30, 40)				
Date:	6/21/2017	Time:	8:54:39 PM	Test ID:	ILT_12_Mr_SG_pt15
Tested By:	DW, HG, PV, JV	Location:	TS_14_SG	Sta.:	NA
Latitude, N:	41.983845	Longitude, W:	88.014992	Elev. (ft):	723
Comments:	Subgrade testing, east bound Thorndale Ave. west of Hamilton Lakes Dr.				

Step	N	σ_{cyclic} [psi]	M_{r-comp} [psi]	M_{r-comp} (pred.) [psi]	δ_p [in.]	$\Delta\delta_p$ [in.]	$d = \frac{\Delta\log(\delta_p)}{\Delta\log(N)}$	Near-linear Elastic
Conditioning	500	14.67	---	---	0.0482	---	0.173	---
1	100	4.69	16,619	16,472	0.0474	-0.0008	-0.423	Y
2	100	9.94	11,812	12,211	0.0479	-0.0003	0.351	Y
3	100	14.67	10,383	10,202	0.0486	0.0004	0.368	Y
4	100	19.71	8,945	8,760	0.0579	0.0097	0.776	N
5	100	29.37	6,814	6,932	0.1086	0.0604	0.655	N
6	100	39.12	5,736	5,719	0.1861	0.1379	0.787	N



Model: AASHTO (2015)

$$M_{r-comp} = k_1^* P_a \left(\frac{\theta}{P_a}\right)^{k_2^*} \left(1 + \frac{\tau_{oct}}{P_a}\right)^{k_3^*}$$

Parameter	Value	P-Value
k_1^*	1,096.6	1.68E-07
k_2^*	-0.303	1.48E-02
k_3^*	-1.383	4.40E-02
Adj. R ²	0.996	
Std. Error [psi]	255	

M_{r-comp} (pred.)-BP [psi]	19,321
$\sigma_{cyclic-BP}$ [psi]	3.0

No image.

In-situ Resilient Modulus [Mr]: Cyclic Loading, Composite, Stress-Dependent

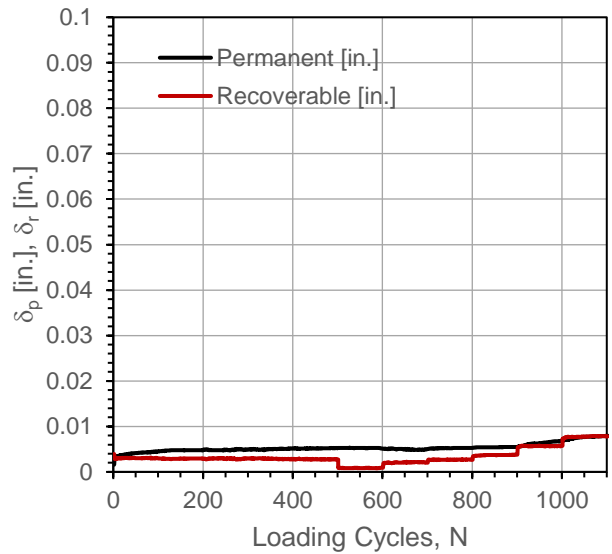
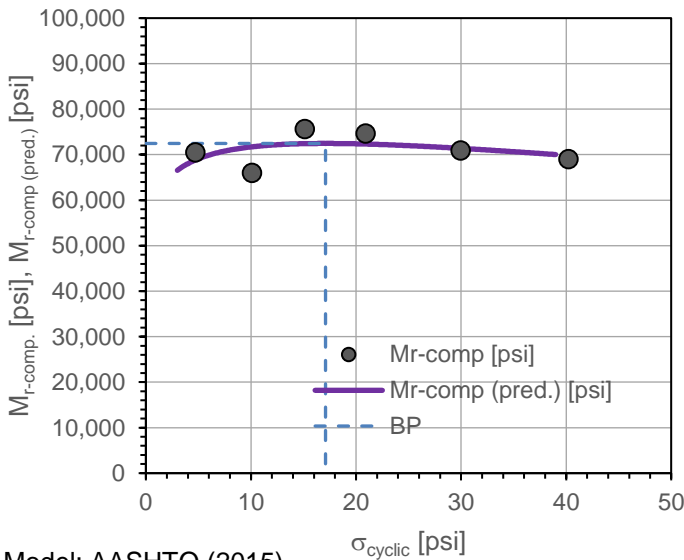
Project Name: Illinois Tollway - IC Research
 Project ID: Elgin O'Hare Extension - IL Tollway
 Location: IL390 (West of O'Hare), Itasca, IL



Automated Plate Load Test [APLT]

Test:	In-situ Resilient Modulus [Mr]: Cyclic Loading, Composite, Stress-Dependent (5, 10, 15, 20, 30, 40)				
Date:	6/21/2017	Time:	10:08:12 PM	Test ID:	ILT_12_Mr_SG_pt16
Tested By:	DW, HG, PV, JV	Location:	TS_14_SG	Sta.:	NA
Latitude, N:	41.983742	Longitude, W:	88.015060	Elev. (ft):	719
Comments:	Subgrade testing, east bound Thorndale Ave. west of Hamilton Lakes Dr.				

Step	N	σ_{cyclic} [psi]	M_{r-comp} [psi]	M_{r-comp} (pred.) [psi]	δ_p [in.]	$\Delta\delta_p$ [in.]	$d = \Delta\log(\delta_p) / \Delta\log(N)$	Near-linear Elastic
Conditioning	500	15.13	---	---	0.0052	---	0.109	---
1	100	4.71	70,528	68,815	0.0052	-0.0001	-0.025	Y
2	100	10.10	66,028	71,722	0.0050	-0.0002	-0.291	Y
3	100	15.13	75,646	72,417	0.0053	0.0001	0.243	Y
4	100	20.91	74,644	72,330	0.0055	0.0002	0.172	Y
5	100	29.97	70,970	71,378	0.0068	0.0016	0.552	Y
6	100	40.24	69,035	69,817	0.0079	0.0027	0.521	Y



Model: AASHTO (2015)

$$M_{r-comp} = k_1^* P_a \left(\frac{\theta}{P_a}\right)^{k_2^*} \left(1 + \frac{\tau_{oct}}{P_a}\right)^{k_3^*}$$

Parameter	Value	P-Value
k_1^*	4,973.0	9.07E-07
k_2^*	0.099	4.94E-01
k_3^*	-0.643	5.14E-01
Adj. R^2	-0.020	
Std. Error [psi]	1,469	

M_{r-comp} (pred.)-BP [psi]	72,461
$\sigma_{cyclic-BP}$ [psi]	17.1



In-situ Resilient Modulus [Mr]: Cyclic Loading, Composite, Stress-Dependent

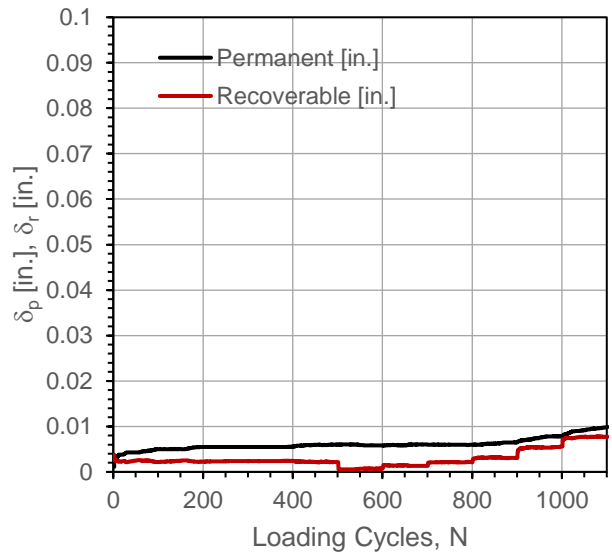
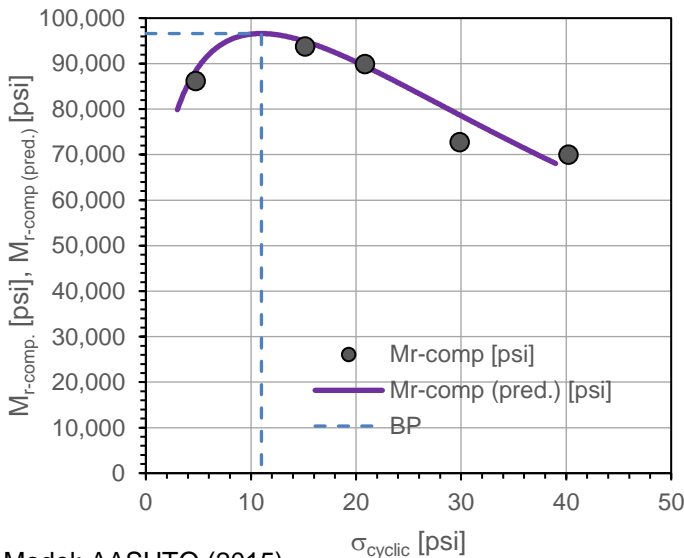
Project Name: Illinois Tollway - IC Research
 Project ID: Elgin O'Hare Extension - IL Tollway
 Location: IL390 (West of O'Hare), Itasca, IL



Automated Plate Load Test [APLT]

Test:	In-situ Resilient Modulus [Mr]: Cyclic Loading, Composite, Stress-Dependent (5, 10, 15, 20, 30, 40)				
Date:	6/21/2017	Time:	10:39:01 PM	Test ID:	ILT_12_Mr_SG_pt17
Tested By:	DW, HG, PV, JV	Location:	TS_14_SG	Sta.:	NA
Latitude, N:	41.983746	Longitude, W:	88.015297	Elev. (ft):	720
Comments:	Subgrade testing, east bound Thorndale Ave. west of Hamilton Lakes Dr.				

Step	N	σ_{cyclic} [psi]	M_{r-comp} [psi]	M_{r-comp} (pred.) [psi]	δ_p [in.]	$\Delta\delta_p$ [in.]	$d = \Delta\log(\delta_p) / \Delta\log(N)$	Near-linear Elastic
Conditioning	500	15.15	---	---	0.0060	---	0.143	---
1	100	4.73	86,195	88,357	0.0058	-0.0002	-0.355	Y
2	100	10.07	102,541	96,502	0.0060	0.0000	0.273	Y
3	100	15.15	93,819	94,895	0.0060	0.0000	-0.059	Y
4	100	20.86	89,899	89,442	0.0065	0.0005	0.539	Y
5	100	29.87	72,801	78,718	0.0078	0.0018	0.558	Y
6	100	40.22	70,044	66,726	0.0098	0.0038	0.530	Y



Model: AASHTO (2015)

$$M_{r-comp} = k_1^* P_a \left(\frac{\theta}{P_a}\right)^{k_2^*} \left(1 + \frac{\tau_{oct}}{P_a}\right)^{k_3^*}$$

Parameter	Value	P-Value
k_1^*	7,841.6	1.06E-06
k_2^*	0.352	9.01E-02
k_3^*	-3.351	4.08E-02
Adj. R^2	0.860	
Std. Error [psi]	4,200	

M_{r-comp} (pred.)-BP [psi]	96,609
$\sigma_{cyclic-BP}$ [psi]	11.0



In-situ Resilient Modulus [Mr]: Cyclic Loading, Composite, Stress-Dependent

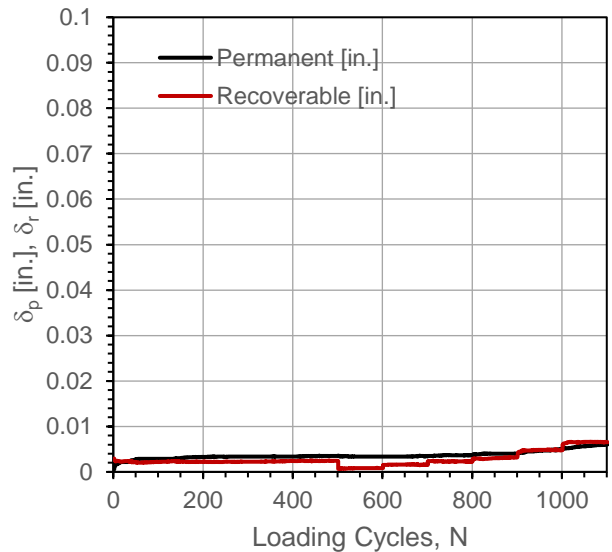
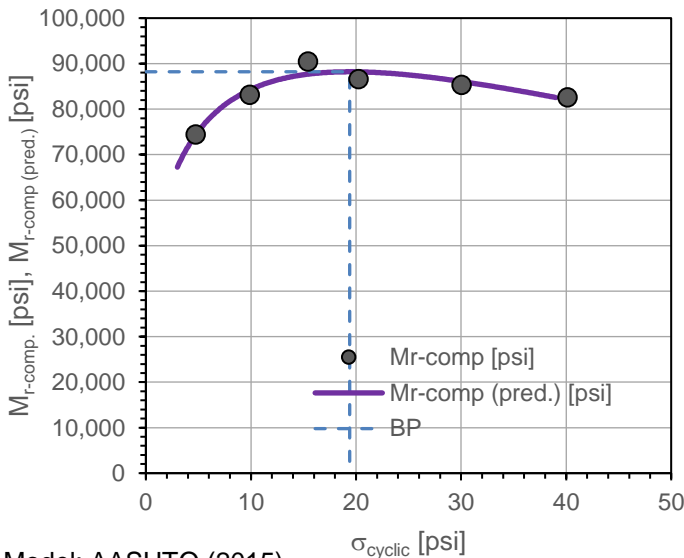
Project Name: Illinois Tollway - IC Research
 Project ID: Elgin O'Hare Extension - IL Tollway
 Location: IL390 (West of O'Hare), Itasca, IL



Automated Plate Load Test [APLT]

Test:	In-situ Resilient Modulus [Mr]: Cyclic Loading, Composite, Stress-Dependent (5, 10, 15, 20, 30, 40)				
Date:	6/22/2017	Time:	11:11:50 PM	Test ID:	ILT_12_Mr_SG_pt18
Tested By:	DW, HG, PV, JV	Location:	TS_14_SG	Sta.:	NA
Latitude, N:	41.983788	Longitude, W:	88.015327	Elev. (ft):	716
Comments:	Subgrade testing, east bound Thorndale Ave. west of Hamilton Lakes Dr.				

Step	N	σ_{cyclic} [psi]	M_{r-comp} [psi]	M_{r-comp} (pred.) [psi]	δ_p [in.]	$\Delta\delta_p$ [in.]	$d = \Delta\log(\delta_p) / \Delta\log(N)$	Near-linear Elastic
Conditioning	500	15.43	---	---	0.0035	---	0.167	---
1	100	4.74	74,425	74,360	0.0034	-0.0001	-0.224	Y
2	100	9.90	83,208	84,245	0.0035	0.0000	0.139	Y
3	100	15.43	90,494	87,690	0.0037	0.0002	0.255	Y
4	100	20.24	86,637	88,194	0.0040	0.0005	0.210	Y
5	100	30.06	85,356	86,069	0.0051	0.0016	0.486	Y
6	100	40.12	82,602	82,093	0.0061	0.0026	0.631	Y



Model: AASHTO (2015)

$$M_{r-comp} = k_1^* P_a \left(\frac{\theta}{P_a}\right)^{k_2^*} \left(1 + \frac{\tau_{oct}}{P_a}\right)^{k_3^*}$$

Parameter	Value	P-Value
k_1^*	5,951.7	4.91E-08
k_2^*	0.284	1.06E-02
k_3^*	-1.653	1.64E-02
Adj. R^2	0.895	
Std. Error [psi]	1,660	

M_{r-comp} (pred.)-BP [psi]	88,211
$\sigma_{cyclic-BP}$ [psi]	19.4



In-situ Resilient Modulus [Mr]: Cyclic Loading, Composite, Stress-Dependent

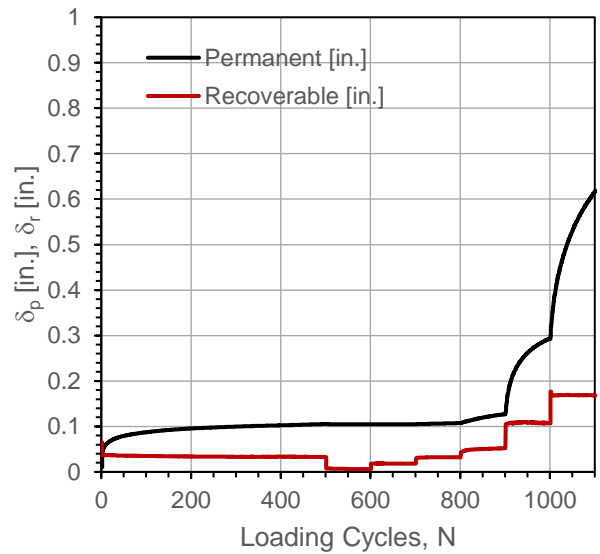
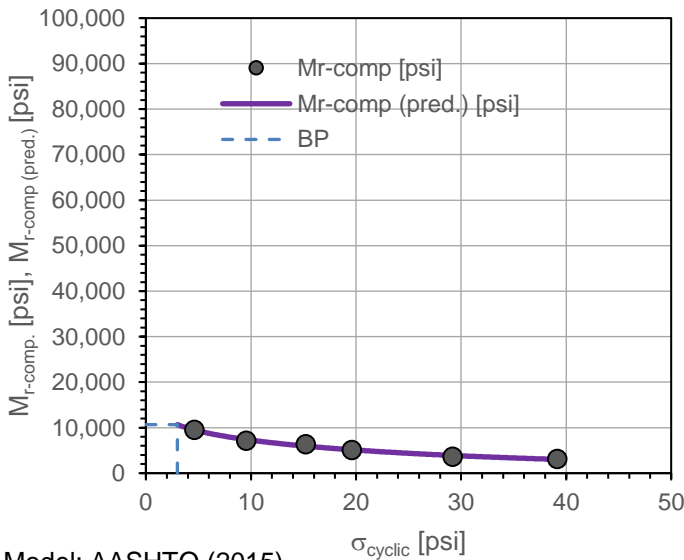
Project Name: Illinois Tollway - IC Research
 Project ID: Elgin O'Hare Extension - IL Tollway
 Location: IL390 (West of O'Hare), Itasca, IL



Automated Plate Load Test [APLT]

Test:	In-situ Resilient Modulus [Mr]: Cyclic Loading, Composite, Stress-Dependent (5, 10, 15, 20, 30, 40)				
Date:	6/21/2017	Time:	9:32:07 PM	Test ID:	ILT_12_Mr_SG_pt19
Tested By:	DW, HG, PV, JV	Location:	TS_14_SG	Sta.:	NA
Latitude, N:	41.983627	Longitude, W:	88.015259	Elev. (ft):	726
Comments:	Subgrade testing, east bound Thorndale Ave. west of Hamilton Lakes Dr.				

Step	N	σ_{cyclic} [psi]	M_{r-comp} [psi]	M_{r-comp} (pred.) [psi]	δ_p [in.]	$\Delta\delta_p$ [in.]	$d = \Delta\log(\delta_p) / \Delta\log(N)$	Near-linear Elastic
Conditioning	500	15.21	---	---	0.1052	---	0.154	---
1	100	4.63	9,516	9,492	0.1046	-0.0006	-0.307	Y
2	100	9.57	7,133	7,387	0.1050	-0.0002	0.169	Y
3	100	15.21	6,399	5,946	0.1075	0.0023	0.654	N
4	100	19.62	5,090	5,138	0.1269	0.0217	0.929	N
5	100	29.19	3,649	3,891	0.2932	0.1880	0.757	N
6	100	39.17	3,125	3,023	0.6155	0.5103	0.951	N



Model: AASHTO (2015)

$$M_{r-comp} = k_1^* P_a \left(\frac{\theta}{P_a}\right)^{k_2^*} \left(1 + \frac{\tau_{oct}}{P_a}\right)^{k_3^*}$$

Parameter	Value	P-Value
k_1^*	694.2	2.62E-06
k_2^*	-0.170	3.01E-01
k_3^*	-2.590	7.21E-02
Adj. R^2	0.985	
Std. Error [psi]	291	

M_{r-comp} (pred.)-BP [psi]	10,668
$\sigma_{cyclic-BP}$ [psi]	3.0



In-situ Resilient Modulus [Mr]: Cyclic Loading, Composite, Stress-Dependent

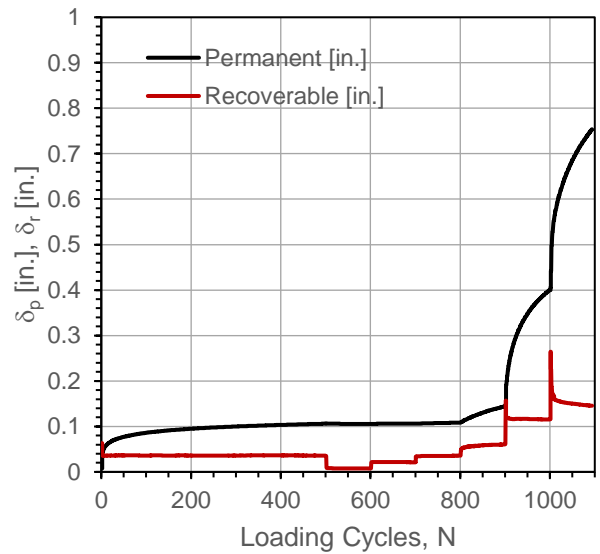
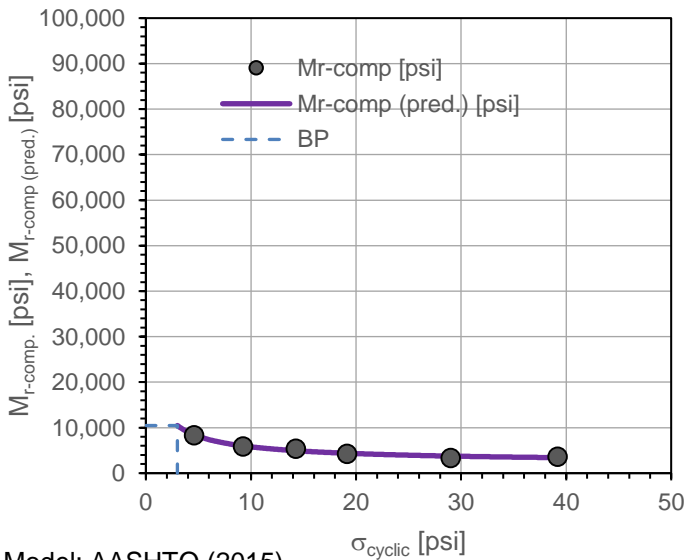
Project Name: Illinois Tollway - IC Research
 Project ID: Elgin O'Hare Extension - IL Tollway
 Location: IL390 (West of O'Hare), Itasca, IL



Automated Plate Load Test [APLT]

Test:	In-situ Resilient Modulus [Mr]: Cyclic Loading, Composite, Stress-Dependent (5, 10, 15, 20, 30, 40)				
Date:	6/22/2017	Time:	11:52:27 PM	Test ID:	ILT_12_Mr_SG_pt20
Tested By:	DW, HG, PV, JV	Location:	TS_14_SG	Sta.:	NA
Latitude, N:	41.983650	Longitude, W:	88.015404	Elev. (ft):	705
Comments:	Subgrade testing, east bound Thorndale Ave. west of Hamilton Lakes Dr.				

Step	N	σ_{cyclic} [psi]	M_{r-comp} [psi]	M_{r-comp} (pred.) [psi]	δ_p [in.]	$\Delta\delta_p$ [in.]	$d = \frac{\Delta\log(\delta_p)}{\Delta\log(N)}$	Near-linear Elastic
Conditioning	500	14.28	---	---	0.1060	---	0.171	---
1	100	4.59	8,344	8,430	0.1054	-0.0006	-0.847	Y
2	100	9.24	5,887	5,998	0.1062	0.0003	0.386	Y
3	100	14.28	5,422	4,938	0.1083	0.0023	0.617	Y
4	100	19.14	4,292	4,375	0.1439	0.0379	0.920	N
5	100	29.00	3,378	3,755	0.4005	0.2945	0.853	N
6	100	39.19	3,629	3,417	0.7608	0.6548	0.780	N



Model: AASHTO (2015)

$$M_{r-comp} = k_1^* P_a \left(\frac{\theta}{P_a}\right)^{k_2^*} \left(1 + \frac{\tau_{oct}}{P_a}\right)^{k_3^*}$$

Parameter	Value	P-Value
k_1^*	463.1	8.95E-06
k_2^*	-0.543	6.82E-02
k_3^*	0.867	5.67E-01
Adj. R^2	0.967	
Std. Error [psi]	334	

M_{r-comp} (pred.)-BP [psi]	10,467
$\sigma_{cyclic-BP}$ [psi]	3.0



In-situ Resilient Modulus [Mr]: Cyclic Loading, Composite, Stress-Dependent

Project Name: IC
 Project ID: ILT
 Location: Itasca, IL



Automated Plate Load Test [APLT]

Test:	In-Situ Static Plate Load Test: Two Loading Cycles.				
Date:	6/22/2017	Time:	6:37:55 PM	Test ID:	TS15_PT1
Tested By:	DW, HG, PV	Location:	TS15_PGE	Sta.:	NA
Latitude:	41.98370	Longitude:	88.01403	Elev. (ft):	NA
Comments:	Test on compacted nominal 6 in. thick PGE placed over subgrade.				

Cycle	Stage	Load Step	Target Applied Load (lbs)	Target Applied Stress (psi)	Actual Applied Stress (psi)	Deformation (in.)			Average Def. (in.)
						Sensor 1	Sensor 2	Sensor 3	
0	Seating	0	707	1	1.31	0.0190	0.0116	0.0086	0.0131
<i>Zero load and deformation sensors after applying the seating stress.</i>									
1	Seating	0	0	0	0.00	0.0000	0.0000	0.0000	0.0000
1	Load	1	1767	2.5	2.49	0.0278	0.0188	0.0163	0.0210
1	Load	2	3534	5	4.98	0.0451	0.0316	0.0271	0.0346
1	Load	3	5301	7.5	7.48	0.0568	0.0403	0.0426	0.0466
1	Load	4	7069	10	9.97	0.0712	0.0471	0.0496	0.0559
1	Load	5	10603	15	14.96	0.0939	0.0637	0.0680	0.0752
1	Load	6	7069	10	9.97	0.0902	0.0615	0.0643	0.0720
1	Unload	7	1767	2.5	2.56	0.0797	0.0517	0.0554	0.0622
1	Unload	8	3534	5	5.00	0.0828	0.0528	0.0590	0.0649
1	Unload	9	7069	10	9.97	0.0888	0.0582	0.0646	0.0705
2	Load	10	10603	15	14.65	0.0958	0.0650	0.0707	0.0772
2	Load	11	3534	5	4.75	0.0868	0.0561	0.0629	0.0686
2	Load	12	0	0	0.00	0.0764	0.0478	0.0533	0.0591

Plate Diameter:	30.0	in.			
Shape factor:	2.67				
Material Type:	B		A = Cohesive, B = Granular, C = Intermediate		
Poisson's ratio:	0.35				
Design Stress: (assumed)	10.0	psi	AASHTO T222 Method PCA Design Criteria	k_{u1} (pci) @ design stress: k_u (pci) @ $\delta = 0.05$ in.:	169
Target Deformation:	0.05	in.			149

Modulus at target deformation

Stress @ $\delta = 0.05$ in. (psi) 7.4

E ₁ (psi)	NA
k' _u (pci)	NA
k _u (pci)	NA

Modulus at target/design applied stress

First Loading Cycle

δ_1 (in.)	0.0564
E ₁ (psi)	5,922
k' _{u1} (pci)	177
k _{u1} (pci)	169

Second Loading Cycle

δ_2 (in.)	0.0106
E ₂ (psi)	22,210
k' _{u2} (pci)	940
k _{u2} (pci)	633

E₂ / E₁ or k₂ / k₁ Ratio 3.8

Plate Bending Correction for

$$k_u \geq 100 \text{ and } 1,000 \text{ pci}$$

$$k_u = -39.9178 + 5.5076 [k'_u]^{0.7019}$$

In-situ Modulus of Subgrade Reaction (k) and Elastic Modulus

Project Name: Illinois Tollway - IC Research
 Project ID: Elgin O'Hare Extension - IL Tollway
 Location: IL390 (West of O'Hare), Itasca, IL



Polynomial Fit Parameters

First Cycle

a ₁	-1.57E-04
a ₂	7.21E-03
R ²	1.00

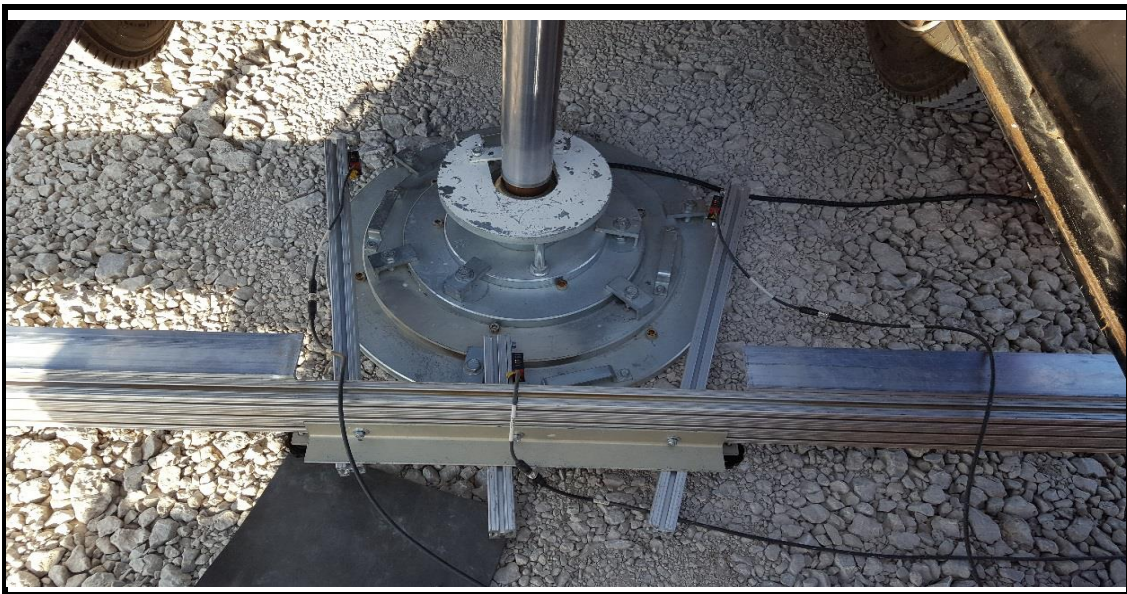
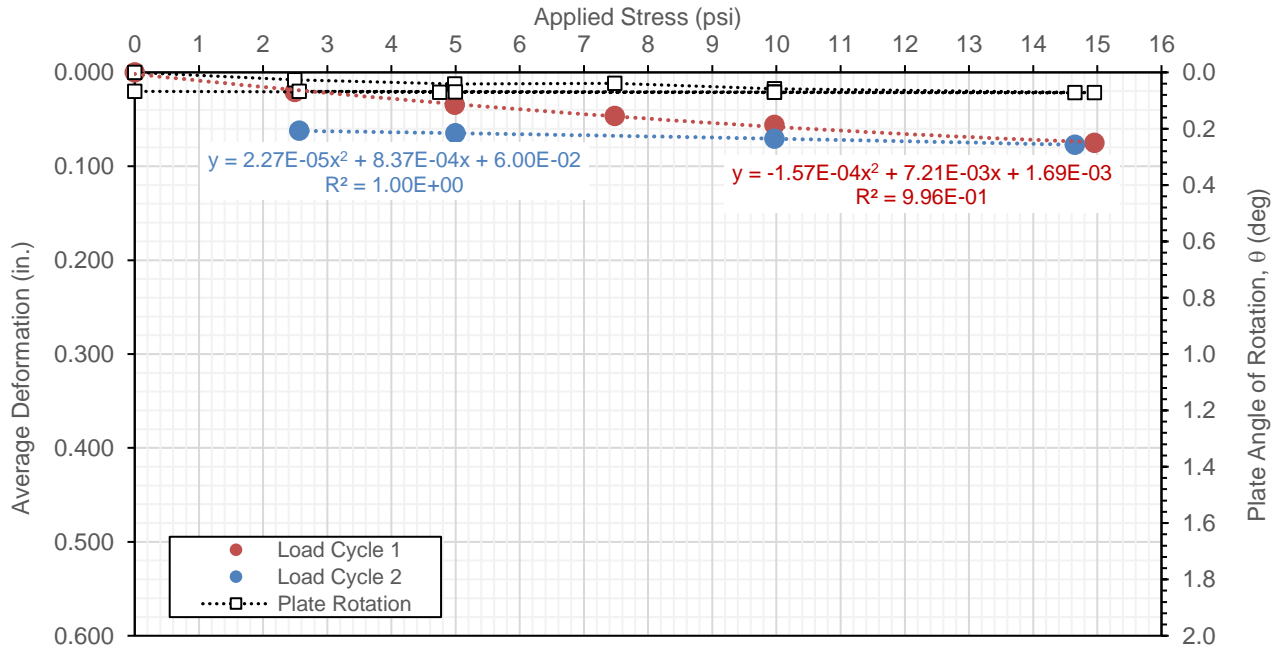
Second Cycle

a ₁	2.27E-05
a ₂	8.37E-04
R ²	1.00

θ_{max} (deg) **0.0723**

NOTES:

- Test performed per AASHTO T222/ASTM D1196.
- k-value determined using:
 - calculated stress at 0.05 in. plate deformation (d) for first loading cycle, per PCA design guidelines, and
 - for a defined target stress and calculating corresponding plate deformations using polynomial fit parameters.



Automated Plate Load Test [APLT]

Test:	In-Situ Static Plate Load Test: Two Loading Cycles.				
Date:	6/22/2017	Time:	7:09:53 PM	Test ID:	TS15_PT2
Tested By:	DW, HG, PV	Location:	TS15_PGE	Sta.:	NA
Latitude:	41.98369	Longitude:	88.01438	Elev. (ft):	NA
Comments:	Test on compacted nominal 6 in. thick PGE placed over subgrade.				

Cycle	Stage	Load Step	Target Applied Load (lbs)	Target Applied Stress (psi)	Actual Applied Stress (psi)	Deformation (in.)			Average Def. (in.)
						Sensor 1	Sensor 2	Sensor 3	
0	Seating	0	707	1	1.40	0.0224	0.0334	0.0159	0.0239
<i>Zero load and deformation sensors after applying the seating stress.</i>									
1	Seating	0	0	0	0.00	0.0000	0.0000	0.0000	0.0000
1	Load	1	1767	2.5	2.49	0.0223	0.0423	0.0248	0.0298
1	Load	2	3534	5	4.97	0.0354	0.0681	0.0482	0.0506
1	Load	3	5301	7.5	7.46	0.0490	0.0901	0.0669	0.0687
1	Load	4	7069	10	9.96	0.0625	0.1105	0.0875	0.0868
1	Load	5	10603	15	14.92	0.0873	0.1458	0.1174	0.1168
1	Load	6	7069	10	9.95	0.0835	0.1413	0.1134	0.1128
1	Unload	7	1767	2.5	2.48	0.0693	0.1252	0.0986	0.0977
1	Unload	8	3534	5	4.97	0.0717	0.1278	0.1012	0.1002
1	Unload	9	7069	10	9.94	0.0788	0.1370	0.1087	0.1081
2	Load	10	10603	15	14.92	0.0886	0.1503	0.1202	0.1197
2	Load	11	3534	5	0.00	0.0638	0.1201	0.0938	0.0926
2	Load	12	0	0	0.00	0.0580	0.1151	0.0871	0.0867

Plate Diameter:	30.0	in.				
Shape factor:	2.67					
Material Type:	B		A = Cohesive, B = Granular, C = Intermediate			
Poisson's ratio:	0.35					
Design Stress: (assumed)	10.0	psi	AASHTO T222 Method	k_{u1} (pci) @ design stress:	115	
Target Deformation:	0.05	in.	PCA Design Criteria	k_u (pci) @ $\delta = 0.05$ in.:	104	

Modulus at target deformation

Stress @ $\delta = 0.05$ in. (psi) 5.2

E ₁ (psi)	NA
k' _u (pci)	NA
k _u (pci)	NA

Modulus at target/design applied stress

First Loading Cycle

δ_1 (in.)	0.0863
E ₁ (psi)	4,029
k' _{u1} (pci)	116
k _{u1} (pci)	115

Second Loading Cycle

δ_2 (in.)	0.0123
E ₂ (psi)	19,974
k' _{u2} (pci)	816
k _{u2} (pci)	569
E ₂ / E ₁ or k ₂ / k ₁ Ratio	5.0

Plate Bending Correction for

$$k_u \geq 100 \text{ and } 1,000 \text{ pci}$$

$$k_u = -39.9178 + 5.5076 [k'_u]^{0.7019}$$

In-situ Modulus of Subgrade Reaction (k) and Elastic Modulus

Project Name: Illinois Tollway - IC Research
 Project ID: Elgin O'Hare Extension - IL Tollway
 Location: IL390 (West of O'Hare), Itasca, IL



Polynomial Fit Parameters

First Cycle

a ₁	-1.98E-04
a ₂	1.06E-02
R ²	1.00

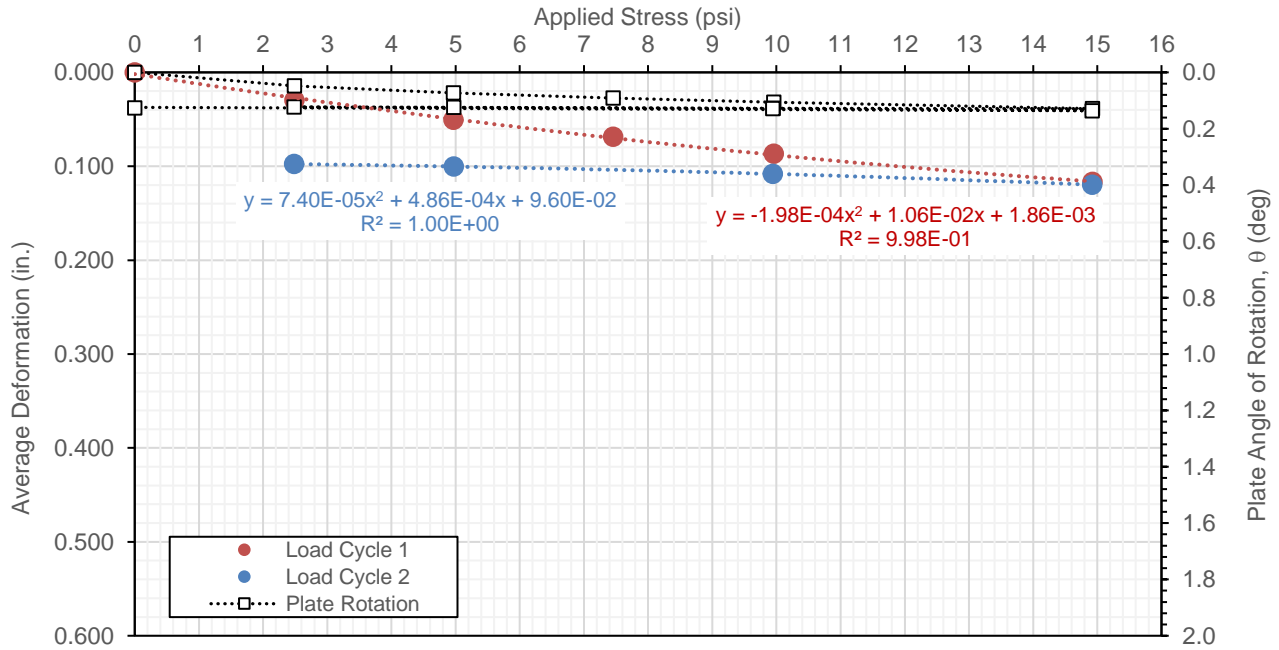
Second Cycle

a ₁	7.40E-05
a ₂	4.86E-04
R ²	1.00

θ_{max} (deg) **0.1361**

NOTES:

1. Test performed per AASHTO T222/ASTM D1196.
2. k-value determined using:
 - (a) calculated stress at 0.05 in. plate deformation (d) for first loading cycle, per PCA design guidelines, and
 - (b) for a defined target stress and calculating corresponding plate deformations using polynomial fit parameters.



Automated Plate Load Test [APLT]

Test:	In-Situ Static Plate Load Test: Two Loading Cycles.				
Date:	6/22/2017	Time:	7:54:27 PM	Test ID:	TS15_PT3
Tested By:	DW, HG, PV	Location:	TS15_PGE	Sta.:	NA
Latitude:	41.98375	Longitude:	88.01477	Elev. (ft):	NA
Comments:	Test on compacted nominal 6 in. thick PGE placed over subgrade.				

Cycle	Stage	Load Step	Target Applied Load (lbs)	Target Applied Stress (psi)	Actual Applied Stress (psi)	Deformation (in.)			Average Def. (in.)
						Sensor 1	Sensor 2	Sensor 3	
0	Seating	0	707	1	1.40	0.0137	0.0252	0.0230	0.0207
<i>Zero load and deformation sensors after applying the seating stress.</i>									
1	Seating	0	0	0	0.00	0.0000	0.0000	0.0000	0.0000
1	Load	1	1767	2.5	2.50	0.0115	0.0204	0.0144	0.0154
1	Load	2	3534	5	4.97	0.0199	0.0339	0.0238	0.0259
1	Load	3	5301	7.5	7.58	0.0267	0.0427	0.0300	0.0331
1	Load	4	7069	10	9.95	0.0309	0.0499	0.0359	0.0389
1	Load	5	10603	15	14.68	0.0382	0.0628	0.0461	0.0490
1	Load	6	7069	10	9.95	0.0372	0.0613	0.0445	0.0476
1	Unload	7	1767	2.5	2.49	0.0336	0.0569	0.0403	0.0436
1	Unload	8	3534	5	5.05	0.0345	0.0577	0.0410	0.0444
1	Unload	9	7069	10	9.94	0.0367	0.0605	0.0437	0.0470
2	Load	10	10603	15	14.93	0.0389	0.0648	0.0475	0.0504
2	Load	11	3534	5	0.00	0.0333	0.0555	0.0388	0.0426
2	Load	12	0	0	0.00	0.0317	0.0532	0.0361	0.0403

Plate Diameter:	30.0	in.			
Shape factor:	2.67				
Material Type:	B	A = Cohesive, B = Granular, C = Intermediate			
Poisson's ratio:	0.35				
Design Stress: (assumed)	10.0	psi	AASHTO T222 Method	k_{u1} (pci) @ design stress:	229
Target Deformation:	0.05	in.	PCA Design Criteria	k_u (pci) @ $\delta = 0.05$ in.:	NA*

Modulus at target deformation

Stress @ $\delta = 0.05$ in. (psi) NA*

**0.05 in. deformation not achieved*

E ₁ (psi)	NA
k' _u (pci)	NA
k _u (pci)	NA

Modulus at target/design applied stress

First Loading Cycle

δ_1 (in.)	0.0392
E ₁ (psi)	8,046
k' _{u1} (pci)	255
k _{u1} (pci)	229

Second Loading Cycle

δ_2 (in.)	0.0040
E ₂ (psi)	45,547
k' _{u2} (pci)	2,503
k _{u2} (pci)	1,298

E₂ / E₁ or k₂ / k₁ Ratio 5.7

Plate Bending Correction for

$$k_u \geq 100 \text{ and } 1,000 \text{ pci}$$

$$k_u = -39.9178 + 5.5076 [k'_u]^{0.7019}$$

In-situ Modulus of Subgrade Reaction (k) and Elastic Modulus

Project Name: Illinois Tollway - IC Research
 Project ID: Elgin O'Hare Extension - IL Tollway
 Location: IL390 (West of O'Hare), Itasca, IL



Polynomial Fit Parameters

First Cycle

a ₁	-1.53E-04
a ₂	5.45E-03
R ²	0.99

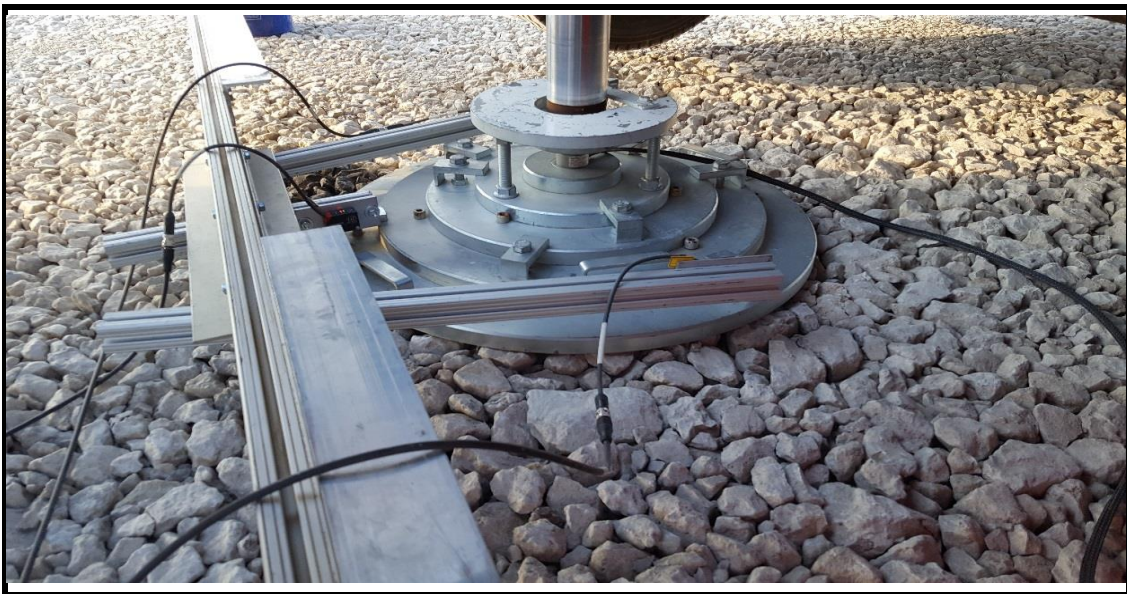
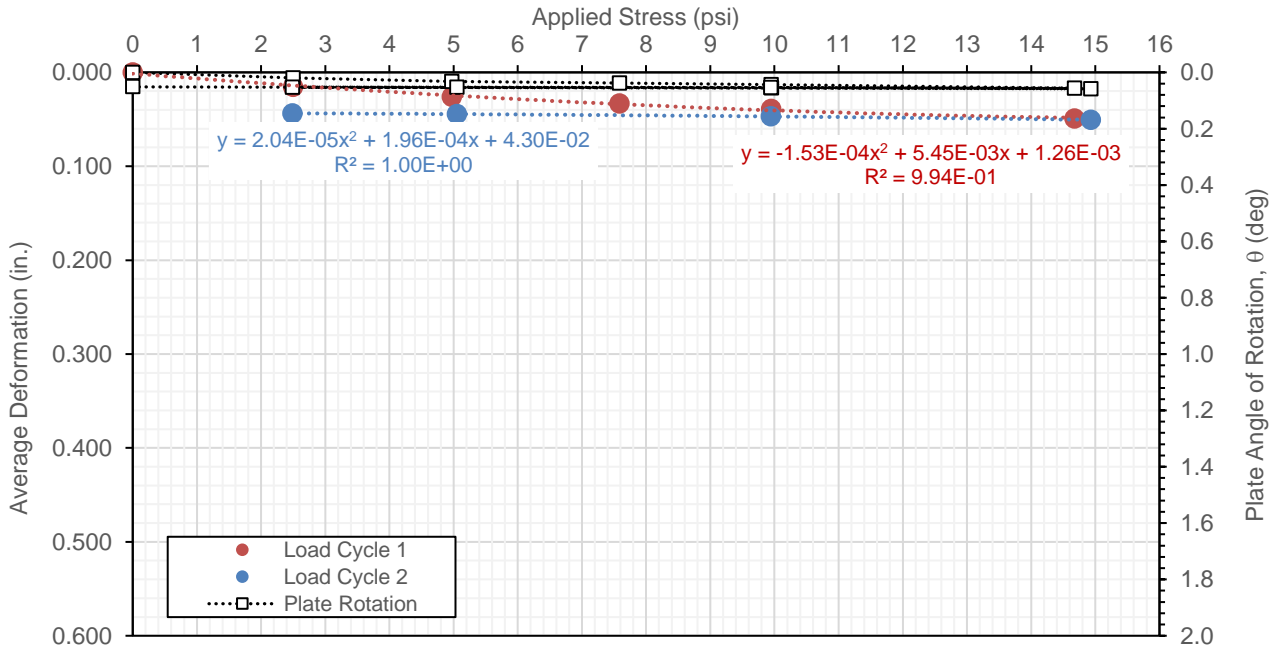
Second Cycle

a ₁	2.04E-05
a ₂	1.96E-04
R ²	1.00

θ_{max} (deg) **0.0582**

NOTES:

1. Test performed per AASHTO T222/ASTM D1196.
2. k-value determined using:
 - (a) calculated stress at 0.05 in. plate deformation (d) for first loading cycle, per PCA design guidelines, and
 - (b) for a defined target stress and calculating corresponding plate deformations using polynomial fit parameters.



Automated Plate Load Test [APLT]

Test:	In-Situ Static Plate Load Test: Two Loading Cycles.				
Date:	6/22/2017	Time:	8:32:59 PM	Test ID:	TS15_PT4
Tested By:	DW, HG, PV	Location:	TS15_PGE	Sta.:	NA
Latitude:	41.98377	Longitude:	88.01497	Elev. (ft):	NA
Comments:	Test on compacted nominal 6 in. thick PGE placed over subgrade.				

Cycle	Stage	Load Step	Target Applied Load (lbs)	Target Applied Stress (psi)	Actual Applied Stress (psi)	Deformation (in.)			Average Def. (in.)
						Sensor 1	Sensor 2	Sensor 3	
0	Seating	0	707	1	1.40	0.0142	0.0247	0.0297	0.0228
<i>Zero load and deformation sensors after applying the seating stress.</i>									
1	Seating	0	0	0	0.00	0.0000	0.0000	0.0000	0.0000
1	Load	1	1767	2.5	2.49	0.0195	0.0216	0.0231	0.0214
1	Load	2	3534	5	4.98	0.0332	0.0358	0.0409	0.0366
1	Load	3	5301	7.5	7.46	0.0455	0.0469	0.0545	0.0489
1	Load	4	7069	10	9.96	0.0575	0.0555	0.0661	0.0597
1	Load	5	10603	15	14.93	0.0792	0.0715	0.0884	0.0797
1	Load	6	7069	10	9.96	0.0765	0.0693	0.0858	0.0772
1	Unload	7	1767	2.5	2.49	0.0679	0.0608	0.0783	0.0690
1	Unload	8	3534	5	4.97	0.0699	0.0623	0.0803	0.0709
1	Unload	9	7069	10	9.94	0.0745	0.0673	0.0841	0.0753
2	Load	10	10603	15	14.92	0.0817	0.0739	0.0906	0.0821
2	Load	11	3534	5	0.00	0.0649	0.0575	0.0756	0.0660
2	Load	12	0	0	0.00	0.0608	0.0546	0.0731	0.0628

Plate Diameter:	30.0	in.			
Shape factor:	2.67				
Material Type:	B		A = Cohesive, B = Granular, C = Intermediate		
Poisson's ratio:	0.35				
Design Stress: (assumed)	10.0	psi	AASHTO T222 Method PCA Design Criteria	k_{u1} (pci) @ design stress: k_u (pci) @ $\delta = 0.05$ in.:	160
Target Deformation:	0.05	in.			169

Modulus at target deformation

Stress @ $\delta = 0.05$ in. (psi) 7.9

E ₁ (psi)	NA
k' _u (pci)	NA
k _u (pci)	NA

Modulus at target/design applied stress

First Loading Cycle

δ_1 (in.)	0.0601
E ₁ (psi)	5,601
k' _{u1} (pci)	166
k _{u1} (pci)	160

Second Loading Cycle

δ_2 (in.)	0.0075
E ₂ (psi)	28,798
k' _{u2} (pci)	1,335
k _{u2} (pci)	820
E ₂ / E ₁ or k ₂ / k ₁ Ratio	5.1

Plate Bending Correction for

$$k_u \geq 100 \text{ and } 1,000 \text{ pci}$$

$$k_u = -39.9178 + 5.5076 [k'_u]^{0.7019}$$

In-situ Modulus of Subgrade Reaction (k) and Elastic Modulus

Project Name: Illinois Tollway - IC Research
 Project ID: Elgin O'Hare Extension - IL Tollway
 Location: IL390 (West of O'Hare), Itasca, IL



Polynomial Fit Parameters

First Cycle

a ₁	-1.66E-04
a ₂	7.67E-03
R ²	1.00

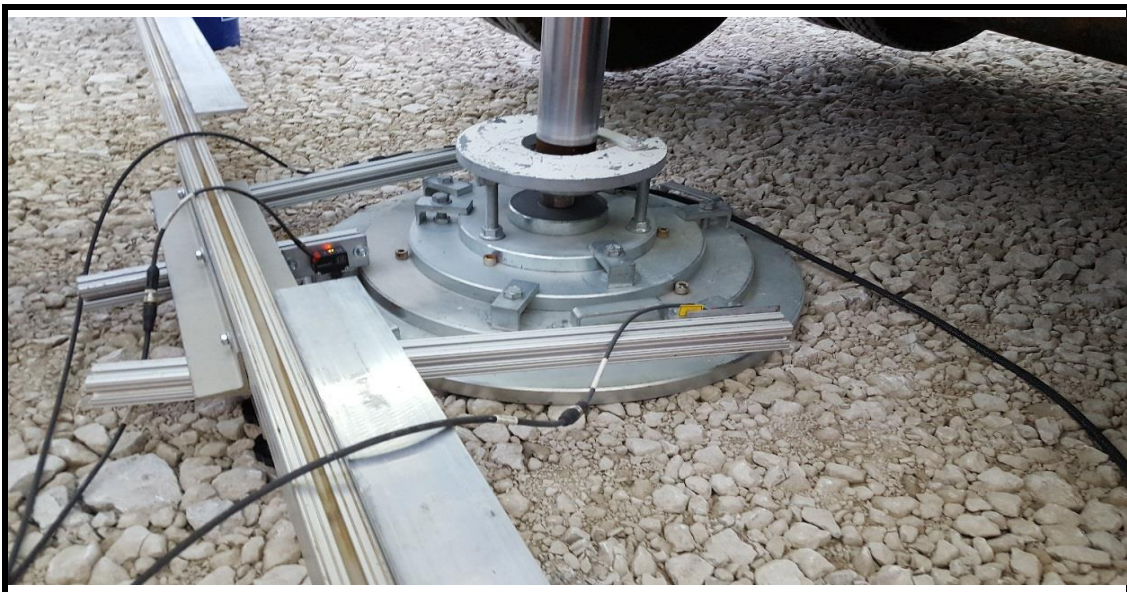
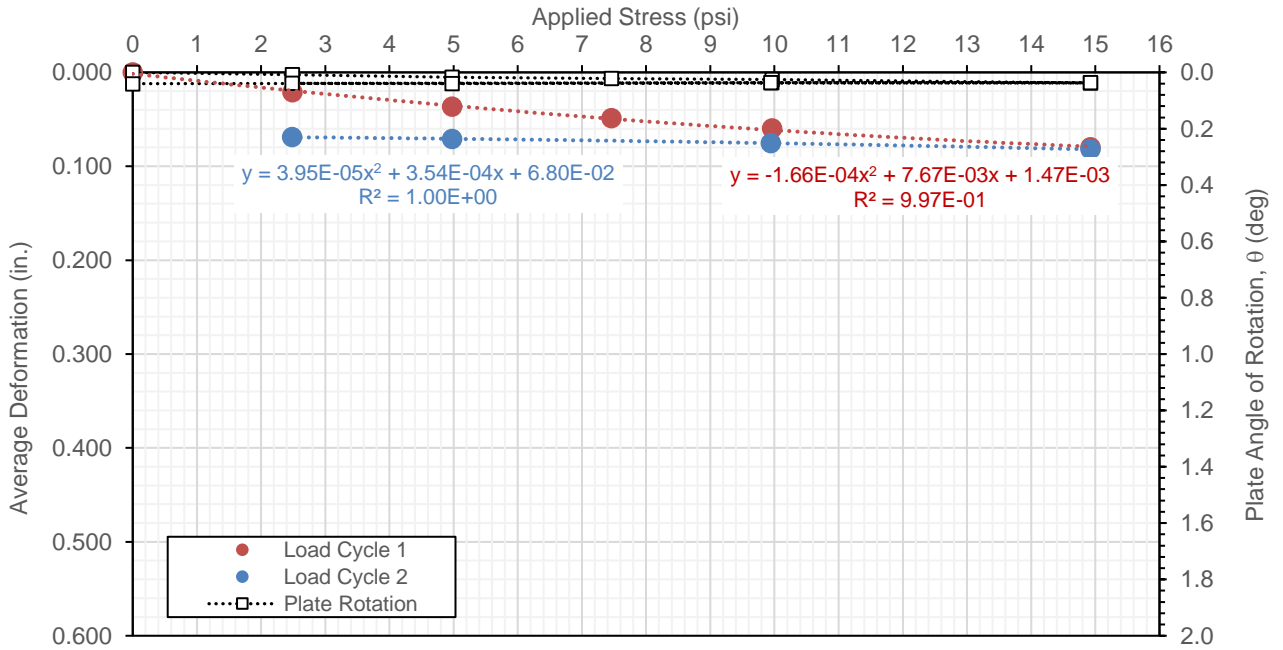
Second Cycle

a ₁	3.95E-05
a ₂	3.54E-04
R ²	1.00

θ_{max} (deg) **0.0416**

NOTES:

- Test performed per AASHTO T222/ASTM D1196.
- k-value determined using:
 - calculated stress at 0.05 in. plate deformation (d) for first loading cycle, per PCA design guidelines, and
 - for a defined target stress and calculating corresponding plate deformations using polynomial fit parameters.



Automated Plate Load Test [APLT]

Test:	In-Situ Static Plate Load Test: Two Loading Cycles.				
Date:	6/22/2017	Time:	11:15:00 PM	Test ID:	TS15_PT5
Tested By:	DW, HG, PV	Location:	TS15_PGE	Sta.:	NA
Latitude:	41.98375	Longitude:	88.01515	Elev. (ft):	NA
Comments:	Test on compacted nominal 6 in. thick PGE placed over subgrade.				

Cycle	Stage	Load Step	Target Applied Load (lbs)	Target Applied Stress (psi)	Actual Applied Stress (psi)	Deformation (in.)			Average Def. (in.)
						Sensor 1	Sensor 2	Sensor 3	
0	Seating	0	707	1	1.40	0.0084	0.0206	0.0159	0.0150
<i>Zero load and deformation sensors after applying the seating stress.</i>									
1	Seating	0	0	0	0.00	0.0000	0.0000	0.0000	0.0000
1	Load	1	1767	2.5	2.49	0.0078	0.0166	0.0129	0.0124
1	Load	2	3534	5	5.07	0.0147	0.0262	0.0202	0.0204
1	Load	3	5301	7.5	7.63	0.0211	0.0340	0.0258	0.0270
1	Load	4	7069	10	9.95	0.0265	0.0412	0.0296	0.0324
1	Load	5	10603	15	14.93	0.0362	0.0548	0.0368	0.0426
1	Load	6	7069	10	9.95	0.0346	0.0534	0.0355	0.0412
1	Unload	7	1767	2.5	2.55	0.0288	0.0480	0.0332	0.0367
1	Unload	8	3534	5	4.97	0.0308	0.0501	0.0335	0.0381
1	Unload	9	7069	10	9.95	0.0341	0.0525	0.0360	0.0409
2	Load	10	10603	15	14.93	0.0383	0.0578	0.0395	0.0452
2	Load	11	3534	5	0.00	0.0263	0.0467	0.0335	0.0355
2	Load	12	0	0	0.00	0.0235	0.0435	0.0324	0.0332

Plate Diameter:	30.0	in.				
Shape factor:	2.67					
Material Type:	B		A = Cohesive, B = Granular, C = Intermediate			
Poisson's ratio:	0.35					
Design Stress: (assumed)	10.0	psi	AASHTO T222 Method	k_{u1} (pci) @ design stress:	268	
Target Deformation:	0.05	in.	PCA Design Criteria	k_u (pci) @ $\delta = 0.05$ in.:	NA*	

Modulus at target deformation

Stress @ $\delta = 0.05$ in. (psi)	NA*
*0.05 in. deformation not achieved	
E_1 (psi)	NA
k'_{u1} (pci)	NA
k_{u1} (pci)	NA

Modulus at target/design applied stress

<i>First Loading Cycle</i>	
δ_1 (in.)	0.0324
E_1 (psi)	9,411
k'_{u1} (pci)	309
k_{u1} (pci)	268
<i>Second Loading Cycle</i>	
δ_2 (in.)	0.0052
E_2 (psi)	37,521
k'_{u2} (pci)	1,916
k_{u2} (pci)	1,069
E_2 / E_1 or k_2 / k_1 Ratio	4.0

Plate Bending Correction for

$$k_u \geq 100 \text{ and } 1,000 \text{ pci}$$

$$k_u = -39.9178 + 5.5076 [k'_u]^{0.7019}$$

In-situ Modulus of Subgrade Reaction (k) and Elastic Modulus	
Project Name: Illinois Tollway - IC Research	
Project ID: Elgin O'Hare Extension - IL Tollway	
Location: IL390 (West of O'Hare), Itasca, IL	

Polynomial Fit Parameters

First Cycle

a ₁	-9.73E-05
a ₂	4.21E-03
R ²	1.00

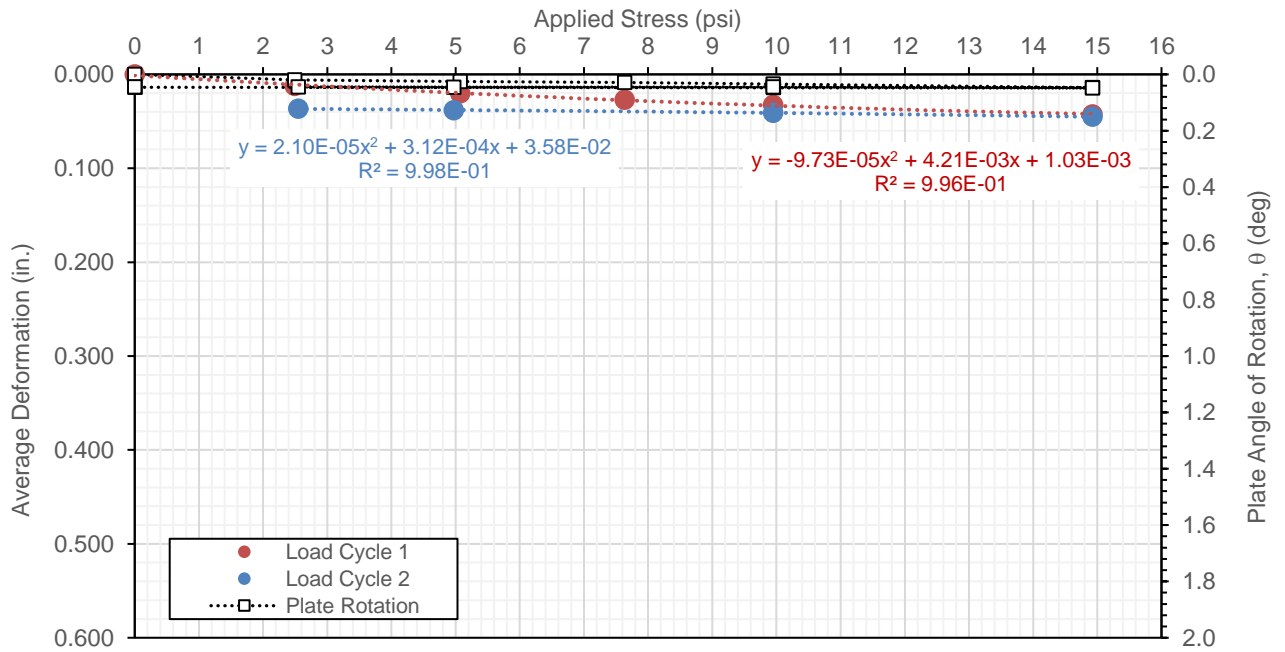
Second Cycle

a ₁	2.10E-05
a ₂	3.12E-04
R ²	1.00

θ_{max} (deg) **0.0482**

NOTES:

1. Test performed per AASHTO T222/ASTM D1196.
2. k-value determined using:
 - (a) calculated stress at 0.05 in. plate deformation (d) for first loading cycle, per PCA design guidelines, and
 - (b) for a defined target stress and calculating corresponding plate deformations using polynomial fit parameters.



Automated Plate Load Test [APLT]

Test:	In-Situ Static Plate Load Test: Two Loading Cycles.				
Date:	6/22/2017	Time:	11:56:26 PM	Test ID:	TS15_PT6
Tested By:	DW, HG, PV	Location:	TS15_PGE	Sta.:	NA
Latitude:	41.98377	Longitude:	88.01528	Elev. (ft):	NA
Comments:	Test on compacted nominal 6 in. thick PGE placed over subgrade.				

Cycle	Stage	Load Step	Target Applied Load (lbs)	Target Applied Stress (psi)	Actual Applied Stress (psi)	Deformation (in.)			Average Def. (in.)
						Sensor 1	Sensor 2	Sensor 3	
0	Seating	0	707	1	1.40	0.0222	0.0219	0.0484	0.0309
<i>Zero load and deformation sensors after applying the seating stress.</i>									
1	Seating	0	0	0	0.00	0.0000	0.0000	0.0000	0.0000
1	Load	1	1767	2.5	2.48	0.0252	0.0236	0.0293	0.0260
1	Load	2	3534	5	5.07	0.0365	0.0428	0.0492	0.0428
1	Load	3	5301	7.5	7.53	0.0439	0.0532	0.0612	0.0528
1	Load	4	7069	10	9.95	0.0512	0.0602	0.0722	0.0612
1	Load	5	10603	15	14.92	0.0642	0.0780	0.0875	0.0766
1	Load	6	7069	10	9.95	0.0634	0.0756	0.0864	0.0751
1	Unload	7	1767	2.5	2.48	0.0605	0.0687	0.0833	0.0708
1	Unload	8	3534	5	4.97	0.0612	0.0705	0.0845	0.0721
1	Unload	9	7069	10	10.06	0.0630	0.0748	0.0877	0.0752
2	Load	10	10603	15	14.92	0.0667	0.0799	0.0921	0.0795
2	Load	11	3534	5	-0.01	0.0592	0.0706	0.0854	0.0717
2	Load	12	0	0	0.00	0.0578	0.0675	0.0834	0.0696

Plate Diameter:	30.0	in.				
Shape factor:	2.67					
Material Type:	B	A = Cohesive, B = Granular, C = Intermediate				
Poisson's ratio:	0.35					
Design Stress: (assumed)	10.0	psi	AASHTO T222 Method	k_{u1} (pci) @ design stress:	156	
Target Deformation:	0.05	in.	PCA Design Criteria	k_u (pci) @ $\delta = 0.05$ in.:	156	

Modulus at target deformation

Stress @ $\delta = 0.05$ in. (psi) 7.2

E ₁ (psi)	NA
k' _u (pci)	NA
k _u (pci)	NA

Modulus at target/design applied stress

First Loading Cycle

δ_1 (in.)	0.0617
E ₁ (psi)	5,472
k' _{u1} (pci)	162
k _{u1} (pci)	156

Second Loading Cycle

δ_2 (in.)	0.0051
E ₂ (psi)	38,155
k' _{u2} (pci)	1,961
k _{u2} (pci)	1,087

E₂ / E₁ or k₂ / k₁ Ratio 7.0

Plate Bending Correction for

$$k'_u \geq 100 \text{ and } 1,000 \text{ pci}$$

$$k_u = -39.9178 + 5.5076 [k'_u]^{0.7019}$$

In-situ Modulus of Subgrade Reaction (k) and Elastic Modulus

Project Name: Illinois Tollway - IC Research
 Project ID: Elgin O'Hare Extension - IL Tollway
 Location: IL390 (West of O'Hare), Itasca, IL



Polynomial Fit Parameters

First Cycle

a ₁	-2.64E-04
a ₂	8.82E-03
R ²	0.99

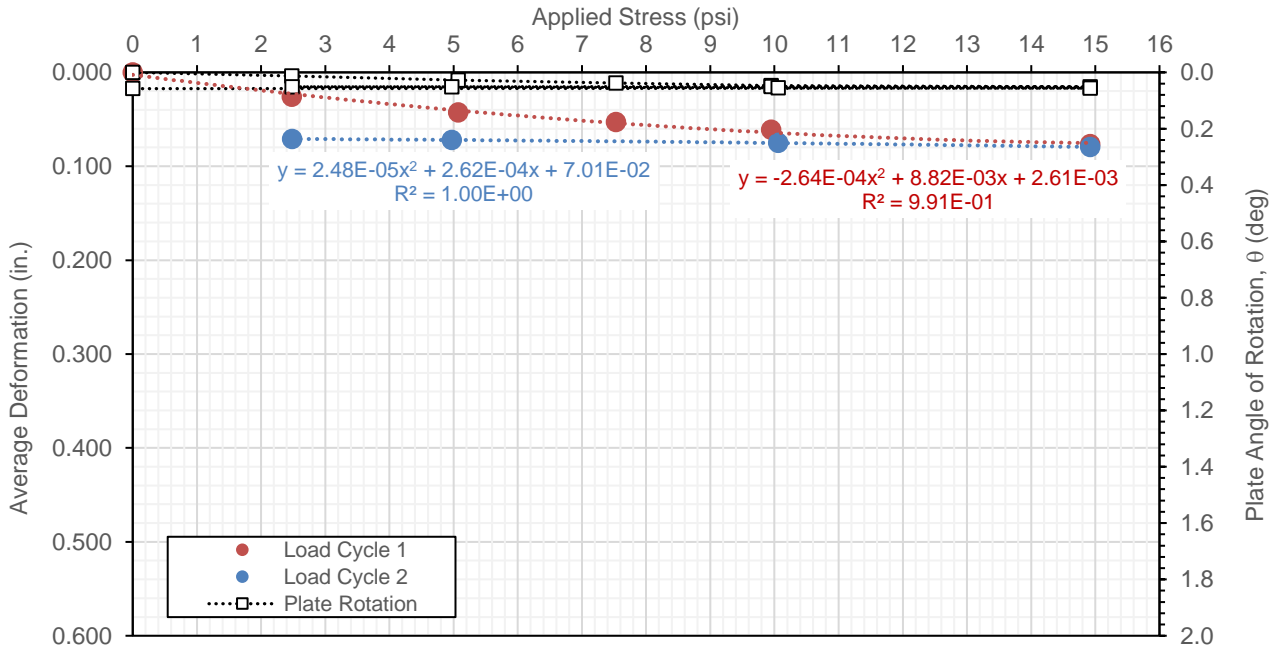
Second Cycle

a ₁	2.48E-05
a ₂	2.62E-04
R ²	1.00

θ_{max} (deg) **0.0579**

NOTES:

1. Test performed per AASHTO T222/ASTM D1196.
2. k-value determined using:
 - (a) calculated stress at 0.05 in. plate deformation (d) for first loading cycle, per PCA design guidelines, and
 - (b) for a defined target stress and calculating corresponding plate deformations using polynomial fit parameters.



Automated Plate Load Test [APLT]

Test:	In-Situ Static Plate Load Test: Two Loading Cycles.				
Date:	6/23/2017	Time:	12:41:16 AM	Test ID:	TS15_PT7
Tested By:	DW, HG, PV	Location:	TS15_PGE	Sta.:	NA
Latitude:	41.98375	Longitude:	88.01539	Elev. (ft):	NA
Comments:	Test on compacted nominal 6 in. thick PGE placed over subgrade.				

Cycle	Stage	Load Step	Target Applied Load (lbs)	Target Applied Stress (psi)	Actual Applied Stress (psi)	Deformation (in.)			Average Def. (in.)
						Sensor 1	Sensor 2	Sensor 3	
0	Seating	0	707	1	1.40	0.0101	0.0207	0.0094	0.0134
<i>Zero load and deformation sensors after applying the seating stress.</i>									
1	Seating	0	0	0	0.00	0.0000	0.0000	0.0000	0.0000
1	Load	1	1767	2.5	2.49	0.0158	0.0257	0.0158	0.0191
1	Load	2	3534	5	4.97	0.0288	0.0401	0.0300	0.0330
1	Load	3	5301	7.5	7.48	0.0376	0.0557	0.0402	0.0445
1	Load	4	7069	10	9.95	0.0464	0.0658	0.0483	0.0535
1	Load	5	10603	15	14.92	0.0647	0.0819	0.0615	0.0694
1	Load	6	7069	10	9.95	0.0627	0.0802	0.0599	0.0676
1	Unload	7	1767	2.5	2.49	0.0572	0.0759	0.0547	0.0626
1	Unload	8	3534	5	4.97	0.0577	0.0768	0.0562	0.0636
1	Unload	9	7069	10	9.95	0.0617	0.0798	0.0596	0.0671
2	Load	10	10603	15	14.93	0.0678	0.0847	0.0648	0.0724
2	Load	11	3534	5	0.00	0.0579	0.0764	0.0548	0.0630
2	Load	12	0	0	0.00	0.0561	0.0747	0.0527	0.0612

Plate Diameter:	30.0	in.			
Shape factor:	2.67				
Material Type:	B		A = Cohesive, B = Granular, C = Intermediate		
Poisson's ratio:	0.35				
Design Stress: (assumed)	10.0	psi	AASHTO T222 Method PCA Design Criteria	k_{u1} (pci) @ design stress:	175
Target Deformation:	0.05	in.		k_u (pci) @ $\delta = 0.05$ in.:	193

Modulus at target deformation

Stress @ $\delta = 0.05$ in. (psi) 9.0

E ₁ (psi)	NA
k' _u (pci)	NA
k _u (pci)	NA

Modulus at target/design applied stress

First Loading Cycle

δ_1 (in.)	0.0540
E ₁ (psi)	6,151
k' _{u1} (pci)	185
k _{u1} (pci)	175

Second Loading Cycle

δ_2 (in.)	0.0050
E ₂ (psi)	38,523
k' _{u2} (pci)	1,987
k _{u2} (pci)	1,098

E₂ / E₁ or k₂ / k₁ Ratio 6.3

Plate Bending Correction for

$$k_u \geq 100 \text{ and } 1,000 \text{ pci}$$

$$k_u = -39.9178 + 5.5076 [k'_u]^{0.7019}$$

In-situ Modulus of Subgrade Reaction (k) and Elastic Modulus

Project Name: Illinois Tollway - IC Research
 Project ID: Elgin O'Hare Extension - IL Tollway
 Location: IL390 (West of O'Hare), Itasca, IL



Polynomial Fit Parameters

First Cycle

a ₁	-1.73E-04
a ₂	7.13E-03
R ²	1.00

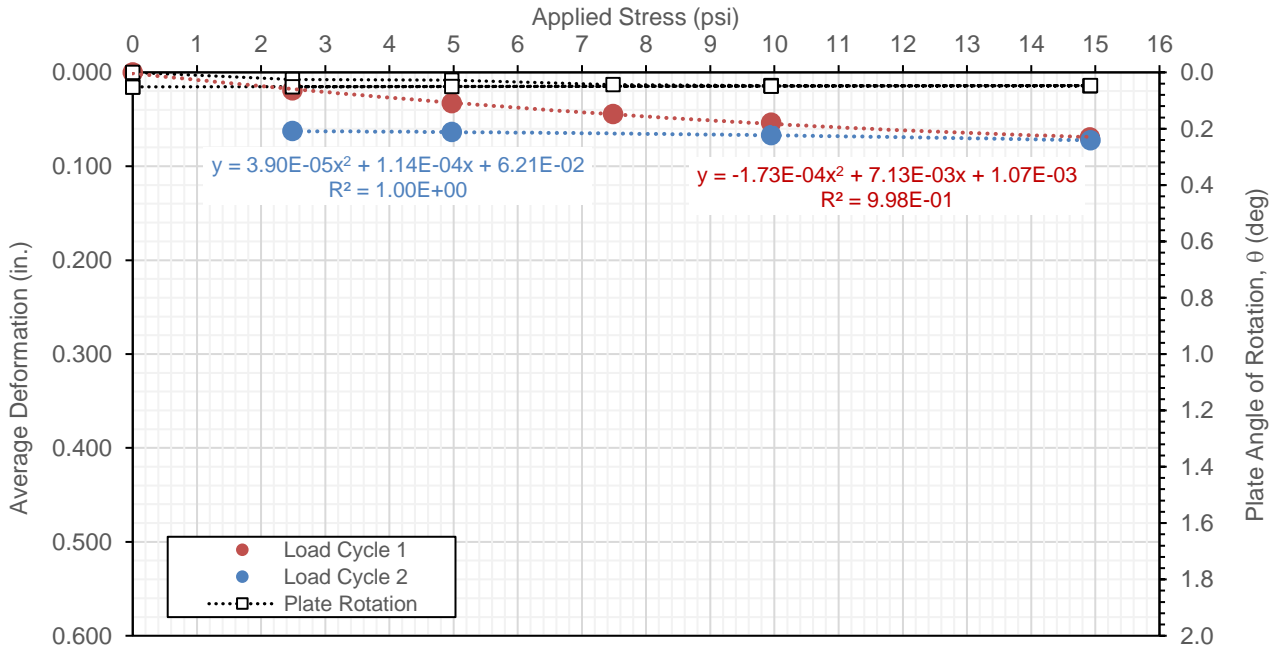
Second Cycle

a ₁	3.90E-05
a ₂	1.14E-04
R ²	1.00

θ_{max} (deg) **0.0521**

NOTES:

1. Test performed per AASHTO T222/ASTM D1196.
2. k-value determined using:
 - (a) calculated stress at 0.05 in. plate deformation (d) for first loading cycle, per PCA design guidelines, and
 - (b) for a defined target stress and calculating corresponding plate deformations using polynomial fit parameters.



Automated Plate Load Test [APLT]

Test:	In-Situ Static Plate Load Test: Two Loading Cycles.				
Date:	6/22/2017	Time:	10:32:48 PM	Test ID:	TS15_PT8
Tested By:	DW, HG, PV	Location:	TS15_PGE	Sta.:	NA
Latitude:	41.98365	Longitude:	88.01546	Elev. (ft):	NA
Comments:	Test on compacted nominal 6 in. thick PGE placed over subgrade.				

Cycle	Stage	Load Step	Target Applied Load (lbs)	Target Applied Stress (psi)	Actual Applied Stress (psi)	Deformation (in.)			Average Def. (in.)
						Sensor 1	Sensor 2	Sensor 3	
0	Seating	0	707	1	1.40	0.0241	0.0364	0.0332	0.0312
<i>Zero load and deformation sensors after applying the seating stress.</i>									
1	Seating	0	0	0	0.00	0.0000	0.0000	0.0000	0.0000
1	Load	1	1767	2.5	2.48	0.0419	0.0379	0.0439	0.0412
1	Load	2	3534	5	4.97	0.0856	0.0687	0.0799	0.0781
1	Load	3	5301	7.5	7.45	0.1279	0.0950	0.1109	0.1113
1	Load	4	7069	10	9.94	0.1705	0.1190	0.1432	0.1442
1	Load	5	10603	15	14.92	0.2534	0.1565	0.1987	0.2029
1	Load	6	7069	10	9.95	0.2457	0.1520	0.1931	0.1969
1	Unload	7	1767	2.5	2.58	0.2107	0.1342	0.1685	0.1711
1	Unload	8	3534	5	5.02	0.2185	0.1385	0.1743	0.1771
1	Unload	9	7069	10	9.94	0.2385	0.1499	0.1894	0.1926
2	Load	10	10603	15	14.91	0.2652	0.1622	0.2039	0.2104
2	Load	11	3534	5	-0.01	0.2000	0.1273	0.1567	0.1613
2	Load	12	0	0					

Plate Diameter:	30.0	in.			
Shape factor:	2.67				
Material Type:	B		A = Cohesive, B = Granular, C = Intermediate		
Poisson's ratio:	0.35				
Design Stress: (assumed)	10.0	psi	AASHTO T222 Method PCA Design Criteria	k_{u1} (pci) @ design stress:	69
Target Deformation:	0.05	in.			k_u (pci) @ $\delta = 0.05$ in.:

Modulus at target deformation

Stress @ $\delta = 0.05$ in. (psi) 3.2

E ₁ (psi)	NA
k' _u (pci)	NA
k _u (pci)	NA

Modulus at target/design applied stress

First Loading Cycle

δ_1 (in.)	0.1446
E ₁ (psi)	2,427
k' _{u1} (pci)	69
k _{u1} (pci)	69

Second Loading Cycle

δ_2 (in.)	0.0276
E ₂ (psi)	10,685
k' _{u2} (pci)	362
k _{u2} (pci)	304

E₂ / E₁ or k₂ / k₁ Ratio

E ₂ / E ₁ or k ₂ / k ₁ Ratio	4.4
--	-----

Plate Bending Correction for

$$k'_u \geq 100 \text{ and } 1,000 \text{ pci}$$

$$k_u = -39.9178 + 5.5076 [k'_u]^{0.7019}$$

In-situ Modulus of Subgrade Reaction (k) and Elastic Modulus

Project Name: Illinois Tollway - IC Research
 Project ID: Elgin O'Hare Extension - IL Tollway
 Location: IL390 (West of O'Hare), Itasca, IL



Polynomial Fit Parameters

First Cycle

a ₁	-1.89E-04
a ₂	1.64E-02
R ²	1.00

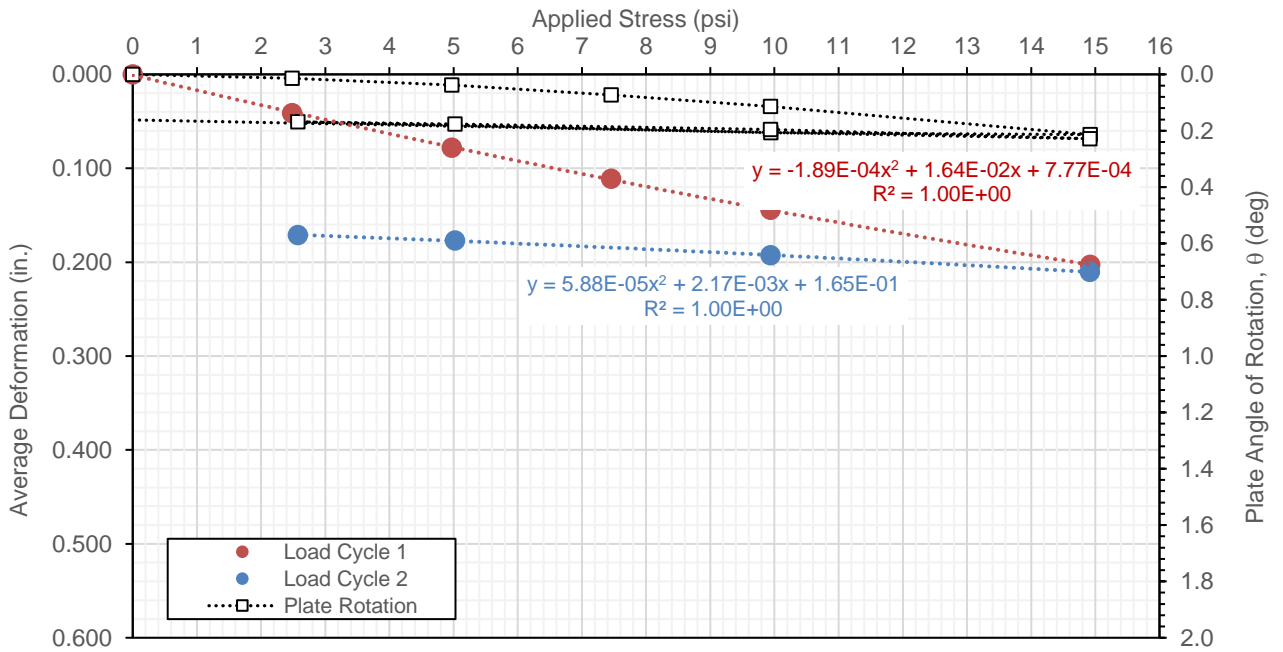
Second Cycle

a ₁	5.88E-05
a ₂	2.17E-03
R ²	#VALUE!

θ_{max} (deg) **0.2284**

NOTES:

1. Test performed per AASHTO T222/ASTM D1196.
2. k-value determined using:
 - (a) calculated stress at 0.05 in. plate deformation (d) for first loading cycle, per PCA design guidelines, and
 - (b) for a defined target stress and calculating corresponding plate deformations using polynomial fit parameters.



Automated Plate Load Test [APLT]

Test:	In-Situ Static Plate Load Test: Two Loading Cycles.				
Date:	6/22/2017	Time:	7:53:33 PM	Test ID:	TS15_PT9
Tested By:	DW, HG, PV	Location:	TS15_PGE	Sta.:	NA
Latitude:	41.98362	Longitude:	88.01536	Elev. (ft):	NA
Comments:	Test on compacted nominal 6 in. thick PGE placed over subgrade.				

Cycle	Stage	Load Step	Target Applied Load (lbs)	Target Applied Stress (psi)	Actual Applied Stress (psi)	Deformation (in.)			Average Def. (in.)
						Sensor 1	Sensor 2	Sensor 3	
0	Seating	0	707	1	1.40	0.0094	0.0058	0.0131	0.0094
<i>Zero load and deformation sensors after applying the seating stress.</i>									
1	Seating	0	0	0	0.00	0.0000	0.0000	0.0000	0.0000
1	Load	1	1767	2.5	2.49	0.0298	0.0260	0.0354	0.0304
1	Load	2	3534	5	4.99	0.0745	0.0722	0.0837	0.0768
1	Load	3	5301	7.5	7.46	0.1133	0.1153	0.1261	0.1182
1	Load	4	7069	10	9.95	0.1627	0.1701	0.1802	0.1710
1	Load	5	10603	15	14.79	0.2566	0.2675	0.2732	0.2658
1	Load	6	7069	10	9.94	0.2466	0.2580	0.2627	0.2557
1	Unload	7	1767	2.5	2.48	0.2075	0.2149	0.2250	0.2158
1	Unload	8	3534	5	5.00	0.2143	0.2228	0.2321	0.2231
1	Unload	9	7069	10	9.95	0.2380	0.2484	0.2541	0.2468
2	Load	10	10603	15	14.81	0.2714	0.2823	0.2858	0.2798
2	Load	11	3534	5	0.01	0.1951	0.2010	0.2108	0.2023
2	Load	12	0	0	0.00	0.1802	0.1888	0.1951	0.1880

Plate Diameter:	30.0	in.				
Shape factor:	2.67					
Material Type:	B		A = Cohesive, B = Granular, C = Intermediate			
Poisson's ratio:	0.35					
Design Stress: (assumed)	10.0	psi	AASHTO T222 Method PCA Design Criteria	k_{u1} (pci) @ design stress:	59	
Target Deformation:	0.05	in.			k_u (pci) @ $\delta = 0.05$ in.:	70

Modulus at target deformation

Stress @ $\delta = 0.05$ in. (psi) 3.2

E ₁ (psi)	NA
k' _u (pci)	NA
k _u (pci)	NA

Modulus at target/design applied stress

First Loading Cycle

δ_1 (in.)	0.1708
E ₁ (psi)	2,055
k' _{u1} (pci)	59
k _{u1} (pci)	59

Second Loading Cycle

δ_2 (in.)	0.0362
E ₂ (psi)	8,597
k' _{u2} (pci)	276
k _{u2} (pci)	245
E ₂ / E ₁ or k ₂ / k ₁ Ratio	4.2

Plate Bending Correction for

$$k_u \geq 100 \text{ and } 1,000 \text{ pci}$$

$$k_u = -39.9178 + 5.5076 [k'_u]^{0.7019}$$

In-situ Modulus of Subgrade Reaction (k) and Elastic Modulus

Project Name: Illinois Tollway - IC Research
 Project ID: Elgin O'Hare Extension - IL Tollway
 Location: IL390 (West of O'Hare), Itasca, IL



Polynomial Fit Parameters

First Cycle

a ₁	2.46E-04
a ₂	1.46E-02
R ²	1.00

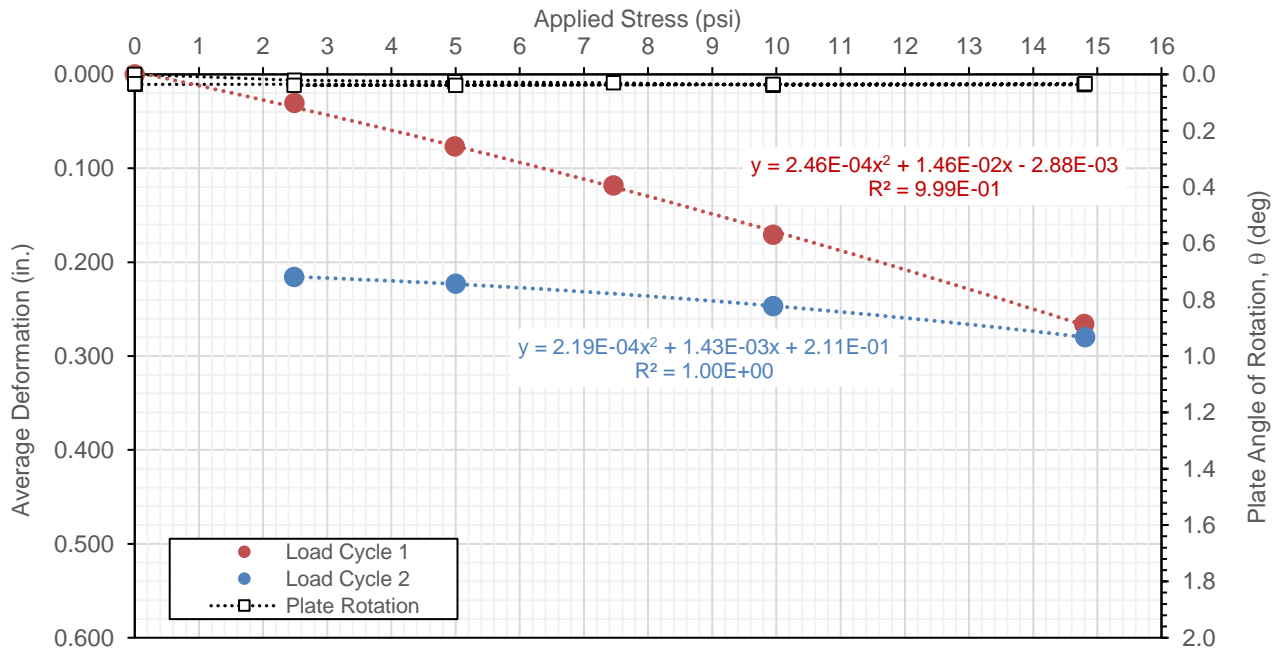
Second Cycle

a ₁	2.19E-04
a ₂	1.43E-03
R ²	1.00

θ_{max} (deg) **0.0391**

NOTES:

1. Test performed per AASHTO T222/ASTM D1196.
2. k-value determined using:
 - (a) calculated stress at 0.05 in. plate deformation (d) for first loading cycle, per PCA design guidelines, and
 - (b) for a defined target stress and calculating corresponding plate deformations using polynomial fit parameters.



Automated Plate Load Test [APLT]

Test:	In-Situ Static Plate Load Test: Two Loading Cycles.				
Date:	6/22/2017	Time:	9:13:00 PM	Test ID:	TS15_PT10
Tested By:	DW, HG, PV	Location:	TS15_PGE	Sta.:	NA
Latitude:	41.98361	Longitude:	88.01528	Elev. (ft):	NA
Comments:	Test on compacted nominal 6 in. thick PGE placed over subgrade.				

Cycle	Stage	Load Step	Target Applied Load (lbs)	Target Applied Stress (psi)	Actual Applied Stress (psi)	Deformation (in.)			Average Def. (in.)
						Sensor 1	Sensor 2	Sensor 3	
0	Seating	0	707	1	1.40	0.0165	0.0440	0.0383	0.0330
<i>Zero load and deformation sensors after applying the seating stress.</i>									
1	Seating	0	0	0	0.00	0.0000	0.0000	0.0000	0.0000
1	Load	1	1767	2.5	2.49	0.0667	0.1258	0.1098	0.1007
1	Load	2	3534	5	4.98	0.1283	0.2595	0.2224	0.2034
1	Load	3	5301	7.5	7.48	0.1904	0.3890	0.3292	0.3029
1	Load	4	7069	10	9.96	0.2520	0.4816	0.4037	0.3791
1	Load	5	10603	15	14.93	0.3754	0.6306	0.5449	0.5170
1	Load	6	7069	10	9.95	0.3630	0.6163	0.5338	0.5044
1	Unload	7	1767	2.5	2.54	0.3179	0.5514	0.4834	0.4509
1	Unload	8	3534	5	4.98	0.3258	0.5650	0.4943	0.4617
1	Unload	9	7069	10	9.95	0.3507	0.6013	0.5230	0.4917
2	Load	10	10603	15	14.93	0.3885	0.6523	0.5620	0.5343
2	Load	11	3534	5	-0.02	0.2983	0.5314	0.4640	0.4312
2	Load	12	0	0					

Plate Diameter:	30.0	in.			
Shape factor:	2.67				
Material Type:	B		A = Cohesive, B = Granular, C = Intermediate		
Poisson's ratio:	0.35				
Design Stress: (assumed)	10.0	psi	AASHTO T222 Method PCA Design Criteria	k_{u1} (pci) @ design stress:	26
Target Deformation:	0.05	in.			k_u (pci) @ $\delta = 0.05$ in.:

Modulus at target deformation

Stress @ $\delta = 0.05$ in. (psi) 1.1

E ₁ (psi)	NA
k' _u (pci)	NA
k _u (pci)	NA

Modulus at target/design applied stress

First Loading Cycle

δ ₁ (in.)	0.3842
E ₁ (psi)	914
k' _{u1} (pci)	26
k _{u1} (pci)	26

Second Loading Cycle

δ ₂ (in.)	0.0489
E ₂ (psi)	6,688
k' _{u2} (pci)	204
k _{u2} (pci)	191

E₂ / E₁ or k₂ / k₁ Ratio 7.3

Plate Bending Correction for

$$k'_u \geq 100 \text{ and } 1,000 \text{ pci}$$

$$k_u = -39.9178 + 5.5076 [k'_u]^{0.7019}$$

In-situ Modulus of Subgrade Reaction (k) and Elastic Modulus		
Project Name:	Illinois Tollway - IC Research	
Project ID:	Elgin O'Hare Extension - IL Tollway	
Location:	IL390 (West of O'Hare), Itasca, IL	

Polynomial Fit Parameters

First Cycle

a ₁	-7.14E-04
a ₂	4.56E-02
R ²	1.00

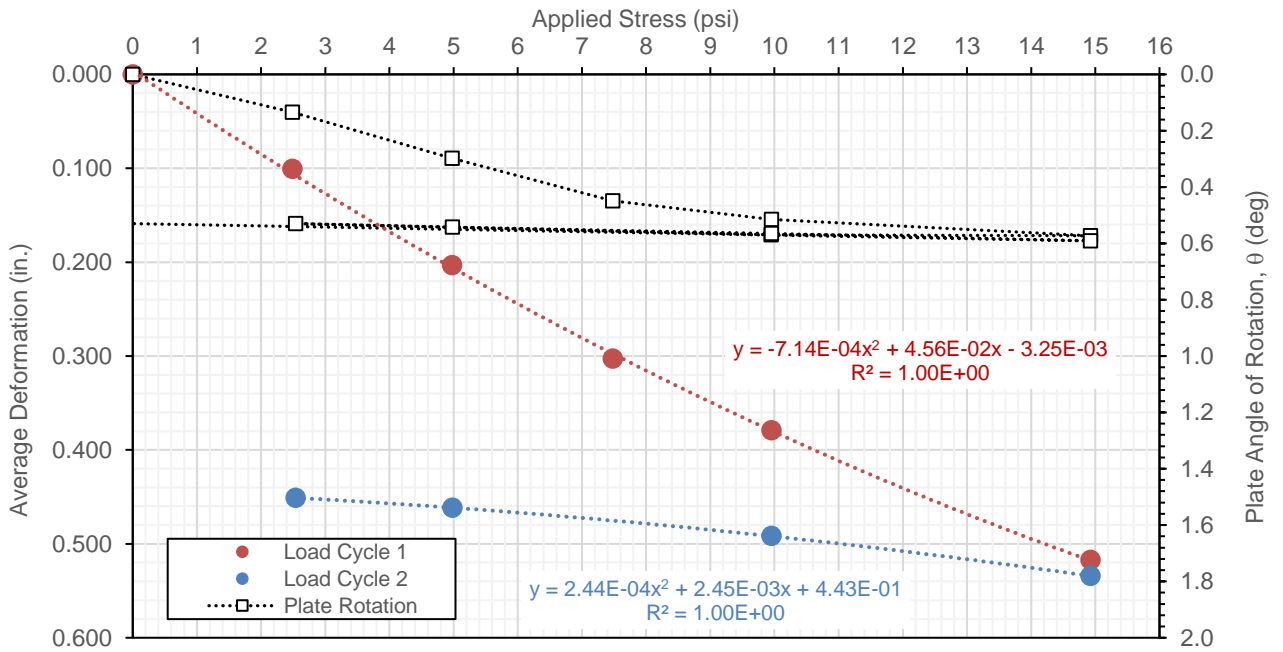
Second Cycle

a ₁	2.44E-04
a ₂	2.45E-03
R ²	1.00

θ_{max} (deg) **0.5911**

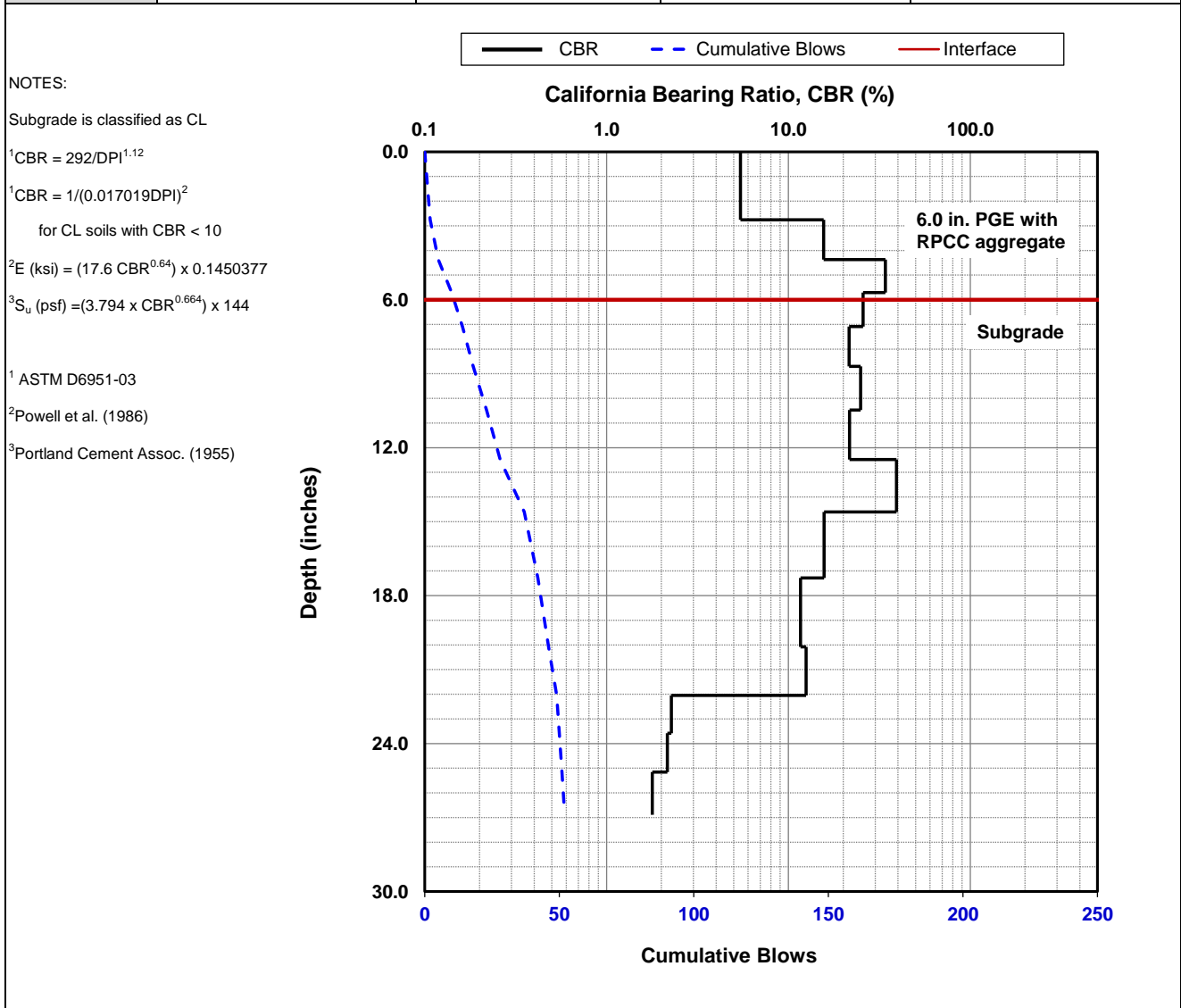
NOTES:

1. Test performed per AASHTO T222/ASTM D1196.
2. k-value determined using:
 - (a) calculated stress at 0.05 in. plate deformation (d) for first loading cycle, per PCA design guidelines, and
 - (b) for a defined target stress and calculating corresponding plate deformations using polynomial fit parameters.



Date of Test	10/13/2016	Test ID	Pt. 26	Operator	DW/PV	ASTM	D6951
Latitude	41.98382	Longitude	-87.97592	Elevation (ft)	NA		
Location	Section 4642 (PGE)	Station	NA				
Comments	Nominal 6 in. of compacted PGE with RPCC crushed aggregate. <i>Subgrade assumed as CL clay.</i>						

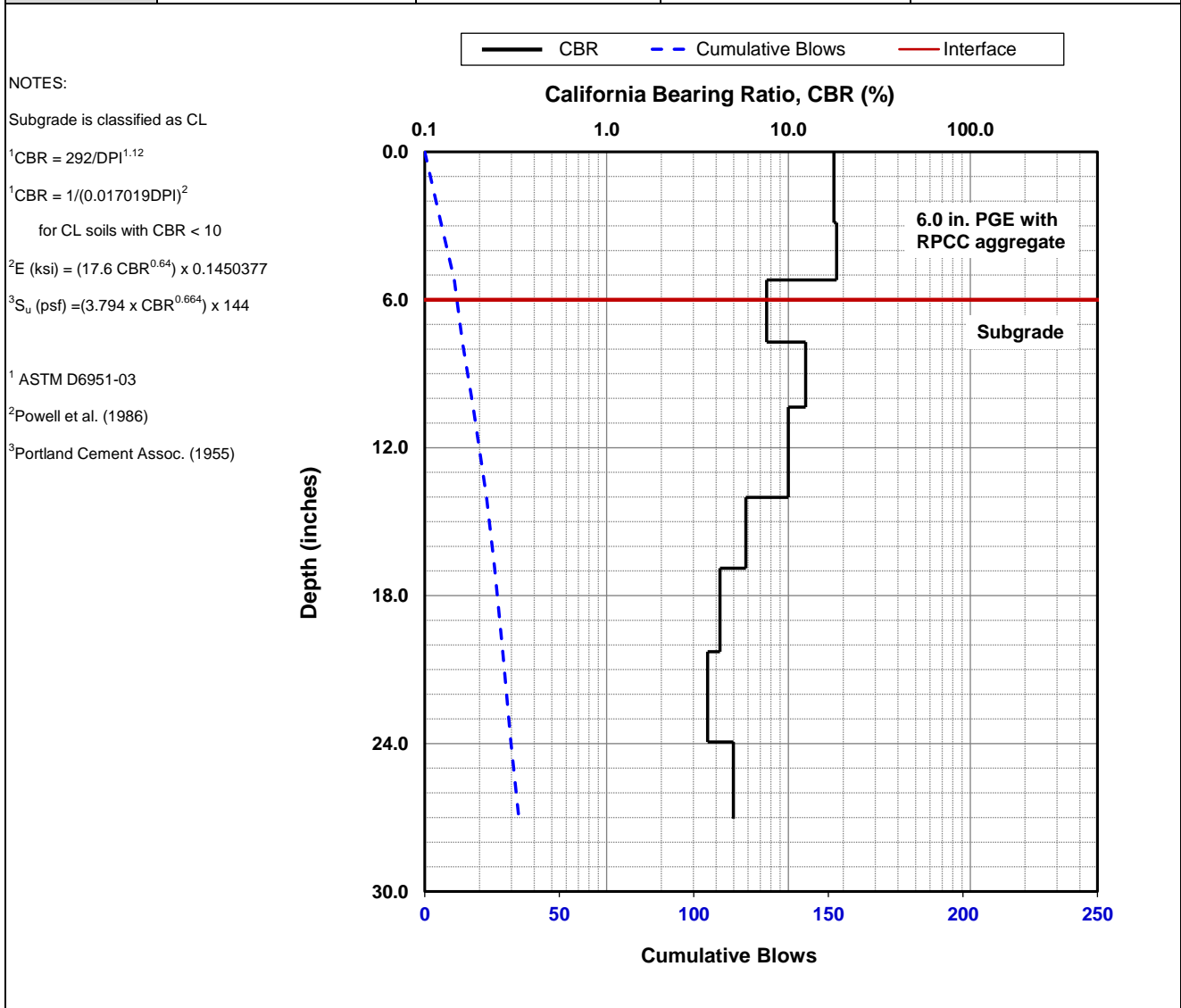
Parameter	DPI (mm/blow)	CBR (%)	E _{CBR} , Elastic Modulus (ksi) (non stress-dependent)	S _{u-CBR} , Bearing Capacity (psf)
Avg. PGE Layer [0 to 6.0 in.]	14.5	14.6	14.2	3,242
Avg. Subgrade Layer [6.0 to 18.0 in.]	9.2	24.4	19.7	4,552
Ratio of Avg. Top/Bottom Layer	1.6	0.6	0.7	0.7
Std. Dev. PGE Layer [0 to 6.0 in.]	14.6	13.5	13.5	3,079
Std. Dev. Subgrade Layer [6.0 to 18.0 in.]	2.5	7.9	9.6	2,157



Dynamic Cone Penetrometer (DCP) Test Results		
Project Name:	Illinois Tollway - IC Research	
Project ID:	Elgin O'Hare Extension - IL Tollway	
Location:	IL390 (West of O'Hare)	

Date of Test	10/13/2016	Test ID	Pt. 27	Operator	DW/PV	ASTM	D6951
Latitude	41.98369	Longitude	-87.97578	Elevation (ft)	NA		
Location	Section 4642 (PGE)	Station	NA				
Comments	Nominal 6 in. of compacted PGE with RPCC crushed aggregate. <i>Subgrade assumed as CL clay.</i>						

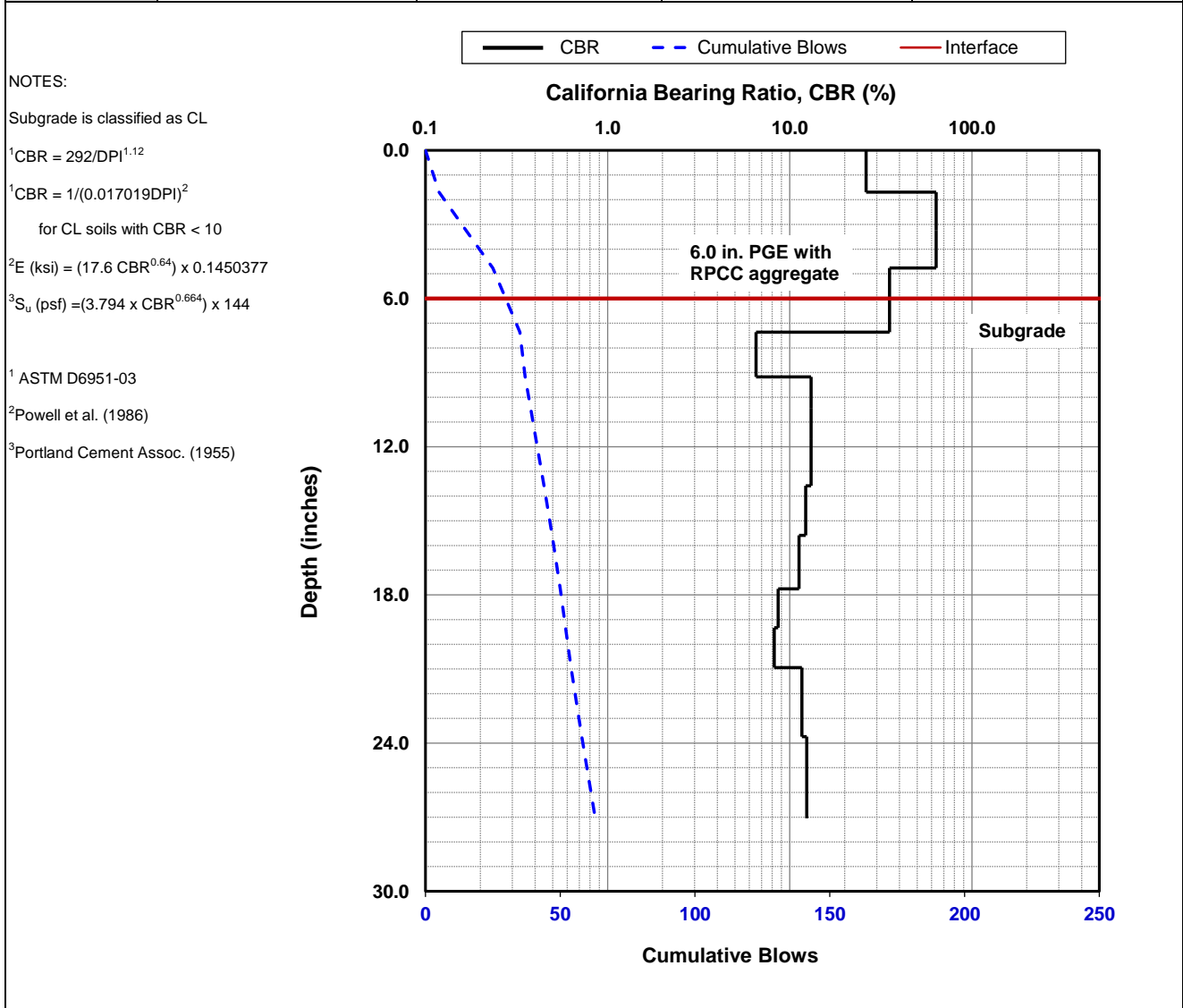
Parameter	DPI (mm/blow)	CBR (%)	E _{CBR} , Elastic Modulus (ksi) (non stress-dependent)	S _{u-CBR} , Bearing Capacity (psf)
Avg. PGE Layer [0 to 6.0 in.]	12.0	18.1	16.3	3,732
Avg. Subgrade Layer [6.0 to 18.0 in.]	19.8	8.8	10.3	2,316
Ratio of Avg. Top/Bottom Layer	0.6	2.1	1.6	1.6
Std. Dev. PGE Layer [0 to 6.0 in.]	0.2	0.4	1.3	276
Std. Dev. Subgrade Layer [6.0 to 18.0 in.]	3.3	2.9	5.0	1,101



Dynamic Cone Penetrometer (DCP) Test Results		
Project Name:	Illinois Tollway - IC Research	
Project ID:	Elgin O'Hare Extension - IL Tollway	
Location:	IL390 (West of O'Hare)	

Date of Test	10/13/2016	Test ID	Pt. 28	Operator	DW/PV	ASTM	D6951
Latitude	41.98373	Longitude		-87.97569	Elevation (ft)	NA	
Location	Section 4642 (PGE)	Station		NA			
Comments	Nominal 6 in. of compacted PGE with RPCC crushed aggregate. <i>Subgrade assumed as CL clay.</i>						

Parameter	DPI (mm/blow)	CBR (%)	E _{CBR} , Elastic Modulus (ksi) (non stress-dependent)	S _{u-CBR} , Bearing Capacity (psf)
Avg. PGE Layer [0 to 6.0 in.]	5.3	44.7	29.1	6,812
Avg. Subgrade Layer [6.0 to 18.0 in.]	17.6	11.8	12.4	2,807
Ratio of Avg. Top/Bottom Layer	0.3	3.8	2.4	2.4
Std. Dev. PGE Layer [0 to 6.0 in.]	2.4	19.2	16.9	3,883
Std. Dev. Subgrade Layer [6.0 to 18.0 in.]	2.7	2.6	4.7	1,021



Dynamic Cone Penetrometer (DCP) Test Results	
Project Name:	Illinois Tollway - IC Research
Project ID:	Elgin O'Hare Extension - IL Tollway
Location:	IL390 (West of O'Hare)



Date of Test	10/13/2016	Test ID	Pt. 29	Operator	DW/PV	ASTM	D6951
Latitude	41.98370	Longitude	-87.97566	Elevation (ft)	NA		
Location	Section 4642 (PGE)	Station	NA				
Comments	Nominal 6 in. of compacted PGE with RPCC crushed aggregate. <i>Subgrade assumed as CL clay.</i>						

Parameter	DPI (mm/blow)	CBR (%)	E _{CBR} , Elastic Modulus (ksi) (non stress-dependent)	S _{u-CBR} , Bearing Capacity (psf)
Avg. PGE Layer [0 to 6.0 in.]	9.4	23.8	19.4	4,484
Avg. Subgrade Layer [6.0 to 18.0 in.]	20.9	7.9	9.6	2,162
Ratio of Avg. Top/Bottom Layer	0.4	3.0	2.0	2.1
Std. Dev. PGE Layer [0 to 6.0 in.]	1.2	3.2	5.4	1,194
Std. Dev. Subgrade Layer [6.0 to 18.0 in.]	6.1	3.8	6.0	1,316

NOTES:

Subgrade is classified as CL

¹CBR = 292/DPI^{1.12}

¹CBR = 1/(0.017019DPI)²
for CL soils with CBR < 10

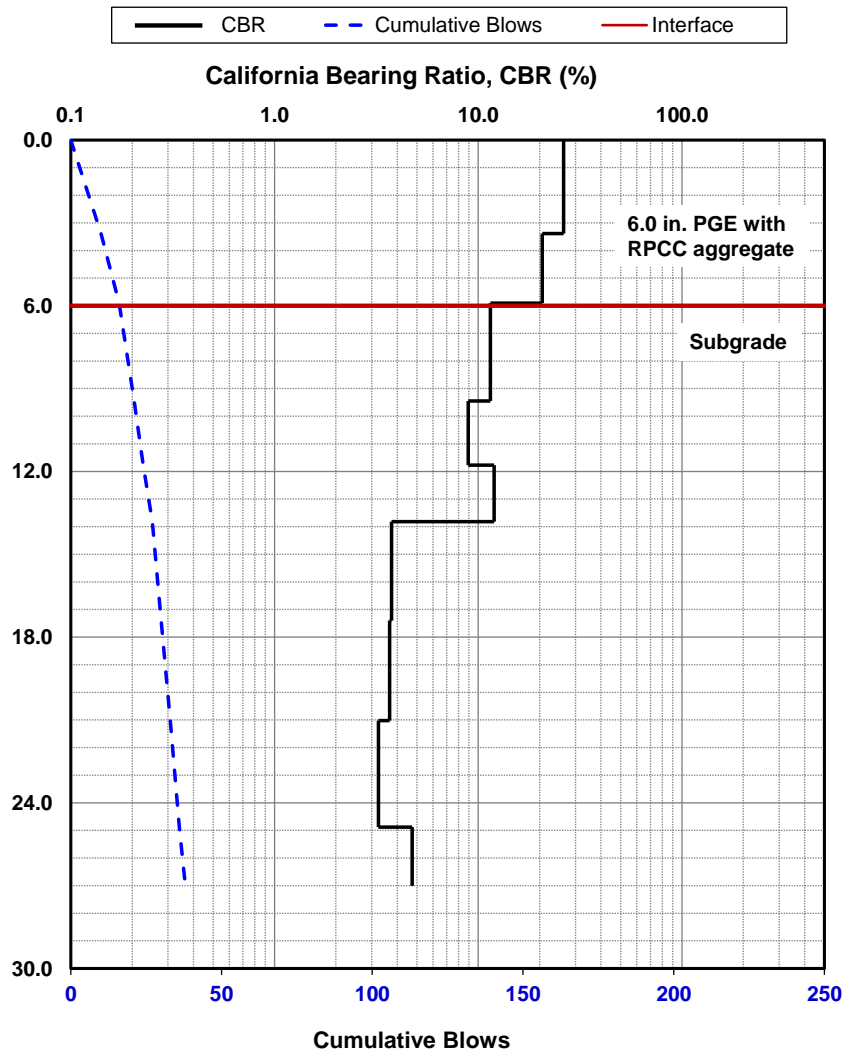
²E (ksi) = (17.6 CBR^{0.64}) x 0.1450377

³S_u (psf) = (3.794 x CBR^{0.664}) x 144

¹ ASTM D6951-03

² Powell et al. (1986)

³ Portland Cement Assoc. (1955)



Dynamic Cone Penetrometer (DCP) Test Results	
Project Name:	Illinois Tollway - IC Research
Project ID:	Elgin O'Hare Extension - IL Tollway
Location:	IL390 (West of O'Hare)



Date of Test	10/13/2016	Test ID	Pt. 30	Operator	DW/PV	ASTM	D6951
Latitude	41.98380	Longitude	-87.97553	Elevation (ft)	NA		
Location	Section 4642 (PGE)	Station	NA				
Comments	Nominal 6 in. of compacted PGE with RPCC crushed aggregate. <i>Subgrade assumed as CL clay.</i>						

Parameter	DPI (mm/blow)	CBR (%)	E _{CBR} , Elastic Modulus (ksi) (non stress-dependent)	S _{u-CBR} , Bearing Capacity (psf)
Avg. PGE Layer [0 to 6.0 in.]	13.7	15.6	14.8	3,382
Avg. Subgrade Layer [6.0 to 18.0 in.]	34.7	2.9	5.0	1,101
Ratio of Avg. Top/Bottom Layer	0.4	5.4	2.9	3.1
Std. Dev. PGE Layer [0 to 6.0 in.]	1.5	1.9	3.9	845
Std. Dev. Subgrade Layer [6.0 to 18.0 in.]	3.5	0.5	1.7	350

NOTES:

Subgrade is classified as CL

¹CBR = 292/DPI^{1.12}

¹CBR = 1/(0.017019DPI)²
for CL soils with CBR < 10

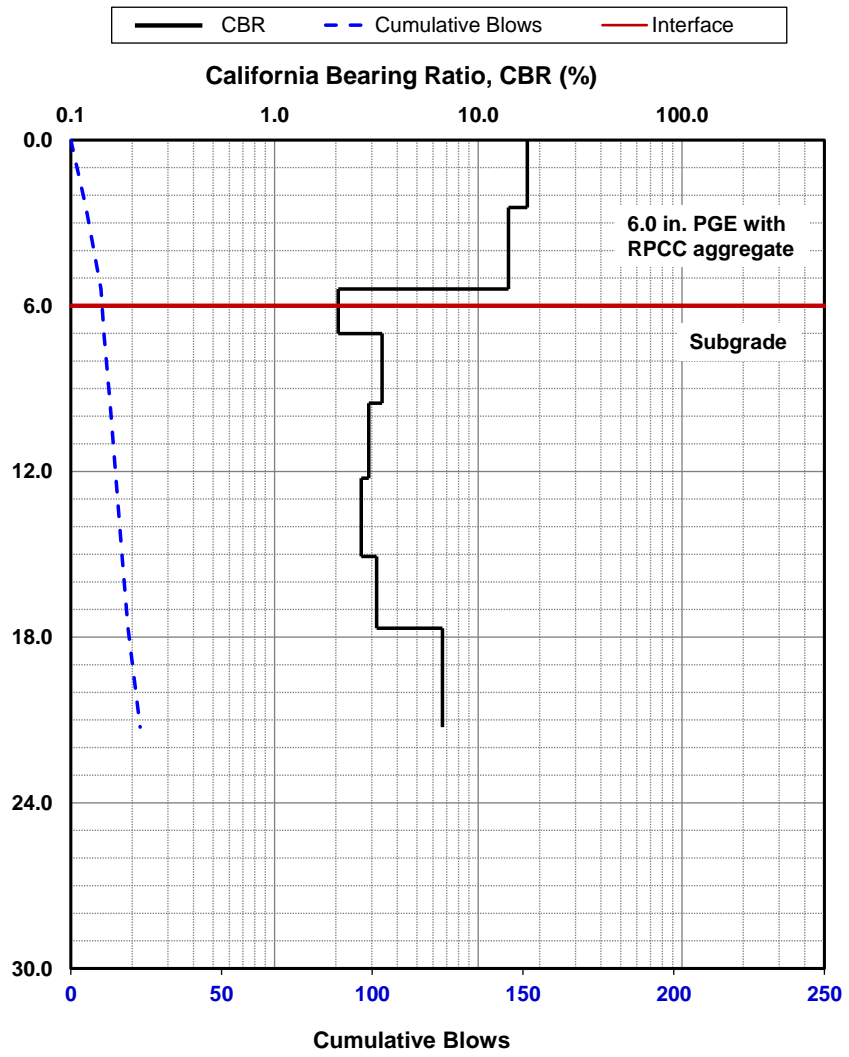
²E (ksi) = (17.6 CBR^{0.64}) x 0.1450377

³S_u (psf) = (3.794 x CBR^{0.664}) x 144

¹ ASTM D6951-03

² Powell et al. (1986)

³ Portland Cement Assoc. (1955)

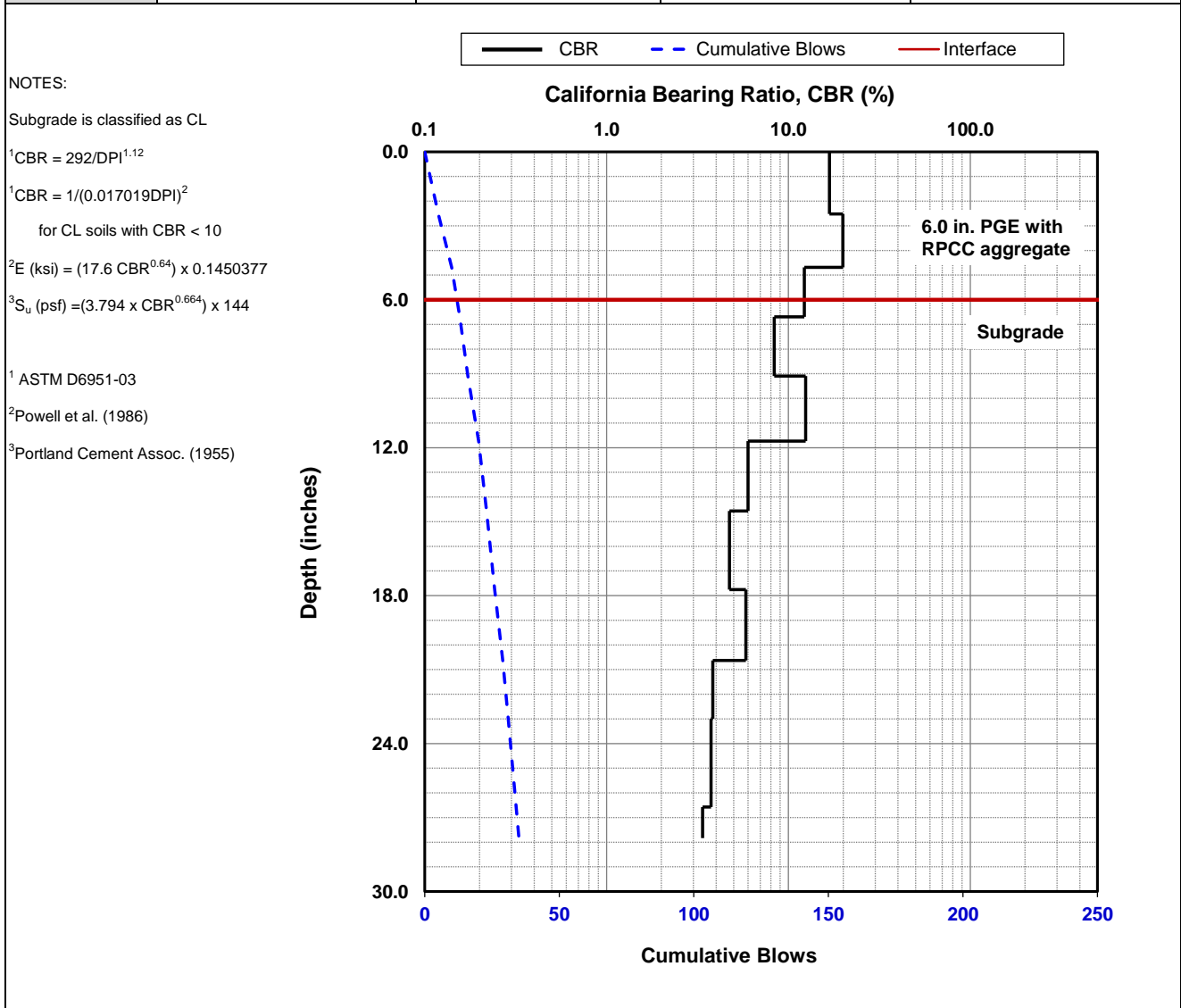


Dynamic Cone Penetrometer (DCP) Test Results	
Project Name:	Illinois Tollway - IC Research
Project ID:	Elgin O'Hare Extension - IL Tollway
Location:	IL390 (West of O'Hare)



Date of Test	10/13/2016	Test ID	Pt. 31	Operator	DW/PV	ASTM	D6951
Latitude	41.98378	Longitude	-87.97534	Elevation (ft)	NA		
Location	Section 4642 (PGE)	Station	NA				
Comments	Nominal 6 in. of compacted PGE with RPCC crushed aggregate. <i>Subgrade assumed as CL clay.</i>						

Parameter	DPI (mm/blow)	CBR (%)	E _{CBR} , Elastic Modulus (ksi) (non stress-dependent)	S _{u-CBR} , Bearing Capacity (psf)
Avg. PGE Layer [0 to 6.0 in.]	13.1	16.4	15.3	3,501
Avg. Subgrade Layer [6.0 to 18.0 in.]	21.6	7.4	9.2	2,062
Ratio of Avg. Top/Bottom Layer	0.6	2.2	1.7	1.7
Std. Dev. PGE Layer [0 to 6.0 in.]	2.5	3.2	5.3	1,174
Std. Dev. Subgrade Layer [6.0 to 18.0 in.]	4.4	3.4	5.6	1,228

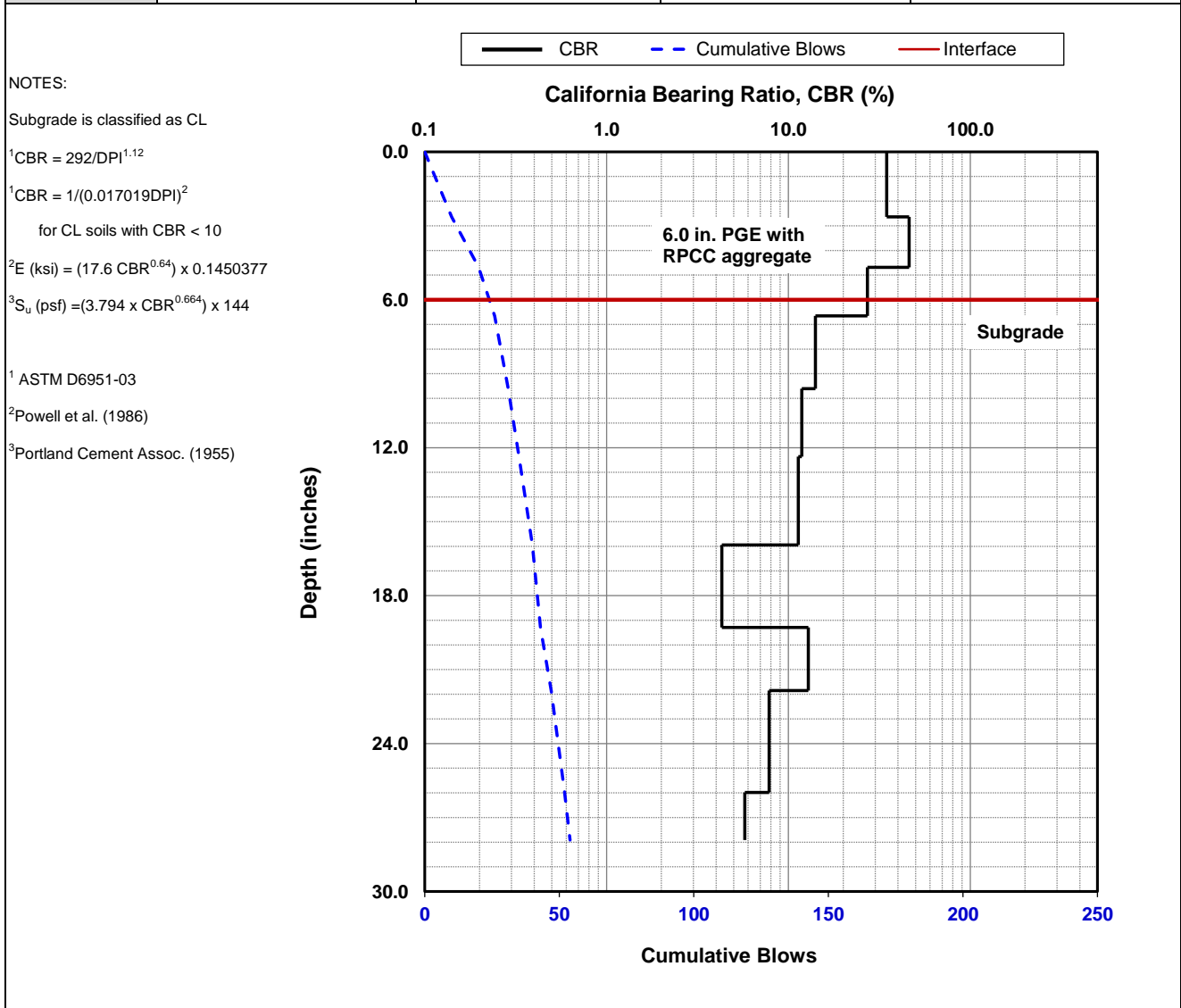


Dynamic Cone Penetrometer (DCP) Test Results	
Project Name:	Illinois Tollway - IC Research
Project ID:	Elgin O'Hare Extension - IL Tollway
Location:	IL390 (West of O'Hare)



Date of Test	10/13/2016	Test ID	Pt. 32	Operator	DW/PV	ASTM	D6951
Latitude	41.98374	Longitude	-87.97528	Elevation (ft)	NA		
Location	Section 4642 (PGE)	Station	NA				
Comments	Nominal 6 in. of compacted PGE with RPCC crushed aggregate. <i>Subgrade assumed as CL clay.</i>						

Parameter	DPI (mm/blow)	CBR (%)	E _{CBR} , Elastic Modulus (ksi) (non stress-dependent)	S _{u-CBR} , Bearing Capacity (psf)
Avg. PGE Layer [0 to 6.0 in.]	6.5	35.9	25.2	5,887
Avg. Subgrade Layer [6.0 to 18.0 in.]	18.9	9.7	10.9	2,467
Ratio of Avg. Top/Bottom Layer	0.3	3.7	2.3	2.4
Std. Dev. PGE Layer [0 to 6.0 in.]	1.3	7.8	9.5	2,137
Std. Dev. Subgrade Layer [6.0 to 18.0 in.]	5.9	4.2	6.4	1,422

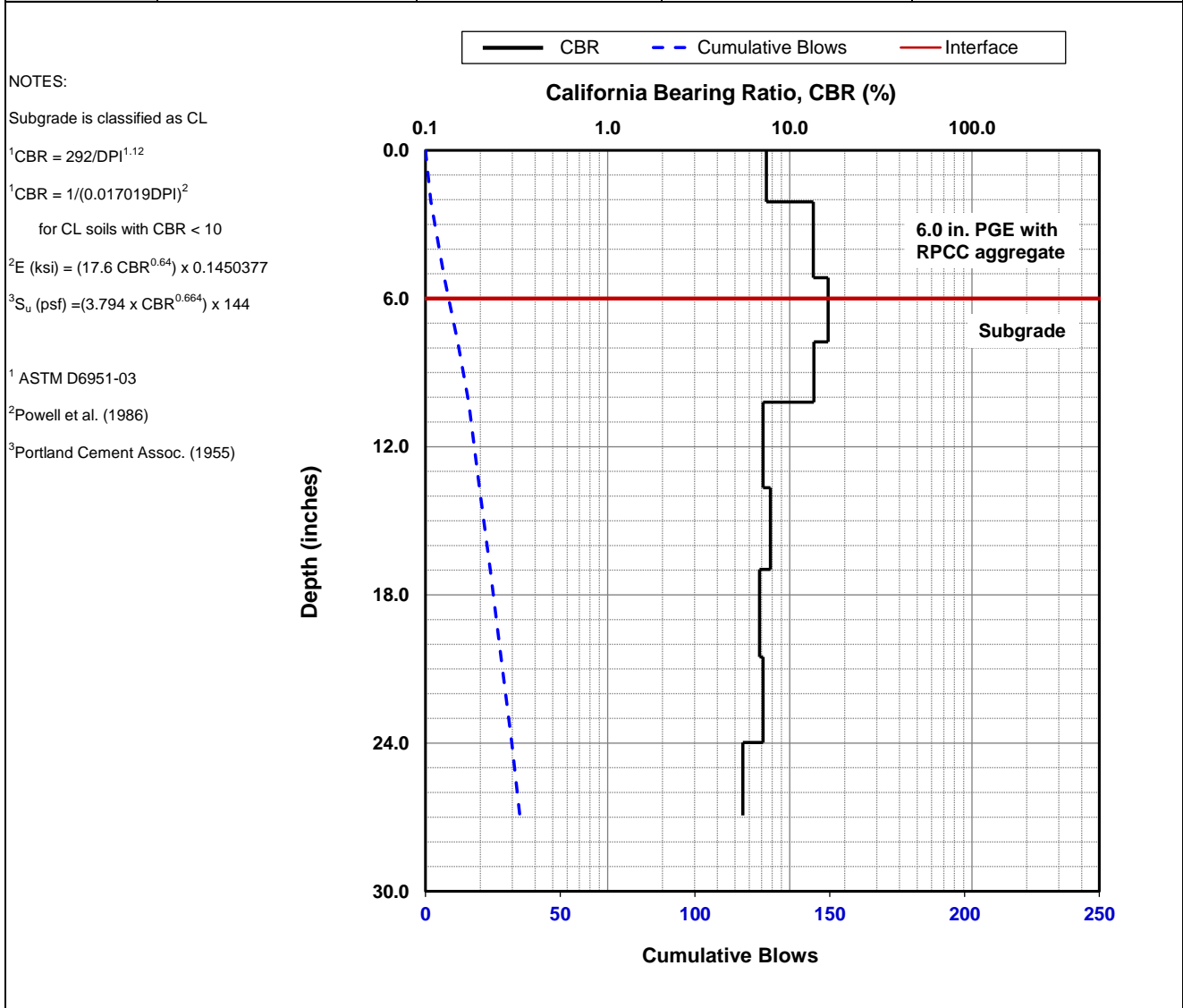


Dynamic Cone Penetrometer (DCP) Test Results	
Project Name:	Illinois Tollway - IC Research
Project ID:	Elgin O'Hare Extension - IL Tollway
Location:	IL390 (West of O'Hare)



Date of Test	10/13/2016	Test ID	Pt. 33	Operator	DW/PV	ASTM	D6951
Latitude	41.98365	Longitude	-87.97505	Elevation (ft)	NA		
Location	Section 4642 (PGE)	Station	NA				
Comments	Nominal 6 in. of compacted PGE with RPCC crushed aggregate. <i>Subgrade assumed as CL clay.</i>						

Parameter	DPI (mm/blow)	CBR (%)	E _{CBR} , Elastic Modulus (ksi) (non stress-dependent)	S _{u-CBR} , Bearing Capacity (psf)
Avg. PGE Layer [0 to 6.0 in.]	18.7	11.0	11.8	2,682
Avg. Subgrade Layer [6.0 to 18.0 in.]	17.6	11.7	12.3	2,801
Ratio of Avg. Top/Bottom Layer	1.1	0.9	1.0	1.0
Std. Dev. PGE Layer [0 to 6.0 in.]	6.3	3.5	5.7	1,250
Std. Dev. Subgrade Layer [6.0 to 18.0 in.]	4.3	4.4	6.6	1,467

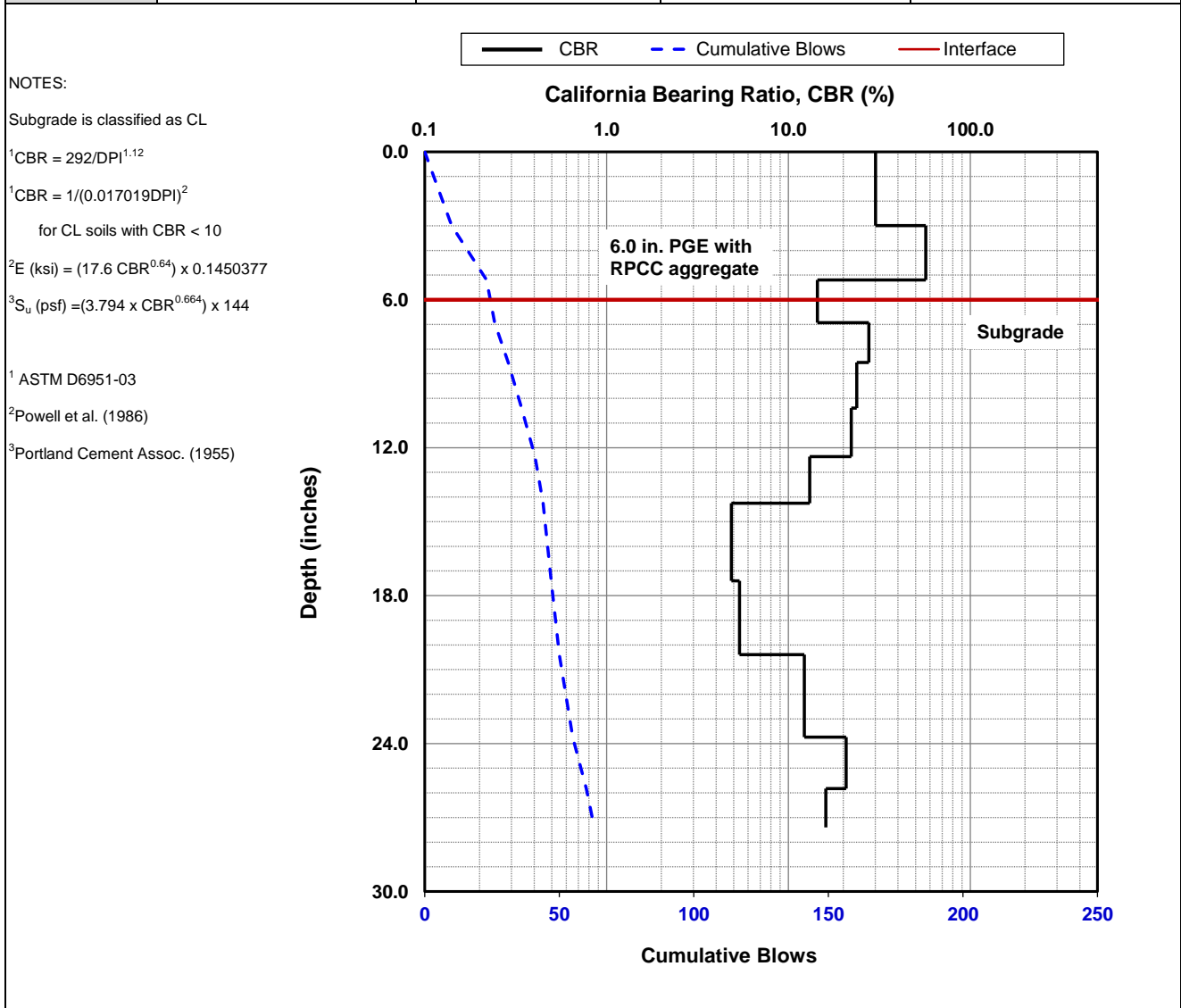


Dynamic Cone Penetrometer (DCP) Test Results	
Project Name:	Illinois Tollway - IC Research
Project ID:	Elgin O'Hare Extension - IL Tollway
Location:	IL390 (West of O'Hare)



Date of Test	10/13/2016	Test ID	Pt. 34	Operator	DW/PV	ASTM	D6951
Latitude	41.98370	Longitude	-87.97479	Elevation (ft)	NA		
Location	Section 4642 (PGE)	Station	NA				
Comments	Nominal 6 in. of compacted PGE with RPCC crushed aggregate. <i>Subgrade assumed as CL clay.</i>						

Parameter	DPI (mm/blow)	CBR (%)	E _{CBR} , Elastic Modulus (ksi) (non stress-dependent)	S _{u-CBR} , Bearing Capacity (psf)
Avg. PGE Layer [0 to 6.0 in.]	5.7	41.3	27.6	6,459
Avg. Subgrade Layer [6.0 to 18.0 in.]	12.9	16.6	15.4	3,533
Ratio of Avg. Top/Bottom Layer	0.4	2.5	1.8	1.8
Std. Dev. PGE Layer [0 to 6.0 in.]	1.9	15.5	14.7	3,365
Std. Dev. Subgrade Layer [6.0 to 18.0 in.]	6.9	8.4	10.0	2,244



Dynamic Cone Penetrometer (DCP) Test Results	
Project Name:	Illinois Tollway - IC Research
Project ID:	Elgin O'Hare Extension - IL Tollway
Location:	IL390 (West of O'Hare)



Date of Test	10/13/2016	Test ID	Pt. 35	Operator	DW/PV	ASTM	D6951
Latitude	41.98375	Longitude	-87.97478	Elevation (ft)	NA		
Location	Section 4642 (PGE)	Station	NA				
Comments	Nominal 6 in. of compacted PGE with RPCC crushed aggregate. <i>Subgrade assumed as CL clay.</i>						

Parameter	DPI (mm/blow)	CBR (%)	E _{CBR} , Elastic Modulus (ksi) (non stress-dependent)	S _{u-CBR} , Bearing Capacity (psf)
Avg. PGE Layer [0 to 6.0 in.]	7.1	32.4	23.6	5,502
Avg. Subgrade Layer [6.0 to 18.0 in.]	9.0	24.8	19.9	4,610
Ratio of Avg. Top/Bottom Layer	0.8	1.3	1.2	1.2
Std. Dev. PGE Layer [0 to 6.0 in.]	5.3	17.6	16.0	3,664
Std. Dev. Subgrade Layer [6.0 to 18.0 in.]	2.8	8.9	10.3	2,328

NOTES:

Subgrade is classified as CL

¹CBR = 292/DPI^{1.12}

¹CBR = 1/(0.017019DPI)²

for CL soils with CBR < 10

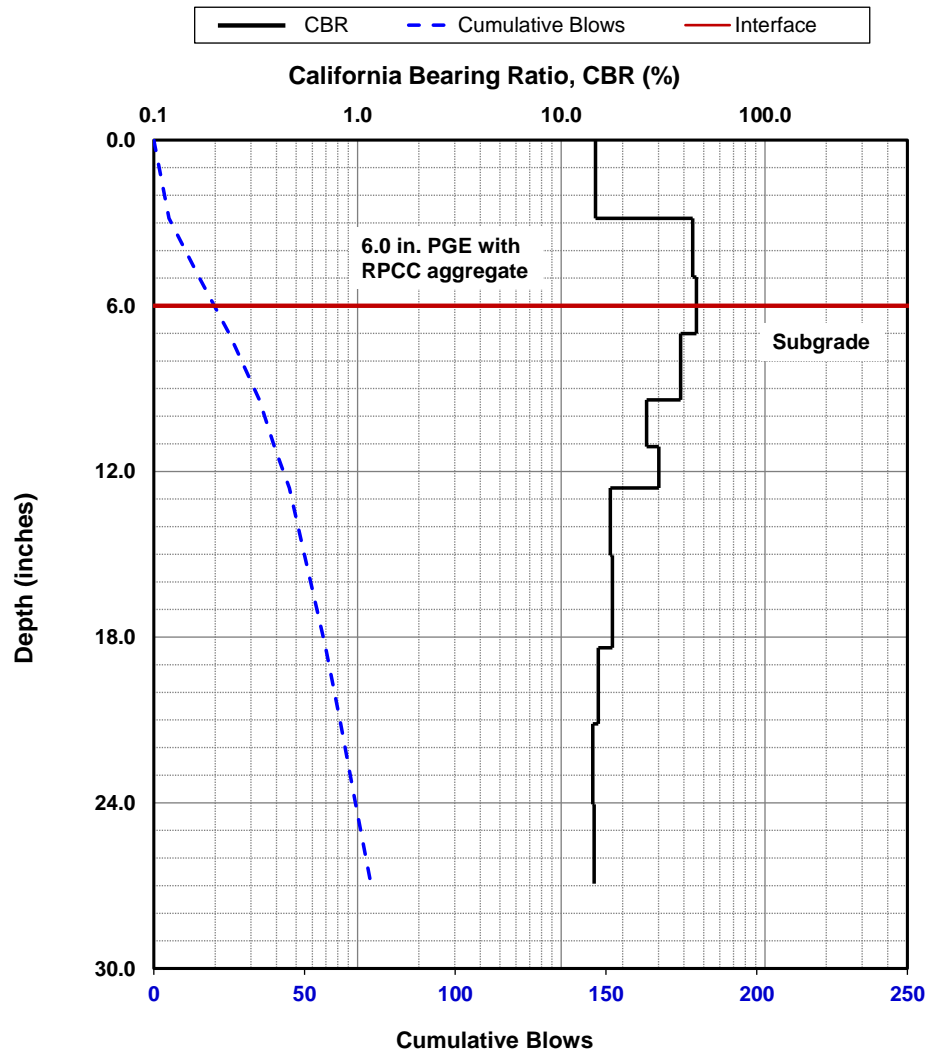
²E (ksi) = (17.6 CBR^{0.64}) x 0.1450377

³S_u (psf) = (3.794 x CBR^{0.664}) x 144

¹ ASTM D6951-03

² Powell et al. (1986)

³ Portland Cement Assoc. (1955)



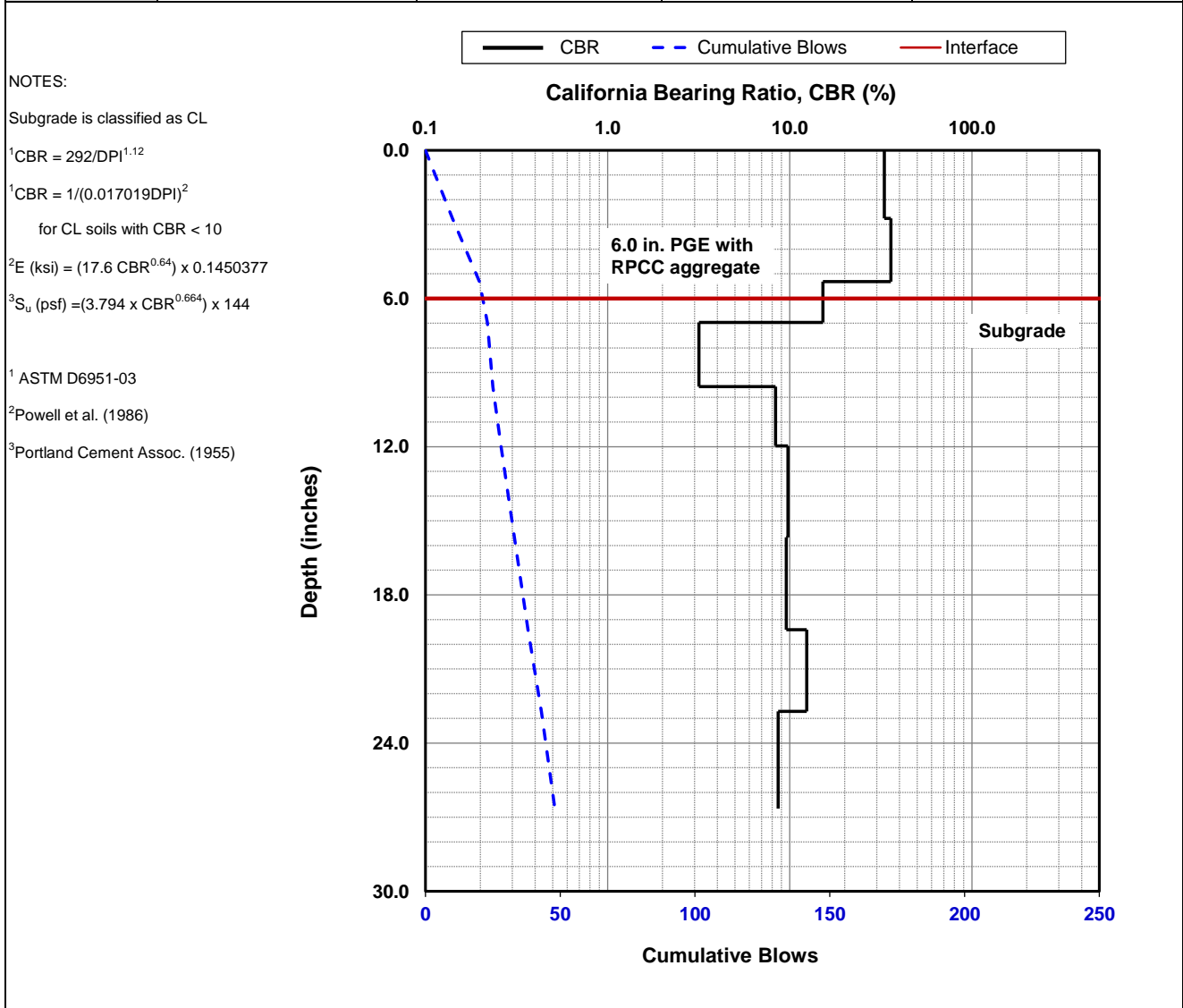
Dynamic Cone Penetrometer (DCP) Test Results

Project Name: Illinois Tollway - IC Research
 Project ID: Elgin O'Hare Extension - IL Tollway
 Location: IL390 (West of O'Hare)



Date of Test	10/13/2016	Test ID	Pt. 36	Operator	DW/PV	ASTM	D6951
Latitude	41.98370	Longitude	-87.97456	Elevation (ft)	NA		
Location	Section 4642 (PGE)	Station	NA				
Comments	Nominal 6 in. of compacted PGE with RPCC crushed aggregate. <i>Subgrade assumed as CL clay.</i>						

Parameter	DPI (mm/blow)	CBR (%)	E _{CBR} , Elastic Modulus (ksi) (non stress-dependent)	S _{u-CBR} , Bearing Capacity (psf)
Avg. PGE Layer [0 to 6.0 in.]	7.7	29.7	22.4	5,193
Avg. Subgrade Layer [6.0 to 18.0 in.]	21.1	7.8	9.5	2,133
Ratio of Avg. Top/Bottom Layer	0.4	3.8	2.4	2.4
Std. Dev. PGE Layer [0 to 6.0 in.]	3.6	9.5	10.8	2,434
Std. Dev. Subgrade Layer [6.0 to 18.0 in.]	6.8	3.1	5.3	1,156

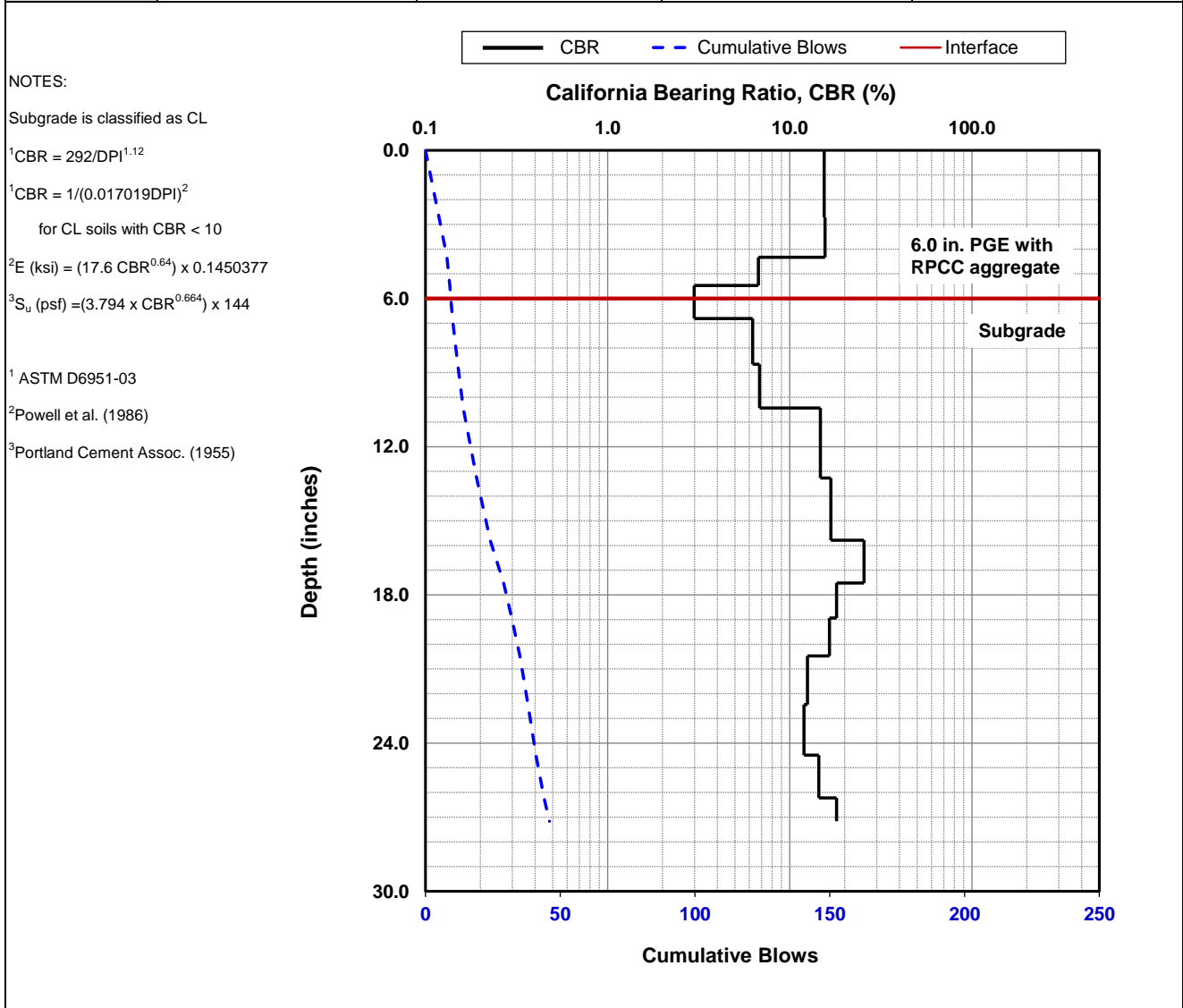


Dynamic Cone Penetrometer (DCP) Test Results	
Project Name:	Illinois Tollway - IC Research
Project ID:	Elgin O'Hare Extension - IL Tollway
Location:	IL390 (West of O'Hare)



Date of Test	10/13/2016	Test ID	Pt. 37	Operator	DW/PV	ASTM	D6951
Latitude	41.98366	Longitude	-87.97433	Elevation (ft)	NA		
Location	Section 4642 (PGE)	Station	NA				
Comments	Nominal 6 in. of compacted PGE with RPCC crushed aggregate. <i>Subgrade assumed as CL clay.</i>						

Parameter	DPI (mm/blow)	CBR (%)	E _{CBR} , Elastic Modulus (ksi) (non stress-dependent)	S _{u-CBR} , Bearing Capacity (psf)
Avg. PGE Layer [0 to 6.0 in.]	15.4	13.6	13.6	3,093
Avg. Subgrade Layer [6.0 to 18.0 in.]	15.3	13.8	13.7	3,115
Ratio of Avg. Top/Bottom Layer	1.0	1.0	1.0	1.0
Std. Dev. PGE Layer [0 to 6.0 in.]	7.6	4.4	6.6	1,459
Std. Dev. Subgrade Layer [6.0 to 18.0 in.]	9.2	8.4	10.0	2,250



Dynamic Cone Penetrometer (DCP) Test Results		
Project Name:	Illinois Tollway - IC Research	
Project ID:	Elgin O'Hare Extension - IL Tollway	
Location:	IL390 (West of O'Hare)	

Date of Test	10/13/2016	Test ID	Pt. 38	Operator	DW/PV	ASTM	D6951
Latitude	41.98371	Longitude	-87.97425	Elevation (ft)	NA		
Location	Section 4642 (PGE)	Station	NA				
Comments	Nominal 6 in. of compacted PGE with RPCC crushed aggregate. <i>Subgrade assumed as CL clay.</i>						

Parameter	DPI (mm/blow)	CBR (%)	E _{CBR} , Elastic Modulus (ksi) (non stress-dependent)	S _{u-CBR} , Bearing Capacity (psf)
Avg. PGE Layer [0 to 6.0 in.]	11.4	19.2	16.9	3,881
Avg. Subgrade Layer [6.0 to 18.0 in.]	12.7	17.0	15.6	3,579
Ratio of Avg. Top/Bottom Layer	0.9	1.1	1.1	1.1
Std. Dev. PGE Layer [0 to 6.0 in.]	2.0	3.7	5.9	1,293
Std. Dev. Subgrade Layer [6.0 to 18.0 in.]	1.3	1.7	3.6	781

NOTES:

Subgrade is classified as CL

¹CBR = 292/DPI^{1.12}

¹CBR = 1/(0.017019DPI)²
for CL soils with CBR < 10

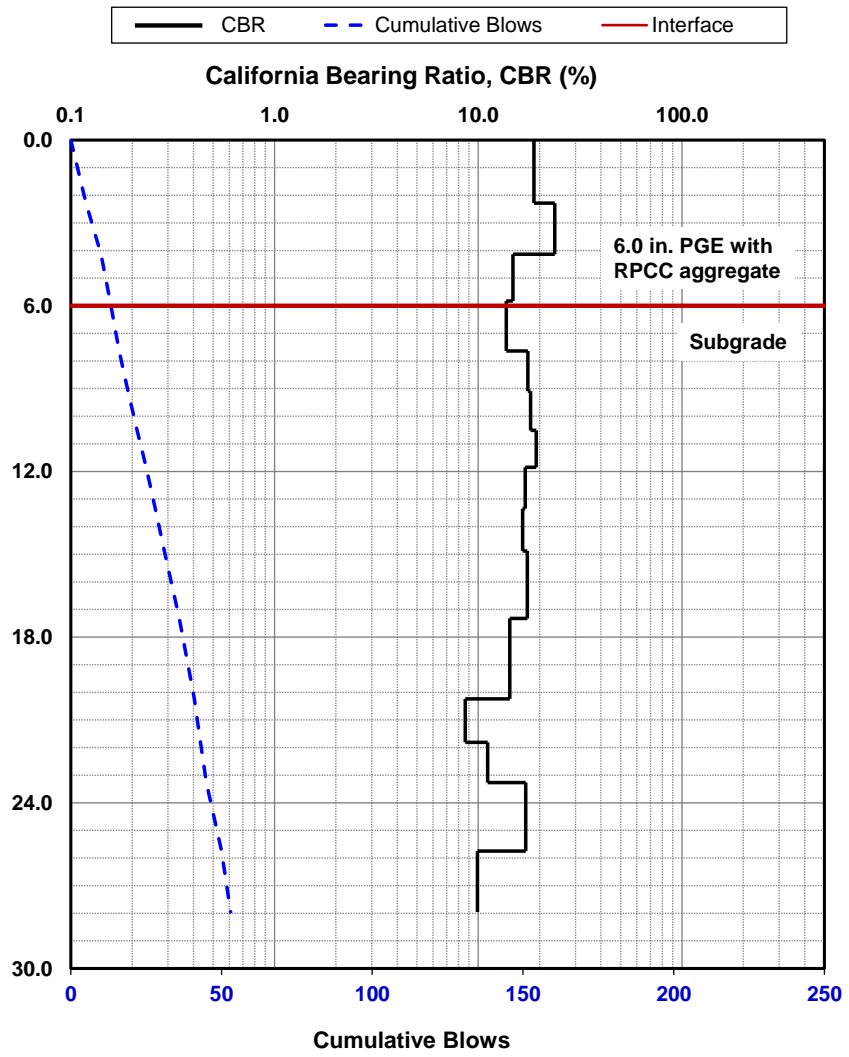
²E (ksi) = (17.6 CBR^{0.64}) x 0.1450377

³S_u (psf) = (3.794 x CBR^{0.664}) x 144

¹ ASTM D6951-03

² Powell et al. (1986)

³ Portland Cement Assoc. (1955)



Dynamic Cone Penetrometer (DCP) Test Results		
Project Name:	Illinois Tollway - IC Research	
Project ID:	Elgin O'Hare Extension - IL Tollway	
Location:	IL390 (West of O'Hare)	

Date of Test	10/13/2016	Test ID	Pt. 39	Operator	DW/PV	ASTM	D6951
Latitude	41.98367	Longitude	-87.97409	Elevation (ft)	NA		
Location	Section 4642 (PGE)	Station	NA				
Comments	Nominal 6 in. of compacted PGE with RPCC crushed aggregate. <i>Subgrade assumed as CL clay.</i>						

Parameter	DPI (mm/blow)	CBR (%)	E _{CBR} , Elastic Modulus (ksi) (non stress-dependent)	S _{u-CBR} , Bearing Capacity (psf)
Avg. PGE Layer [0 to 6.0 in.]	7.6	30.2	22.6	5,256
Avg. Subgrade Layer [6.0 to 18.0 in.]	14.3	14.8	14.3	3,275
Ratio of Avg. Top/Bottom Layer	0.5	2.0	1.6	1.6
Std. Dev. PGE Layer [0 to 6.0 in.]	1.7	9.9	11.1	2,512
Std. Dev. Subgrade Layer [6.0 to 18.0 in.]	3.1	3.3	5.5	1,204

NOTES:

Subgrade is classified as CL

¹CBR = 292/DPI^{1.12}

¹CBR = 1/((0.017019DPI)²)
for CL soils with CBR < 10

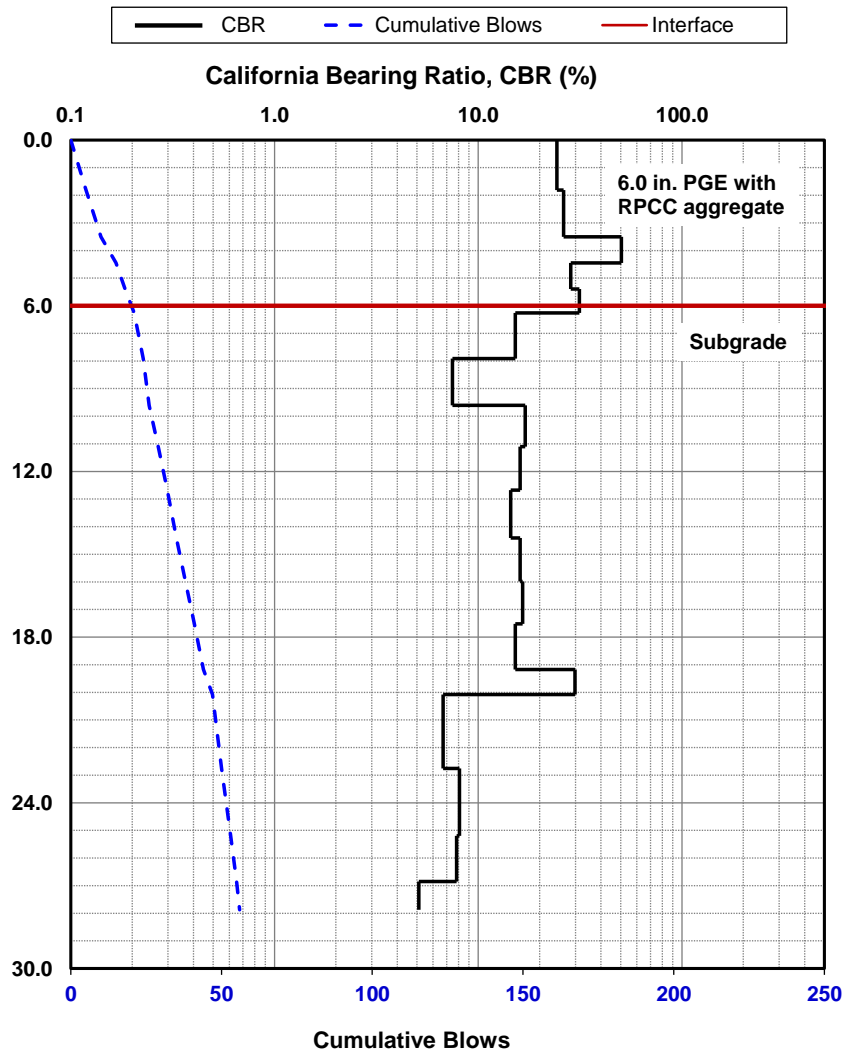
²E (ksi) = (17.6 CBR^{0.64}) x 0.1450377

³S_u (psf) = (3.794 x CBR^{0.664}) x 144

¹ ASTM D6951-03

² Powell et al. (1986)

³ Portland Cement Assoc. (1955)



Dynamic Cone Penetrometer (DCP) Test Results	
Project Name:	Illinois Tollway - IC Research
Project ID:	Elgin O'Hare Extension - IL Tollway
Location:	IL390 (West of O'Hare)



Date of Test	10/13/2016	Test ID	Pt. 40	Operator	DW/PV	ASTM	D6951
Latitude	41.98371	Longitude	-87.97591	Elevation (ft)	NA		
Location	Section 4642 (PGE)	Station	NA				
Comments	Nominal 6 in. of compacted PGE with RPCC crushed aggregate. <i>Subgrade assumed as CL clay.</i>						

Parameter	DPI (mm/blow)	CBR (%)	E _{CBR} , Elastic Modulus (ksi) (non stress-dependent)	S _{u-CBR} , Bearing Capacity (psf)
Avg. PGE Layer [0 to 6.0 in.]	5.8	40.8	27.4	6,408
Avg. Subgrade Layer [6.0 to 18.0 in.]	5.8	40.7	27.4	6,405
Ratio of Avg. Top/Bottom Layer	1.0	1.0	1.0	1.0
Std. Dev. PGE Layer [0 to 6.0 in.]	3.3	19.7	17.2	3,954
Std. Dev. Subgrade Layer [6.0 to 18.0 in.]	1.5	11.0	11.9	2,687

NOTES:

Subgrade is classified as CL

¹CBR = 292/DPI^{1.12}

¹CBR = 1/(0.017019DPI)²
for CL soils with CBR < 10

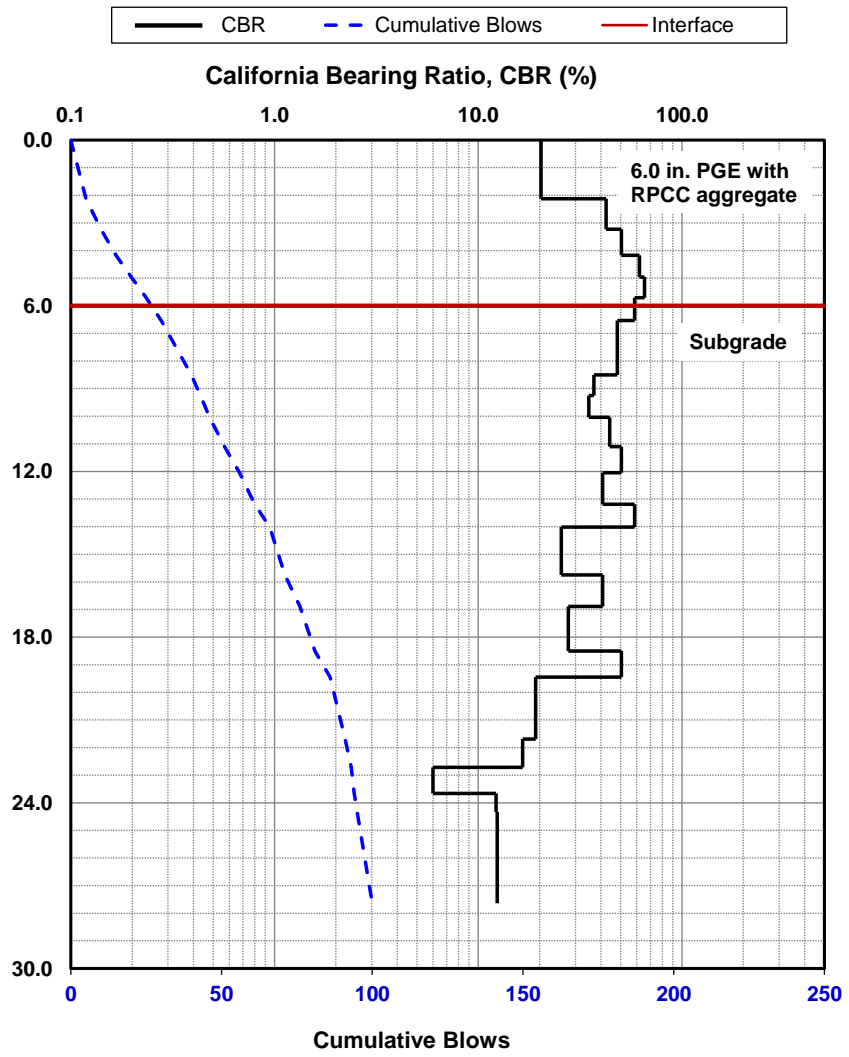
²E (ksi) = (17.6 CBR^{0.64}) x 0.1450377

³S_u (psf) = (3.794 x CBR^{0.664}) x 144

¹ ASTM D6951-03

² Powell et al. (1986)

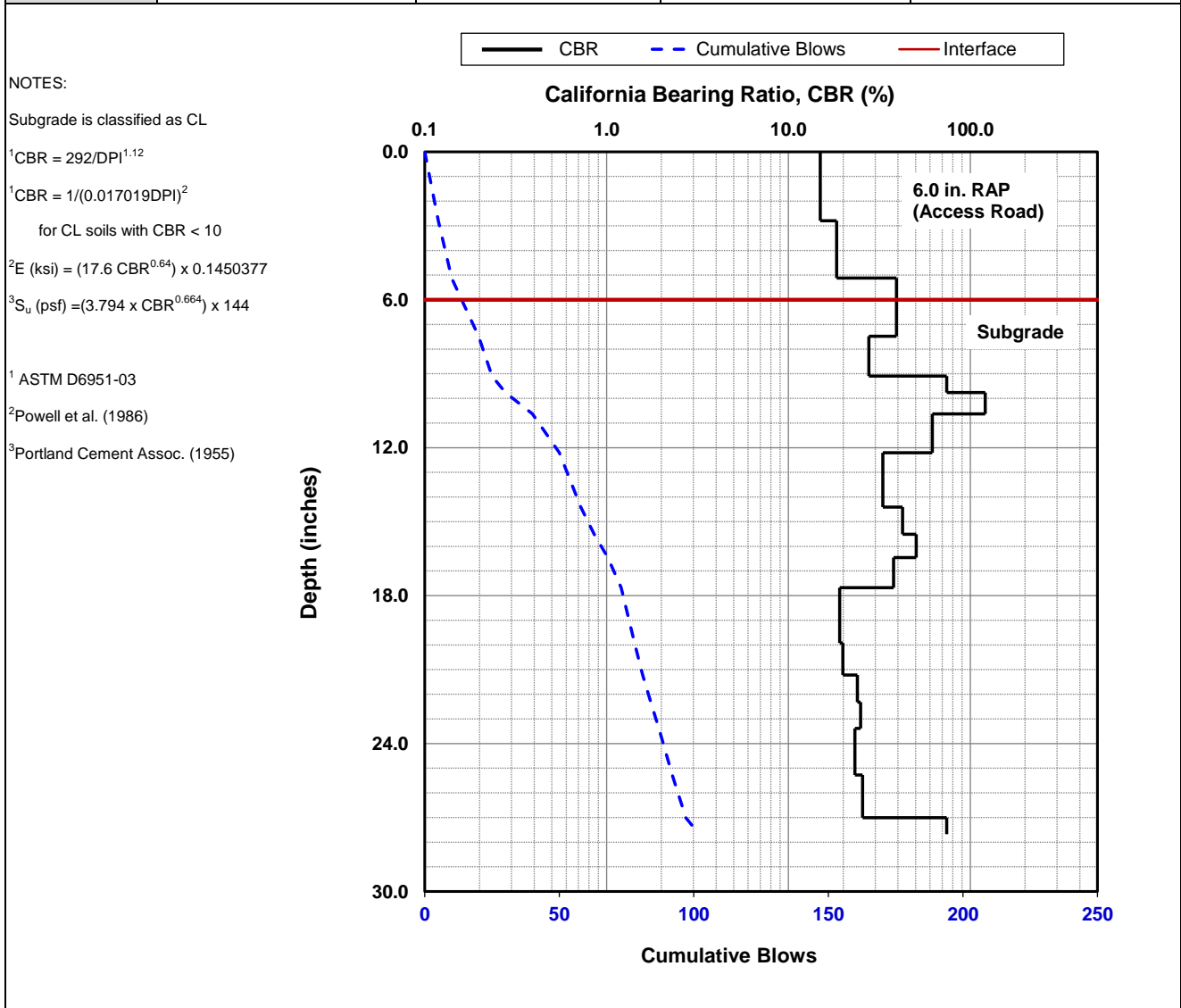
³ Portland Cement Assoc. (1955)



Dynamic Cone Penetrometer (DCP) Test Results		
Project Name:	Illinois Tollway - IC Research	
Project ID:	Elgin O'Hare Extension - IL Tollway	
Location:	IL390 (West of O'Hare)	

Date of Test	10/13/2016	Test ID	Pt. 41	Operator	DW/PV	ASTM	D6951
Latitude	41.98329	Longitude	-87.97246	Elevation (ft)	NA		
Location	Section 4642 (RAP Access Road)	Station	NA				
Comments	Access road with RAP material with nominal 6 in. in thickness. <i>Subgrade assumed as CL clay.</i>						

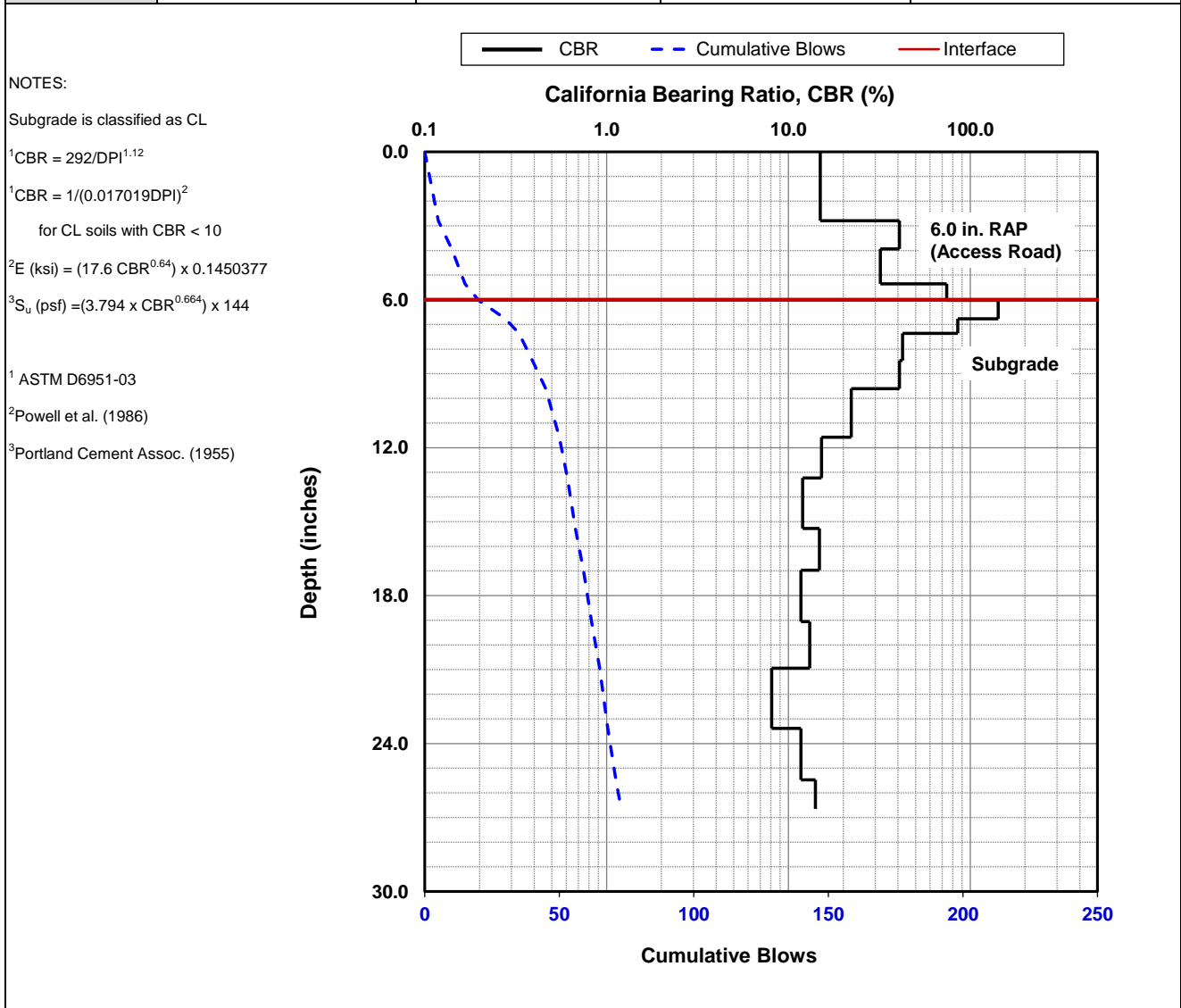
Parameter	DPI (mm/blow)	CBR (%)	E _{CBR} , Elastic Modulus (ksi) (non stress-dependent)	S _{u-CBR} , Bearing Capacity (psf)
Avg. PGE Layer [0 to 6.0 in.]	10.7	20.6	17.7	4,073
Avg. Subgrade Layer [6.0 to 18.0 in.]	5.0	48.3	30.5	7,174
Ratio of Avg. Top/Bottom Layer	2.1	0.4	0.6	0.6
Std. Dev. PGE Layer [0 to 6.0 in.]	3.9	11.7	12.3	2,795
Std. Dev. Subgrade Layer [6.0 to 18.0 in.]	1.9	28.9	22.0	5,099



Dynamic Cone Penetrometer (DCP) Test Results		
Project Name:	Illinois Tollway - IC Research	
Project ID:	Elgin O'Hare Extension - IL Tollway	
Location:	IL390 (West of O'Hare)	

Date of Test	10/13/2016	Test ID	Pt. 42	Operator	DW/PV	ASTM	D6951
Latitude	41.98334	Longitude	-87.97260	Elevation (ft)	NA		
Location	Section 4642 (RAP Access Road)	Station	NA				
Comments	Access road with RAP material with nominal 6 in. in thickness. <i>Subgrade assumed as CL clay.</i>						

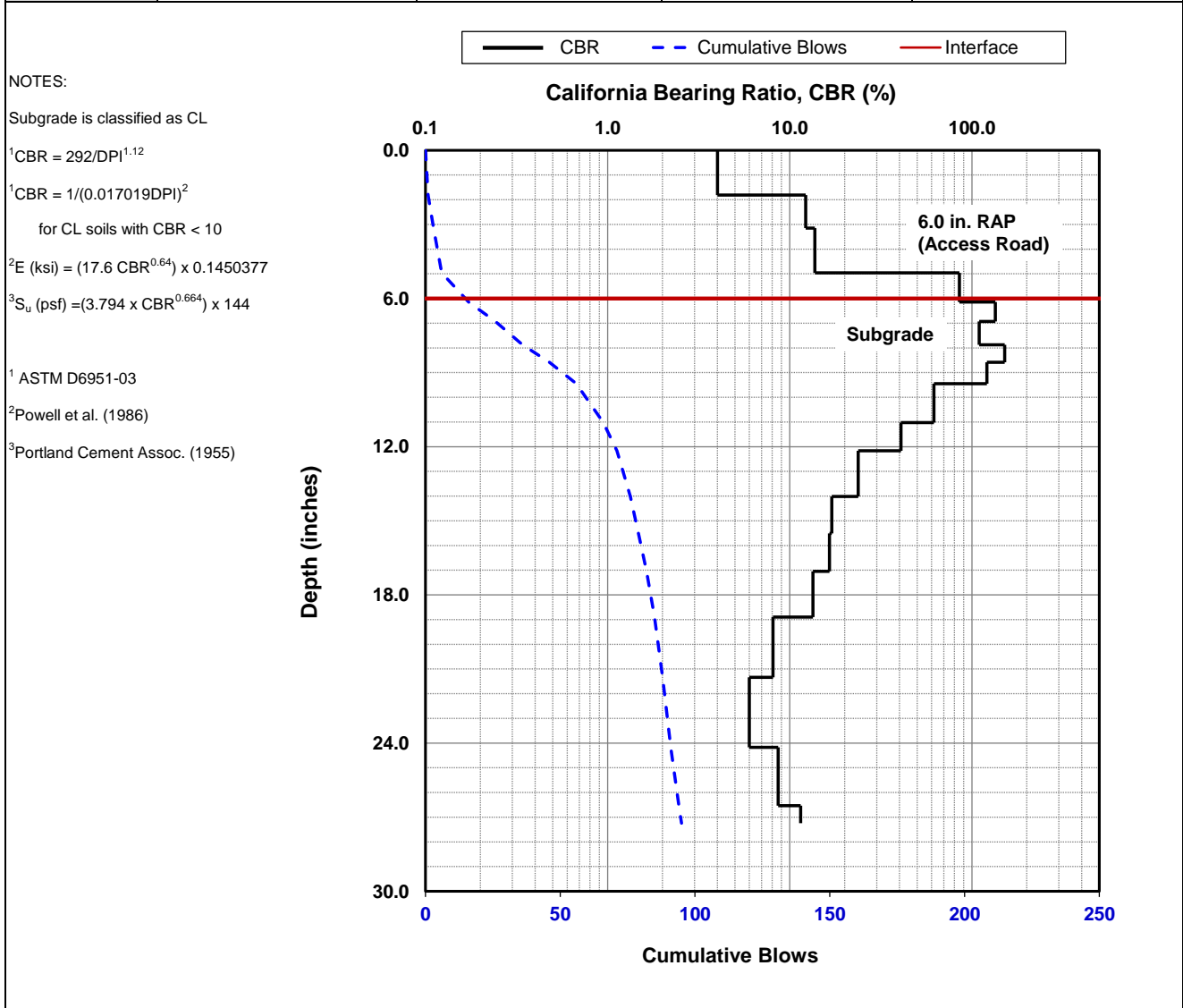
Parameter	DPI (mm/blow)	CBR (%)	E _{CBR} , Elastic Modulus (ksi) (non stress-dependent)	S _{u-CBR} , Bearing Capacity (psf)
Avg. PGE Layer [0 to 6.0 in.]	7.7	29.9	22.5	5,216
Avg. Subgrade Layer [6.0 to 18.0 in.]	7.1	32.4	23.6	5,497
Ratio of Avg. Top/Bottom Layer	1.1	0.9	1.0	0.9
Std. Dev. PGE Layer [0 to 6.0 in.]	5.0	24.4	19.7	4,555
Std. Dev. Subgrade Layer [6.0 to 18.0 in.]	5.8	45.5	29.4	6,894



Dynamic Cone Penetrometer (DCP) Test Results		
Project Name:	Illinois Tollway - IC Research	
Project ID:	Elgin O'Hare Extension - IL Tollway	
Location:	IL390 (West of O'Hare)	

Date of Test	10/13/2016	Test ID	Pt. 43	Operator	DW/PV	ASTM	D6951
Latitude	41.98329	Longitude	-87.97266	Elevation (ft)	NA		
Location	Section 4642 (RAP Access Road)	Station	NA				
Comments	Access road with RAP material with nominal 6 in. in thickness. <i>Subgrade assumed as CL clay.</i>						

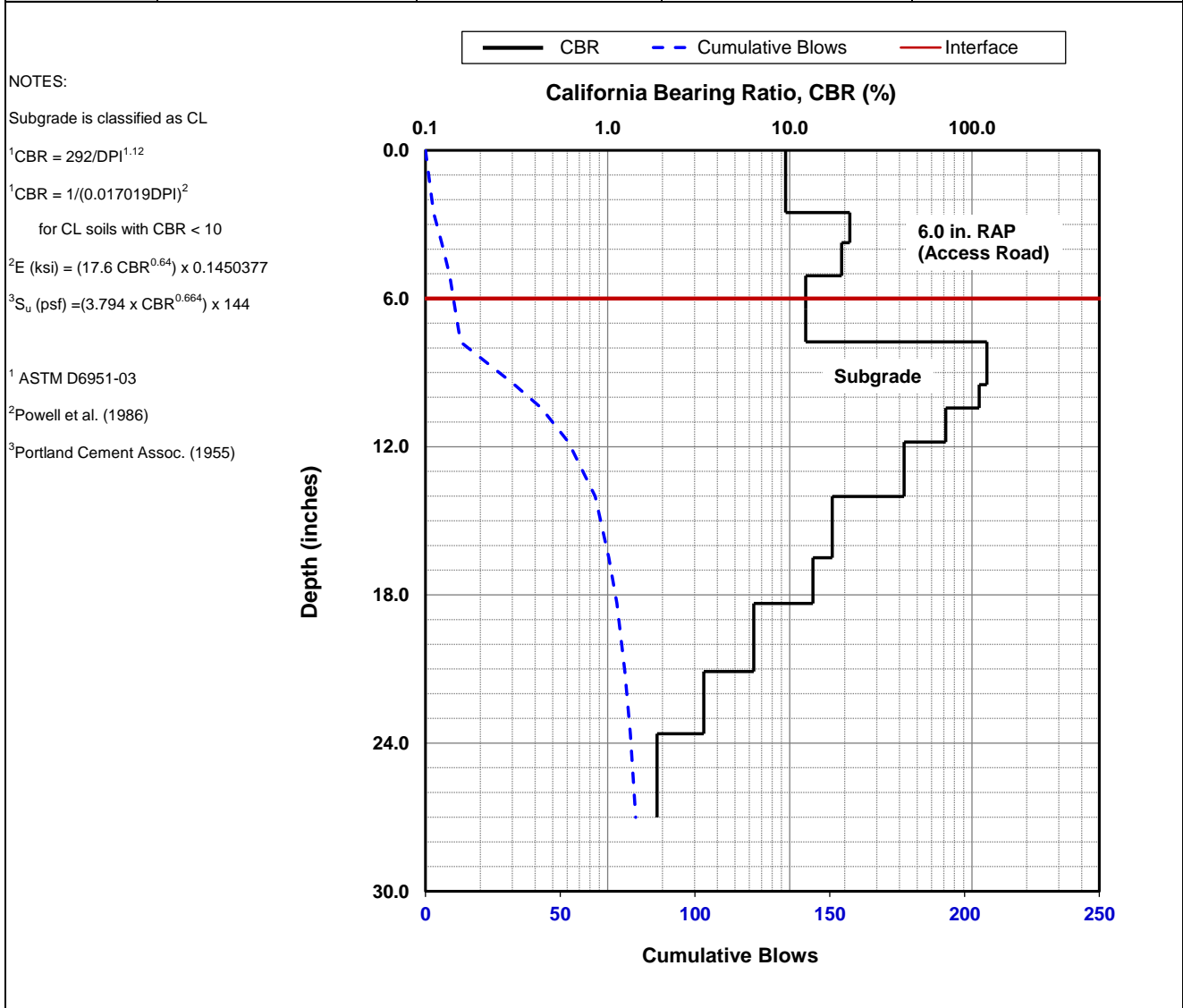
Parameter	DPI (mm/blow)	CBR (%)	E _{CBR} , Elastic Modulus (ksi) (non stress-dependent)	S _{u-CBR} , Bearing Capacity (psf)
Avg. PGE Layer [0 to 6.0 in.]	9.8	22.8	18.9	4,355
Avg. Subgrade Layer [6.0 to 18.0 in.]	4.7	51.7	31.9	7,498
Ratio of Avg. Top/Bottom Layer	2.1	0.4	0.6	0.6
Std. Dev. PGE Layer [0 to 6.0 in.]	19.5	34.6	24.7	5,752
Std. Dev. Subgrade Layer [6.0 to 18.0 in.]	5.3	54.6	33.0	7,776



Dynamic Cone Penetrometer (DCP) Test Results		
Project Name:	Illinois Tollway - IC Research	
Project ID:	Elgin O'Hare Extension - IL Tollway	
Location:	IL390 (West of O'Hare)	

Date of Test	10/13/2016	Test ID	Pt. 44	Operator	DW/PV	ASTM	D6951
Latitude	41.98333	Longitude		-87.97272	Elevation (ft)	NA	
Location	Section 4642 (RAP Access Road)	Station		NA			
Comments	Access road with RAP material with nominal 6 in. in thickness. <i>Subgrade assumed as CL clay.</i>						

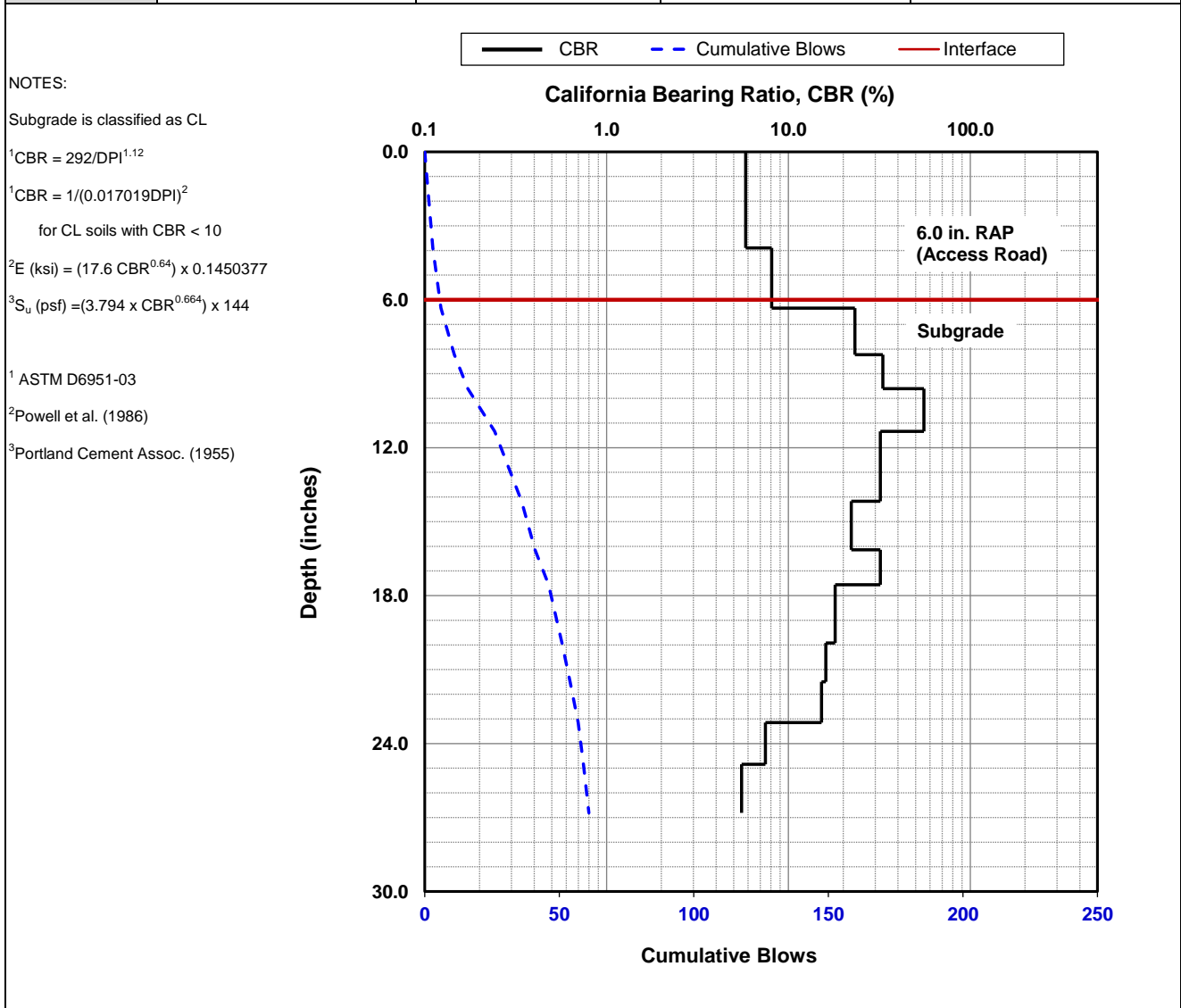
Parameter	DPI (mm/blow)	CBR (%)	E _{CBR} , Elastic Modulus (ksi) (non stress-dependent)	S _{u-CBR} , Bearing Capacity (psf)
Avg. PGE Layer [0 to 6.0 in.]	14.8	14.3	14.0	3,190
Avg. Subgrade Layer [6.0 to 18.0 in.]	5.1	47.6	30.2	7,103
Ratio of Avg. Top/Bottom Layer	2.9	0.3	0.5	0.4
Std. Dev. PGE Layer [0 to 6.0 in.]	5.3	5.6	7.7	1,713
Std. Dev. Subgrade Layer [6.0 to 18.0 in.]	6.5	46.1	29.6	6,949



Dynamic Cone Penetrometer (DCP) Test Results		
Project Name:	Illinois Tollway - IC Research	
Project ID:	Elgin O'Hare Extension - IL Tollway	
Location:	IL390 (West of O'Hare)	

Date of Test	10/13/2016	Test ID	Pt. 45	Operator	DW/PV	ASTM	D6951
Latitude	41.98330	Longitude	-87.97279	Elevation (ft)	NA		
Location	Section 4642 (RAP Access Road)	Station	NA				
Comments	Access road with RAP material with nominal 6 in. in thickness. <i>Subgrade assumed as CL clay.</i>						

Parameter	DPI (mm/blow)	CBR (%)	E _{CBR} , Elastic Modulus (ksi) (non stress-dependent)	S _{u-CBR} , Bearing Capacity (psf)
Avg. PGE Layer [0 to 6.0 in.]	26.8	7.3	9.1	2,051
Avg. Subgrade Layer [6.0 to 18.0 in.]	7.1	32.4	23.6	5,499
Ratio of Avg. Top/Bottom Layer	3.8	0.2	0.4	0.4
Std. Dev. PGE Layer [0 to 6.0 in.]	7.1	1.3	3.0	653
Std. Dev. Subgrade Layer [6.0 to 18.0 in.]	2.0	12.0	12.5	2,851



Dynamic Cone Penetrometer (DCP) Test Results		
Project Name:	Illinois Tollway - IC Research	
Project ID:	Elgin O'Hare Extension - IL Tollway	
Location:	IL390 (West of O'Hare)	

Date of Test	10/13/2016	Test ID	Pt. 46	Operator	DW/PV	ASTM	D6951
Latitude	41.98337	Longitude	-87.97288	Elevation (ft)	NA		
Location	Section 4642 (RAP Access Road)	Station	NA				
Comments	Access road with RAP material with nominal 6 in. in thickness. <i>Subgrade assumed as CL clay.</i>						

Parameter	DPI (mm/blow)	CBR (%)	E _{CBR} , Elastic Modulus (ksi) (non stress-dependent)	S _{u-CBR} , Bearing Capacity (psf)
Avg. PGE Layer [0 to 6.0 in.]	26.3	7.5	9.3	2,083
Avg. Subgrade Layer [6.0 to 18.0 in.]	9.1	24.5	19.8	4,570
Ratio of Avg. Top/Bottom Layer	2.9	0.3	0.5	0.5
Std. Dev. PGE Layer [0 to 6.0 in.]	11.2	4.0	6.2	1,376
Std. Dev. Subgrade Layer [6.0 to 18.0 in.]	2.0	6.3	8.3	1,855

NOTES:

Subgrade is classified as CL

¹CBR = 292/DPI^{1.12}

¹CBR = 1/(0.017019DPI)²

for CL soils with CBR < 10

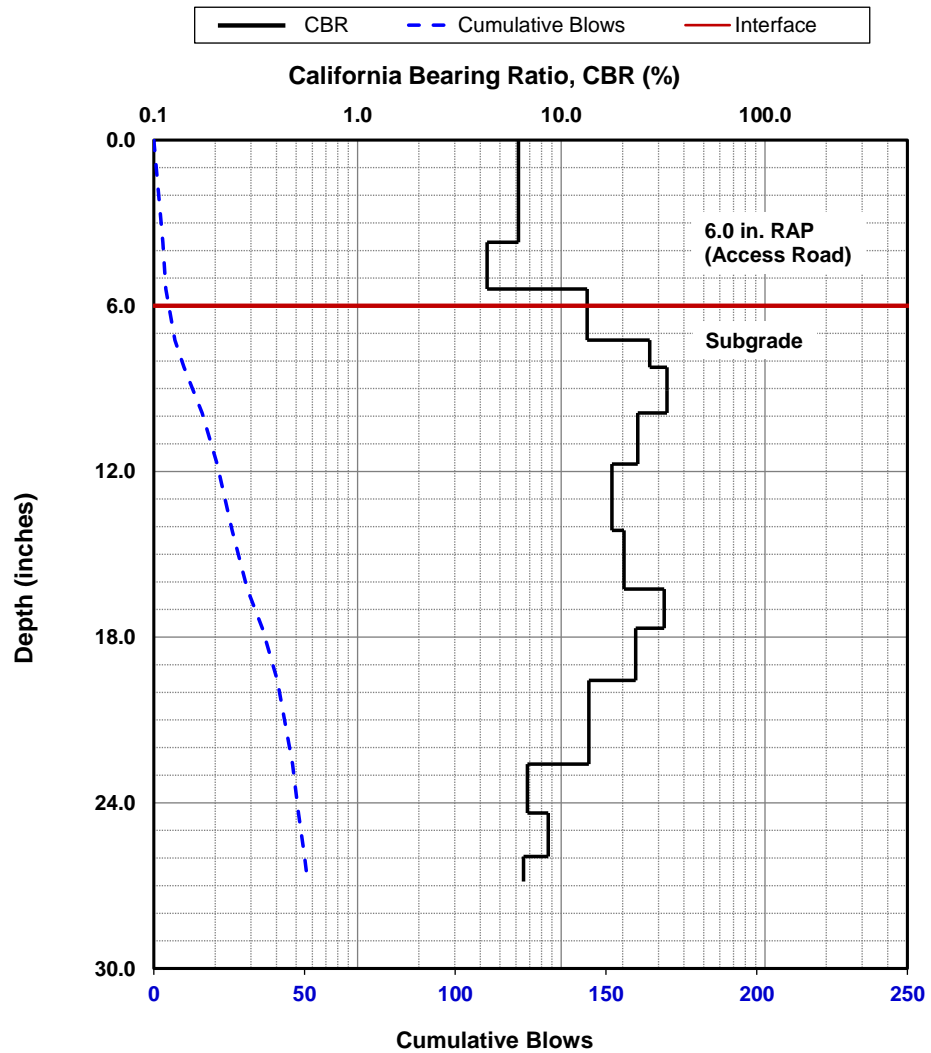
²E (ksi) = (17.6 CBR^{0.64}) x 0.1450377

³S_u (psf) = (3.794 x CBR^{0.664}) x 144

¹ ASTM D6951-03

² Powell et al. (1986)

³ Portland Cement Assoc. (1955)



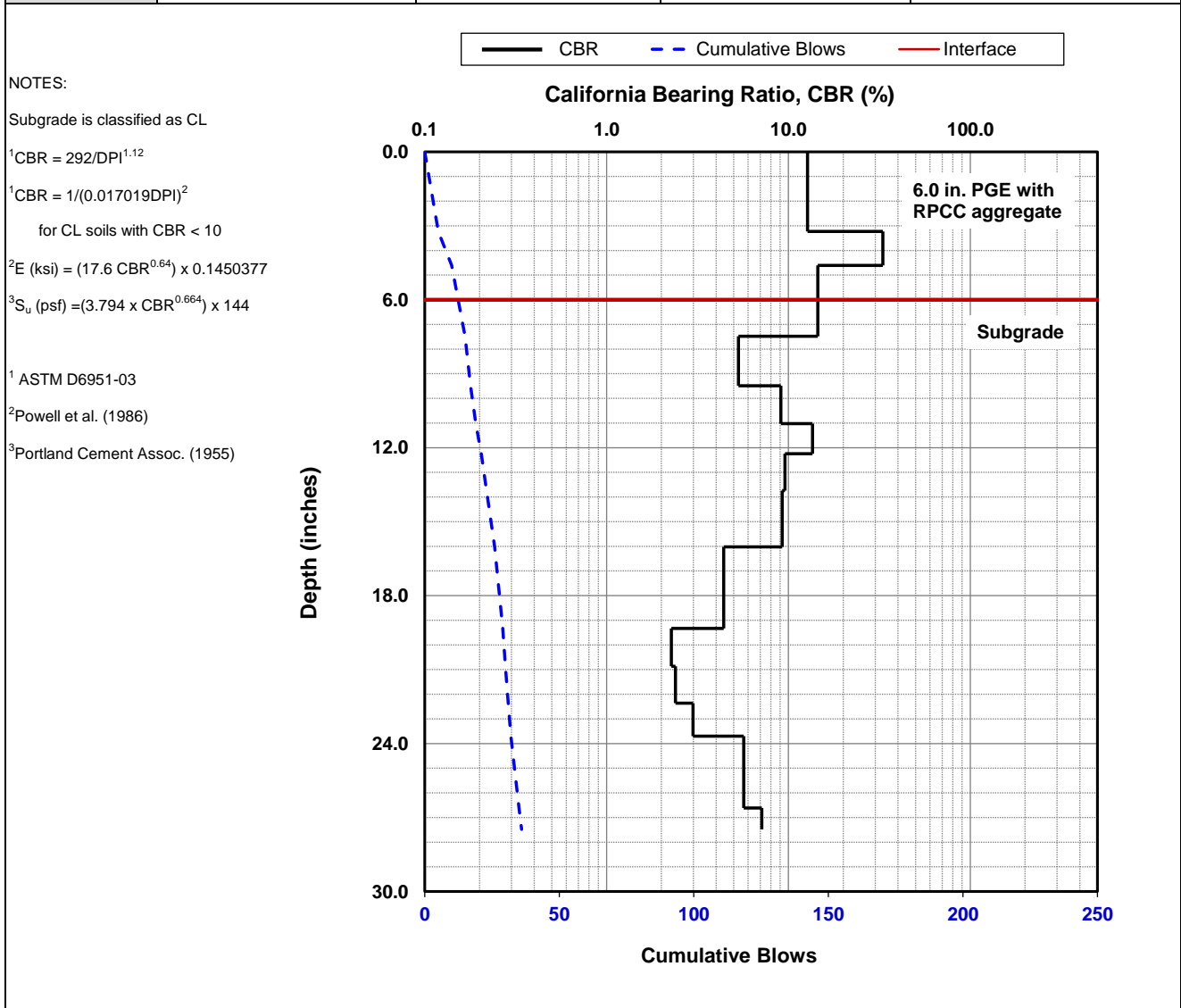
Dynamic Cone Penetrometer (DCP) Test Results

Project Name: Illinois Tollway - IC Research
 Project ID: Elgin O'Hare Extension - IL Tollway
 Location: IL390 (West of O'Hare)



Date of Test	10/13/2016	Test ID	Pt. 47	Operator	DW/PV	ASTM	D6951
Latitude	41.98323	Longitude	-87.97329	Elevation (ft)	NA		
Location	Section 4642 (PGE)	Station	NA				
Comments	Nominal 6 in. of compacted PGE with RPCC crushed aggregate. <i>Subgrade assumed as CL clay.</i>						

Parameter	DPI (mm/blow)	CBR (%)	E _{CBR} , Elastic Modulus (ksi) (non stress-dependent)	S _{u-CBR} , Bearing Capacity (psf)
Avg. PGE Layer [0 to 6.0 in.]	12.7	17.0	15.6	3,585
Avg. Subgrade Layer [6.0 to 18.0 in.]	21.5	7.5	9.2	2,076
Ratio of Avg. Top/Bottom Layer	0.6	2.3	1.7	1.7
Std. Dev. PGE Layer [0 to 6.0 in.]	4.5	9.9	11.1	2,502
Std. Dev. Subgrade Layer [6.0 to 18.0 in.]	4.7	3.3	5.5	1,208



Dynamic Cone Penetrometer (DCP) Test Results	
Project Name:	Illinois Tollway - IC Research
Project ID:	Elgin O'Hare Extension - IL Tollway
Location:	IL390 (West of O'Hare)



Date of Test	10/13/2016	Test ID	Pt. 48	Operator	DW/PV	ASTM	D6951
Latitude	41.98331	Longitude	-87.97341	Elevation (ft)	NA		
Location	Section 4642 (PGE)	Station	NA				
Comments	Nominal 6 in. of compacted PGE with RPCC crushed aggregate. <i>Subgrade assumed as CL clay.</i>						

Parameter	DPI (mm/blow)	CBR (%)	E _{CBR} , Elastic Modulus (ksi) (non stress-dependent)	S _{u-CBR} , Bearing Capacity (psf)
Avg. PGE Layer [0 to 6.0 in.]	5.8	40.6	27.3	6,391
Avg. Subgrade Layer [6.0 to 18.0 in.]	12.3	17.6	16.0	3,666
Ratio of Avg. Top/Bottom Layer	0.5	2.3	1.7	1.7
Std. Dev. PGE Layer [0 to 6.0 in.]	2.9	16.8	15.5	3,556
Std. Dev. Subgrade Layer [6.0 to 18.0 in.]	1.9	3.3	5.5	1,213

NOTES:

Subgrade is classified as CL

¹CBR = 292/DPI^{1.12}

¹CBR = 1/(0.017019DPI)²

for CL soils with CBR < 10

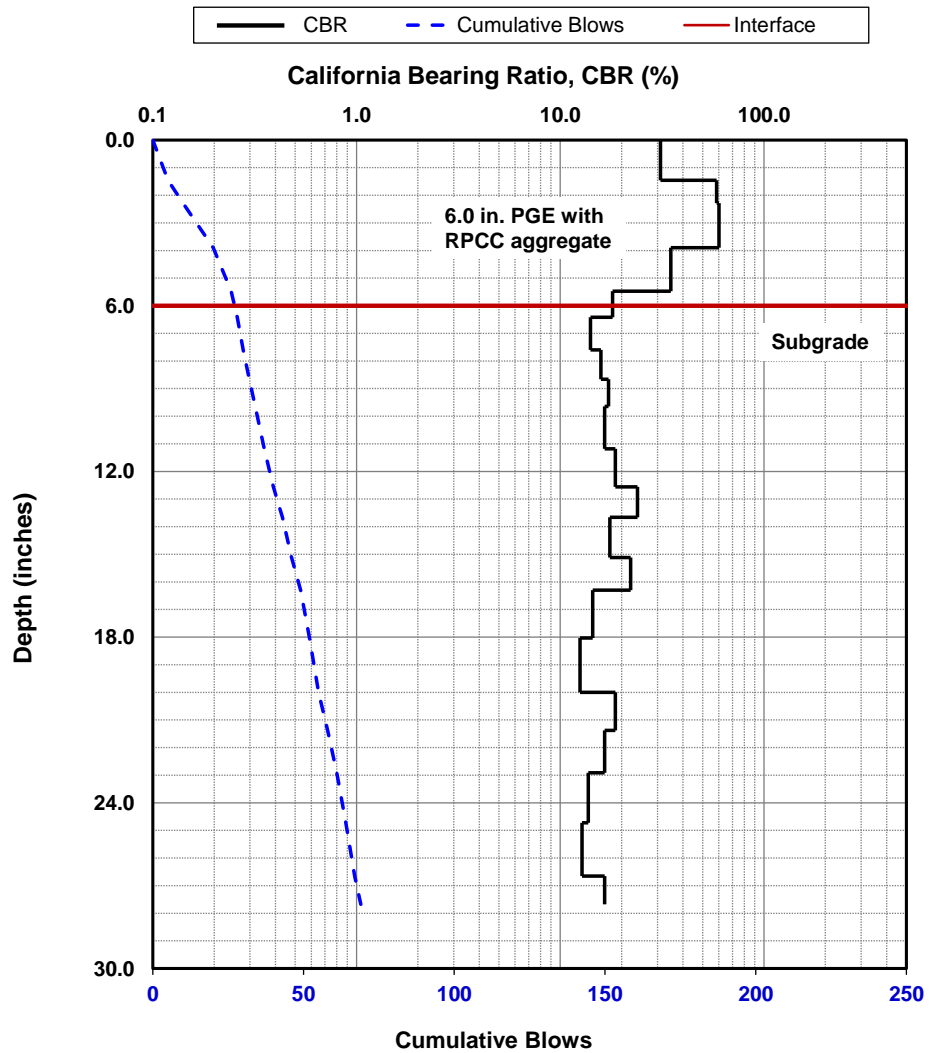
²E (ksi) = (17.6 CBR^{0.64}) x 0.1450377

³S_u (psf) = (3.794 x CBR^{0.664}) x 144

¹ ASTM D6951-03

² Powell et al. (1986)

³ Portland Cement Assoc. (1955)



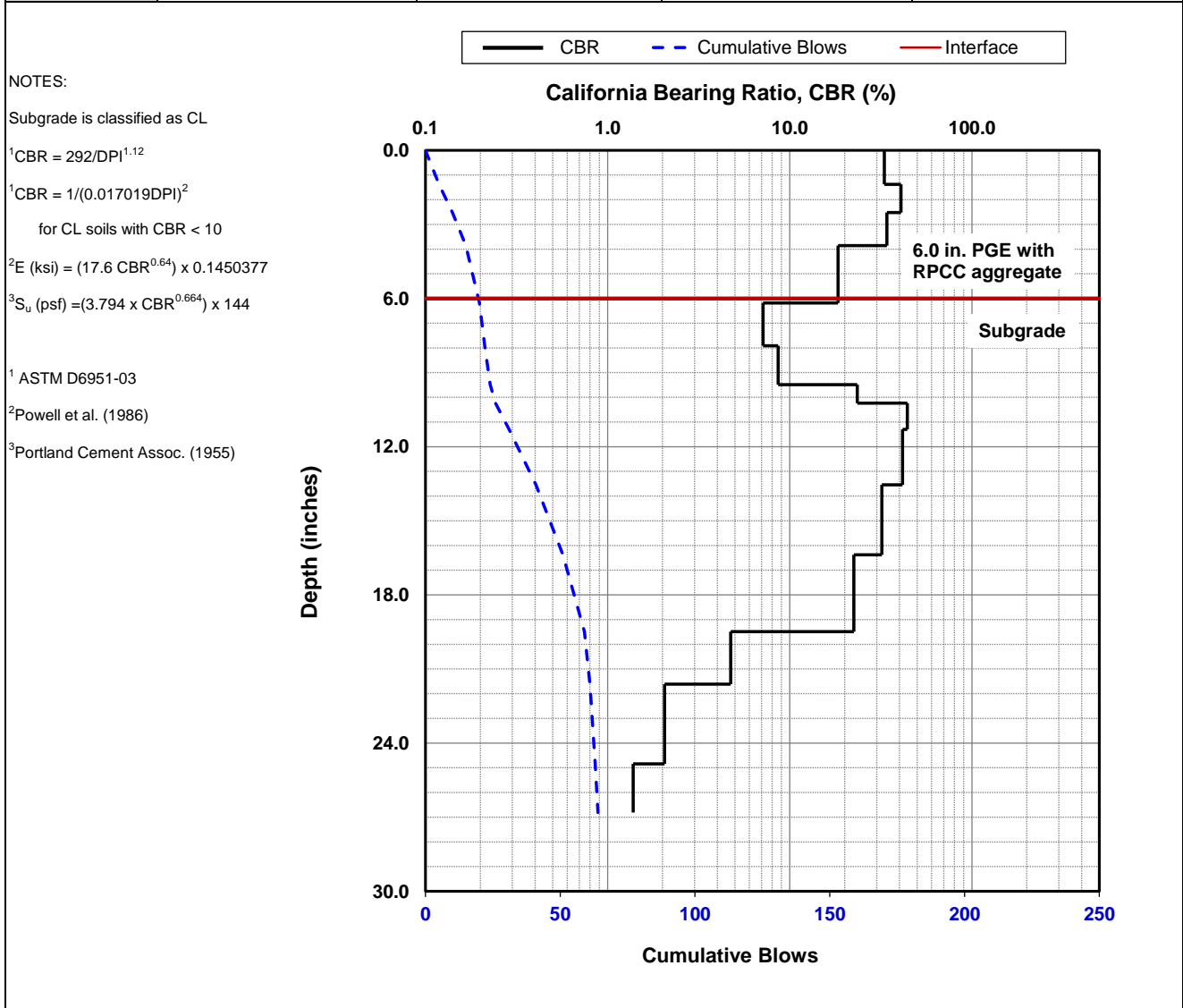
Dynamic Cone Penetrometer (DCP) Test Results

Project Name: Illinois Tollway - IC Research
 Project ID: Elgin O'Hare Extension - IL Tollway
 Location: IL390 (West of O'Hare)



Date of Test	10/13/2016	Test ID	Pt. 49	Operator	DW/PV	ASTM	D6951
Latitude	41.98337	Longitude	-87.97389	Elevation (ft)	NA		
Location	Section 4642 (PGE)	Station	NA				
Comments	Nominal 6 in. of compacted PGE with RPCC crushed aggregate. <i>Subgrade assumed as CL clay.</i>						

Parameter	DPI (mm/blow)	CBR (%)	E _{CBR} , Elastic Modulus (ksi) (non stress-dependent)	S _{u-CBR} , Bearing Capacity (psf)
Avg. PGE Layer [0 to 6.0 in.]	7.9	29.0	22.0	5,117
Avg. Subgrade Layer [6.0 to 18.0 in.]	8.7	26.0	20.5	4,753
Ratio of Avg. Top/Bottom Layer	0.9	1.1	1.1	1.1
Std. Dev. PGE Layer [0 to 6.0 in.]	2.4	8.2	9.8	2,207
Std. Dev. Subgrade Layer [6.0 to 18.0 in.]	6.8	14.6	14.2	3,245

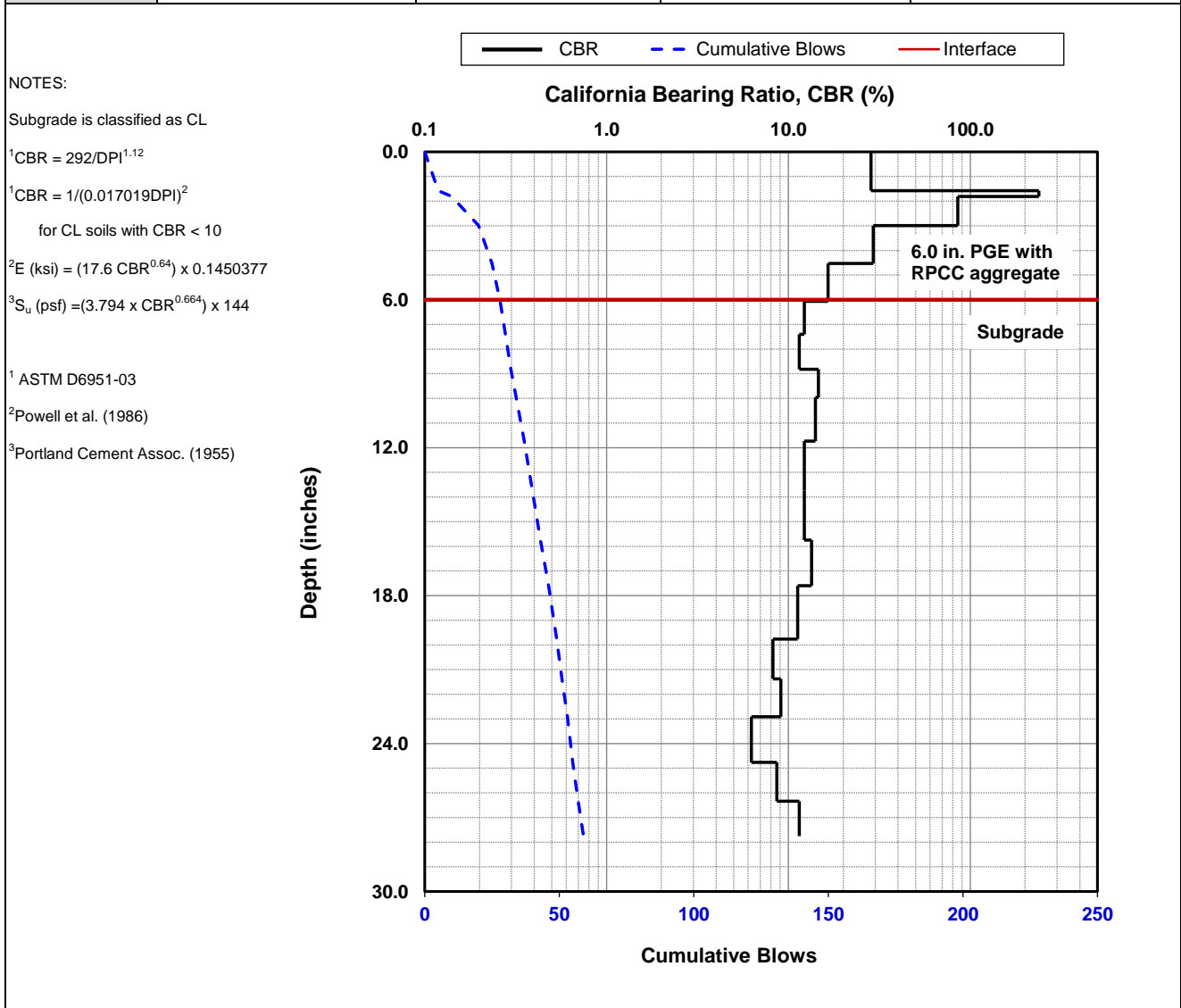


Dynamic Cone Penetrometer (DCP) Test Results	
Project Name:	Illinois Tollway - IC Research
Project ID:	Elgin O'Hare Extension - IL Tollway
Location:	IL390 (West of O'Hare)



Date of Test	10/13/2016	Test ID	Pt. 50	Operator	DW/PV	ASTM	D6951
Latitude	41.98322	Longitude	-87.97409	Elevation (ft)	NA		
Location	Section 4642 (PGE)	Station	NA				
Comments	Nominal 6 in. of compacted PGE with RPCC crushed aggregate. <i>Subgrade assumed as CL clay.</i>						

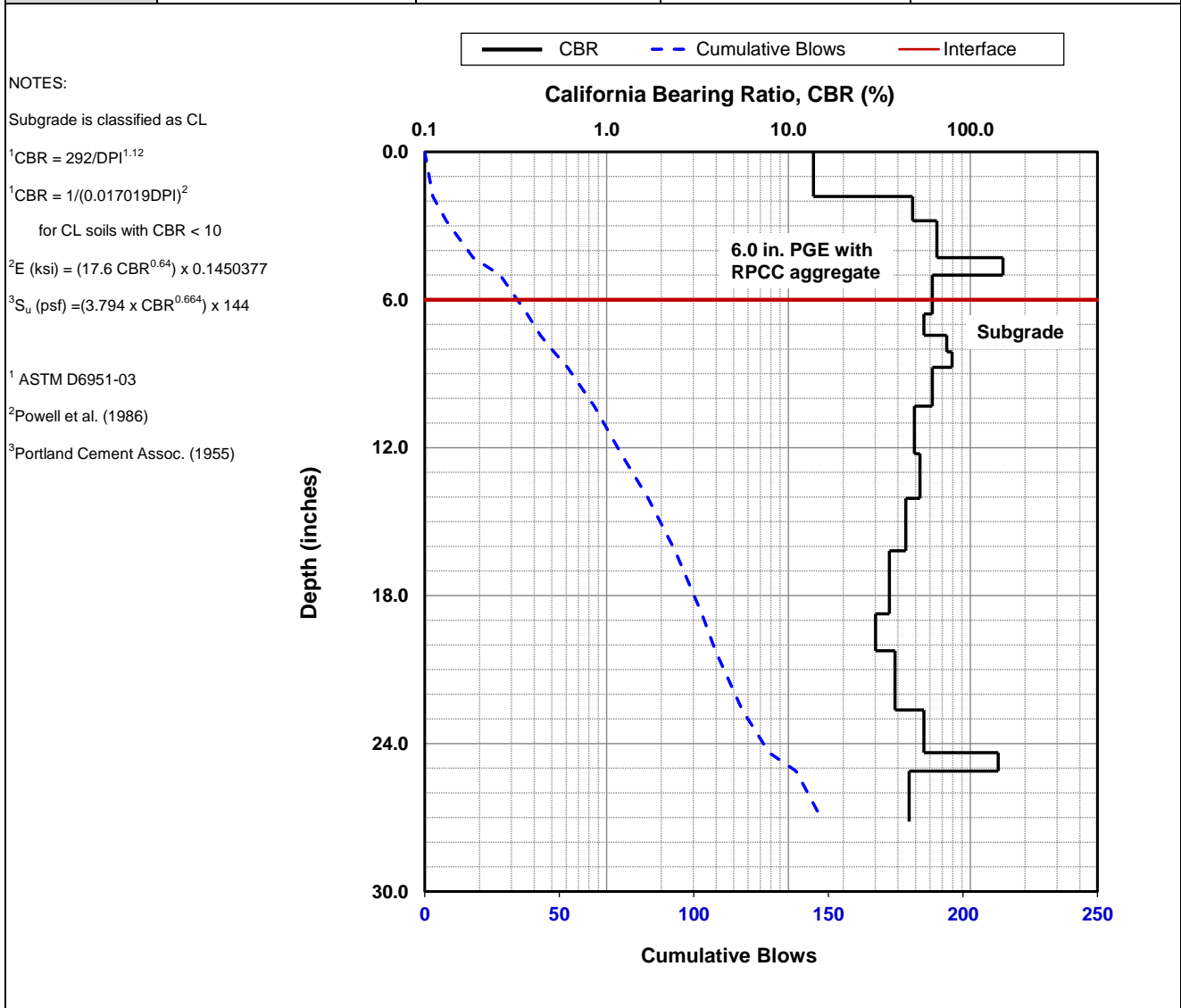
Parameter	DPI (mm/blow)	CBR (%)	E _{CBR} , Elastic Modulus (ksi) (non stress-dependent)	S _{u-CBR} , Bearing Capacity (psf)
Avg. PGE Layer [0 to 6.0 in.]	5.5	43.3	28.5	6,666
Avg. Subgrade Layer [6.0 to 18.0 in.]	16.3	12.8	13.1	2,975
Ratio of Avg. Top/Bottom Layer	0.3	3.4	2.2	2.2
Std. Dev. PGE Layer [0 to 6.0 in.]	4.2	85.4	44.0	10,469
Std. Dev. Subgrade Layer [6.0 to 18.0 in.]	1.3	1.2	2.8	600



Dynamic Cone Penetrometer (DCP) Test Results		
Project Name:	Illinois Tollway - IC Research	
Project ID:	Elgin O'Hare Extension - IL Tollway	
Location:	IL390 (West of O'Hare)	

Date of Test	10/13/2016	Test ID	Pt. 51	Operator	DW/PV	ASTM	D6951
Latitude	41.98324	Longitude	-87.97643	Elevation (ft)	NA		
Location	Section 4642 (PGE)	Station	NA				
Comments	Nominal 6 in. of compacted PGE with RPCC crushed aggregate. <i>Subgrade assumed as CL clay.</i>						

Parameter	DPI (mm/blow)	CBR (%)	E _{CBR} , Elastic Modulus (ksi) (non stress-dependent)	S _{u-CBR} , Bearing Capacity (psf)
Avg. PGE Layer [0 to 6.0 in.]	4.4	55.6	33.4	7,877
Avg. Subgrade Layer [6.0 to 18.0 in.]	4.8	50.9	31.6	7,430
Ratio of Avg. Top/Bottom Layer	0.9	1.1	1.1	1.1
Std. Dev. PGE Layer [0 to 6.0 in.]	6.1	50.5	31.4	7,389
Std. Dev. Subgrade Layer [6.0 to 18.0 in.]	1.1	14.7	14.2	3,250

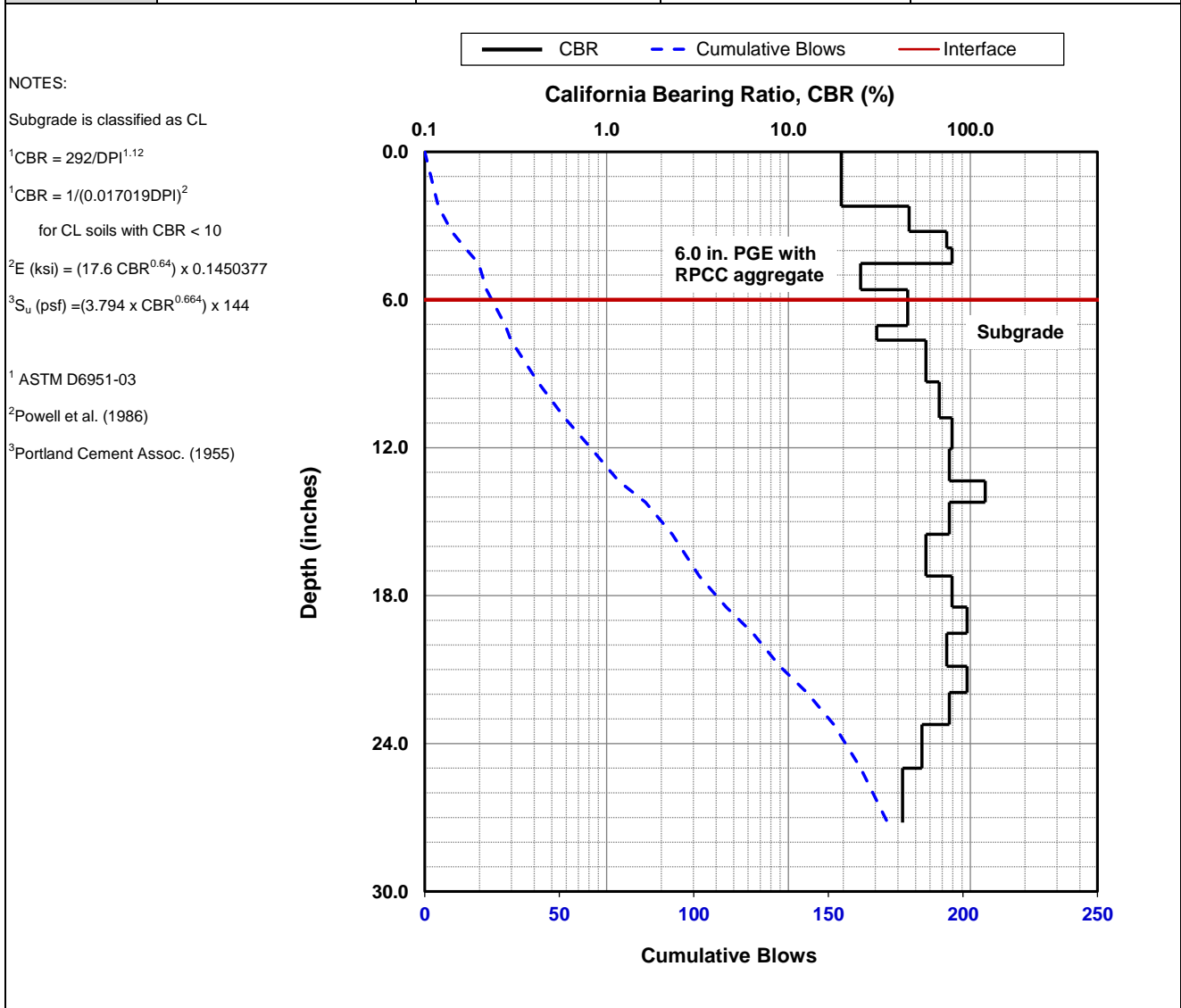


Dynamic Cone Penetrometer (DCP) Test Results	
Project Name:	Illinois Tollway - IC Research
Project ID:	Elgin O'Hare Extension - IL Tollway
Location:	IL390 (West of O'Hare)



Date of Test	10/13/2016	Test ID	Pt. 52	Operator	DW/PV	ASTM	D6951
Latitude	41.98321	Longitude	-87.97654	Elevation (ft)	NA		
Location	Section 4642 (PGE)	Station	NA				
Comments	Nominal 6 in. of compacted PGE with RPCC crushed aggregate. <i>Subgrade assumed as CL clay.</i>						

Parameter	DPI (mm/blow)	CBR (%)	E _{CBR} , Elastic Modulus (ksi) (non stress-dependent)	S _{u-CBR} , Bearing Capacity (psf)
Avg. PGE Layer [0 to 6.0 in.]	6.2	38.0	26.2	6,117
Avg. Subgrade Layer [6.0 to 18.0 in.]	3.7	68.0	38.0	8,999
Ratio of Avg. Top/Bottom Layer	1.7	0.6	0.7	0.7
Std. Dev. PGE Layer [0 to 6.0 in.]	3.7	27.3	21.2	4,910
Std. Dev. Subgrade Layer [6.0 to 18.0 in.]	1.5	24.4	19.7	4,552

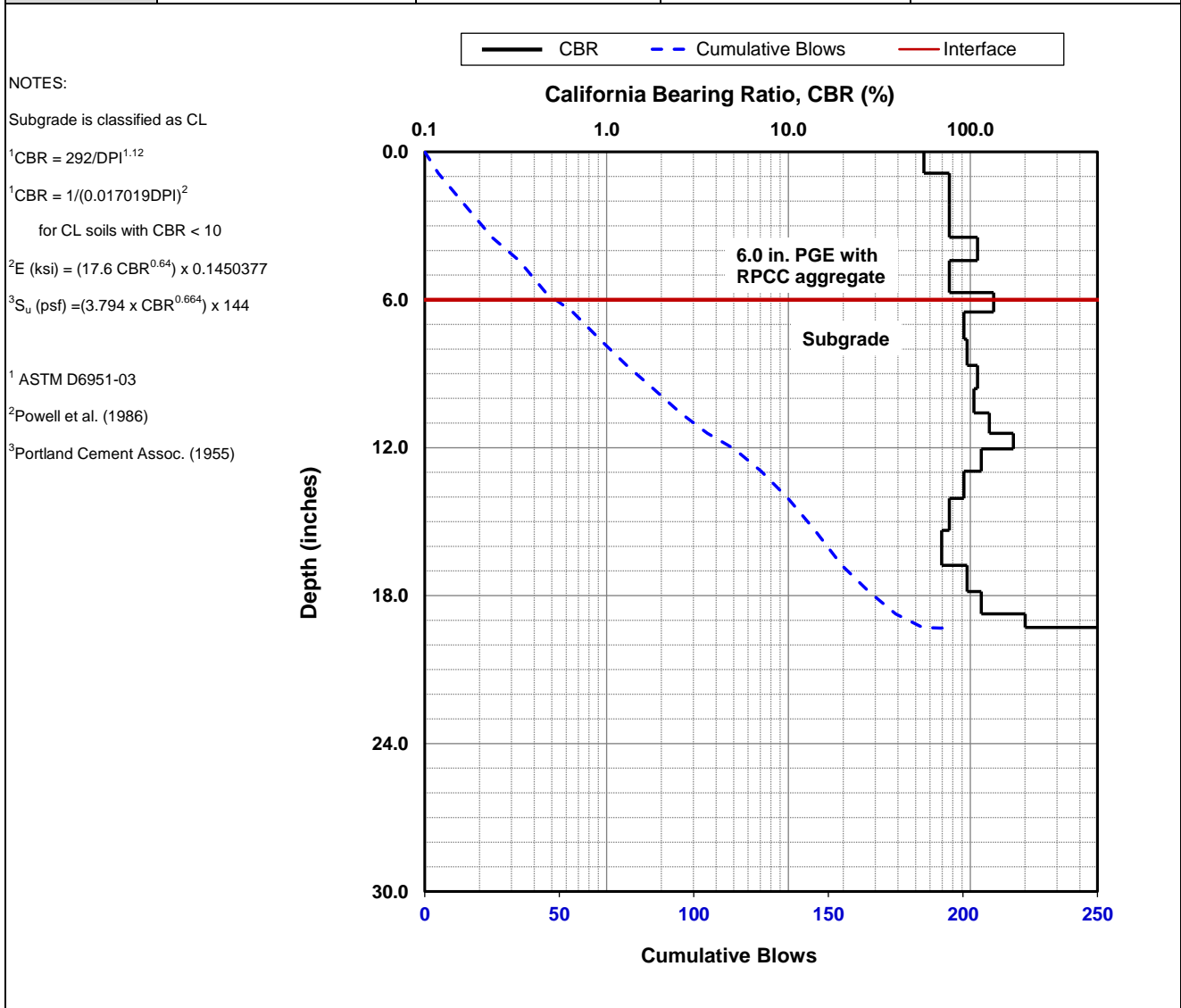


Dynamic Cone Penetrometer (DCP) Test Results	
Project Name:	Illinois Tollway - IC Research
Project ID:	Elgin O'Hare Extension - IL Tollway
Location:	IL390 (West of O'Hare)



Date of Test	10/13/2016	Test ID	Pt. 53	Operator	DW/PV	ASTM	D6951
Latitude	41.98324	Longitude	-87.97666	Elevation (ft)	NA		
Location	Section 4642 (PGE)	Station	NA				
Comments	Nominal 6 in. of compacted PGE with RPCC crushed aggregate. <i>Subgrade assumed as CL clay.</i>						

Parameter	DPI (mm/blow)	CBR (%)	E _{CBR} , Elastic Modulus (ksi) (non stress-dependent)	S _{u-CBR} , Bearing Capacity (psf)
Avg. PGE Layer [0 to 6.0 in.]	3.0	85.3	43.9	10,463
Avg. Subgrade Layer [6.0 to 18.0 in.]	2.6	99.4	48.4	11,578
Ratio of Avg. Top/Bottom Layer	1.1	0.9	0.9	0.9
Std. Dev. PGE Layer [0 to 6.0 in.]	0.9	28.8	21.9	5,083
Std. Dev. Subgrade Layer [6.0 to 18.0 in.]	0.5	27.8	21.4	4,967

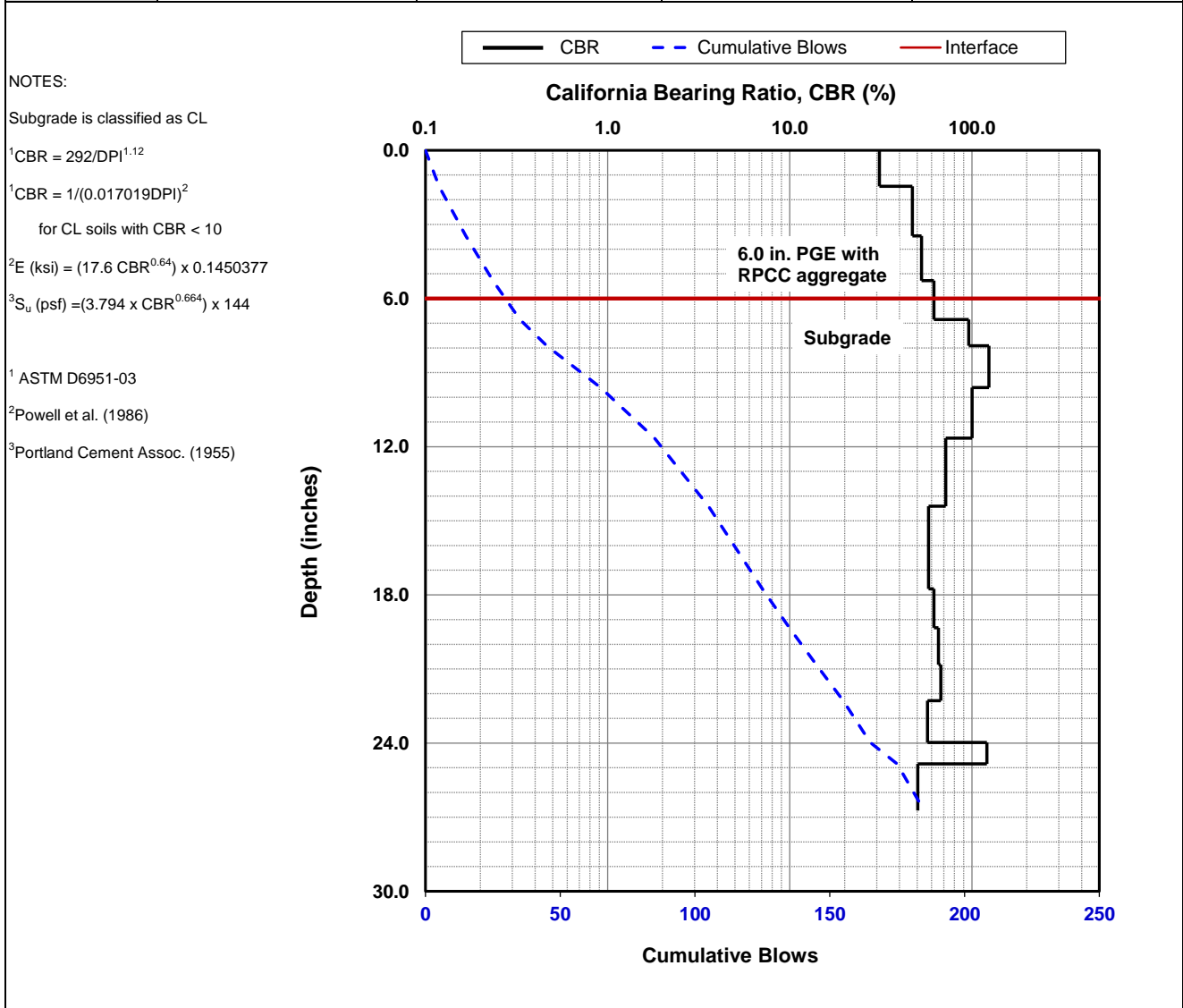


Dynamic Cone Penetrometer (DCP) Test Results	
Project Name:	Illinois Tollway - IC Research
Project ID:	Elgin O'Hare Extension - IL Tollway
Location:	IL390 (West of O'Hare)



Date of Test	10/13/2016	Test ID	Pt. 54	Operator	DW/PV	ASTM	D6951
Latitude	41.98320	Longitude		-87.97666	Elevation (ft)	NA	
Location	Section 4642 (PGE)	Station		NA			
Comments	Nominal 6 in. of compacted PGE with RPCC crushed aggregate. <i>Subgrade assumed as CL clay.</i>						

Parameter	DPI (mm/blow)	CBR (%)	E _{CBR} , Elastic Modulus (ksi) (non stress-dependent)	S _{u-CBR} , Bearing Capacity (psf)
Avg. PGE Layer [0 to 6.0 in.]	5.0	48.5	30.6	7,186
Avg. Subgrade Layer [6.0 to 18.0 in.]	3.1	82.9	43.1	10,266
Ratio of Avg. Top/Bottom Layer	1.6	0.6	0.7	0.7
Std. Dev. PGE Layer [0 to 6.0 in.]	1.6	13.6	13.6	3,089
Std. Dev. Subgrade Layer [6.0 to 18.0 in.]	0.8	25.8	20.4	4,727



Dynamic Cone Penetrometer (DCP) Test Results		
Project Name:	Illinois Tollway - IC Research	
Project ID:	Elgin O'Hare Extension - IL Tollway	
Location:	IL390 (West of O'Hare)	

Date of Test	10/13/2016	Test ID	Pt. 55	Operator	DW/PV	ASTM	D6951
Latitude	41.98319	Longitude	-87.97678	Elevation (ft)	NA		
Location	Section 4642 (PGE)	Station	NA				
Comments	Nominal 6 in. of compacted PGE with RPCC crushed aggregate. <i>Subgrade assumed as CL clay.</i>						

Parameter	DPI (mm/blow)	CBR (%)	E _{CBR} , Elastic Modulus (ksi) (non stress-dependent)	S _{u-CBR} , Bearing Capacity (psf)
Avg. PGE Layer [0 to 6.0 in.]	5.6	42.7	28.2	6,607
Avg. Subgrade Layer [6.0 to 18.0 in.]	2.0	136.1	59.2	14,267
Ratio of Avg. Top/Bottom Layer	2.8	0.3	0.5	0.5
Std. Dev. PGE Layer [0 to 6.0 in.]	3.6	23.8	19.4	4,479
Std. Dev. Subgrade Layer [6.0 to 18.0 in.]	0.6	64.5	36.7	8,689

NOTES:

Subgrade is classified as CL

¹CBR = 292/DPI^{1.12}

¹CBR = 1/(0.017019DPI)²

for CL soils with CBR < 10

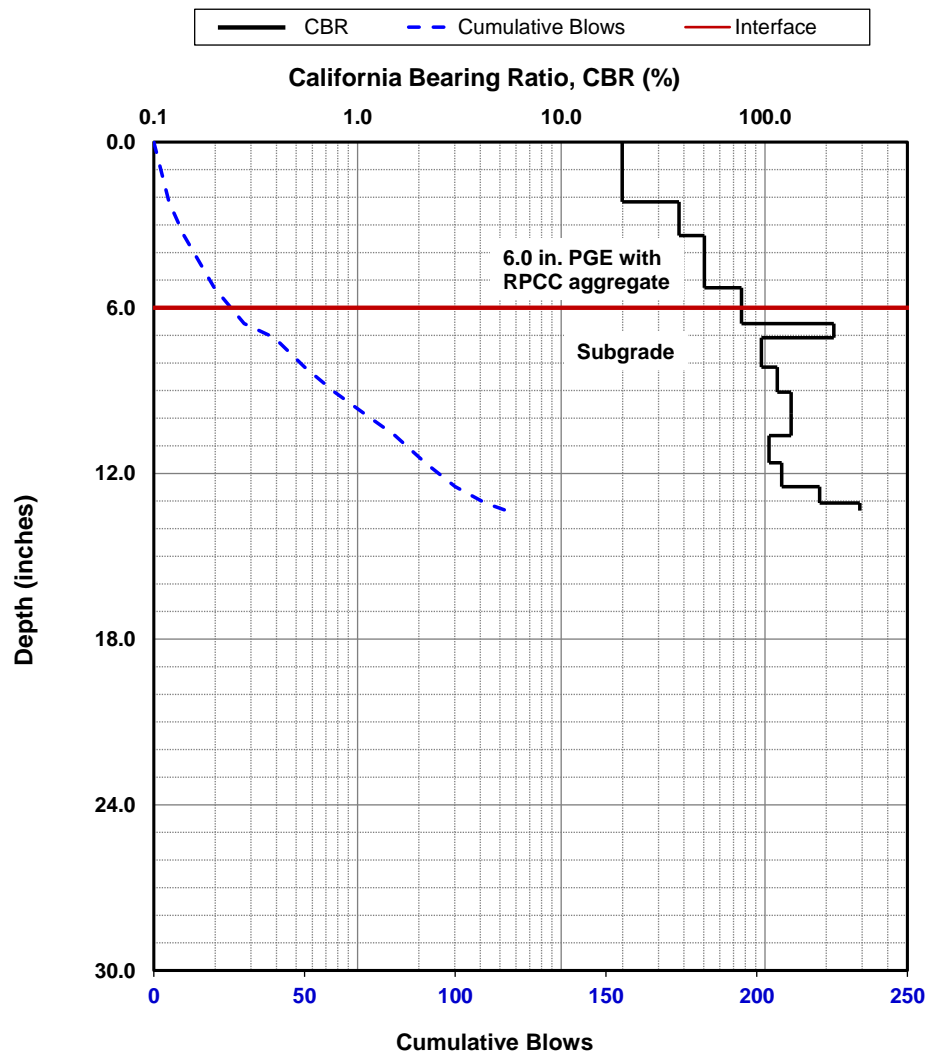
²E (ksi) = (17.6 CBR^{0.64}) x 0.1450377

³S_u (psf) = (3.794 x CBR^{0.664}) x 144

¹ ASTM D6951-03

² Powell et al. (1986)

³ Portland Cement Assoc. (1955)



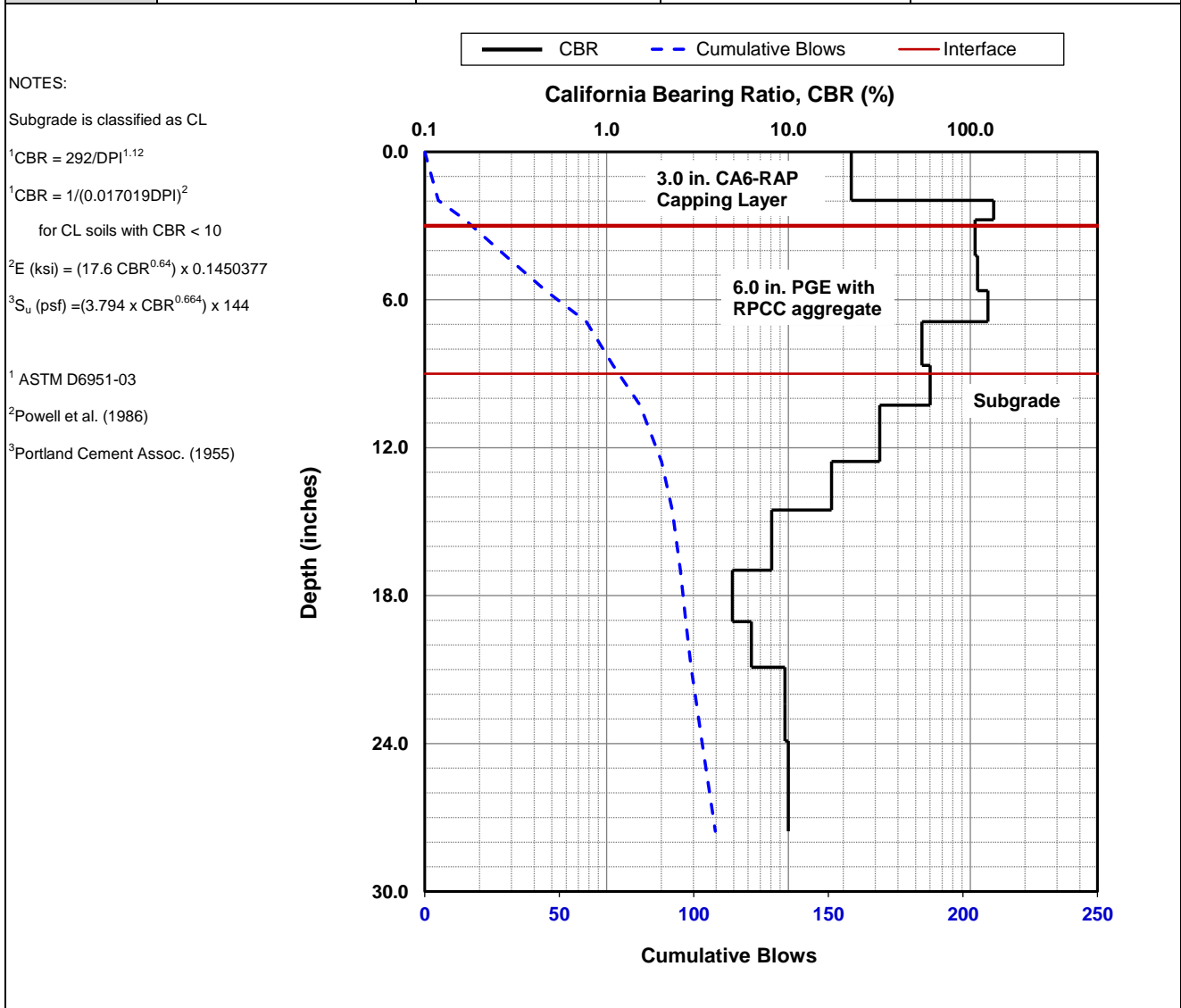
Dynamic Cone Penetrometer (DCP) Test Results

Project Name: Illinois Tollway - IC Research
 Project ID: Elgin O'Hare Extension - IL Tollway
 Location: IL390 (West of O'Hare)



Date of Test	10/14/2016	Test ID	Pt. 57	Operator	DW/PV	ASTM	D6951
Latitude	41.98340	Longitude	-87.98164	Elevation (ft)	NA		
Location	Section 4642 (CA6 Capping)	Station	NA				
Comments	Nominal 3 in. of CA6 -RAP capping layer over nominal 6 in. of compacted PGE with RPCC crushed aggregate. <i>Subgrade assumed as CL clay.</i>						

Parameter	DPI (mm/blow)	CBR (%)	E _{CBR} , Elastic Modulus (ksi) (non stress-dependent)	S _{u-CBR} , Bearing Capacity (psf)
Avg. PGE+CA6 Layer [0 to 9.0 in.]	3.1	81.0	42.5	10,107
Avg. Subgrade Layer [9.0 to 21.0 in.]	10.7	20.5	17.6	4,057
Ratio of Avg. Top/Bottom Layer	0.3	4.0	2.4	2.5
Std.Dev.PGE+CA6 Layer [0 to 9 in.]	3.7	48.1	30.4	7,150
Std. Dev. Subgrade Layer [9.0 to 21.0 in.]	9.1	21.5	18.2	4,185

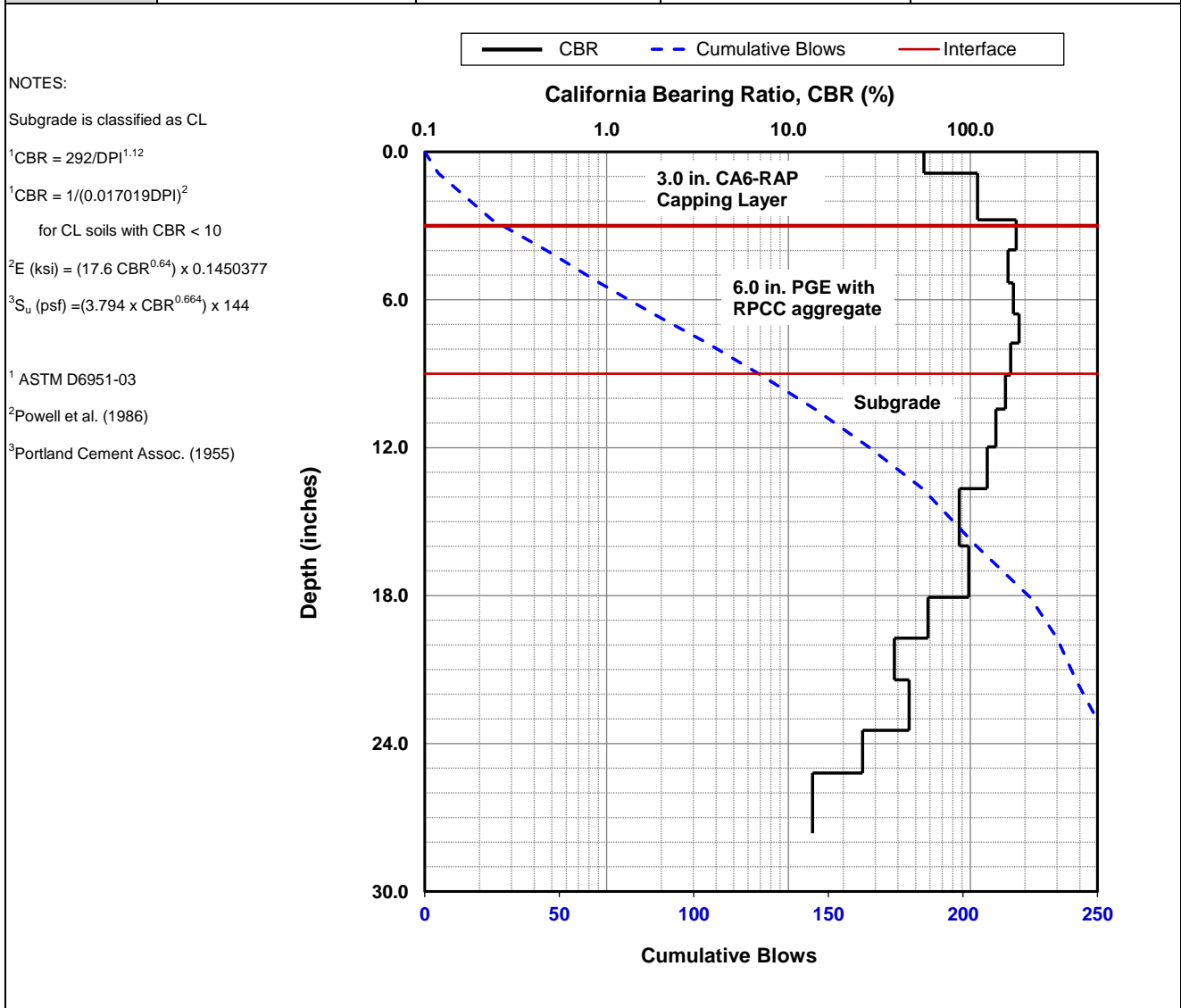


Dynamic Cone Penetrometer (DCP) Test Results	
Project Name:	Illinois Tollway - IC Research
Project ID:	Elgin O'Hare Extension - IL Tollway
Location:	IL390 (West of O'Hare)



Date of Test	10/14/2016	Test ID	Pt. 60	Operator	DW/PV	ASTM	D6951
Latitude	41.98338	Longitude	-87.98219	Elevation (ft)	NA		
Location	Section 4642 (CA6 Capping)	Station	NA				
Comments	Nominal 3 in. of CA6 -RAP capping layer over nominal 6 in. of compacted PGE with RPCC crushed aggregate. <i>Subgrade assumed as CL clay.</i>						

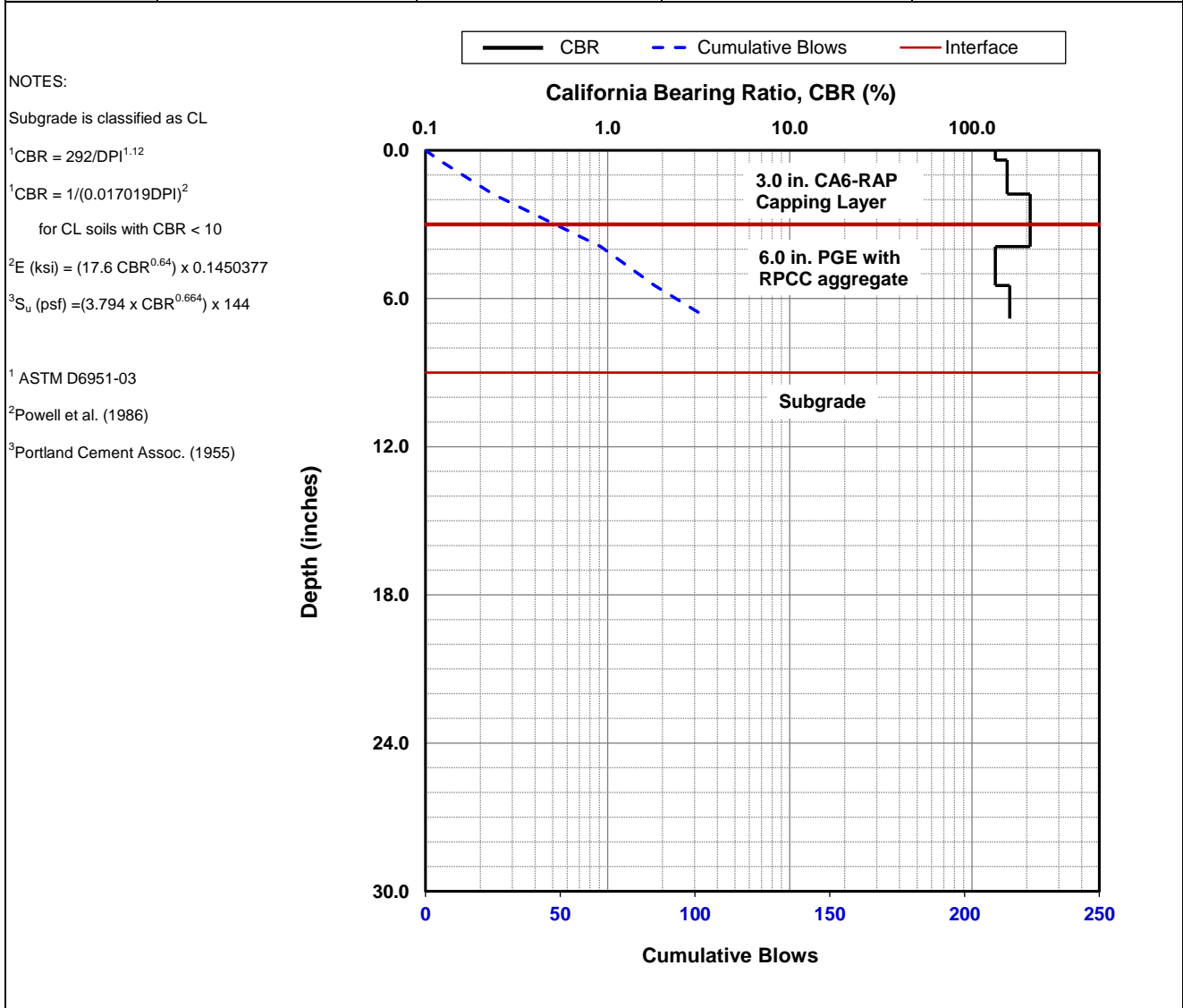
Parameter	DPI (mm/blow)	CBR (%)	E _{CBR} , Elastic Modulus (ksi) (non stress-dependent)	S _{u-CBR} , Bearing Capacity (psf)
Avg. PGE+CA6 Layer [0 to 9.0 in.]	1.8	147.5	62.4	15,050
Avg. Subgrade Layer [9.0 to 21.0 in.]	2.7	96.6	47.6	11,366
Ratio of Avg. Top/Bottom Layer	0.7	1.5	1.3	1.3
Std.Dev.PGE+CA6 Layer [0 to 9 in.]	1.3	54.5	33.0	7,773
Std. Dev. Subgrade Layer [9.0 to 21.0 in.]	1.6	42.6	28.2	6,596



Dynamic Cone Penetrometer (DCP) Test Results		
Project Name:	Illinois Tollway - IC Research	
Project ID:	Elgin O'Hare Extension - IL Tollway	
Location:	IL390 (West of O'Hare)	

Date of Test	10/14/2016	Test ID	Pt. 63	Operator	DW/PV	ASTM	D6951
Latitude	41.98340	Longitude	-87.98250	Elevation (ft)	NA		
Location	Section 4642 (CA6 Capping)	Station	NA				
Comments	Nominal 3 in. of CA6 -RAP capping layer over nominal 6 in. of compacted PGE with RPCC crushed aggregate. <i>Subgrade assumed as CL clay.</i>						

Parameter	DPI (mm/blow)	CBR (%)	E _{CBR} , Elastic Modulus (ksi) (non stress-dependent)	S _{u-CBR} , Bearing Capacity (psf)
Avg. PGE+CA6 Layer [0 to 9.0 in.]	1.6	166.9	67.5	16,338
Avg. Subgrade Layer [9.0 to 21.0 in.]	Refusal	Refusal	Refusal	Refusal
Ratio of Avg. Top/Bottom Layer	NA	NA	NA	NA
Std.Dev.PGE+CA6 Layer [0 to 9 in.]	0.3	33.4	24.1	5,610
Std. Dev. Subgrade Layer [9.0 to 21.0 in.]	NA	NA	NA	NA

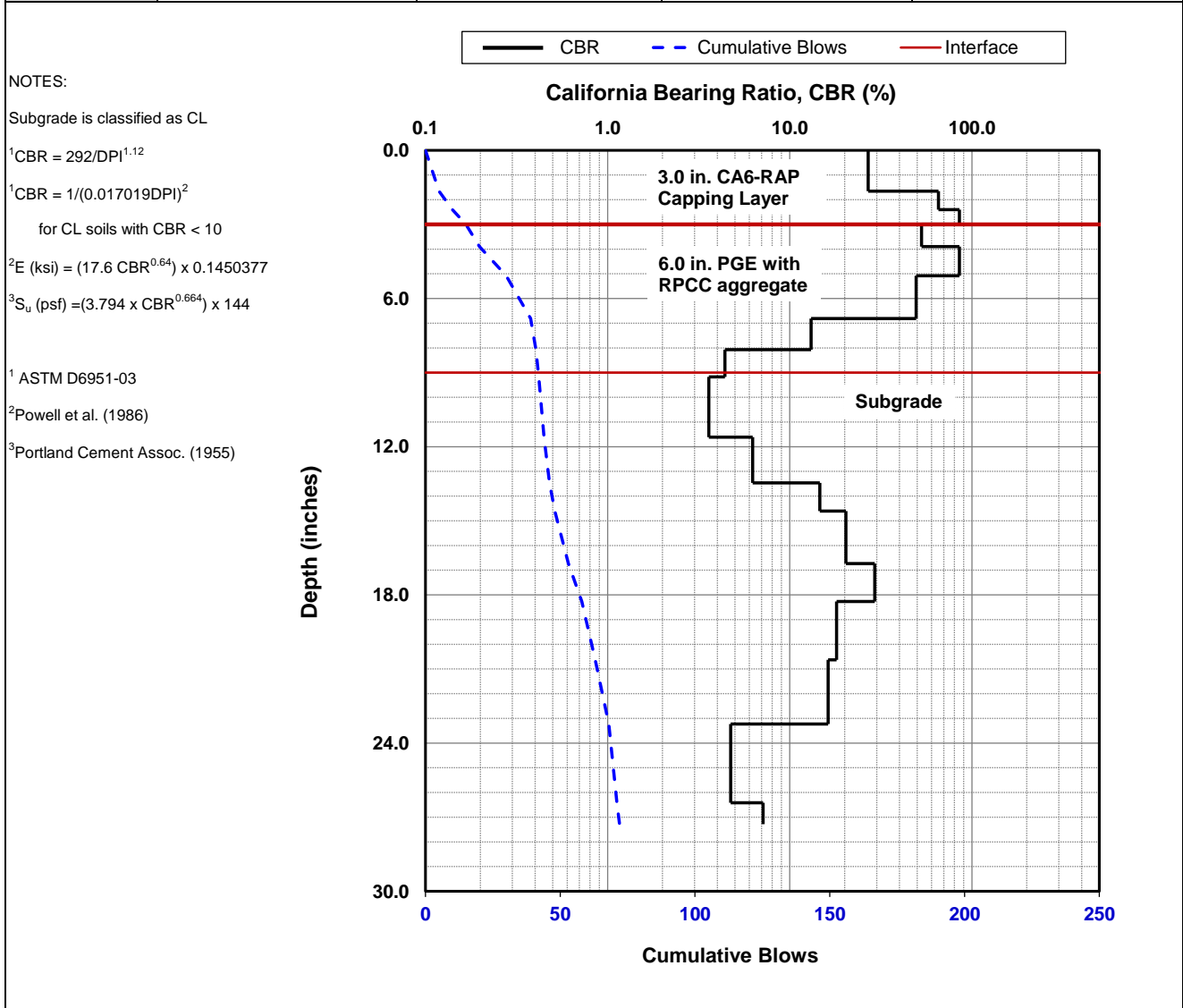


Dynamic Cone Penetrometer (DCP) Test Results	
Project Name:	Illinois Tollway - IC Research
Project ID:	Elgin O'Hare Extension - IL Tollway
Location:	IL390 (West of O'Hare)



Date of Test	10/14/2016	Test ID	Pt. 64	Operator	DW/PV	ASTM	D6951
Latitude	41.98343	Longitude	-87.98274	Elevation (ft)	NA		
Location	Section 4642 (CA6 Capping)	Station	NA				
Comments	Nominal 3 in. of CA6 -RAP capping layer over nominal 6 in. of compacted PGE with RPCC crushed aggregate. <i>Subgrade assumed as CL clay.</i>						

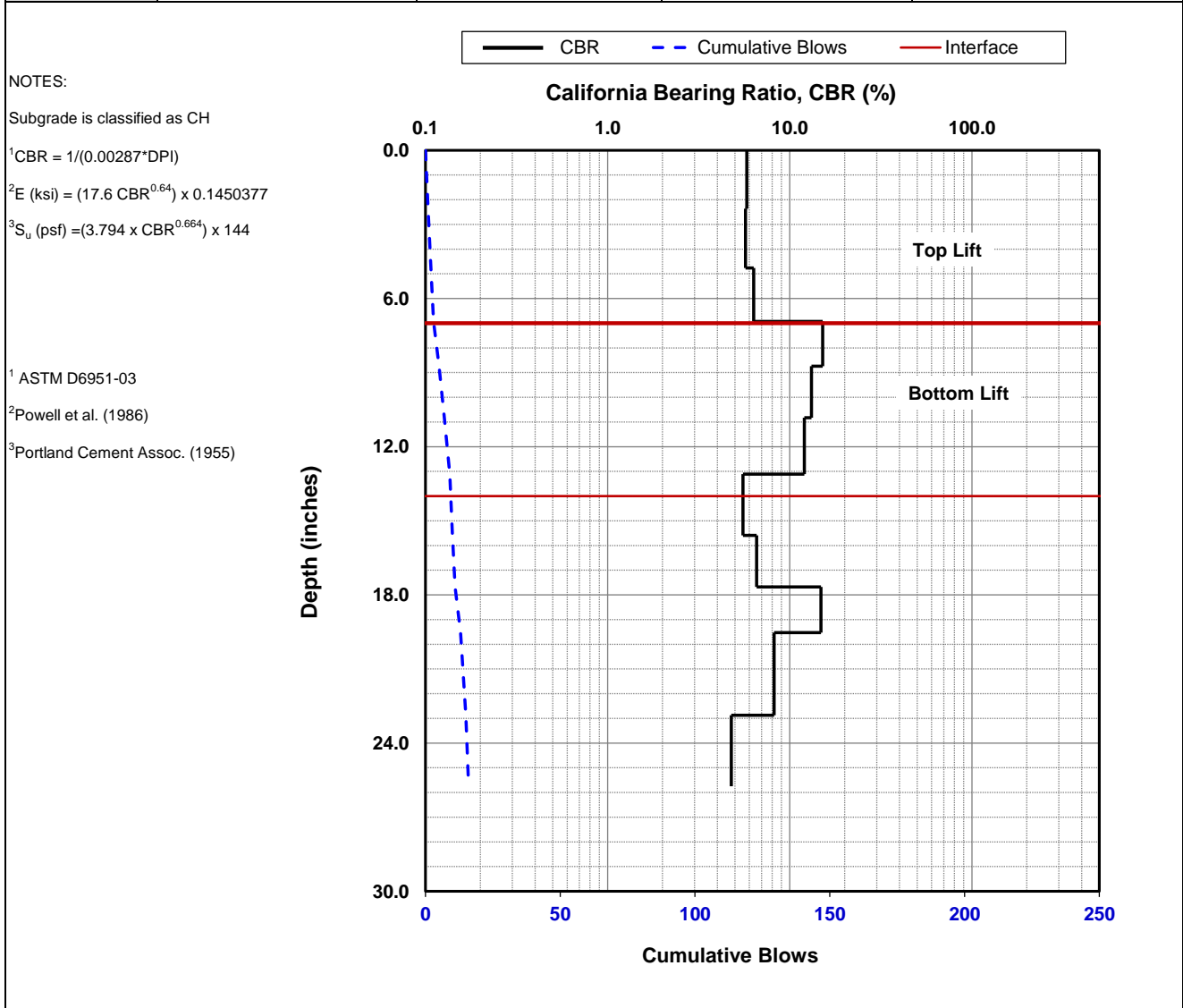
Parameter	DPI (mm/blow)	CBR (%)	E _{CBR} , Elastic Modulus (ksi) (non stress-dependent)	S _{u-CBR} , Bearing Capacity (psf)
Avg. PGE+CA6 Layer [0 to 9.0 in.]	5.5	42.9	28.3	6,624
Avg. Subgrade Layer [9.0 to 21.0 in.]	13.9	15.4	14.7	3,353
Ratio of Avg. Top/Bottom Layer	0.4	2.8	1.9	2.0
Std.Dev.PGE+CA6 Layer [0 to 9 in.]	8.3	29.7	22.4	5,195
Std. Dev. Subgrade Layer [9.0 to 21.0 in.]	8.9	9.5	10.8	2,428



Dynamic Cone Penetrometer (DCP) Test Results		
Project Name:	Illinois Tollway - IC Research	
Project ID:	Elgin O'Hare Extension - IL Tollway	
Location:	IL390 (West of O'Hare)	

Date of Test	10/14/2016	Test ID	Pt. 66	Operator	DW/PV	ASTM	D6951
Latitude	41°58'50.02069"N		Longitude	87°56'24.88866"W		Elevation (ft)	NA
Location	Section 4662 (Embankment fill)		Station	NA			
Comments	Embankment fill placed with nominal 8 in. loose lift thickness (assumed as 7 in. compacted lift thickness). Per lab test results provided by Interra Services, subgrade classified as CH clay.						

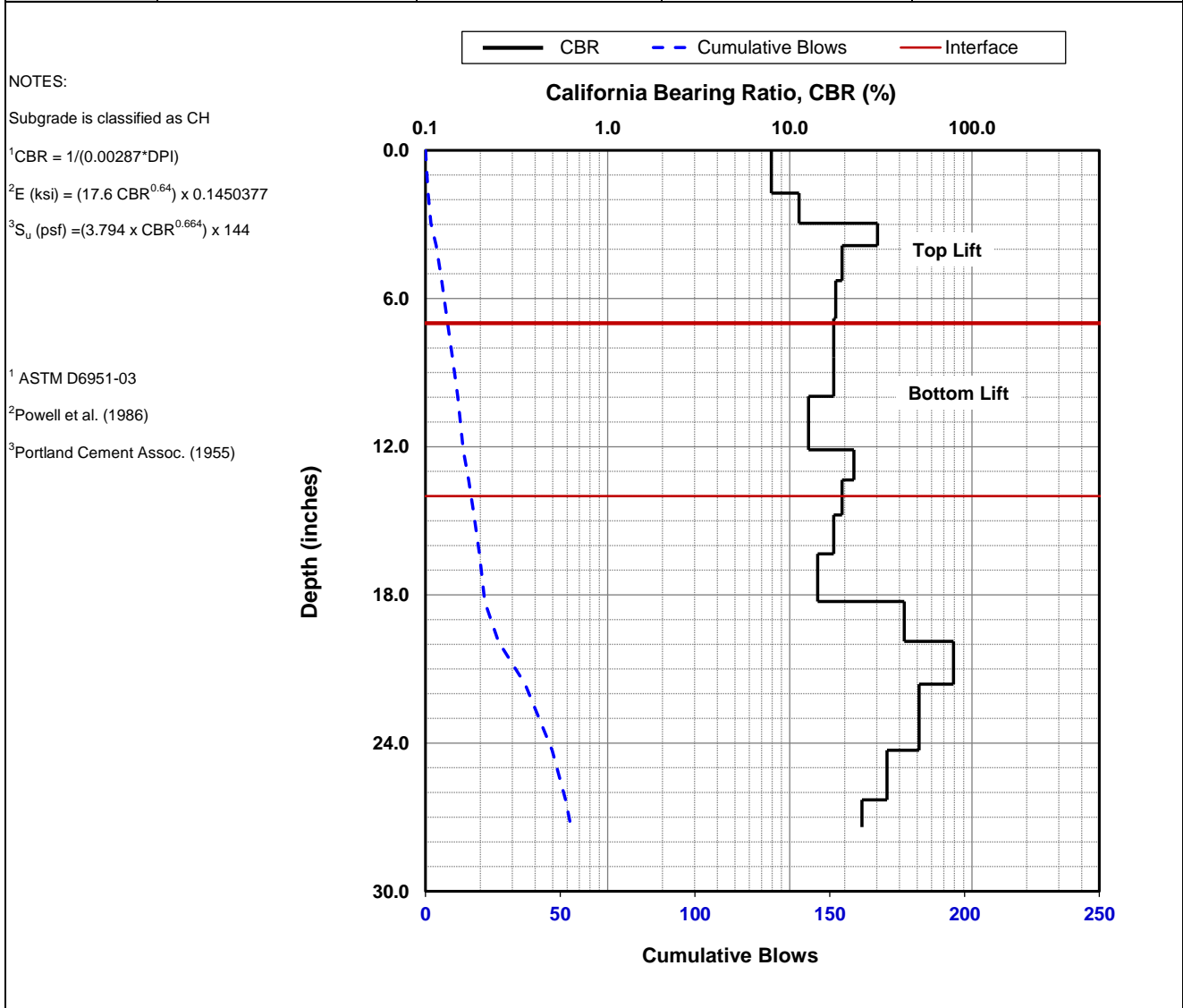
Parameter	DPI (mm/blow)	CBR (%)	E _{CBR} , Elastic Modulus (ksi) (non stress-dependent)	S _{u-CBR} , Bearing Capacity (psf)
Avg. Top Lift [0 to 7.0 in.]	58.7	5.9	8.0	1,783
Avg. Bottom Lift [7.0 to 14.0 in.]	26.2	13.3	13.4	3,048
Ratio of Avg. Top/Bottom Lift	2.2	0.4	0.6	0.6
Std. Dev. Top Lift [0 to 7.0 in.]	2.7	0.3	1.1	237
Std. Dev. Bottom Lift [7.0 to 14.0 in.]	3.0	1.6	3.4	742



Dynamic Cone Penetrometer (DCP) Test Results		
Project Name:	Illinois Tollway - IC Research	
Project ID:	Elgin O'Hare Extension - IL Tollway	
Location:	IL390 (West of O'Hare)	

Date of Test	10/14/2016	Test ID	Pt. 67	Operator	DW/PV	ASTM	D6951
Latitude	41°58'50.23744"N		Longitude	87°56'25.08738"W		Elevation (ft)	NA
Location	Section 4662 (Embankment fill)		Station	NA			
Comments	Embankment fill placed with nominal 8 in. loose lift thickness (assumed as 7 in. compacted lift thickness). Per lab test results provided by Interra Services, subgrade clasified as CH clay.						

Parameter	DPI (mm/blow)	CBR (%)	E _{CBR} , Elastic Modulus (ksi) (non stress-dependent)	S _{u-CBR} , Bearing Capacity (psf)
Avg. Top Lift [0 to 7.0 in.]	21.6	16.1	15.1	3,460
Avg. Bottom Lift [7.0 to 14.0 in.]	20.2	17.2	15.8	3,620
Ratio of Avg. Top/Bottom Lift	1.1	0.9	1.0	1.0
Std. Dev. Top Lift [0 to 7.0 in.]	13.9	8.6	10.1	2,285
Std. Dev. Bottom Lift [7.0 to 14.0 in.]	4.5	3.6	5.8	1,271

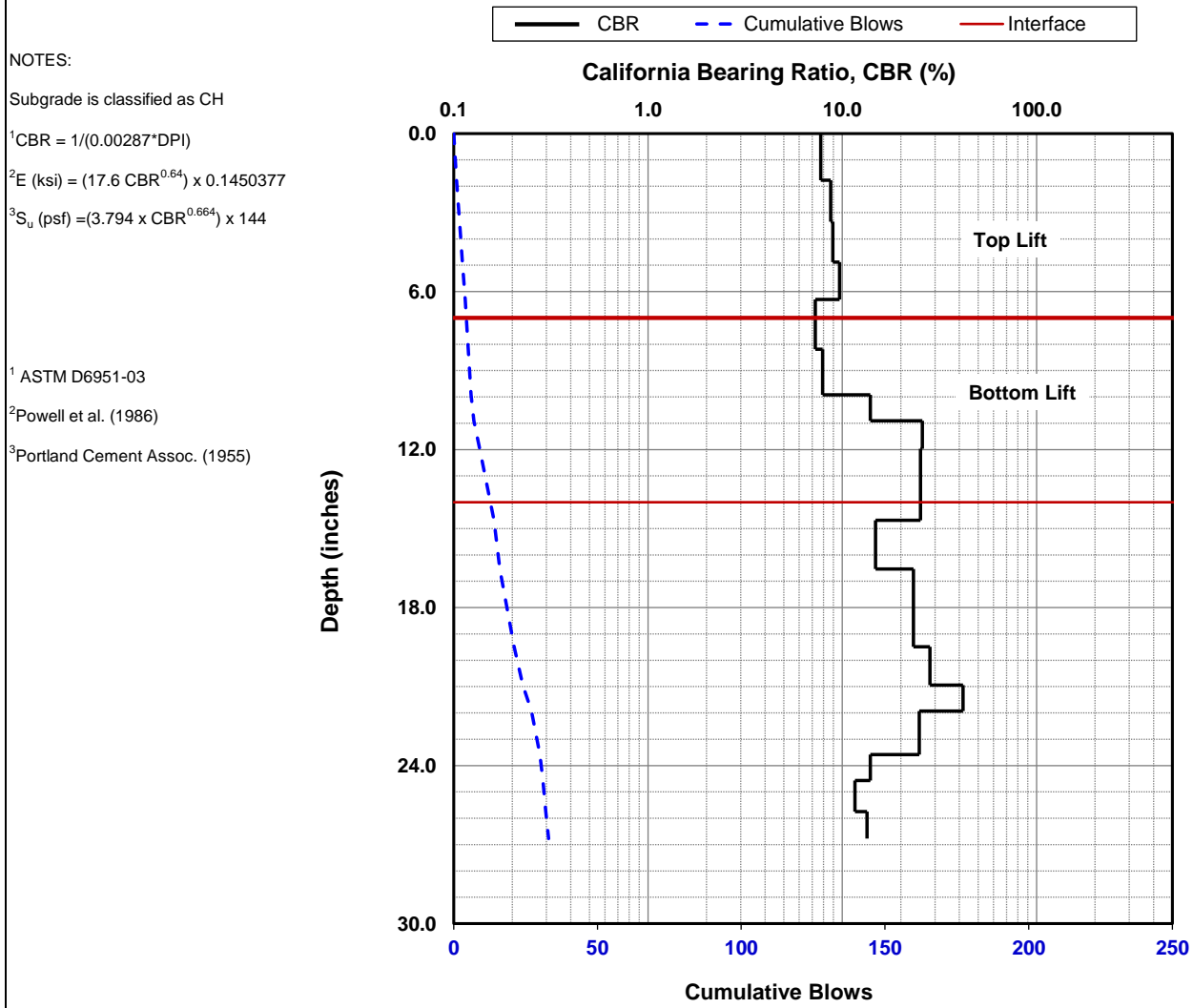


Dynamic Cone Penetrometer (DCP) Test Results	
Project Name:	Illinois Tollway - IC Research
Project ID:	Elgin O'Hare Extension - IL Tollway
Location:	IL390 (West of O'Hare)



Date of Test	10/14/2016	Test ID	Pt. 68	Operator	DW/PV	ASTM	D6951
Latitude	41°58'50.42781"N		Longitude	87°56'25.08597"W		Elevation (ft)	NA
Location	Section 4662 (Embankment fill)		Station	NA			
Comments	Embankment fill placed with nominal 8 in. loose lift thickness (assumed as 7 in. compacted lift thickness). Per lab test results provided by Interra Services, subgrade clasified as CH clay.						

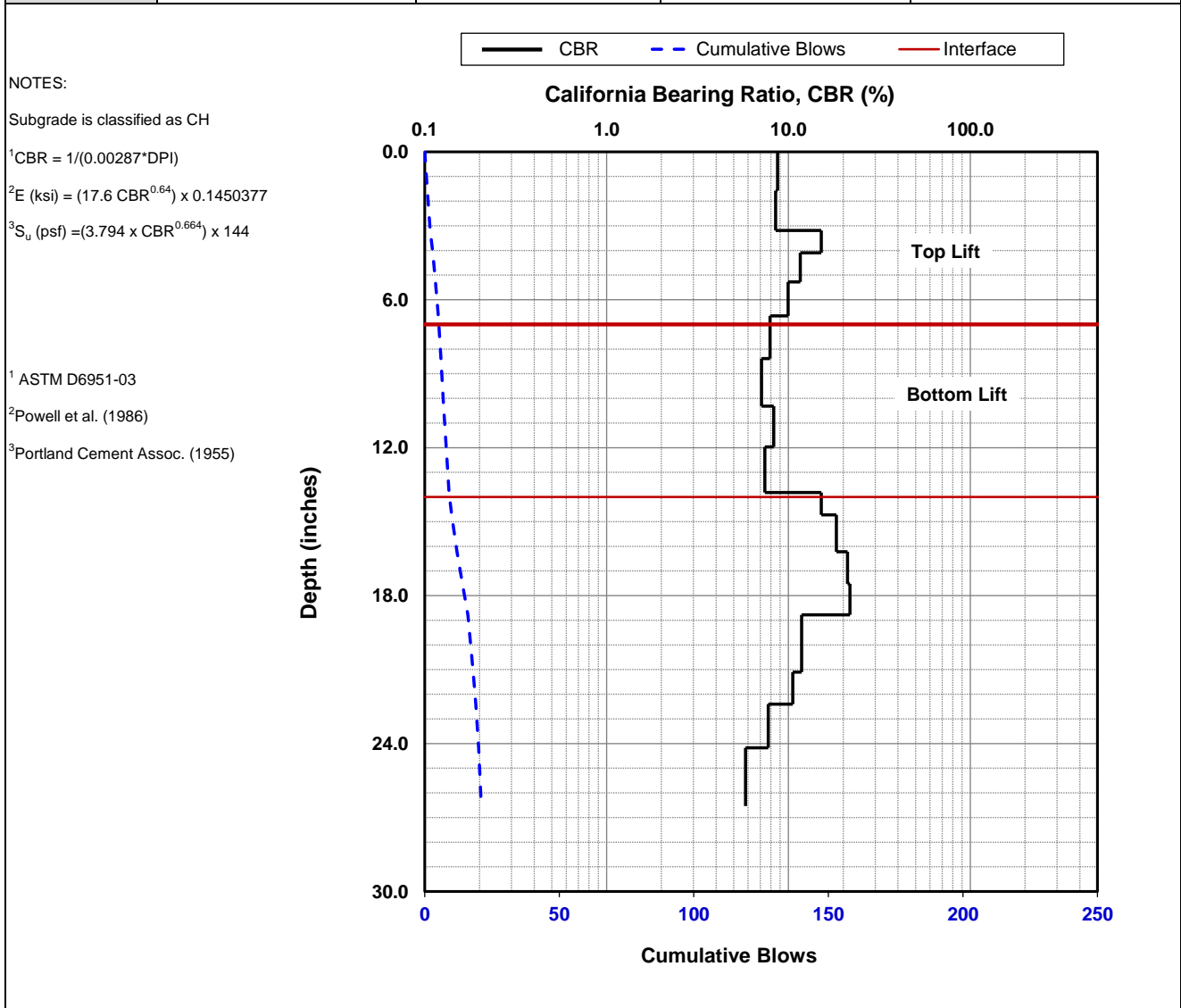
Parameter	DPI (mm/blow)	CBR (%)	E _{CBR} , Elastic Modulus (ksi) (non stress-dependent)	S _{u-CBR} , Bearing Capacity (psf)
Avg. Top Lift [0 to 7.0 in.]	40.0	8.7	10.2	2,300
Avg. Bottom Lift [7.0 to 14.0 in.]	21.3	16.4	15.3	3,494
Ratio of Avg. Top/Bottom Lift	1.9	0.5	0.7	0.7
Std. Dev. Top Lift [0 to 7.0 in.]	3.9	0.8	2.3	482
Std. Dev. Bottom Lift [7.0 to 14.0 in.]	16.4	9.1	10.5	2,359



Dynamic Cone Penetrometer (DCP) Test Results		
Project Name:	Illinois Tollway - IC Research	
Project ID:	Elgin O'Hare Extension - IL Tollway	
Location:	IL390 (West of O'Hare)	

Date of Test	10/14/2016	Test ID	Pt. 69	Operator	DW/PV	ASTM	D6951
Latitude	41°58'50.68561"N		Longitude	87°56'25.08232"W		Elevation (ft)	NA
Location	Section 4662 (Embankment fill)		Station	NA			
Comments	Embankment fill placed with nominal 8 in. loose lift thickness (assumed as 7 in. compacted lift thickness). Per lab test results provided by Interra Services, subgrade clasified as CH clay.						

Parameter	DPI (mm/blow)	CBR (%)	E _{CBR} , Elastic Modulus (ksi) (non stress-dependent)	S _{u-CBR} , Bearing Capacity (psf)
Avg. Top Lift [0 to 7.0 in.]	33.8	10.3	11.4	2,572
Avg. Bottom Lift [7.0 to 14.0 in.]	45.5	7.7	9.4	2,111
Ratio of Avg. Top/Bottom Lift	0.7	1.3	1.2	1.2
Std. Dev. Top Lift [0 to 7.0 in.]	7.1	2.6	4.7	1,028
Std. Dev. Bottom Lift [7.0 to 14.0 in.]	10.4	3.4	5.6	1,224



Dynamic Cone Penetrometer (DCP) Test Results	
Project Name:	Illinois Tollway - IC Research
Project ID:	Elgin O'Hare Extension - IL Tollway
Location:	IL390 (West of O'Hare)

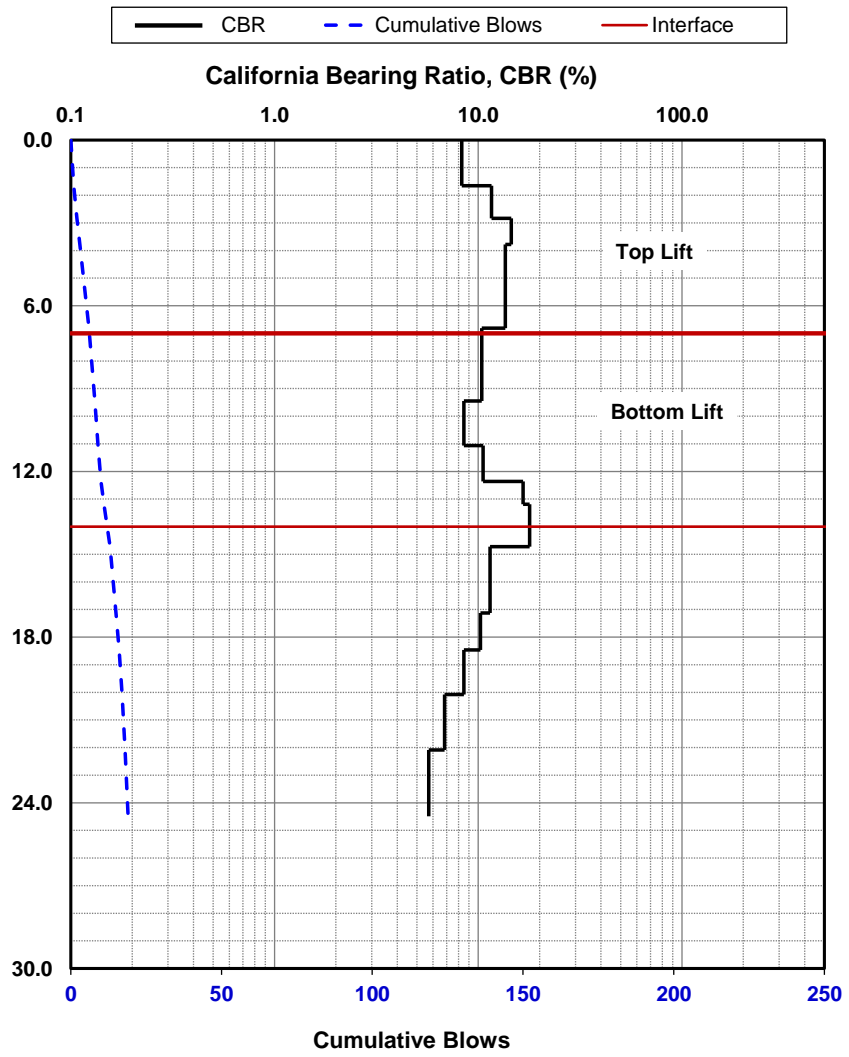


Date of Test	10/14/2016	Test ID	Pt. 70	Operator	DW/PV	ASTM	D6951
Latitude	41°58'50.64107"N		Longitude	87°56'24.93070"W		Elevation (ft)	NA
Location	Section 4662 (Embankment fill)		Station	NA			
Comments	Embankment fill placed with nominal 8 in. loose lift thickness (assumed as 7 in. compacted lift thickness). Per lab test results provided by Interra Services, subgrade clasified as CH clay.						

Parameter	DPI (mm/blow)	CBR (%)	E _{CBR} , Elastic Modulus (ksi) (non stress-dependent)	S _{u-CBR} , Bearing Capacity (psf)
Avg. Top Lift [0 to 7.0 in.]	28.8	12.1	12.6	2,858
Avg. Bottom Lift [7.0 to 14.0 in.]	28.7	12.1	12.6	2,866
Ratio of Avg. Top/Bottom Lift	1.0	1.0	1.0	1.0
Std. Dev. Top Lift [0 to 7.0 in.]	8.7	2.9	5.0	1,108
Std. Dev. Bottom Lift [7.0 to 14.0 in.]	9.1	4.2	6.4	1,409

NOTES:
 Subgrade is classified as CH
¹CBR = 1/(0.00287*DPI)
²E (ksi) = (17.6 CBR^{0.64}) x 0.1450377
³S_u (psf) =(3.794 x CBR^{0.664}) x 144

¹ ASTM D6951-03
²Powell et al. (1986)
³Portland Cement Assoc. (1955)

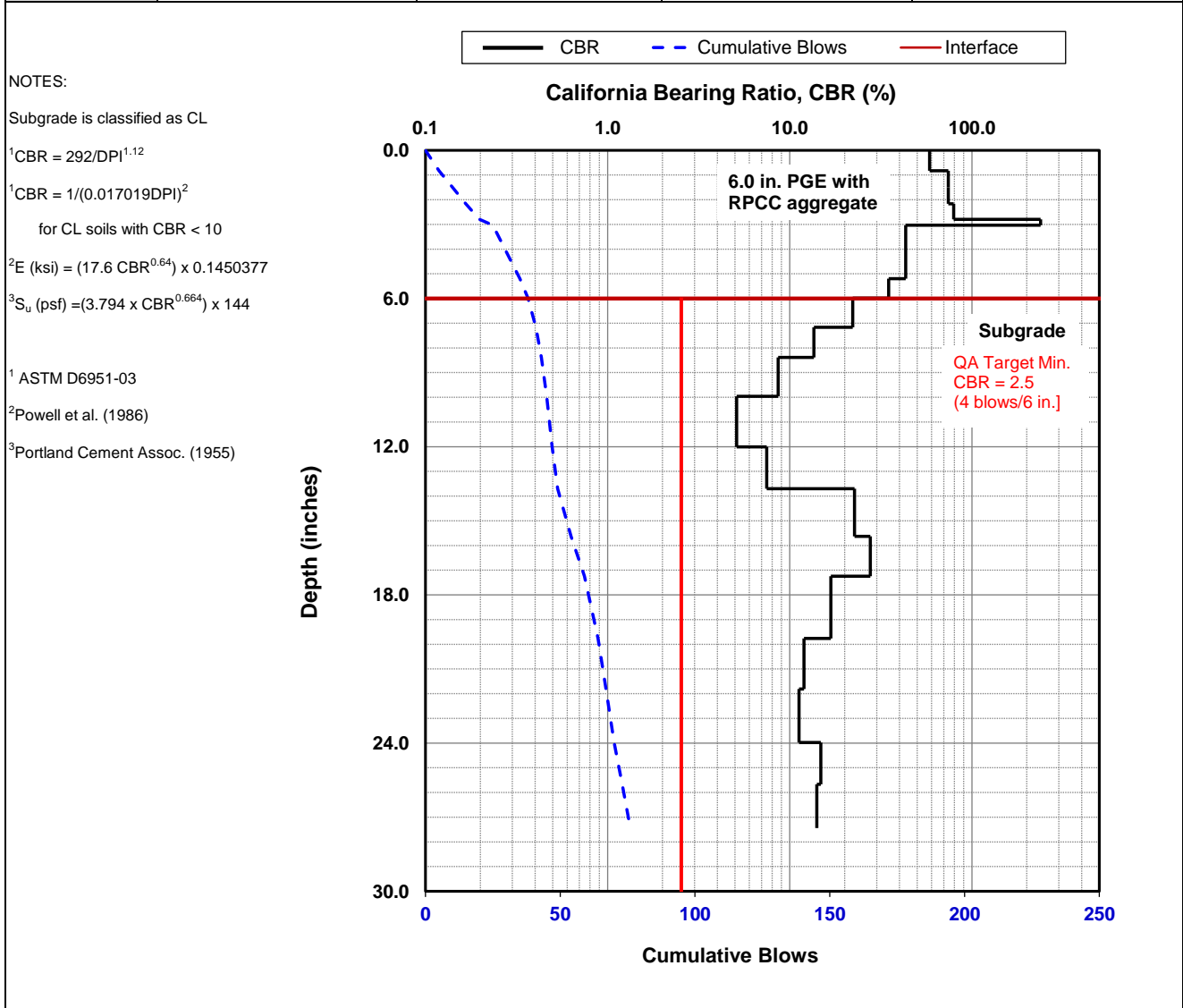


Dynamic Cone Penetrometer (DCP) Test Results	
Project Name:	Illinois Tollway - IC Research
Project ID:	Elgin O'Hare Extension - IL Tollway
Location:	IL390 (West of O'Hare)



Date of Test	4/11/2017	Test ID	TS6_Pt. 1	Operator	PV	ASTM	D6951
Latitude	41.9837096	Longitude	-87.9737274	Elevation (ft)	NA		
Location	Section 4642 (PGE)	Station	NA				
Comments	Nominal 6 in. of compacted PGE with RPCC crushed aggregate. <i>Subgrade assumed as CL clay.</i> PGE prepared in Fall 2016.						

Parameter	DPI (mm/blow)	CBR (%)	E _{CBR} , Elastic Modulus (ksi) (non stress-dependent)	S _{u-CBR} , Bearing Capacity (psf)
Avg. PGE Layer [0 to 6.0 in.]	4.0	61.8	35.8	8,448
Avg. Subgrade Layer [6.0 to 18.0 in.]	13.5	15.9	15.0	3,426
Ratio of Avg. Top/Bottom Layer	0.3	3.9	2.4	2.5
Std. Dev. PGE Layer [0 to 6.0 in.]	1.6	64.7	36.8	8,708
Std. Dev. Subgrade Layer [6.0 to 18.0 in.]	6.4	8.2	9.8	2,206



Dynamic Cone Penetrometer (DCP) Test Results	
Project Name:	Illinois Tollway - IC Research
Project ID:	Elgin O'Hare Extension - IL Tollway
Location:	IL390 (West of O'Hare)



Date of Test	4/11/2017	Test ID	TS6_Pt. 2	Operator	PV	ASTM	D6951
Latitude	41.9837489	Longitude	-87.9738580	Elevation (ft)	NA		
Location	Section 4642 (PGE)	Station	NA				
Comments	Nominal 6 in. of compacted PGE with RPCC crushed aggregate. <i>Subgrade assumed as CL clay.</i> PGE prepared in Fall 2016.						

Parameter	DPI (mm/blow)	CBR (%)	E _{CBR} , Elastic Modulus (ksi) (non stress-dependent)	S _{u-CBR} , Bearing Capacity (psf)
Avg. PGE Layer [0 to 6.0 in.]	13.6	15.7	14.8	3,393
Avg. Subgrade Layer [6.0 to 18.0 in.]	19.6	9.0	10.4	2,344
Ratio of Avg. Top/Bottom Layer	0.7	1.7	1.4	1.4
Std. Dev. PGE Layer [0 to 6.0 in.]	3.1	3.8	6.0	1,323
Std. Dev. Subgrade Layer [6.0 to 18.0 in.]	5.0	3.9	6.1	1,351

NOTES:

Subgrade is classified as CL

¹CBR = 292/DPI^{1.12}

¹CBR = 1/(0.017019DPI)²
for CL soils with CBR < 10

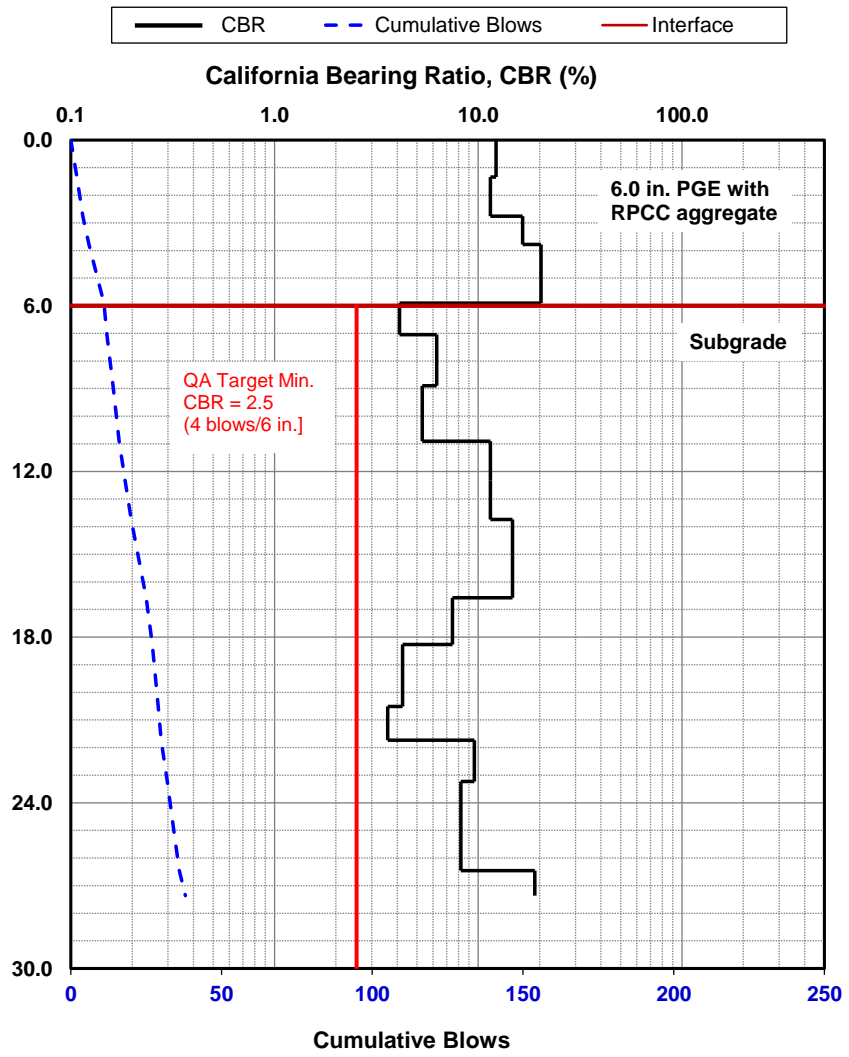
²E (ksi) = (17.6 CBR^{0.64}) x 0.1450377

³S_u (psf) = (3.794 x CBR^{0.664}) x 144

¹ ASTM D6951-03

² Powell et al. (1986)

³ Portland Cement Assoc. (1955)

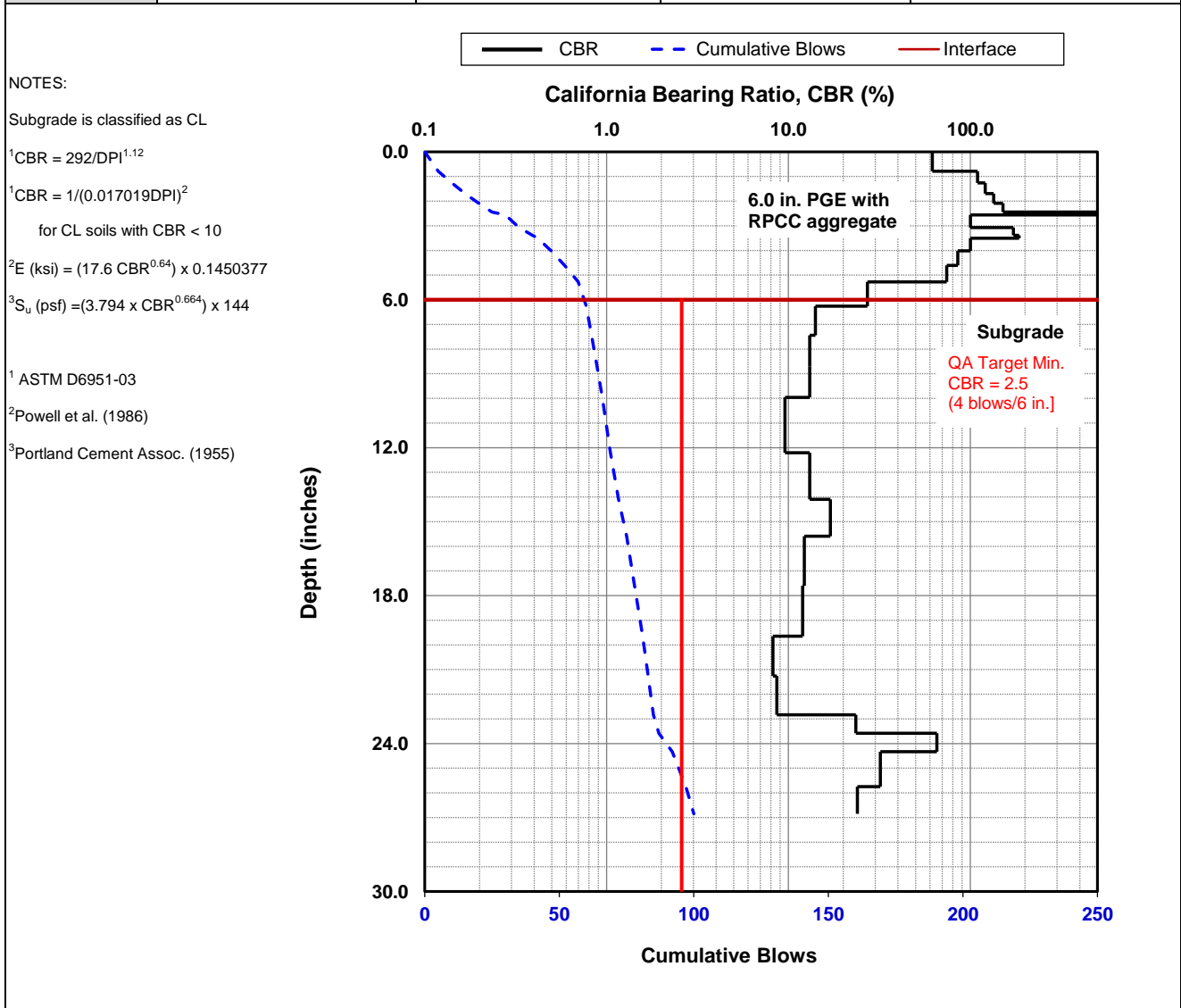


Dynamic Cone Penetrometer (DCP) Test Results	
Project Name:	Illinois Tollway - IC Research
Project ID:	Elgin O'Hare Extension - IL Tollway
Location:	IL390 (West of O'Hare)



Date of Test	4/11/2017	Test ID	TS6_Pt. 3	Operator	PV	ASTM	D6951
Latitude	41.9836796	Longitude	-87.97409220	Elevation (ft)	NA		
Location	Section 4642 (PGE)	Station	NA				
Comments	Nominal 6 in. of compacted PGE with RPCC crushed aggregate. <i>Subgrade assumed as CL clay.</i> PGE prepared in Fall 2016.						

Parameter	DPI (mm/blow)	CBR (%)	E _{CBR} , Elastic Modulus (ksi) (non stress-dependent)	S _{u-CBR} , Bearing Capacity (psf)
Avg. PGE Layer [0 to 6.0 in.]	2.7	98.0	48.0	11,474
Avg. Subgrade Layer [6.0 to 18.0 in.]	16.0	13.1	13.2	3,013
Ratio of Avg. Top/Bottom Layer	0.2	7.5	3.6	3.8
Std. Dev. PGE Layer [0 to 6.0 in.]	1.8	118.4	54.2	13,007
Std. Dev. Subgrade Layer [6.0 to 18.0 in.]	1.9	2.2	4.2	926

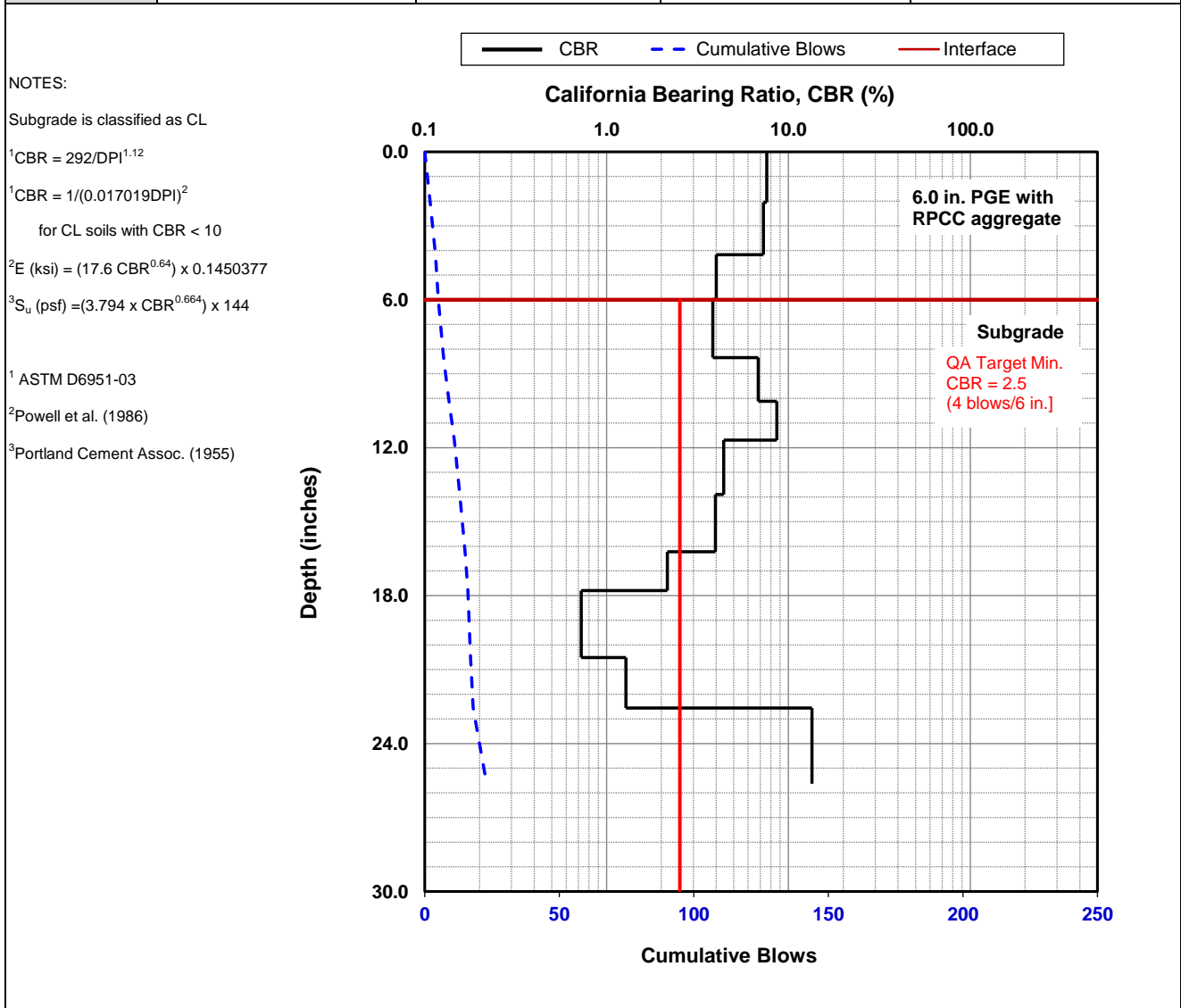


Dynamic Cone Penetrometer (DCP) Test Results	
Project Name:	Illinois Tollway - IC Research
Project ID:	Elgin O'Hare Extension - IL Tollway
Location:	IL390 (West of O'Hare)



Date of Test	4/11/2017	Test ID	TS6_Pt. 4	Operator	PV	ASTM	D6951
Latitude	41.9837630	Longitude	-87.9741493	Elevation (ft)	NA		
Location	Section 4642 (PGE)	Station	NA				
Comments	Nominal 6 in. of compacted PGE with RPCC crushed aggregate. <i>Subgrade assumed as CL clay.</i> PGE prepared in Fall 2016.						

Parameter	DPI (mm/blow)	CBR (%)	E _{CBR} , Elastic Modulus (ksi) (non stress-dependent)	S _{u-CBR} , Bearing Capacity (psf)
Avg. PGE Layer [0 to 6.0 in.]	30.4	6.4	8.4	1,869
Avg. Subgrade Layer [6.0 to 18.0 in.]	27.3	4.6	6.8	1,514
Ratio of Avg. Top/Bottom Layer	1.1	1.4	1.2	1.2
Std. Dev. PGE Layer [0 to 6.0 in.]	9.8	1.7	3.6	791
Std. Dev. Subgrade Layer [6.0 to 18.0 in.]	7.0	2.3	4.4	960

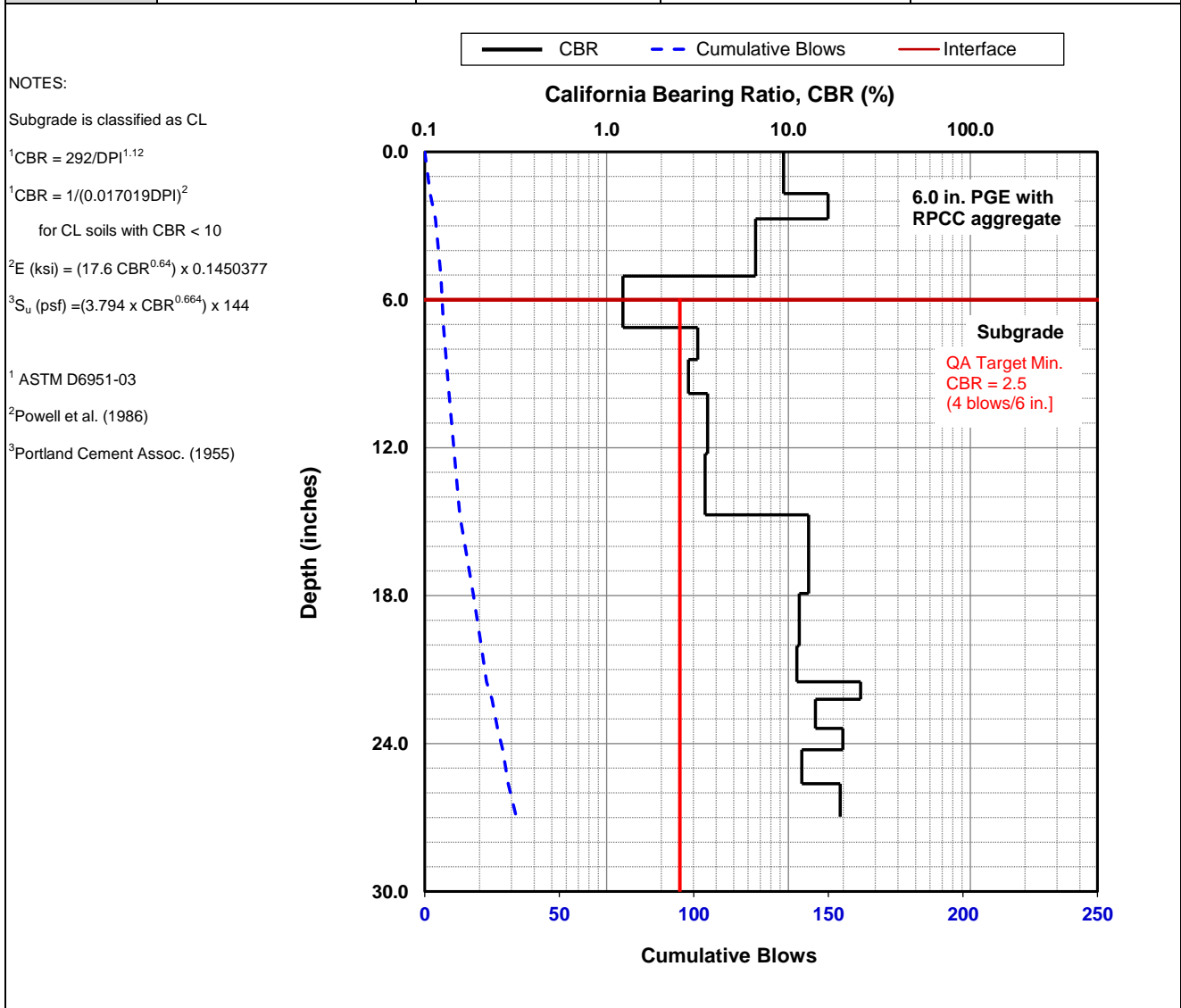


Dynamic Cone Penetrometer (DCP) Test Results	
Project Name:	Illinois Tollway - IC Research
Project ID:	Elgin O'Hare Extension - IL Tollway
Location:	IL390 (West of O'Hare)



Date of Test	4/11/2017	Test ID	TS6_Pt. 5	Operator	PV	ASTM	D6951
Latitude	41.9837612	Longitude	-87.9744120	Elevation (ft)	NA		
Location	Section 4642 (PGE)	Station	NA				
Comments	Nominal 6 in. of compacted PGE with RPCC crushed aggregate. <i>Subgrade assumed as CL clay.</i> PGE prepared in Fall 2016.						

Parameter	DPI (mm/blow)	CBR (%)	E _{CBR} , Elastic Modulus (ksi) (non stress-dependent)	S _{u-CBR} , Bearing Capacity (psf)
Avg. PGE Layer [0 to 6.0 in.]	21.3	9.5	10.8	2,433
Avg. Subgrade Layer [6.0 to 18.0 in.]	27.3	4.6	6.8	1,516
Ratio of Avg. Top/Bottom Layer	0.8	2.0	1.6	1.6
Std. Dev. PGE Layer [0 to 6.0 in.]	6.7	4.2	6.4	1,425
Std. Dev. Subgrade Layer [6.0 to 18.0 in.]	11.8	4.2	6.4	1,415



Dynamic Cone Penetrometer (DCP) Test Results	
Project Name:	Illinois Tollway - IC Research
Project ID:	Elgin O'Hare Extension - IL Tollway
Location:	IL390 (West of O'Hare)



Date of Test	4/11/2017	Test ID	TS6_Pt. 6	Operator	PV	ASTM	D6951
Latitude	41.9836917	Longitude	-87.9746838	Elevation (ft)	NA		
Location	Section 4642 (PGE)	Station	NA				
Comments	Nominal 6 in. of compacted PGE with RPCC crushed aggregate. <i>Subgrade assumed as CL clay.</i> PGE prepared in Fall 2016.						

Parameter	DPI (mm/blow)	CBR (%)	E _{CBR} , Elastic Modulus (ksi) (non stress-dependent)	S _{u-CBR} , Bearing Capacity (psf)
Avg. PGE Layer [0 to 6.0 in.]	4.8	50.0	31.2	7,339
Avg. Subgrade Layer [6.0 to 18.0 in.]	20.9	7.9	9.6	2,158
Ratio of Avg. Top/Bottom Layer	0.2	6.3	3.3	3.4
Std. Dev. PGE Layer [0 to 6.0 in.]	0.7	7.4	9.2	2,067
Std. Dev. Subgrade Layer [6.0 to 18.0 in.]	12.8	10.8	11.7	2,650

NOTES:

Subgrade is classified as CL

¹CBR = 292/DPI^{1.12}

¹CBR = 1/(0.017019DPI)²

for CL soils with CBR < 10

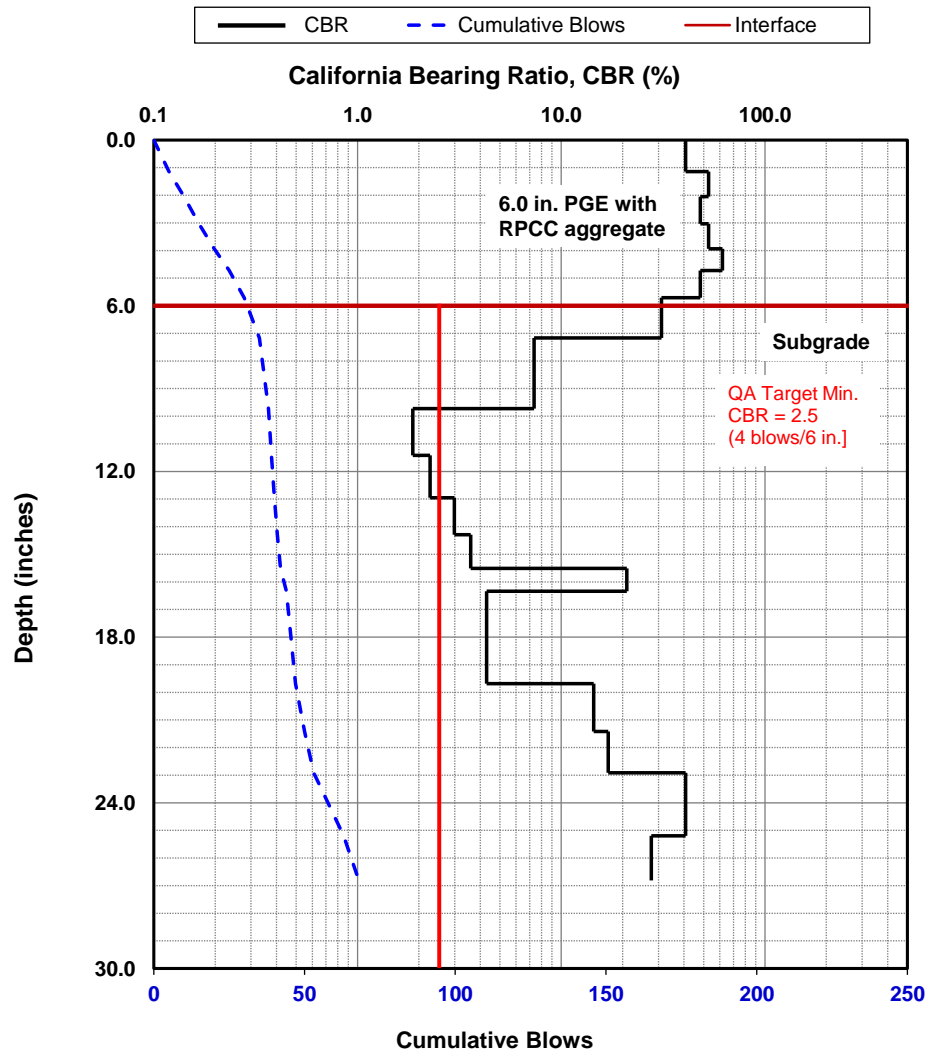
²E (ksi) = (17.6 CBR^{0.64}) x 0.1450377

³S_u (psf) = (3.794 x CBR^{0.664}) x 144

¹ ASTM D6951-03

² Powell et al. (1986)

³ Portland Cement Assoc. (1955)



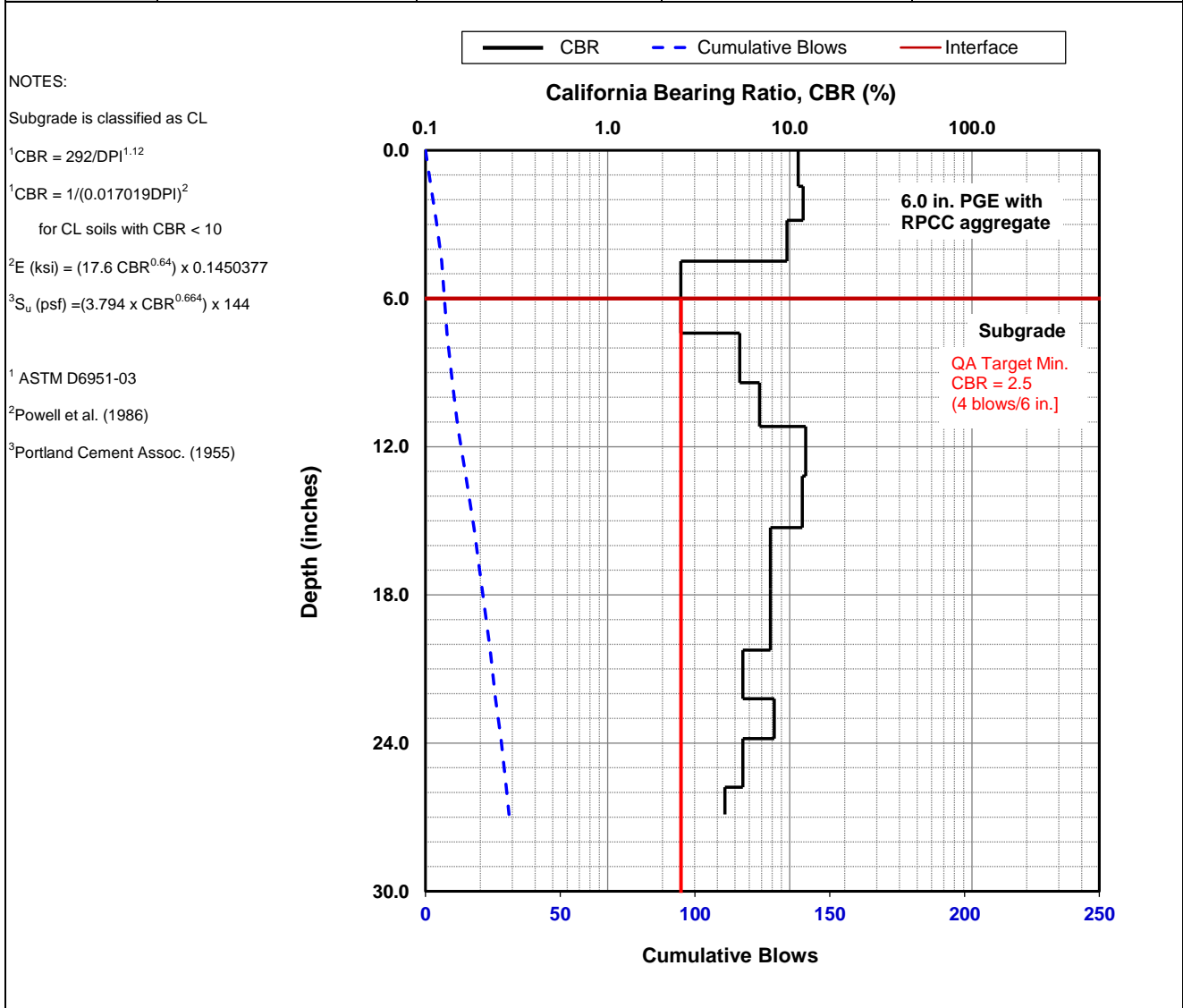
Dynamic Cone Penetrometer (DCP) Test Results

Project Name: Illinois Tollway - IC Research
 Project ID: Elgin O'Hare Extension - IL Tollway
 Location: IL390 (West of O'Hare)



Date of Test	4/11/2017	Test ID	TS6_Pt. 7	Operator	PV	ASTM	D6951
Latitude	41.9837554	Longitude	-87.9748499	Elevation (ft)	NA		
Location	Section 4642 (PGE)	Station	NA				
Comments	Nominal 6 in. of compacted PGE with RPCC crushed aggregate. <i>Subgrade assumed as CL clay.</i> PGE prepared in Fall 2016.						

Parameter	DPI (mm/blow)	CBR (%)	E _{CBR} , Elastic Modulus (ksi) (non stress-dependent)	S _{u-CBR} , Bearing Capacity (psf)
Avg. PGE Layer [0 to 6.0 in.]	23.5	8.5	10.0	2,264
Avg. Subgrade Layer [6.0 to 18.0 in.]	20.2	8.4	10.0	2,251
Ratio of Avg. Top/Bottom Layer	1.2	1.0	1.0	1.0
Std. Dev. PGE Layer [0 to 6.0 in.]	8.2	3.8	6.0	1,336
Std. Dev. Subgrade Layer [6.0 to 18.0 in.]	3.5	3.1	5.2	1,146



Dynamic Cone Penetrometer (DCP) Test Results	
Project Name:	Illinois Tollway - IC Research
Project ID:	Elgin O'Hare Extension - IL Tollway
Location:	IL390 (West of O'Hare)



Date of Test	4/11/2017	Test ID	TS6_Pt. 8	Operator	PV	ASTM	D6951
Latitude	41.9837359	Longitude	-87.9752143	Elevation (ft)	NA		
Location	Section 4642 (PGE)	Station	NA				
Comments	Nominal 6 in. of compacted PGE with RPCC crushed aggregate. <i>Subgrade assumed as CL clay.</i> PGE prepared in Fall 2016.						

Parameter	DPI (mm/blow)	CBR (%)	E _{CBR} , Elastic Modulus (ksi) (non stress-dependent)	S _{u-CBR} , Bearing Capacity (psf)
Avg. PGE Layer [0 to 6.0 in.]	4.0	61.3	35.6	8,403
Avg. Subgrade Layer [6.0 to 18.0 in.]	17.6	11.8	12.4	2,809
Ratio of Avg. Top/Bottom Layer	0.2	5.2	2.9	3.0
Std. Dev. PGE Layer [0 to 6.0 in.]	0.4	6.4	8.4	1,873
Std. Dev. Subgrade Layer [6.0 to 18.0 in.]	5.8	7.5	9.3	2,090

NOTES:

Subgrade is classified as CL

¹CBR = 292/DPI^{1.12}

¹CBR = 1/(0.017019DPI)²

for CL soils with CBR < 10

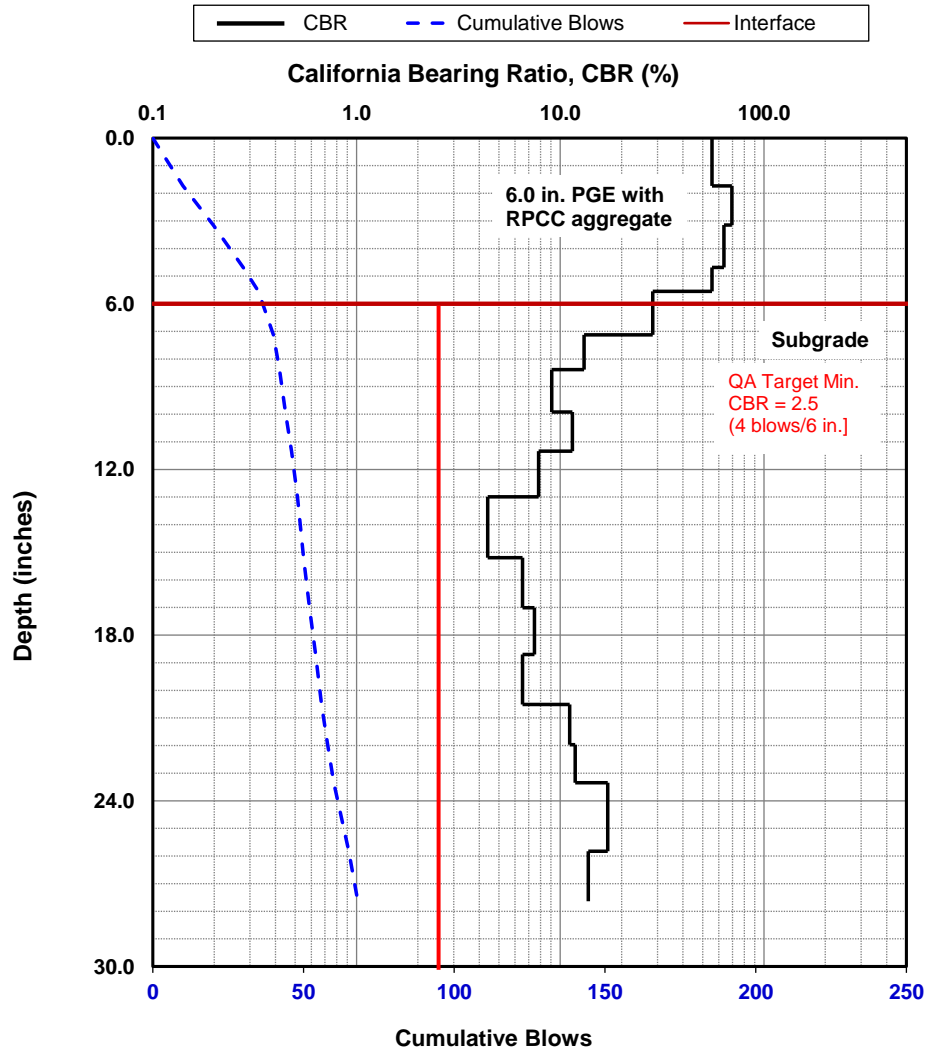
²E (ksi) = (17.6 CBR^{0.64}) x 0.1450377

³S_u (psf) = (3.794 x CBR^{0.664}) x 144

¹ ASTM D6951-03

² Powell et al. (1986)

³ Portland Cement Assoc. (1955)



Dynamic Cone Penetrometer (DCP) Test Results

Project Name: Illinois Tollway - IC Research
 Project ID: Elgin O'Hare Extension - IL Tollway
 Location: IL390 (West of O'Hare)



Date of Test	4/11/2017	Test ID	TS6_Pt. 9	Operator	PV	ASTM	D6951
Latitude	41.9837096	Longitude	-87.9755314	Elevation (ft)	NA		
Location	Section 4642 (PGE)	Station	NA				
Comments	Nominal 6 in. of compacted PGE with RPCC crushed aggregate. <i>Subgrade assumed as CL clay.</i> PGE prepared in Fall 2016.						

Parameter	DPI (mm/blow)	CBR (%)	E _{CBR} , Elastic Modulus (ksi) (non stress-dependent)	S _{u-CBR} , Bearing Capacity (psf)
Avg. PGE Layer [0 to 6.0 in.]	4.4	55.6	33.4	7,878
Avg. Subgrade Layer [6.0 to 18.0 in.]	26.3	5.0	7.2	1,593
Ratio of Avg. Top/Bottom Layer	0.2	11.1	4.7	4.9
Std. Dev. PGE Layer [0 to 6.0 in.]	1.2	14.4	14.1	3,212
Std. Dev. Subgrade Layer [6.0 to 18.0 in.]	5.8	4.0	6.2	1,377

NOTES:

Subgrade is classified as CL

¹CBR = 292/DPI^{1.12}

¹CBR = 1/(0.017019DPI)²

for CL soils with CBR < 10

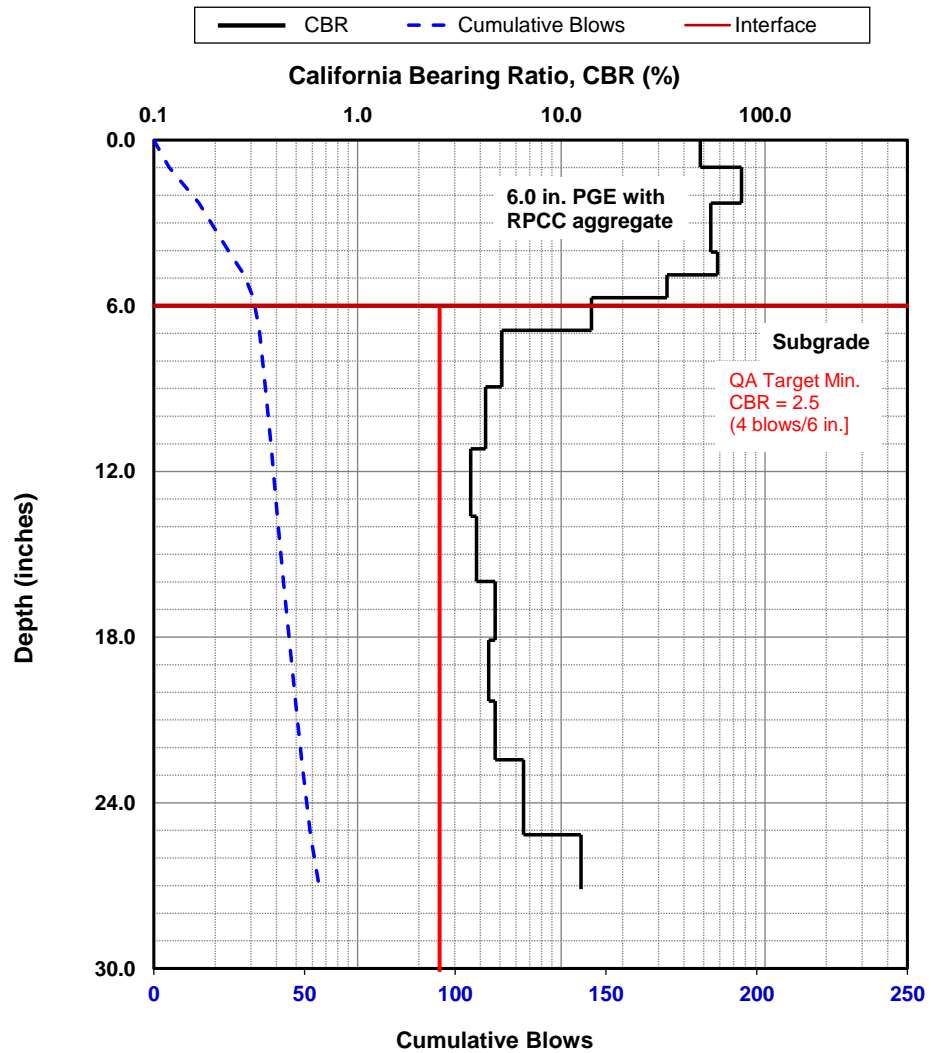
²E (ksi) = (17.6 CBR^{0.64}) x 0.1450377

³S_u (psf) = (3.794 x CBR^{0.664}) x 144

¹ ASTM D6951-03

² Powell et al. (1986)

³ Portland Cement Assoc. (1955)



Dynamic Cone Penetrometer (DCP) Test Results

Project Name: Illinois Tollway - IC Research
 Project ID: Elgin O'Hare Extension - IL Tollway
 Location: IL390 (West of O'Hare)



Date of Test	4/11/2017	Test ID	TS6_Pt. 10	Operator	PV	ASTM	D6951
Latitude	41.9837832	Longitude	-87.9757277	Elevation (ft)	NA		
Location	Section 4642 (PGE)	Station	NA				
Comments	Nominal 6 in. of compacted PGE with RPCC crushed aggregate. <i>Subgrade assumed as CL clay.</i> PGE prepared in Fall 2016.						

Parameter	DPI (mm/blow)	CBR (%)	E _{CBR} , Elastic Modulus (ksi) (non stress-dependent)	S _{u-CBR} , Bearing Capacity (psf)
Avg. PGE Layer [0 to 6.0 in.]	15.9	13.2	13.3	3,027
Avg. Subgrade Layer [6.0 to 18.0 in.]	35.0	2.8	5.0	1,087
Ratio of Avg. Top/Bottom Layer	0.5	4.7	2.7	2.8
Std. Dev. PGE Layer [0 to 6.0 in.]	4.7	5.1	7.2	1,604
Std. Dev. Subgrade Layer [6.0 to 18.0 in.]	9.2	1.3	3.0	644

NOTES:

Subgrade is classified as CL

¹CBR = 292/DPI^{1.12}

¹CBR = 1/(0.017019DPI)²

for CL soils with CBR < 10

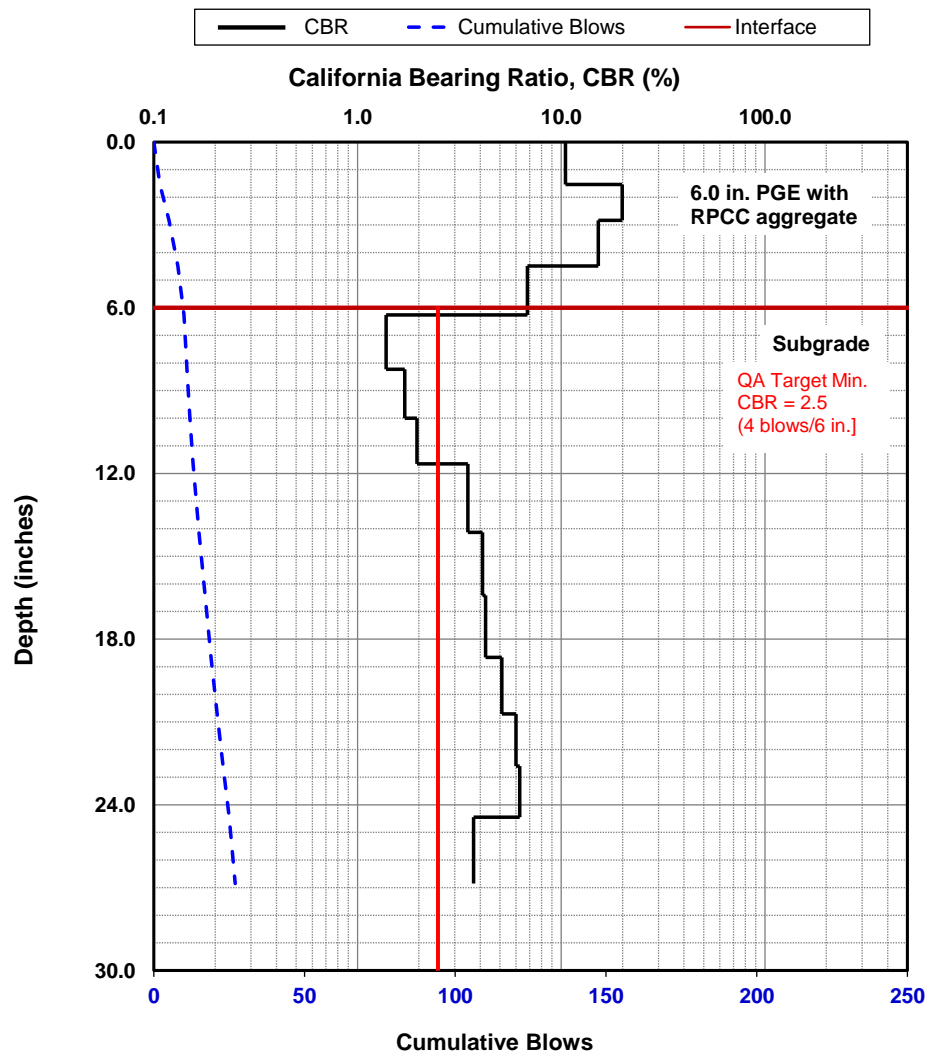
²E (ksi) = (17.6 CBR^{0.64}) x 0.1450377

³S_u (psf) = (3.794 x CBR^{0.664}) x 144

¹ ASTM D6951-03

² Powell et al. (1986)

³ Portland Cement Assoc. (1955)



Dynamic Cone Penetrometer (DCP) Test Results

Project Name: Illinois Tollway - IC Research
 Project ID: Elgin O'Hare Extension - IL Tollway
 Location: IL390 (West of O'Hare)



Date of Test	4/11/2017	Test ID	TS6_Pt. 11	Operator	PV	ASTM	D6951
Latitude	41.9837736	Longitude	-87.9762332	Elevation (ft)	NA		
Location	Section 4642 (PGE)	Station	NA				
Comments	Nominal 6 in. of compacted PGE with RPCC crushed aggregate. <i>Subgrade assumed as CL clay.</i> PGE prepared in Fall 2016.						

Parameter	DPI (mm/blow)	CBR (%)	E _{CBR} , Elastic Modulus (ksi) (non stress-dependent)	S _{u-CBR} , Bearing Capacity (psf)
Avg. PGE Layer [0 to 6.0 in.]	7.0	33.0	23.9	5,572
Avg. Subgrade Layer [6.0 to 18.0 in.]	NA (refusal - rock)	NA (refusal - rock)	NA (refusal - rock)	NA (refusal - rock)
Ratio of Avg. Top/Bottom Layer	NA	NA	NA	NA
Std. Dev. PGE Layer [0 to 6.0 in.]	3.6	22.9	19.0	4,373
Std. Dev. Subgrade Layer [6.0 to 18.0 in.]	NA (refusal - rock)	NA (refusal - rock)	NA (refusal - rock)	NA (refusal - rock)

NOTES:

Subgrade is classified as CL

¹CBR = 292/DPI^{1.12}

¹CBR = 1/(0.017019DPI)²

for CL soils with CBR < 10

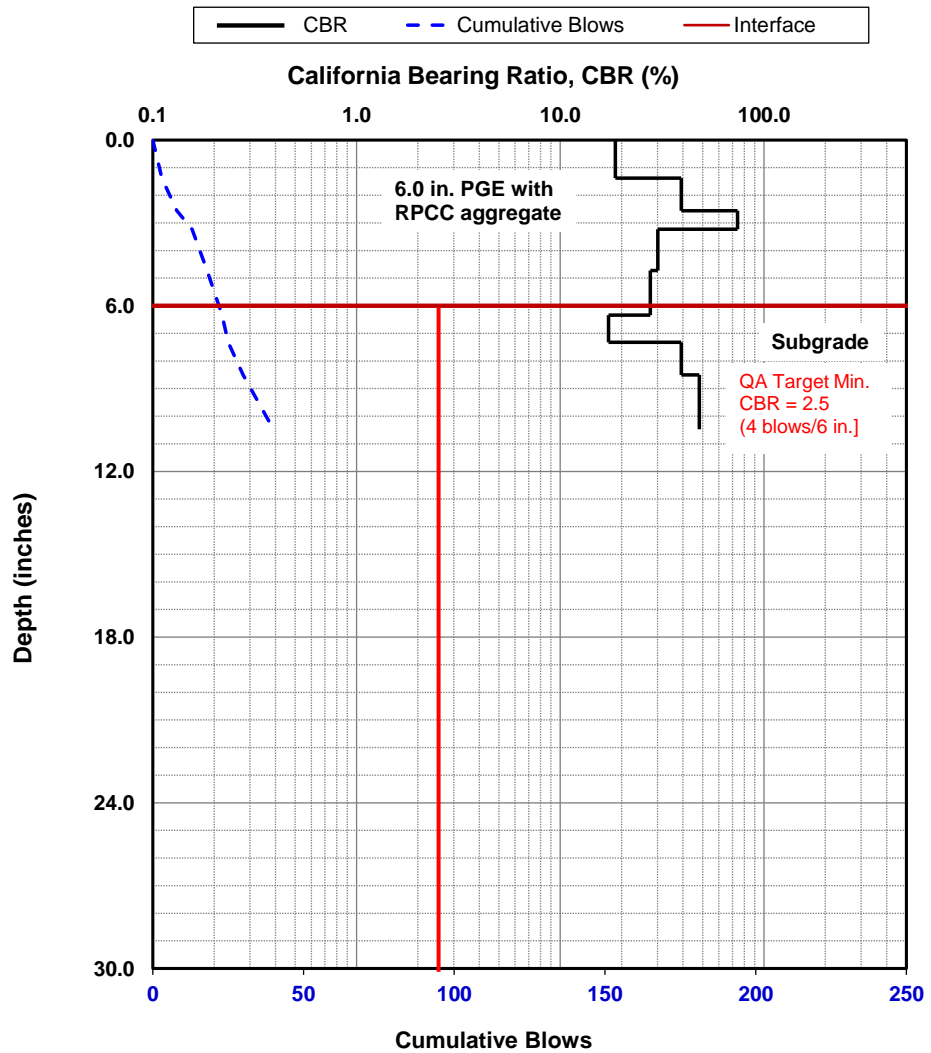
²E (ksi) = (17.6 CBR^{0.64}) x 0.1450377

³S_u (psf) = (3.794 x CBR^{0.664}) x 144

¹ ASTM D6951-03

²Powell et al. (1986)

³Portland Cement Assoc. (1955)



Dynamic Cone Penetrometer (DCP) Test Results

Project Name: Illinois Tollway - IC Research
 Project ID: Elgin O'Hare Extension - IL Tollway
 Location: IL390 (West of O'Hare)



Date of Test	4/11/2017	Test ID	TS6_Pt. 12	Operator	PV	ASTM	D6951
Latitude	41.9838130	Longitude	-87.9765663	Elevation (ft)	NA		
Location	Section 4642 (PGE)	Station	NA				
Comments	Nominal 6 in. of compacted PGE with RPCC crushed aggregate. <i>Subgrade assumed as CL clay.</i> PGE prepared in Fall 2016.						

Parameter	DPI (mm/blow)	CBR (%)	E _{CBR} , Elastic Modulus (ksi) (non stress-dependent)	S _{u-CBR} , Bearing Capacity (psf)
Avg. PGE Layer [0 to 6.0 in.]	6.4	36.6	25.6	5,969
Avg. Subgrade Layer [6.0 to 18.0 in.]	21.3	7.6	9.4	2,107
Ratio of Avg. Top/Bottom Layer	0.3	4.8	2.7	2.8
Std. Dev. PGE Layer [0 to 6.0 in.]	2.3	13.3	13.4	3,044
Std. Dev. Subgrade Layer [6.0 to 18.0 in.]	5.5	4.0	6.2	1,363

NOTES:

Subgrade is classified as CL

¹CBR = 292/DPI^{1.12}

¹CBR = 1/(0.017019DPI)²
for CL soils with CBR < 10

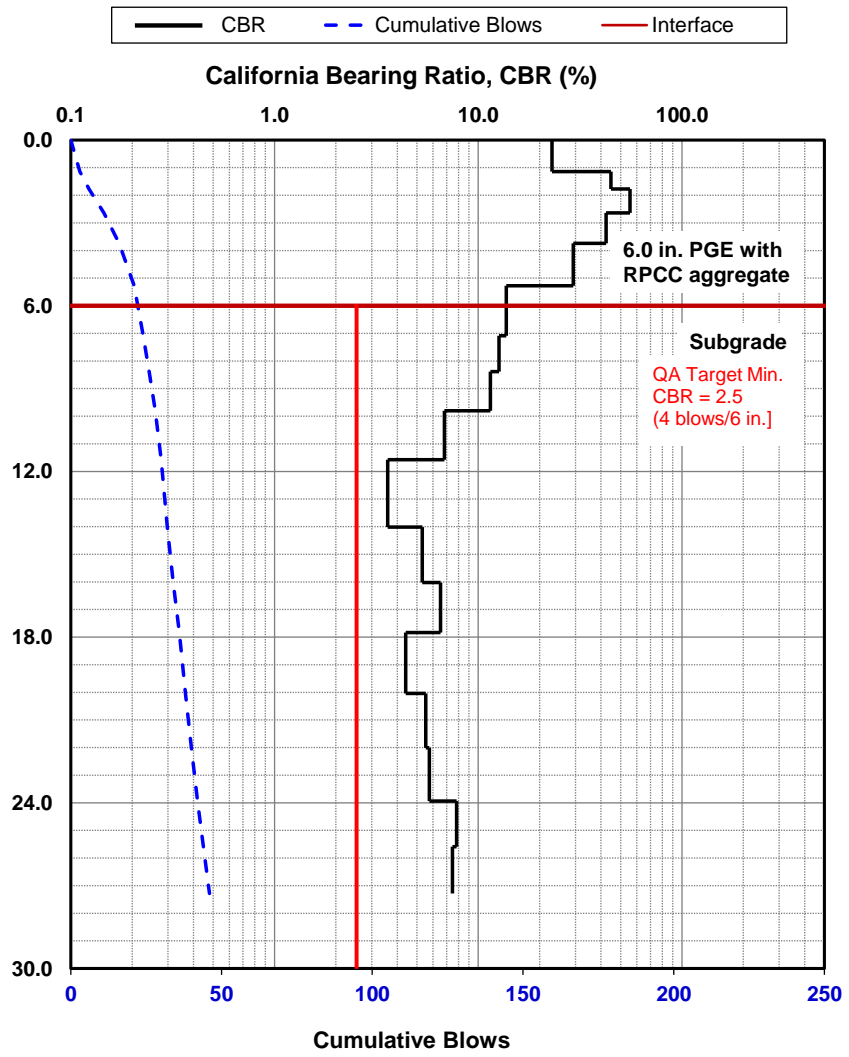
²E (ksi) = (17.6 CBR^{0.64}) x 0.1450377

³S_u (psf) = (3.794 x CBR^{0.664}) x 144

¹ ASTM D6951-03

²Powell et al. (1986)

³Portland Cement Assoc. (1955)

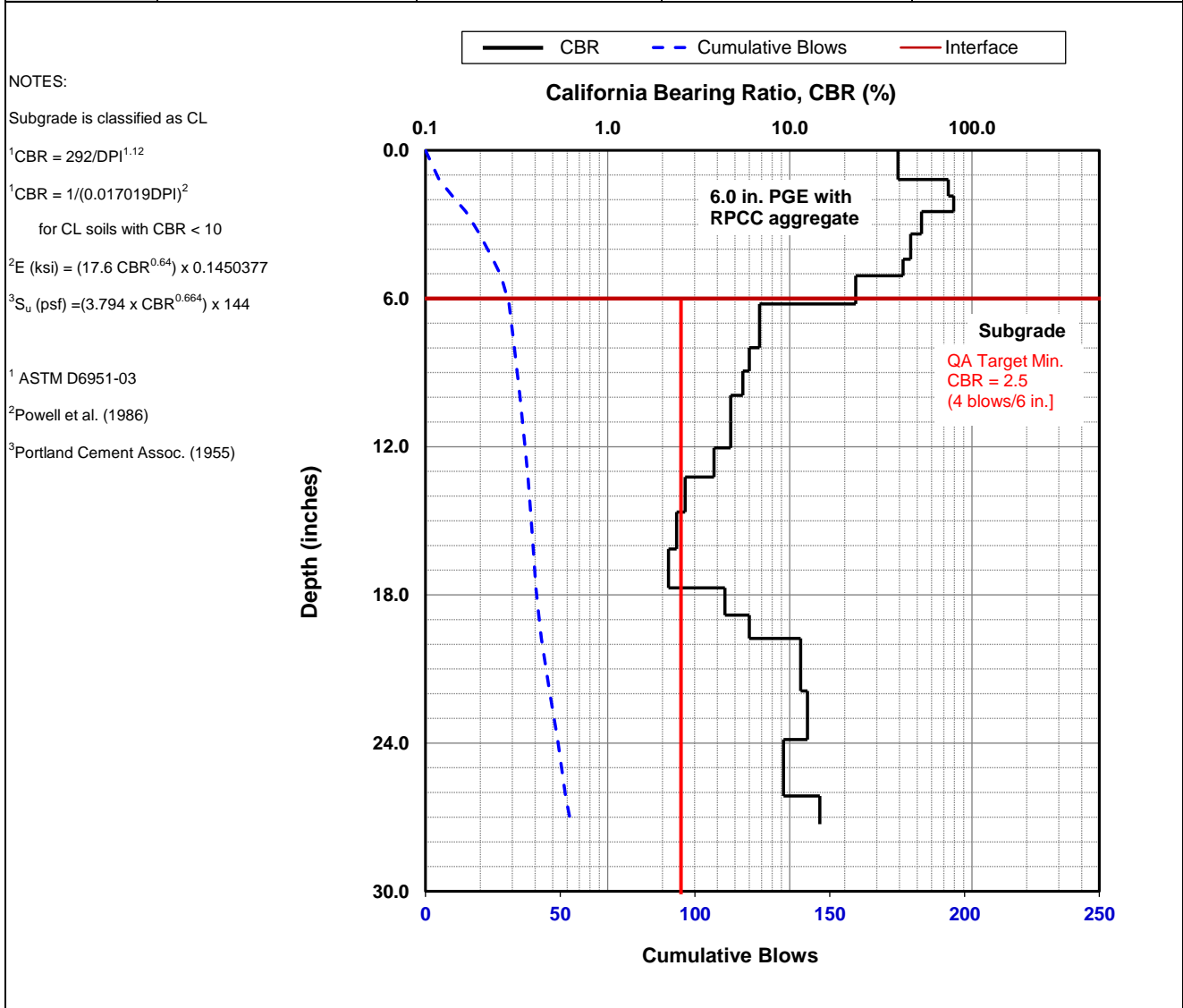


Dynamic Cone Penetrometer (DCP) Test Results	
Project Name:	Illinois Tollway - IC Research
Project ID:	Elgin O'Hare Extension - IL Tollway
Location:	IL390 (West of O'Hare)



Date of Test	4/11/2017	Test ID	TS6_Pt. 13	Operator	PV	ASTM	D6951
Latitude	41.9837620	Longitude	-87.9765652	Elevation (ft)	NA		
Location	Section 4642 (PGE)	Station	NA				
Comments	Nominal 6 in. of compacted PGE with RPCC crushed aggregate. <i>Subgrade assumed as CL clay.</i> PGE prepared in Fall 2016.						

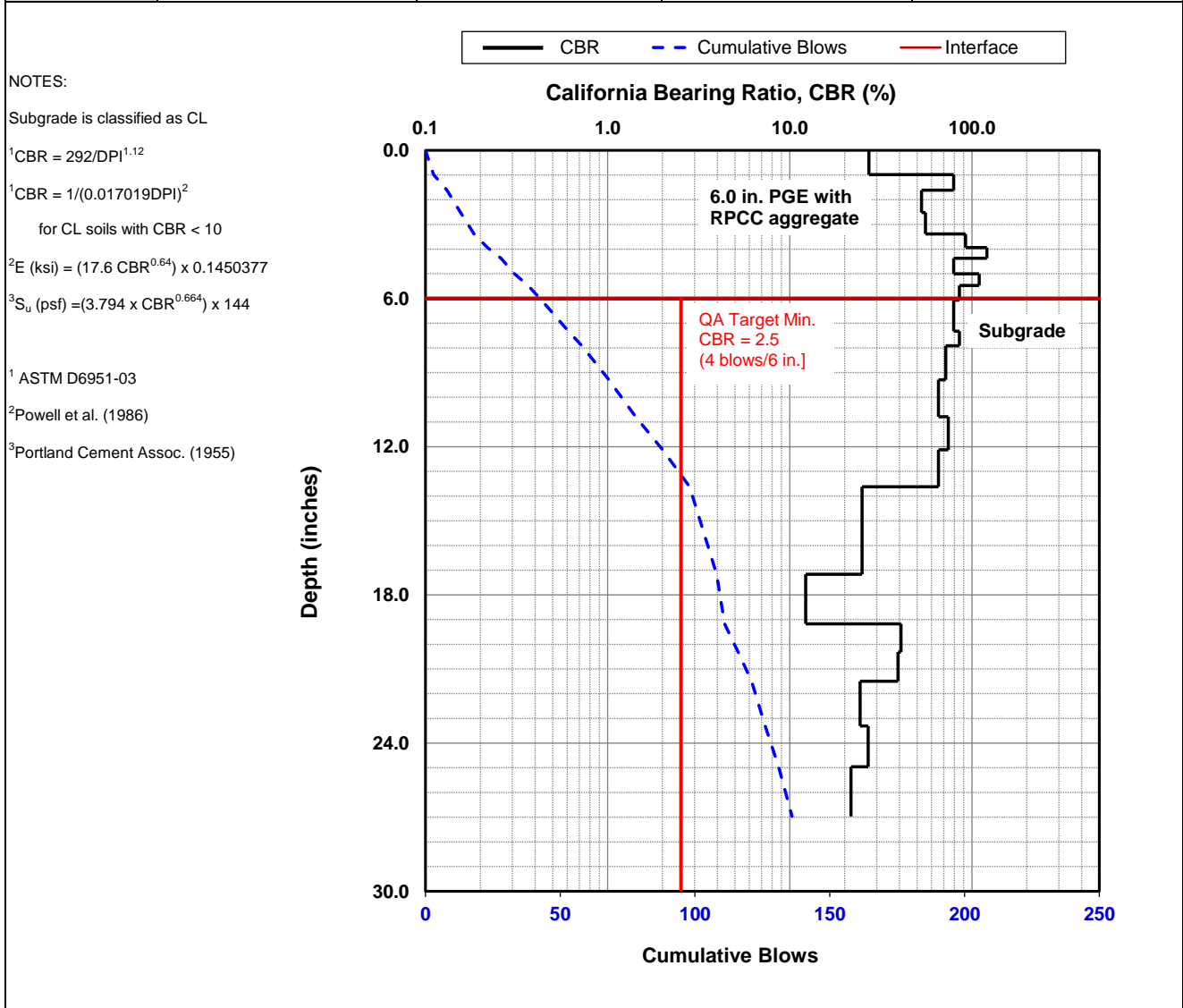
Parameter	DPI (mm/blow)	CBR (%)	E _{CBR} , Elastic Modulus (ksi) (non stress-dependent)	S _{u-CBR} , Bearing Capacity (psf)
Avg. PGE Layer [0 to 6.0 in.]	5.1	47.1	30.1	7,055
Avg. Subgrade Layer [6.0 to 18.0 in.]	29.2	4.0	6.2	1,383
Ratio of Avg. Top/Bottom Layer	0.2	11.6	4.8	5.1
Std. Dev. PGE Layer [0 to 6.0 in.]	2.0	18.9	16.7	3,842
Std. Dev. Subgrade Layer [6.0 to 18.0 in.]	6.5	1.7	3.5	767



Dynamic Cone Penetrometer (DCP) Test Results		
Project Name:	Illinois Tollway - IC Research	
Project ID:	Elgin O'Hare Extension - IL Tollway	
Location:	IL390 (West of O'Hare)	

Date of Test	4/11/2017	Test ID	TS6_Pt. 14	Operator	PV	ASTM	D6951
Latitude	41.9837265	Longitude	-87.9764412	Elevation (ft)	NA		
Location	Section 4642 (PGE)	Station	NA				
Comments	Nominal 6 in. of compacted PGE with RPCC crushed aggregate. <i>Subgrade assumed as CL clay.</i> PGE prepared in Fall 2016.						

Parameter	DPI (mm/blow)	CBR (%)	E _{CBR} , Elastic Modulus (ksi) (non stress-dependent)	S _{u-CBR} , Bearing Capacity (psf)
Avg. PGE Layer [0 to 6.0 in.]	3.6	70.0	38.7	9,171
Avg. Subgrade Layer [6.0 to 18.0 in.]	4.9	49.3	30.9	7,267
Ratio of Avg. Top/Bottom Layer	0.7	1.4	1.3	1.3
Std. Dev. PGE Layer [0 to 6.0 in.]	2.3	31.8	23.4	5,438
Std. Dev. Subgrade Layer [6.0 to 18.0 in.]	4.9	26.5	20.8	4,818



Dynamic Cone Penetrometer (DCP) Test Results	
Project Name:	Illinois Tollway - IC Research
Project ID:	Elgin O'Hare Extension - IL Tollway
Location:	IL390 (West of O'Hare)



Date of Test	4/12/2017	Test ID	TS7_Pt. 23	Operator	PV	ASTM	D6951
Latitude	41.9837849	Longitude	-87.9803137	Elevation (ft)	NA		
Location	Section 4642 (PGE)	Station	NA				
Comments	Nominal 3 in. of CA6-RAP compacted over nominal 6 in. PGE with RPCC crushed aggregate. <i>Subgrade assumed as CL clay.</i> PGE prepared in Fall 2016. CA6-RAP placed and compacted on 04/11/2016.						

Parameter	DPI (mm/blow)	CBR (%)	E_{CBR} , Elastic Modulus (ksi) (non stress-dependent)	S_{u-CBR} , Bearing Capacity (psf)
Avg. PGE+CA6 Layer [0 to 9.0 in.]	8.6	26.4	20.7	4,797
Avg. Subgrade Layer [9.0 to 21.0 in.]	2.2	118.2	54.1	12,989
Ratio of Avg. Top/Bottom Layer	3.8	0.2	0.4	0.4
Std.Dev.PGE+CA6 Layer [0 to 9 in.]	2.1	6.7	8.6	1,924
Std. Dev. Subgrade Layer [9.0 to 21.0 in.]	2.2	71.0	39.1	9,259

NOTES:

Subgrade is classified as CL

¹CBR = 292/DPI^{1.12}

¹CBR = 1/(0.017019DPI)²
for CL soils with CBR < 10

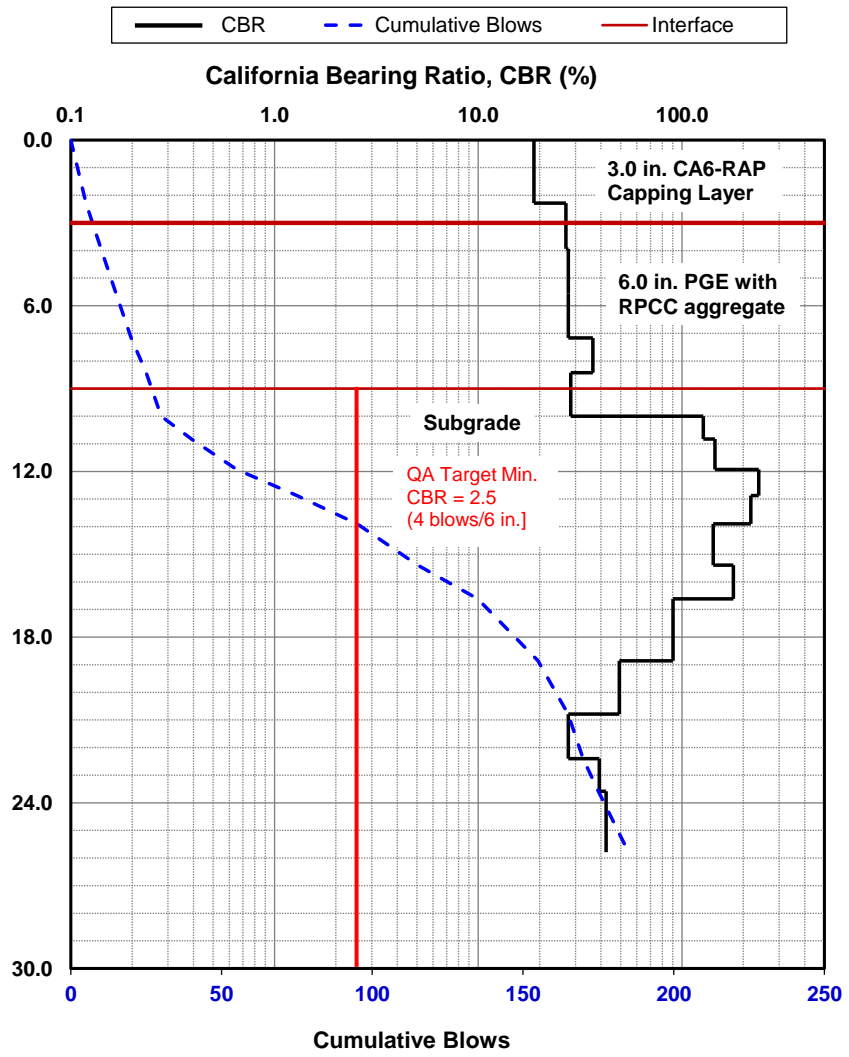
²E (ksi) = (17.6 CBR^{0.64}) x 0.1450377

³S_u (psf) = (3.794 x CBR^{0.664}) x 144

¹ ASTM D6951-03

² Powell et al. (1986)

³ Portland Cement Assoc. (1955)

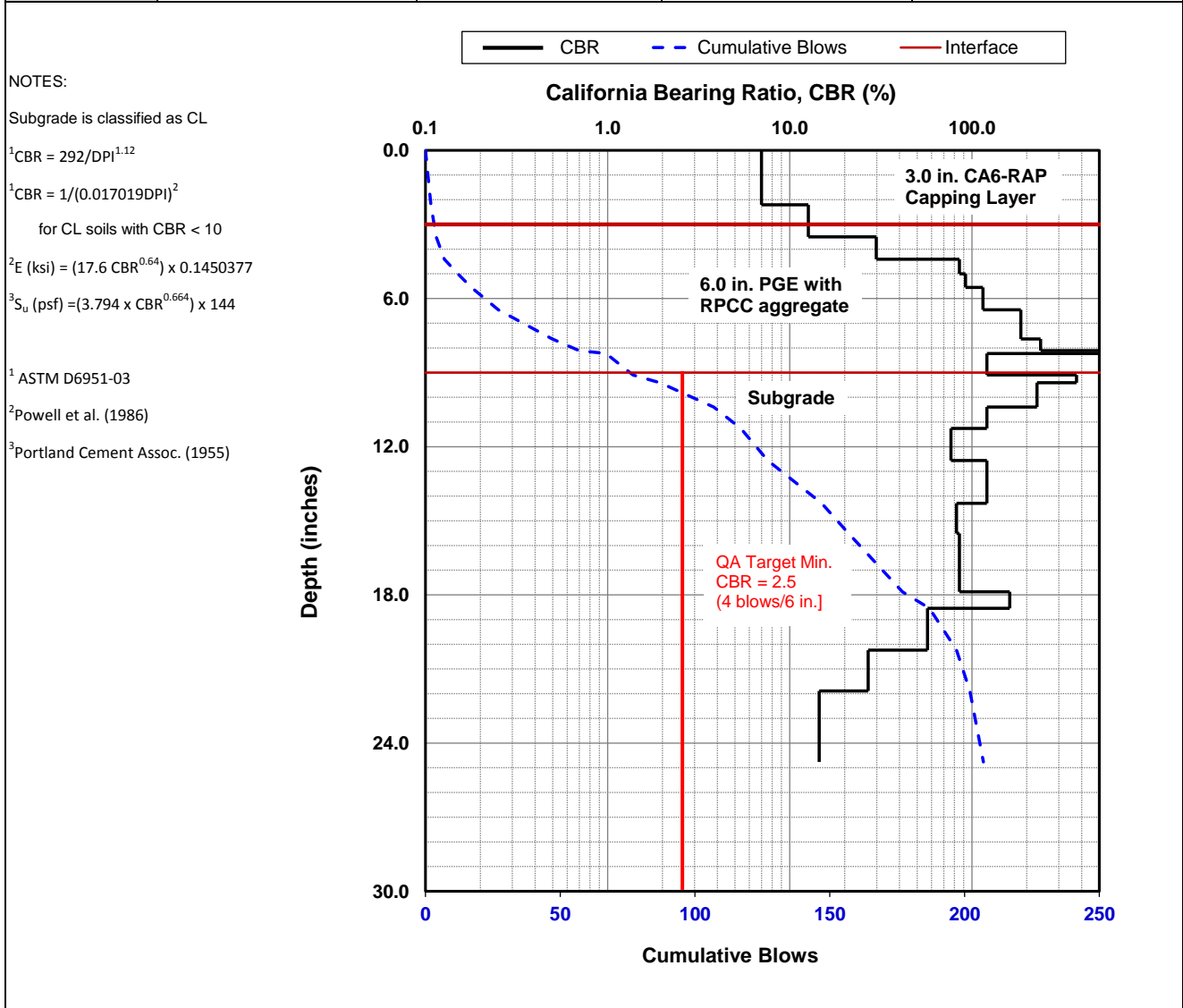


Dynamic Cone Penetrometer (DCP) Test Results	
Project Name:	Illinois Tollway - IC Research
Project ID:	Elgin O'Hare Extension - IL Tollway
Location:	IL390 (West of O'Hare)



Date of Test	4/12/2017	Test ID	TS7_Pt. 26	Operator	PV	ASTM	D6951
Latitude	41.9837317	Longitude	-87.9813417	Elevation (ft)	NA		
Location	Section 4642 (PGE)	Station	NA				
Comments	Nominal 3 in. of CA6-RAP compacted over nominal 6 in. PGE with RPCC crushed aggregate. <i>Subgrade assumed as CL clay.</i> PGE prepared in Fall 2016. CA6-RAP placed and compacted on 04/11/2016.						

Parameter	DPI (mm/blow)	CBR (%)	E _{CBR} , Elastic Modulus (ksi) (non stress-dependent)	S _{u-CBR} , Bearing Capacity (psf)
Avg. PGE+CA6 Layer [0 to 9.0 in.]	3.0	85.3	43.9	10,463
Avg. Subgrade Layer [9.0 to 21.0 in.]	2.6	100.1	48.7	11,638
Ratio of Avg. Top/Bottom Layer	1.2	0.9	0.9	0.9
Std.Dev.PGE+CA6 Layer [0 to 9 in.]	10.7	321.0	102.6	25,222
Std. Dev. Subgrade Layer [9.0 to 21.0 in.]	2.2	102.0	49.3	11,778

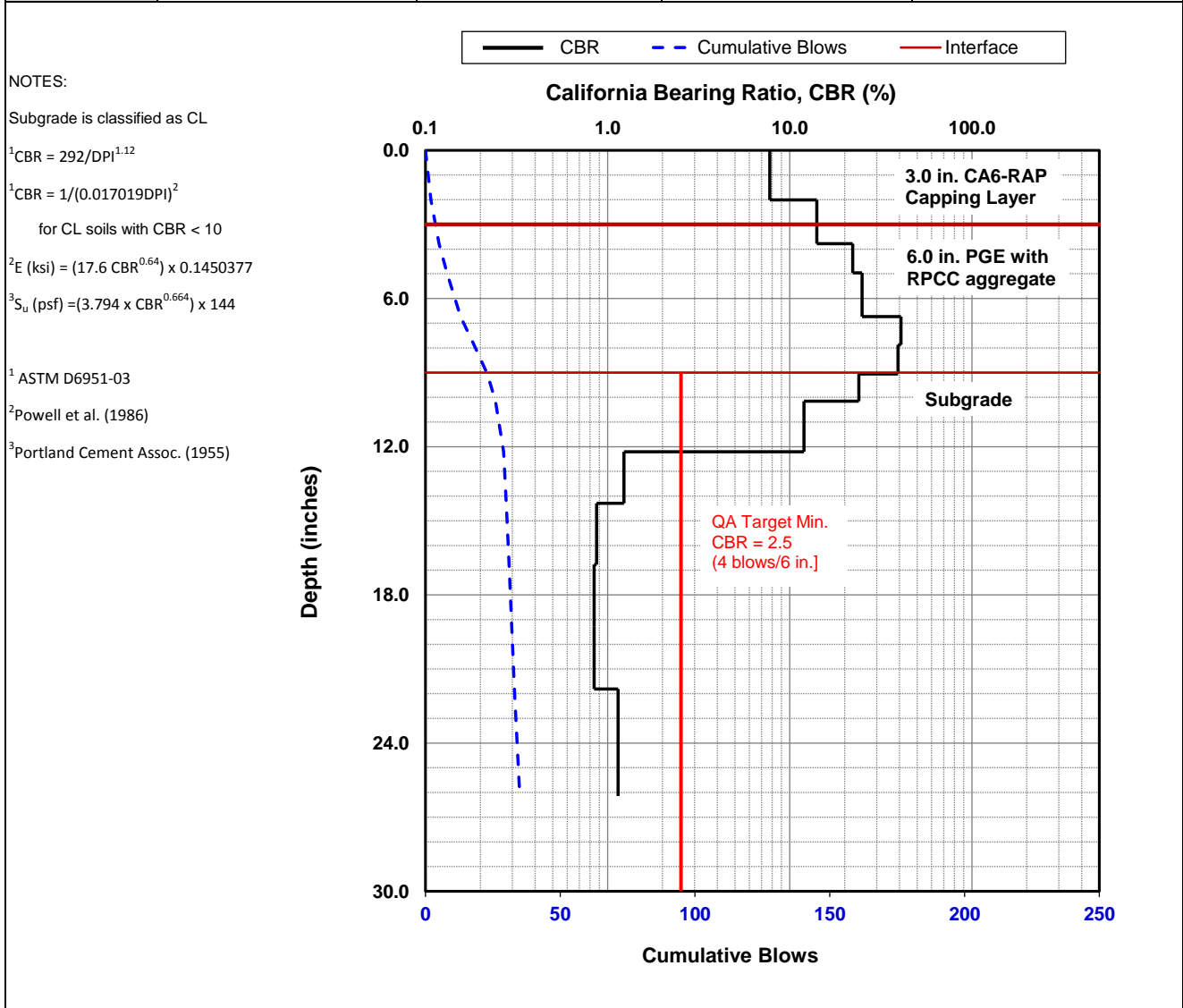


Dynamic Cone Penetrometer (DCP) Test Results	
Project Name:	Illinois Tollway - IC Research
Project ID:	Elgin O'Hare Extension - IL Tollway
Location:	IL390 (West of O'Hare)



Date of Test	4/12/2017	Test ID	TS7_Pt. 27	Operator	PV	ASTM	D6951
Latitude	41.9837919	Longitude	-87.9813360	Elevation (ft)	NA		
Location	Section 4642 (PGE)	Station	NA				
Comments	Nominal 3 in. of CA6-RAP compacted over nominal 6 in. PGE with RPCC crushed aggregate. <i>Subgrade assumed as CL clay.</i> PGE prepared in Fall 2016. CA6-RAP placed and compacted on 04/11/2016.						

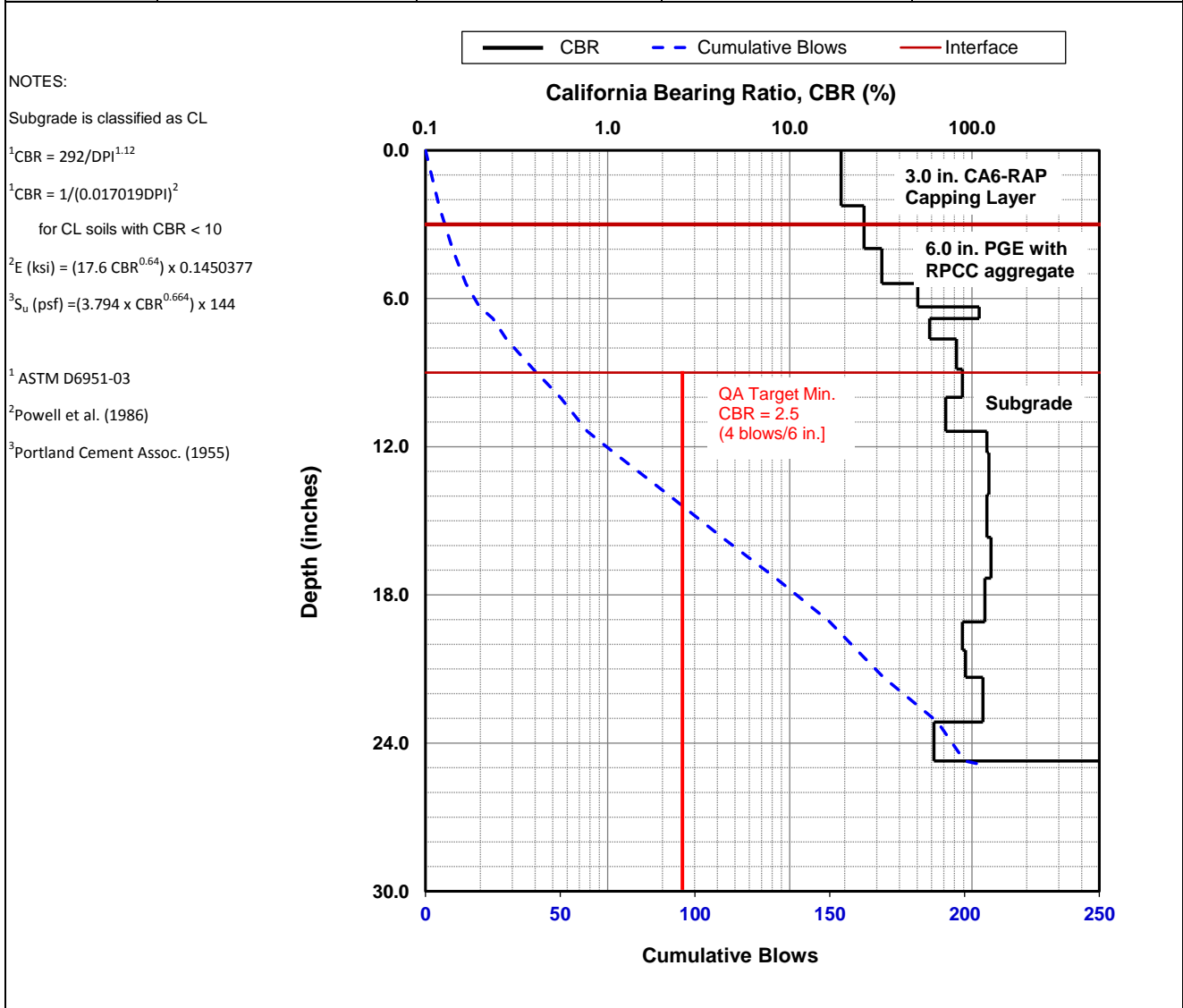
Parameter	DPI (mm/blow)	CBR (%)	E_{CBR} , Elastic Modulus (ksi) (non stress-dependent)	S_{u-CBR} , Bearing Capacity (psf)
Avg. PGE+CA6 Layer [0 to 9.0 in.]	10.0	22.2	18.5	4,274
Avg. Subgrade Layer [9.0 to 21.0 in.]	32.4	3.3	5.5	1,204
Ratio of Avg. Top/Bottom Layer	0.3	6.7	3.4	3.5
Std.Dev.PGE+CA6 Layer [0 to 9 in.]	8.5	13.7	13.6	3,106
Std. Dev. Subgrade Layer [9.0 to 21.0 in.]	25.1	9.6	10.8	2,446



Dynamic Cone Penetrometer (DCP) Test Results		
Project Name:	Illinois Tollway - IC Research	
Project ID:	Elgin O'Hare Extension - IL Tollway	
Location:	IL390 (West of O'Hare)	

Date of Test	4/12/2017	Test ID	TS7_Pt. 29	Operator	PV	ASTM	D6951
Latitude	41.9837316	Longitude	-87.9816384	Elevation (ft)	NA		
Location	Section 4642 (PGE)	Station	NA				
Comments	Nominal 3 in. of CA6-RAP compacted over nominal 6 in. PGE with RPCC crushed aggregate. <i>Subgrade assumed as CL clay.</i> PGE prepared in Fall 2016. CA6-RAP placed and compacted on 04/11/2016.						

Parameter	DPI (mm/blow)	CBR (%)	E_{CBR} , Elastic Modulus (ksi) (non stress-dependent)	S_{u-CBR} , Bearing Capacity (psf)
Avg. PGE+CA6 Layer [0 to 9.0 in.]	5.6	42.2	28.0	6,556
Avg. Subgrade Layer [9.0 to 21.0 in.]	2.4	107.6	51.0	12,206
Ratio of Avg. Top/Bottom Layer	2.3	0.4	0.5	0.5
Std.Dev.PGE+CA6 Layer [0 to 9 in.]	3.6	32.7	23.8	5,534
Std. Dev. Subgrade Layer [9.0 to 21.0 in.]	0.5	20.3	17.6	4,038

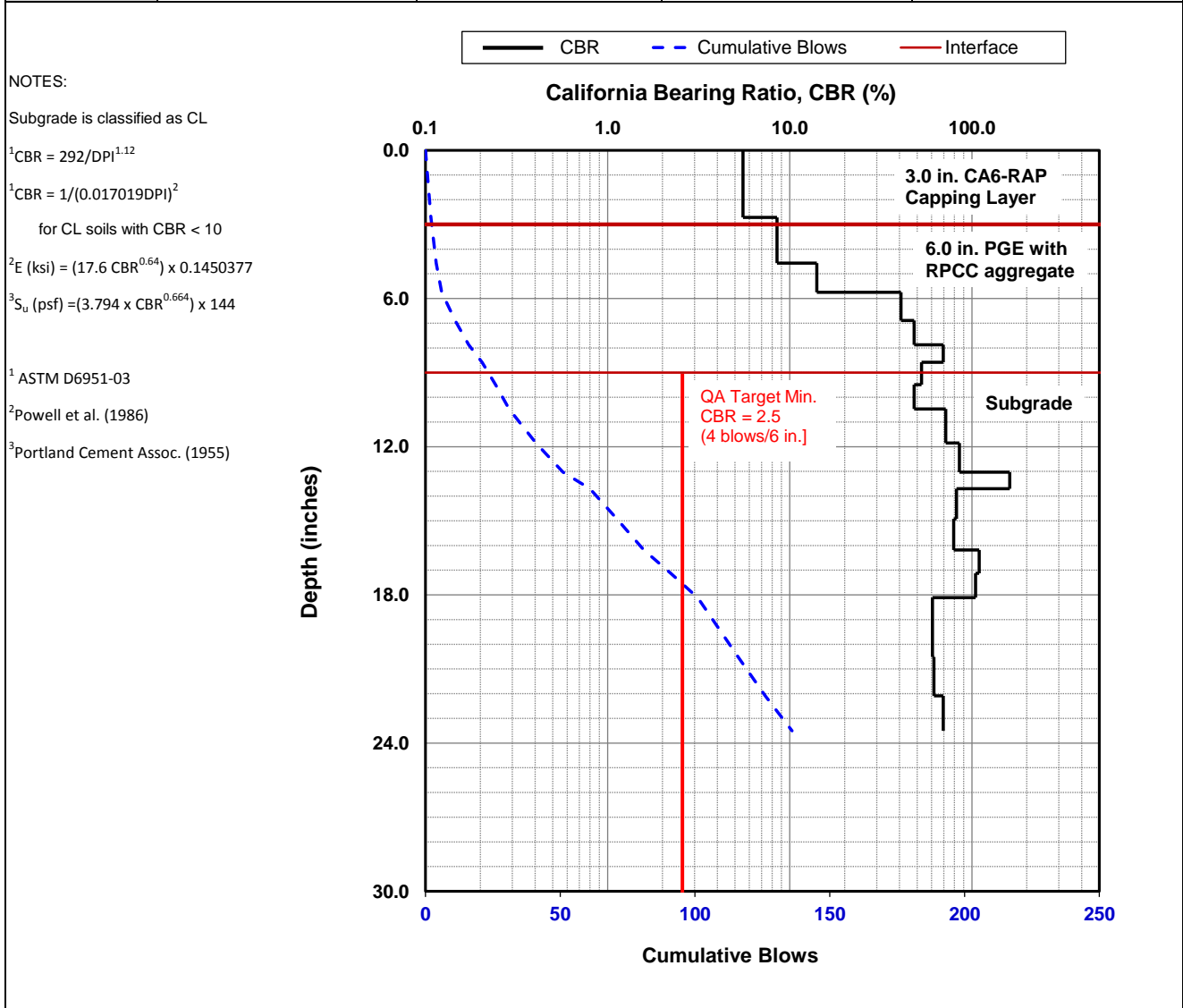


Dynamic Cone Penetrometer (DCP) Test Results	
Project Name:	Illinois Tollway - IC Research
Project ID:	Elgin O'Hare Extension - IL Tollway
Location:	IL390 (West of O'Hare)



Date of Test	4/12/2017	Test ID	TS7_Pt. 30	Operator	PV	ASTM	D6951
Latitude	41.9838090	Longitude	-87.9817281	Elevation (ft)	NA		
Location	Section 4642 (PGE)	Station	NA				
Comments	Nominal 3 in. of CA6-RAP compacted over nominal 6 in. PGE with RPCC crushed aggregate. <i>Subgrade assumed as CL clay.</i> PGE prepared in Fall 2016. CA6-RAP placed and compacted on 04/11/2016.						

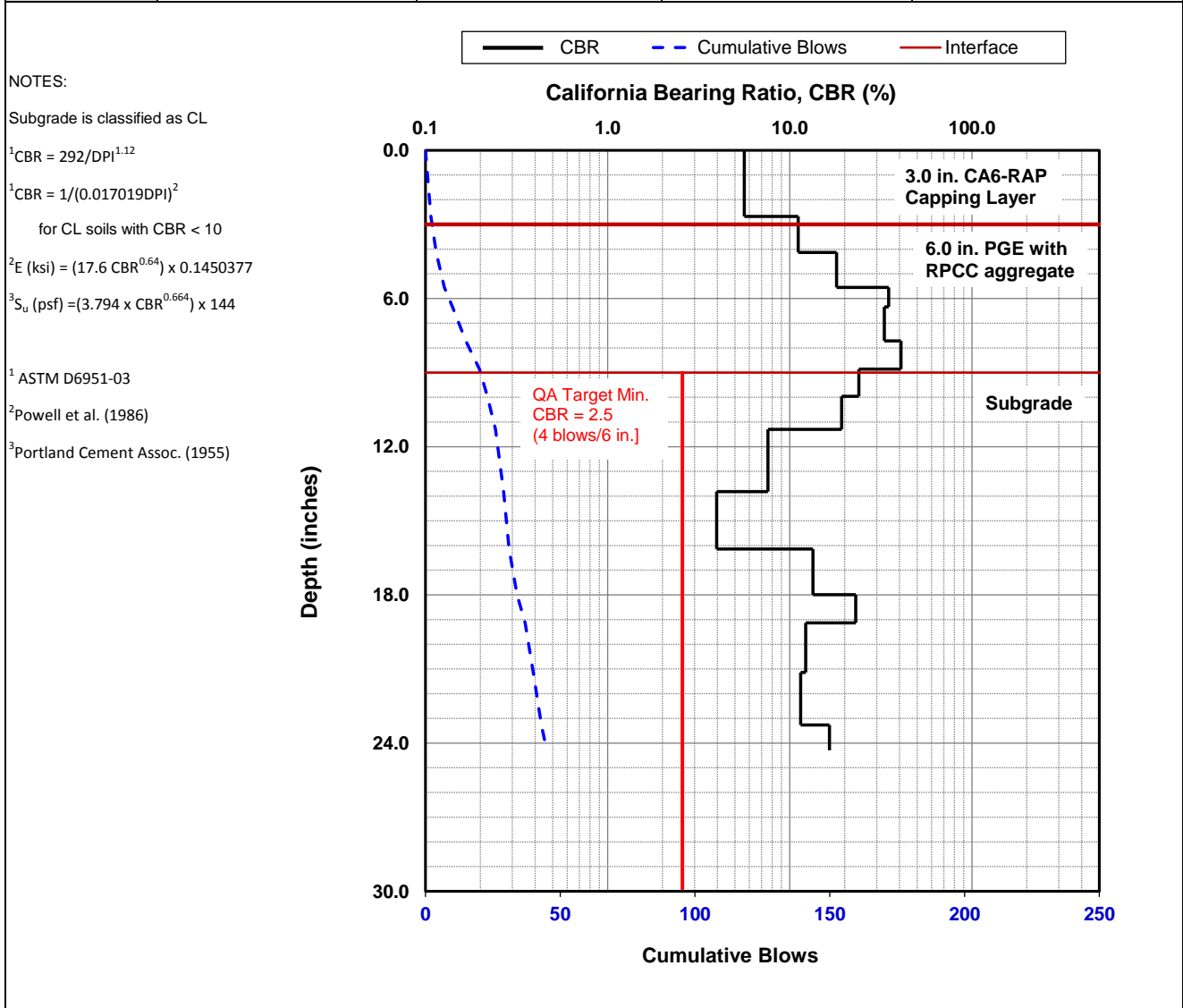
Parameter	DPI (mm/blow)	CBR (%)	E_{CBR} , Elastic Modulus (ksi) (non stress-dependent)	S_{u-CBR} , Bearing Capacity (psf)
Avg. PGE+CA6 Layer [0 to 9.0 in.]	9.3	24.1	19.6	4,522
Avg. Subgrade Layer [9.0 to 21.0 in.]	3.1	81.9	42.8	10,184
Ratio of Avg. Top/Bottom Layer	3.0	0.3	0.5	0.4
Std.Dev.PGE+CA6 Layer [0 to 9 in.]	13.4	25.2	20.1	4,655
Std. Dev. Subgrade Layer [9.0 to 21.0 in.]	1.0	33.2	24.0	5,586



Dynamic Cone Penetrometer (DCP) Test Results		
Project Name:	Illinois Tollway - IC Research	
Project ID:	Elgin O'Hare Extension - IL Tollway	
Location:	IL390 (West of O'Hare)	

Date of Test	4/12/2017	Test ID	TS7_Pt. 37	Operator	PV	ASTM	D6951
Latitude	41.9837481	Longitude	-87.9846995	Elevation (ft)	NA		
Location	Section 4642 (PGE)	Station	NA				
Comments	Nominal 3 in. of CA6-RAP compacted over nominal 6 in. PGE with RPCC crushed aggregate. <i>Subgrade assumed as CL clay.</i> PGE prepared in Fall 2016. CA6-RAP placed and compacted on 04/11/2016.						

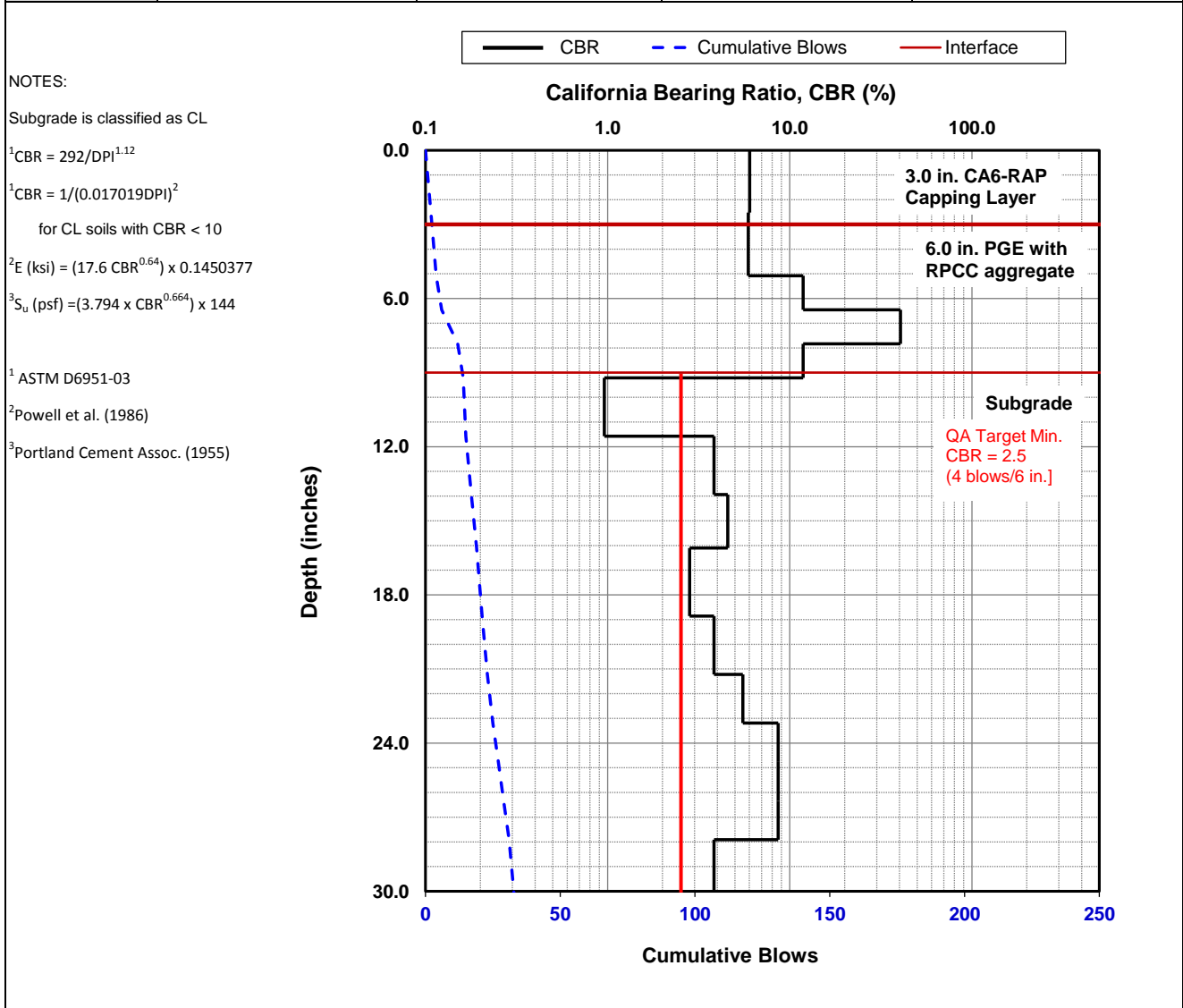
Parameter	DPI (mm/blow)	CBR (%)	E _{CBR} , Elastic Modulus (ksi) (non stress-dependent)	S _{u-CBR} , Bearing Capacity (psf)
Avg. PGE+CA6 Layer [0 to 9.0 in.]	11.3	19.4	17.0	3,915
Avg. Subgrade Layer [9.0 to 21.0 in.]	15.6	13.5	13.5	3,070
Ratio of Avg. Top/Bottom Layer	0.7	1.4	1.3	1.3
Std.Dev.PGE+CA6 Layer [0 to 9 in.]	12.5	14.8	14.3	3,263
Std. Dev. Subgrade Layer [9.0 to 21.0 in.]	7.3	7.6	9.4	2,104



Dynamic Cone Penetrometer (DCP) Test Results		
Project Name:	Illinois Tollway - IC Research	
Project ID:	Elgin O'Hare Extension - IL Tollway	
Location:	IL390 (West of O'Hare)	

Date of Test	4/18/2017	Test ID	TS9_Pt. 2	Operator	PV	ASTM	D6951
Latitude	41.9833819	Longitude	-87.9933858	Elevation (ft)	NA		
Location	Section 4642 (PGE)	Station	NA				
Comments	Nominal 3 in. of CA6-RAP compacted over nominal 6 in. PGE with RPCC crushed aggregate. <i>Subgrade assumed as CL clay.</i> PGE prepared in Fall 2016. CA6-RAP placed and compacted on 04/18/16 over west half of the area, east half was placed prior to 04/10/16.						

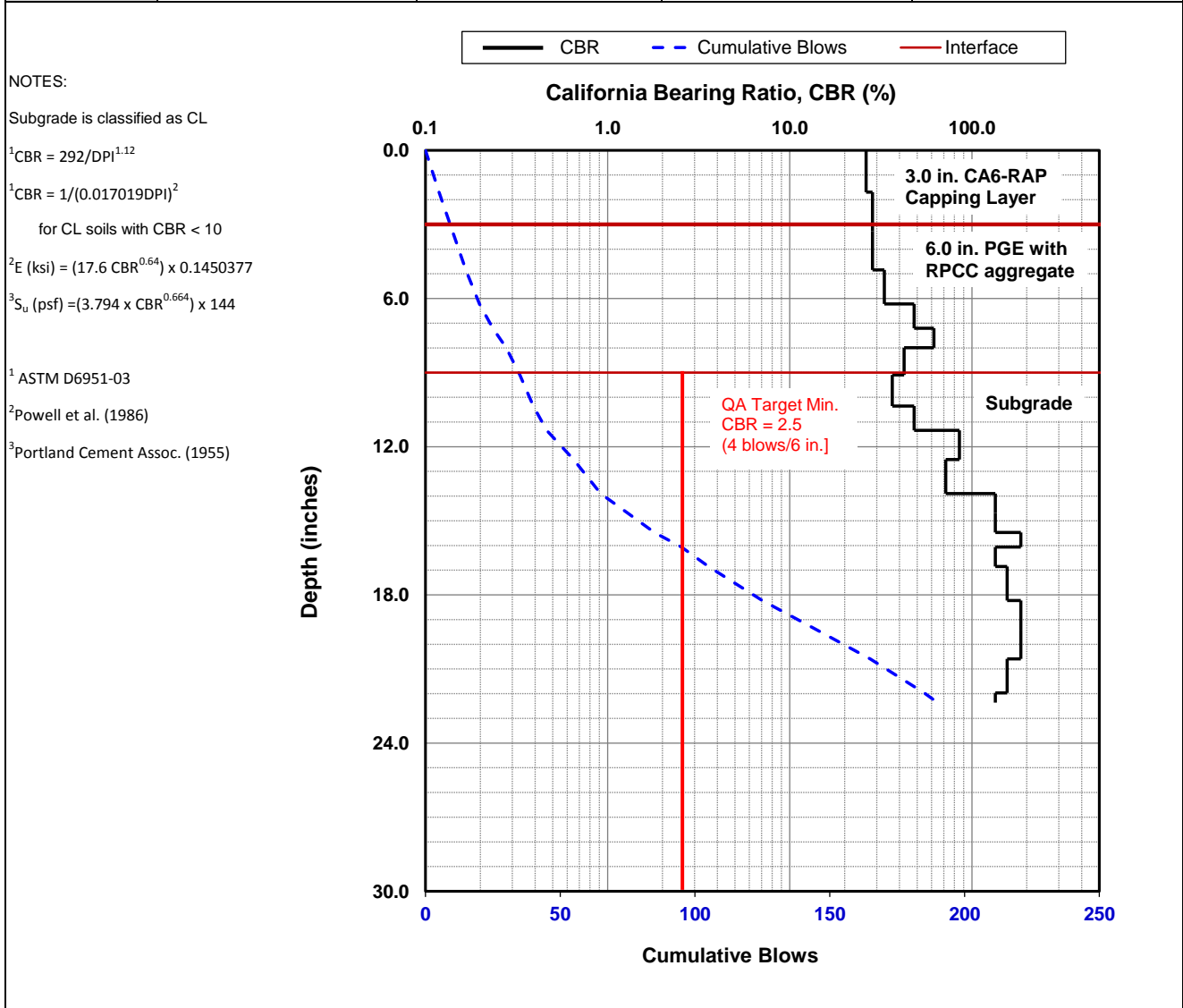
Parameter	DPI (mm/blow)	CBR (%)	E _{CBR} , Elastic Modulus (ksi) (non stress-dependent)	S _{u-CBR} , Bearing Capacity (psf)
Avg. PGE+CA6 Layer [0 to 9.0 in.]	16.7	12.5	12.8	2,917
Avg. Subgrade Layer [9.0 to 21.0 in.]	33.9	3.0	5.2	1,135
Ratio of Avg. Top/Bottom Layer	0.5	4.1	2.5	2.6
Std.Dev.PGE+CA6 Layer [0 to 9 in.]	11.0	13.4	13.5	3,068
Std. Dev. Subgrade Layer [9.0 to 21.0 in.]	13.4	1.4	3.2	683



Dynamic Cone Penetrometer (DCP) Test Results		
Project Name:	Illinois Tollway - IC Research	
Project ID:	Elgin O'Hare Extension - IL Tollway	
Location:	IL390 (West of O'Hare)	

Date of Test	4/18/2017	Test ID	TS9_Pt. 3	Operator	PV	ASTM	D6951
Latitude	41.9835128	Longitude	-87.9935268	Elevation (ft)	NA		
Location	Section 4642 (PGE)	Station	NA				
Comments	Nominal 3 in. of CA6-RAP compacted over nominal 6 in. PGE with RPCC crushed aggregate. <i>Subgrade assumed as CL clay.</i> PGE prepared in Fall 2016. CA6-RAP placed and compacted on 04/18/16 over west half of the area, east half was placed prior to 04/10/16.						

Parameter	DPI (mm/blow)	CBR (%)	E _{CBR} , Elastic Modulus (ksi) (non stress-dependent)	S _{u-CBR} , Bearing Capacity (psf)
Avg. PGE+CA6 Layer [0 to 9.0 in.]	6.6	35.3	25.0	5,821
Avg. Subgrade Layer [9.0 to 21.0 in.]	2.2	118.0	54.1	12,975
Ratio of Avg. Top/Bottom Layer	2.9	0.3	0.5	0.4
Std.Dev.PGE+CA6 Layer [0 to 9 in.]	1.8	12.9	13.1	2,983
Std. Dev. Subgrade Layer [9.0 to 21.0 in.]	1.6	55.0	33.2	7,821

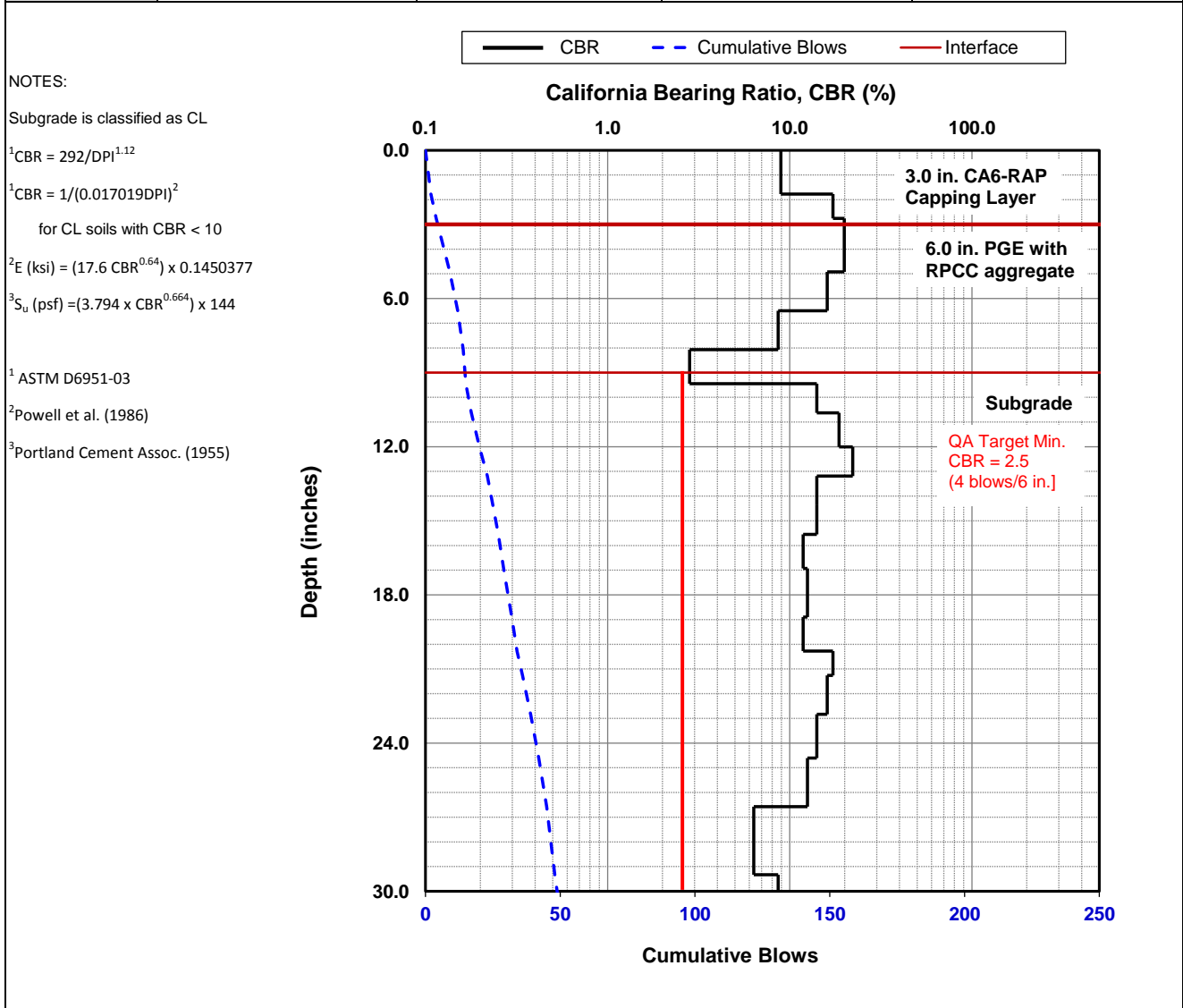


Dynamic Cone Penetrometer (DCP) Test Results	
Project Name:	Illinois Tollway - IC Research
Project ID:	Elgin O'Hare Extension - IL Tollway
Location:	IL390 (West of O'Hare)



Date of Test	4/18/2017	Test ID	TS9_Pt. 11	Operator	PV	ASTM	D6951
Latitude	41.9834479	Longitude	-87.9941266	Elevation (ft)	NA		
Location	Section 4642 (PGE)	Station	NA				
Comments	Nominal 3 in. of CA6-RAP compacted over nominal 6 in. PGE with RPCC crushed aggregate. <i>Subgrade assumed as CL clay.</i> PGE prepared in Fall 2016. CA6-RAP placed and compacted on 04/18/16 over west half of the area, east half was placed prior to 04/10/16.						

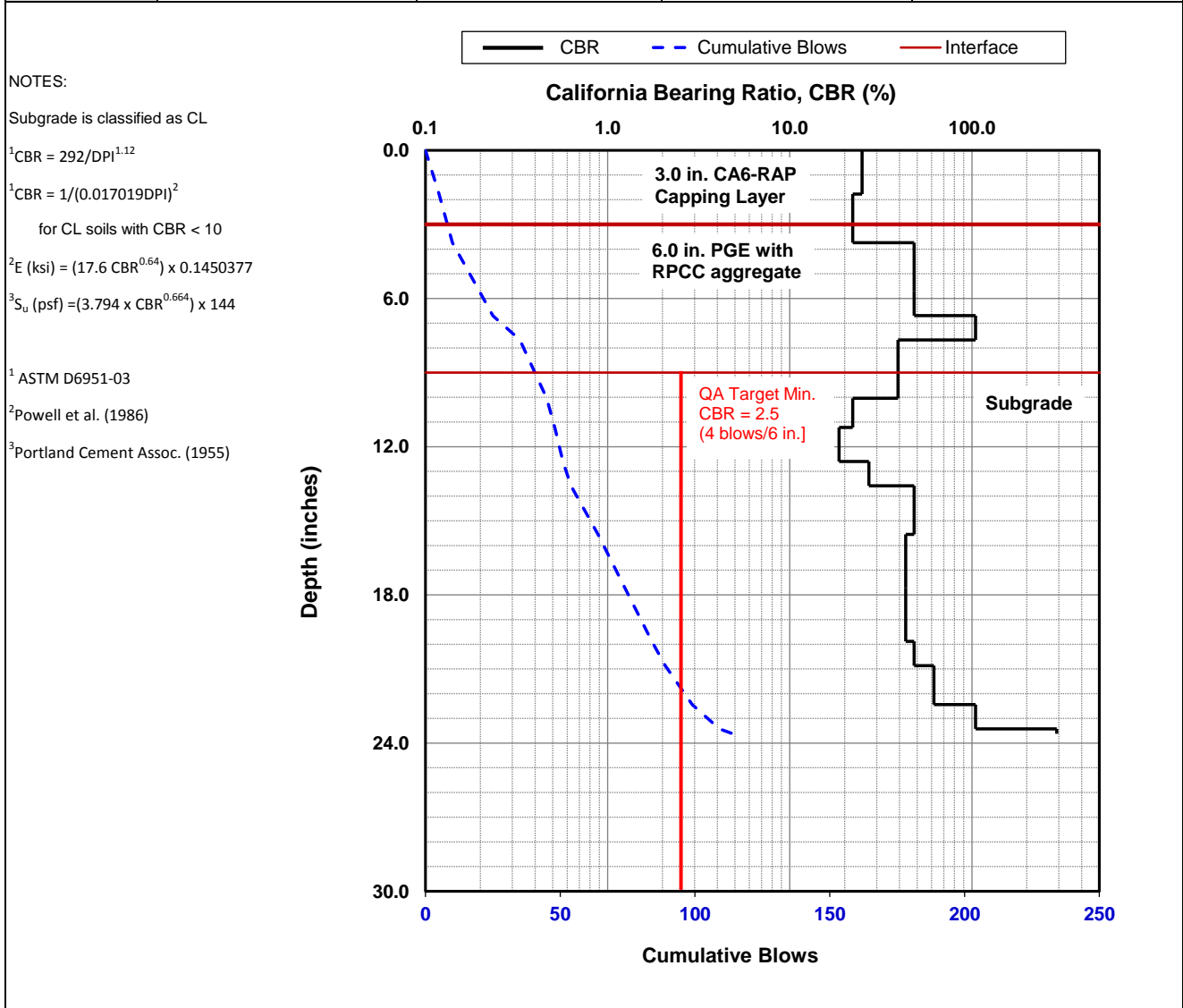
Parameter	DPI (mm/blow)	CBR (%)	E _{CBR} , Elastic Modulus (ksi) (non stress-dependent)	S _{u-CBR} , Bearing Capacity (psf)
Avg. PGE+CA6 Layer [0 to 9.0 in.]	16.0	13.1	13.2	3,013
Avg. Subgrade Layer [9.0 to 21.0 in.]	14.3	14.9	14.4	3,278
Ratio of Avg. Top/Bottom Layer	1.1	0.9	0.9	0.9
Std.Dev.PGE+CA6 Layer [0 to 9 in.]	8.3	6.1	8.1	1,808
Std. Dev. Subgrade Layer [9.0 to 21.0 in.]	2.6	3.5	5.7	1,256



Dynamic Cone Penetrometer (DCP) Test Results	
Project Name:	Illinois Tollway - IC Research
Project ID:	Elgin O'Hare Extension - IL Tollway
Location:	IL390 (West of O'Hare)

Date of Test	4/18/2017	Test ID	TS9_Pt. 12	Operator	PV	ASTM	D6951
Latitude	41.9834456	Longitude	-87.9938381	Elevation (ft)	NA		
Location	Section 4642 (PGE)	Station	NA				
Comments	Nominal 3 in. of CA6-RAP compacted over nominal 6 in. PGE with RPCC crushed aggregate. <i>Subgrade assumed as CL clay.</i> PGE prepared in Fall 2016. CA6-RAP placed and compacted on 04/18/16 over west half of the area, east half was placed prior to 04/10/16.						

Parameter	DPI (mm/blow)	CBR (%)	E_{CBR} , Elastic Modulus (ksi) (non stress-dependent)	S_{u-CBR} , Bearing Capacity (psf)
Avg. PGE+CA6 Layer [0 to 9.0 in.]	5.7	41.8	27.9	6,520
Avg. Subgrade Layer [9.0 to 21.0 in.]	6.3	37.5	26.0	6,062
Ratio of Avg. Top/Bottom Layer	0.9	1.1	1.1	1.1
Std.Dev.PGE+CA6 Layer [0 to 9 in.]	2.7	28.7	21.9	5,074
Std. Dev. Subgrade Layer [9.0 to 21.0 in.]	2.7	12.7	13.0	2,958

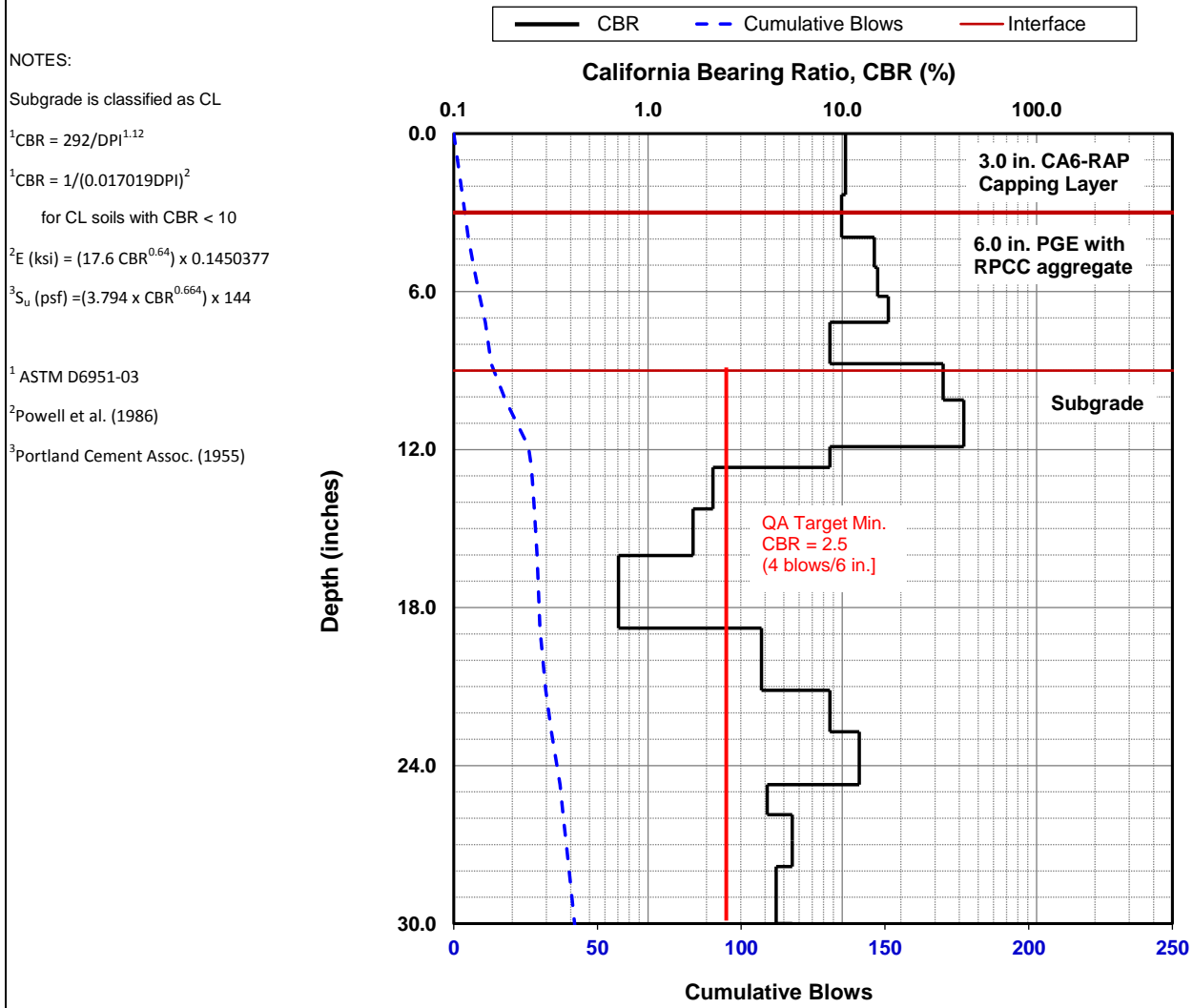


Dynamic Cone Penetrometer (DCP) Test Results	
Project Name:	Illinois Tollway - IC Research
Project ID:	Elgin O'Hare Extension - IL Tollway
Location:	IL390 (West of O'Hare)



Date of Test	4/18/2017	Test ID	TS9_Pt. 15	Operator	PV	ASTM	D6951
Latitude	41.9835510	Longitude	-87.9924287	Elevation (ft)	NA		
Location	Section 4642 (PGE)	Station	NA				
Comments	Nominal 3 in. of CA6-RAP compacted over nominal 6 in. PGE with RPCC crushed aggregate. <i>Subgrade assumed as CL clay.</i> PGE prepared in Fall 2016. CA6-RAP placed and compacted on 04/18/16 over west half of the area, east half was placed prior to 04/10/16.						

Parameter	DPI (mm/blow)	CBR (%)	E_{CBR} , Elastic Modulus (ksi) (non stress-dependent)	S_{u-CBR} , Bearing Capacity (psf)
Avg. PGE+CA6 Layer [0 to 9.0 in.]	17.1	12.2	12.6	2,870
Avg. Subgrade Layer [9.0 to 21.0 in.]	16.6	12.6	12.9	2,934
Ratio of Avg. Top/Bottom Layer	1.0	1.0	1.0	1.0
Std.Dev.PGE+CA6 Layer [0 to 9 in.]	3.4	3.3	5.5	1,203
Std. Dev. Subgrade Layer [9.0 to 21.0 in.]	22.9	17.1	15.7	3,598

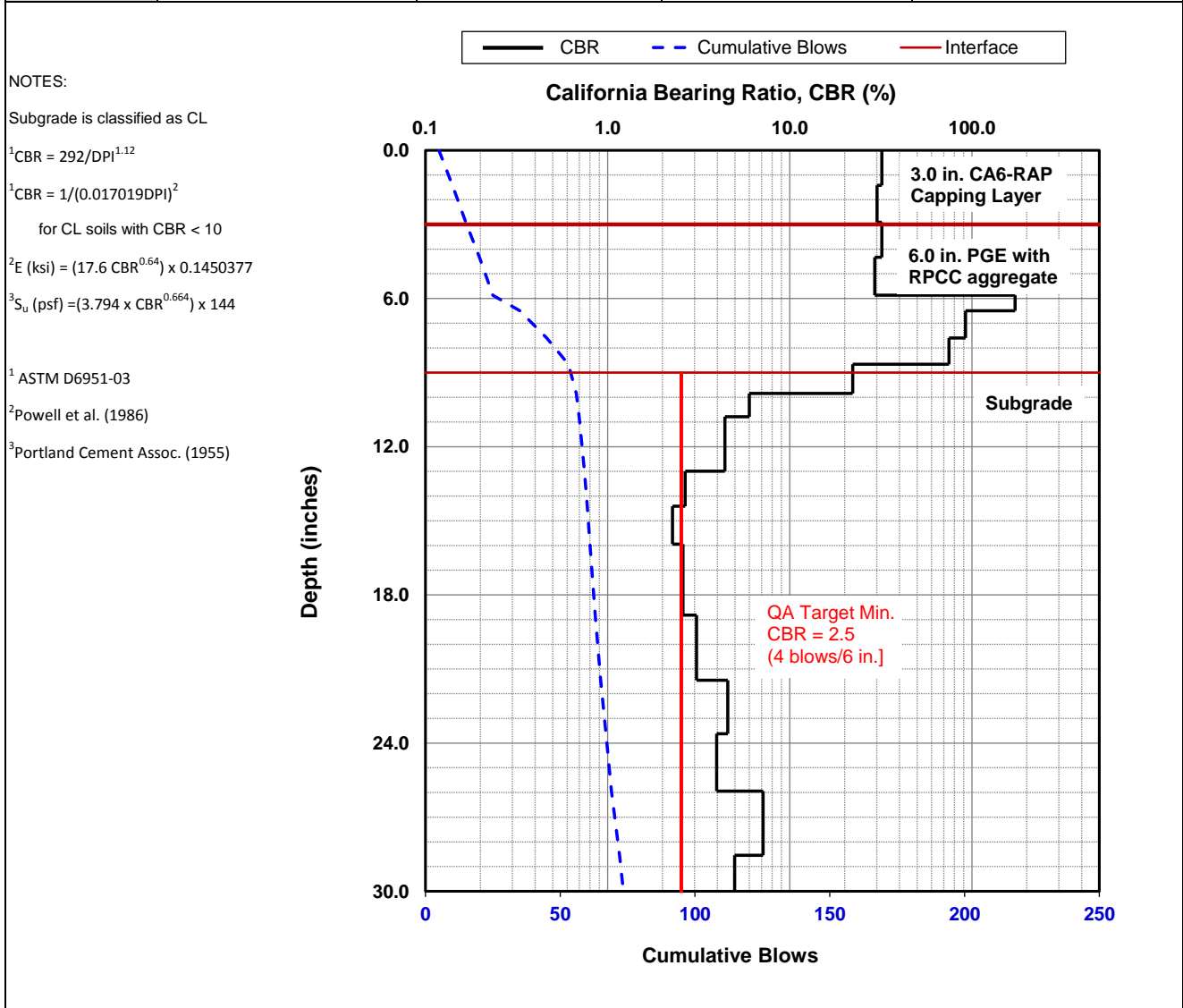


Dynamic Cone Penetrometer (DCP) Test Results	
Project Name:	Illinois Tollway - IC Research
Project ID:	Elgin O'Hare Extension - IL Tollway
Location:	IL390 (West of O'Hare)



Date of Test	5/4/2017	Test ID	TS12_Pt. 1	Operator	PV	ASTM	D6951
Latitude	41.9831190	Longitude	-87.9643397	Elevation (ft)	NA		
Location	Section 4644 (RAP)	Station	NA				
Comments	Nominal 3 in. of CA6-RAP compacted over nominal 6 in. PGE with RPCC crushed aggregate. <i>Subgrade assumed as CL clay.</i> PGE prepared end of April 2017. CA6-RAP placed and compacted on 05/02 to 05/03/17.						

Parameter	DPI (mm/blow)	CBR (%)	E_{CBR} , Elastic Modulus (ksi) (non stress-dependent)	S_{u-CBR} , Bearing Capacity (psf)
Avg. PGE+CA6 Layer [0 to 9.0 in.]	4.2	59.3	34.8	8,218
Avg. Subgrade Layer [9.0 to 21.0 in.]	27.1	4.7	6.9	1,528
Ratio of Avg. Top/Bottom Layer	0.2	12.6	5.1	5.4
Std.Dev.PGE+CA6 Layer [0 to 9 in.]	2.5	50.8	31.5	7,416
Std. Dev. Subgrade Layer [9.0 to 21.0 in.]	10.1	7.2	9.0	2,021

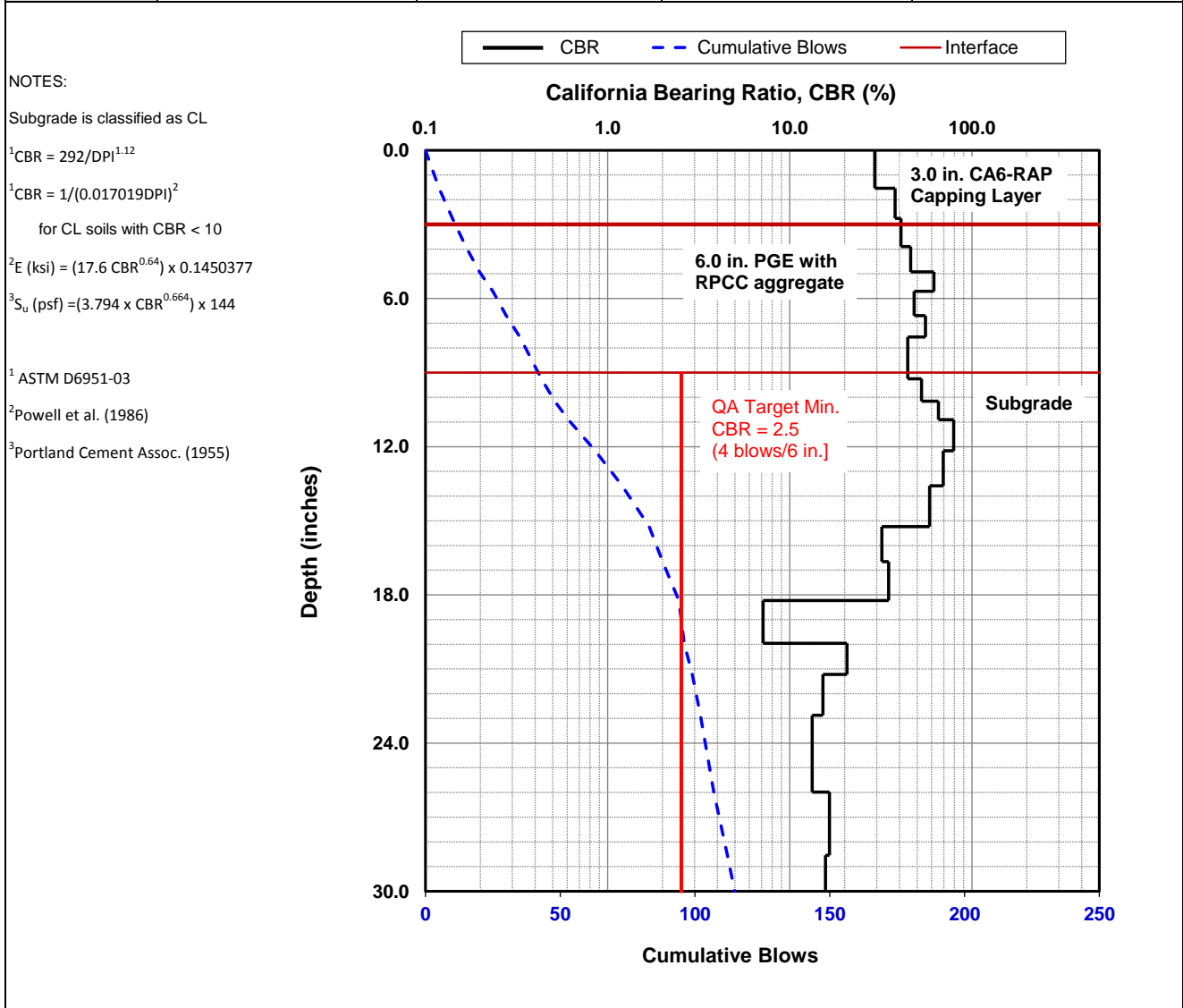


Dynamic Cone Penetrometer (DCP) Test Results	
Project Name:	Illinois Tollway - IC Research
Project ID:	Elgin O'Hare Extension - IL Tollway
Location:	IL390 (West of O'Hare)



Date of Test	5/4/2017	Test ID	TS12_Pt. 2	Operator	PV	ASTM	D6951
Latitude	41.9831100	Longitude	-87.9640995	Elevation (ft)	NA		
Location	Section 4644 (RAP)	Station	NA				
Comments	Nominal 3 in. of CA6-RAP compacted over nominal 6 in. PGE with RPCC crushed aggregate. <i>Subgrade assumed as CL clay.</i> PGE prepared end of April 2017. CA6-RAP placed and compacted on 05/02 to 05/03/17.						

Parameter	DPI (mm/blow)	CBR (%)	E_{CBR} , Elastic Modulus (ksi) (non stress-dependent)	S_{u-CBR} , Bearing Capacity (psf)
Avg. PGE+CA6 Layer [0 to 9.0 in.]	5.5	43.6	28.6	6,698
Avg. Subgrade Layer [9.0 to 21.0 in.]	5.4	43.9	28.7	6,731
Ratio of Avg. Top/Bottom Layer	1.0	1.0	1.0	1.0
Std.Dev.PGE+CA6 Layer [0 to 9 in.]	1.3	10.9	11.8	2,673
Std. Dev. Subgrade Layer [9.0 to 21.0 in.]	6.0	24.3	19.7	4,544

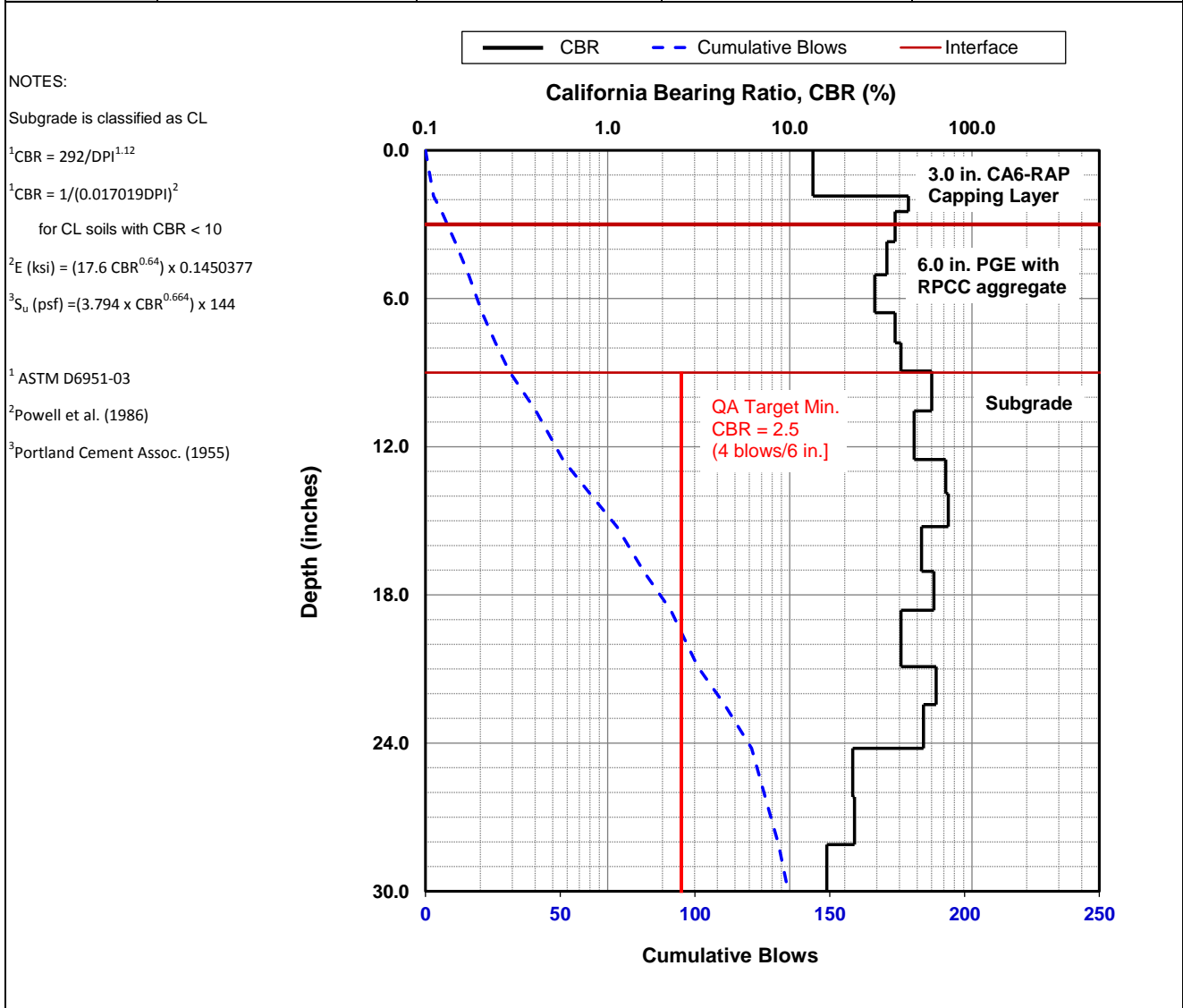


Dynamic Cone Penetrometer (DCP) Test Results	
Project Name:	Illinois Tollway - IC Research
Project ID:	Elgin O'Hare Extension - IL Tollway
Location:	IL390 (West of O'Hare)



Date of Test	5/4/2017	Test ID	TS12_Pt. 3	Operator	PV	ASTM	D6951
Latitude	41.9830886	Longitude	-87.9640234	Elevation (ft)	NA		
Location	Section 4644 (RAP)	Station	NA				
Comments	Nominal 3 in. of CA6-RAP compacted over nominal 6 in. PGE with RPCC crushed aggregate. <i>Subgrade assumed as CL clay.</i> PGE prepared end of April 2017. CA6-RAP placed and compacted on 05/02 to 05/03/17.						

Parameter	DPI (mm/blow)	CBR (%)	E_{CBR} , Elastic Modulus (ksi) (non stress-dependent)	S_{u-CBR} , Bearing Capacity (psf)
Avg. PGE+CA6 Layer [0 to 9.0 in.]	7.3	31.4	23.2	5,388
Avg. Subgrade Layer [9.0 to 21.0 in.]	4.3	56.4	33.7	7,946
Ratio of Avg. Top/Bottom Layer	1.7	0.6	0.7	0.7
Std.Dev.PGE+CA6 Layer [0 to 9 in.]	4.4	12.0	12.5	2,847
Std. Dev. Subgrade Layer [9.0 to 21.0 in.]	0.9	12.2	12.6	2,871

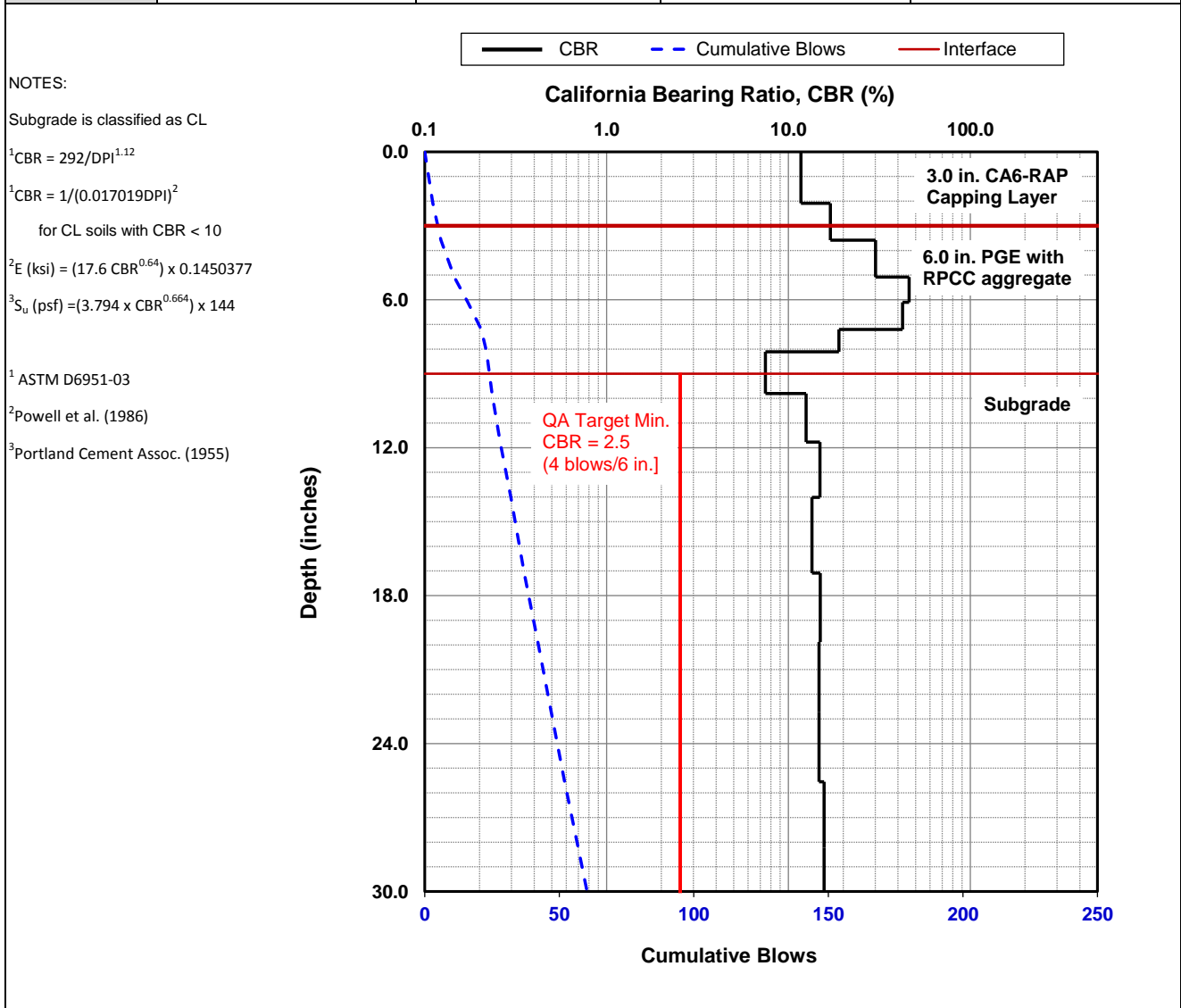


Dynamic Cone Penetrometer (DCP) Test Results	
Project Name:	Illinois Tollway - IC Research
Project ID:	Elgin O'Hare Extension - IL Tollway
Location:	IL390 (West of O'Hare)



Date of Test	5/4/2017	Test ID	TS12_Pt. 4	Operator	PV	ASTM	D6951
Latitude	41.9830145	Longitude	-87.9636936	Elevation (ft)	NA		
Location	Section 4644 (RAP)	Station	NA				
Comments	Nominal 3 in. of CA6-RAP compacted over nominal 6 in. PGE with RPCC crushed aggregate. <i>Subgrade assumed as CL clay.</i> PGE prepared end of April 2017. CA6-RAP placed and compacted on 05/02 to 05/03/17.						

Parameter	DPI (mm/blow)	CBR (%)	E_{CBR} , Elastic Modulus (ksi) (non stress-dependent)	S_{u-CBR} , Bearing Capacity (psf)
Avg. PGE+CA6 Layer [0 to 9.0 in.]	10.0	22.3	18.6	4,286
Avg. Subgrade Layer [9.0 to 21.0 in.]	14.6	14.5	14.1	3,221
Ratio of Avg. Top/Bottom Layer	0.7	1.5	1.3	1.3
Std.Dev.PGE+CA6 Layer [0 to 9 in.]	6.1	14.7	14.2	3,252
Std. Dev. Subgrade Layer [9.0 to 21.0 in.]	1.0	1.1	2.7	573

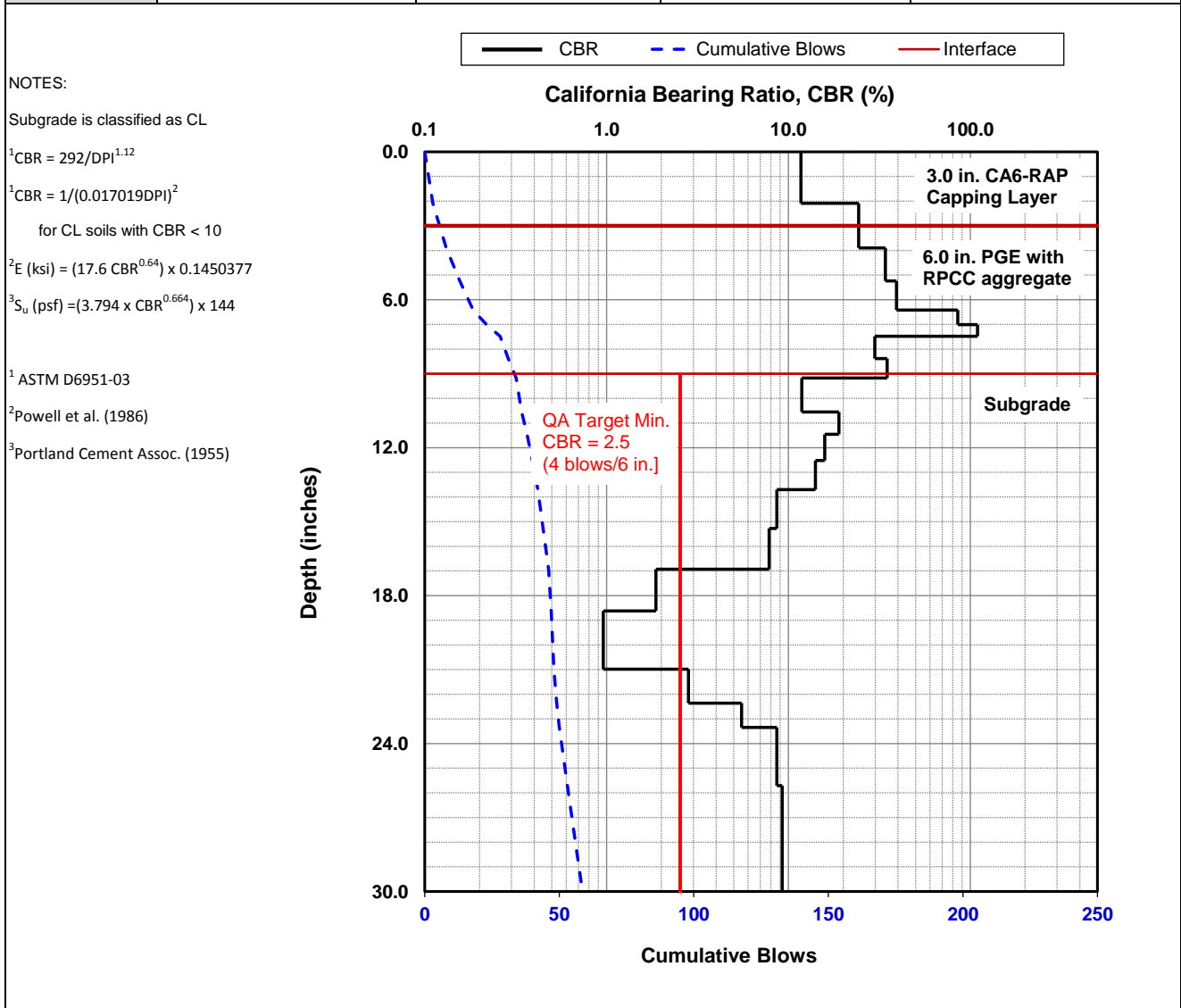


Dynamic Cone Penetrometer (DCP) Test Results	
Project Name:	Illinois Tollway - IC Research
Project ID:	Elgin O'Hare Extension - IL Tollway
Location:	IL390 (West of O'Hare)



Date of Test	5/4/2017	Test ID	TS12_Pt. 5	Operator	PV	ASTM	D6951
Latitude	41.9830028	Longitude	-87.9634073	Elevation (ft)	NA		
Location	Section 4644 (RAP)	Station	NA				
Comments	Nominal 3 in. of CA6-RAP compacted over nominal 6 in. PGE with RPCC crushed aggregate. <i>Subgrade assumed as CL clay.</i> PGE prepared end of April 2017. CA6-RAP placed and compacted on 05/02 to 05/03/17.						

Parameter	DPI (mm/blow)	CBR (%)	E_{CBR} , Elastic Modulus (ksi) (non stress-dependent)	S_{u-CBR} , Bearing Capacity (psf)
Avg. PGE+CA6 Layer [0 to 9.0 in.]	6.9	33.8	24.3	5,660
Avg. Subgrade Layer [9.0 to 21.0 in.]	21.4	7.5	9.3	2,086
Ratio of Avg. Top/Bottom Layer	0.3	4.5	2.6	2.7
Std.Dev.PGE+CA6 Layer [0 to 9 in.]	5.6	33.3	24.0	5,598
Std. Dev. Subgrade Layer [9.0 to 21.0 in.]	17.2	6.4	8.4	1,877

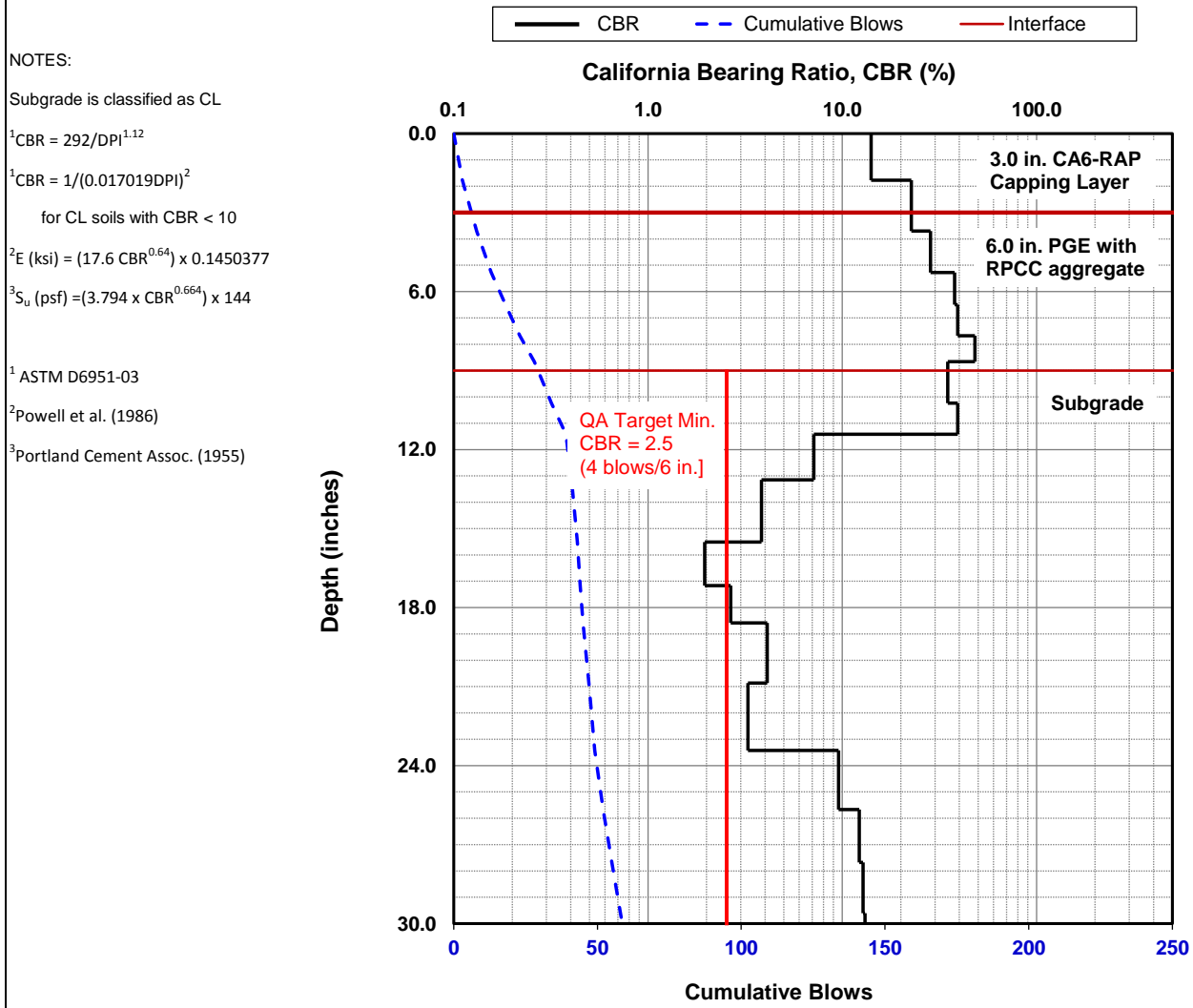


Dynamic Cone Penetrometer (DCP) Test Results	
Project Name:	Illinois Tollway - IC Research
Project ID:	Elgin O'Hare Extension - IL Tollway
Location:	IL390 (West of O'Hare)



Date of Test	5/4/2017	Test ID	TS12_Pt. 6	Operator	PV	ASTM	D6951
Latitude	41.9830379	Longitude	-87.9632648	Elevation (ft)	NA		
Location	Section 4644 (RAP)	Station	NA				
Comments	Nominal 3 in. of CA6-RAP compacted over nominal 6 in. PGE with RPCC crushed aggregate. <i>Subgrade assumed as CL clay.</i> PGE prepared end of April 2017. CA6-RAP placed and compacted on 05/02 to 05/03/17.						

Parameter	DPI (mm/blow)	CBR (%)	E _{CBR} , Elastic Modulus (ksi) (non stress-dependent)	S _{u-CBR} , Bearing Capacity (psf)
Avg. PGE+CA6 Layer [0 to 9.0 in.]	7.9	29.0	22.0	5,113
Avg. Subgrade Layer [9.0 to 21.0 in.]	16.3	12.8	13.1	2,969
Ratio of Avg. Top/Bottom Layer	0.5	2.3	1.7	1.7
Std.Dev.PGE+CA6 Layer [0 to 9 in.]	4.2	13.1	13.3	3,021
Std. Dev. Subgrade Layer [9.0 to 21.0 in.]	14.3	16.9	15.6	3,569

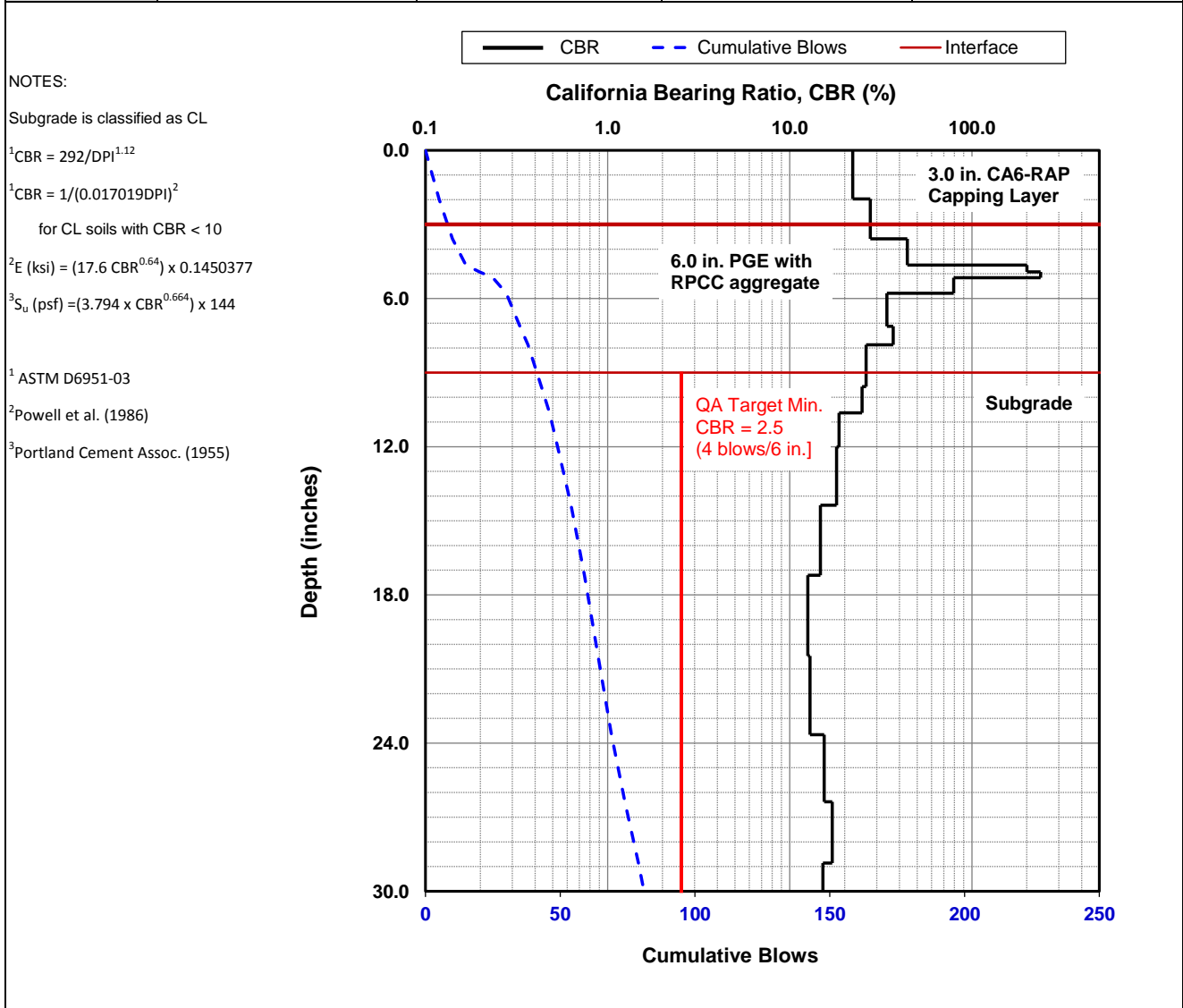


Dynamic Cone Penetrometer (DCP) Test Results	
Project Name:	Illinois Tollway - IC Research
Project ID:	Elgin O'Hare Extension - IL Tollway
Location:	IL390 (West of O'Hare)



Date of Test	5/4/2017	Test ID	TS12_Pt. 7	Operator	PV	ASTM	D6951
Latitude	41.9831111	Longitude	-87.9634161	Elevation (ft)	NA		
Location	Section 4644 (RAP)	Station	NA				
Comments	Nominal 3 in. of CA6-RAP compacted over nominal 6 in. PGE with RPCC crushed aggregate. <i>Subgrade assumed as CL clay.</i> PGE prepared end of April 2017. CA6-RAP placed and compacted on 05/02 to 05/03/17.						

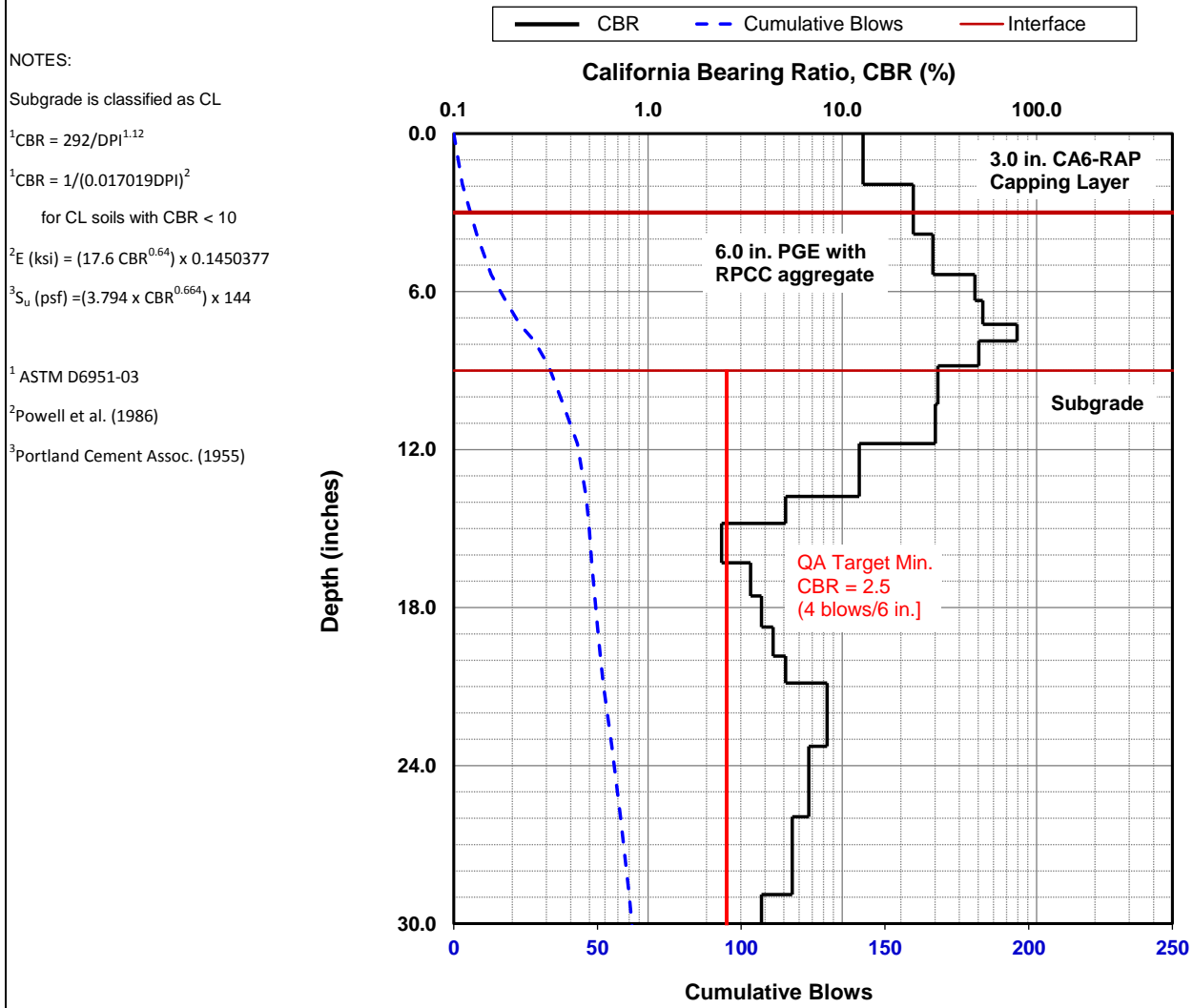
Parameter	DPI (mm/blow)	CBR (%)	E _{CBR} , Elastic Modulus (ksi) (non stress-dependent)	S _{u-CBR} , Bearing Capacity (psf)
Avg. PGE+CA6 Layer [0 to 9.0 in.]	5.7	42.0	27.9	6,533
Avg. Subgrade Layer [9.0 to 21.0 in.]	13.2	16.2	15.2	3,478
Ratio of Avg. Top/Bottom Layer	0.4	2.6	1.8	1.9
Std.Dev.PGE+CA6 Layer [0 to 9 in.]	3.3	79.3	41.9	9,965
Std. Dev. Subgrade Layer [9.0 to 21.0 in.]	2.9	4.7	6.9	1,527



Dynamic Cone Penetrometer (DCP) Test Results	
Project Name:	Illinois Tollway - IC Research
Project ID:	Elgin O'Hare Extension - IL Tollway
Location:	IL390 (West of O'Hare)

Date of Test	5/4/2017	Test ID	TS12_Pt. 8	Operator	PV	ASTM	D6951
Latitude	41.9830090	Longitude	-87.9628502	Elevation (ft)	NA		
Location	Section 4644 (RAP)	Station	NA				
Comments	Nominal 3 in. of CA6-RAP compacted over nominal 6 in. PGE with RPCC crushed aggregate. <i>Subgrade assumed as CL clay.</i> PGE prepared end of April 2017. CA6-RAP placed and compacted on 05/02 to 05/03/17.						

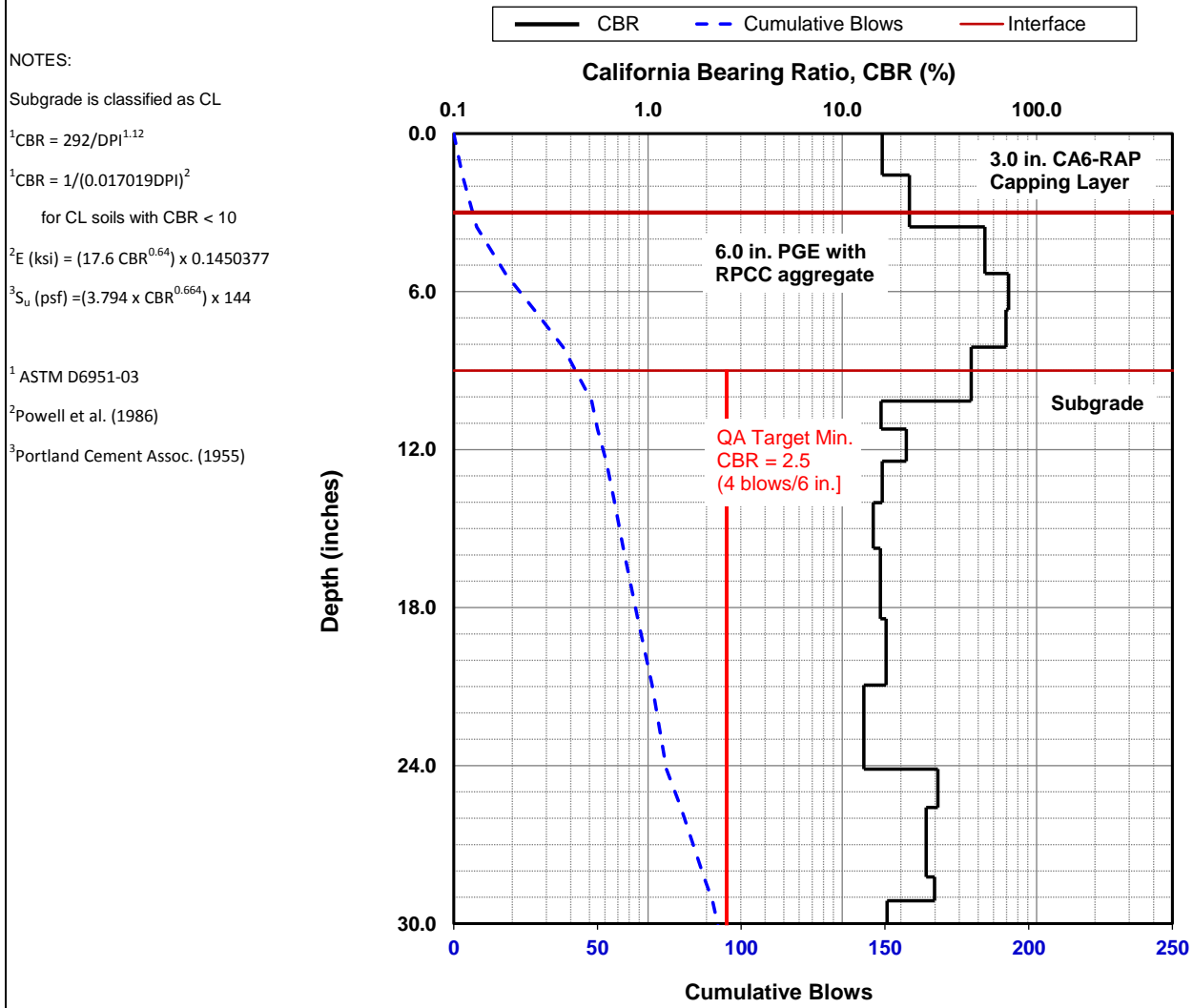
Parameter	DPI (mm/blow)	CBR (%)	E _{CBR} , Elastic Modulus (ksi) (non stress-dependent)	S _{u-CBR} , Bearing Capacity (psf)
Avg. PGE+CA6 Layer [0 to 9.0 in.]	6.8	34.2	24.5	5,701
Avg. Subgrade Layer [9.0 to 21.0 in.]	16.1	13.0	13.2	2,998
Ratio of Avg. Top/Bottom Layer	0.4	2.6	1.9	1.9
Std.Dev.PGE+CA6 Layer [0 to 9 in.]	5.3	23.2	19.1	4,401
Std. Dev. Subgrade Layer [9.0 to 21.0 in.]	10.7	11.5	12.2	2,771



Dynamic Cone Penetrometer (DCP) Test Results		
Project Name:	Illinois Tollway - IC Research	
Project ID:	Elgin O'Hare Extension - IL Tollway	
Location:	IL390 (West of O'Hare)	

Date of Test	5/4/2017	Test ID	TS12_Pt. 9	Operator	PV	ASTM	D6951
Latitude	41.9830025	Longitude	-87.9626853	Elevation (ft)	NA		
Location	Section 4644 (RAP)	Station	NA				
Comments	Nominal 3 in. of CA6-RAP compacted over nominal 6 in. PGE with RPCC crushed aggregate. <i>Subgrade assumed as CL clay.</i> PGE prepared end of April 2017. CA6-RAP placed and compacted on 05/02 to 05/03/17.						

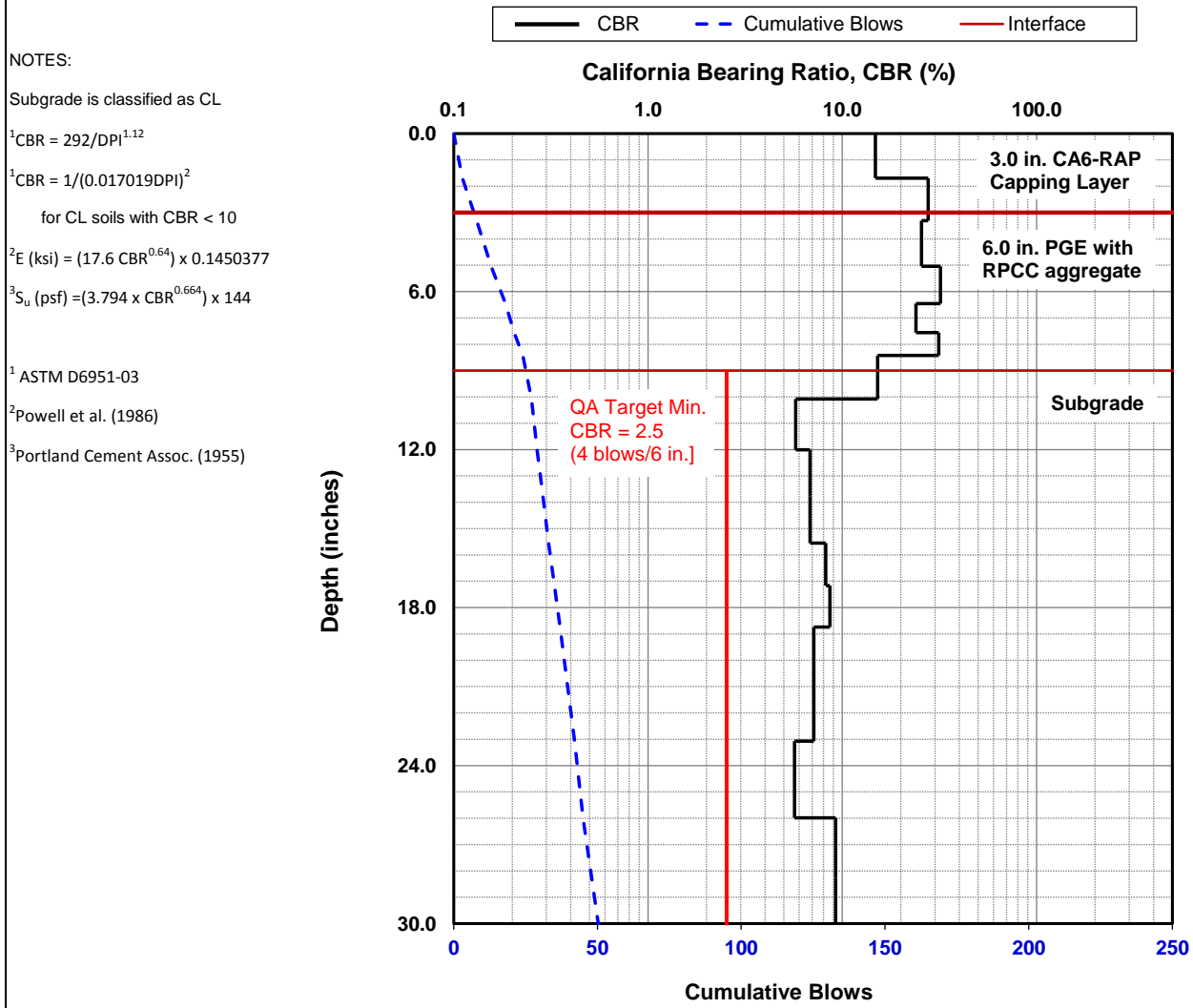
Parameter	DPI (mm/blow)	CBR (%)	E_{CBR} , Elastic Modulus (ksi) (non stress-dependent)	S_{u-CBR} , Bearing Capacity (psf)
Avg. PGE+CA6 Layer [0 to 9.0 in.]	5.4	44.0	28.8	6,738
Avg. Subgrade Layer [9.0 to 21.0 in.]	13.0	16.4	15.3	3,507
Ratio of Avg. Top/Bottom Layer	0.4	2.7	1.9	1.9
Std.Dev.PGE+CA6 Layer [0 to 9 in.]	4.7	26.6	20.8	4,824
Std. Dev. Subgrade Layer [9.0 to 21.0 in.]	3.2	11.3	12.1	2,737



Dynamic Cone Penetrometer (DCP) Test Results	
Project Name:	Illinois Tollway - IC Research
Project ID:	Elgin O'Hare Extension - IL Tollway
Location:	IL390 (West of O'Hare)

Date of Test	5/4/2017	Test ID	TS12_Pt. 10	Operator	PV	ASTM	D6951
Latitude	41.9829712	Longitude	-87.9623447	Elevation (ft)	NA		
Location	Section 4644 (RAP)	Station	NA				
Comments	Nominal 3 in. of CA6-RAP compacted over nominal 6 in. PGE with RPCC crushed aggregate. <i>Subgrade assumed as CL clay.</i> PGE prepared end of April 2017. CA6-RAP placed and compacted on 05/02 to 05/03/17.						

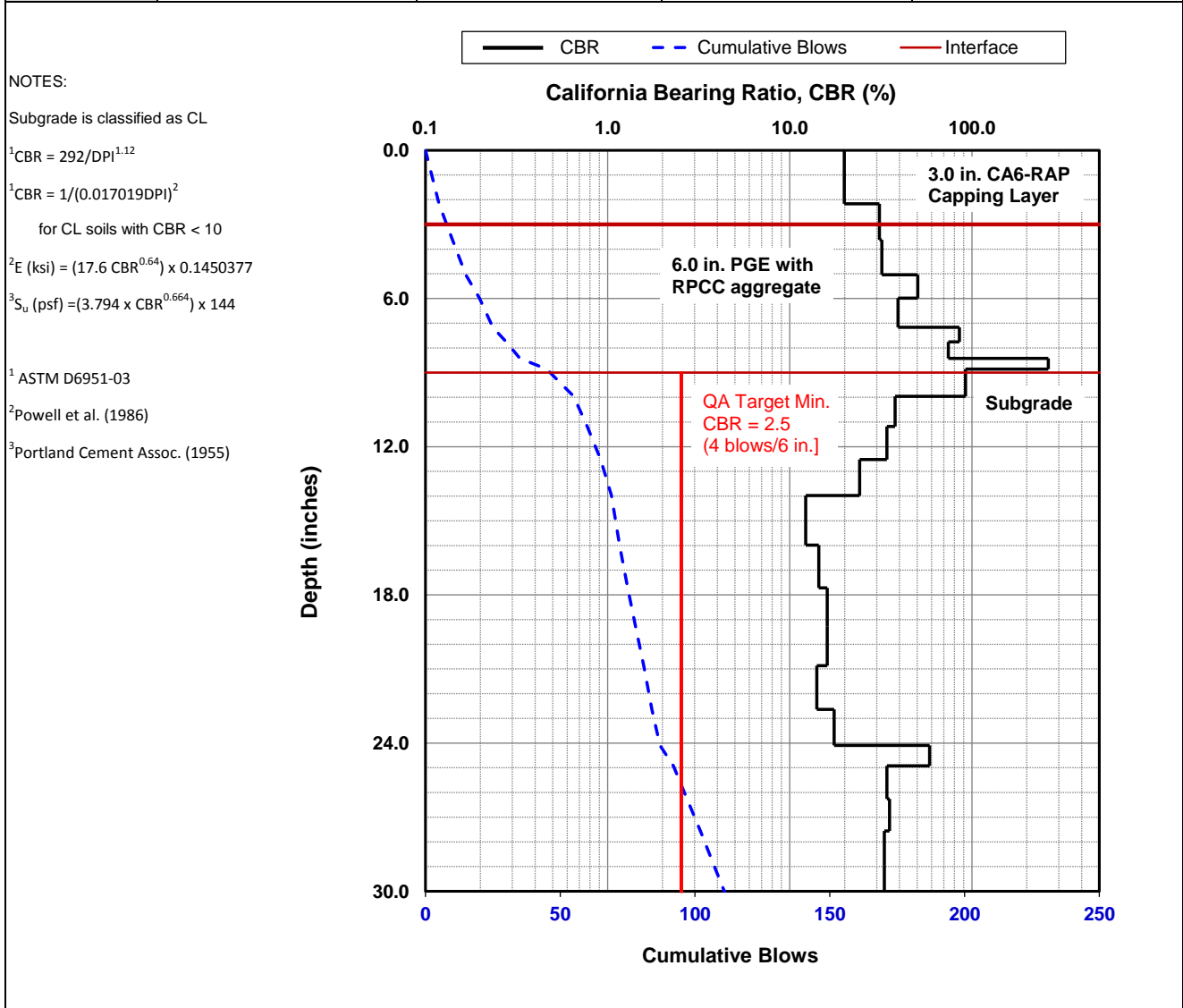
Parameter	DPI (mm/blow)	CBR (%)	E _{CBR} , Elastic Modulus (ksi) (non stress-dependent)	S _{u-CBR} , Bearing Capacity (psf)
Avg. PGE+CA6 Layer [0 to 9.0 in.]	8.9	25.2	20.1	4,654
Avg. Subgrade Layer [9.0 to 21.0 in.]	22.0	7.1	9.0	2,014
Ratio of Avg. Top/Bottom Layer	0.4	3.5	2.2	2.3
Std.Dev.PGE+CA6 Layer [0 to 9 in.]	3.1	7.1	9.0	2,008
Std. Dev. Subgrade Layer [9.0 to 21.0 in.]	3.4	3.2	5.3	1,173



Dynamic Cone Penetrometer (DCP) Test Results		
Project Name:	Illinois Tollway - IC Research	
Project ID:	Elgin O'Hare Extension - IL Tollway	
Location:	IL390 (West of O'Hare)	

Date of Test	5/4/2017	Test ID	TS12_Pt. 11	Operator	PV	ASTM	D6951
Latitude	41.9830280	Longitude	-87.9619420	Elevation (ft)	NA		
Location	Section 4644 (RAP)	Station	NA				
Comments	Nominal 3 in. of CA6-RAP compacted over nominal 6 in. PGE with RPCC crushed aggregate. <i>Subgrade assumed as CL clay.</i> PGE prepared end of April 2017. CA6-RAP placed and compacted on 05/02 to 05/03/17.						

Parameter	DPI (mm/blow)	CBR (%)	E_{CBR} , Elastic Modulus (ksi) (non stress-dependent)	S_{u-CBR} , Bearing Capacity (psf)
Avg. PGE+CA6 Layer [0 to 9.0 in.]	5.0	48.1	30.5	7,156
Avg. Subgrade Layer [9.0 to 21.0 in.]	8.5	26.7	20.9	4,834
Ratio of Avg. Top/Bottom Layer	0.6	1.8	1.5	1.5
Std.Dev.PGE+CA6 Layer [0 to 9 in.]	3.4	76.3	40.9	9,715
Std. Dev. Subgrade Layer [9.0 to 21.0 in.]	4.9	26.5	20.8	4,815

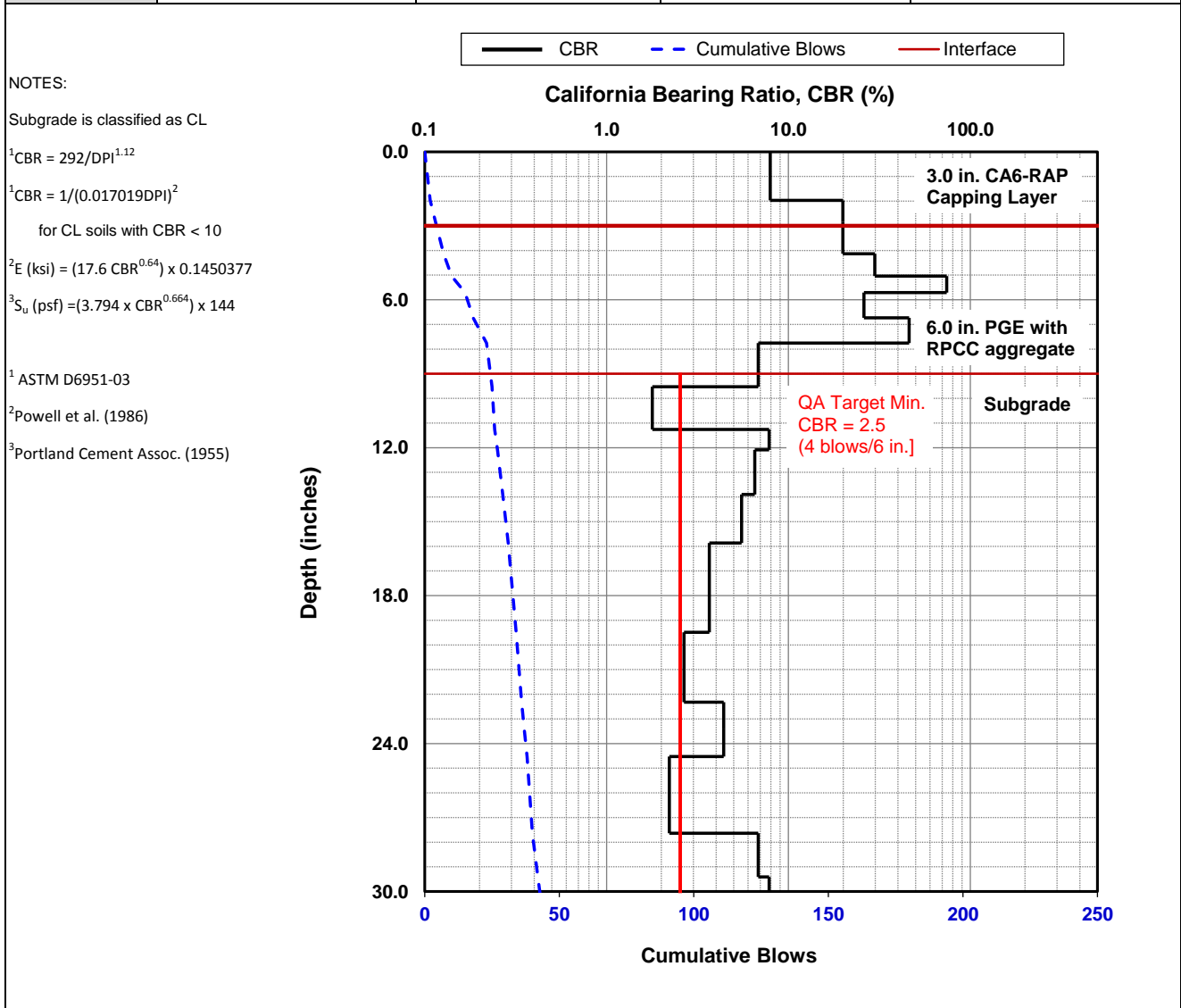


Dynamic Cone Penetrometer (DCP) Test Results	
Project Name:	Illinois Tollway - IC Research
Project ID:	Elgin O'Hare Extension - IL Tollway
Location:	IL390 (West of O'Hare)



Date of Test	5/4/2017	Test ID	TS12_Pt. 12	Operator	PV	ASTM	D6951
Latitude	41.9830816	Longitude	-87.9618267	Elevation (ft)	NA		
Location	Section 4644 (RAP)	Station	NA				
Comments	Nominal 3 in. of CA6-RAP compacted over nominal 6 in. PGE with RPCC crushed aggregate. <i>Subgrade assumed as CL clay.</i> PGE prepared end of April 2017. CA6-RAP placed and compacted on 05/02 to 05/03/17.						

Parameter	DPI (mm/blow)	CBR (%)	E_{CBR} , Elastic Modulus (ksi) (non stress-dependent)	S_{u-CBR} , Bearing Capacity (psf)
Avg. PGE+CA6 Layer [0 to 9.0 in.]	9.7	23.0	19.0	4,378
Avg. Subgrade Layer [9.0 to 21.0 in.]	28.1	4.4	6.6	1,454
Ratio of Avg. Top/Bottom Layer	0.3	5.3	2.9	3.0
Std.Dev.PGE+CA6 Layer [0 to 9 in.]	8.6	21.9	18.4	4,238
Std. Dev. Subgrade Layer [9.0 to 21.0 in.]	9.3	2.4	4.4	972

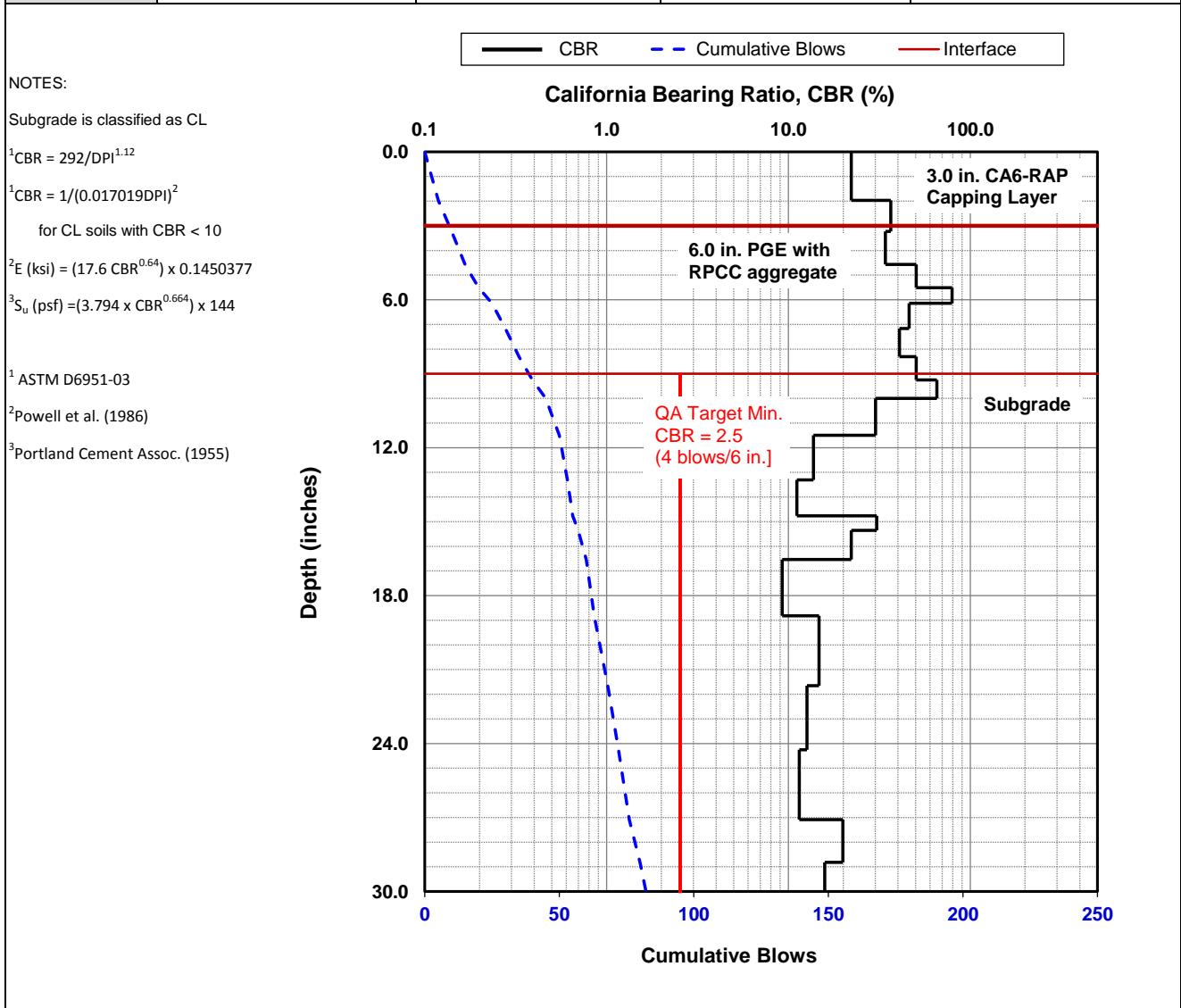


Dynamic Cone Penetrometer (DCP) Test Results	
Project Name:	Illinois Tollway - IC Research
Project ID:	Elgin O'Hare Extension - IL Tollway
Location:	IL390 (West of O'Hare)



Date of Test	5/4/2017	Test ID	TS12_Pt. 13	Operator	PV	ASTM	D6951
Latitude	41.9829641	Longitude	-87.9614688	Elevation (ft)	NA		
Location	Section 4644 (RAP)	Station	NA				
Comments	Nominal 3 in. of CA6-RAP compacted over nominal 6 in. PGE with RPCC crushed aggregate. <i>Subgrade assumed as CL clay.</i> PGE prepared end of April 2017. CA6-RAP placed and compacted on 05/02 to 05/03/17.						

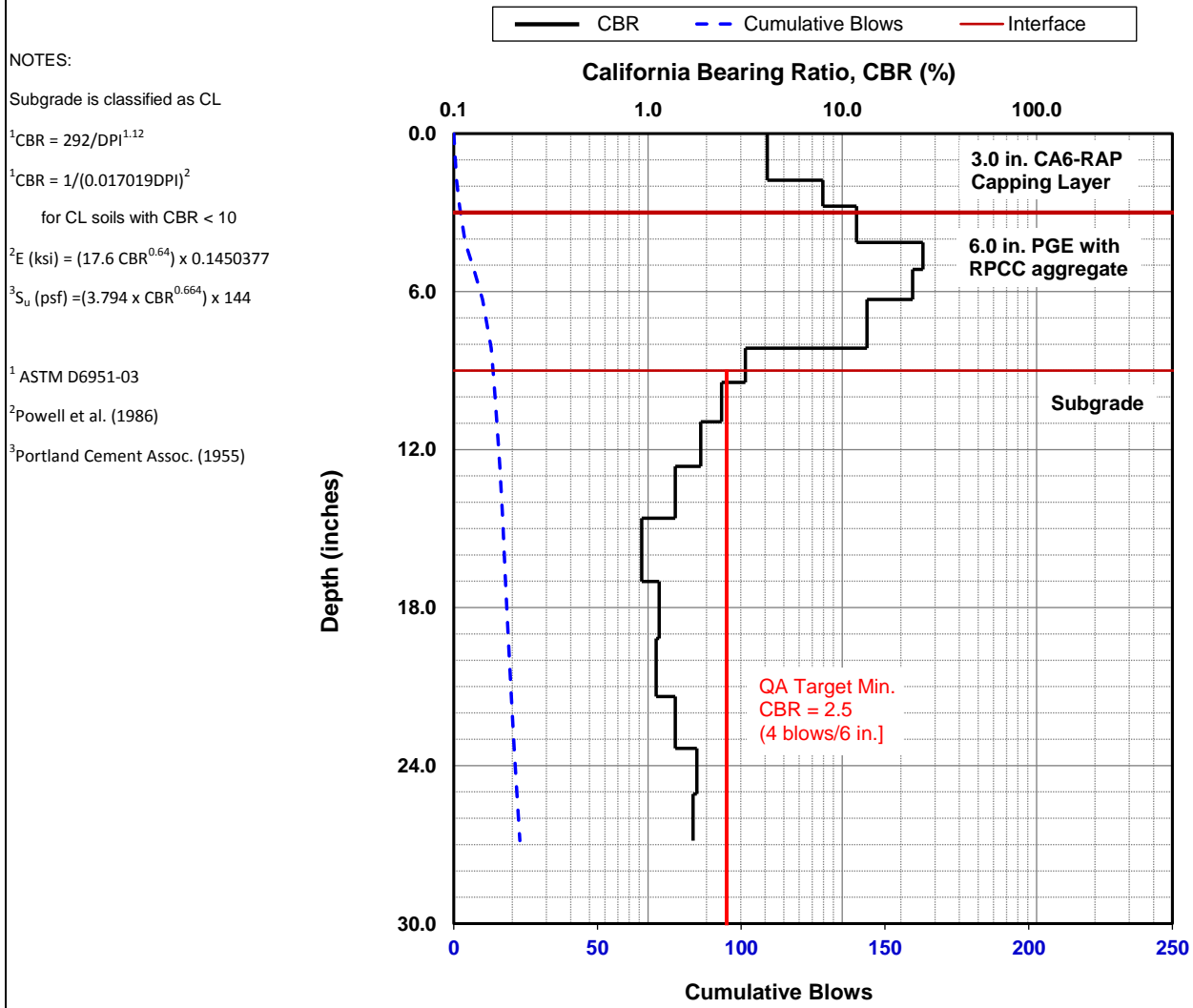
Parameter	DPI (mm/blow)	CBR (%)	E_{CBR} , Elastic Modulus (ksi) (non stress-dependent)	S_{u-CBR} , Bearing Capacity (psf)
Avg. PGE+CA6 Layer [0 to 9.0 in.]	5.9	40.2	27.1	6,347
Avg. Subgrade Layer [9.0 to 21.0 in.]	11.3	19.4	17.0	3,915
Ratio of Avg. Top/Bottom Layer	0.5	2.1	1.6	1.6
Std.Dev.PGE+CA6 Layer [0 to 9 in.]	2.3	17.4	15.9	3,646
Std. Dev. Subgrade Layer [9.0 to 21.0 in.]	5.7	18.4	16.5	3,781



Dynamic Cone Penetrometer (DCP) Test Results		
Project Name:	Illinois Tollway - IC Research	
Project ID:	Elgin O'Hare Extension - IL Tollway	
Location:	IL390 (West of O'Hare)	

Date of Test	5/4/2017	Test ID	TS12_Pt. 14	Operator	PV	ASTM	D6951
Latitude	41.9830497	Longitude	-87.9612512	Elevation (ft)	NA		
Location	Section 4644 (RAP)	Station	NA				
Comments	Nominal 3 in. of CA6-RAP compacted over nominal 6 in. PGE with RPCC crushed aggregate. <i>Subgrade assumed as CL clay.</i> PGE prepared end of April 2017. CA6-RAP placed and compacted on 05/02 to 05/03/17.						

Parameter	DPI (mm/blow)	CBR (%)	E_{CBR} , Elastic Modulus (ksi) (non stress-dependent)	S_{u-CBR} , Bearing Capacity (psf)
Avg. PGE+CA6 Layer [0 to 9.0 in.]	17.1	12.1	12.6	2,862
Avg. Subgrade Layer [9.0 to 21.0 in.]	50.5	1.4	3.1	668
Ratio of Avg. Top/Bottom Layer	0.3	8.9	4.1	4.3
Std.Dev.PGE+CA6 Layer [0 to 9 in.]	14.7	8.8	10.2	2,309
Std. Dev. Subgrade Layer [9.0 to 21.0 in.]	10.3	0.8	2.2	479

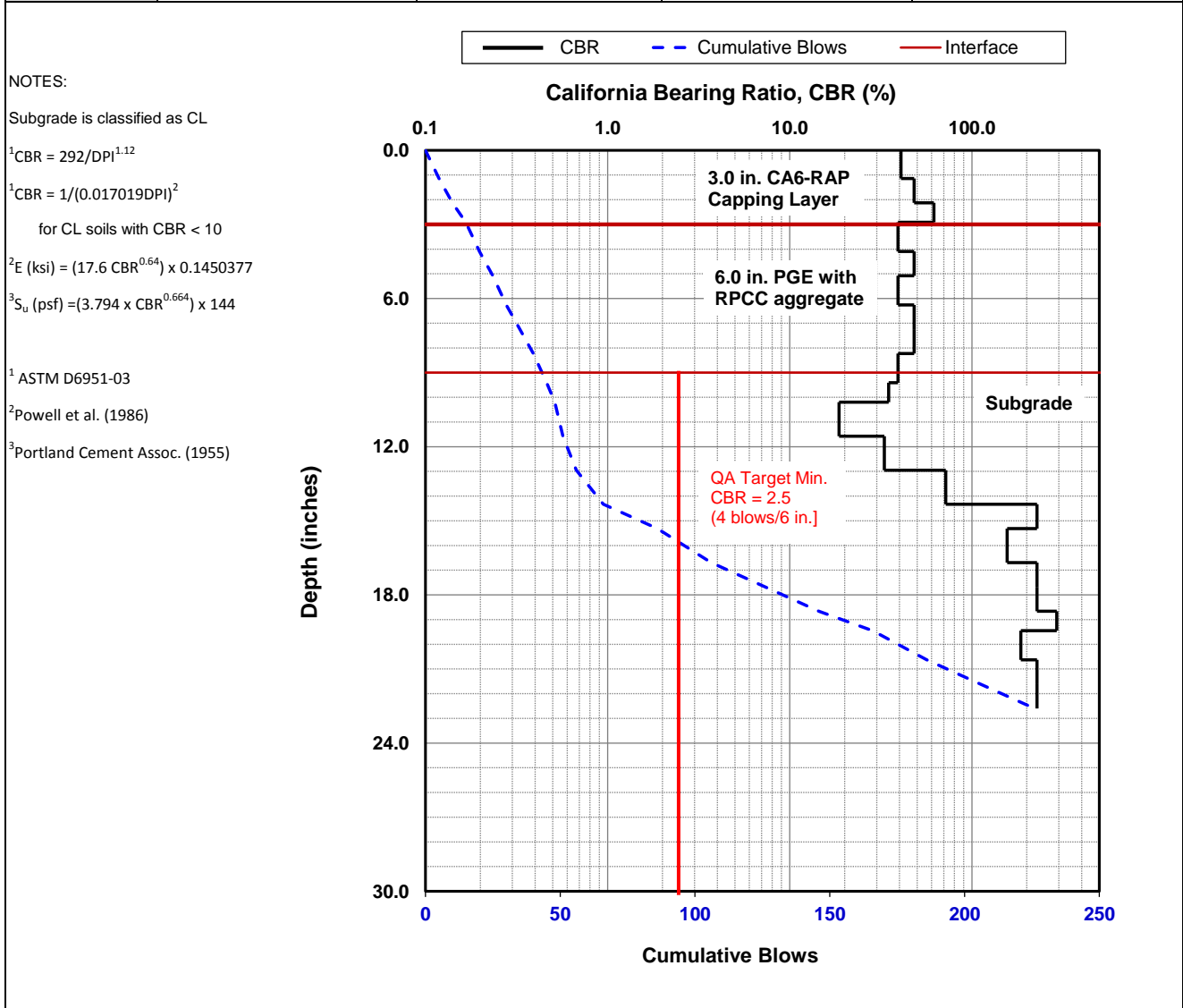


Dynamic Cone Penetrometer (DCP) Test Results	
Project Name:	Illinois Tollway - IC Research
Project ID:	Elgin O'Hare Extension - IL Tollway
Location:	IL390 (West of O'Hare)



Date of Test	5/4/2017	Test ID	TS12_Pt. 15	Operator	PV	ASTM	D6951
Latitude	41.9830231	Longitude	-87.9649881	Elevation (ft)	NA		
Location	Section 4644 (RAP)	Station	NA				
Comments	Nominal 3 in. of CA6-RAP compacted over nominal 6 in. PGE with RPCC crushed aggregate. <i>Subgrade assumed as CL clay.</i> PGE prepared end of April 2017. CA6-RAP placed and compacted on 05/02 to 05/03/17.						

Parameter	DPI (mm/blow)	CBR (%)	E_{CBR} , Elastic Modulus (ksi) (non stress-dependent)	S_{u-CBR} , Bearing Capacity (psf)
Avg. PGE+CA6 Layer [0 to 9.0 in.]	5.3	45.0	29.2	6,842
Avg. Subgrade Layer [9.0 to 21.0 in.]	2.0	132.8	58.3	14,034
Ratio of Avg. Top/Bottom Layer	2.6	0.3	0.5	0.5
Std.Dev.PGE+CA6 Layer [0 to 9 in.]	0.7	7.1	9.0	2,011
Std. Dev. Subgrade Layer [9.0 to 21.0 in.]	3.6	99.8	48.6	11,613

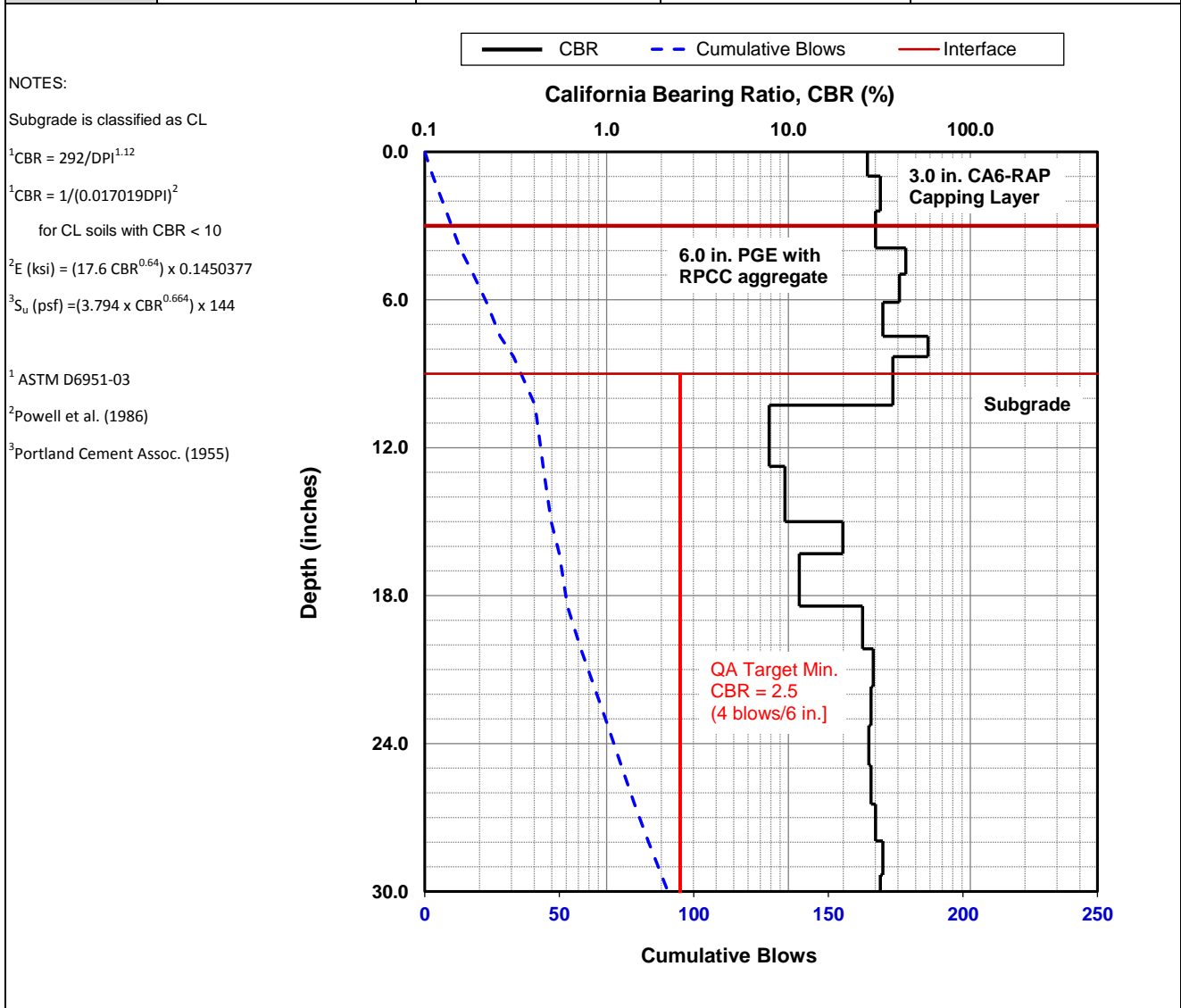


Dynamic Cone Penetrometer (DCP) Test Results	
Project Name:	Illinois Tollway - IC Research
Project ID:	Elgin O'Hare Extension - IL Tollway
Location:	IL390 (West of O'Hare)



Date of Test	6/21/2017	Test ID	TS13_Pt1	Operator	PV	ASTM	D6951
Latitude	-87.9924287		Longitude	0.0000000		Elevation (ft)	NA
Location	EB Thorndale Ave. between Hamilton Lakes Dr. and North Arlington Heights Rd		Station	NA			
Comments	Nominal 3 in. of CA6-RAP compacted over nominal 6 in. PGE with RPCC crushed aggregate. <i>Subgrade assumed as CL clay.</i>						

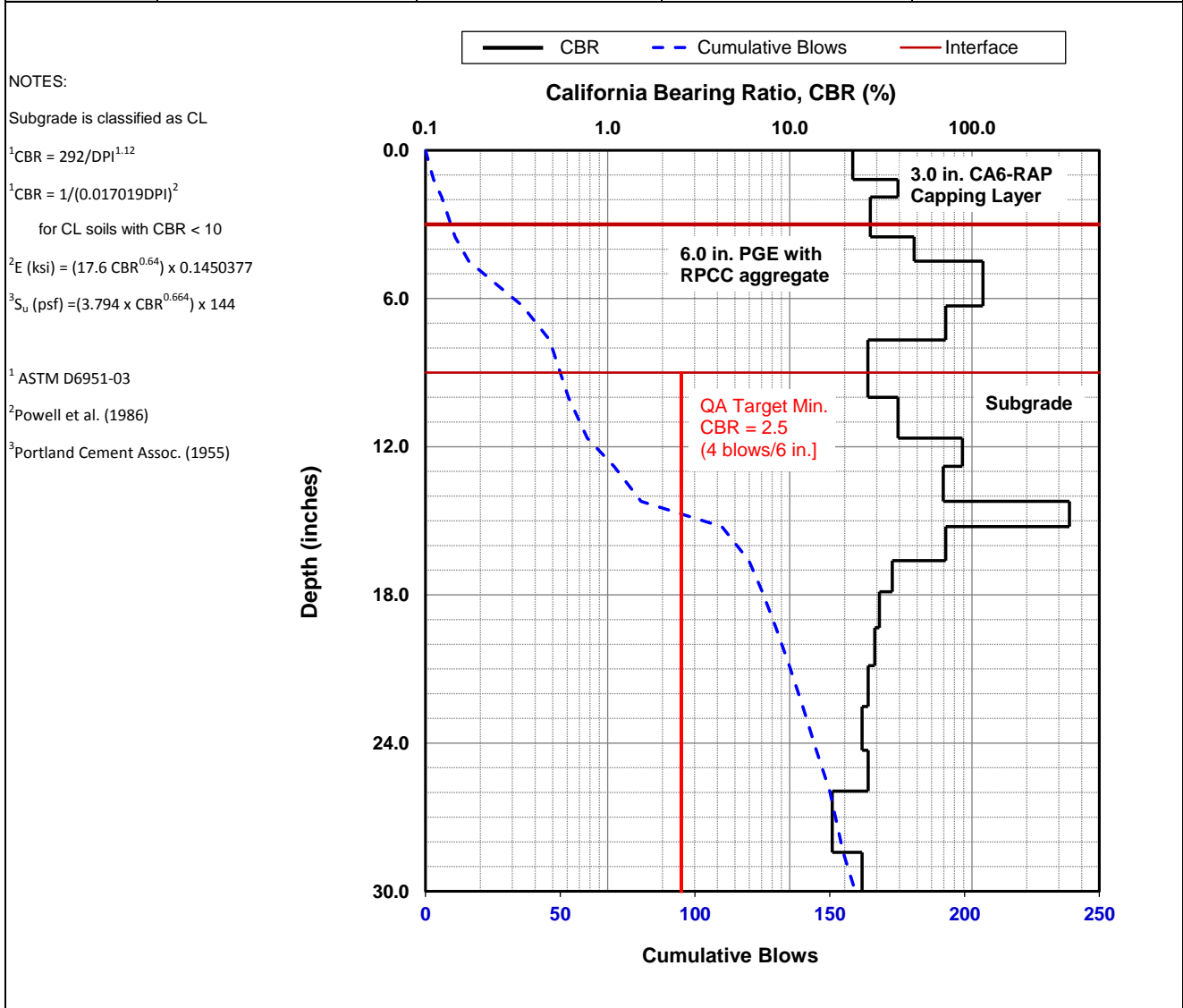
Parameter	DPI (mm/blow)	CBR (%)	E_{CBR} , Elastic Modulus (ksi) (non stress-dependent)	S_{u-CBR} , Bearing Capacity (psf)
Avg. PGE+CA6 Layer [0 to 9.0 in.]	6.4	36.6	25.5	5,960
Avg. Subgrade Layer [9.0 to 21.0 in.]	11.3	19.3	16.9	3,894
Ratio of Avg. Top/Bottom Layer	0.6	1.9	1.5	1.5
Std.Dev.PGE+CA6 Layer [0 to 9 in.]	1.5	10.8	11.7	2,645
Std. Dev. Subgrade Layer [9.0 to 21.0 in.]	6.4	17.1	15.7	3,595



Dynamic Cone Penetrometer (DCP) Test Results	
Project Name:	Illinois Tollway - IC Research
Project ID:	Elgin O'Hare Extension - IL Tollway
Location:	IL390 (West of O'Hare)

Date of Test	6/21/2017	Test ID	TS13_Pt2	Operator	HG/JV	ASTM	D6951
Latitude	41.9837800		Longitude	88.0114210		Elevation (ft)	NA
Location	EB Thorndale Ave. between Hamilton Lakes Dr. and North Arlington Heights Rd		Station	NA			
Comments	Nominal 3 in. of CA6-RAP compacted over nominal 6 in. PGE with RPCC crushed aggregate. <i>Subgrade assumed as CL clay.</i>						

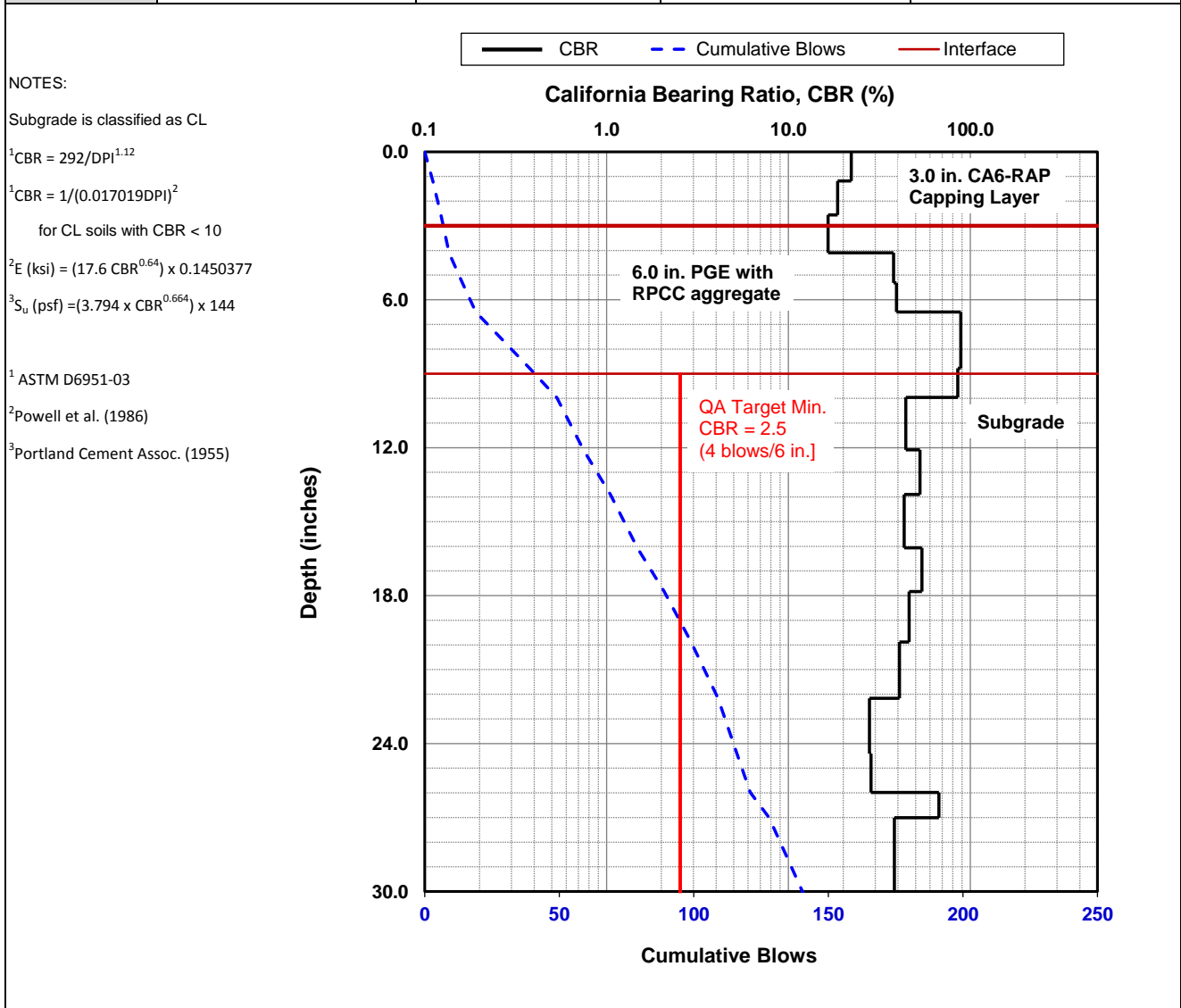
Parameter	DPI (mm/blow)	CBR (%)	E_{CBR} , Elastic Modulus (ksi) (non stress-dependent)	S_{u-CBR} , Bearing Capacity (psf)
Avg. PGE+CA6 Layer [0 to 9.0 in.]	4.8	50.5	31.4	7,385
Avg. Subgrade Layer [9.0 to 21.0 in.]	3.9	62.8	36.1	8,534
Ratio of Avg. Top/Bottom Layer	1.2	0.8	0.9	0.9
Std.Dev.PGE+CA6 Layer [0 to 9 in.]	3.1	37.8	26.1	6,096
Std. Dev. Subgrade Layer [9.0 to 21.0 in.]	2.7	92.6	46.3	11,047



Dynamic Cone Penetrometer (DCP) Test Results		
Project Name:	Illinois Tollway - IC Research	
Project ID:	Elgin O'Hare Extension - IL Tollway	
Location:	IL390 (West of O'Hare)	

Date of Test	6/21/2017	Test ID	TS13_Pt3	Operator	HG/JV	ASTM	D6951
Latitude	41.9838100	Longitude		88.0114520		Elevation (ft)	NA
Location	EB Thorndale Ave. between Hamilton Lakes Dr. and North Arlington Heights Rd		Station	NA			
Comments	Nominal 3 in. of CA6-RAP compacted over nominal 6 in. PGE with RPCC crushed aggregate. <i>Subgrade assumed as CL clay.</i>						

Parameter	DPI (mm/blow)	CBR (%)	E_{CBR} , Elastic Modulus (ksi) (non stress-dependent)	S_{u-CBR} , Bearing Capacity (psf)
Avg. PGE+CA6 Layer [0 to 9.0 in.]	5.2	46.4	29.8	6,987
Avg. Subgrade Layer [9.0 to 21.0 in.]	5.6	42.6	28.2	6,594
Ratio of Avg. Top/Bottom Layer	0.9	1.1	1.1	1.1
Std.Dev.PGE+CA6 Layer [0 to 9 in.]	4.0	31.7	23.3	5,423
Std. Dev. Subgrade Layer [9.0 to 21.0 in.]	1.6	16.7	15.5	3,546

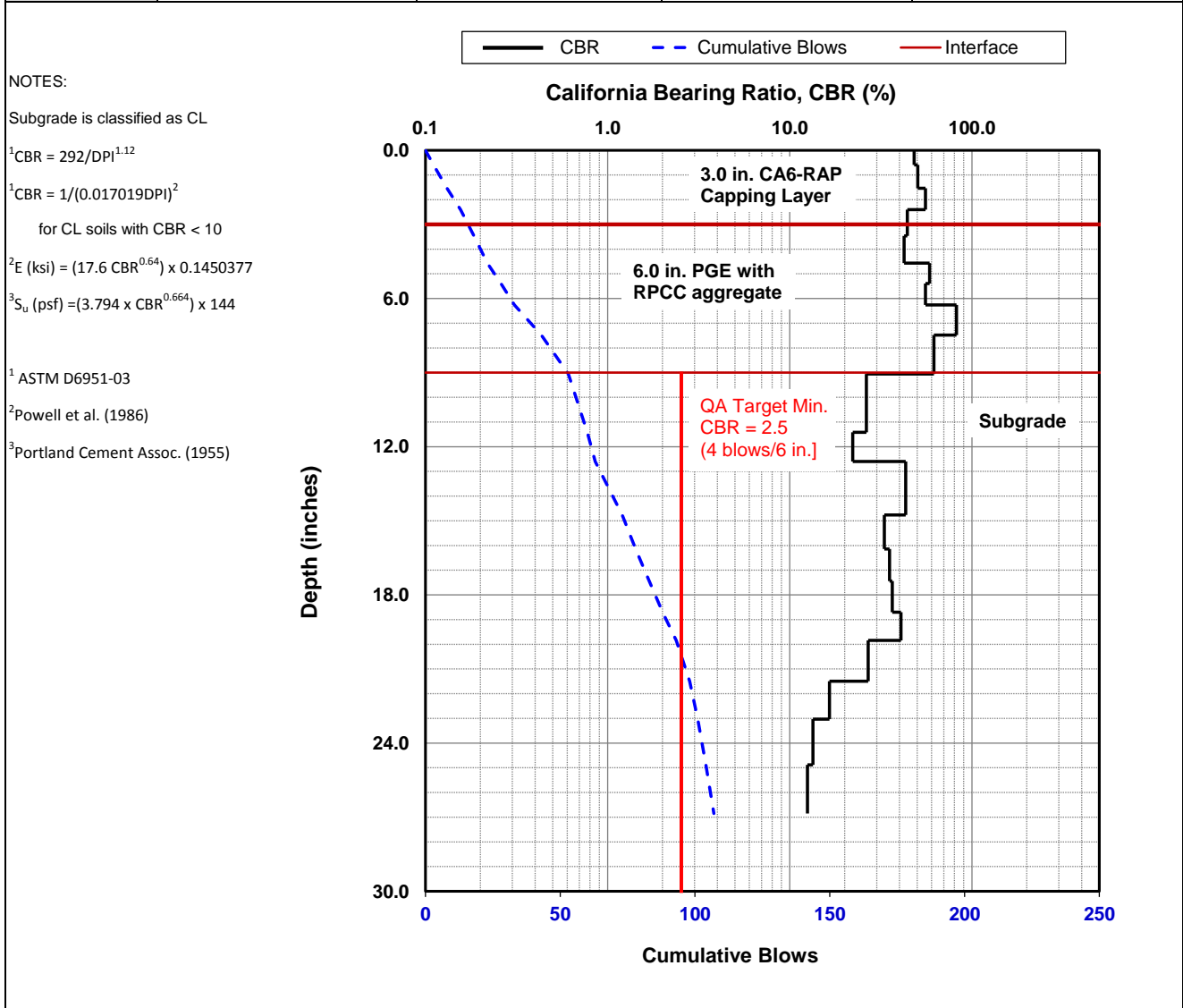


Dynamic Cone Penetrometer (DCP) Test Results	
Project Name:	Illinois Tollway - IC Research
Project ID:	Elgin O'Hare Extension - IL Tollway
Location:	IL390 (West of O'Hare)



Date of Test	6/21/2017	Test ID	TS13_Pt4	Operator	HG/JV	ASTM	D6951
Latitude	41.9838030		Longitude	88.0110170		Elevation (ft)	NA
Location	EB Thorndale Ave. between Hamilton Lakes Dr. and North Arlington Heights Rd		Station	NA			
Comments	Nominal 3 in. of CA6-RAP compacted over nominal 6 in. PGE with RPCC crushed aggregate. <i>Subgrade assumed as CL clay.</i>						

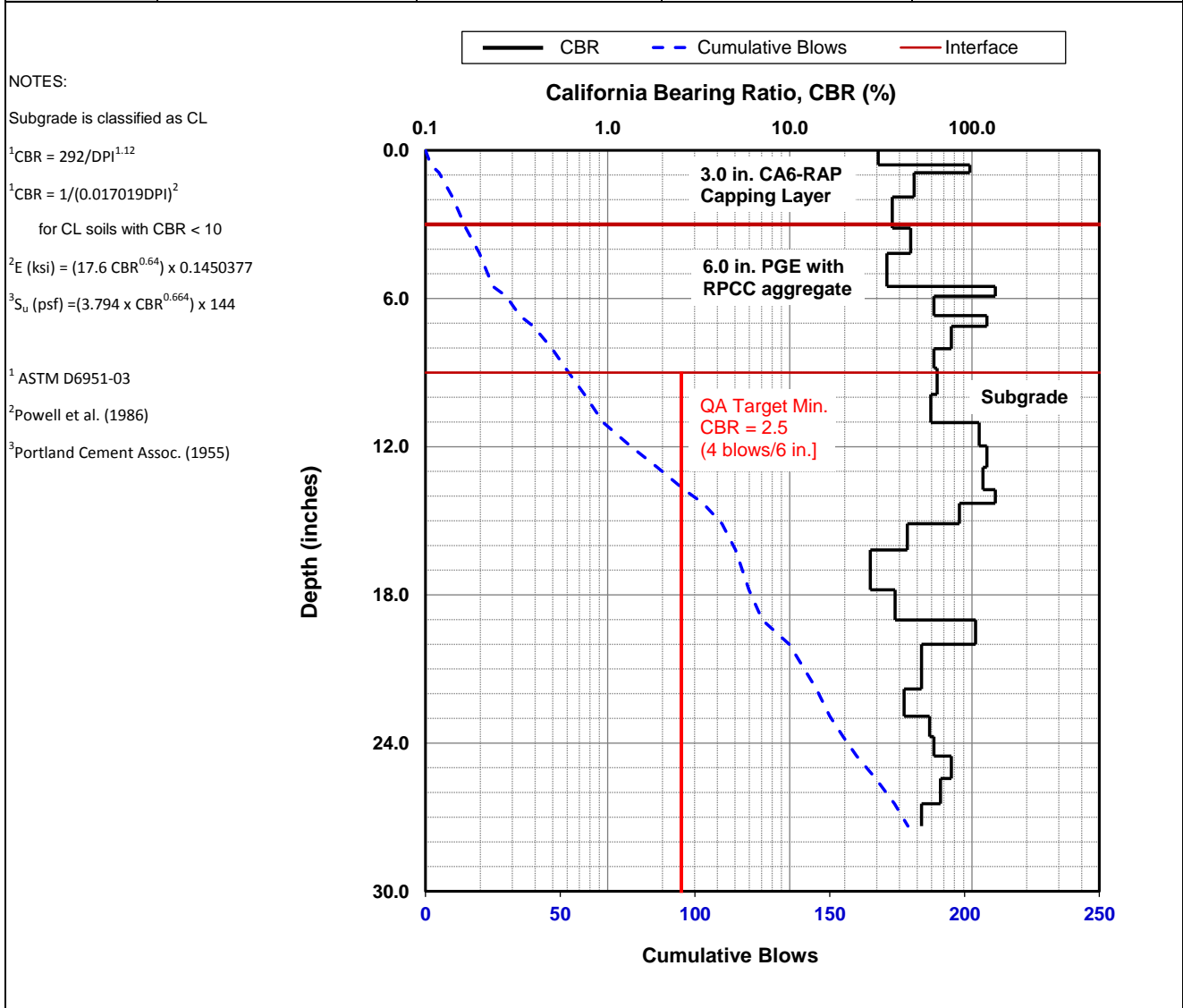
Parameter	DPI (mm/blow)	CBR (%)	E_{CBR} , Elastic Modulus (ksi) (non stress-dependent)	S_{u-CBR} , Bearing Capacity (psf)
Avg. PGE+CA6 Layer [0 to 9.0 in.]	4.3	56.4	33.7	7,951
Avg. Subgrade Layer [9.0 to 21.0 in.]	7.0	32.9	23.9	5,559
Ratio of Avg. Top/Bottom Layer	0.6	1.7	1.4	1.4
Std.Dev.PGE+CA6 Layer [0 to 9 in.]	0.7	11.5	12.2	2,766
Std. Dev. Subgrade Layer [9.0 to 21.0 in.]	1.6	7.4	9.2	2,062



Dynamic Cone Penetrometer (DCP) Test Results		
Project Name:	Illinois Tollway - IC Research	
Project ID:	Elgin O'Hare Extension - IL Tollway	
Location:	IL390 (West of O'Hare)	

Date of Test	6/21/2017	Test ID	TS13_Pt5	Operator	HG/JV	ASTM	D6951
Latitude	41.9837720		Longitude	88.0107270		Elevation (ft)	NA
Location	EB Thorndale Ave. between Hamilton Lakes Dr. and North Arlington Heights Rd		Station	NA			
Comments	Nominal 3 in. of CA6-RAP compacted over nominal 6 in. PGE with RPCC crushed aggregate. <i>Subgrade assumed as CL clay.</i>						

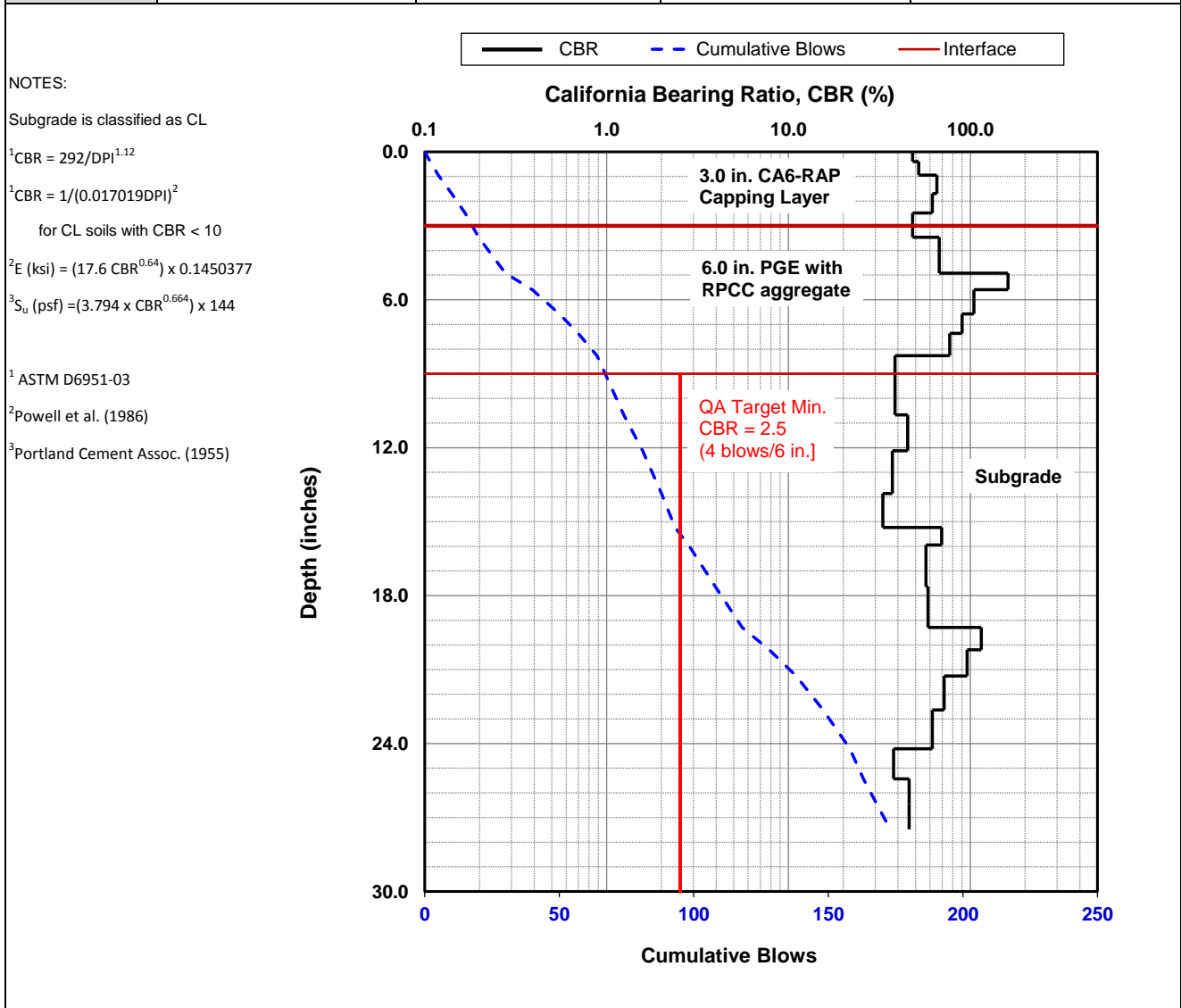
Parameter	DPI (mm/blow)	CBR (%)	E_{CBR} , Elastic Modulus (ksi) (non stress-dependent)	S_{u-CBR} , Bearing Capacity (psf)
Avg. PGE+CA6 Layer [0 to 9.0 in.]	4.3	56.9	33.9	7,995
Avg. Subgrade Layer [9.0 to 21.0 in.]	2.9	88.6	45.0	10,730
Ratio of Avg. Top/Bottom Layer	1.5	0.6	0.8	0.7
Std.Dev.PGE+CA6 Layer [0 to 9 in.]	2.0	35.6	25.1	5,851
Std. Dev. Subgrade Layer [9.0 to 21.0 in.]	1.9	36.4	25.5	5,939



Dynamic Cone Penetrometer (DCP) Test Results		
Project Name:	Illinois Tollway - IC Research	
Project ID:	Elgin O'Hare Extension - IL Tollway	
Location:	IL390 (West of O'Hare)	

Date of Test	6/21/2017	Test ID	TS13_Pt6	Operator	HG/JV	ASTM	D6951
Latitude	41.9837760	Longitude	88.0107270	Elevation (ft)	NA		
Location	EB Thorndale Ave. between Hamilton Lakes Dr. and North Arlington Heights Rd		Station	NA			
Comments	Nominal 3 in. of CA6-RAP compacted over nominal 6 in. PGE with RPCC crushed aggregate. <i>Subgrade assumed as CL clay.</i>						

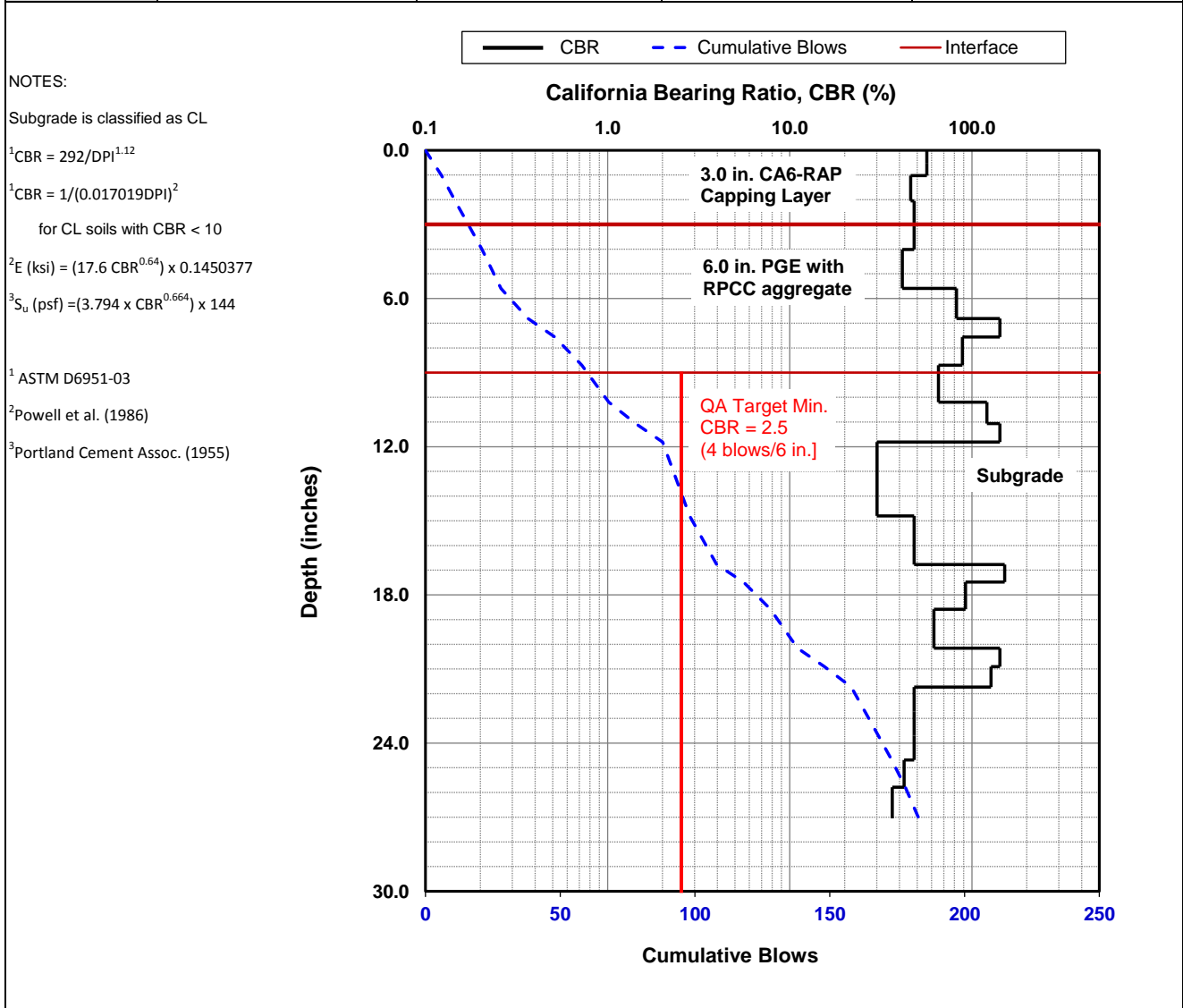
Parameter	DPI (mm/blow)	CBR (%)	E_{CBR} , Elastic Modulus (ksi) (non stress-dependent)	S_{u-CBR} , Bearing Capacity (psf)
Avg. PGE+CA6 Layer [0 to 9.0 in.]	3.3	77.2	41.2	9,789
Avg. Subgrade Layer [9.0 to 21.0 in.]	4.6	53.0	32.4	7,624
Ratio of Avg. Top/Bottom Layer	0.7	1.5	1.3	1.3
Std.Dev.PGE+CA6 Layer [0 to 9 in.]	1.2	35.8	25.2	5,880
Std. Dev. Subgrade Layer [9.0 to 21.0 in.]	1.6	25.8	20.4	4,727



Dynamic Cone Penetrometer (DCP) Test Results		
Project Name:	Illinois Tollway - IC Research	
Project ID:	Elgin O'Hare Extension - IL Tollway	
Location:	IL390 (West of O'Hare)	

Date of Test	6/21/2017	Test ID	TS13_Pt7	Operator	HG/JV	ASTM	D6951
Latitude	41.9838140	Longitude	88.0107190	Elevation (ft)	708		
Location	EB Thorndale Ave. between Hamilton Lakes Dr. and North Arlington Heights Rd	Station	NA				
Comments	Nominal 3 in. of CA6-RAP compacted over nominal 6 in. PGE with RPCC crushed aggregate. <i>Subgrade assumed as CL clay.</i>						

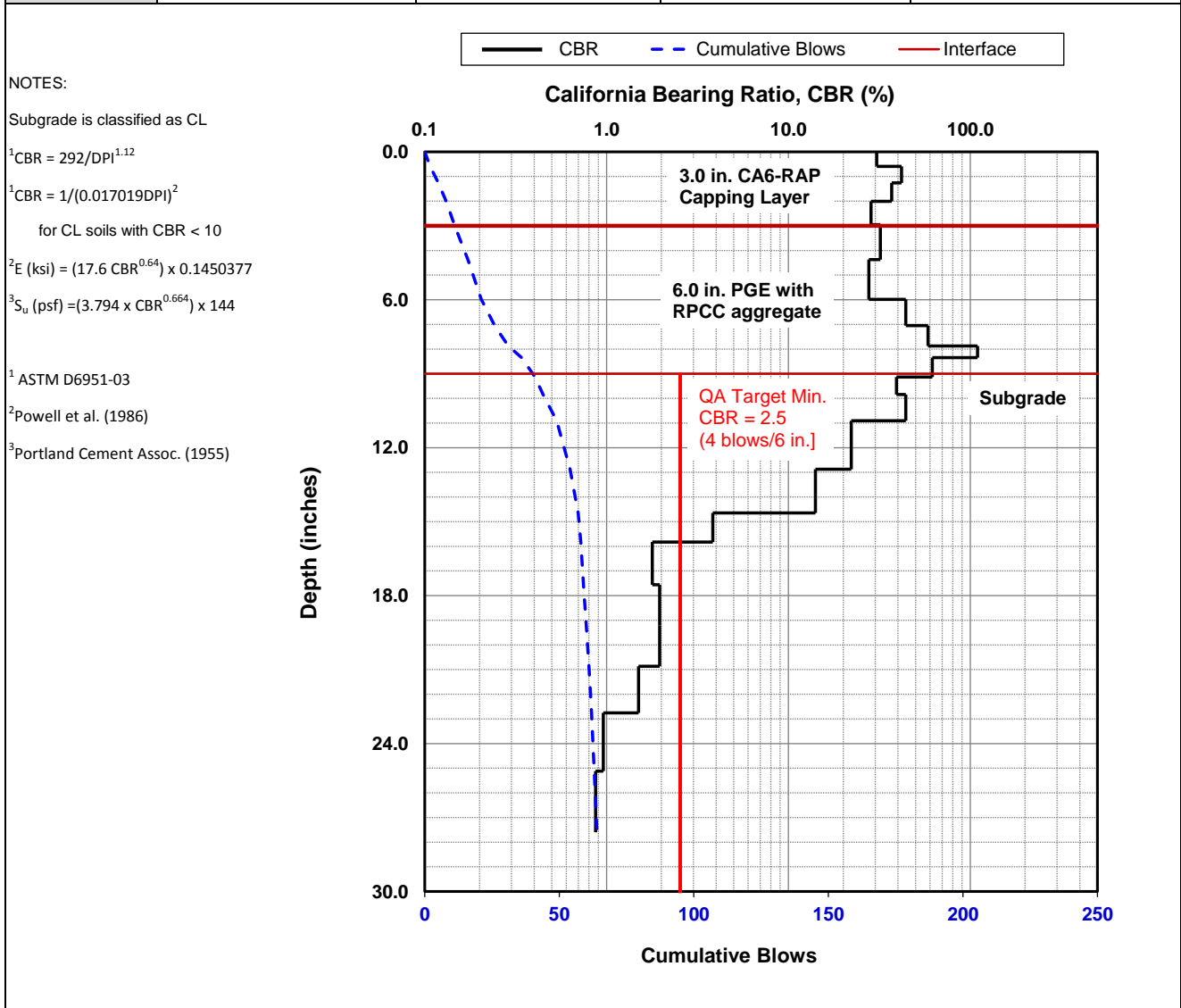
Parameter	DPI (mm/blow)	CBR (%)	E_{CBR} , Elastic Modulus (ksi) (non stress-dependent)	S_{u-CBR} , Bearing Capacity (psf)
Avg. PGE+CA6 Layer [0 to 9.0 in.]	3.8	65.3	37.0	8,758
Avg. Subgrade Layer [9.0 to 21.0 in.]	3.4	73.1	39.8	9,441
Ratio of Avg. Top/Bottom Layer	1.1	0.9	0.9	0.9
Std.Dev.PGE+CA6 Layer [0 to 9 in.]	1.2	30.7	22.9	5,311
Std. Dev. Subgrade Layer [9.0 to 21.0 in.]	1.9	45.7	29.5	6,908



Dynamic Cone Penetrometer (DCP) Test Results		
Project Name:	Illinois Tollway - IC Research	
Project ID:	Elgin O'Hare Extension - IL Tollway	
Location:	IL390 (West of O'Hare)	

Date of Test	6/21/2017	Test ID	TS13_Pt8	Operator	HG/JV	ASTM	D6951
Latitude	41.9837490	Longitude		88.0104830		Elevation (ft)	NA
Location	EB Thorndale Ave. between Hamilton Lakes Dr. and North Arlington Heights Rd	Station		NA			
Comments	Nominal 3 in. of CA6-RAP compacted over nominal 6 in. PGE with RPCC crushed aggregate. <i>Subgrade assumed as CL clay.</i>						

Parameter	DPI (mm/blow)	CBR (%)	E_{CBR} , Elastic Modulus (ksi) (non stress-dependent)	S_{u-CBR} , Bearing Capacity (psf)
Avg. PGE+CA6 Layer [0 to 9.0 in.]	5.7	41.9	27.9	6,527
Avg. Subgrade Layer [9.0 to 21.0 in.]	14.9	14.2	13.9	3,177
Ratio of Avg. Top/Bottom Layer	0.4	3.0	2.0	2.1
Std.Dev.PGE+CA6 Layer [0 to 9 in.]	1.9	24.2	19.6	4,533
Std. Dev. Subgrade Layer [9.0 to 21.0 in.]	17.0	17.4	15.9	3,641

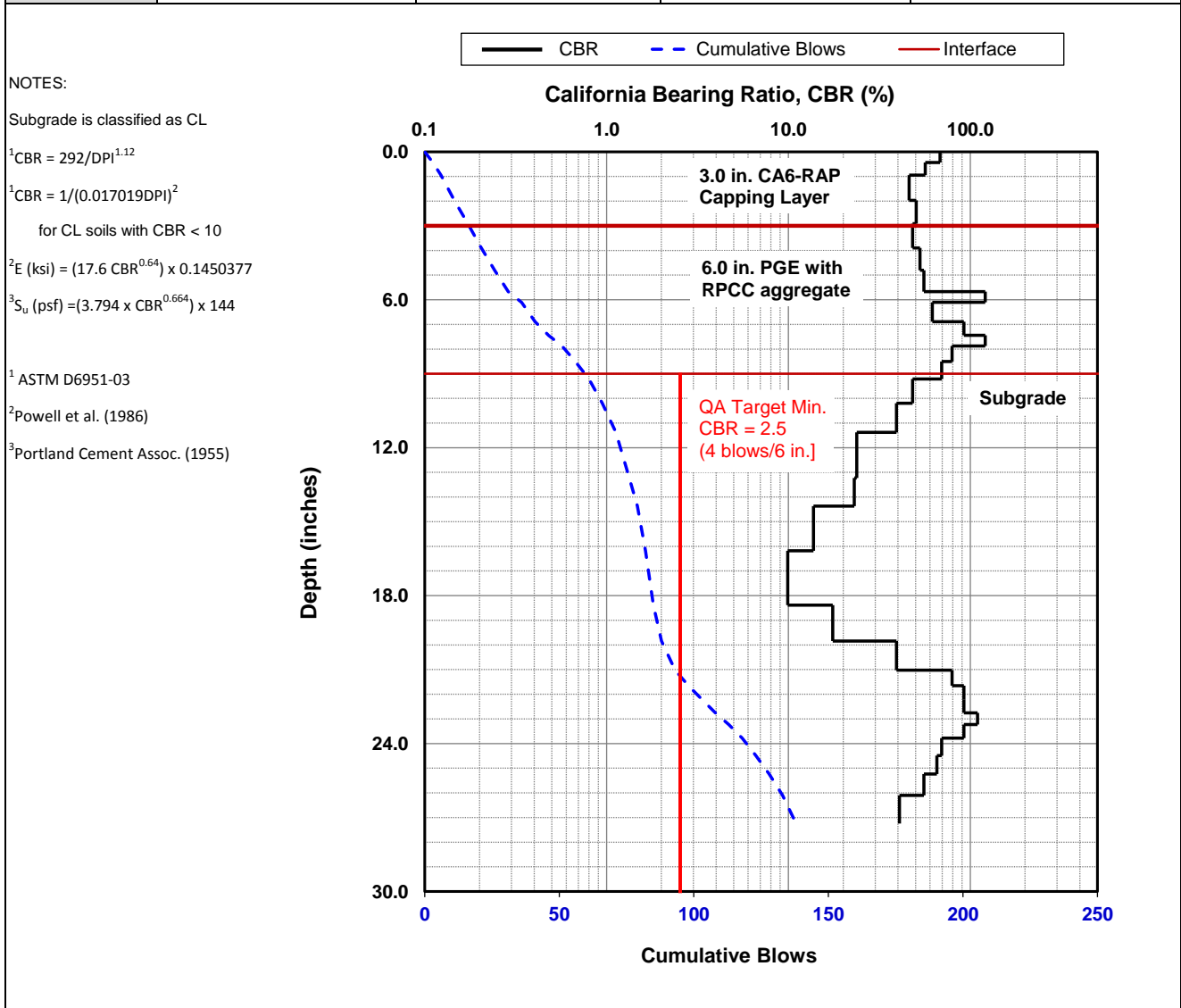


Dynamic Cone Penetrometer (DCP) Test Results	
Project Name:	Illinois Tollway - IC Research
Project ID:	Elgin O'Hare Extension - IL Tollway
Location:	IL390 (West of O'Hare)



Date of Test	6/21/2017	Test ID	TS13_Pt9	Operator	HG/JV	ASTM	D6951
Latitude	41.9837680	Longitude		88.0104980		Elevation (ft)	NA
Location	EB Thorndale Ave. between Hamilton Lakes Dr. and North Arlington Heights Rd	Station		NA			
Comments	Nominal 3 in. of CA6-RAP compacted over nominal 6 in. PGE with RPCC crushed aggregate. <i>Subgrade assumed as CL clay.</i>						

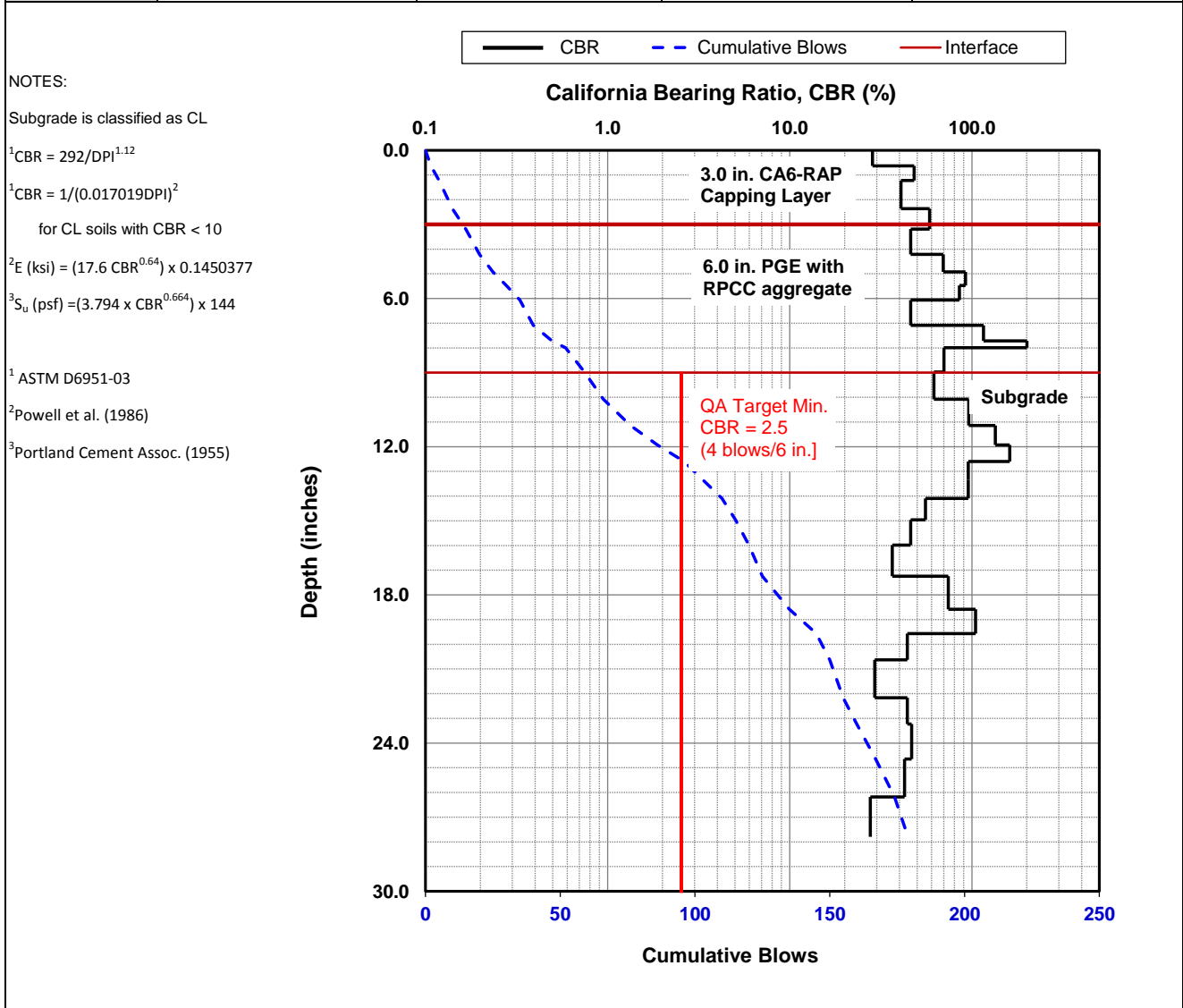
Parameter	DPI (mm/blow)	CBR (%)	E_{CBR} , Elastic Modulus (ksi) (non stress-dependent)	S_{u-CBR} , Bearing Capacity (psf)
Avg. PGE+CA6 Layer [0 to 9.0 in.]	3.8	64.8	36.8	8,715
Avg. Subgrade Layer [9.0 to 21.0 in.]	9.4	23.8	19.4	4,484
Ratio of Avg. Top/Bottom Layer	0.4	2.7	1.9	1.9
Std.Dev.PGE+CA6 Layer [0 to 9 in.]	1.0	24.7	19.9	4,591
Std. Dev. Subgrade Layer [9.0 to 21.0 in.]	4.9	13.8	13.7	3,120



Dynamic Cone Penetrometer (DCP) Test Results		
Project Name:	Illinois Tollway - IC Research	
Project ID:	Elgin O'Hare Extension - IL Tollway	
Location:	IL390 (West of O'Hare)	

Date of Test	6/21/2017	Test ID	TS13_Pt10	Operator	PV	ASTM	D6951
Latitude	41.9837880	Longitude	88.0104680	Elevation (ft)	NA		
Location	EB Thorndale Ave. between Hamilton Lakes Dr. and North Arlington Heights Rd		Station	NA			
Comments	Nominal 3 in. of CA6-RAP compacted over nominal 6 in. PGE with RPCC crushed aggregate. <i>Subgrade assumed as CL clay.</i>						

Parameter	DPI (mm/blow)	CBR (%)	E_{CBR} , Elastic Modulus (ksi) (non stress-dependent)	S_{u-CBR} , Bearing Capacity (psf)
Avg. PGE+CA6 Layer [0 to 9.0 in.]	3.9	64.2	36.6	8,667
Avg. Subgrade Layer [9.0 to 21.0 in.]	3.3	77.9	41.5	9,852
Ratio of Avg. Top/Bottom Layer	1.2	0.8	0.9	0.9
Std.Dev.PGE+CA6 Layer [0 to 9 in.]	2.0	46.4	29.8	6,982
Std. Dev. Subgrade Layer [9.0 to 21.0 in.]	1.5	38.1	26.2	6,130



Dynamic Cone Penetrometer (DCP) Test Results	
Project Name:	Illinois Tollway - IC Research
Project ID:	Elgin O'Hare Extension - IL Tollway
Location:	IL390 (West of O'Hare)



Date of Test	6/21/2017	Test ID	TS13_Pt11	Operator	HG/JV	ASTM	D6951
Latitude	41.9837760	Longitude		88.0103000		Elevation (ft)	NA
Location	EB Thorndale Ave. between Hamilton Lakes Dr. and North Arlington Heights Rd	Station		NA			
Comments	Nominal 3 in. of CA6-RAP compacted over nominal 6 in. PGE with RPCC crushed aggregate. <i>Subgrade assumed as CL clay.</i>						

Parameter	DPI (mm/blow)	CBR (%)	E_{CBR} , Elastic Modulus (ksi) (non stress-dependent)	S_{u-CBR} , Bearing Capacity (psf)
Avg. PGE+CA6 Layer [0 to 9.0 in.]	4.6	52.8	32.3	7,609
Avg. Subgrade Layer [9.0 to 21.0 in.]	6.3	36.9	25.7	5,998
Ratio of Avg. Top/Bottom Layer	0.7	1.4	1.3	1.3
Std.Dev.PGE+CA6 Layer [0 to 9 in.]	1.4	20.0	17.4	3,995
Std. Dev. Subgrade Layer [9.0 to 21.0 in.]	3.5	22.9	18.9	4,370

NOTES:

Subgrade is classified as CL

¹CBR = 292/DPI^{1.12}

¹CBR = 1/(0.017019DPI)²
for CL soils with CBR < 10

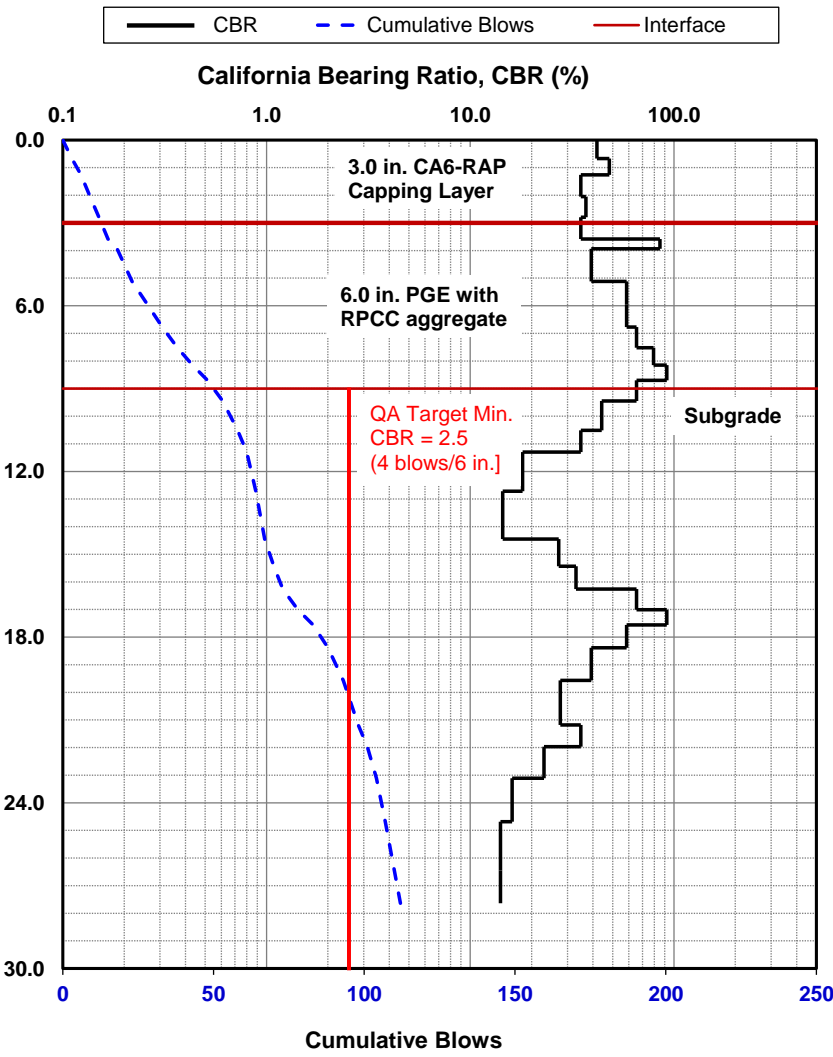
²E (ksi) = (17.6 CBR^{0.64}) x 0.1450377

³S_u (psf) = (3.794 x CBR^{0.664}) x 144

¹ ASTM D6951-03

² Powell et al. (1986)

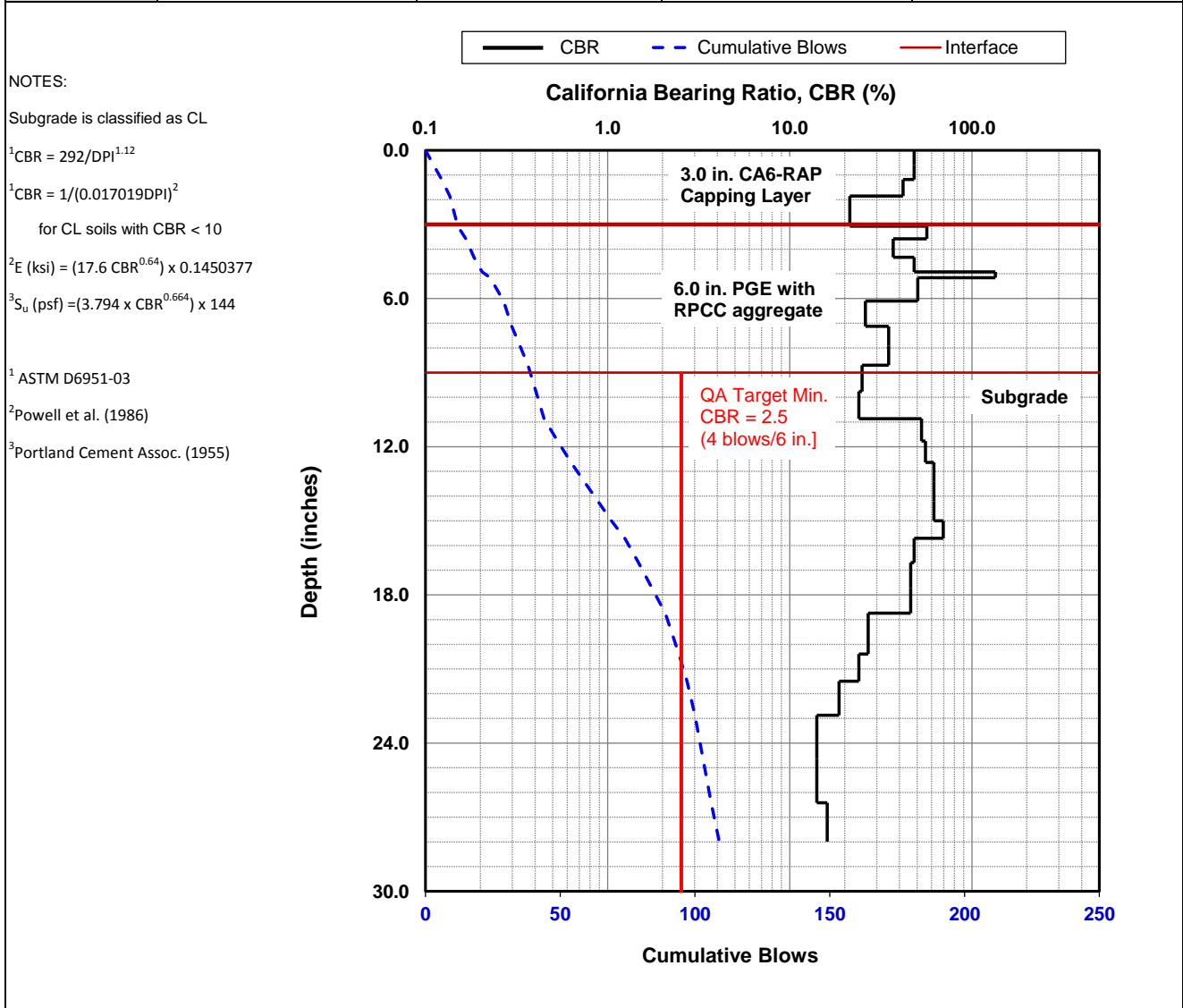
³ Portland Cement Assoc. (1955)



Dynamic Cone Penetrometer (DCP) Test Results		
Project Name:	Illinois Tollway - IC Research	
Project ID:	Elgin O'Hare Extension - IL Tollway	
Location:	IL390 (West of O'Hare)	

Date of Test	6/21/2017	Test ID	TS13_Pt12	Operator	HG/JV	ASTM	D6951
Latitude	41.9838100	Longitude		88.0102920		Elevation (ft)	NA
Location	EB Thorndale Ave. between Hamilton Lakes Dr. and North Arlington Heights Rd	Station		NA			
Comments	Nominal 3 in. of CA6-RAP compacted over nominal 6 in. PGE with RPCC crushed aggregate. <i>Subgrade assumed as CL clay.</i>						

Parameter	DPI (mm/blow)	CBR (%)	E_{CBR} , Elastic Modulus (ksi) (non stress-dependent)	S_{u-CBR} , Bearing Capacity (psf)
Avg. PGE+CA6 Layer [0 to 9.0 in.]	5.8	40.6	27.3	6,395
Avg. Subgrade Layer [9.0 to 21.0 in.]	5.5	43.2	28.4	6,659
Ratio of Avg. Top/Bottom Layer	1.1	0.9	1.0	1.0
Std.Dev.PGE+CA6 Layer [0 to 9 in.]	2.1	27.7	21.4	4,962
Std. Dev. Subgrade Layer [9.0 to 21.0 in.]	2.3	16.4	15.3	3,500

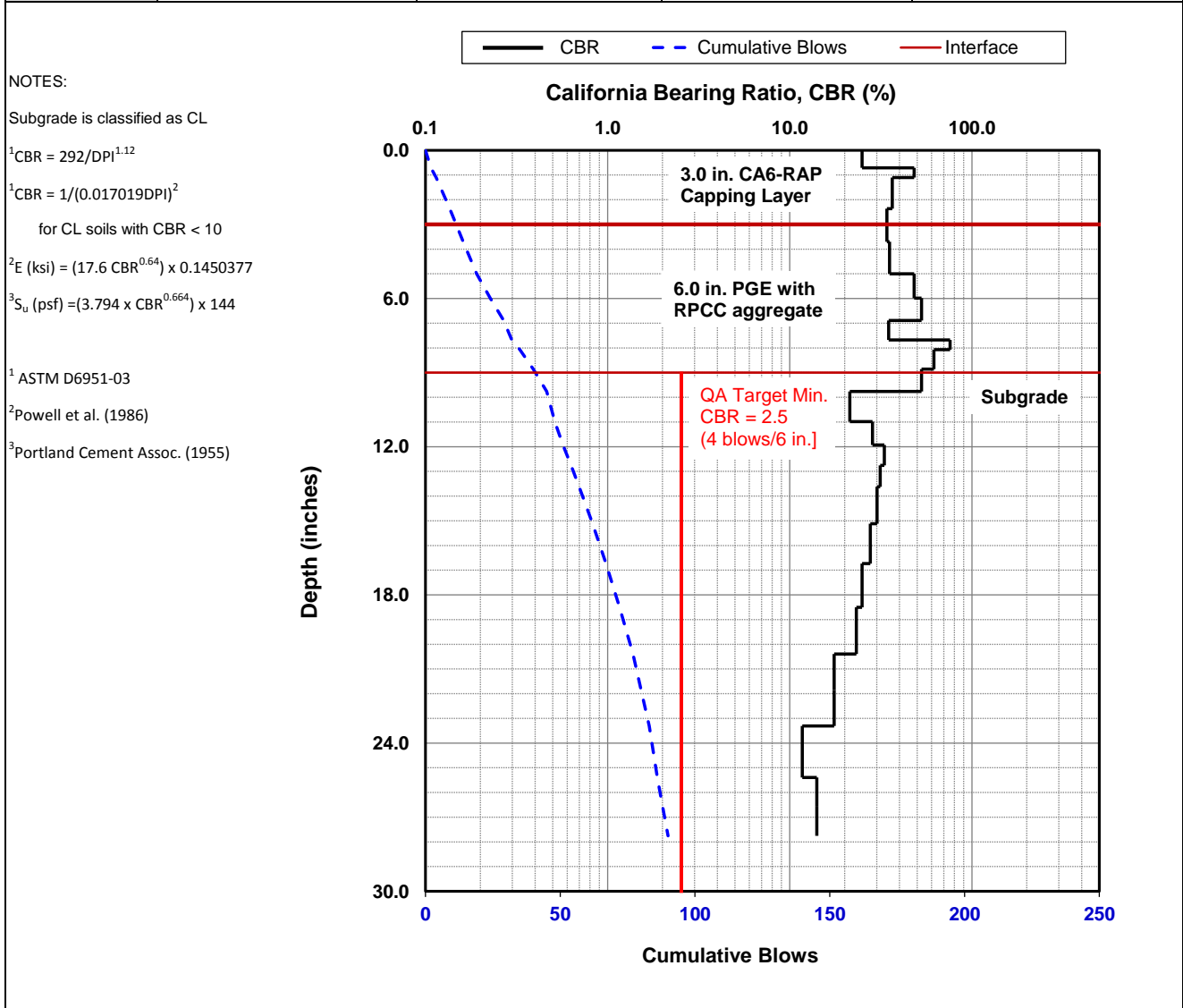


Dynamic Cone Penetrometer (DCP) Test Results	
Project Name:	Illinois Tollway - IC Research
Project ID:	Elgin O'Hare Extension - IL Tollway
Location:	IL390 (West of O'Hare)



Date of Test	6/21/2017	Test ID	TS13_Pt13	Operator	HG/JV	ASTM	D6951
Latitude	41.9838260	Longitude		88.0097050		Elevation (ft)	NA
Location	EB Thorndale Ave. between Hamilton Lakes Dr. and North Arlington Heights Rd		Station	NA			
Comments	Nominal 3 in. of CA6-RAP compacted over nominal 6 in. PGE with RPCC crushed aggregate. <i>Subgrade assumed as CL clay.</i>						

Parameter	DPI (mm/blow)	CBR (%)	E_{CBR} , Elastic Modulus (ksi) (non stress-dependent)	S_{u-CBR} , Bearing Capacity (psf)
Avg. PGE+CA6 Layer [0 to 9.0 in.]	5.6	42.2	28.0	6,556
Avg. Subgrade Layer [9.0 to 21.0 in.]	7.9	28.8	21.9	5,083
Ratio of Avg. Top/Bottom Layer	0.7	1.5	1.3	1.3
Std.Dev.PGE+CA6 Layer [0 to 9 in.]	1.9	15.7	14.9	3,407
Std. Dev. Subgrade Layer [9.0 to 21.0 in.]	1.7	9.3	10.6	2,396

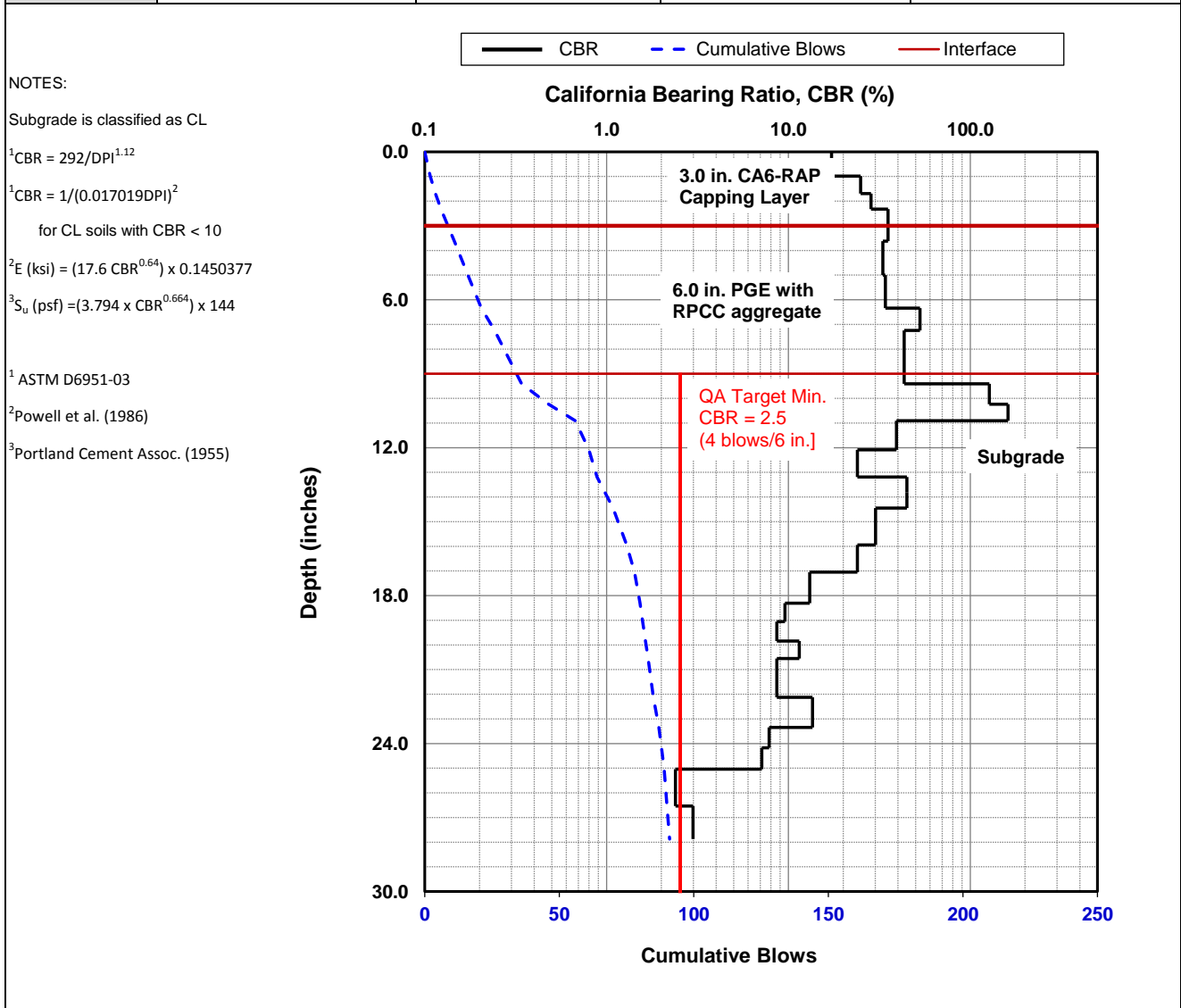


Dynamic Cone Penetrometer (DCP) Test Results	
Project Name:	Illinois Tollway - IC Research
Project ID:	Elgin O'Hare Extension - IL Tollway
Location:	IL390 (West of O'Hare)



Date of Test	6/21/2017	Test ID	TS13_Pt14	Operator	HG/JV	ASTM	D6951
Latitude	41.9838450	Longitude		88.0096890		Elevation (ft)	NA
Location	EB Thorndale Ave. between Hamilton Lakes Dr. and North Arlington Heights Rd		Station	NA			
Comments	Nominal 3 in. of CA6-RAP compacted over nominal 6 in. PGE with RPCC crushed aggregate. <i>Subgrade assumed as CL clay.</i>						

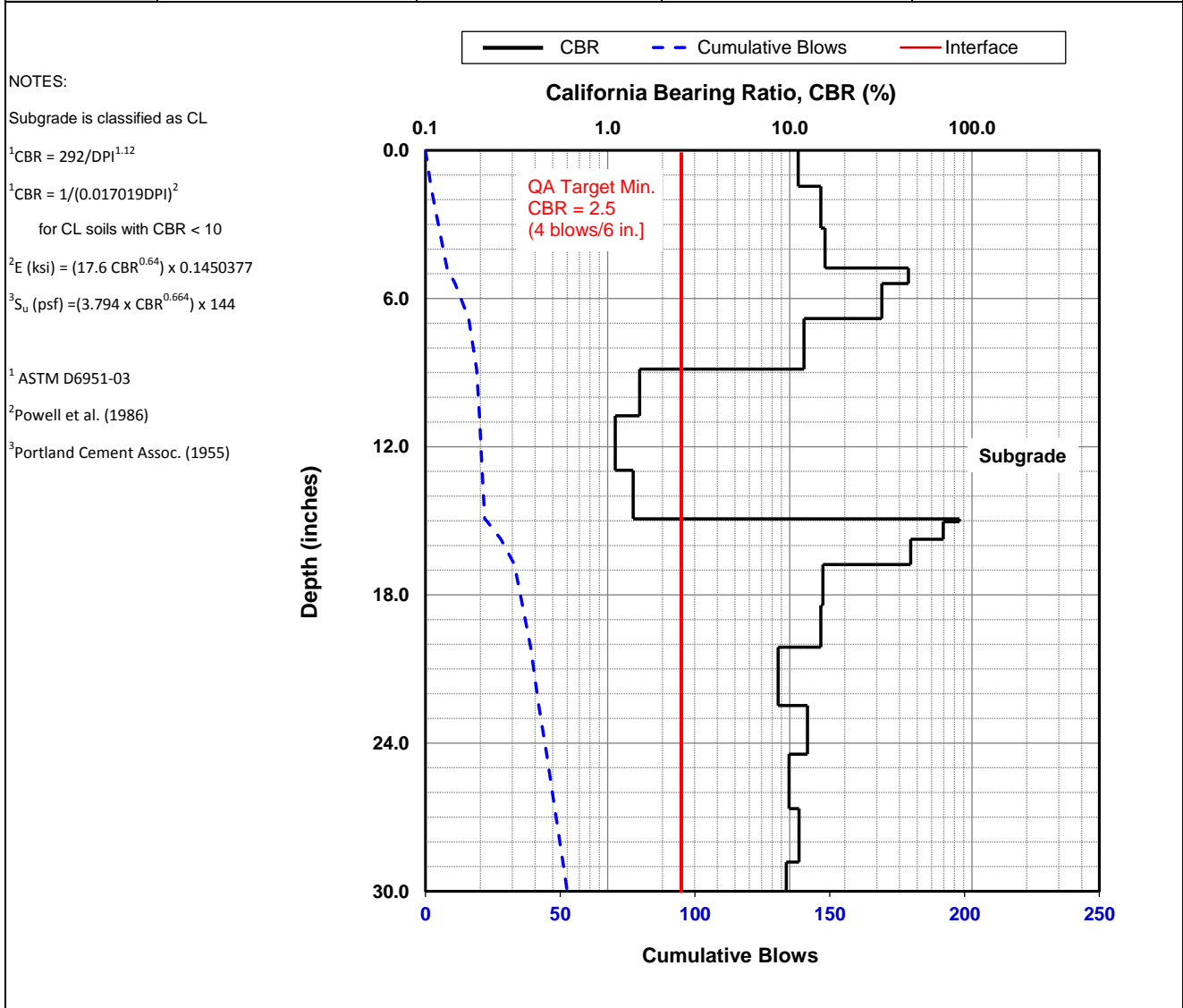
Parameter	DPI (mm/blow)	CBR (%)	E_{CBR} , Elastic Modulus (ksi) (non stress-dependent)	S_{u-CBR} , Bearing Capacity (psf)
Avg. PGE+CA6 Layer [0 to 9.0 in.]	6.6	35.0	24.9	5,796
Avg. Subgrade Layer [9.0 to 21.0 in.]	6.0	39.1	26.7	6,232
Ratio of Avg. Top/Bottom Layer	1.1	0.9	0.9	0.9
Std.Dev.PGE+CA6 Layer [0 to 9 in.]	2.8	11.6	12.3	2,781
Std. Dev. Subgrade Layer [9.0 to 21.0 in.]	6.6	48.7	30.7	7,213



Dynamic Cone Penetrometer (DCP) Test Results		
Project Name:	Illinois Tollway - IC Research	
Project ID:	Elgin O'Hare Extension - IL Tollway	
Location:	IL390 (West of O'Hare)	

Date of Test	6/21/2017	Test ID	TS14_Pt15	Operator	PV	ASTM	D6951
Latitude	41.9838450	Longitude	88.0149920	Elevation (ft)	NA		
Location	EB Thorndale Ave. west of Hamilton Lakes Dr. Bridge	Station	NA				
Comments	Compacted Subgrade (passed proofrolling on 06/22/17)						

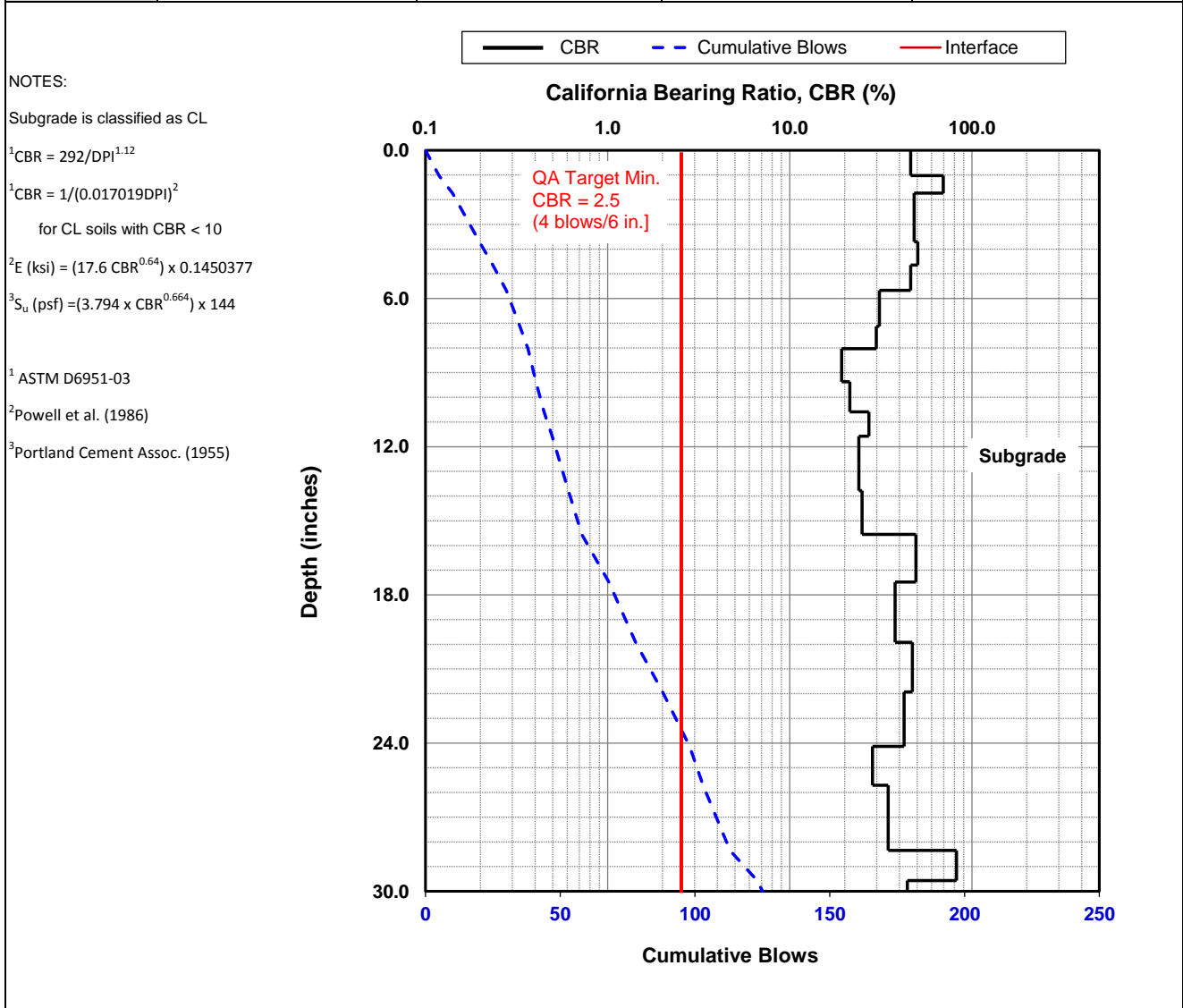
Parameter	DPI (mm/blow)	CBR (%)	E_{CBR} , Elastic Modulus (ksi) (non stress-dependent)	S_{u-CBR} , Bearing Capacity (psf)
Avg. Top Lift [0 to 7.0 in.]	10.8	20.3	17.5	4,032
Avg. Bottom Lift [7.0 to 14.0 in.]	29.9	3.9	6.1	1,343
Ratio of Avg. Top/Bottom Lift	0.4	5.2	2.9	3.0
Std. Dev. Top Lift [0 to 7.0 in.]	5.6	13.8	13.7	3,116
Std. Dev. Bottom Lift [7.0 to 14.0 in.]	23.3	36.7	25.6	5,972



Dynamic Cone Penetrometer (DCP) Test Results		
Project Name:	Illinois Tollway - IC Research	
Project ID:	Elgin O'Hare Extension - IL Tollway	
Location:	IL390 (West of O'Hare)	

Date of Test	6/21/2017	Test ID	TS14_Pt16	Operator	PV	ASTM	D6951
Latitude	41.9837420	Longitude		88.0150600		Elevation (ft)	NA
Location	EB Thorndale Ave. west of Hamilton Lakes Dr. Bridge	Station		NA			
Comments	Compacted Subgrade (passed proofrolling on 06/22/17)						

Parameter	DPI (mm/blow)	CBR (%)	E_{CBR} , Elastic Modulus (ksi) (non stress-dependent)	S_{u-CBR} , Bearing Capacity (psf)
Avg. Top Lift [0 to 7.0 in.]	5.2	46.4	29.7	6,979
Avg. Bottom Lift [7.0 to 14.0 in.]	9.4	23.8	19.4	4,479
Ratio of Avg. Top/Bottom Lift	0.6	2.0	1.5	1.6
Std. Dev. Top Lift [0 to 7.0 in.]	1.1	11.3	12.1	2,737
Std. Dev. Bottom Lift [7.0 to 14.0 in.]	1.3	3.8	6.0	1,332

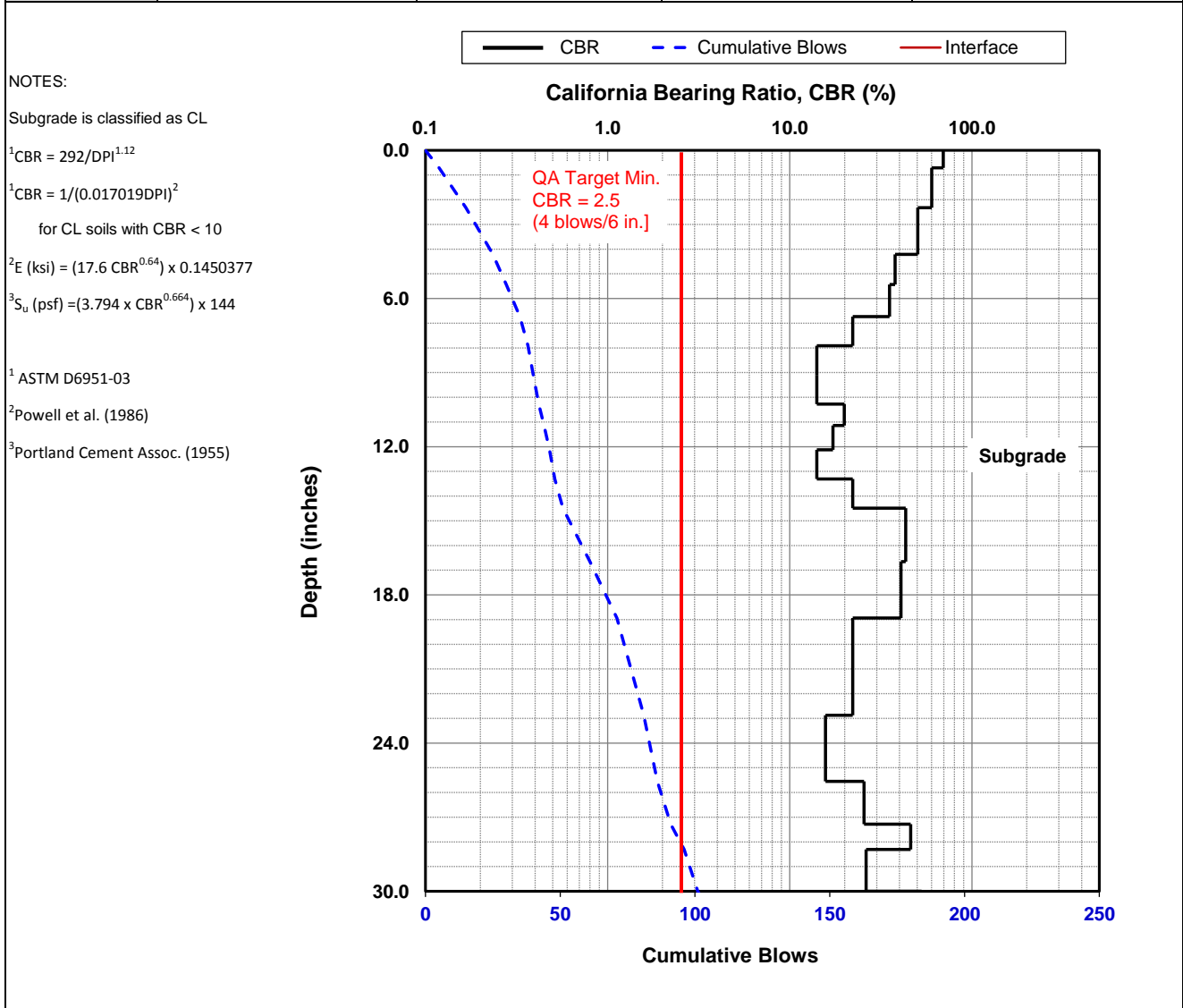


Dynamic Cone Penetrometer (DCP) Test Results	
Project Name:	Illinois Tollway - IC Research
Project ID:	Elgin O'Hare Extension - IL Tollway
Location:	IL390 (West of O'Hare)



Date of Test	6/21/2017	Test ID	TS14_Pt17	Operator	PV	ASTM	D6951
Latitude	41.9837460	Longitude		88.0152970		Elevation (ft)	NA
Location	EB Thorndale Ave. west of Hamilton Lakes Dr. Bridge	Station		NA			
Comments	Compacted Subgrade (passed proofrolling on 06/22/17)						

Parameter	DPI (mm/blow)	CBR (%)	E_{CBR} , Elastic Modulus (ksi) (non stress-dependent)	S_{u-CBR} , Bearing Capacity (psf)
Avg. Top Lift [0 to 7.0 in.]	4.9	49.4	31.0	7,280
Avg. Bottom Lift [7.0 to 14.0 in.]	12.3	17.5	16.0	3,661
Ratio of Avg. Top/Bottom Lift	0.4	2.8	1.9	2.0
Std. Dev. Top Lift [0 to 7.0 in.]	1.3	15.1	14.5	3,319
Std. Dev. Bottom Lift [7.0 to 14.0 in.]	2.4	3.7	5.9	1,314

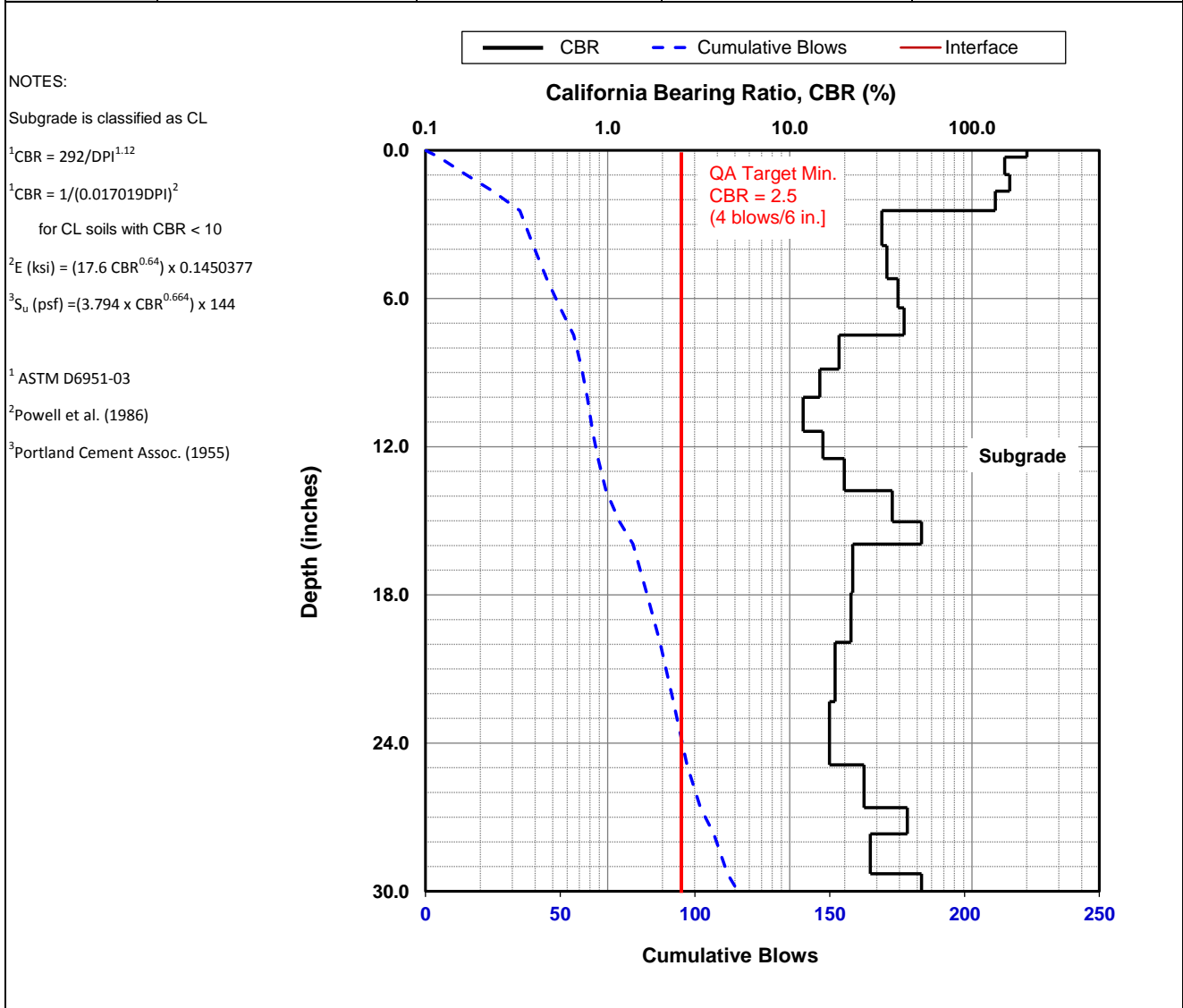


Dynamic Cone Penetrometer (DCP) Test Results	
Project Name:	Illinois Tollway - IC Research
Project ID:	Elgin O'Hare Extension - IL Tollway
Location:	IL390 (West of O'Hare)



Date of Test	6/21/2017	Test ID	TS14_Pt18	Operator	PV	ASTM	D6951
Latitude	41.9837880	Longitude		88.0153270		Elevation (ft)	NA
Location	EB Thorndale Ave. west of Hamilton Lakes Dr. Bridge	Station		NA			
Comments	Compacted Subgrade (passed proofrolling on 06/22/17)						

Parameter	DPI (mm/blow)	CBR (%)	E_{CBR} , Elastic Modulus (ksi) (non stress-dependent)	S_{u-CBR} , Bearing Capacity (psf)
Avg. Top Lift [0 to 7.0 in.]	3.5	72.8	39.7	9,421
Avg. Bottom Lift [7.0 to 14.0 in.]	13.3	16.0	15.1	3,450
Ratio of Avg. Top/Bottom Lift	0.3	4.5	2.6	2.7
Std. Dev. Top Lift [0 to 7.0 in.]	2.5	73.0	39.8	9,434
Std. Dev. Bottom Lift [7.0 to 14.0 in.]	2.6	3.2	5.4	1,194

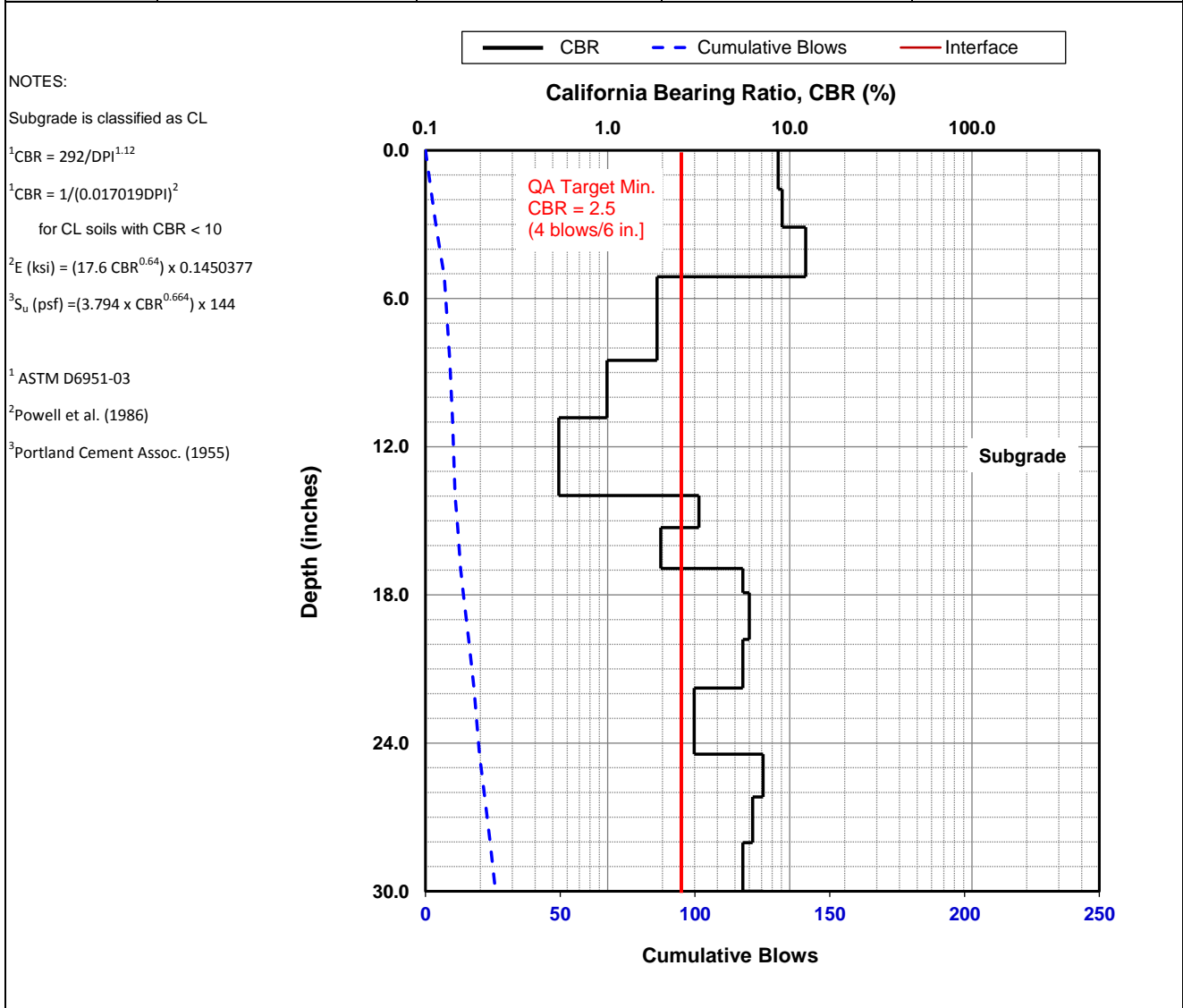


Dynamic Cone Penetrometer (DCP) Test Results	
Project Name:	Illinois Tollway - IC Research
Project ID:	Elgin O'Hare Extension - IL Tollway
Location:	IL390 (West of O'Hare)



Date of Test	6/21/2017	Test ID	TS14_Pt19	Operator	PV	ASTM	D6951
Latitude	41.9836270	Longitude	88.0152590	Elevation (ft)	NA		
Location	EB Thorndale Ave. west of Hamilton Lakes Dr. Bridge	Station	NA				
Comments	Compacted Subgrade (passed proofrolling on 06/22/17)						

Parameter	DPI (mm/blow)	CBR (%)	E_{CBR} , Elastic Modulus (ksi) (non stress-dependent)	S_{u-CBR} , Bearing Capacity (psf)
Avg. Top Lift [0 to 7.0 in.]	18.6	11.1	11.9	2,697
Avg. Bottom Lift [7.0 to 14.0 in.]	56.3	1.1	2.7	579
Ratio of Avg. Top/Bottom Lift	0.3	10.1	4.4	4.7
Std. Dev. Top Lift [0 to 7.0 in.]	1.4	1.7	3.6	788
Std. Dev. Bottom Lift [7.0 to 14.0 in.]	18.6	0.7	2.0	421



Dynamic Cone Penetrometer (DCP) Test Results		
Project Name:	Illinois Tollway - IC Research	
Project ID:	Elgin O'Hare Extension - IL Tollway	
Location:	IL390 (West of O'Hare)	

Date of Test	6/21/2017	Test ID	TS14_Pt20	Operator	PV	ASTM	D6951
Latitude	41.9836500	Longitude		88.0154040		Elevation (ft)	NA
Location	EB Thorndale Ave. west of Hamilton Lakes Dr. Bridge	Station		NA			
Comments	Compacted Subgrade (passed proofrolling on 06/22/17)						

Parameter	DPI (mm/blow)	CBR (%)	E_{CBR} , Elastic Modulus (ksi) (non stress-dependent)	S_{u-CBR} , Bearing Capacity (psf)
Avg. Top Lift [0 to 7.0 in.]	47.0	3.9	6.1	1,352
Avg. Bottom Lift [7.0 to 14.0 in.]	19.5	9.0	10.4	2,357
Ratio of Avg. Top/Bottom Lift	2.4	0.4	0.6	0.6
Std. Dev. Top Lift [0 to 7.0 in.]	9.7	0.8	2.2	477
Std. Dev. Bottom Lift [7.0 to 14.0 in.]	7.0	6.1	8.1	1,818

NOTES:

Subgrade is classified as CL

¹CBR = 292/DPI^{1.12}

¹CBR = 1/(0.017019DPI)²

for CL soils with CBR < 10

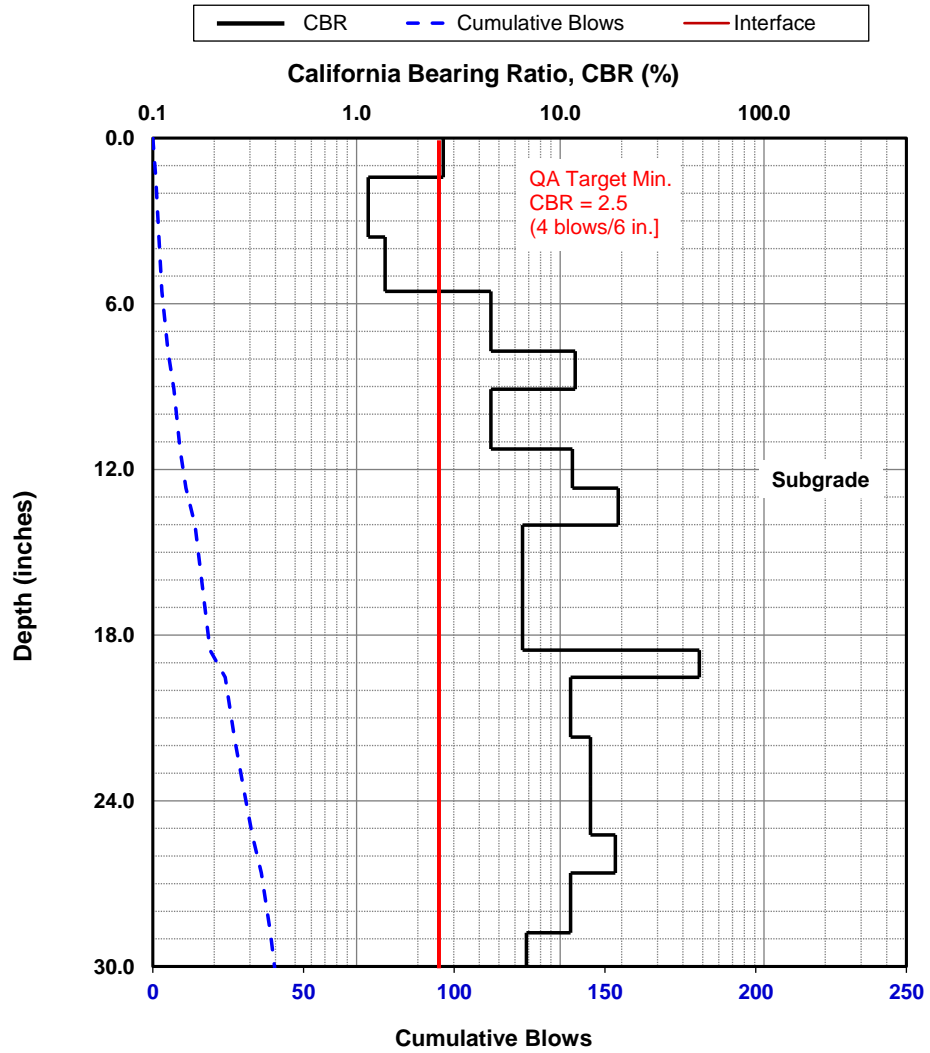
²E (ksi) = (17.6 CBR^{0.64}) x 0.1450377

³S_u (psf) = (3.794 x CBR^{0.664}) x 144

¹ ASTM D6951-03

² Powell et al. (1986)

³ Portland Cement Assoc. (1955)



Dynamic Cone Penetrometer (DCP) Test Results

Project Name: Illinois Tollway - IC Research
 Project ID: Elgin O'Hare Extension - IL Tollway
 Location: IL390 (West of O'Hare)



APPENDIX D: GUIDE SPECIFICATION

SECTION xxx

TOLLWAY SPECIAL PROVISION [Draft_v2]

INTELLIGENT COMPACTION STIFFNESS MAPPING FOR EMBANKMENT AND PAVEMENT FOUNDATION LAYERS

Xxx-1.0 DESCRIPTION

Provide Intelligent Compaction (IC) stiffness mapping on the surface of completed compaction layers (i.e., embankment, subgrade, base, and sub-base layers). Validate the IC roller result by demonstrating calibration to stiffness of soil and aggregate layers. Submit data acquisition records, completed IC mapping reports, and calibration results. The measurements obtained using the IC roller will not be used by the Engineer for acceptance of the compaction layers.

Xxx-2.0 MATERIALS

None

Xxx-3.0 GENERAL

DEFINITIONS

IC Roller: The intelligent Compaction (IC) roller is defined as a self-propelled smooth drum roller that is capable of measuring and recording in-situ stiffness of the compaction layers along with roller position (RTK-GNSS) and a time stamp.

Mapping Area: The test area is typically a portion of the project covered by one subplot of compaction materials, limited to a single lift. It may also be a test strip with dimensions stated in the specifications.

IC Stiffness Mapping: The mapping of a test area with IC rollers that have been calibrated with the stiffness units for each material type mapped. Such mapping is typically performed with a final full coverage pass of the test area by the IC roller after the required compaction has been achieved.

System Calibration: The Contractor shall have the IC system certified and independently calibrated, upon selected materials, by the Contractor's IC technology professional or independent experienced professional. The Contractor shall have the IC results independently calibrated to read out in stiffness values. Certified calibration test results comparing predicted and measured IC stiffness measured values should demonstrate a coefficient of determination (R^2) ≥ 0.85 . The Contractor's technology provider shall provide training for Contractor and Tollway project staff on use of IC data and mapping reports.

Real-Time Display, Reports: The IC results must be displayed to the roller operator on a color-coded computer screen in real-time and the data must be saved on board for viewing. Results shall also be available for viewing remotely during the rolling operations. IC stiffness mapping reports shall be prepared and submitted by the Contractor or Contractor's IC technology provider.

HAPS: The IC roller will be equipped with a High Accuracy Positioning System (HAPS), typically Real Time Kinematic Global Navigation Satellite System (RTK-GNSS) or Robotic Total Station (RTS), to document the rollers position.

IC stiffness mapping will be required on the surface of all completed compaction layers. Acceptance of the IC results by the Engineer will be based on submitting the data and calibrated mapping report for each layer.

The contractor must submit to the Engineer an IC Stiffness Mapping Work Plan at least two weeks prior to the Preconstruction Meeting. The work plan shall include the following:

1. IC roller make, model, dimensions, weight, and operating parameters (i.e., speed, vibration frequency and amplitude setting(s)).
2. Description of IC measurement system and evidence of previous field calibration results with in-situ stiffness values and a description of the test methods.\
3. Description of IC roller calibration protocols (i.e., description testing procedure(s), number of test locations, and frequency of calibrations).
4. Credentials of the Contractor's IC technology provider.
5. IC stiffness mapping report format, submittal process and timing, and responsible personnel. Provide an example of an IC stiffness mapping report that shows geospatially located and color-coded stiffness values.
6. A contingency plan in case of equipment breakdown or IC system malfunctions during the project.
7. Procedure for transferring IC data to the Engineer and provision for real-time monitoring during IC operations.

Xxx-4.0 EQUIPMENT

1. IC Roller

The IC roller shall meet the following minimum requirements:

- a. Machine Type: Self-propelled smooth drum vibratory roller.
- b. Weight: Operating weight of at least 22,000 lbs.
- c. Drum Width: 7 feet.
- d. Vibration Settings: Amplitude range of 0.029" to 0.075" and frequency range of 30 to 40 Hz.
- e. IC system: Integrated or retrofitted (with a computer screen in the roller cab for real-time viewing of geo-referenced spatial color-coded maps and data storage).
- f. HAPS: HAPS mounted on the roller to report data at the drum center. The HAPS Unit shall receive corrections from a local base station to report RTK-GNSS measurements of northing, easing, and elevation.

2. High Accuracy Positioning System

The Contractor shall provide the High Accuracy Positioning System (HAPS) that meets the following requirements. The goal of the HAPS requirements is to achieve accurate and consistent HAPS measurements among all HAPS devices on the same project. Conversions of HAPS data need to be minimized to avoid errors introduced during the process.

Real Time Kinematic Global Navigation Satellite System (RTK-GNSS)

-or-

Robotic Total Station (RTS)

- a. GNSS Base Station - Local or virtual GNSS base receiver that acquires satellite signals from the GNSS and GLONASS constellations. The GNSS base station shall broadcast updated correction data to the GNSS receivers on the IC rollers during operations.
- b. RTS – A robotic total station set up over a control point determines the position of the targets mounted on the IC Roller(s) and Rover.
- c. Rover - A hand-held GNSS receiver or active RTS target on a survey rod with controller shall be provided and operated by the contractor, for in-situ point measurements in conjunction with the IC roller, at the direction of the Engineer.
- d. GNSS or RTS systems will use the local coordinates of the project control, as established by the surveyor. Accuracy must be verified to within 1 ft between the IC rollers and rovers.
- e. The data from the IC roller shall be displayed to the roller operator on a color-coded computer screen in “real time” during the roller operation and the data shall be saved for transferring and viewing by the Engineer. The color coding will be based on calibration to stiffness values. Target stiffness values will be provided from the Engineer.

Xxx-5.0 OPERATIONS

1. IC Stiffness Mapping

The IC Stiffness mapping shall be performed on all compaction layers, and prior to placing of new fill layer. Mapping must be performed in such a way that it covers the full extent of the compaction work area. Overlapping between adjacent roller lanes shall be limited to 10% or less. Keep roller speed and vibration settings (frequency and amplitude) constant during roller operations and within range of what was used during calibration. Permitted variation in vibration frequency is +/-2Hz and permitted variation in roller speed is +/- 0.5 mph. Record IC stiffness mapping results in the forward direction only unless the roller is calibrated for mapping in reverse direction.

Check, verify and expand the field calibrated results for the IC equipment to ensure proper performance. If the IC results fall outside the limits set initial field calibration, additional tests shall be performed to further expand the calibration. Operate the machine according to the IC technology provider and roller manufacturer’s recommendations to provide reliable and repeatable measurements. A minimum of 12 test points will be required to establish the IC stiffness calibration, and certified calibration test results comparing predicted and measured IC stiffness values should demonstrate a coefficient of determination (R^2) ≥ 0.85 .

2. Equipment Breakdowns

In the event of equipment breakdowns/IC system malfunctions/GNSS problems, the Contractor shall have a contingency plan to acquire the equipment or unit necessary in 3 days, but it is intended that IC stiffness mapping data shall be collected and provided for a minimum 80% of all compaction layers.

Xxx-6.0 IC MEASUREMENTS, OUTPUT, AND REPORTING

1. IC Measurements

The reported IC measurements shall be in situ design stiffness value(s) (modulus of subgrade reaction, elastic modulus, or resilient modulus as provided from the Engineer) that are calibrated using independent in situ testing. Calibration shall be performed over the full range of ground stiffness conditions anticipated on the project site. Calibration work shall be performed by the IC technology professional or independent experienced professional.

2. **Data Collection, Export, and Onboard Display**

Electronic copies of the following shall be provided to the engineer:

- a. Calibration report(s) that summarizes:
 - i. Dates of testing,
 - ii. Names of field personnel conducting tests,
 - iii. Description of tests,
 - iv. Plots of test results,
 - v. Calibration test results comparing IC measurements and stiffness values and a record of certification.

- b. IC stiffness mapping reports that summarizes:
 - i. Dates of testing,
 - ii. Names of field personnel conducting roller operations and in situ verification tests,
 - iii. Description of verification tests, if any,
 - iv. Geo-referenced spatial color-coded maps of in situ stiffness values covering the entire mapping area overlaid on a recent aerial photo of the project.

- c. IC data shall be exported from the vendor's software in mapping data files. Contractor to provide a laptop to the Department with applicable software installed for their sole use during the project to evaluate data and observe real-time results.
 - i. Minimum Computer Specifications:
 - ii. Processor - Intel i5 (or equivalent) Dual Core
 - iii. Graphics Card – AMD Radeon R7 M360 (or equivalent)
 - iv. Memory – 12GB RAM
 - v. Hard Drive – 128GB SSD

Xxx-7.0 PRE-PRODUCTION TEST SECTION(S)

HAPS Correlation and Verification. Prior to the start of mapping, the Contractor, HAPS representative and/or IC roller technology provider shall conduct the following to check the proper setup of the HAPS and IC roller(s) using the same datum:

1. On a location, nearby or within the project limits, as approved by the Engineer, the HAPS to be used on the project shall be set up and calibrated. Verification that the roller positioning system is working properly and that there is communication with all HAPS.
2. The coordinates of the roller from the on-board display shall be recorded.
3. The coordinates for both sides of the front drum shall be measured with a rover, and recorded.
4. The roller and rover coordinates shall be compared to confirm horizontal accuracy of no more than 1 ft. Work shall not begin until proper verification has been obtained.

5. Accuracy verification testing shall be conducted as requested by the Engineer during production operations.

Xxx-8.0 PERSONNEL

The Contractor shall coordinate for on-site technical assistance from the IC technology provider during the initial three (3) days of production and then as needed during the remaining operations. As a minimum, the roller representative shall be present during the initial setup and verification testing of the IC roller(s). The roller representative shall also assist the Contractor and the Engineer with data management using the data analysis software including IC data input and processing.

Xxx-9.0 TRAINING

The Contractor shall coordinate for on-site training for Contractor's and Tollway project personnel related to operation of the IC technology. Contractor's personnel shall include the IC Field manager or IC Program Administrator, IC technician(s), and roller operator(s). Tollway personnel shall include the Project Engineer and field inspector(s). Tollway will provide a location for the training. Training shall be at least 4 hours duration.

Topics shall include the following as a minimum;

1. Background information for the specific IC system(s) to be used.
2. Setup and checks for IC system(s), GNSS or RTS equipment operation. Operation of the IC systems on the roller, i.e. setup data collection, start/stop of data recording, and on-board display options.
3. Operation of analysis software to review IC coverage maps, compare point test data, perform statistics analysis, and produce reports for project requirements.
4. Coverage and uniformity requirements.

Xxx-10.0 ACCEPTANCE OF WORK

IC Roller Data: The procedure for obtaining the IC roller data shall be established between the contractor and the Engineer prior to the pre-construction meeting. The frequency of obtaining the data from each roller shall be a minimum of once each day of compaction or at the completion of each lift in each construction area, whichever is greater. The data is to be date/time stamped, to allow review later, and an electronic compaction report showing the color-coded mapping results from each roller is to be provided to the Engineer.

Xxx-11.0 METHOD OF MEASUREMENT

Progress payments will be made based on a schedule of values approved by the Engineer up to 80% of the bid amount. The remaining 20% of the bid amount will be paid after all submittals required are: submitted, in compliance with this special provision, and accepted by the Engineer.

Xxx-12.0 BASIS OF PAYMENT

1. Payment for Intelligent Compaction stiffness mapping will be the lump sum contract price.
2. Payment is full compensation for all work associated with providing IC equipment, training, reports, and in situ calibration testing.

Payment will be made under:

Pay Item	Pay Unit
Intelligent Compaction (IC) Stiffness Mapping	Lump Sum